

Visible Light Photocatalysis in the Chemistry of Radical Ions and Triplet Nitrenes

By

Elliot Patrick Farney

A dissertation submitted in partial fulfillment of
the requirements for the degree of

Doctor of Philosophy
(Chemistry)

at the

UNIVERSITY OF WISCONSIN–MADISON

2015

Date of final oral examination: 5/21/2015

The dissertation is approved by the following members of the Final Oral Committee:

Tehshik P. Yoon, Professor, Chemistry

Clark R. Landis, Professor, Chemistry

Steven D. Burke, Professor, Chemistry

Jennifer M. Schomaker, Associate Professor, Chemistry

Randall H. Goldsmith, Assistant Professor, Chemistry

Visible Light Photocatalysis in the Chemistry of Radical Ions and Triplet Nitrenes

Elliot Patrick Farney

Under the supervision of Professor Tehshik P. Yoon

At the University of Wisconsin–Madison

The Yoon group has recently pioneered methods to access the chemistry of radical ions using transition metal photocatalysts. The research presented herein describes the development of a radical anion cycloaddition that overcomes the thermodynamic constraints of electron transfer as well as novel strategies towards an enantioselective radical cation Diels–Alder cycloaddition. Observations made in the latter study led to the unexpected discovery that the photocatalyst counteranion has marked effects on the photophysical properties of polypyridyl ruthenium complexes. Attempting to utilize photoinduced electron transfer to generate nitrene radical anions, we obtained evidence consistent with the intermediacy of free triplet nitrenes. Further studies demonstrating the feasibility of energy transfer from photoexcited transition metal complexes to organic azides led to the development of an intermolecular olefin aziridination methodology and an intramolecular cyclization strategy to access a variety of nitrogen-containing heterocycles.

Acknowledgments

This is the most important part of my dissertation. I thank my advisor, Prof. Tehshik Yoon. I met him in the fall of 2009, when I was a naïve “first year” and he was a rising superstar. Intellectually, Tehshik has been an ideal mentor. He has always encouraged me to explore my hypotheses, and he has always guided me in the right direction. Perhaps his greatest quality is his willingness to serve as a sounding board for any ideas, both crazy and reasonable. His ability to see the “big picture” of not just an individual project but an entire research program is something I’m still learning. Tehshik’s tireless work ethic is inspiring, and his excitement for all things chemistry is contagious. Whenever I was losing motivation for a project, I knew that a short conversation with him would be all the encouragement I needed. Lastly, I thank him for his generous support during the tough times and throughout my search for a postgraduate position.

I also thank Prof. Jennifer Schomaker. Mistaking her for an incredibly enthusiastic postdoc during a poster session at a recruiting weekend, she was the first person I met at UW-Madison. She also served as my first mentor in graduate school during a brief three-week rotation in her brand new research group. I don’t think I’ll ever see someone run more simultaneous reactions than Jen, and she has always been a source of inspiration to work harder no matter what. I also thank Prof. Clark Landis, Prof. Steve Burke, and Prof. Randy Goldsmith for taking the time to sit on my dissertation committee. I have learned much from them through supergroups and teaching appointments.

I thank all of the incredible people in the Yoon group for their support, their enthusiasm to discuss science, and their friendship over the past six years. The friendships I have developed with the entire Yoon group (past and present) will last a lifetime. Special thanks goes to the guys in the “Broffice”, namely Kevin, Spencer, Adrian, Evan, and Jim. They made the day-to-day grind that much more tolerable through eclectic musical tastes, paper airplanes, “Farnago”, and only the most serious of scientific discussions. Kevin was a great source of

knowledge and taught me the ropes in my early days of graduate school. Him and Liz offered guidance and always knew how to make me laugh, something of immeasurable value on the ultra-marathon that is graduate school.

The chemistry department at UW-Madison has a great support staff. I thank all of them, especially Charlie Fry for his willingness to help with NMR experiments at all hours of the day, Martha Vestling for her assistance with mass spectrometry, and Tracy Drier for expertly crafting and repairing critical pieces of glassware on short notice.

I thank the most important people in my life, my parents. I could not imagine this journey without their support and guidance. They have sacrificed so much to ensure that I would always be able to strive for my goals. From the weekend visits to the sporting events to the great food to their constant source of encouragement, they have done an incredible amount for me throughout graduate school. They deserve this Ph.D. as much as I do.

Table of Contents

| | |
|---|------|
| Abstract | i |
| Acknowledgments | ii |
| Table of Contents | iv |
| List of Figures | viii |
| List of Schemes | ix |
| List of Tables | xii |
| Chapter 1. Development and Applications of Transition Metal and Photogenerated Nitrenes in Organic Synthesis | 1 |
| 1.1 Introduction | 2 |
| 1.1.1 Reactivity and Spin Multiplicity of Nitrenes | 2 |
| 1.1.2 Formation of Nitrenes | 3 |
| 1.2 Classes of Nitrenes and General Reactivity Trends | 3 |
| 1.2.1 Alkylnitrenes | 3 |
| 1.2.2 Vinylnitrenes | 5 |
| 1.2.3 Arylnitrenes | 8 |
| 1.2.3.1 Elucidating the Photophysics and Reactivity Profile of Phenylnitrene | 8 |
| 1.2.3.2 A Brief Survey of Arylnitrenes in Synthetic Chemistry | 11 |
| 1.2.4 Carbonylnitrenes | 12 |
| 1.2.4.1 Olefin Aziridination as a Mechanistic Probe | 13 |
| 1.2.4.2 C(sp ³)-H Insertion | 15 |
| 1.2.5 Sulfonylnitrenes | 18 |
| 1.3 Harnessing the Reactivity of Nitrenes | 21 |
| 1.4 Introduction to Metallonitrene Chemistry | 22 |
| 1.5 Further Advances in Metallonitrene Additions | 26 |

| | |
|---|----|
| 1.6 Mechanistic Studies on Metallonitrene Chemistry | 29 |
| 1.7 Triplet Sensitized Aziridination and Conclusions | 31 |
| 1.8 References | 32 |
| Chapter 2. Cleavable Redox Auxiliaries in Photocatalyzed Intermolecular [2+2] Cyclobutanations | 40 |
| 2.1 Introduction | 41 |
| 2.2 Results and Discussion | 44 |
| 2.3 Conclusions | 48 |
| 2.4 Contributions | 49 |
| 2.5 Experimental | 49 |
| 2.5.1 General Information | 49 |
| 2.5.2 Synthesis and Characterization of Starting Materials | 50 |
| 2.5.3 Photocycloadditions | 55 |
| 2.5.4 Cleavage of the Auxiliary Group | 66 |
| 2.5.5 Stereochemical Assignments by nOe | 70 |
| 2.6 References | 71 |
| Chapter 3. Photogenerated Nitrenes for Intermolecular Olefin Aziridination | 75 |
| 3.1 Introduction | 76 |
| 3.2 System Design | 77 |
| 3.3 Initial Results | 79 |
| 3.4 Optimization Studies | 80 |
| 3.5 Mechanistic Studies | 83 |
| 3.5.1 Proposal for the Intermediacy of a Nitrene Radical Anion | 83 |
| 3.5.2 Preliminary Exploration of Substrate Scope | 89 |
| 3.5.3 Proposal for the Intermediacy of a Free Nitrene via Energy Transfer | 91 |

| | |
|--|------------|
| 3.6 Conclusions | 94 |
| 3.7 References | 94 |
| Chapter 4. Visible-Light Sensitization of Vinyl Azides by Transition-Metal Photocatalysis | 98 |
| 4.1 Introduction | 99 |
| 4.2 Reaction Design | 100 |
| 4.3 Results and Discussion | 103 |
| 4.4 Mechanistic Studies and Considerations | 107 |
| 4.4.1 Sensitization of Vinyl Azides | 107 |
| 4.4.2 Sensitization of Aryl Azides | 109 |
| 4.4.3 Photophysical Considerations | 110 |
| 4.5 Conclusions | 112 |
| 4.6 Experimental | 114 |
| 4.6.1 General Information | 114 |
| 4.6.2 Synthesis of Cyclization Substrates | 115 |
| 4.6.3 Cyclizations of Vinyl and Aryl Azides | 124 |
| 4.6.4 nOe Studies and Manipulation of the Azirine Intermediate | 132 |
| 4.7 References | 135 |
| Chapter 5. Towards a Photocatalytic Enantioselective Radical Cation Diels–Alder Cycloaddition | 140 |
| 5.1 Introduction | 141 |
| 5.2 System Design: First-Generation Approach | 143 |
| 5.3 Results and Discussion: First-Generation Approach | 145 |
| 5.4 Second-Generation Approach | 150 |
| 5.5 Results and Discussion: Second-Generation Approach | 153 |
| 5.5.1 Jacobsen-Type Ureas as H-Bond Donors | 155 |

| | |
|---|------------|
| 5.5.2 Diaminocyclohexyl Ureas: Impetus and Structure-Activity Relationships | 157 |
| 5.5.3 Pyridinium and Quinolinium Ureas as H-Bond Donors | 162 |
| 5.5.4 C ₃ -Symmetric Phosphotriamides and Synthesis of Non-Symmetric Derivatives for Introduction of Chirality | 164 |
| 5.6 Concluding Remarks and Future Directions | 170 |
| 5.7 Experimental | 173 |
| 5.7.1 General Information | 173 |
| 5.7.2 Synthesis of Polypyridyl Ru(II) Complexes | 174 |
| 5.8 References | 181 |
| Chapter 6. Counteranion Effects on the Properties of Polypyridyl Ru(II) Complexes | 187 |
| 6.1 Introduction | 188 |
| 6.2 Results and Discussion | 189 |
| 6.2.1 Photophysical Studies and the Kinetics of Excited State Quenching | 189 |
| 6.2.2 Electrochemical Studies | 192 |
| 6.2.3 Free Energy of Electron Transfer and the Kinetics of Excited State Quenching | 194 |
| 6.2.4 Counteranion Effects on Chain Propagation | 197 |
| 6.3 Conclusions | 199 |
| 6.4 Experimental | 200 |
| 6.4.1 General Information | 200 |
| 6.4.2 Radical Cation Diels–Alder Cycloadditions | 201 |
| 6.4.3 UV-Vis, Phosphorescence Spectra, and Chain Length Measurements | 202 |
| 6.4.4 Cyclic Voltammetry Experiments | 209 |
| 6.5 References | 213 |
| Appendix. NMR Spectra for New Compounds | 216 |

List of Figures**Chapter 1**

Figure 1-1. Spin multiplicity of nitrenes 2

Chapter 2

Figure 2-1. Cyclobutane-containing natural products 41

Chapter 5

Figure 5-1. Expanded SAR studies for peptidomimetic and diaminocyclohexyl urea scaffolds 161

List of Schemes

Chapter 1

| | |
|---|----|
| Scheme 1-1. Intramolecular energy transfer sensitization in formation of triplet alkylnitrenes | 4 |
| Scheme 1-2. Vinylnitrene trapping in thermal azirine decomposition | 6 |
| Scheme 1-3. Solution phase decomposition of vinylnitrene precursors | 7 |
| Scheme 1-4. Preliminary observations in arylnitrene chemistry | 9 |
| Scheme 1-5. Solution-phase photochemistry of phenyl azide and phenylnitrene | 11 |
| Scheme 1-6. General classes of carbonylnitrenes | 13 |
| Scheme 1-7. Stereochemistry of olefin aziridination by a carbalkoxynitrene | 14 |
| Scheme 1-8. Experiments probing spin multiplicity and stereospecificity in C-H insertion | 16 |
| Scheme 1-9. Comparison of alkanoylnitrene and carbethoxynitrene cyclizations | 17 |
| Scheme 1-10. Dibenzothiophene sulfilimines as sulfonylnitrene precursors | 19 |
| Scheme 1-11. Photolysis of 2-naphthylsulfonyl azide and excited state rearrangement | 20 |
| Scheme 1-12. Cu-catalyzed decomposition of benzenesulfonyl azide | 22 |
| Scheme 1-13. Early studies on metallonitrene transfer chemistry by Breslow and Gellman | 24 |
| Scheme 1-14. Manganese porphyrins for imido group transfer to olefins | 25 |
| Scheme 1-15. Evans' Cu-catalyzed aziridination | 26 |
| Scheme 1-16. Jacobsen's Cu-catalyzed aziridination and mechanistic proposal | 27 |
| Scheme 1-17. Proposed mechanism of aziridination via a metallonitrene intermediate | 30 |

Chapter 2

| | |
|---|----|
| Scheme 2-1. Photosensitized cyclobutanation of cyclic enones | 42 |
| Scheme 2-2. Cyclobutanation by controlled potential electrolysis | 42 |
| Scheme 2-3. Intermolecular cycloaddition of acyclic enones by photocatalysis | 43 |

| | |
|---|-----|
| Scheme 2-4. Dimerization of candidate enones | 44 |
| Chapter 3 | |
| Scheme 3-1. Photochemical reduction of aryl azides by Ru(bpy) ₃ ²⁺ | 78 |
| Scheme 3-2. Azide reduction with iridium complex 3-8 in the absence of reductive quencher | 80 |
| Scheme 3-3. Proposed mechanism for photocatalyzed aziridination via a nitrene radical anion | 83 |
| Scheme 3-4. Sensitization and electron transfer steps in nitrene radical anion formation | 88 |
| Scheme 3-5. Aziridination of allylsilane 3-35 | 89 |
| Scheme 3-6. Electron transfer versus concerted electron exchange | 91 |
| Scheme 3-7. Probing reactivity of the photogenerated intermediate | 93 |
| Chapter 4 | |
| Scheme 4-1. 2 <i>H</i> -Azirine trapping experiment in the presence of cyclopentadiene | 105 |
| Scheme 4-2. Isolation and manipulation of 2 <i>H</i> -azirine 4-40 | 106 |
| Scheme 4-3. Pathways for generation of azirine 4-11 | 107 |
| Scheme 4-4. Pathways for conversion of azirine 4-11 to pyrrole 4-3 | 108 |
| Scheme 4-5. Energy transfer mechanism from [Ru] sensitizer to azidoacrylates | 110 |
| Scheme 4-6. Jablonski diagram for triplet energy transfer | 111 |
| Chapter 5 | |
| Scheme 5-1. Arene(poly)carboxylate-sensitized addition of alcohol nucleophiles | 143 |
| Scheme 5-2. Mechanistic proposal for a photocatalyzed radical cation Diels–Alder cycloaddition | 144 |
| Scheme 5-3. Synthesis of substituted BINOL 5-10 and derivatization | 146 |

| | |
|---|-----|
| Scheme 5-4. Photoanation chemistry of polypyridyl Ru(II) complexes in nonpolar solvents | 149 |
| Scheme 5-5. Mechanistic constructs for enantioselective Diels-Alder reactions | 150 |
| Scheme 5-6. Anion-binding strategy applied to a radical cation intermediate | 151 |
| Scheme 5-7. Photocatalyzed intermolecular radical cation Diels-Alder reaction | 152 |
| Scheme 5-8. Survey of sulfonamide, sulfonamide, and sulfamoyl ureas | 158 |
| Scheme 5-9. Asymmetric induction for an intermolecular, sulfonate-catalyzed Povarov reaction | 158 |
| Scheme 5-10. Pyridinium ureas as hydrogen-bond donors in nitroolefin/indole addition | 162 |
| Scheme 5-11. Phosphotriamides as sulfonate anion-binding scaffolds in an ionic cycloaddition | 165 |
| Scheme 5-12. Syntheses of novel, non-symmetric phosphotriamides | 167 |
| Scheme 5-13. Synthesis of tris-aryl phosphotriamides and [Diels-Alder studies] | 168 |
| Scheme 5-14. Attempted syntheses of substituted phosphotriamides | 169 |
| Scheme 5-15. Comparison between first- and second-generation approaches | 171 |

List of Tables

Chapter 2

| | |
|---|----|
| Table 2-1. Optimization studies on the crossed, intermolecular [2+2] cycloaddition | 45 |
| Table 2-2. Substrate scope of the intermolecular [2+2] cycloaddition | 46 |
| Table 2-3. Substrate scope of the intramolecular [2+2] cycloaddition | 47 |
| Table 2-4. Cleavage of the redox auxiliary | 48 |

Chapter 3

| | |
|--|----|
| Table 3-1. Concentration and scale-up studies | 81 |
| Table 3-2. Survey of sulfonyl azides | 84 |
| Table 3-3. Survey of olefins in photosensitized aziridination | 85 |
| Table 3-4. Survey of iridium photocatalysts | 87 |
| Table 3-5. Preliminary exploration of substrate scope | 90 |

Chapter 4

| | |
|--|-----|
| Table 4-1. Initial investigations on triplet sensitization of dienyl azide 4-1 | 101 |
| Table 4-2. Pyrrole synthesis substrate scope study | 104 |

Chapter 5

| | |
|--|-----|
| Table 5-1. Chiral catalyst and oxidative quencher screen | 147 |
| Table 5-2. Counteranion survey with Ru(dfmb) ₃ ²⁺ complexes | 154 |
| Table 5-3. Hydrogen-bond donor studies | 156 |
| Table 5-4. Evaluation of chiral diaminocyclohexyl urea scaffolds | 160 |
| Table 5-5. Pyridinium and quinolinium ureas as H-bond donors and PET sensitizers | 163 |
| Table 5-6. Phosphotriamide and thiophosphotriamide study | 166 |
| Table S5-1. Substrate survey in the radical cation Diels-Alder cycloaddition | 180 |

Chapter 6

| | |
|--|-----|
| Table 6-1. Counteranion survey with Ru(dfmb) ₃ ²⁺ complexes | 190 |
| Table 6-2. Photophysical data for polypyridyl ruthenium sensitizers | 191 |
| Table 6-3. Electrochemical data in CH ₂ Cl ₂ and the dependence on counteranion | 193 |
| Table 6-4. Empirical and computed thermochemical and kinetic data for excited state quenching | 196 |
| Table 6-5. Quantum yield and chain length determinations | 199 |

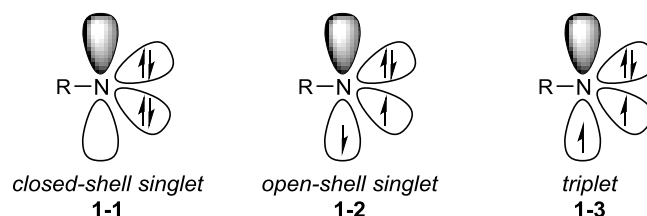
**Chapter 1. Development and Applications of Transition Metal and Photogenerated
Nitrenes in Organic Synthesis**

1.1 Introduction

1.1.1. Reactivity and Spin Multiplicity of Nitrenes

Nitrenes are neutral, electrophilic, hypovalent, nitrogen-centered species¹ that tend to exhibit higher reactivity than their well-studied, isoelectronic carbene counterparts, due in part to the increased electron affinity of nitrogen compared to carbon.^{2a} Often implicated as non-isolable intermediates, the reactivity profile of nitrenes derives from the fact that nitrogen possesses only six valence electrons. Two electrons are present in a covalent bond with a hydrogen atom or R group, and two electrons constitute a nitrogen lone pair. As shown in Figure 1-1, the remaining two electrons can be spin-paired in a single p-orbital (closed-shell singlet nitrene, **1-1**), be spin-paired in separate orbitals (open-shell singlet nitrene, **1-2**), or exist in separate orbitals with parallel spins (triplet nitrene, **1-3**).^{2b}

Figure 1-1. Spin multiplicity of nitrenes



Generally, the spin state of a nitrene largely controls its reactivity. Singlet nitrenes are short-lived, highly electrophilic species that tend to undergo insertion into unactivated carbon-hydrogen bonds, add in a stereospecific fashion to olefins to form aziridines, and undergo nucleophilic attack by alcohols and other polarized species. Contrastingly, triplet nitrenes tend to be far less reactive, with reactivity best characterized as that of a 1,1-diradical; thus, they undergo non-stereospecific additions to olefins and perform hydrogen-atom abstraction in lieu of C-H insertion.

However, it is not only the electronic configuration that controls the reactivity of a nitrene but also its substituents. Accordingly, Section 1.2 will be devoted to a discussion of those nitrenes that have been central to the development of both free nitrene chemistry and the field

of metallonitrene chemistry. We will focus on the fundamental properties of the respective nitrenes, as elucidated by careful mechanistic and photophysical studies, and place substantially less emphasis on myriad heterocyclic architectures that have been synthesized with nitrene chemistry.

1.1.2. Formation of Nitrenes

Generation of nitrenes can be accomplished in a variety of ways, but nitrenes discussed in this review are typically formed by thermolysis or photolysis of an appropriate azide with subsequent extrusion of molecular nitrogen from the thermally perturbed or photochemically excited azide in its singlet state; both methods afford a mixture of singlet and triplet nitrenes. Removal of two singly bonded groups to nitrogen via α -elimination leads to singlet nitrenes. Triplet nitrenes can be generated by azide photolysis in the presence of a triplet sensitizer such as benzophenone or acetophenone or by intersystem crossing (ISC) from a singlet excited state. It should be noted that the latter method is often not suitable for accessing the reactivity of triplet nitrenes because, unlike their carbene counterparts, triplet nitrenes are formed by very inefficient ISC.³

1.2 Classes of Nitrenes and General Reactivity Trends

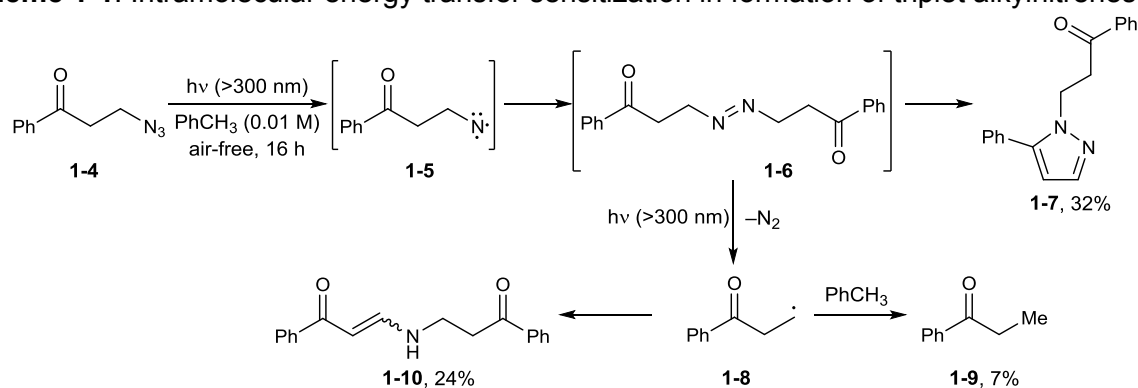
1.2.1. Alkylnitrenes

Alkylnitrenes have long been proposed as intermediates in a wide range of rearrangements.⁴ Studies by Stieglitz near the turn of the 20th century suggested that hypovalent nitrogen-derived species were intermediates in the Beckmann rearrangement, the decomposition of trityl azide to benzophenone phenylimine, and the rearrangement of *N*-halo amines to afford imines.⁵ However, efforts to spectroscopically characterize alkylnitrenes were unsuccessful until 1964, when Wasserman reported electron paramagnetic resonance (EPR)

studies of a variety of alkylnitrenes generated from UV-photolysis of alkyl azides in glass matrices at 4 K.⁶ Low temperatures promote intersystem crossing over intramolecular rearrangement, enabling triplet nitrenes to be efficiently formed and observed. These nitrenes exhibited long lifetimes and EPR values consistent with triplet imidogen (NH) and were thus assigned as alkylnitrenes having a triplet ground state. Alkylnitrenes were among the first species to be investigated by flash photolysis, thus paving the way for spectroscopic analysis of nitrenes in general.⁷

Triplet alkyl nitrenes have been calculated to be ~35 kcal/mol more stable than their singlet counterparts and have long lifetimes ($\tau \sim 27$ ms) due to the inability of a triplet alkyl nitrene to rearrange to the singlet imine.^{8a} However, triplet alkyl nitrenes have not been studied extensively in solution phase, in part because they are difficult to generate selectively due to the large singlet/triplet energy gap, and consequently, slow rate of ISC. In fact, Gudmundsdóttir and co-workers recently reported the only conclusive solution phase studies on triplet alkyl nitrenes.^{8b} They hypothesized that triplet alkyl nitrenes could be selectively generated by intramolecular energy transfer from acetophenone, a well-studied sensitizer exhibiting very efficient intersystem crossing from the singlet to triplet manifold (10^{11} s^{-1}) with a quantum yield near unity.

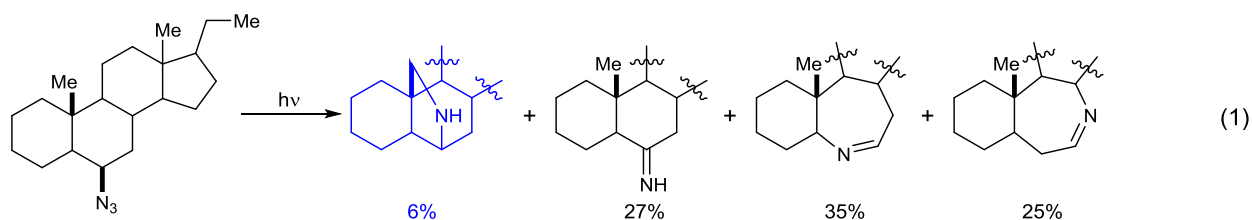
Scheme 1-1. Intramolecular energy transfer sensitization in formation of triplet alkylnitrenes



Indeed, incorporation of acetophenone and an alkyl azide within the same molecule (**1-4**, Scheme 1-1) led to selective generation of triplet alkyl nitrene **1-5** when **1-4** was submitted to

laser flash photolysis in solution (excimer laser, 17 ns, 150 mJ, 308 nm).⁸ In a separate experiment, prolonged irradiation of triplet alkyl nitrene **1-5** primarily formed azo dimer **1-6** that cyclized to pyrazole **1-7** and formed propiophenone radical **1-8** that further reacted to afford propiophenone **1-9** or enaminone **1-10**.

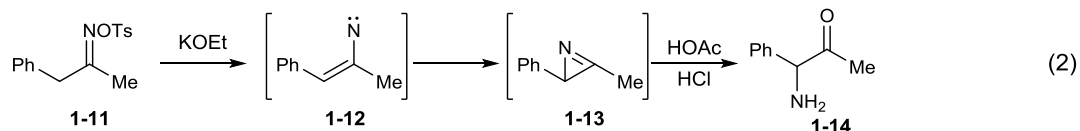
No evidence for the existence of singlet alkyl nitrenes, however, has ever been obtained. This is likely due to the fact that alkylnitrenes possess α -hydrogen atoms, thus enabling very rapid 1,2-hydrogen or alkyl migration before intersystem crossing to the triplet state can occur. Additionally, 1,2-hydrogen or alkyl migration are hypothesized to proceed directly from the singlet excited azide and bypass the singlet nitrene altogether.⁹ These rearrangements are rapid and unselective and have thus severely complicated efforts to utilize alkylnitrenes in synthesis (eq. 1).¹⁰



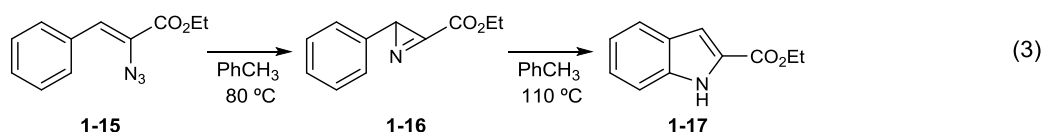
Overall, alkylnitrenes have experienced very little utility in empirically-viable, solution phase chemistry. Indeed, rapid rearrangement upon photolysis precludes intermolecular reactivity and effectively obviates C-H insertion or oxidative functionalization processes that are common to other classes of nitrenes to be discussed in this review.

1.2.2 Vinylnitrenes

Vinylnitrenes were first postulated as intermediates in the rearrangement of ketoximes to α -amino ketones (the Neber rearrangement).¹¹ The work of Cram^{12a} and House^{12b} demonstrated that γ -elimination from **1-11** formed non-isolable azirine **1-13** via the putative vinylnitrene **1-12**; subsequent azirine hydrolysis furnished the α -amino ketone **1-14**.

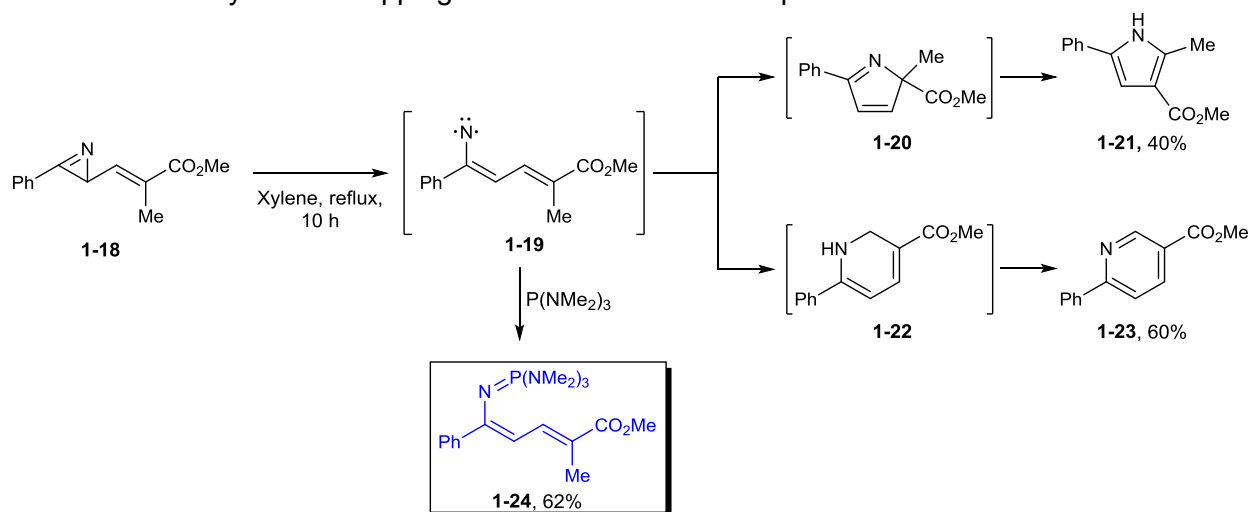


While a concerted γ -elimination to give azirine **1-13** was ruled out based on the requirement for front-side displacement of a *syn*-oxime tosylate, conclusive evidence for the presence of a vinylnitrene was never obtained.¹³ Nevertheless, this study spurred considerable interest in the possibility that vinylnitrenes might be utilized in a variety of synthetically useful transformations.



Indeed, seminal reports by Hassner,¹³ Taniguchi,^{14a} and Hemetsberger^{14b} demonstrated that *2H*-azirines **1-16** could be isolated from thermolysis of styrenyl azides and α -azidocinnamates **1-15** (eq. 3). Interestingly, re-subjecting azirines such as **1-16** to a higher reaction temperature led to the corresponding indole **1-17**. Subsequently, it was discovered that oxazoles,^{15a} quinones,^{15b} pyrazoles,^{15c} β -lactams,^{15d} and azepines^{15e} could also be synthesized from readily prepared azirines.

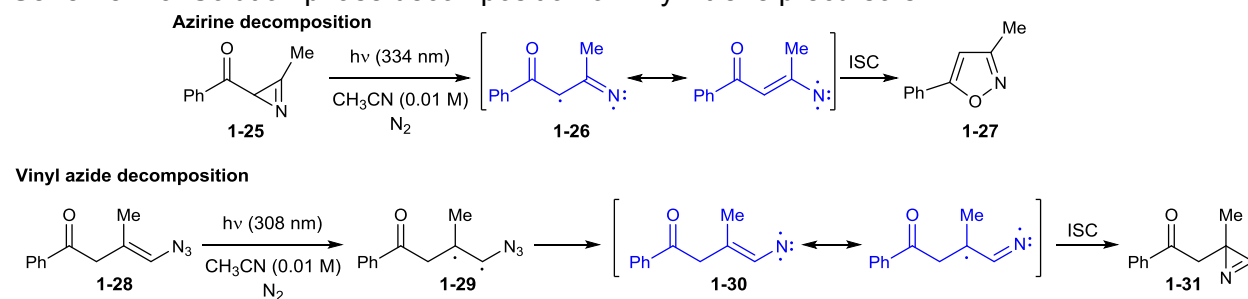
Scheme 1-2. Vinylnitrene trapping in thermal azirine decomposition



Padwa's investigations on methacryloyl α -2*H*-azirine **1-18** provided the first substantive support for the intermediacy of a vinylnitrene in azirine decomposition and rearrangement (Scheme 1-2).¹⁶ The direct thermolysis of **1-18** produced pyrrole **1-21** and pyridine **1-23**, presumably via dihydropyrrole **1-20** and dihydropyridine **1-21**. However, when **1-18** was thermolyzed in the presence of tris(dimethylamino)phosphine,¹⁷ phosphineimine **1-24** was isolated as the sole product of the reaction. This experiment provided evidence for singlet vinylnitrene **1-19** as a common intermediate in formation of dihydropyrrole **1-20** and dihydropyridine **1-22**.¹⁸

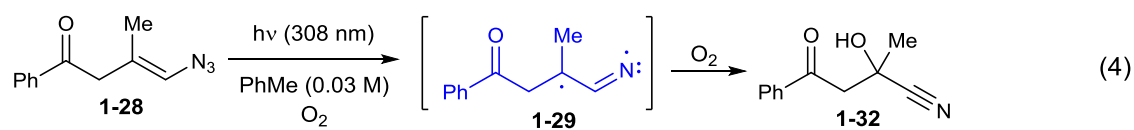
Until recently, there were no examples of the direct detection or characterization of vinylnitrenes. Parasuk and Cramer calculated that triplet vinylnitrene is 15 kcal/mol more stable than the lowest energy singlet state.¹⁹ The lowest energy singlet state is open shell and resembles a 1,3-biradical. When compared to the 35 kcal/mol singlet–triplet gap for alkylnitrenes (Section 1.2.1), it is evident that (a) the vinyl group stabilizes the singlet state by delocalizing an unpaired spin and (b) due to the open-shell character of the singlet, less electron-electron repulsions exist than for closed-shell singlet alkylnitrenes. Thus, it was hypothesized that triplet vinylnitrenes would be even more stable than triplet alkylnitrenes.

Scheme 1-3. Solution phase decomposition of vinylnitrene precursors



Surprisingly, this hypothesis was refuted by experimental data. Applying the intramolecular triplet energy transfer strategy discussed in Section 1.2.1, Gudmundsdóttir and coworkers performed laser flash photolysis on 2*H*-azirine **1-25** and obtained solution phase spectroscopic data supporting the existence of triplet vinylnitrenes **1-26** (Scheme 1-3).^{20,21}

Despite the apparent increased stability relative to alkylnitrenes, it was discovered that ground state triplet vinylnitrene **1-26** decays to isoxazole **1-27** by fast (10^6 s^{-1}) intersystem crossing relative to the 27 ms lifetime of triplet alkylnitrenes. In a later study, evidence was provided for the intermediacy of a vinylnitrene following *azide* decomposition.²² Indeed, intramolecular energy transfer from the acetophenone sensitizer in vinyl azide **1-28** resulted in biradical **1-29** that subsequently formed vinylnitrene **1-30**. This species was detected by transient absorption spectroscopy and was found to undergo ISC to form azirine **1-31**.



Unlike triplet alkyl or aryl nitrenes, triplet vinylnitrenes do not dimerize, perform H-atom abstraction, or react slowly (10^4 – $10^7 \text{ M}^{-1}\text{s}^{-1}$) with O_2 to yield nitro compounds. Instead, the highly delocalized spin density inherent to vinylnitrenes imparts fascinating reactivity upon these short-lived intermediates, whereby photolysis of **1-28** in O_2 -saturated solution led to rapid ($7 \times 10^8 \text{ M}^{-1}\text{s}^{-1}$) C-O bond formation at the tertiary β -carbon to afford **1-32** (eq. 4).²⁶ Therefore, this experiment and those in Scheme 1-3 demonstrate that the reactivity of triplet vinylnitrenes is best described as an iminyl biradical, a species exhibiting reactivity of a carbon-centered radical.

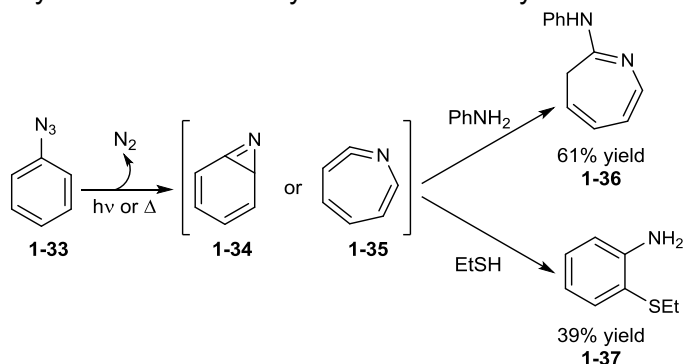
1.2.3 Arylnitrenes

1.2.3.1 Elucidating the photophysics and reactivity profile of phenylnitrene

The complex photochemistry of aryl nitrenes has long been the subject of intense study.²³ Even before elucidation of the photophysical decomposition and rearrangement pathways available to aryl nitrenes, thermolysis and photolysis of aryl azides followed by intramolecular cyclization²⁴ was used for the syntheses of many nitrogenous heterocycles. Indeed, this is perhaps the most prevalent use of aryl- and heteroarylnitrenes. This vast collection of reactions

is best left to several reviews,²⁵ though a few examples will be discussed here. This section will primarily be devoted to the *solution-phase* photochemistry of aryl nitrenes. In the last two decades, this area has received increased attention due to the importance of aryl nitrenes in photoaffinity labeling and photocrosslinking to determine the higher order structure of RNA and RNA-protein complexes.²⁶

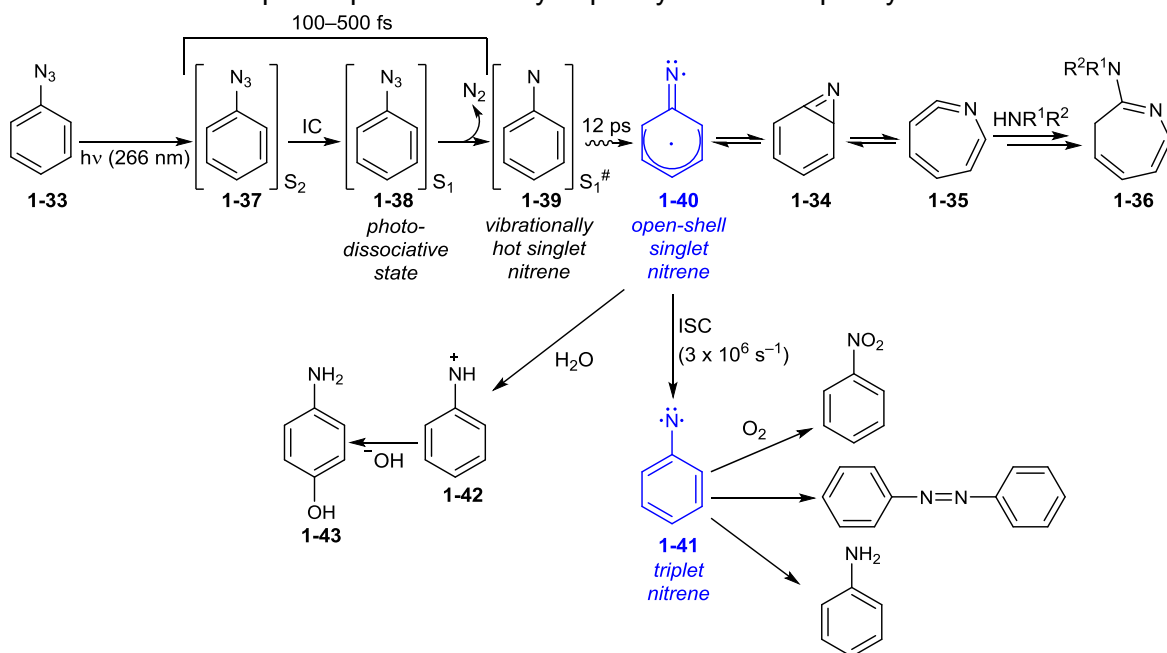
Scheme 1-4. Preliminary observations in aryl nitrene chemistry



The earliest investigations on aryl nitrenes were not promising. The direct photolysis and thermolysis of phenyl azide and most of its derivatives at concentrations $>10^{-3}$ M in benzene, cyclohexene, or acetonitrile leads to polymeric tars and low yields ($<5\%$) of azobenzene in lieu of C-H insertion products and aziridines.²⁷ Huisgen^{28a,b} discovered that thermolysis of phenyl azide **1-33** in the presence of aniline afforded 3*H*-azepine **1-36**; Doering^{28c} also observed its formation under photolytic conditions (Scheme 1-4). It was originally hypothesized that **1-36** could be derived from nucleophilic attack on heterocumulene **1-35**. However, this hypothesis failed to explain the formation of *o*-thioalkoxyaniline **1-37** when phenyl azide was photolyzed in the presence of thiols. Thus, benzazirine **1-34** was postulated as another potential intermediate in aryl azide decomposition.²⁹ Unfortunately, the relationship between benzazirine **1-34** and 1,2-didehydroazepine **1-35** was unclear, but more troubling was that the precursor to either **1-34** or **1-35** was not known. Interestingly, reactions initiated by triplet sensitization in the presence of diethylamine gave azobenzene and aniline instead of the corresponding 3*H*-azepine,³⁰ suggesting that azobenzene and aniline arise from a triplet nitrene.³¹ Benzazirine **1-34**, 1,2-

didehydroazepine **1-35**, and 3*H*-azepine **1-36**, therefore, must arise from a precursor of singlet spin multiplicity.

The advent of transient absorption spectroscopy was critical to unifying all the empirical data regarding arylnitrene reactivity. In 1997, Platz^{32a} and Wirz^{32b} were finally able to detect singlet phenylnitrene ($\tau = 1$ ns) by laser flash photolysis, which provided the critical link to explaining the formation of all primary photoproducts arising from photolysis of phenyl azide. A follow-up study reported the observation of triplet phenylnitrene and revealed that its spectroscopic signature exhibited great similarity to singlet phenylnitrene, consistent with these two species having very similar open-shell electronic configurations.³³ Indeed, high-level calculations had shown that open-shell singlet phenylnitrene is 18 kcal/mol lower in energy than closed-shell singlet phenylnitrene.³⁴ This confirms that singlet phenylnitrene is the logical precursor to benzazirine **1-34**, as the biradical nature of the open-shell singlet nitrene facilitates its cyclization to benzazirine. Observation of benzazirine **1-34** proved a formidable challenge, but Platz obtained absorption data consistent with a *t*-butyl substituted benzazirine with a lifetime of 62 ns in solution at room temperature as a transient precursor to the corresponding 1,2-didehydroazepine.^{35a} More recently, Inui and McMahon reported unprecedented, direct observation of 4-methoxy- and 4-methylthiobenzazirine in argon matrices at 10 K.^{35b} Finally, 1,2-didehydroazepine **1-35** was independently detected by solution phase time-resolved IR and UV-vis spectroscopy.³⁶

Scheme 1-5. Solution-phase photochemistry of phenyl azide and phenylnitrene

A mechanistic picture consistent with all these data is presented in Scheme 1-5. It has recently been shown by femtosecond UV-vis analysis that initial azide excitation gives rise to the second singlet excited azide **1-37** that undergoes rapid internal conversion (IC) to the photo-dissociative first singlet excited azide **1-38**.³⁷ Extrusion of N₂ affords a vibrationally hot singlet nitrene **1-39** that relaxes to open-shell singlet nitrene **1-40**. From here, formation of either benzazirine **1-34** or triplet nitrene **1-41** can occur. The last notable reaction resulting from photolysis of phenyl azide was the formation of nitrenium ion **1-42** ($\tau = 110$ ps). This species is the only known trapped product of singlet phenylnitrene and undergoes further reaction to yield substituted aniline **1-43**.

1.2.3.2 A brief survey of arylnitrenes in synthetic chemistry

The vast majority of reactions involving free arylnitrenes in preparative chemistry are intramolecular cyclizations onto aryl, heteroaryl, and alkenyl groups appended *ortho* to the nitrene moiety.²⁵ These cyclizations proceed with retention of configuration and typically work best when synthesizing 5- and 6-membered heterocycles. Carbazoles,^{38a} benzimidazoles,^{38b}

indoles,^{38c} phenothiazines,^{38d} carbolines,^{38e} thienopyrroles,^{38f} and strained aziridines^{38g} can all be formed from either thermolysis or photolysis of arylnitrene precursors.

A select number of intermolecular processes have also been studied. Arylnitrenes have been shown to undergo intermolecular C-H insertion with excellent selectivity for insertion into tertiary C-H bonds [$\sim 200:7:1$ ($3^\circ:2^\circ:1^\circ$)], amounting to the highest chemoselectivity among all nitrenes due to stabilization of the free nitrene by electron donation from the aromatic ring.^{39a} While preparative studies on this reaction are rare due to poor yields and copious aniline formation, it is interesting to note that conclusive evidence exists for C-H insertion by the *triplet* phenylnitrene instead of the singlet phenylnitrene.^{39b} This is unique to arylnitrenes. Reports of intermolecular olefin aziridination via a free arylnitrene intermediate are also very scarce, likely due to the complex solution phase chemistry discussed in Section 1.2.3.1. While aryl azides can add to olefins to give a triazoline that is subsequently decomposed to the aziridine under UV-irradiation, this is only feasible for strained olefins such as norbornene.⁴⁰ Thus, the vast majority of methods for olefin aziridination by a nitrene involve metallonitrene intermediates (Section 1.4).

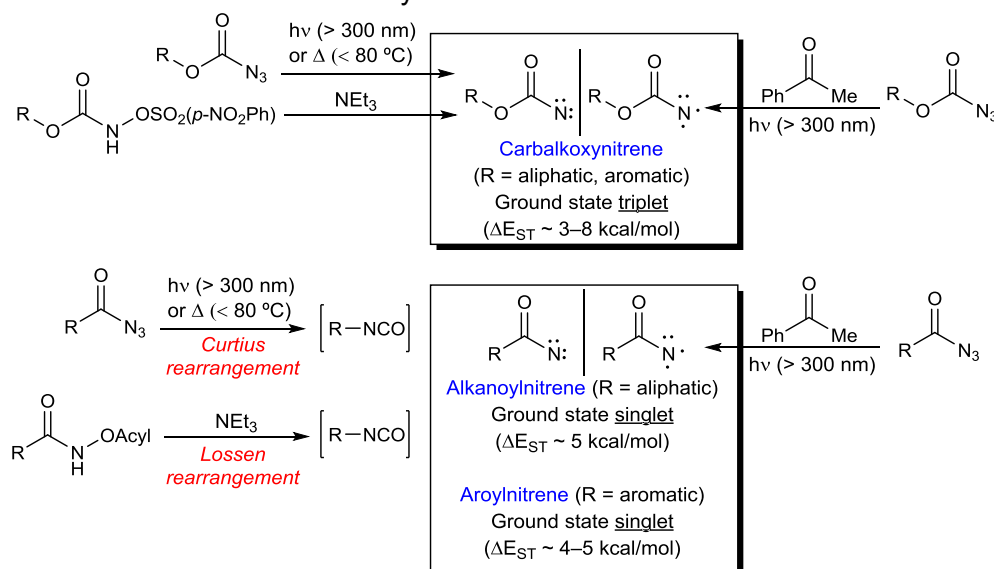
1.2.4 Carbonylnitrenes

The general categorization of “carbonylnitrenes” encompasses carbalkoxy-, alkanoyl- and aroylnitrenes (Scheme 1-6).⁴¹ While carbalkoxynitrenes can be formed by thermolysis, direct photolysis, sensitized photolysis, or α -elimination of azides, alkanoyl and aroylnitrenes can only be formed by sensitized photolysis. Thermolysis, direct photolysis, or α -elimination of the latter two species affords isocyanates arising from Curtius or Lossen rearrangements. Unfortunately, these rearrangements appear to arise from the excited azide and therefore are highly competitive with nitrene formation, often affording isocyanate to the exclusion of nitrene.

Because carbalkoxynitrenes are typically not prone to the intramolecular rearrangement and decomposition pathways that hamper many classes of nitrenes, carbalkoxynitrenes have

been employed in synthetic applications. In particular, nitrene addition to olefins installs an aziridine, a versatile carbon electrophile that can be used to construct myriad nitrogenous architectures. Olefin aziridination has also served as a valuable mechanistic probe for elucidating nitrene spin multiplicity. Originally developed by Skell and Woodward for carbenes,⁴² Lwowski applied this probe to nitrenes, and the resulting studies were of paramount importance in understanding nitrene reactivity.

Scheme 1-6. General classes of carbonylnitrenes

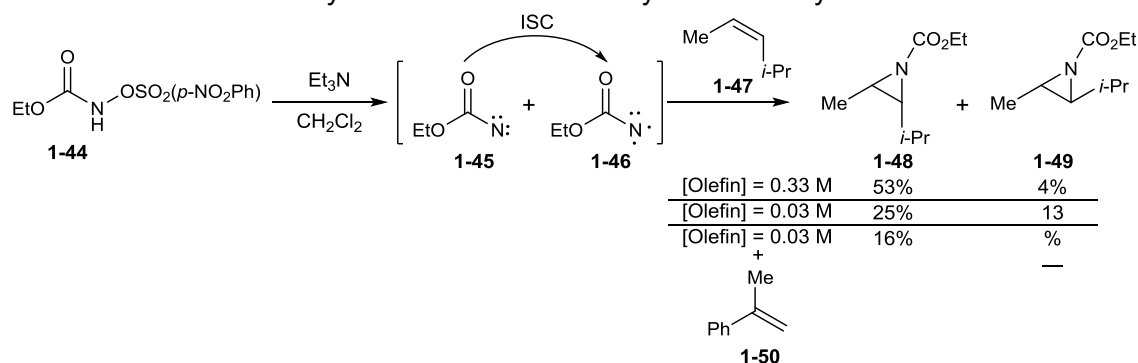


1.2.4.1 Olefin Aziridination as a Mechanistic Probe

Indeed, Lwowski and co-workers found the stereospecificity of carbalkoxynitrene addition to olefins to be dependent on the following variables: a) mode of nitrene generation, b) olefin concentration, and c) olefin identity (Scheme 1-7).⁴³ First, generating carbalkoxynitrenes by photolysis led to poor stereospecificity, as approximately one-third of nitrene was directly generated as the triplet. On the other hand, high stereospecificity in olefin aziridination by carbalkoxynitrenes could be achieved by α -elimination, as from **1-44** in Scheme 1-7. Second, the stereoselectivity of aziridination increased with the concentration of olefin **1-47**. This is in accord with Lwowski's adaptation of Skell-Woodworth theory, which states that singlet nitrenes

add to olefins in a single, concerted step to afford stereospecific aziridination; triplet nitrenes add to olefins in two steps via a long-lived 1,3-diradical intermediate, and thus undergo nonstereospecific aziridination. The observed concentration dependence on stereoselectivity can be rationalized as a consequence of the fact that higher olefin concentration results in a higher probability of intercepting the singlet nitrene **1-45** (stereospecific addition to afford **1-48**) before ISC to the triplet manifold **1-46** (non-stereospecific addition to afford **1-48** and **1-49**).

Scheme 1-7. Stereochemistry of olefin aziridination by a carbalkoxynitrene



Finally, α -methylstyrene **1-50** was investigated as a “triplet trap.” It was predicted that addition of nitrene **1-46** to styrenyl olefin **1-50** would proceed faster than addition of **1-46** to aliphatic olefin **1-47** due to formation of a highly stabilized benzylic radical in the latter case. Indeed, *trans*-aziridine **1-49** was not observed upon addition of **1-50**, consistent with selective consumption of triplet **1-46** by **1-50**, leaving only singlet **1-45** to perform stereospecific aziridination of **1-47**.

These experiments combined with EPR spectroscopy provide excellent circumstantial evidence for nitrene spin multiplicity. As just discussed, (ethoxycarbonyl)nitrene, which is known by EPR spectroscopy to have a triplet ground state, gives both the *cis*- and *trans*-aziridines from reaction with *cis*-4-methyl-2-pentene. In contrast, nitrogen- and sulfur-substituted nitrenes ($R_2NN:$ and $RSN:$) are believed to have singlet ground states and exhibit retention of stereochemistry upon olefin addition.⁴⁴

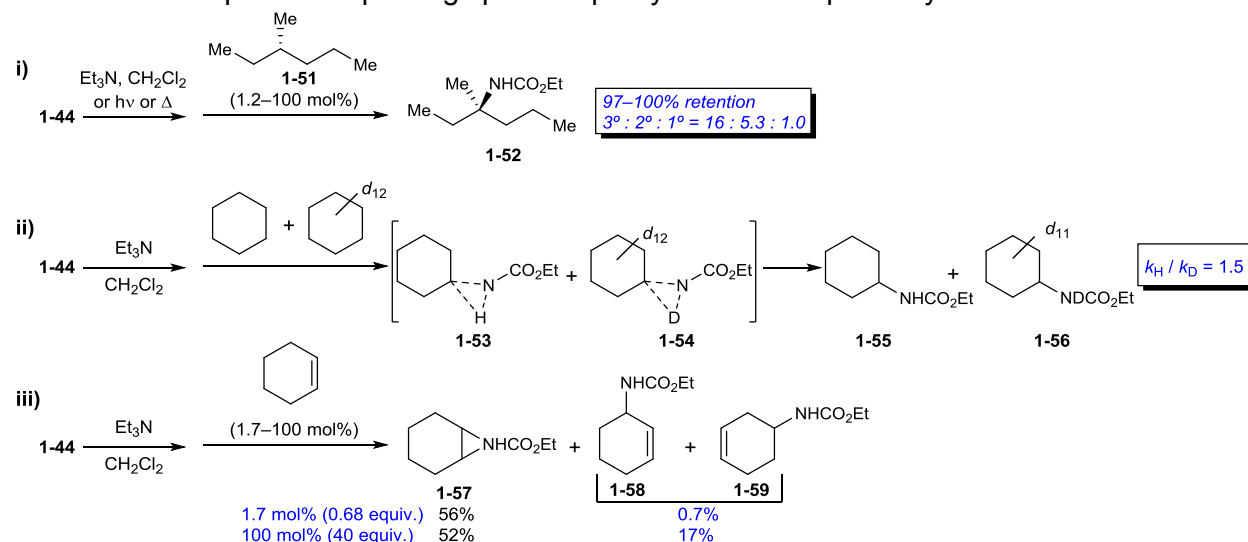
Schuster and co-workers have shown that *both* direct photolysis *and* triplet sensitized photolysis of β -naphthoyl azide in solutions containing *cis*- or *trans*-4-methyl-2-pentene, α -deuteriostyrene, or (*E*)- β -deuterio- α -methylstyrene gave exclusively retention of olefin stereochemistry, consistent with the reacting species being a *singlet* nitrene.⁴⁵ Since there are no experiments (such as the Curie law test for triplets) able to unambiguously confirm the existence of a singlet ground state for a transient intermediate, further circumstantial evidence in favor of the hypothesis was provided. A long-lived singlet nitrene reacting with olefin before the triplet ground state could be reached was ruled out by determining that this singlet state would have to exhibit an unreasonably long lifetime of 200 ns. Furthermore, the species produced in these experiments does not form azo dimer and exhibits no reactivity with O₂, which is inconsistent with the reactivity of a triplet nitrene (see Sections 1.2.1 and 1.2.2). Therefore, it was concluded that the data support ground state singlet multiplicity for aroylnitrenes with a small triplet/singlet gap, a necessary requirement to account for rapid ISC, as no reactivity arising from the higher energy triplet state was ever observed. Recent work by Platz has confirmed the ground state nature of aroylnitrenes, established the very short lifetime (120 ps) of the singlet excited azide, and confirmed that isocyanate formation does not arise from nitrene rearrangement but instead from photo-Curtius rearrangement in the lowest singlet excited state of the aroylazide.⁴⁶

1.2.4.2 C(sp³)-H Insertion

Most nitrenes exhibit some degree of chemoselectivity with respect to insertion into unactivated C-H bonds. Even though substantial evidence demonstrates that nitrene C-H insertion occurs in a concerted fashion from the singlet manifold (see below) and thus does not proceed via homolytic bond cleavage, the general order of reactivity correlates well to C-H bond dissociation energies. For example, the rate of insertion generally decreases in the order 3° > 2° > 1°; this has been found to equate to approximately a 30:9:1 (3°:2°:1°) ratio of C-H

bond reactivity towards a carbonylnitrene.^{43b} However, while C-H insertion is possible for all nitrenes, this reaction is only preparatively feasible for using carbalkoxynitrenes or sulfonylnitrenes, as most other nitrenes cannot be generated in a selective manner without first undergoing rearrangement or decomposition. Studies on C-H insertion by nitrenes have also elucidated fundamental principles that guided synthetic efforts, and as such, the discussion of C-H insertion will begin with a mechanistic picture.

Scheme 1-8. Experiments probing spin multiplicity and stereospecificity in C-H insertion

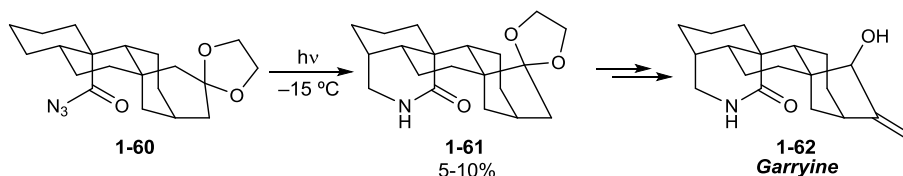


Seminal studies by Lwowski and co-workers (Scheme 1-8) found that (i) nitrene insertion into the optically active methine carbon of (*S*)-(+)-3-methylhexane **1-51** to afford **1-52** proceeded with complete retention of configuration *regardless* of the mode by which the putative nitrene was generated, and the selectivity of insertion was not dependent upon olefin concentration (note: not all insertion products are depicted).^{47a} In experiments (ii) involving equimolar cyclohexane and cyclohexane-*d*₁₂, a primary kinetic isotope effect of 1.5 was observed, and the combined yield of C-H insertion products **1-55** and **1-56** was dependent on nitrene concentration.^{47b} Finally (iii), a concentration dependence on nitrene was observed in addition to cyclohexene, wherein higher olefin concentrations led to greater amounts of C-H insertion products **1-58** and **1-59** over aziridine **1-57**.^{47c} Taken together, these data provide strong

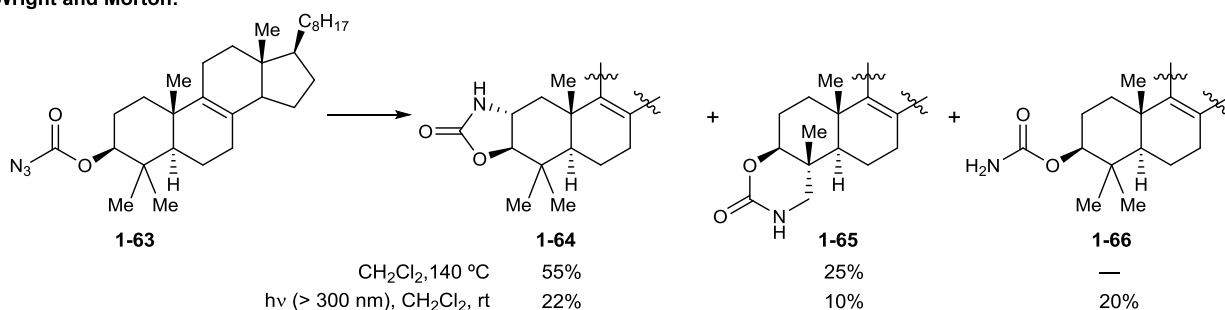
support for C-H insertion by a singlet carbalkoxynitrene via an unsymmetrical transition state, as in **1-53** and **1-54**. These studies established a firm understanding of carbalkoxynitrene reactivity, and due to the absence of competing rearrangement pathways, these species were applied to synthesis.

Scheme 1-9. Comparison of alkanoylnitrene and carbethoxynitrene cyclizations

Masamune:



Wright and Morton:



Indeed, the most popular use for carbalkoxynitrenes has been cyclization to lactams via C-H insertion, and installation of this moiety in a controlled, potentially stereoselective fashion spurred investigations on nitrene cyclizations in the synthesis of diterpene alkaloids and steroidal frameworks. Early work by Masamune on the total synthesis of Garryine **1-62** featured an alkanoylnitrene cyclization as the key step (Scheme 1-9).⁴⁸ Unfortunately, photo-Curtius rearrangement of **1-60** was the dominant process, resulting in quite poor yields of the desired product **1-61**. Wright and Morton studied the high-pressure thermolysis⁴⁹ and photolysis of 3 β -lanost-8-enyl azidoformate **1-63** and obtained a mixture of δ -lactam **1-64** and γ -lactam **1-65** arising from nitrene insertion into the α -methylene and α -methyl group, respectively.⁵⁰ These cyclization events occur on the concave face of the steroid backbone, and unlike similar alkanoylnitrene cyclizations, this azidoformate cyclization avoids isocyanate formation. Interestingly, photolysis gave a similar ratio of cyclized products, but considerable quantities of

formate ester **1-66** were produced, presumably from the triplet nitrene. However, the low chemoselectivity obtained is typical of carbalkoxynitrene cyclizations and has greatly limited their use beyond highly contrived substrates in which there are very few sites for C-H insertion.⁵¹ In this regard, metallocarbalkoxynitrenes have fared far better (Section 1.7).

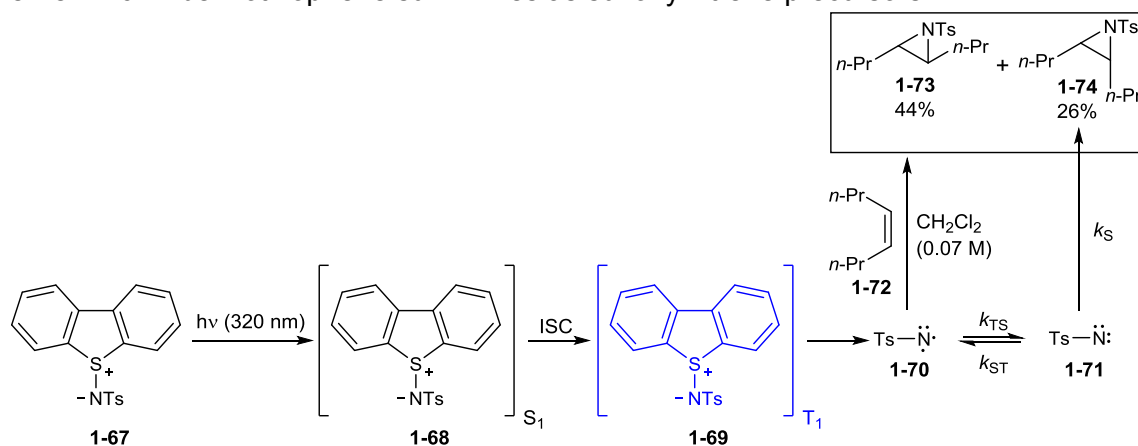
1.2.5 Sulfonylnitrenes

The chemistry of sulfonylnitrenes has received somewhat less attention than the other nitrenes discussed in this review. Much of this has been due to the difficulty in effecting clean formation of sulfonylnitrenes. Indeed, rearrangement of singlet sulfonylnitrene through a pseudo-Curtius pathway has been reported. Furthermore, some thermolytic studies have shown decomposition of aliphatic sulfonyl azides to hydrocarbon, SO₂, and N₂, apparently catalyzed by free radicals of unknown identity, whereas aromatic sulfonyl azides do not exhibit this behavior.⁵² More problematic is that these eliminations can, depending on azide structure, occur from either the azide precursor or the nitrene. The mechanistic proposals that emerge for transformations involving sulfonylnitrenes are confusing, as well. Contrary to some of the older literature on this topic, sulfonylnitrenes are often not involved in reactions as kinetically competent species.⁵³ Further, both ground state and excited state azides may react to yield the same products as nitrenes. While many of these empirical difficulties and mechanistic ambiguities could potentially be solved by utilizing other precursors to free sulfonylnitrenes,⁵⁴ such as *N*-halosulfonamides, *N*-hydroxysulfonamides, or sulfonylimino-iodanes, there have been surprisingly few studies involving these species.⁵⁵ Sulfonyl azides have been used for the vast majority of studies.⁵⁶

Photolysis of sulfonyl azides to generate free nitrenes is complex, but has allowed for the determination of important aspects of sulfonylnitrene chemistry. Smolinsky, Wasserman, and Yager investigated the photodecomposition of aromatic sulfonyl azides by EPR at 77 K and identified a long-lived resonance (18 h at 77 K) for each azide.⁵⁷ Furthermore, the zero-field

splitting parameters were of much greater magnitude than for aryl azides, suggesting significant interaction of unpaired spins on a ground state triplet nitrene. This is an interesting result, especially when considering that the ground state of seemingly related aroylnitrenes has singlet multiplicity (see Section 1.2.4.2). This has been attributed to an $n \rightarrow \pi^*$ stereoelectronic interaction between the oxygen lone pair and an empty orbital on nitrogen in the closed-shell singlet aroylnitrene, thereby affording a species having bonding character intermediate between that of an oxazirine and a free acyl nitrene. Such an effect acts to stabilize the singlet nitrene; this interaction is apparently attenuated for sulfonylnitrenes.⁴¹

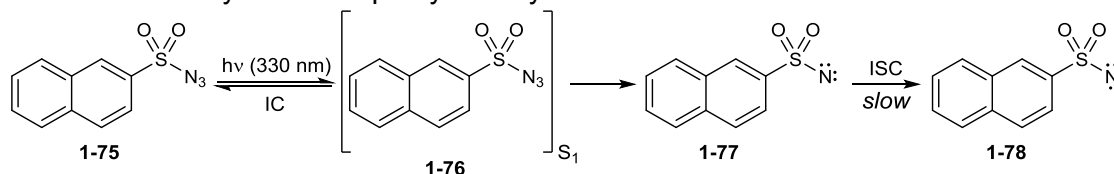
Scheme 1-10. Dibenzothiophene sulfilimines as sulfonylnitrene precursors



Recently, Toscano and Jenks designed dibenzothiophene sulfilimines (such as **1-67**) as sulfonylnitrene precursors to circumvent issues arising from thermolytic or photolytic decomposition of sulfonyl azides (Scheme 1-10).⁵⁸ While photolysis of tosyl azides followed by oxidative olefin functionalization led to an intractable mixture of products, photolysis of **1-67** gave efficient olefin aziridination. However, the chemistry of these sulfilimines was found to contain its own remarkable eccentricities. Reactions with *cis*-oct-4-ene **1-72** gave predominantly *trans*-aziridine **1-73** and a *loss* of stereospecificity was observed as the olefin concentration was *increased*. While these results could be construed as evidence for a nitrene ground state of singlet multiplicity, arylsulfonylnitrenes are known to be ground state triplets. Therefore, these results can be explained by invoking several postulates: (a) little, if any, singlet

nitrene **1-71** is formed on direct photolysis, (b) triplet sulfonylnitrene **1-70** exclusively arises from triplet **1-69** that forms by ISC from **1-68**, (c) ISC from triplet **1-70** to singlet **1-71** is somewhat endergonic, (d) the rate of singlet quenching by olefin (k_S) is markedly faster than ISC back to triplet nitrene (k_{ST}), and (e) $k_S > k_T$. Thus, raising the concentration of **1-72** leads to essentially irreversible ISC, and given that $k_S > k_T$, a decrease in retention would be expected. This study is unique in that the triplet nitrene is hypothesized to be the exclusive, initial nitrene species produced from photolysis of a singlet precursor. In lieu of utilizing a triplet sensitizer for azide decomposition (Chapters 3 and 4), dibenzothiophene sulfilimines represent a potentially valuable method for selective generation of triplet sulfonylnitrenes.

Scheme 1-11. Photolysis of 2-naphthylsulfonyl azide



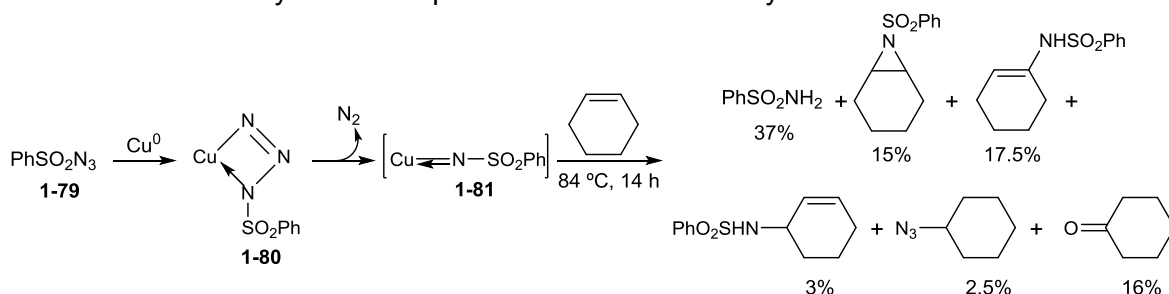
The sequence of events involved in the photolysis of sulfonylazides remained an enigma until Platz's recent investigations on the excited state chemistry of arylsulfonylnitrenes (Scheme 1-11).⁵⁹ Upon excitation at 330 nm, 2-naphthylsulfonyl azide **1-75** exclusively formed its S_1 state **1-76** ($\tau = 32$ ps), the first time this state had ever been observed. Contrast this to acyl azides, which upon photolysis produce azide S_1 ($\tau = 690$ ps) and small amounts of the corresponding azide T_1 state,⁴⁶ as evidenced by product distributions arising from the subsequent transformation into triplet nitrene (see Section 1.2.4). Internal conversion (IC) was found to be very efficient, with a quantum yield of 0.42 and a rate constant of $1.3 \times 10^{10} \text{ s}^{-1}$; such efficient IC is not typical for excited azides. After extrusion of N_2 , the closed-shell singlet nitrene **1-77** ($\tau = 700 \pm 300$ ps) was formed followed by slow ISC ($\sim 6 \times 10^7 \text{ s}^{-1}$) to triplet nitrene **1-78**. This serves to reinforce the point that unlike carbenes, triplet nitrenes are formed by inefficient ISC. The results of these studies are further supported by the fact that photolysis of

sulfonyl azides generally leads to negligible amounts of triplet-nitrene-derived products, as the singlet state reacts or decays far faster than ISC.

There are few known preparative reactions of free sulfonylnitrenes. While C-H insertion of a sulfonylnitrene, for example, is a concerted reaction involving singlet nitrene, the selectivities for C-H insertion are much lower than that for carbalkoxynitrenes.⁶⁰ Taking the canonical example of 2-methylbutane, ethoxycarbonylnitrene exhibits 32:10:1 selectivity (3°:2°:1°), while mesylnitrene shows a 9.6:4.2:1 selectivity; the latter is very poor selectivity when considering the bond dissociation energies of these C-H bonds. Therefore, sulfonylnitrenes are far less selective, and thus, far more reactive than carbalkoxynitrenes. Indeed, this raised the important issue of how to attenuate the reactivity of nitrenes, and this topic will be the subject of the remainder of the review.

1.3 Harnessing the Reactivity of Nitrenes

Despite the rich mechanistic chemistry investigated with the aforementioned classes of nitrenes, most are not useful for intermolecular processes in synthetic chemistry. Alkyl nitrenes are highly unstable and typically undergo undesired intramolecular rearrangements before productive chemistry can occur. Vinyl- and aryl nitrenes are most useful in the synthesis of nitrogenous heterocycles from intramolecular cyclization events. While aryl nitrenes exhibit excellent selectivity in C-H insertion reactions, the complex chemistry of the precursor azides render them unsuitable for intermolecular olefin functionalization or C-H insertion. Alkanoyl and aroyl nitrenes suffer from photo- and thermal-Claisen and Lossen rearrangements, and tend to give copious isocyanate even in the most favorable cases. Carbalkoxynitrenes exhibit good selectivity for C-H insertion, but are typically only used for olefin aziridination where the olefin is present in large excess. Sulfonylnitrenes are generally too reactive for useful levels of selectivity in C-H insertion, and applications to olefin functionalization are scarce.

Scheme 1-12. Cu-catalyzed decomposition of benzenesulfonyl azide

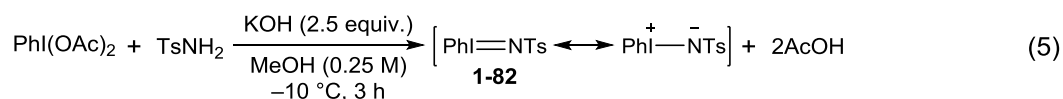
At this point, one must consider the origins of nitrene chemistry. The entire field arose out of the desire to compare the reactivity of monovalent nitrogen with that of divalent carbon. Therefore, advances in nitrene chemistry closely mirrored carbene chemistry. This is perhaps most clearly seen in 1967 reports by Kwart and Khan.⁶¹ Attempting to correlate the well-known decomposition of diazoalkanes and diazocarbonyl compounds by copper to afford stabilized copper-carbene complexes, Kwart and Khan studied the reaction of benzenesulfonyl azide **1-79** with cyclohexene in the presence of stoichiometric copper-bronze (Scheme 1-12). In analogy to carbene chemistry, they proposed that the aziridination, vinylic and allylic insertion products obtained were consistent with reaction of cyclohexene with a dative copper-imido species **1-81** obtained from the decomposition of copper-azide complex **1-80**. This first report on putative metallonitrene chemistry laid the groundwork for research a decade later.

The following three sections will place particular emphasis upon olefin aziridination as a vehicle for the development of metallonitrene chemistry. This was done in lieu of an extensive discussion on C-H amidation chemistry so as to parallel many of the concepts discussed in Chapters 3 and 4.

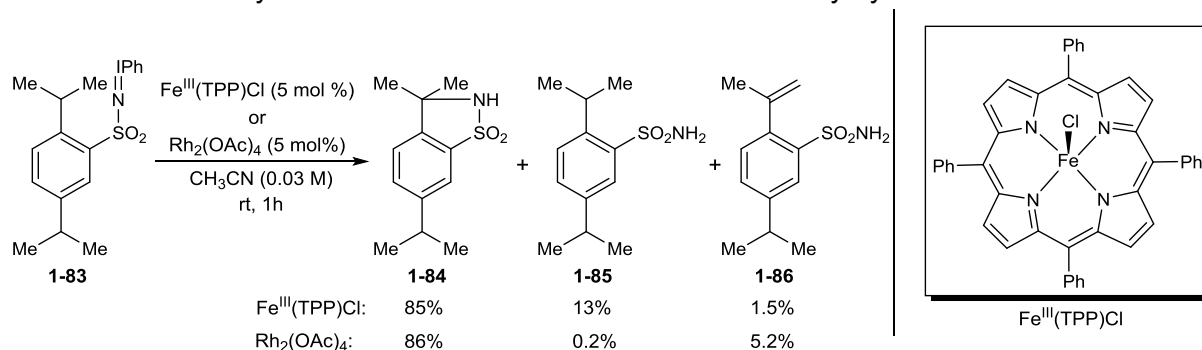
1.4 Introduction to Metallonitrene Chemistry

The complex, often non-selective reactivity arising from photogeneration of free nitrenes prompted investigations on attenuating and controlling the reactivity of these electrophilic intermediates. Ways in which this might be achieved derived inspiration from pioneering studies

by Wittig, who showed that phosphorus ylides participate in 1,2-addition to carbonyl compounds to afford an overall carbonyl olefination reaction.⁶² In essence, the reactivity of a formally carbanionic C1-synthon is modulated to that of a carbene via covalent bonding to a Lewis acidic phosphorus nucleus. This “ylide”, therefore, demonstrated that formation of dipolarophilic compounds constitutes a methodology by which to control the innate reactivity of hypervalent carbon-centered intermediates. This notion was extended to hypovalent nitrogen-centered intermediates when Yamada and co-workers established that reaction of an equimolar mixture of (diacetoxyiodo)benzene and *p*-toluenesulfonamide afforded *N*-tosyliminoaryliodinane **1-82** (PhI=NTs), a novel I-N ylide (eq. 5).⁶³



This ylide, the tosylimide analogue of iodosobenzene, was found to exhibit electrophilic character in stoichiometric reactions with thioanisole and triphenylphosphine; therefore, it was postulated that a nitrenoid was an intermediate in these reactions. This result was largely overlooked in the literature until Groves demonstrated that iron(III) porphyrins catalysed the insertion of oxygen from iodosobenzene into the C-H bonds of hydrocarbons, presumably via the intermediacy of a high-valent Fe(V) oxo compound.⁶⁴ Also around this time, Sharpless reported that metal-oxo chemistry could be mimicked by species in which oxygen is replaced by a tosylimide group; these studies on osmium-catalyzed oxyamination of olefins by Chloramine-T represented the first reports of formal metal-catalyzed nitrene transfer.⁶⁵ Taken together, the reports by Groves and Sharpless suggested that imido ylides such as **1-82** could be effectively engaged in the functionalization of hydrocarbons by transformation of the dipolarophilic ylide to a metallonitrene.⁶⁶

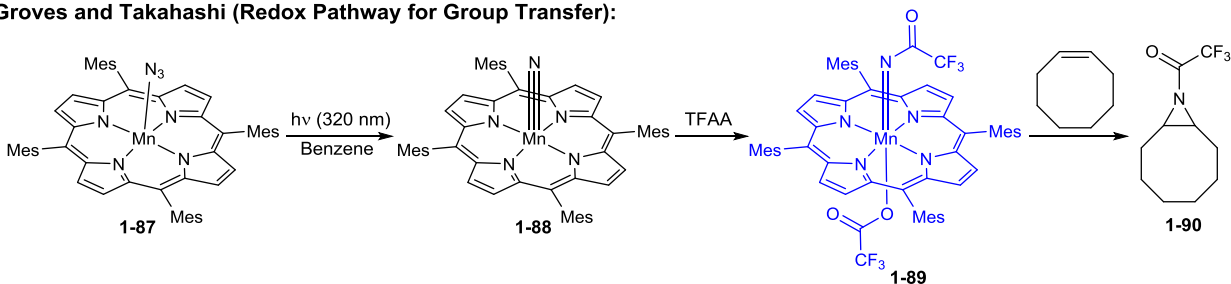
Scheme 1-13. Early studies on metallonitrene transfer chemistry by Breslow and Gellman


Indeed, seminal work by Breslow and Gellman found that Yamada's PhI=NTs ylide **1-82** underwent tosylamidation of cyclohexane in the presence of Fe(III) and Mn(III) porphyrins.^{67a} While the yields of intermolecular amidation products were low for both classes of porphyrins, the benzylic amidation of **1-83** occurred in high yield to afford benzosultam **1-84**, sulfonamide **1-85**, and olefin **1-86** (Scheme 1-13).^{68b} Interestingly, further studies revealed that microsomal cytochrome P-450-LM2 purified from rabbit liver catalyzed inter- and intramolecular amidation reactions in similar yields.^{68c} The proposed catalytically-active intermediates are high-valent Fe(V) and Mn(V) imido complexes, analogous to the cytochrome P450 hydroxylation chemistry discussed above.

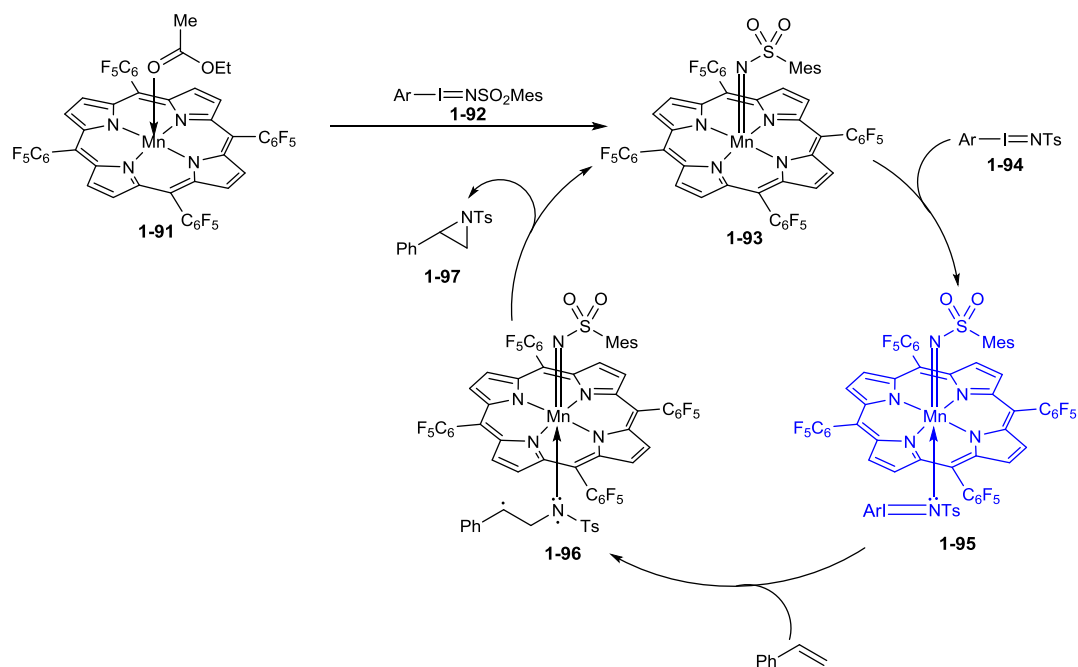
These reports on catalytic nitrene transfer began an active area of study on nitrogen atom transfer to alkenes via metal-nitrene intermediates. Groves and Takahashi synthesized and photolyzed Mn(III) azide **1-87** to give Mn(V) nitride **1-88** (Scheme 1-14).⁶⁸ Exposing this stable complex to trifluoroacetic anhydride (TFAA) gave acylimidomanganese (V) trifluoroacetate **1-89**; upon reaction with 11 equiv. of cyclooctene, azirine **1-90** was produced in 82–94% yield, thereby demonstrating the first aziridination utilizing a metallonitrene complex. Inspired by this study, Mansuy and co-workers developed Fe(TPP)-catalyzed imido group transfer from PhI=NTs to styrenyl olefins.⁶⁹

Scheme 1-14. Manganese porphyrins for imido group transfer to olefins

Groves and Takahashi (Redox Pathway for Group Transfer):



Abu-Omar and Zdilla (Non-Redox Pathway for Group Transfer):



Such studies raised important mechanistic questions regarding imido group transfer (Scheme 1-14), and two possible scenarios can be envisioned. In the “redox” pathway, the metal imido complex is the active imido group transfer reagent. In the “non-redox” pathway, the high-valent metal-imido species serves only as a Lewis acid catalyst for the activation of the nitrene transfer reagent, and the *datively* bound imido species is preferentially transferred to substrate.⁷⁰ These pathways have important implications on the imido group transfer step. For instance, in a recent study on catalytic aziridination with Mn(V) imido complexes by Abu-Omar and Zdilla, reaction of solvent-ligated species **1-91** with ylide **1-92** ($\text{Ar} = 2\text{-}(tert\text{-butylsulfonyl})\text{benzene}$) afforded stable Mn(V) complex **1-93** (Scheme 1-14).⁷¹ This

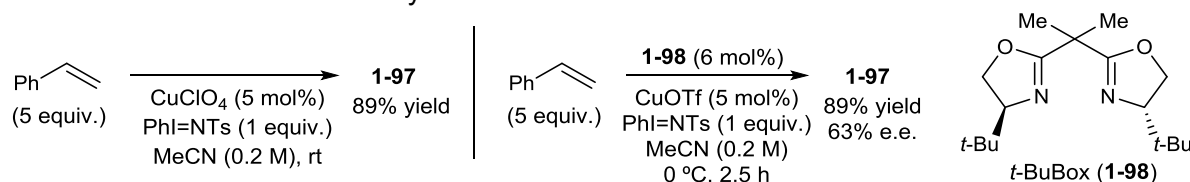
complex failed to aziridinate olefins. Thereafter, the inactive complex was exposed to ArI=NTs **1-94**, resulting in the irreversible formation of putative adduct **1-95**. When reacted with styrene, tosylated aziridine **1-97** was formed in lieu of the mesitylsulfonyl aziridine, indicating that complex **1-95** does not transfer its imido ligand, but rather the datively coordinated nitrenoid moiety. In accordance with Hammett studies (and with computational studies discussed in Section 1.6), the mechanism for olefin addition is proposed to occur via a radical pathway through biradical **1-96**. In contrast to many aziridination protocols, this methodology used the olefin as the limiting reagent, though only styrenyl olefins were competent substrates.

Other porphyrin complexes besides those of iron and manganese have proven useful for oxidative olefin functionalization. In particular, Zhang has highlighted the utility of electron-deficient, sterically-hindered cobalt(II) porphyrins in catalyzing aziridination of alkenes.⁷² A variety of nitrene precursors, including bromamine-T,^{72a} diphenylphosphoryl azide,^{72b} and arylsulfonyl azides^{72c,d} were shown to participate in aziridination reactions.

1.5 Further Advances in Metallonitrene Additions

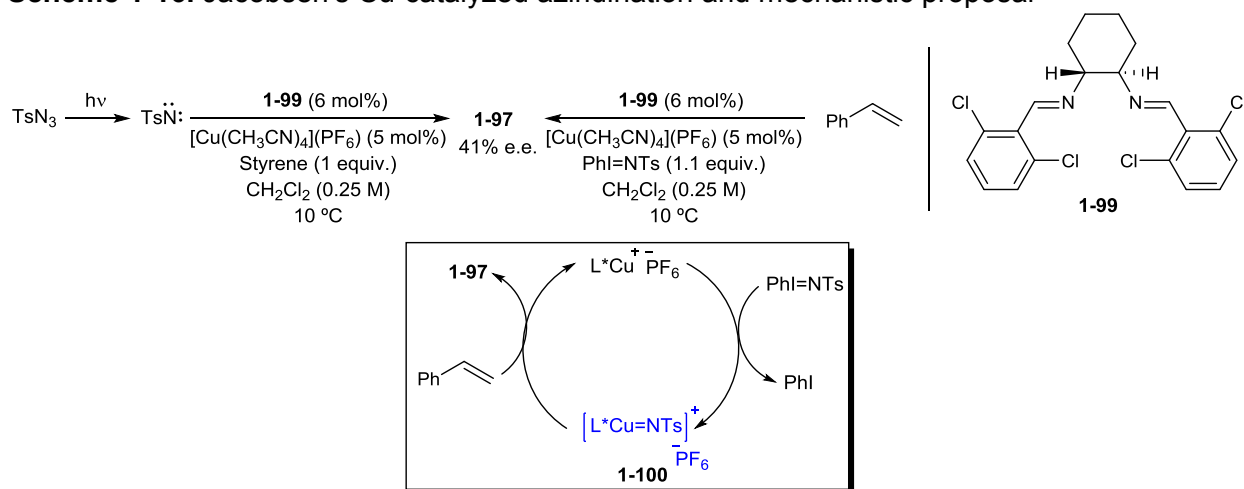
In an effort to generalize the scope of transition-metal catalyzed aziridination and to exercise control over product stereochemistry, Evans surmised that Cu(I) precatalysts employed in cyclopropanation would afford efficient imido group transfer from I-N ylides to olefins (Scheme 1-15). Indeed, exposure of PhI=NTs and olefin to catalytic CuOTf in MeCN led to efficient aziridination.⁷³ Aliphatic olefins, acrylates, cinnamates, and enol silanes were competent substrates under these mild conditions. An enantioselective aziridination was developed by introducing a chiral bisoxazoline (box) ligand **1-98** to the reaction conditions.

Scheme 1-15. Evans' Cu-catalyzed aziridination



While aziridination was stereospecific with *cis*- and *trans*-oct-4-ene, a dramatic counteranion dependence was observed for aziridination of *cis*- β -methylstyrene. Near stereospecificity in the latter reaction was obtained when the weakly coordinating ClO_4^- counteranion was complexed to Cu(I); more Lewis basic counteranions such as acetylacetonate (acac) and Br^- led to a non-stereospecific addition. Additionally, *cis*-stilbene could not be aziridinated in a stereospecific manner under any conditions. These studies signaled a substantial difference in reaction mechanism for aliphatic and aryl-substituted olefins (see Section 1.6 for a complete discussion).

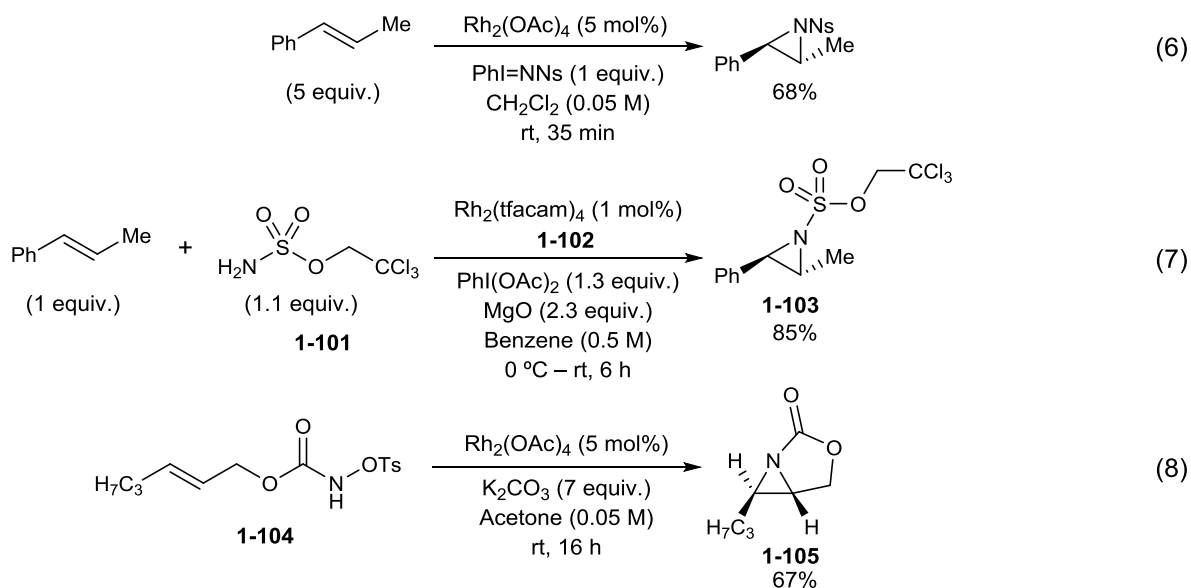
Scheme 1-16. Jacobsen's Cu-catalyzed aziridination and mechanistic proposal



Jacobsen concurrently demonstrated that chiral, monomeric (diimine)copper(I) complexes based on the “salen” (*N,N'*-bis(salicylideneamino)ethane) ligand architecture **1-99** effect enantioselective olefin aziridination (Scheme 1-16).⁷⁴ However, the identity of the catalytically active copper-derived imido transfer species in this system and the one developed by Evans was not clear. The mechanism could proceed via a dative complex such as **1-95** (Scheme 1-14) or via a discrete (diimine) $\text{Cu}=\text{NTs}$ intermediate. To probe this question, several hypervalent iodine ylides were synthesized in which the aryl group appended to iodine was varied to increase steric bulk. In no case was a change in enantioselectivity observed, indicating that the aryl iodide was fully dissociated from the active imido transfer agent prior to

enantiodetermining bond formation. Further, reaction of photochemically generated closed-shell tosylnitrene under the optimized conditions gave identical enantioselectivity to the catalytic aziridination reaction. Therefore, these two experiments provide strong evidence for common copper-nitrene intermediate **1-100**.

The ability for mid to late transition metal imido complexes to effect oxidative hydrocarbon functionalization was realized at an early stage in the development of metallonitrene chemistry. In fact, Breslow and Gellman observed that $\text{Rh}_2(\text{OAc})_4$ catalyzed intramolecular amidation (Scheme 1-13). Inspired by this study and by those of Doyle⁷⁵ on asymmetric, intermolecular cyclopropanations of allylic diazoacetates catalyzed by chiral Rh(II) carboxamides, Müller speculated that intermolecular nitrene transfer could be catalyzed by Rh(II).⁷⁶ After extensive optimization, it was discovered that changing the hypervalent iodonium ylide from $\text{PhI}=\text{NTs}$ to $\text{PhI}=\text{NNs}$ (Ns = *p*-nitrobenzenesulfonyl) afforded stereospecific aziridination of styrenyl and aliphatic olefins in good yields (eq. 6).



Du Bois reported that electrophilic Rh-carboxamide catalyst **1-102** (tfacam = CF_3CONH) catalyzed an intermolecular olefin aziridination to give **1-103** using trichlorosulfamate ester **1-101** as the metallonitrene precursor (eq. 7).⁷⁷ Unlike most intermolecular nitrene transfer

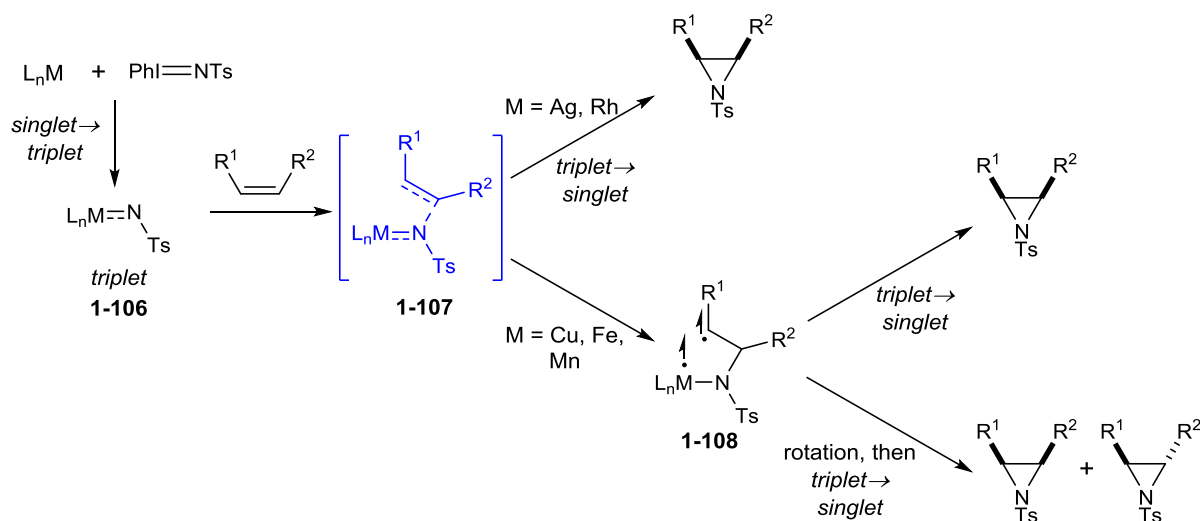
reactions, the hypervalent iodonium ylide was generated in-situ. Further, other sulfamate esters and phosphoramidates were tolerated in the aziridination event, though protecting group removal at the aziridine stage was not investigated.

This chemistry was subsequently studied by Lebel, who demonstrated that α -elimination from *N*-tosyloxycarbamate **1-104** to afford a putative singlet carbalkoxynitrene in the presence of $\text{Rh}_2(\text{OAc})_4$ effected intramolecular aziridination, affording **1-105** (eq. 8).^{78a} Given that a hypervalent iodine oxidant is not required for nitrene formation, this methodology can be used in scenarios where competitive functional group oxidation might pose an issue. Additionally, iodobenzene is not generated as a stoichiometric byproduct. Lebel later developed closely related aziridination conditions in which the dinuclear rhodium catalyst was replaced by $\text{Cu}(\text{pyridine})_4(\text{BF}_4)_2$.^{78b} While styrenyl and aliphatic olefins were efficiently aziridinated, a loss of stereospecificity was observed.

Significantly, all of the Rh-catalyzed aziridinations discussed above occurred in a stereospecific manner, while Mn, Fe, Co, and Cu catalysts typically afford non-stereospecific aziridination for styrenyl olefins and stilbenes. Since metallonitrene complexes are believed to exist in a triplet spin configuration, it must be the case that spin inversion followed by the second C-N bond forming event is faster than C-C bond rotation when employing Rh.

1.6 Mechanistic Studies on Metallonitrene Chemistry

Until this point, little consideration has been given to the spin state of the metal nitrene. However, as discussed in the previous section, it has been observed that the identity of the metal is directly responsible for the mechanisms by which these metal nitrene reactions proceed. For Cu, Fe, and Mn catalysts, loss of stereospecificity is often observed when aromatic substitution is introduced on the olefin, whereas Rh and Ag catalysts maintain stereospecificity.

Scheme 1-17. Proposed mechanism of aziridination via a metallonitrene intermediate

A thorough study on Cu and Ag catalysts in the presence of $PhI=NTs$ revealed that both metals form *triplet* metal nitrenes **1-106** ($L_nCu^II N^+Ts$ and L_nAgNTs) to begin the reaction (Scheme 1-17).⁷⁹ The metallonitrene subsequently attacks the olefin to give activated complex **1-107** having triplet multiplicity (parallel spins on N and C) en route to formation of the first C-N bond. From here, the mechanisms diverge. In the case of Ag (and likely Rh), the energy required to cross from the triplet manifold to the singlet manifold (minimum energy crossing point (MECP)) followed by the second C-N bond formation is substantially *lower* than the pathway involving C-C bond rotation in **1-107**. Therefore, the second C-N bond forms before C-C bond rotation can occur and thus stereospecificity is maintained in a concerted but asynchronous pathway.

For Cu (and likely Fe and Mn), however, discrete triplet biradical intermediate **1-108** forms from **1-107**, and the *relative* values of the corresponding MECP and the barrier for rotation around the C-N bond will control the stereochemistry. Therefore, when styrenyl substrates are employed, a benzylic radical is formed in species **1-108**. This radical is stabilized by delocalization into the aryl ring, allowing C-C bond rotation to occur before closure to the aziridine, resulting in a loss of stereospecificity. On the other hand, alkyl radicals are not

stabilized by resonance delocalization, thereby destabilizing **1-108** relative to a benzylic radical and affecting a faster rate of ring closure before C-C bond rotation can occur.

1.7 Triplet Sensitized Aziridination and Conclusions

Arguably the most straightforward method to synthesize aziridines involves the addition of nitrene intermediates to olefins. As discussed in the first half of this chapter, these electrophilic, hypovalent species are most directly formed *in situ* via photodecomposition of organic azides. However, these photochemical methods suffer from low yields of the desired aziridine and poor chemoselectivity due to competing hydrogen atom abstraction and C-H insertion pathways arising from multiple electronic excited states of the nitrene. Indeed, the initial sensitization event affords singlet nitrene that often reacts far faster than ISC to the triplet manifold. Though it appears plausible to hypothesize that some of this complexity could be avoided by selective generation of triplet nitrene, no methods affecting a single-step aziridination in this manner have been reported.

However, Gudmundsdottir has demonstrated that triplet alkyl- and vinylnitrenes can be selectively synthesized by intramolecular energy transfer from an acetophenone sensitizer, thereby circumventing the singlet manifold entirely. While these nitrenes simply dimerize, decompose, or rearrange, sulfonylnitrenes and carbalkoxynitrenes are far less prone to these unproductive events. Jenks reported the only known literature method that currently exists for selectively generating sulfonylnitrenes in their triplet state, and carbonylnitrenes had never previously succumbed to triplet sensitization.

Recent investigations in our laboratory have shown that sulfonylnitrenes (Chapter 3), arylnitrenes (Chapter 4), and carbonylnitrenes can be selectively generated with putative triplet spin multiplicity from azide precursors. These methodologies, based upon visible light-induced energy transfer from polypyridyl transition metal sensitizers, effectively avoid the highly reactive

singlet manifold and offer a means by which to study the reactivity inherent to free triplet nitrenes without use of intramolecular energy transfer. We believe that this unexplored area in nitrene chemistry offers significant synthetic advances while potentially having a profound impact on solution phase spectroscopic studies of these versatile intermediates.

1.8 References

¹ For comprehensive reviews on nitrene chemistry, see (a) *Azides and Nitrenes, Reactivity and Utility*; Scriven, E. F. V., Ed.; Academic: New York, 1984; (b) Lwowski, W. *Nitrenes*; Lwowski, W., Ed.; Interscience: New York, 1970.

² (a) Platz, M. S. Nitrenes. In *Reactive Intermediates*; Moss, R. A., Platz, M. S., Jones, M., Jr., Eds.; Wiley-Interscience: 2004; Chapter 11, p 501. (b) *Nitrenes and Nitrenium Ions*; Falvey, D. E., Gudmundsdottir, A. D., Eds.; Wiley Series on Reactive Intermediates in Chemistry and Biology; John Wiley & Sons, Inc.: New York, 2013; Vol. 6.

³ Poe, R.; Grayzar, J.; Young, J. T.; Leyva, E.; Schnapp, K. A.; Platz, M. S. Remarkable catalysis of intersystem crossing of singlet (pentafluorophenyl)nitrene. *J. Am. Chem. Soc.* **1991**, *113*, 3209–3211.

⁴ Tiemann, F. Ueber die Einwirkung von Benzolsulfonsäurechlorid auf Amidoxime. *Ber. Dtsch. Chem. Ges.* **1891**, *24*, 4162–4167.

⁵ (a) Stieglitz, J.; Leech, P. N. Die molekulare Umlagerung von triphenylmethyl-hydroxylamin. *Chem. Ber.* **1913**, *46*, 2147. (b) Stieglitz, J. Leech, P. N. The molecular rearrangement of triarylmethylhydroxylamines and the “Beckmann” rearrangement of ketoximes. *J. Am. Chem. Soc.* **1914**, *36*, 272–301.

⁶ Wasserman, E.; Smolinski, G.; Yager, W. A. Electron spin resonance of alkyl nitrenes. *J. Am. Chem. Soc.* **1964**, *86*, 3166–3167.

⁷ Dixon, R. N. The 0-0 and 1-0 bands of the $A(^3\Pi_g^-)-X(^3\Sigma_g^-)$ system of NH. *Can. J. Phys.* **1959**, *37*, 1171–1186.

⁸ (a) Mandel, S. M.; Krause Bauer, J. A.; Gudmundsdóttir, A. D. Photolysis of α -azidoacetophenones: trapping of triplet alkyl nitrenes in solution. *Org. Lett.* **2001**, *3*, 523–526. (b) Singh, P. N. D.; Mandel, S. M.; Sankaranarayanan, J.; Luthukrishnan, S.; Chang, M.; Robinson, R. M.; Lahti, P. M.; Ault, B. S.; Gudmundsdóttir, A. D. Selective formation of triplet alkyl nitrenes from photolysis of β -azido-propiofenone and their reactivity. *J. Am. Chem. Soc.* **2007**, *129*, 16263–16272.

⁹ (a) Moriarty, R. M.; Serridge, P. Thermal decomposition of germinal diazides. *J. Am. Chem. Soc.* **1971**, *93*, 1534–1535. (b) Abramovitch, R. M.; Kyba, E. P. Photodecomposition of alkyl

azides. Absence of freedom of choice and nonnitrene mechanism. *J. Am. Chem. Soc.* **1971**, *93*, 1537–1538.

¹⁰ Pancrazi, A.; Khuong-Huu, Q. Alcaloides steroidiques—CLXXII: Photochemie d'azido-steroides. *Tetrahedron* **1975**, *31*, 2041–2048.

¹¹ Neber, P. W.; Friedolsheim, A. Uber eine neue art der umlagerung von Oximen. *Ann.* **1926**, *449*, 109–134.

¹² (a) Cram, D. J.; Hatch, M. J. The problem of the unsaturated three-membered ring containing nitrogen. *J. Am. Chem. Soc.* **1953**, *75*, 33–38. (b) House, H. O.; Berkowitz, W. F. The neber rearrangement of substituted desoxybenzoin oxime tosylates. *J. Org. Chem.* **1963**, *28*, 307–311.

¹³ Hassner, A.; Fowler, F. W. Stereochemistry. XXXII. Synthesis and reactions of 1-azirines. *J. Am. Chem. Soc.* **1968**, *90*, 2869–2875.

¹⁴ (a) Isomura, K.; Kobayashi, S.; Taniguchi, H. Indole formation by pyrolysis of β -styrylazides. *Tetrahedron Lett.* **1968**, *31*, 3499–3502. (b) Hemetsberger, H.; Knittel, D.; Weidmann, H. Enazide, 3. Mitt.: Thermolyse von α -azidozimestern; synthese von indolderivaten. *Monatsh. Chem.* **1970**, *101*, 161–165.

¹⁵ (a) Padwa, A.; Smolanoff, J.; Tremper, A. Photochemical transformations of small ring heterocyclic systems. LXV. Intramolecular cycloaddition reactions of vinyl-substituted 2*H*-azirines. *J. Am. Chem. Soc.* **1975**, *97*, 4682–4691. (b) Gemeraad, P.; Moore, H. W. Rearrangements of azidoquinones. XII. Thermal conversion of 2-azido-3-vinyl-1,4,-quinones to indolequinones. *J. Org. Chem.* **1974**, *39*, 774–780. (c) Padwa, A.; Carlsen, P. H. J. Thermal rearrangement of allyl substituted 2*H*-azirines to 3-azabicyclo[3.2.0]hex-2-enes. *J. Org. Chem.* **1976**, *41*, 180–182. (d) Weyler, W.; Duncan, W. G.; Moore, H. W. Rearrangements of azidoquinones. XVI. Thermal and photolytic rearrangements of 2,5-diazido-1,4,-quinones. Synthesis and chemistry of cyanoketenes. *J. Am. Chem. Soc.* **1975**, *97*, 6187–6192. (e) Anderson, D. J.; Hassner, A. Chemistry of small ring heterocycles. XVIII. 3*H*-azepines from azirines and cyclopentadienones. *J. Am. Chem. Soc.* **1971**, *93*, 4339–4340.

¹⁶ Padwa, A.; Smalanoff, J.; Tremper, A. Photochemical transformations of small ring heterocyclic compounds. 71. Intramolecular reorganization of some unsaturated 2*H*-azirines. *J. Org. Chem.* **1975**, *41*, 543–549.

¹⁷ (a) Nishiwaki, T.; Nakano, A.; Matsuoka, H. Studies on heterocyclic chemistry. Part VII. Thermally induced dimerization of 5-aminoisoxazoles and 2*H*-azirines and photochemistry of 5-aminoisoxazoles. *J. Chem. Soc. C.* **1970**, 1825–1829. (b) Nishiwaki, T.; Fugiyama, F. Studies on heterocyclic chemistry. Part XIII. Cleavage of 5-benzyl-amino-oxazoles, photoproducts of *N*-benzyl-2*H*-azirine-2-carboxamides, by dialkyl phosphite. *J. Chem. Soc. Perkin Trans. 1* **1972**, 1456–1459.

¹⁸ A recent study demonstrated that rearrangement of α -methyl- β -substituted styrenyl azides under thermolytic conditions does not proceed via the intermediacy of an azirine, but rather through π -assisted rearrangement from the aromatic nucleus. See Taber, D. J.; Tian, W. The Neber route to substituted indoles. *J. Am. Chem. Soc.* **2006**, *128*, 1058–1059.

- ¹⁹ Parasuk, V.; Cramer, C. J. Multireference configuration interaction and second-order perturbation theory calculations for the $1^3A''$, $1^1A''$, and $1^1A'$ electronic states of vinylnitrene and vinylphosphinidene. *Chem. Phys. Lett.* **1996**, *260*, 7–14.
- ²⁰ Rajam, S.; Murthy, R. S.; Jadhav, A. V.; Li, Q.; Keller, C.; Carra, C.; Pace, T. C. S.; Bohne, C.; Ault, B. S.; Gudmundsdóttir, A. D. Photolysis of (3-methyl-2*H*-azirin-2-yl)-phenylmethanone: direct detection of a triplet vinylnitrene intermediate. *J. Org. Chem.* **2011**, *76*, 9934–9945.
- ²¹ Irradiation of azirine 1-x in a frozen matrix led to ketenimine in lieu of the the desired vinylnitrene. A different design principle was used to obtain an azirine-derived triplet vinylnitrene in a cryogenic matrix, which was subsequently characterized by ESR and IR spectroscopy. See Sarkar, S. K.; Sawai, A.; Kanahara, K.; Wentrup, C.; Abe, M.; Gudmundsdóttir, A. D. Direct detection of a triplet vinylnitrene, 1,4-naphthoquinone-2-yl nitrene, in solution and cryogenic matrices. *J. Am. Chem. Soc.* **2015**, *137*, 4207–4214.
- ²² Rajam, S.; Jadhav, A. V.; Li, Q.; Sarkar, S. K.; Singh, P. N. D.; Rohr, A.; Pace, T. C. S.; Li, R.; Krause, J. A.; Bohne, C.; Ault, B. S.; Gudmundsdóttir, A. D. Triplet sensitized photolysis of a vinyl azide: direct detection of a triplet vinyl azide and nitrene. *J. Org. Chem.* **2014**, *79*, 9325–9334.
- ²³ For a comprehensive modern review of aryl nitrene chemistry with an emphasis on aryl nitrene photochemistry, see: Gritsan, N.; Platz, M. Photochemistry of azides: the azide/nitrene interface. In *Organic azides: syntheses and applications*. Bräse, S.; Banert, K., Eds.; John Wiley & Sons: 2010; Chapter 11, pp 327–363.
- ²⁴ For the earliest report on the synthesis of heterocyclic compounds from aryl azides, see Smith, P. A. S.; Brown, B. B. The synthesis of heterocyclic compounds from aryl azides. I. Bromo and nitro carbazoles. *J. Am. Chem. Soc.* **1951**, *73*, 2435–2437.
- ²⁵ For reviews of aryl nitrene chemistry with an emphasis on myriad reactions of aryl nitrenes, see (a) Smith, P. A. S. Aryl nitrenes and formation of nitrenes by rupture of heterocyclic rings. In *Nitrenes*; Lwowski, W., Ed.; Interscience: New York, 1970; Chapter 4, pp 99–162. (b) Smith, P. A. S. Aryl and heteroaryl azides and nitrenes. In *Azides and Nitrenes, Reactivity and Utility*; Scriven, E. F. V., Ed.; Academic: New York, 1984; Chapter 3, pp 95–204.
- ²⁶ For examples of aryl azide photocrosslinking, see (a) Wang, J.-F.; Downs, W. D.; Cech, T. R. *Science* **1993**, *260*, 504–508. (b) Buchmueller, K. L.; Hill, B. T.; Platz, M.; Weeks, K. M. RNA-tethered phenyl azide photocrosslinking via a short-lived indiscriminant electrophile. *J. Am. Chem. Soc.* **2003**, *125*, 10850–10861.
- ²⁷ (a) Abramovitch, R. A.; Davis, B. A. *Chem. Rev.* **1964**, *64*, 149. (b) Abramovitch, R. A.; Kyba, E. P. "The Chemistry of the Azido Group"; Patai, S., Ed.; Wiley: New York, 1971, p. 256. (c) Iddon, B.; Meth-Cohn, O.; Scriven, E. F. V.; Suschitzky, H.; Gallagher, P. T. *Angew. Chem. Int. Ed.* **1979**, *18*, 900.
- ²⁸ (a) Huisgen, R.; Vossius, D.; Appl, M. Die thermolyse des phenylazids in primären aminen; die Konstitution des dibenzamils. *Chem. Ber.* **1958**, *91*, 1–12. (b) Huisgen, R.; Appl, M. Der chemismus der ringerweiterung beim zerfall des phenylazids in anilin. *Chem. Ber.* **1958**, *91*, 12–31. (c) Doering, W. von E.; Odum, R. A. Ring enlargement in the photolysis of phenyl azide. *Tetrahedron* **1966**, *22*, 81–93.

-
- ²⁹ Carrol, S. E.; May, B.; Scriven, E. F. V.; Suschitzky, H.; Thomas, D. R. Decomposition of aromatic azides in ethanethiol. *Tetrahedron Lett.* **1977**, *36*, 3175–3178.
- ³⁰ Splitter, J. S.; Calvin, M. Irradiation of 3-substituted-2-phenyloxaziridines—direct evidence for phenylnitrene. *Tetrahedron Lett.* **1968**, *9*, 1445–1448.
- ³¹ Pritchina, E. A.; Gritsan, N. P. Mechanism of *p*-azidoaniline photolysis in the presence of oxygen. *J. Photochem. Photobiol. A: Chemistry* **1988**, *43*, 165–182.
- ³² (a) Gritsan, N. P.; Yazawa, T.; Platz, M. S. Direct observation of singlet phenylnitrene and measurement of its rate of rearrangement. *J. Am. Chem. Soc.* **1997**, *119*, 5059–5060. (b) Born, R.; Burda, C.; Senn, P.; Wirz, J. Transient absorption spectra and reaction kinetics of singlet phenylnitrene and its 2,4,6-tribromo derivative in solution. *J. Am. Chem. Soc.* **1997**, *119*, 5060–5061.
- ³³ Gritsan, N. P.; Zhu, Z.; Hadad, C. M.; Platz, M. S. Laser flash photolysis and computational study of singlet phenylnitrene. *J. Am. Chem. Soc.* **1999**, *121*, 1202–1207.
- ³⁴ Kim, S.-J.; Hamilton, T. P.; Schaefer, H. F. Phenylnitrene: energetics, vibrational frequencies, and molecular structures. *J. Am. Chem. Soc.* **1992**, *114*, 5349–5355. (b) Hrovat, D. A.; Waali, E. E.; Borden, W. T. Ab initio calculations of the singlet-triplet energy difference in phenylnitrene. *J. Am. Chem. Soc.* **1992**, *114*, 8698–8699.
- ³⁵ (a) Tsao, M.-L.; Platz, M. S. Photochemistry of ortho,ortho' dialkyl phenyl azides. *J. Am. Chem. Soc.* **2003**, *125*, 12014–12025. (b) Inui, H.; Sawada, K.; Oishi, S.; Ushida, K.; McMahon, R. Aryl nitrene rearrangements: spectroscopic observation of a benzazirine and its ring expansion to a ketenimine by heavy-atom tunneling. *J. Am. Chem. Soc.* **2013**, *135*, 10246–10249.
- ³⁶ Li, Y.-Z.; Kirby, J. P.; George, M. W.; Poliakoff, M.; Schuster, G. B. 1,2-didehydroazepines from the photolysis of substituted aryl azides. Analysis of their chemical and physical properties by time-resolved spectroscopic methods. *J. Am. Chem. Soc.* **1988**, *110*, 8092–8098.
- ³⁷ Burdzinski, G.; Hackett, J. C.; Wang, J.; Gustafson, T. L.; Hadad, C. M.; Platz, M. S. Early events in the photochemistry of aryl azides from femtosecond UV/Vis spectroscopy and quantum chemical calculations. *J. Am. Chem. Soc.* **2006**, *128*, 13402–13411.
- ³⁸ (a) Swenton, J. S.; Ikeler, T. J.; Williams, B. W. Photochemistry of singlet and triplet azide excited states. *J. Am. Chem. Soc.* **1970**, *92*, 3103–3109. (b) Hall, J. H.; Kamm, D. R. Synthesis of benzimidazoles from anils of *o*-azidoaniline. *J. Org. Chem.* **1965**, *30*, 2092–2093. (c) Smith, P. A. S.; Rowe, C. D.; Hansen, D. W., Jr. Stereochemistry in the cyclization of *o*-azidophenylalkenes to indoles. *Tetrahedron Lett.* **1983**, *24*, 5169–5172. (d) Cadogan, J. I. G.; Mackie, R. K.; Modd, M. J. Reductive cyclization of nitro-compounds by triethyl phosphite: new syntheses of phenothiazines and anthranils. *J. Chem. Soc. Chem. Commun.* **1966**, 491a. (e) Abramovitch, R. A.; Kalinowski, J. Pyrido[1,2-*b*]indazole and its derivatives. *J. Heterocycl. Chem.* **1974**, *11*, 857–861. (f) Moody, C. J.; Rees, C. W.; Tsoi, S. C. Ring cleavage of 3-azidothiophens; a novel extrusion of acetylene. *J. Chem. Soc. Chem. Commun.* **1981**, 550–551. (g) Fukuyama, T.; Yang, L. Total synthesis of (±)-mitomycins via isomitomycin A. *J. Am. Chem. Soc.* **1987**, *109*, 7881–7882.

-
- ³⁹ (a) Hall, J. H.; Hill, J. W.; Tasi, H.-C. Insertion reactions of aryl nitrenes. *Tetrahedron Lett.* **1965**, *26*, 2211–2216. (b) Hall, J. H.; Hill, J. W.; Fargher, J. M. Evidence for the involvement of triplet phenyl nitrene in intermolecular C-H insertion. *J. Am. Chem. Soc.* **1968**, *90*, 5313–5314.
- ⁴⁰ Paquette, L. A.; Kesselmayr, M. A.; Rogers, R. D. Quantitation of proximity effects on rate. A case study involving dyotropic hydrogen migration within syn-sesquinorbornene disulfones carrying central substituents having different spatial demands. *J. Am. Chem. Soc.* **1990**, *112*, 284–291.
- ⁴¹ The singlet–triplet gap of carbalkoxynitrenes has been estimated to be 3–8 kcal/mol. See Scott, A. P.; Platz, M. S.; Radom, J. *J. Am. Chem. Soc.* **2001**, *123*, 6069. The singlet-triplet gap of alkanoyl- and aroylnitrenes has been estimated to be 4–5 kcal/mol. See Liu, J.; Mandel, S.; Hadad, C. M.; Platz, M. S. A comparison of acetyl- and methoxycarbonylnitrenes by computational methods and a laser flash photolysis study of benzoylnitrene. *J. Org. Chem.* **2004**, *69*, 8583–8593.
- ⁴² Woodworth, R. C.; Skell, P. S. Methylene, CH₂. Stereospecific reaction with *cis*- and *trans*-2-butene. *J. Am. Chem. Soc.* **1959**, *81*, 3383.
- ⁴³ (a) McConaghy, J. S., Jr.; Lwowski, W. Singlet and triplet nitrenes. I. Carbethoxynitrene generated by α -elimination. *J. Am. Chem. Soc.* **1967**, *89*, 2537–2364. (b) McConaghy, J. S., Jr.; Lwowski, W. Singlet and triplet nitrenes. II. Carbethoxynitrene generated from ethyl azidoformate. *J. Am. Chem. Soc.* **1967**, *89*, 4450–4456.
- ⁴⁴ (a) Atkinson, R. S.; Rees, C. W. Reactive intermediates. Part VII. Oxidation of 3-aminobenzoxazolin-2-one; stereospecific addition of the amino-nitrene to olefins. *J. Chem. Soc. C.* **1969**, 772–778. (b) Atkinson, R. S.; Judkins, B. D.; Khan, N. 2,4-dinitrobenzenesulphenylnitrene: addition to (*Z*)- and (*E*)-1-phenylpropene. *J. Chem. Soc., Perkin Trans 1* **1982**, 2491–2497.
- ⁴⁵ Autrey, T.; Schuster, G. B. Are aroxynitrenes ground-state singlets? Photochemistry of β -naphthoyl azide. *J. Am. Chem. Soc.* **1987**, *109*, 5814–5820.
- ⁴⁶ Kubicki, J.; Zhang, Y.; Vyas, S.; Burdzinski, G.; Luk, H. L.; Wang, J.; Xue, J.; Peng, H.-L.; Pritchina, E. A.; Sliwa, M.; Buntinx, G.; Gritsan, N. P.; Hadad, C. M.; Platz, M. S. Photochemistry of 2-naphthoyl azide. An ultrafast time-resolved UV-Vis and IR spectroscopic and computational study. *J. Am. Chem. Soc.* **2011**, *133*, 9751–9761.
- ⁴⁷ (a) Simson, J. M.; Lwowski, W. Carbethoxynitrene. The stereochemistry of the intermolecular singlet carbon-hydrogen insertion. *J. Am. Chem. Soc.* **1969**, *91*, 5107–5113. (b) Lwowski, W.; Maricich, T. J. Carbethoxynitrene by α -elimination. Reactions with hydrocarbons. *J. Am. Chem. Soc.* **1965**, *87*, 3630–3637. (c) Lwowski, W.; Woerner, F. P. Carbethoxynitrene. Control of chemical reactivity. *J. Am. Chem. Soc.* **1965**, *87*, 5491–5492.
- ⁴⁸ Masamune, S. Total synthesis of diterpenes and diterpene alkaloids. IV. Garryine. *J. Am. Chem. Soc.* **1964**, *86*, 290–291.

- ⁴⁹ Dichloromethane has been shown to stabilize the singlet state of nitrenes. See (a) Felt, G. R.; Linke, S.; Lwowski, W. Alkanoylnitrenes: stabilization of the singlet state by dichloromethane. *Tetrahedron Lett.* **1972**, *13*, 2037–2040. (b) Belloli, R. C.; Whitehead, M. A.; Wollenberg, R. H.; LaBohn, V. A. Effect of dichloromethane on the reaction of carbethoxynitrene with trans-1,2,-dimethylcyclohexane. *J. Org. Chem.* **1974**, *39*, 2128–2130.
- ⁵⁰ Wright, J. J.; Morton, J. B. Thermolysis and photolysis of 3 β -lanostenyl azidocarbonate: functionalization of the 4 α -methyl group. *J. Chem. Soc. Chem. Commun.* **1976**, 668–670.
- ⁵¹ See ref. 1a, pg. 231 and Moody, C. J. Oxidation by nitrene insertion. In *Comprehensive organic synthesis: selectivity, strategy, and efficiency in modern organic chemistry. Vol. 7: Oxidation*; Trost, B. M.; Fleming, I.; Ley, S. V., Eds.; Elsevier: 1991; Chapter 1.2, p. 25.
- ⁵² (a) Breslow, D. S.; Sloan, M. F.; Newburg, N. R.; Renfrow, W. B. *J. Am. Chem. Soc.* **1969**, *91*, 2293. (b) Leffler, J. E.; Tsuno, Y. *J. Org. Chem.* **1963**, *28*, 190.
- ⁵³ Smith, M. B.; March, J. In *March's Advanced Organic Chemistry. Reactions, Mechanisms, and Structure*, 6th ed., Wiley & Sons, Hoboken, New Jersey, 2007, 2357 (p. 294).
- ⁵⁴ Garay, J.-C.; Maloney, V.; Marlow, M.; Small, P. Spectroscopy and kinetics of triplet 4-methylbenzenesulfonylnitrene. *J. Phys. Chem.* **1996**, *100*, 5788–5793.
- ⁵⁵ Shainyan, B. A.; Kuzmin, A. V. Sulfonyl nitrenes from different sources: computational study of formation and transformations. *J. Phys. Org. Chem.* **2013**, *27*, 156–162.
- ⁵⁶ Breslow, D. S. Sulfonylnitrenes. In *Nitrenes*; Lwowski, W., Ed.; Interscience: New York, 1970; Chapter 8, pp 245–303.
- ⁵⁷ Smolinsky, G.; Wasserman, E.; Yager, W. A. The EPR of ground state triplet nitrenes. *J. Am. Chem. Soc.* **1962**, *84*, 3220–3221.
- ⁵⁸ Desikan, V.; Liu, Y.; Toscano, J. P.; Jenks, W. S. Photochemistry of *N*-acetyl-, *N*-trifluoroacetyl-, *N*-mesyl-, and *N*-tosyldibenzothiophene sulfilimines. *J. Org. Chem.* **2008**, *73*, 4398–4414.
- ⁵⁹ Kubicki, J.; Luk, H. L.; Zhang, Y.; Vyas, S.; Peng, H.-L.; Hadad, C. M.; Platz, M. S. Direct observation of a sulfonyl azide excited state and its decay processes by ultrafast time-resolved IR spectroscopy. *J. Am. Chem. Soc.* **2012**, *134*, 7036–7044.
- ⁶⁰ Breslow, D. S.; Edwards, E. I.; Linsay, E. C.; Omura, H. Insertion of sulfonylnitrenes into the carbon-hydrogen bonds of saturated hydrocarbons. Acid-catalyzed thermolysis of *N*-alkyl sulfonamides. *J. Am. Chem. Soc.* **1976**, *98*, 4268–4275.
- ⁶¹ (a) Kwart, H.; Kahn, A. A. Copper-catalyzed decomposition of benzenesulfonyl azide in hydroxylic media. *J. Am. Chem. Soc.* **1967**, *89*, 1950–1951. (b) Kwart, H.; Kahn, A. A. Copper-catalyzed decomposition of benzenesulfonyl azide in cyclohexene solution. *J. Am. Chem. Soc.* **1967**, *89*, 1951–1953.

⁶² (a) Wittig, G.; Schollkopf, U. Über Triphenyl-phosphin-methylene als olefinbildende Reagenzien I. *Chem. Ber.* **1954**, *87*, 1318–1330. (b) Wittig, G.; Haag, W. Über Triphenyl-phosphin-methylene als olefinbildende Reagenzien II. *Chem. Ber.* **1955**, *88*, 1654–1666.

⁶³ Yamada, Y.; Yamamoto, T.; Okawara, M. Synthesis and reaction of new I–N ylide, N-tosyliminoiodinane. *Chem. Lett.* **1975**, 361–362.

⁶⁴ (a) Groves, J.T.; Nemo, T.E.; Myers, R.S. Hydroxylation and epoxidation catalyzed by iron-porphine complexes. Oxygen transfer from iodosylbenzene. *J. Am. Chem. Soc.* **1979**, *101*, 1032–1033. (b) Hill, C.L.; Schardt, B.C. Alkane activation and functionalization under mild conditions by a homogeneous manganese(III)porphyrin-iodosylbenzene oxidizing system. *J. Am. Chem. Soc.* **1980**, *102*, 6374–6375. (c) Groves, J.T.; Kruper, W.J.; Haushalter, R.C. Hydrocarbon oxidations with oxometalloporphyrins. Isolation and reactions of a (porphyrinato)manganese(V) complex. *J. Am. Chem. Soc.* **1980**, *102*, 6375–6377. (d) Groves, J.T.; Haushalter, R.C.; Nakamura, M.; Nemo, T.E.; Evans, B.J. High-valent iron-porphyrin complexes related to peroxidase and cytochrome P-450. *J. Am. Chem. Soc.* **1981**, *103*, 2884–2886.

⁶⁵ (a) Sharpless, K. B.; Patrick, D. W.; Truesdale, L. K.; Biller, S. A. A new reaction. stereospecific vicinal oxyamination of olefins by alkyl imido osmium compounds. *J. Am. Chem. Soc.* **1975**, *97*, 2305–2307. (b) Sharpless, K. B.; Chong, A. O.; Oshima, K. Osmium-catalyzed vicinal oxyamination of olefins by chloramine-T. *J. Org. Chem.* **1976**, *41*, 177–179.

⁶⁶ Groves, J.T.; Takahashi, T. Activation and transfer of nitrogen from a nitridomanganese(V) porphyrin complex. The aza analogue of epoxidation. *J. Am. Chem. Soc.* **1983**, *105*, 2073–2074.

⁶⁷ (a) Breslow, R.; Gellman, S.H. Tosylamidation of cyclohexane by a cytochrome P-450 model. *J. Chem. Soc., Chem. Commun.* **1982**, 1400–1401. (b) Breslow, R.; Gellman, S.H. Intramolecular nitrene C–H insertions mediated by transition-metal complexes as nitrogen analogues of cytochrome P-450 reactions. *J. Am. Chem. Soc.* **1983**, *105*, 6728–6729. (c) Svastits, E. W.; Dawson, J. H.; Breslow, R.; Gellman, S. H. Functionalized nitrogen atom transfer catalyzed by cytochrome P-450. *J. Am. Chem. Soc.* **1985**, *107*, 6427–6428.

⁶⁸ Groves, J. T.; Takahashi, T. Activation and transfer of nitrogen from a nitridomanganese(V) porphyrin complex. The aza analogue of epoxidation. *J. Am. Chem. Soc.* **1983**, *105*, 2074–2075.

⁶⁹ (a) Mansuy, D.; Mahy, J.-P.; Dureault, A.; Bedi, G.; Battioni, P. Iron- and manganese-porphyrin catalyzed aziridination of alkenes by tosyl- and acyl-iminoiodobenzene. *J. Chem. Soc., Chem. Commun.* **1984**, 1161–1163. (b) Mahy, J.-P.; Bedi, G.; Battioni, P.; Mansuy, D. *Tetrahedron Lett.* **1988**, *29*, 1927–1930.

⁷⁰ This is in accordance with Goldberg's "third oxidant" in high-valent porphyrinoid oxidations. See: Wang, S. H.; Mandimutsira, B. S.; Todd, R.; Ramdhanie, B.; Fox, J. P.; Goldberg, D. P. Catalytic sulfoxidation and epoxidation with a Mn(III) triazacorrole: evidence for a "third oxidant" in high-valent porphyrinoid oxidations. *J. Am. Chem. Soc.* **2004**, *126*, 18–19.

⁷¹ Zdilla, M. J.; Abu-Omar, M. M. Mechanism of catalytic aziridination with manganese corrole: the often postulated high-valent Mn(V) is not the group transfer reagent. *J. Am. Chem. Soc.* **2006**, *128*, 16971–16979.

⁷² (a) Gao, G.-Y.; Harden, J.D.; Zhang, X.P. Cobalt-catalyzed efficient aziridination of alkenes. *Org. Lett.* **2005**, *7*, 3191–3193. (b) Gao, G.-Y.; Jones, J.E.; Vyas, R.; Harden, J.D.; Zhang, X.P. Cobalt-catalyzed aziridination with diphenylphosphoryl azide (DPAA): Direct synthesis of *N*-phosphorus-substituted aziridines from alkenes. *J. Org. Chem.* **2006**, *71*, 6655–6658. (c) Ruppel, J.V.; Kamble, R.M.; Zhang, X.P. Cobalt-catalyzed intramolecular C-H amination with arylsulfonyl azides. *Org. Lett.* **2007**, *9*, 4889–4892. (d) Ruppel, J.V.; Jones, J.E.; Huff, C.A.; Kamble, R.M.; Chen, Y.; Zhang, X.P. A highly effective cobalt catalyst for olefin aziridination with azides: hydrogen bonding guided catalyst design. *Org. Lett.* **2008**, *10*, 1995–1998.

⁷³ (a) Evans, D.A.; Faul, M.M.; Bilodeau, M.T. Copper-catalyzed aziridination of olefins by (*N*-(*p*-toluenesulfonyl)imino)phenyliodine. *J. Org. Chem.* **1991**, *56*, 6744–6746. (b) Evans, D.A.; Faul, M.M.; Bilodeau, M.T.; Anderson, B.A.; Barnes, D.M. Bis(oxazoline)-copper complexes as chiral catalysts for the enantioselective aziridination of olefins. *J. Am. Chem. Soc.* **1993**, *115*, 5328–5329. (c) Evans, D.A.; Faul, M.M.; Bilodeau, M.T. Development of the copper-catalyzed olefin aziridination reaction. *J. Am. Chem. Soc.* **1994**, *116*, 2742–2753.

⁷⁴ Li, Z.; Conser, K.R.; Jacobsen, E.N. Asymmetric alkene aziridination with readily available chiral diimine-based catalysts. *J. Am. Chem. Soc.* **1993**, *115*, 5326–5327. Li, Z.; Quan, R.W.; Jacobsen, E.N. Mechanism of the (diimine)copper-catalyzed asymmetric aziridination of alkenes. Nitrene transfer via ligand-accelerated catalysis. *J. Am. Chem. Soc.* **1995**, *117*, 5889–5890.

⁷⁵ Doyle, M. P.; Pieters, R. J.; Martin, S. F.; Austin, R. E.; Oalmann, C. J.; Müller, P. High enantioselectivity in the intramolecular cyclopropanation of allyl diazoacetates using a novel rhodium(II) catalyst. *J. Am. Chem. Soc.* **1991**, *113*, 1423–1424.

⁷⁶ Müller, P.; Baud, C.; Jacquier, Y.; Moran, M.; Nägeli, I. Rhodium(II)-catalyzed aziridinations and CH insertions with [*N*-(*p*-nitrobenzenesulfonyl)imino]phenyliodine. *J. Phys. Org. Chem.* **1996**, *9*, 341–347.

⁷⁷ (a) Guthikonda, K.; Du Bois, J. A unique and highly efficient method for catalytic olefin aziridination. *J. Am. Chem. Soc.* **2002**, *124*, 13672–13673. (b) Guthikonda, K.; When, P.M.; Caliendo, B.J.; Du Bois, J. Rh-catalyzed alkene oxidation: a highly efficient and selective process for preparing *N*-alkoxysulfonyl aziridines. *Tetrahedron* **2006**, *62*, 11331–11342.

⁷⁸ (a) Lebel, H.; Huard, K.; Lectard, S. *N*-tosyloxycarbamates as a source of metal nitrenes: rhodium-catalyzed C-H insertion and aziridination reactions. *J. Am. Chem. Soc.* **2005**, *127*, 14198–14199. (b) Lebel, H.; Lectard, S.; Parmentier, M. Copper-catalyzed alkene aziridination with *N*-tosyloxycarbamates. *Org. Lett.* **2007**, *9*, 4797–4800.

⁷⁹ Maestre, L.; Sameera, W.M.C.; Mar Díaz-Requejo, M.; Maseras, F.; Pérez, P.J. A general mechanism for the copper- and silver-catalyzed olefin aziridination reactions: concomitant involvement of the singlet and triplet pathways. *J. Am. Chem. Soc.* **2013**, *135*, 1338–1348.

Chapter 2. Cleavable Redox Auxiliaries in Photocatalyzed Intermolecular [2+2] Cyclobutanations

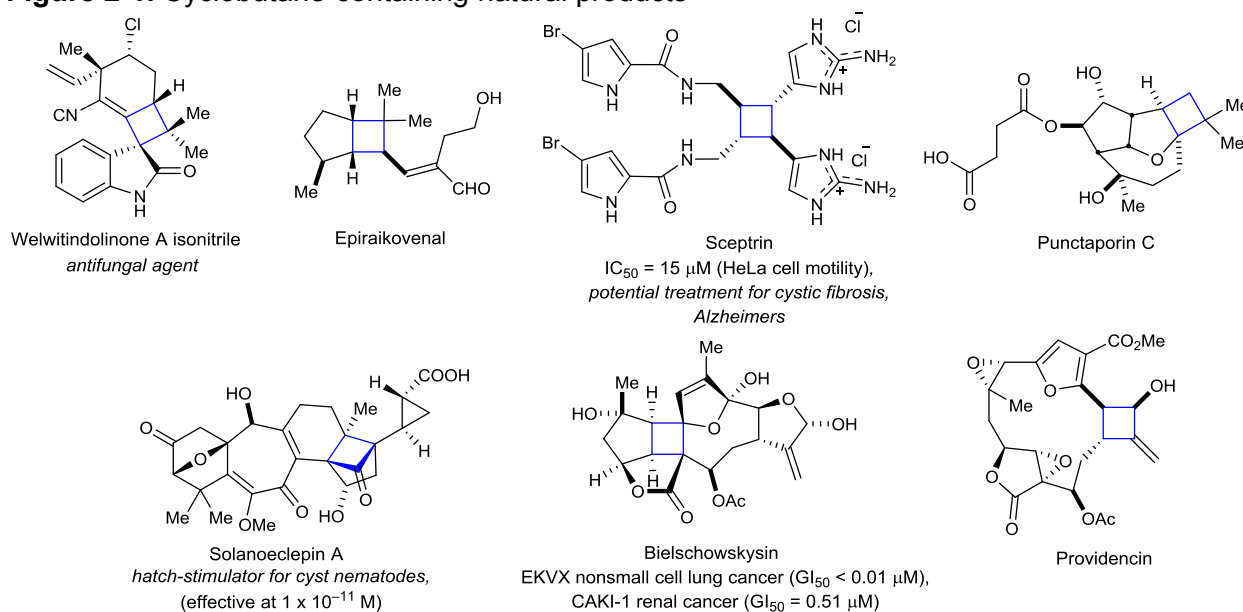
Portions of this work have previously been published:

Tyson, E. L.; Farney, E. P.; Yoon, T. P. Photocatalytic [2+2] cycloadditions of enones with cleavable redox auxiliaries. *Org. Lett.* **2012**, *14*(4), 1110–1113.

2.1 Introduction

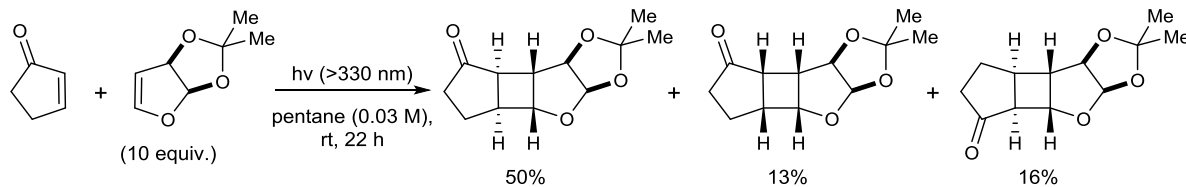
Cyclobutanes are synthetically valuable due to their prevalence in a diverse range of natural products¹ as well as their utility in generating expanded carbocyclic frameworks via strain-releasing fragmentation reactions.² Synthesis of these strained carbocycles, however, remains challenging, and having access to the nearly 1900 cyclobutane-containing natural products would greatly expand the pool of structures available for diversification in the pharmaceutical industry.

Figure 2-1. Cyclobutane-containing natural products



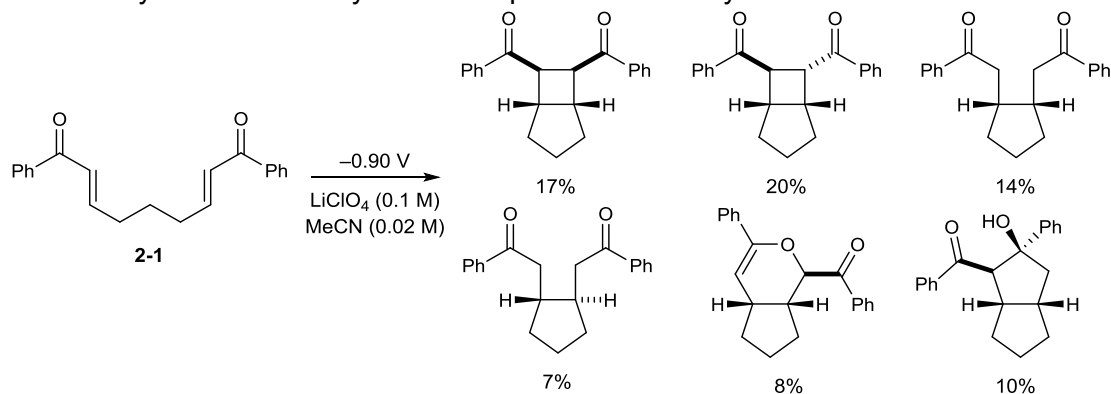
One of the most widely-employed methods for generating the cyclobutane motif is photoinitiated formal [2+2] cycloaddition³ of *cyclic* enones with ultraviolet (UV) light (Scheme 2-1).⁴ UV photoexcitation of an enone forms the enone singlet excited state (S_1) followed by intersystem crossing (ISC) to the first triplet excited state (T_1). Reaction of the newly formed triplet intermediate with an acceptor alkene affords a 1,4-biradical intermediate that participates in a second-bond forming event to effect the formal cyclobutanation.

Scheme 2-1. Photosensitized cyclobutane of cyclic enones



Attempts to extend this chemistry to significantly more versatile *acyclic* enones have generally not been successful, primarily due to energy-wasting *cis-trans* isomerization that occurs in the T_1 state and interferes with productive cycloaddition.⁵ Further, selectivity in photochemical cyclobutane reactions can be poorly defined; complex mixtures of head-to-head and head-to-tail regioisomeric products can be formed, along with mixtures of *trans*-fused and *cis*-fused stereoisomers (Scheme 2-1).⁶ Thus, efficient, high-yielding, stereocontrolled cycloadditions of acyclic enones is a challenging problem.

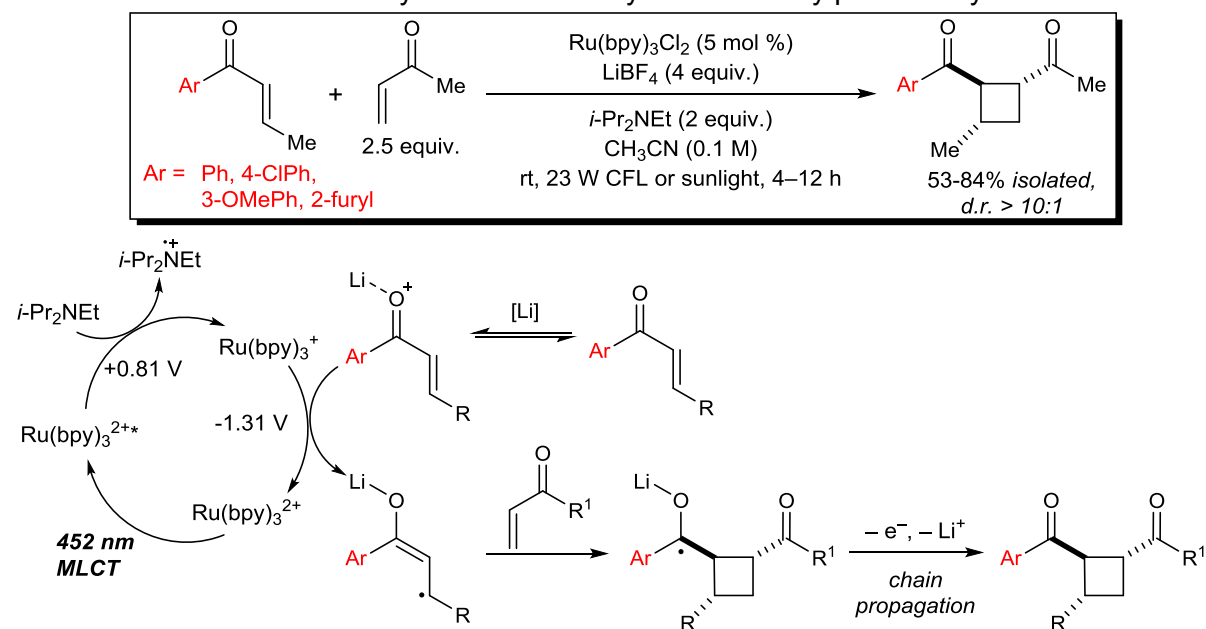
Scheme 2-2. Cyclobutane by controlled potential electrolysis



In the search for a potentially generalizable solution, our research group was inspired by the work of Krische and Bauld on electrochemically-induced radical anion cyclizations of tethered bis-enones **2-1** (Scheme 2-2).⁷ Indeed, this method avoids formation of the problematic triplet excited state of the enone and thus can be applied to acyclic enones.⁸ Single-electron reduction of an aromatic enone affords a putative radical anion intermediate that participates in stepwise bond forming events with an appropriate Michael acceptor. However, controlled potential electrolysis led to a high concentration of radical anion intermediate,⁹ and a multitude of products arising from undesired pathways was observed. We found that this redox

neutral, intramolecular, formal cyclobutanation could be better effected by visible-light photocatalysis¹⁰ using polypyridyl ruthenium(II) sensitizers in the presence of a tertiary amine reductive quencher and subsequently extended our initial publication to intermolecular systems¹¹ (Scheme 2-3).

Scheme 2-3. Intermolecular cycloaddition of acyclic enones by photocatalysis



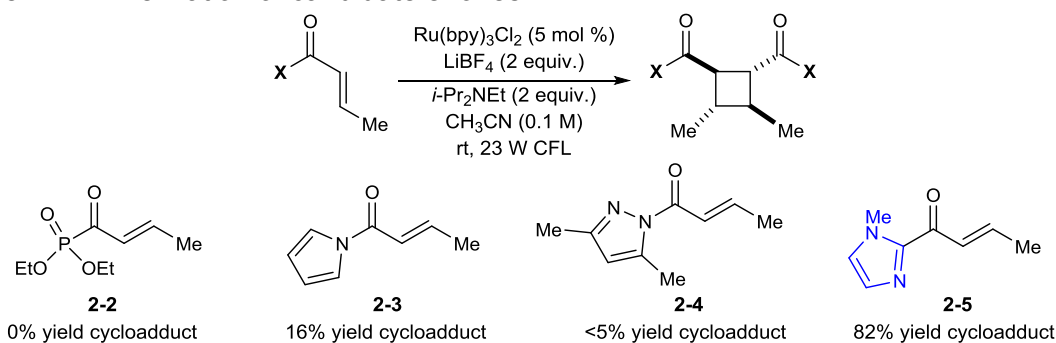
This methodology presumably generates very low concentrations of the putative radical anion intermediate and thus affords controlled cycloadditions to give cyclobutanes in high yields.¹² Additionally, we were pleased to observe excellent control of regiochemistry and relative stereochemistry in cyclobutane formation. However, we found the involvement of an aryl enone in the reaction to be a strict requirement for successful cycloaddition. In turn, this restricted our methodology to the synthesis of cyclobutanes containing an aryl ketone, a functional group not amenable to rapid, facile diversification. We proposed a mechanism for the cycloaddition that rationalizes this constraint. The key reactive intermediate in this process is an enone radical anion generated by single electron transfer from a photogenerated Ru(bpy)₃⁺ complex to a Lewis acid-activated enone. The one-electron reduction of aryl enones is significantly more facile than the corresponding reduction of less-conjugated enone substrates.

Enoate esters, for example, possess reduction potentials ~ 700 mV more negative than aryl enones,¹³ which precludes formation of the corresponding enoate radical anions under these photocatalytic conditions.

2.2 Results and Discussion

We sought to address this limitation via the use of a cleavable “redox auxiliary”,^{14,15} a motif that temporarily modulates the reduction potential of an otherwise redox inactive enoate substrate, facilitating reduction and cycloaddition prior to its cleavage from the cyclobutane product. Ideally, this strategy would enable access to cyclobutane carboxamides, esters, thioesters, and acids – products otherwise inaccessible without the aid of the cleavable auxiliary. To begin, we examined the homodimerization of α,β -unsaturated carbonyl compounds that have been validated as surrogates of carboxylate esters in other synthetic methods (Scheme 2-4).

Scheme 2-4. Dimerization of candidate enones



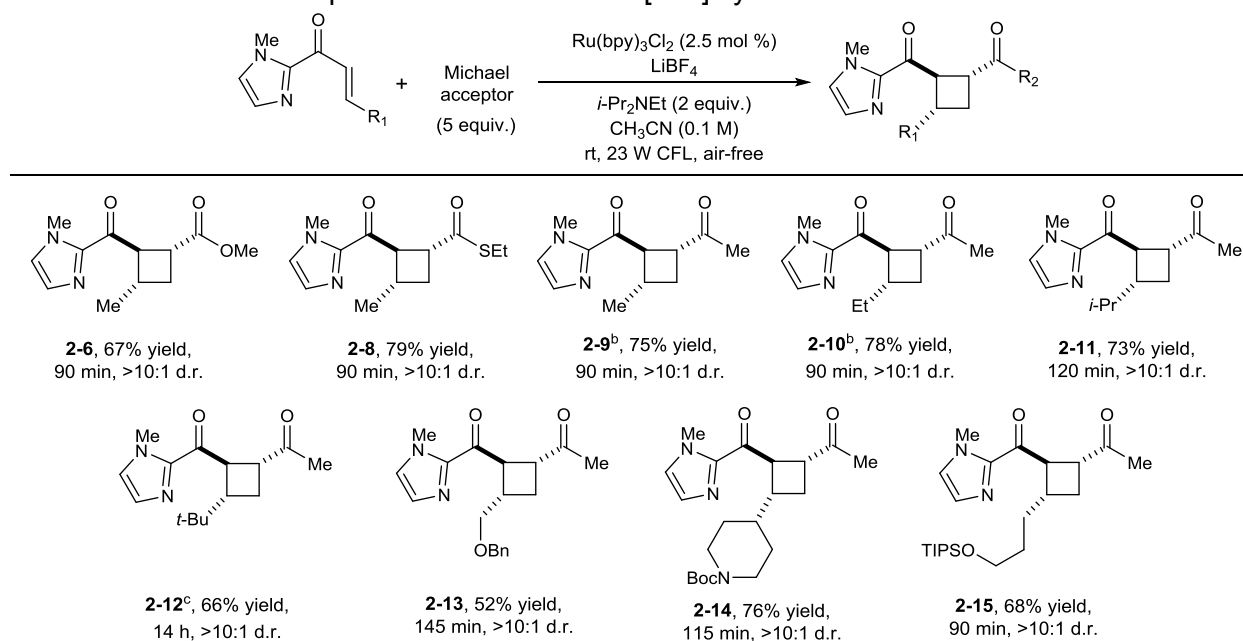
Upon exposure to the conditions we had optimized for intermolecular [2+2] cycloaddition of aryl enones, unsaturated acyl phosphonates¹⁶ **2-2** underwent rapid decomposition. *N*-acyl pyrroles¹⁷ **2-3** and pyrazoles¹⁸ **2-4** reacted sluggishly and gave unsatisfactory yields of the corresponding dimerized cyclobutanes. On the other hand, α,β -unsaturated 2-acylimidazoles¹⁹ **2-5** reacted smoothly and furnished the desired [2+2] cyclodimer in 82% yield.²⁰ We therefore elected to continue our studies using enones bearing an *N*-methylimidazol-2-yl auxiliary group.

Table 2-1. Optimization studies on the crossed, intermolecular [2+2] cycloaddition

| entry | Ru(bpy) ₃ Cl ₂ (mol%) ^a | LiBF ₄ (equiv.) ^a | time (min) | yield ^b 2-6 (d.r.) | yield ^b 2-7 |
|-------|---|--|------------|---|-------------------------------|
| 1 | 5.0 | 2 | 90 | 43% (5:1) | 24% |
| 2 | 5.0 | 4 | 90 | 42% (10:1) | 13% |
| 3 | 5.0 | 0.5 | 120 | 21% (2:1) | 50% |
| 4 | 2.5 | 2 | 150 | 51% (5:1) | 19% |
| 5 | 2.5 | 2 | 90 | 67% (>10:1) | <5% |

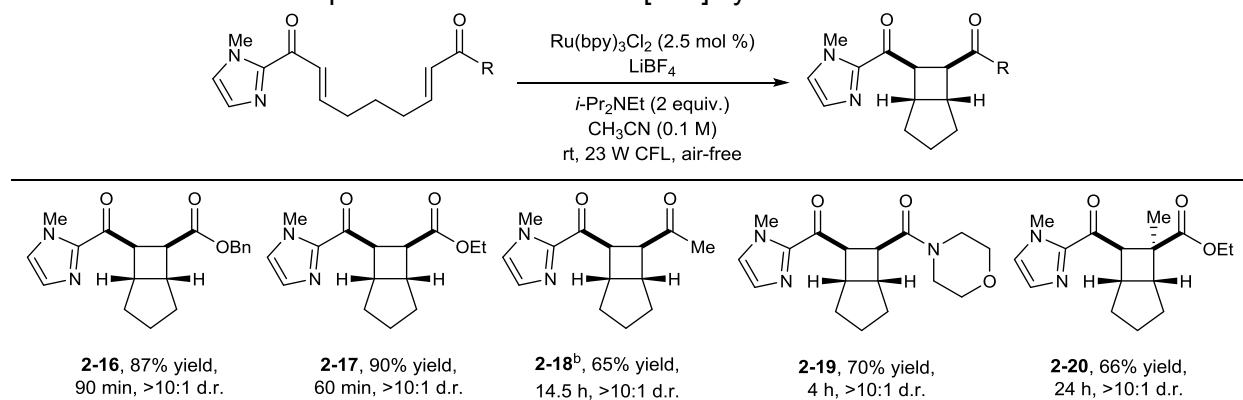
^aAmounts of photocatalyst and LiBF₄ are with respect to the theoretical yield of product **2-6**. ^bAryl enone added dropwise over a 45 min period.

Next, we studied the crossed intermolecular [2+2] cyclization of acyl imidazole **2-5** with methyl acrylate (Table 2-1). The conditions we had previously reported for [2+2] cycloaddition of phenyl enones with methyl acrylate afforded only 43% of the desired crossed cycloadduct in 5:1 d.r.; the undesired homodimerization of **2-5** to afford **2-7** was a significant competitive process (entry 1). Higher concentrations of the Lewis acidic additive (LiBF₄) increased the d.r. without increasing the yield of **2-6** (entry 2), while lower Lewis acid loading favored homodimerization (entry 3). We observed a modest increase in selectivity for the heterodimer when the catalyst loading was lowered to 2.5 mol % (entry 4). The best yield and highest diastereoselectivity were obtained when **2-5** was added slowly via syringe pump to the reaction mixture, which presumably minimizes the homodimerization by minimizing the concentration of **2-5** with respect to methyl acrylate while keeping the ratio of Lewis acid to substrate high. By using this slow addition protocol, the desired heterodimer **2-6** could be isolated in 67% yield and with excellent diastereoselectivity (entry 5).

Table 2-2. Substrate scope of the intermolecular [2+2] cycloaddition^a

^aUnless otherwise noted, reactions were performed with 5.0 equiv. Michael acceptor with respect to 1.0 equiv. aryl enone, 2.5 mol% $\text{Ru}(\text{bpy})_3\text{Cl}_2$, 2.0 equiv. LiBF_4 , and 2.0 equiv. $i\text{-Pr}_2\text{NEt}$ in MeCN (0.1 M with respect to aryl enone); aryl enone was added dropwise over a period of 45 min. Isolated yields and diastereomer ratios are the averaged results of two reproducible experiments. ^b0.5 equiv. LiBF_4 was used. ^c4.0 equiv. LiBF_4 was used; aryl enone was added in one portion.

Table 2-2 summarizes experiments probing the scope of the crossed intermolecular [2+2] cycloaddition using 2-acyl imidazoles. A variety of Michael acceptors, including α,β -unsaturated esters (**2-6**), thioesters, (**2-8**), and ketones (**2-9**) provided good yields and high diastereoselectivities in cycloadditions with **2-5**. As we had observed in our previous studies, high selectivity for the crossed cycloadduct requires the use of α,β -unsubstituted Michael acceptor as the reaction partner. However, β -substitution on the acyl imidazole is easily accommodated. Substrates of increased steric demand worked well in this reaction (**2-10**, **2-11**, and **2-12**), and protected heteroatom functional groups were tolerated under optimized reaction conditions (**2-13**, **2-14**, and **2-15**).

Table 2-3. Substrate scope of the intramolecular [2+2] cycloaddition^a

^aUnless otherwise noted, reactions were performed using 2.5 mol% Ru(bpy)₃Cl₂, 0.5 equiv. LiBF₄, and 2.0 equiv. *i*-Pr₂NEt in MeCN (0.1 M with respect to substrate). Isolated yields and diastereomer ratios are the averaged results of two reproducible experiments. ^b0.5 equiv. *i*-Pr₂NEt was used.

We also explored intramolecular [2+2] cycloadditions of 2-acylimidazoles (Table 2-3). In these experiments, we observed somewhat higher yields when the loading of LiBF₄ was reduced to 0.5 equiv. These conditions enabled intramolecular cycloadditions with a variety of acceptor moieties, including esters (**2-16**, **2-17**), ketones (**2-18**), and amides (**2-19**). The use of an α -substituted Michael acceptor required prolonged reaction times, but the expected cycloadduct bearing a quaternary stereocenter (**2-20**) was produced with excellent diastereoselectivity.

Finally, we investigated conditions for transformation of the 2-acylimidazole moiety into carboxylic acid derivatives (Table 2-4).¹⁹ The auxiliary group of cycloadduct **2-16** can easily be *N*-alkylated with MeOTf to afford the corresponding imidazolium salt. Upon recrystallization, this white crystalline material is stable to prolonged storage on the bench for at least six months.²¹ Displacement of the imidazolyl group proceeds smoothly with a variety of oxygen nucleophiles without loss of stereochemical integrity (entries 1-3). While bulky tertiary alcohols did not react with the imidazolium salt (entry 4), the more nucleophilic *tert*-butyl thiol produced the corresponding thioester in quantitative yield (entry 5). Finally, the 2-acylimidazolium moiety could be transformed into an amide functional group upon treatment with either primary or secondary amines (entries 6 and 7). Thus, the use of this redox auxiliary strategy enables the

synthesis of a variety of cyclobutane carboxylic acid derivatives that would not otherwise be accessible using our previously reported photocatalytic [2+2] cycloaddition methodology.

Table 2-4. Cleavage of the redox auxiliary^a



| entry | NucH | yield ^b | d.r. |
|----------------|-------------------|--------------------|-------|
| 1 ^c | H ₂ O | 52% ^c | >10:1 |
| 2 ^c | MeOH | 86% ^c | >10:1 |
| 3 | <i>i</i> -PrOH | 88% ^c | >10:1 |
| 4 | <i>t</i> -BuOH | 0% | — |
| 5 | <i>t</i> -BuSH | 99% | >10:1 |
| 6 ^d | BnNH ₂ | 98% | >10:1 |
| 7 ^d | pyrrolidine | 75% | >10:1 |

^aUnless otherwise noted, cleavage of the imidazolium group was conducted using an excess of the nucleophile and 3.5 equiv. DBU in CH₂Cl₂. ^bIsolated yields. ^cCleavage conducted in Et₂O. ^dNo DBU added.

2.3 Conclusions

We have circumvented a limitation in the scope of the photocatalytic [2+2] cycloaddition developed in our laboratory by using unsaturated 2-acylimidazole groups as redox auxiliaries. These heteroaryl groups facilitate the reduction of the enone substrate to the key radical anion intermediate required for cycloaddition and are then susceptible to cleavage with a variety of nucleophiles under mild conditions. This redox auxiliary approach could be applied to other reactions that involve the reduction of carbonyl compounds to the corresponding radical anions. Continued studies in our laboratory will apply these concepts to other reactions of photogenerated radical ions.

2.4 Contributions

Dr. Liz Tyson performed the experiments in Scheme 2-4. She also carried out the experiments in Tables 2-3 and 2-4.

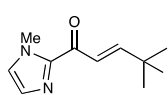
2.5 Experimental

2.5.1 General Information

A 23 W GE compact fluorescent light bulb was used for all photochemical reactions. *i*-Pr₂NEt was purified by distillation from CaH₂ immediately prior to use. Ru(bpy)₃Cl₂·6H₂O was purchased from commercial sources and used without further purification. Methyl acrylate was washed with aqueous NaOH, distilled water, brine, dried over CaCl₂, and fractionally distilled immediately prior to use. Benzene, CH₂Cl₂, THF, and MeCN were purified by elution through alumina. All other reagents were purchased from commercial sources and purified immediately prior to use. Chromatography was performed with Purasil 60Å silica gel (230–400 mesh). All glassware was oven-dried for at least 1 h before use. Diastereomer ratios for all compounds were determined by ¹H NMR analysis of the unpurified reaction mixtures. ¹H and ¹³C NMR data for all previously uncharacterized compounds were obtained using Varian Inova-500 and Varian Unity-500 spectrometers and are referenced to TMS (0.00 ppm) and CDCl₃ (77 ppm), respectively. IR spectral data were obtained using a Bruker Vector 22 spectrometer (thin film on NaCl). Mass spectrometry was performed with a Micromass LCT (electrospray ionization, time-of-flight analyzer or electron impact). These facilities are funded by the NSF (CHE-9974839, CHE-9304546) and the University of Wisconsin. Cyclic voltammograms (CV) were taken on a BAS Epsilon-EC instrument using MeCN with 0.1 M tetrabutylammonium hexafluorophosphate (*n*-Bu₄NPF₆) and 1 mM substrate. The electrodes were as follows: glassy carbon (working), Pt wire (auxiliary) and Ag/AgNO₃ (0.1 M *n*Bu₄NPF₆, 0.01 M Ag/AgNO₃) (reference). The potentials were referenced versus the ferrocene/ferrocenium redox couple, by externally added ferrocene.

2.5.2 Synthesis and Characterization of Starting Materials

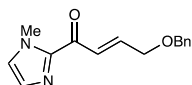
(E)-4,4-Dimethyl-1-(1-methyl-1*H*-imidazol-2-yl)pent-2-en-1-one (2-21): To a flame-dried 100



mL round bottomed flask was added 1-(1-methyl-1*H*-imidazole-2-yl)-2-(triphenylphosphoranylidene)-ethanone²² (1.33 g, 3.45 mmol), benzene (18 mL),

and freshly distilled trimethylacetaldehyde (2.97 g, 34.5 mmol). The reaction was heated to 75 °C and stirred for 105 h under N₂. After cooling to room temperature, the solvent was removed *in vacuo*, and the residue was purified by chromatography on a silica gel column (3:1 hexanes:EtOAc) to afford 0.563 g (2.93 mmol, 85 % yield) of a clear, viscous oil. IR (thin film): 2961, 1666, 1619, 1408 cm⁻¹; ¹H NMR: (499.9 MHz, CDCl₃) δ 7.34 (d, J = 16.0 Hz, 1H), 7.18 (d, J = 0.9 Hz, 1H), 7.13 (d, J = 16.0 Hz, 1H), 7.05 (s, 1H), 4.05 (s, 3H), 1.16 (s, 9H); ¹³C NMR: (125.7 MHz, CDCl₃) δ 181.3, 158.5, 143.9, 129.1, 127.1, 121.2, 36.3, 34.1, 28.7; HRMS (EI) calc'd for [C₁₁H₁₆N₂ONa]⁺ requires *m/z* 215.1160, found *m/z* 215.1155.

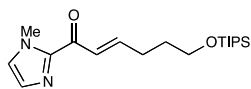
(E)-4-Benzyloxy-1-(1-methyl-1*H*-imidazol-2-yl)but-2-en-1-one (2-22): To a flame-dried 25 mL



round bottomed flask was added 1-(1-methyl-1*H*-imidazole-2-yl)-2-(triphenylphosphoranylidene)-ethanone (0.782 g, 2.03 mmol), benzene (11 mL), and

freshly distilled benzyloxyacetaldehyde (0.336 g, 2.24 mmol). The reaction was heated to 70 °C and stirred for 5 h under N₂. After cooling to room temperature the solvent was removed *in vacuo*, and the residue was purified by chromatography on a silica gel column (3:2 hexanes:EtOAc) to afford 0.485 g (1.89 mmol, 93% yield) of a clear, viscous oil that turned slightly yellow upon standing. IR (thin film): 2922, 1724, 1669, 1625, 1407 cm⁻¹; ¹H NMR: (500.2 MHz, CDCl₃) δ 7.65 (dt, J = 16.0, 2.0 Hz, 1H), 7.36 (m, 4H), 7.29 (m, 1H), 7.17 (d, J = 1.0 Hz, 1H), 7.14 (dt, J = 16.0, 4.5 Hz, 1H), 7.04 (s, 1H), 4.58 (s, 2H), 4.27 (dd, J = 5.0, 2.0 Hz, 2H), 4.03 (s, 3H); ¹³C NMR: (125.7 MHz, CDCl₃) δ 180.3, 143.6, 143.3, 137.9, 129.4, 128.4, 127.8, 127.3, 126.3, 72.7, 69.3, 36.2. HRMS (EI) calc'd for [C₁₅H₁₆N₂O₂Na]⁺ requires *m/z* 279.1109, found *m/z* 279.1104.

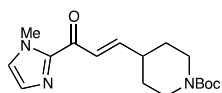
(E)-1-(1-Methyl-1H-imidazol-2-yl)-6-triisopropylsilyloxy-hex-2-en-1-one (2-23): To a



flame-dried 25 mL round bottomed flask was added 1-(1-methyl-1H-imidazole-2-yl)-2-(triphenylphosphoranylidene)-ethanone (0.612 g, 1.59

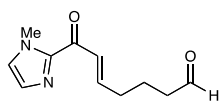
mmol), benzene (8 mL), and 4-((tris(1-methylethyl)silyl)oxy)-butanal²³ (0.389 g, 1.59 mmol). The reaction was warmed to 60 °C and stirred for 22 h under N₂. After cooling to room temperature the solvent was removed *in vacuo*, and the residue was purified by chromatography on a silica gel column (4:1 hexanes:EtOAc) to afford 0.318 g (0.907 mmol, 57% yield) of a clear, viscous oil. IR (thin film): 2943, 2866, 1668, 1622, 1409 cm⁻¹; ¹H NMR: (500.2 MHz, CDCl₃) δ 7.42 (dt, J = 15.7, 1.6 Hz, 1H), 7.17 (dt, J = 15.7, 7.1 Hz, 1H), 7.17 (d, J = 0.7 Hz, 1H), 7.04 (s, 1H), 4.05 (s, 3H), 3.74 (t, J = 6.3 Hz, 1H), 2.42 (ddt, J = 7.3, 7.2, 1.5 Hz, 2H), 1.77 (m, 2H), 1.06 (m, 21H); ¹³C NMR: (125.7 MHz, CDCl₃) δ 180.8, 148.6, 143.8, 129.1, 127.1, 126.2, 62.7, 36.3, 31.6, 29.3, 18.0, 11.9; HRMS (EI) calc'd for [C₁₉H₃₄N₂O₂SiNa]⁺ requires *m/z* 373.2287, found *m/z* 373.2282.

(E)-tert-Butyl-4-(3-(1-methyl-1H-imidazol-2-yl)-3-oxoprop-1-en-1-yl)-piperidine-1-



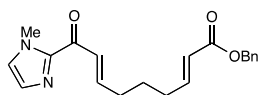
carboxylate (2-24): To a flame-dried 25 mL round-bottomed flask was added 1-(1-methyl-1H-imidazole-2-yl)-2-(triphenylphosphoranylidene)-

ethanone (0.587 g, 1.53 mmol), benzene (8 mL), and 4-formylpiperidine-1-carboxylic acid tert-butyl ester²⁴ (0.391 g, 1.83 mmol). The reaction was heated to 75 °C and was stirred for 44 h under N₂. After cooling to room temperature the solvent was removed *in vacuo*, and the residue was purified by chromatography on a silica gel column (7:3 hexanes:EtOAc) to afford 0.354 g (1.11 mmol, 73% yield) of a clear, viscous oil. IR (thin film): 2934, 1690, 1688, 1621, 1410 cm⁻¹; ¹H NMR: (500.2 MHz, CDCl₃) δ 7.41 (dd, J = 15.8, 1.4 Hz, 1H), 7.18 (d, J = 0.8 Hz, 1H), 7.06 (s, 1H), 7.04 (dd, J = 15.8, 6.7 Hz, 1H), 4.13 (m, 2H), 4.05 (s, 3H), 2.79 (m, 2H), 2.41 (m, 1H), 1.80 (d, J = 12.5 Hz, 2H), 1.45 (m, 10H), 1.40 (ddd, J = 13.2, 5.1, 1.1 Hz, 1H); ¹³C NMR: (125.7 MHz, CDCl₃) δ 180.7, 154.8, 150.8, 143.7, 129.3, 127.2, 124.7, 79.5, 43.5, 39.0, 36.3, 30.7, 28.4; HRMS (EI) calc'd for [C₁₇H₂₅N₃O₃Na]⁺ requires *m/z* 342.1794, found *m/z* 342.1789.

(E)-7-(1-Methyl-1H-imidazol-2-yl)-7-oxohept-5-enal (2-25):

(triphenylphosphoranylidene)-ethanone (5.6 g, 14.6 mmol) was placed in a

100 mL round-bottomed flask with 36 mL (0.4 M) CH_2Cl_2 . 6 mL of a 50 wt. % in water solution of glutaraldehyde (3 g, 30.0 mmol) was added. The mixture was heated to 45 °C and stirred overnight. Upon completion, the reaction was filtered over Celite and the filtrate was concentrated *in vacuo*. The residue was triturated three times with diethyl ether to remove triphenylphosphine oxide. The crude reaction mixture was then purified by chromatography on a silica gel column (2:1 hexanes:acetone) to afford 2.8 g (13.6 mmol, 93% yield) of a light yellow oil. IR (thin film) 2944, 2728, 1720, 1665, 1619, 1408 cm^{-1} ; ^1H NMR: (499.9 MHz, CDCl_3) δ 9.78 (t, $J = 1.4$ Hz, 1H), 7.43 (dt, $J = 15.7, 1.6$ Hz, 1H), 7.18 (s, 1H), 7.07 (m, = 1H), 7.06 (s, 1H), 4.05 (s, 3H), 2.51 (td, $J = 7.4, 1.4$ Hz, 2H), 2.37 (qd, $J = 7.4, 1.4$ Hz, 2H), 1.88 (dq, $J = 7.3, 7.4$ Hz, 2H); ^{13}C NMR: (125.7 MHz, CDCl_3) δ 201.7, 180.4, 146.7, 129.2, 127.2, 127.0, 43.0, 42.7, 36.2, 31.7, 20.5; HRMS (EI) calc'd for $[\text{C}_{11}\text{H}_{14}\text{N}_2\text{O}_2\text{Na}]^+$ requires m/z 229.0948, found m/z 229.0958.

(2E,7E)-Benzyl-9-(1-methyl-1H-imidazol-2-yl)-9-oxonona-2,7-dienoate (2-26):

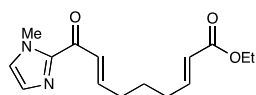
round-bottomed flask was charged with **2-25** (950 mg, 4.6 mmol), benzyl

2-(triphenylphosphoranylidene)acetate²⁵ (2.5 g, 6.1 mmol) and 5 mL (0.9

M) CH_2Cl_2 . The solution was stirred at room temperature for 18 h. The solvent was then removed *in vacuo* and the residue was triturated three times with diethyl ether to remove triphenylphosphine oxide. The crude reaction mixture was then purified by chromatography on a silica gel column (4:1 to 3:1 hexanes:acetone) to afford 1.4 g (4.1 mmol, 90 % yield) of a clear viscous oil. IR (thin film) 2950, 1732, 1670, 1409 cm^{-1} ; ^1H NMR: (499.9 MHz, CDCl_3) δ 7.41 (dt, $J = 15.6, 1.7$ Hz, 1H), 7.37 (m, 5H), 7.17 (d, $J = 0.9$ Hz, 1H), 7.04 (s, 1H), 7.08 (dt, $J = 15.7, 7.2$ Hz, 1H), 7.00 (dt, $J = 16.1, 6.8$ Hz, 1H), 5.89 (dt, $J = 15.6, 1.5$ Hz, 1H), 5.17 (s, $J =$ Hz, 2H), 4.04 (s, 3H), 2.35 (qd, $J = 7.4, 1.7$ Hz, 2H), 2.26 (qd, $J = 7.4, 1.7$ Hz, 2H), 1.69 (m, 2H); ^{13}C NMR:

(125.7 MHz, CDCl₃) δ 180.5, 166.3, 148.9, 147.3, 143.6, 136.1, 129.2, 128.5, 128.2, 128.1, 127.1, 126.8, 121.6, 66.0, 36.3, 31.9, 31.6, 26.4; HRMS (EI) calc'd for [C₂₀H₂₁N₂O₃+H]⁺ requires *m/z* 338.1625, found *m/z* 338.1621.

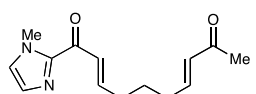
(2E,7E)-Ethyl-9-(1-methyl-1H-imidazol-2-yl)-9-oxonona-2,7-dienoate (2-27): A 25 mL round-



bottomed flask was charged with **2-25** (750 mg, 3.42 mmol), ethyl 2-(triphenylphosphoranylidene)acetate²⁶ (2.03 g, 5.3 mmol) and 6 mL (0.6

M) CH₂Cl₂. The solution was stirred at room temperature for 6 h. The solvent was then removed *in vacuo* and the residue was triturated three times with diethyl ether to remove triphenylphosphine oxide. The crude reaction mixture was then purified by chromatography on a silica gel column (4:1 to 2:1 hexanes:acetone) to afford 810 mg (2.93 mmol, 86% yield) of a light yellow viscous oil. IR (thin film) 2936, 1716, 1667, 1408 cm⁻¹; ¹H NMR: (499.9 MHz, CDCl₃) δ 7.43 (dt, *J* = 15.5, 1.8 Hz, 1H), 7.17 (d, *J* = 0.9 Hz, 1H), 7.09 (dt, *J* = 15.5, 5.7 Hz, 1H), 7.05 (s, 1H), 6.94 (dt, *J* = 15.5, 6.7 Hz), 5.83 (dt, *J* = 15.5, 1.5 Hz, 1H), 4.19 (q, *J* = 7.4 Hz, 2H), 4.05 (s, 3H), 2.35 (qd, *J* = 7.4, 1.8 Hz, 2H), 2.26 (qd, *J* = 7.4, 1.8 Hz, 2H), 1.71 (dt, *J* = 7.4, 7.2 Hz, 2H), 1.29 (t, *J* = 7.1 Hz, 3H); ¹³C NMR: (125.7 MHz, CDCl₃) δ 180.6, 166.6, 148.1, 147.3, 143.6, 129.2, 127.1, 126.8, 121.9, 60.2, 36.25, 31.9, 31.5, 26.5, 14.2; HRMS (EI) calc'd for [C₁₅H₁₉N₂O₃+H]⁺ requires *m/z* 276.1469, found *m/z* 276.1458.

(2E,7E)-1-(1-Methyl-1H-imidazol-2-yl)deca-2,7-diene-1,9-dione (2-28): A 25 mL round-

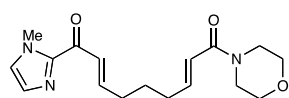


bottomed flask was charged with **2-25** (250 mg, 1.21 mmol), 1-(triphenylphosphoranylidene)propan-2-one²⁷ (660 mg, 2.1 mmol) and 10

mL (0.12 M) CH₂Cl₂. The solution was stirred at room temperature for 12 h. The solvent was then removed *in vacuo* and the crude reaction mixture was loaded directly onto a silica gel column and eluted with 2:1 hexanes:acetone to afford 180 mg (0.73 mmol, 60% yield) of a colorless viscous oil. IR (thin film) 2932, 1667, 1620, 1407, 1362 cm⁻¹; ¹H NMR: (499.9 MHz,

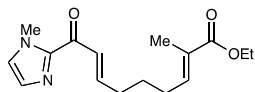
CDCl₃) δ 7.43 (dt, J = 15.7, 1.4 Hz, 1H), 7.18 (d, J = 0.9 Hz, 1H), 7.09 (dt, J = 15.7, 6.8 Hz, 1H), 7.06 (s, 1H), 6.79 (dt, J = 15.7, 6.8 Hz, 1H), 6.09 (dt, J = 15.7, 1.4 Hz, 1H), 4.05 (s, 3H), 2.35 (qd, J = 7.2, 1.7 Hz, 2H), 2.28 (qd, J = 7.2, 1.3 Hz, 2H), 2.25 (s, 3H), 1.73 (m, 2H); ¹³C NMR: (125.7 MHz, CDCl₃) δ 198.5, 180.4, 147.2, 147.1, 143.5, 131.6, 129.2, 127.1, 126.8, 36.2, 31.9, 31.7, 26.8, 26.5; HRMS (EI) calc'd for [C₁₄H₁₈N₂O₂+Na]⁺ requires *m/z* 269.1261, found *m/z* 269.1249.

(2E,7E)-1-(1-Methyl-1H-imidazol-2-yl)-9-morpholinonona-2,7-diene-1,9-dione (2-29): A 25



mL round-bottomed flask was charged with 1.0 equivalent NaH dissolved in 3 mL dry THF at room temperature. Diethyl (2-morpholino-2-oxoethyl)phosphonate²⁸ was added to the stirring solution dropwise (60.5 mg, 0.228 mmol, 1.2 equiv), and the reaction was allowed to stir until solution became clear. A solution of **2-25** (40 mg, 0.194 mmol) in 0.5 mL dry THF was added dropwise, and the reaction was stirred for 15 min. The reaction was then diluted with 5 mL diethyl ether and washed with water. The organic layer was separated and dried over Na₂SO₄. After filtration, the solution was concentrated *in vacuo* and purified by chromatography on a silica gel column (1:1 acetone:hexanes) to afford 35 mg (0.11 mmol, 57% yield) of a colorless oil. IR (thin film) 2858, 1662, 1618, 1407 cm⁻¹; ¹H NMR: (499.9 MHz, CDCl₃) δ 7.42 (dt, J = 15.7, 1.5 Hz, 1H), 7.16 (d, J = 0.9 Hz, 1H), 7.09 (dt, J = 15.7, 6.7 Hz, 1H), 7.05 (s, 1H), 6.89 (dt, J = 15.1, 7.0 Hz, 1H), 6.23 (dt, J = 15.0, 1.5 Hz, 1H), 4.05 (s, 1H), 3.5-3.75 (m, 8H), 2.36 (qd, J = 7.4, 1.7 Hz, 2H), 2.27 (qd, J = 7.4, 1.6 Hz, 2H), 1.72 (m, 2H); ¹³C NMR: (125.7 MHz, CDCl₃) δ 180.5, 165.5, 147.4, 146.0, 143.6, 129.2, 127.2, 126.8, 120.1, 66.8, 46.1, 42.2, 36.3, 31.9, 31.9, 26.7; HRMS (EI) calc'd for [C₁₇H₂₃N₃O₃+H]⁺ requires *m/z* 318.1813, found *m/z* 318.1812.

(2E,7E)-Ethyl-2-methyl-9-(1-methyl-1H-imidazol-2-yl)-9-oxonona-2,7-dienoate (2-30): A 25

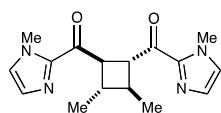


mL round-bottomed flask was charged with **2-25** (470 mg, 1.62 mmol), ethyl 2-(triphenylphosphoranylidene)propanoate²⁹ (1.17 g, 3.23 mmol) and

25 mL (0.06 M) CH₂Cl₂. The solution was stirred at room temperature overnight. The solvent was then removed *in vacuo* and the crude reaction mixture was loaded directly onto a silica gel column and eluted with 3:1 hexanes:acetone to afford 180 mg (0.619 mmol, 38% yield) as a colorless viscous oil. IR (thin film) 2360, 2254, 1700, 1666, 1621 cm⁻¹; ¹H NMR: (499.9 MHz, CDCl₃) δ 7.43 (dt, J = 15.5, 1.9 Hz, 1H), 7.17 (d, J = 1.0 Hz, 1H), 7.11 (dt, J = 15.6, 7.1 Hz, 1H), 7.05 (s, 1H), 6.75 (tq, J = 6.75, 1.7 Hz, 1H), 4.19 (q, J = 7.0 Hz, 2H), 4.05 (s, 3H), 2.36 (qd, J = 7.1, 1.5 Hz, 2H), 2.23 (q, J = 7.3 Hz, 2H), 1.83 (q, J = 1.0 Hz, 3H), 1.70 (dq, J = 7.6, 15.0 Hz, 2H), 1.30 (t, J = 7.0 Hz, 3H); ¹³C NMR: (125.7 MHz, CDCl₃) δ 180.5, 168.1, 147.6, 143.6, 141.1, 129.2, 128.4, 127.1, 126.6, 60.4, 36.2, 32.1, 28.1, 27.1, 14.2, 12.4; HRMS (EI) calc'd for [C₁₆H₂₂N₂O₃+H]⁺ requires *m/z* 291.1704, found *m/z* 291.1712.

2.5.3 Photocycloadditions

(3,4-Dimethylcyclobutane-1,2-diyl)bis((1-methyl-1H-imidazol-2-yl)methanone) (2-7). To an



oven-dried 25 mL Schlenk tube was added 99.6 mg (0.663 mmol) (*E*)-1-(1-methyl-1H-imidazole-2-yl)-but-2-en-1-one, 12.7 mg (0.017 mmol)

Ru(bpy)₃Cl₂·6H₂O, 61.7 mg (0.663 mmol) LiBF₄, 120 μL (0.651 mmol) *i*-Pr₂NEt, and 3.3 mL acetonitrile. The solution was degassed using three freeze-pump-thaw cycles in the dark. The Schlenk tube was backfilled with nitrogen and irradiated for 4 h. Upon completion of the reaction, the reaction was diluted with acetone, passed through a silica plug, and the solvent was removed *in vacuo*. Purified by chromatography (2:1 hexanes:acetone) to afford 82.5 mg (0.275 mmol, 83% yield, >10:1 d.r.) of the cycloadduct. Experiment 2: 99.8 mg (0.664 mmol) enone, 12.6 mg (0.017 mmol) Ru(bpy)₃Cl₂·6H₂O, 61.9 mg (0.666 mmol) LiBF₄, 120 μL (0.651 mmol) *i*-Pr₂NEt, and 3.3 mL acetonitrile. Isolated 80.7 mg (0.269 mmol, 81% yield, >10:1 d.r.).

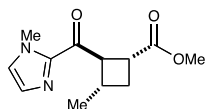
IR (thin film): 2954, 2921, 1665, 1405 cm^{-1} ; ^1H NMR: (500.2 MHz, CDCl_3) δ 6.96 (d, J = 0.7 Hz, 2H), 6.94 (s, 2H), 4.14 (dd, J = 5.6, 3.2 Hz, 2H), 4.00 (s, 6H), 2.18 (m, 2H), 1.21 (m, 6H); ^{13}C NMR: (125.7 MHz, CDCl_3) δ 191.8, 143.1, 129.0, 126.6, 48.9, 38.5, 36.0, 19.1; HRMS (EI) calc'd for $[\text{C}_{16}\text{H}_{20}\text{N}_4\text{O}_2\text{Na}]^+$ requires m/z 323.1484, found m/z 323.1479.

General procedure A: Intermolecular [2+2] cycloadditions (Figure 1): A dry 25 mL Schlenk tube was charged with the Michael acceptor (5 equiv) followed by a solution of $\text{Ru}(\text{bpy})_3\text{Cl}_2 \cdot 6\text{H}_2\text{O}$ (0.025 equiv) and LiBF_4 (0.5–4.0 equiv) in dry MeCN (1.33 M with respect to the Michael acceptor). A second 25 mL Schlenk tube was charged a solution of imidazole enone (1 equiv) in dry MeCN (0.16 M with respect to the aryl enone). $i\text{-Pr}_2\text{NEt}$ (2 equiv) was then added to the first tube. The solutions were degassed using three freeze-pump-thaw cycles under nitrogen in the dark. The Schlenk tubes were then placed in a water bath and irradiated using a 23 W compact fluorescent light bulb placed at a distance of 20 cm. The imidazole enone solution was added dropwise via syringe pump over a period of 45 min to the solution containing the Michael acceptor. Additional time was allowed for the reaction to reach completion (total reaction times listed in Table 3 refer to dropwise addition and subsequent irradiation combined). Upon completion of the reaction, the reaction was diluted with ethyl acetate, passed through a silica plug, and the solvent was removed *in vacuo*. The resulting residue was purified by chromatography on a silica gel column.

General procedure B: Intramolecular [2+2] cycloadditions (Figure 2): A dry 25 mL Schlenk tube was charged with a solution of the bisenone (1 equiv), $\text{Ru}(\text{bpy})_3\text{Cl}_2 \cdot 6\text{H}_2\text{O}$ (0.025 equiv), LiBF_4 (0.5 equiv), and $i\text{-Pr}_2\text{NEt}$ (2 or 0.5 equiv) in acetonitrile (0.1 M). The solution was then degassed using three freeze-pump-thaw cycles under nitrogen in the dark. The Schlenk tube was then irradiated using a 23 W floodlight placed at a distance of 20 cm. Upon completion of the reaction, the reaction was passed through a silica plug using 100% ethyl acetate or acetone

as the eluent, the solvent was removed *in vacuo*, and the residue was purified by chromatography on a silica gel column.

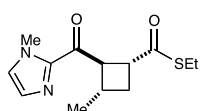
Methyl-3-methyl-2-(1-methyl-1H-imidazole-2-carbonyl) cyclobutanecarboxylate (Table 2-2,



2-6): Prepared according to general procedure **A** using 104.2 mg (0.694 mmol) (*E*)-1-(1-methyl-1*H*-imidazole-2-yl)-but-2-en-1-one, 315 μ L (3.50 mmol)

methyl acrylate, 13.3 mg (0.018 mmol) Ru(bpy)₃Cl₂·6H₂O, 130 mg (1.39 mmol) LiBF₄, 242 μ L (1.39 mmol) *i*-Pr₂NEt, 6.94 mL acetonitrile and an irradiation time of 90 min. Purified by chromatography (23:2 hexanes:acetone) to afford 110 mg (0.466 mmol, 67% yield, >10:1 d.r.) of the cycloadduct as a clear oil. Experiment 2: 104.7 mg (0.697 mmol) enone, 315 μ L (3.50 mmol) methyl acrylate, 13.1 mg (0.017 mmol) Ru(bpy)₃Cl₂·6H₂O, 132 mg (1.41 mmol) LiBF₄, 245 μ L (1.41 mmol) *i*-Pr₂NEt, and 6.97 mL acetonitrile. Isolated 111 mg (0.470 mmol, 67% yield, >10:1 d.r.). IR (thin film): 2954, 1733, 1668, 1411 cm⁻¹; ¹H NMR (499.9 MHz, CDCl₃) δ 7.14 (d, J = 0.9 Hz, 1H), 7.05 (s, 1H), 4.21 (dd, J = 8.9, 8.9 Hz, 1H), 4.02 (s, 3H), 3.66 (s, 3H), 3.46 (ddd, J = 9.0, 9.0, 9.0 Hz, 1H), 2.42 (m, 1H), 2.33 (ddd, J = 10.2, 8.8, 8.8 Hz, 1H), 1.92 (ddd, J = 10.3, 9.4, 9.4 Hz, 1H), 1.26 (d, J = 6.6 Hz, 3H); ¹³C NMR: (125.7 MHz, CDCl₃) δ 190.9, 174.4, 142.6, 129.5, 127.3, 52.2, 51.7, 36.1, 35.1, 32.5, 29.3, 20.8; HRMS (EI) calc'd for [C₁₂H₁₆N₂O₃Na]⁺ requires *m/z* 259.1059, found *m/z* 259.1054.

S-Ethyl 3-methyl-2-(1-methyl-1H-imidazole-2-carbonyl)cyclobutanecarbothioate (Table 2-

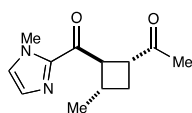


2, 2-8): Prepared according to general procedure **A** using 109.4 mg (0.728 mmol) (*E*)-1-(1-methyl-1*H*-imidazole-2-yl)-but-2-en-1-one, 426 mg (3.67 mmol)

ethyl prop-2-enethioate,¹¹ 13.5 mg (0.018 mmol) Ru(bpy)₃Cl₂·6H₂O, 137 mg (1.46 mmol) LiBF₄, 255 μ L (1.46 mmol) *i*-Pr₂NEt, 7.28 mL acetonitrile and an irradiation time of 90 min. Purified by chromatography (47:3 hexanes:acetone) to afford 150 mg (0.563 mmol, 77% yield, > 10:1 d.r.) of the cycloadduct as a clear oil. Experiment 2: 108.6 mg (0.723 mmol) enone, 421 mg (3.62

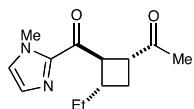
mmol) (S)-ethyl-prop-2-enethioate, 13.4 mg (0.018 mmol) Ru(bpy)₃Cl₂·6H₂O, 136 mg (1.45 mmol) LiBF₄, 255 μL (1.46 mmol) *i*-Pr₂NEt, and 7.23 mL acetonitrile. Isolated 155 mg (0.582 mmol, 80% yield, >10:1 d.r.). IR (thin film): 2963, 2931, 1668, 1410 cm⁻¹; ¹H NMR: (500.2 MHz, CDCl₃) δ 7.15 (s, 1H), 7.06 (s, 1H), 4.26 (dd, J = 8.5, 8.5 Hz, 1H), 4.03 (s, 3H), 3.68 (ddd, J = 8.9, 8.9, 8.9 Hz 1H), 2.86 (q, J = 7.5 Hz, 2H), 2.39 (m, 1H), 2.33 (ddd, J = 10.1, 8.7, 8.7 Hz, 1H), 1.96 (ddd, J = 10.4, 9.3, 9.3 Hz, 1H), 1.26 (d, J = 6.6 Hz, 3H), 1.22 (t, J = 7.5 Hz, 3H); ¹³C NMR: (125.7 MHz, CDCl₃) δ 200.0, 190.7, 142.6, 129.5, 127.3, 52.6, 43.1, 36.1, 32.5, 29.8, 23.0, 20.7, 14.7; HRMS (EI) calc'd for [C₁₃H₁₈N₂O₂SNa]⁺ requires *m/z* 289.0987, found *m/z* 289.0982.

1-(3-Methyl-2-(1-methyl-1H-imidazole-2-carbonyl)cyclobutyl)ethanone (Table 2-2, 2-9):



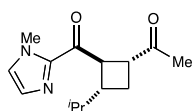
Prepared according to general procedure **A** using 106.8 mg (0.711 mmol) (*E*)-1-(1-methyl-1H-imidazole-2-yl)-but-2-en-1-one, 290 μL (3.57 mmol) 3-buten-2-one, 13.4 mg (0.018 mmol) Ru(bpy)₃Cl₂·6H₂O, 33.6 mg (0.358 mmol) LiBF₄, 250 μL (1.44 mmol) *i*-Pr₂NEt, 7.11 mL acetonitrile and an irradiation time of 90 min. Purified by chromatography (17:3 hexanes:acetone) to afford 119 mg (0.540 mmol, 76% yield, >10:1 d.r.) of the cycloadduct. Experiment 2: 103.4 mg (0.689 mmol) enone, 280 μL (3.45 mmol) 3-buten-2-one, 12.8 mg (0.0171 mmol) Ru(bpy)₃Cl₂·6H₂O, 32.3 mg (0.344 mmol) LiBF₄, 240 μL (1.38 mmol) *i*-Pr₂NEt, and 6.89 mL acetonitrile. Isolated 111 mg (0.504 mmol, 73% yield, >10:1 d.r.) of the cycloadduct as a clear oil. IR (thin film): 2958, 1707, 1665, 1409 cm⁻¹; ¹H NMR: (500.2 MHz, CDCl₃) δ 7.15 (d, J = 0.6 Hz, 1H), 7.05 (s, 1H), 4.13 (dd, J = 8.8, 8.8 Hz, 1H), 4.03 (s, 3H), 3.56 (ddd, J = 9.1, 9.1, 9.1 Hz, 1H), 2.42 (app qq, J = 8.5, 6.8 Hz, 1H), 2.27 (ddd, J = 10.3, 8.9, 8.9 Hz, 1H), 2.08 (s, 3H), 1.84 (ddd, J = 10.4, 9.5, 9.5 Hz, 1H), 1.23 (d, J = 6.7 Hz, 3H); ¹³C NMR: (125.7 MHz, CDCl₃) δ 208.4, 191.4, 142.6, 129.6, 127.3, 51.6, 42.9, 36.1, 32.0, 28.5, 27.5, 20.9; HRMS (EI) calc'd for [C₁₂H₁₆N₂O₂Na]⁺ requires *m/z* 243.1109, found *m/z* 243.1104.

1-(3-Ethyl-2-(1-methyl-1H-imidazole-2-carbonyl)cyclobutyl)ethanone (Table 2-2, **2-10**):



Prepared according to general procedure **A** using 103.5 mg (0.630 mmol) (*E*)-1-(1-methyl-1*H*-imidazole-2-yl)-pent-2-en-1-one, 260 μ L (3.21 mmol) 3-buten-2-one, 11.7 mg (0.016 mmol) Ru(bpy)₃Cl₂·6H₂O, 29.5 mg (0.315 mmol) LiBF₄, 220 μ L (1.26 mmol) *i*-Pr₂NEt, 6.30 mL acetonitrile and an irradiation time of 90 min. Purified by chromatography (17:3 hexanes:acetone) to afford 115 mg (0.491 mmol, 78% yield, >10:1 d.r.) of the cycloadduct as a clear oil. Experiment 2: 103.4 mg (0.630 mmol) enone, 255 μ L (3.15 mmol) 3-buten-2-one, 11.8 mg (0.016 mmol) Ru(bpy)₃Cl₂·6H₂O, 29.5 mg (0.315 mmol) LiBF₄, 220 μ L (1.26 mmol) *i*-Pr₂NEt, and 6.30 mL acetonitrile. Isolated 113 mg (0.482 mmol, 77% yield, >10:1 d.r.). IR (thin film): 2960, 2930, 2874, 1709, 1667, 1410 cm⁻¹; ¹H NMR: (500.2 MHz, CDCl₃) δ 7.14 (s, 1H), 7.07 (s, 1H), 4.22 (dd, *J* = 8.7, 8.7 Hz, 1H), 4.03 (s, 3H), 3.51 (ddd, *J* = 9.2, 9.2, 9.2 Hz, 1H), 2.31 (m, 1H), 2.23 (ddd, *J* = 10.2, 9.2, 9.2 Hz, 1H), 2.08 (s, 3H), 1.83 (ddd, *J* = 10.4, 9.4, 9.4 Hz, 1H), 1.69 (d of quint, *J* = 12.7, 7.3 Hz, 1H), 1.49 (ddq, *J* = 12.8, 7.4, 7.3 Hz, 1H), 0.79 (t, *J* = 7.4 Hz, 3H); ¹³C NMR: (125.7 MHz, CDCl₃) δ 208.5, 191.7, 142.6, 129.5, 127.4, 49.9, 43.5, 37.9, 36.1, 28.5, 27.5, 26.3, 10.8; HRMS (EI) calc'd for [C₁₃H₁₈N₂O₂Na]⁺ requires *m/z* 257.1266, found *m/z* 257.1261.

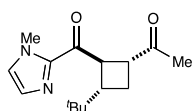
1-(3-iso-Propyl-2-(1-methyl-1H-imidazole-2-carbonyl)cyclobutyl)ethanone (Table 2-2, **2-**



11): Prepared according to general procedure **A** using 108.6 mg (0.609 mmol) (*E*)-4-methyl-1-(1-methyl-1*H*-imidazol-2-yl)-pent-2-en-1-one, 250 μ L (3.08 mmol) 3-buten-2-one, 11.5 mg (0.015 mmol) Ru(bpy)₃Cl₂·6H₂O, 114 mg (1.22 mmol) LiBF₄, 212 μ L (1.22 mmol) *i*-Pr₂NEt, 6.09 mL acetonitrile and an irradiation time of 2 h. Purified by chromatography (23:2 hexanes:acetone) to afford 111 mg (0.447 mmol, 73% yield, >10:1 d.r.) of the cycloadduct as a clear oil. Experiment 2: 106.7 mg (0.599 mmol) enone, 245 μ L (3.02 mmol) 3-buten-2-one, 11.3 mg (0.015 mmol) Ru(bpy)₃Cl₂·6H₂O, 112 mg (1.20 mmol) LiBF₄, 210 μ L (1.20 mmol) *i*-Pr₂NEt, and 5.99 mL acetonitrile. Isolated 110 mg (0.443 mmol, 74% yield,

>10:1 d.r.). IR (thin film): 2957, 2873, 1709, 1665, 1418 cm^{-1} ; ^1H NMR: (500.2 MHz, CDCl_3) δ 7.15 (s, 1H), 7.06 (s, 1H), 4.36 (dd, $J = 8.7, 8.7$ Hz, 1H), 4.02 (s, 3H), 3.32 (ddd, $J = 8.9, 8.9, 8.9$ Hz, 1H), 2.24 (m, 1H), 2.17 (ddd, $J = 10.3, 8.8, 8.8$ Hz, 1H), 2.07 (s, 3H), 1.86 (ddd, $J = 10.3, 9.4, 9.4$ Hz, 1H), 1.64 (m, 1H), 0.83 (d, $J = 6.5$ Hz, 3H), 0.73 (d, $J = 6.5$ Hz, 3H); ^{13}C NMR: (125.7 MHz, CDCl_3) δ 208.3, 192.4, 142.7, 129.5, 127.5, 48.4, 44.5, 42.6, 36.2, 33.4, 27.7, 24.9, 19.6, 18.8; HRMS (EI) calc'd for $[\text{C}_{14}\text{H}_{20}\text{N}_2\text{O}_2\text{Na}]^+$ requires m/z 271.1422, found m/z 271.1417.

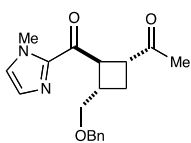
1-(3-(*tert*-Butyl)-2-(1-methyl-1H-imidazole-2-carbonyl)cyclobutyl)ethanone (Table 2-2, **2-**



12): To a 25 mL Schlenk tube that had been evacuated and purged with N_2

was added 106.4 mg (0.553 mmol, 1.0 equiv) (*E*)-4,4-dimethyl-1-(1-methyl-1H-imidazol-2-yl)-pent-2-en-1-one, 112 μL (1.38 mmol, 2.5 equiv) 3-buten-2-one, 10.5 mg (0.014 mmol, 0.025 equiv) $\text{Ru}(\text{bpy})_3\text{Cl}_2 \cdot 6\text{H}_2\text{O}$, 207 mg (2.21 mmol, 4.0 equiv) LiBF_4 , 193 μL (1.11 mmol, 2.0 equiv) *i*- Pr_2NEt , and 5.53 mL acetonitrile. The solution was subsequently degassed using three freeze-pump-thaw cycles under nitrogen in the dark. The Schlenk tube was then placed in a water bath and irradiated for 14 h. Upon completion of the reaction, the reaction was diluted with ethyl acetate, passed through a silica plug, and the solvent was removed *in vacuo*. Purified by chromatography (4:1 hexanes:EtOAc) to afford 97 mg (0.370 mmol, 66% yield, >10:1 d.r.) of the cycloadduct as a clear oil. Experiment 2: 106.3 mg (0.553 mmol) enone, 112 μL (1.38 mmol) 3-buten-2-one, 10.3 mg (0.014 mmol) $\text{Ru}(\text{bpy})_3\text{Cl}_2 \cdot 6\text{H}_2\text{O}$, 206 mg (2.20 mmol) LiBF_4 , 195 μL (1.12 mmol) *i*- Pr_2NEt , and 5.53 mL acetonitrile. Isolated 93 mg (0.354 mmol, 65% yield, >10:1 d.r.). IR (thin film): 2957, 1709, 1666, 1409 cm^{-1} ; ^1H NMR: (500.2 MHz, CDCl_3) δ 7.16 (d, $J = 0.7$ Hz, 1H), 7.06 (s, 1H), 4.53 (dd, $J = 9.2$ Hz, 1H), 4.02 (s, 3H), 3.25 (ddd, $J = 9.2, 9.2, 9.2$ Hz, 1H), 2.43 (ddd, $J = 10.1, 9.0, 9.0$ Hz, 1H), 2.06 (s, 3H), 1.99 (m, 2H), 0.80 (s, 9H); ^{13}C NMR: (125.7 MHz, CDCl_3) δ 208.1, 192.7, 142.8, 129.6, 127.6, 46.4, 45.2, 44.2, 36.1, 31.6, 27.6, 26.4, 21.8; HRMS (EI) calc'd for $[\text{C}_{15}\text{H}_{22}\text{N}_2\text{O}_2\text{Na}]^+$ requires m/z 285.1579, found m/z 285.1574.

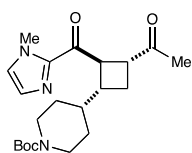
1-(3-((Benzyloxy)methyl)-2-(1-methyl-1H-imidazole-2-carbonyl)cyclobutyl)ethanone (Table



2-2, **2-13**): Prepared according to general procedure **A** using 108.7 mg (0.424 mmol) (*E*)-4-benzyloxy-1-(1-methyl-1*H*-imidazol-2-yl)-but-2-en-1-one, 175 μ L (2.16 mmol) 3-buten-2-one, 7.8 mg (0.010 mmol) Ru(bpy)₃Cl₂·6H₂O, 79.9 mg

(0.852 mmol) LiBF₄, 148 μ L (0.848 mmol) *i*-Pr₂NEt, 4.24 mL acetonitrile and an irradiation time of 145 min. Purified by chromatography (7:3 hexanes:EtOAc) to afford 72 mg (0.221 mmol, 52% yield, >10:1 d.r.) of the cycloadduct as a clear oil. Experiment 2: 108.0 mg (0.723 mmol) enone, 170 μ L (2.10 mmol) 3-buten-2-one, 7.9 mg (0.011 mmol) Ru(bpy)₃Cl₂·6H₂O, 79.1 mg (0.844 mmol) LiBF₄, 147 μ L (0.844 mmol) *i*-Pr₂NEt, and 4.21 mL acetonitrile. Isolated 70 mg (0.214 mmol, 51% yield, >10:1 d.r.). IR (thin film): 2927, 1708, 1666, 1410 cm⁻¹; ¹H NMR: (500.2 MHz, CDCl₃) δ 7.27 (m, 5H), 7.12 (d, *J* = 0.7 Hz, 1H), 7.03 (s, 1H), 4.51 (s, 2H), 4.36 (dd, *J* = 8.7 Hz, 1H), 4.00 (s, 3H), 3.67 (dd, *J* = 9.7, 5.4 Hz, 1H), 3.59 (dd, *J* = 9.6, 6.8 Hz, 1H), 3.55 (ddd, *J* = 9.2, 9.2, 9.2 Hz, 1H), 2.70 (m, 1H), 2.25 (ddd, *J* = 10.3, 9.0, 9.0 Hz, 1H), 2.11 (s, 3H), 2.10 (ddd, *J* = 10.3, 9.4, 9.4 Hz, 1H); ¹³C NMR: (125.7 MHz, CDCl₃) δ 208.2, 191.1, 142.4, 138.5, 129.5, 128.2, 127.5, 127.4, 127.3, 73.1, 72.8, 46.7, 43.6, 36.0, 35.5, 27.5, 24.3; HRMS (EI) calc'd for [C₁₉H₂₂N₂O₃Na]⁺ requires *m/z* 349.1528, found *m/z* 349.1523.

tert-Butyl-4-(3-acetyl-2-(1-methyl-1H-imidazole-2-carbonyl)cyclobutyl)piperidine-1-

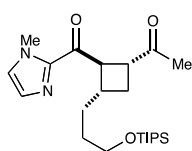


carboxylate (Table 2-2, **2-14**): Due to the hygroscopic nature of the piperidine enone, benzene (3 x 1 mL) was added to the enone, and the volatiles were removed *in vacuo* three times immediately prior to the reaction. Prepared

according to general procedure **B** using 109.5 mg (0.343 mmol) 4-[(*E*)-3-(1-methyl-1*H*-imidazol-2-yl)-3-oxo-propenyl]-piperidine-1-carboxylic acid *tert*-butyl ester, 140 μ L (1.73 mmol) 3-buten-2-one, 6.4 mg (0.009 mmol) Ru(bpy)₃Cl₂·6H₂O, 64.2 mg (0.686 mmol) LiBF₄, 119 μ L (0.686 mmol) *i*-Pr₂NEt, 3.43 mL acetonitrile and an irradiation time of 2 h. Purified by chromatography (2:3 hexanes:EtOAc) to afford 100 mg (0.257 mmol, 75% yield, >10:1 d.r.) of the cycloadduct as a

clear oil. Experiment 2: 111.4 mg (0.349 mmol) enone, 143 μL (1.76 mmol) 3-buten-2-one, 6.5 mg (0.009 mmol) $\text{Ru}(\text{bpy})_3\text{Cl}_2 \cdot 6\text{H}_2\text{O}$, 65.3 mg (0.697 mmol) LiBF_4 , 121 μL (0.698 mmol) *i*- Pr_2NEt , and 3.49 mL acetonitrile. Isolated 105 mg (0.270 mmol, 77% yield, >10:1 d.r.). IR (thin film): 2976, 2930, 2853, 1688, 1667, 1410, 1366 cm^{-1} ; ^1H NMR: (500.2 MHz, CDCl_3) δ 7.14 (s, 1H), 7.07 (s, 1H), 4.37 (dd, $J = 8.7, 8.7$ Hz, 1H), 4.02 (s, 3H), 4.02 (m, 2H), 3.37 (ddd, $J = 9.4, 9.4, 9.4$ Hz, 1H), 2.62 (m, 2H), 2.31 (pent, $J = 8.9$ Hz, 1H), 2.19 (ddd, $J = 10.1, 9.5, 9.5$ Hz, 1H), 2.07 (s, 3H), 1.90 (ddd, $J = 10.2, 9.6, 9.6$ Hz, 1H), 1.66 (m, 1H), 1.50 (m, 2H), 1.42 (s, 9H), 0.99 (qd, $J = 12.5, 4.3$ Hz, 1H), 0.88 (qd, $J = 12.1, 4.2$ Hz, 1H); ^{13}C NMR: (125.7 MHz, CDCl_3) δ 208.0, 191.9, 154.8, 142.4, 129.6, 127.7, 79.2, 47.9, 44.8, 41.3, 39.9, 36.2, 29.1, 28.5, 27.9, 24.7; HRMS (EI) calc'd for $[\text{C}_{21}\text{H}_{31}\text{N}_3\text{O}_4\text{Na}]^+$ requires m/z 412.2212, found m/z 412.2207.

1-(2-(1-Methyl-1H-imidazole-2-carbonyl)-3-(3-((triisopropylsilyl)oxy)propyl)cyclobutyl)ethanone (Table 2-2, 2-15):

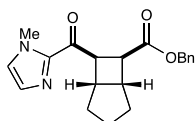


ethanone (Table 2-2, 2-15): Prepared according to general procedure **A** using 112.3 mg (0.320 mmol) (*E*)-1-(1-methyl-1*H*-imidazol-2-yl)-6-triisopropylsilyloxy-hex-2-en-1-one, 130 μL (1.60 mmol) 3-buten-2-one, 6.0

mg (0.008 mmol) $\text{Ru}(\text{bpy})_3\text{Cl}_2 \cdot 6\text{H}_2\text{O}$, 60.4 mg (0.644 mmol) LiBF_4 , 112 μL (0.641 mmol) *i*- Pr_2NEt , 3.20 mL acetonitrile and an irradiation time of 90 min. Purified by chromatography (4:1 hexanes:EtOAc) to afford 92 mg (0.219 mmol, 68% yield, >10:1 d.r.) of the cycloadduct as a clear oil. Experiment 2: 113.2 mg (0.323 mmol) enone, 131 μL (1.61 mmol) 3-buten-2-one, 6.1 mg (0.008 mmol) $\text{Ru}(\text{bpy})_3\text{Cl}_2 \cdot 6\text{H}_2\text{O}$, 60.7 mg (0.647 mmol) LiBF_4 , 113 μL (0.649 mmol) *i*- Pr_2NEt , and 3.23 mL acetonitrile. Isolated 92 mg (0.219 mmol, 68% yield, >10:1 d.r.). IR (thin film): 2942, 2866, 2360, 1711, 1667, 1409 cm^{-1} ; ^1H NMR: (500.2 MHz, CDCl_3) δ 7.13 (s, 1H), 7.04 (s, 1H), 4.22 (dd, $J = 8.8, 8.8$ Hz, 1H), 4.02 (s, 3H), 3.60 (t, $J = 6.7$ Hz, 2H), 3.51 (ddd, $J = 9.2, 9.2, 9.2$ Hz, 1H), 2.39 (m, 1H), 2.24 (ddd, $J = 10.3, 9.4, 9.4$ Hz, 1H), 2.08 (s, 3H), 1.84 (ddd, $J = 10.1, 9.6, 9.6$ Hz, 1H), 1.75 (m, 1H), 1.46 (m, 3H), 1.01 (m, 21H); ^{13}C NMR: (125.7 MHz, CDCl_3) δ 208.3, 191.6, 142.6, 129.6, 127.4, 63.2, 50.2, 43.5, 36.2, 36.1, 31.9, 30.1, 27.5, 26.8,

18.0, 11.9; HRMS (EI) calc'd for $[C_{23}H_{40}N_2O_3SiNa]^+$ requires m/z 443.2706, found m/z 443.2701.

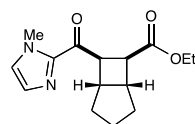
Benzyl 7-(1-methyl-1H-imidazole-2-carbonyl)bicyclo[3.2.0]heptane-6-carboxylate (Table 2-



3, **2-16**): Prepared according to general procedure **B** using 203.3 mg (0.601 mmol) (*2E,7E*)-benzyl 9-(1-methyl-1H-imidazol-2-yl)-9-oxonona-2,7-dienoate,

11.3 mg (0.015 mmol) $Ru(bpy)_3Cl_2 \cdot 6H_2O$, 27.8 mg (0.299 mmol) $LiBF_4$, 220 μL (1.194 mmol) *i*- Pr_2NEt , 6.0 mL acetonitrile, and an irradiation time of 90 min. Purified by chromatography (3:1 hexanes:acetone) to afford 166.7 mg (0.493 mmol, 82% yield, >10:1 d.r.) of the cycloadduct as a clear oil. Experiment 2: 202.6 mg (0.600 mmol) bisenone, 11.5 mg (0.015 mmol) $Ru(bpy)_3Cl_2 \cdot 6H_2O$, 27.7 mg (0.300 mmol) $LiBF_4$, 220 μL (1.19 mmol) *i*- Pr_2NEt , and 6.0 mL acetonitrile. Isolated 160.8 mg (0.476 mmol, 79% yield, >10:1 d.r.). IR (thin film) 2930, 2361, 1667, 1623 cm^{-1} ; 1H NMR: (499.9 MHz, $CDCl_3$) δ 7.26 (m, 3H), 7.16 (m, 2H), 7.03 (d, $J = 0.9$ Hz, 1H), 6.90 (s, 1H), 4.93 (s, 2H), 4.01 (dd, $J = 10.5, 5.7$ Hz, 1H), 3.83 (s, 3H), 3.21 (m, 1H), 3.16 (dd, $J = 10.5, 5.7$ Hz, 1H), 3.02 (m, 1H), 1.90 (m, 2H), 1.73 (m, 2H), 1.58 (m, 2H); ^{13}C NMR: (125.7 MHz, $CDCl_3$) δ 191.5, 173.3, 142.6, 135.8, 128.6, 128.2, 127.8, 127.8, 126.5, 77.3, 77.0, 76.7, 65.9, 46.1, 44.8, 39.5, 37.9, 35.7, 32.3, 32.1, 25.0; HRMS (EI) calc'd for $[C_{20}H_{21}N_2O_3+H]^+$ requires m/z 338.1625, found m/z 338.1614.

Ethyl 7-(1-methyl-1H-imidazole-2-carbonyl)bicyclo[3.2.0]heptane-6-carboxylate (Table 2-3,

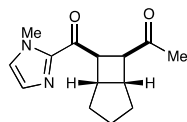


2-17): Prepared according to general procedure **B** using 99.6 mg (0.361 mmol), (*2E,7E*)-ethyl 9-(1-methyl-1H-imidazol-2-yl)-9-oxonona-2,7-dienoate,

6.7 mg (0.009 mmol) $Ru(bpy)_3Cl_2 \cdot 6H_2O$, 16.8 mg (0.181 mmol) $LiBF_4$, 135 μL (0.733 mmol) *i*- Pr_2NEt , 3.6 mL acetonitrile, and an irradiation time of 135 min. Purified by chromatography (2:1 hexanes:acetone) to afford 84 mg (0.493 mmol, 85% yield, >10:1 d.r.) of the cycloadduct as a clear oil. Experiment 2: 101.1 mg (0.366 mmol) bisenone, 6.6 mg (0.009 mmol) $Ru(bpy)_3Cl_2 \cdot 6H_2O$, 16.7 mg (0.179 mmol) $LiBF_4$, 135 μL (0.733 mmol) *i*- Pr_2NEt , and 3.6

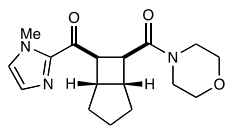
mL acetonitrile. Isolated 82 mg (0.476 mmol, 82% yield, >10:1 d.r.). IR (thin film) 2952, 2855, 1730, 1672, 1409 cm^{-1} ; ^1H NMR: (499.9 MHz, CDCl_3) δ 7.08 (d, $J = 0.9$ Hz, 1H), 6.99 (s, 1H), 4.00 (s, 3H), 3.97 (ddd, $J = 10.2, 5.2, 1.0$ Hz, 1H), 3.93 (dq, $J = 7.3, 0.9$ Hz, 2H), 3.23 (m, 1H), 3.11 (ddd, $J = 10.5, 5.6, 0.9$ Hz, 1H), 2.97 (m, 1H), 1.90 (m, 2H), 1.73 (m, 2H), 1.60 (m, 2H), 1.03 (dd, $J = 7.5, 7.5$ Hz, 3H); ^{13}C NMR: (125.7 MHz, CDCl_3) δ 191.7, 173.5, 142.8, 128.7, 126.4, 60.1, 46.2, 45.1, 39.5, 37.6, 35.9, 32.4, 32.1, 25.0, 13.9; HRMS (EI) calc'd for $[\text{C}_{15}\text{H}_{19}\text{N}_2\text{O}_3+\text{H}]^+$ requires m/z 276.1469, found m/z 276.1461.

1-7-(1-Methyl-1H-imidazole-2-carbonyl)bicyclo[3.2.0]heptan-6-yl)ethanone (Table 2-3, **2-**



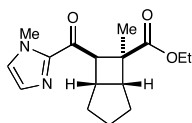
18): Prepared according to general procedure **B** using 101.6 mg (0.413 mmol) (2*E*,7*E*)-1-(1-methyl-1H-imidazol-2-yl)deca-2,7-diene-1,9-dione, 17.5 mg (0.010 mmol) $\text{Ru}(\text{bpy})_3\text{Cl}_2 \cdot 6\text{H}_2\text{O}$, 19.2 mg (0.206 mmol) LiBF_4 , 37 μL (0.201 mmol) *i*-

Pr_2NEt , 4.0 mL acetonitrile, and an irradiation time of 16.5 h. Purified by chromatography (3:1 hexanes:acetone) to afford 66.7 mg (0.271 mmol, 66% yield, >10:1 d.r.) of the cycloadduct as a clear oil. Experiment 2: 100.5 mg (0.408 mmol) bisenone, 7.4 mg (0.010 mmol) $\text{Ru}(\text{bpy})_3\text{Cl}_2 \cdot 6\text{H}_2\text{O}$, 18.7 mg (0.201 mmol) LiBF_4 , 37 μL (0.201 mmol) *i*- Pr_2NEt , and 4.0 mL acetonitrile. Isolated 64.5 mg (0.262 mmol, 65% yield, >10:1 d.r.). IR (thin film) 2949, 2862, 704, 1671, 1409 cm^{-1} ; ^1H NMR: (499.9 MHz, CDCl_3) δ 7.02 (d, $J = 0.9$ Hz, 1H), 6.97 (s, 1H), 4.02 (s, 3H), 3.84 (ddd, $J = 10.2, 5.5, 1.0$ Hz, 1H), 3.33 (dd, $J = 10.2, 5.5$ Hz, 1H), 3.22 (m, 1H), 2.84 (m, 1H), 1.96 (s, 3H), 1.93 (m, 2H), 1.73 (m, 2H), 1.60 (m, 2H); ^{13}C NMR: (125.7 MHz, CDCl_3) δ 207.9, 192.2, 143.2, 128.4, 126.2, 53.8, 46.3, 39.9, 36.6, 35.8, 32.8, 32.0, 26.3, 25.0; HRMS (EI) calc'd for $[\text{C}_{14}\text{H}_{18}\text{N}_2\text{O}_2\text{Na}]^+$ requires m/z 269.1261, found m/z 269.1266.

(1-Methyl-1H-imidazol-2-yl)-7-(morpholine-4-carbonyl)bicyclo[3.2.0]heptan-6-

yl)methanone (Table 2-3, **2-19**): Prepared according to general procedure **B**

using 98.5 mg (0.311 mmol), (*2E,7E*)-1-(1-methyl-1H-imidazol-2-yl)-9-morpholinonona-2,7-diene-1,9-dione, 5.8 mg (0.008 mmol) Ru(bpy)₃Cl₂·6H₂O, 14.7 mg (0.158 mmol) LiBF₄, 110 μL (0.597 mmol) *i*-Pr₂NEt, 3.1 mL acetonitrile, and an irradiation time of 3 h. Purified by chromatography (1:3 hexanes:acetone) to afford 70.0 mg (0.220 mmol, 70% yield, >10:1 d.r.) of the cycloadduct as a light yellow oil. Experiment 2: 100.6 mg (0.317 mmol) bisenone, 6.1 mg (0.008 mmol) Ru(bpy)₃Cl₂·6H₂O, 14.5 mg (0.156 mmol) LiBF₄, 110 μL (0.597 mmol) *i*-Pr₂NEt, and 3.1 mL acetonitrile. Isolated 68.4 mg (0.216 mmol, 68% yield, >10:1 d.r.). IR (thin film) 3055, 2987, 1677, 1636, 1422 cm⁻¹; ¹H NMR: (499.9 MHz, CDCl₃) δ 7.02 (d, J = 0.9 Hz, 1H), 6.97 (s, 1H), 4.01 (s, 3H), 3.83 (ddd, J = 10.1, 5.9, 1.2 Hz, 1H), 3.53 (m, 2H), 3.25-3.47 (m, 8H), 2.91 (m, 1H), 1.92 (m, 2H), 1.53-1.76 (m, 4H); ¹³C NMR: (125.7 MHz, CDCl₃) δ 191.4, 171.6, 143.2, 128.1, 126.0, 66.7, 66.3, 46.0, 45.8, 44.3, 41.9, 39.6, 37.1, 35.8, 32.3, 32.2, 25.2; HRMS (EI) calc'd for [C₁₇H₂₃N₃O₃+H]⁺ requires *m/z* 318.1813, found *m/z* 318.1810.

Ethyl 6-methyl-7-(1-methyl-1H-imidazole-2-carbonyl)bicyclo[3.2.0]heptane-6-carboxylate

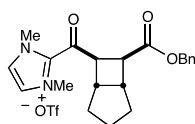
(Table 2-3, **2-20**): Prepared according to general procedure **B** using 88.7 mg

(0.305 mmol) (*2E,7E*)-ethyl 2-methyl-9-(1-methyl-1H-imidazol-2-yl)-9-oxonona-2,7-dienoate, 6.0 mg (0.008 mmol) Ru(bpy)₃Cl₂·6H₂O, 14.3 mg (0.154 mmol) LiBF₄, 115 μL (0.624 mmol) *i*-Pr₂NEt, 3.1 mL acetonitrile, and an irradiation time of 24 h. Purified by chromatography (5:1 hexanes:acetone) to afford 59.0 mg (0.203 mmol, 66% yield, >10:1 d.r.) of the cycloadduct as a light yellow oil. Experiment 2: 84.9 mg (0.294 mmol) bisenone, 5.7 mg (0.008 mmol) Ru(bpy)₃Cl₂·6H₂O, 14.5 mg (0.156 mmol) LiBF₄, 115 μL (0.624 mmol) *i*-Pr₂NEt, and 3.1 mL acetonitrile. Isolated 56.7 mg (0.195 mmol, 66% yield, >10:1 d.r.). IR (thin film) 2956, 2254, 1719, 1669, 1410 cm⁻¹; ¹H NMR: (499.9 MHz, CDCl₃) δ 7.06 (s, 1H), 6.97 (s, 1H), 3.98 (s, 3H), 3.96 (m, 2H), 3.41 (m, 1H), 3.38 (m, 1H), 2.86 (dd, J = 7.7, 7.7 Hz, 1H), 1.89 (m,

2H), 1.79 (m, 1H), 1.64 (dd, $J = 13.4, 6.7$ Hz, 1H), 1.52 (m, 2H), 1.48 (s, 3H), 1.05 (t, $J = 7.2$ Hz, 3H); ^{13}C NMR: (125.7 MHz, CDCl_3) δ 191.8, 176.2, 143.4, 128.6, 126.1, 60.3, 54.2, 48.9, 42.2, 36.4, 35.7, 31.4, 27.0, 26.3, 18.7, 13.9; HRMS (EI) calc'd for $[\text{C}_{16}\text{H}_{22}\text{N}_2\text{O}_3+\text{Na}]^+$ requires m/z 313.1523, found m/z 313.1520.

2.5.4 Cleavage of the Auxiliary Group

2-(7-((Benzyloxy)carbonyl)bicyclo[3.2.0]heptane-6-carbonyl)-1,3-dimethyl-1H-imidazol-3-

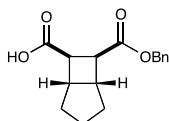


ium triflate (2-31): In an oven-dried round-bottomed flask was placed a

solution of cyclobutane **2-16** (405 mg, 1.20 mmol) in dry dichloromethane (12 mL, 0.1 M). Neat methyl trifluoromethanesulfonate (135 μL , 1.193 mmol) was

added dropwise, and the solution was stirred for 16 h. Upon completion, the reaction was quenched with acetone and the volatiles were removed *in vacuo*. The triflate salt was recrystallized from acetone/diethyl ether to afford 282.5 mg (0.800 mmol, 67%) of a colorless solid (m.p.: 135–140 $^\circ\text{C}$). IR (thin film) 3629, 3093, 2262, 1634 cm^{-1} ; ^1H NMR: (500.2 MHz, CD_3CN) δ 7.30 (m, 5H), 7.19 (m, 2H), 5.00, 4.92 (ABq, 2H, $J_{\text{AB}} = 12$ Hz), 3.87 (s, 6H), 3.54 (ddd, $J = 10.0, 4.4, 0.9$ Hz, 1H), 3.35 (ddd, $J = 10.0, 5.6, 1.0$ Hz, 1H), 3.13 (m, 1H), 3.05 (m, 1H), 1.88 (m, 2H), 1.71 (m, 2H), 1.59 (m, 2H); ^{13}C NMR: (125.7 MHz, CDCl_3) δ 191.4, 171.6, 143.2, 128.1, 126.0, 66.7, 66.3, 46.0, 45.8, 44.3, 41.9, 39.6, 37.1, 35.8, 32.3, 32.2, 25.2; HRMS (EI) calc'd for $[\text{C}_{21}\text{H}_{25}\text{N}_2\text{O}_6]^+$ requires m/z 353.1860, found m/z 353.1851.

7-((Benzyloxy)carbonyl)bicyclo[3.2.0]heptane-6-carboxylic acid (Table 2-4, entry 1, **2-32**):

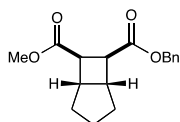


In an oven-dried 1.5 dram vial was placed 49.6 mg (0.099 mmol) of **2-31** in 1.5 mL dry diethyl ether. The vial was sealed with a septum and flushed with a nitrogen atmosphere. 50 μL (0.33 mmol, 3.5 equiv) of DBU was added, and the

reaction was stirred for several minutes before addition of 0.2 mL (11.1 mmol, 111 equiv) H_2O . After 2 h, the solution was acidified with 1 mL acetic acid, concentrated *in vacuo* and purified by

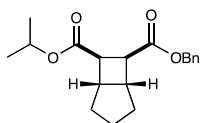
chromatography on a silica column (3:1 Hex:EtOAc + 1% AcOH) to afford 14 mg (0.051 mmol, 52% yield, >10:1 d.r.) of a clear oil. IR(thin film) 3629, 3093, 2262, 1634 cm^{-1} ; ^1H NMR: (499.9 MHz, CDCl_3) δ 7.33 (m, 5H), 5.08, 5.11 (ABq, 2H, $J_{\text{AB}} = 12.6$ Hz), 3.07 (m, 2H), 2.90 (m, 2H), 1.89 (m, 1H), 1.52-1.79 (m, 5H); ^{13}C NMR: (125.7 MHz, CDCl_3) δ 173.0, 135.8, 128.5, 128.3, 128.2, 66.6, 43.2, 39.5, 39.2, 32.1, 24.9; HRMS (EI) calc'd for $[\text{C}_{16}\text{H}_{18}\text{O}_4+\text{H}^+]$ requires m/z 273.1132, found m/z 273.1130.

6-Benzyl 7-methyl bicyclo[3.2.0]heptane-6,7-dicarboxylate (Table 2-4, entry 2, **2-33**): In an



oven-dried 1.5 dram vial was placed 51.4 mg (0.102 mmol) of **2-31** in 1.5 mL dry diethyl ether. The vial was sealed with a septum and flushed with a nitrogen atmosphere. 50 μL (0.33 mmol, 3.5 equiv) of DBU was added, and the reaction was stirred for several minutes before addition of 0.5 mL (12.3 mmol, 111 equiv) methanol. After 2 h, the solution was concentrated *in vacuo* and purified by chromatography on a silica column (10:1 Hex:EtOAc) to afford 25.4 mg (0.088 mmol, 86% yield, >10:1 d.r.) of a clear oil. IR (thin film) 2953, 1731, 1647, 1309 cm^{-1} ; ^1H NMR: (499.9 MHz, CDCl_3) δ 7.34 (m, 5H), 5.13 (s, 2H), 3.69 (s, 3H), 3.59 (dd, $J = 10.4, 8.6$ Hz, 1H), 3.09 (dd, $J = 6.5, 0.8$ Hz, 1H), 2.98 (m, 1H), 2.88 (m, 1H), 1.76 (m, 3H), 1.62-1.42 (m, 3H); ^{13}C NMR: (125.7 MHz, CDCl_3) δ 174.1, 172.4, 136.0, 128.5, 128.1, 128.0, 66.3, 51.5, 41.6, 40.8, 39.7, 38.2, 32.4, 28.5, 25.3; HRMS (EI) calc'd for $[\text{C}_{17}\text{H}_{20}\text{O}_4\text{Na}]^+$ requires m/z 311.1254, found m/z 311.1259.

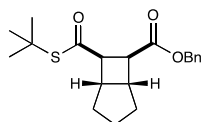
6-Benzyl 7-iso-propyl bicyclo[3.2.0]heptane-6,7-dicarboxylate (Table 2-4, entry 3, **2-34**): In



a 1.5 dram vial was placed 49.2 mg (0.098 mmol) of **2-31** in 1.5 mL dichloromethane. The vial was sealed with a septum and flushed with a nitrogen atmosphere. 50 μL (0.33 mmol, 3.5 equiv) of DBU were added, and the reaction was stirred for several minutes before addition of 0.2 mL (2.59 mmol, 26 equiv) isopropanol. After 2 h, the solution was concentrated *in vacuo* and purified by column

chromatography (9:1 Hex:EtOAc) to afford 27.6 mg (0.087 mmol, 88% yield) of a clear oil. IR (thin film) 2957, 1725, 1263, 1194 cm^{-1} ; ^1H NMR: (499.9 MHz, CDCl_3) δ 7.34 (m, 5H), 5.13 (s, 2H), 5.04 (sept, $J = 6.3$ Hz, 1H), 3.52 (dd, $J = 8.8, 10.1$ Hz, 1H), 3.09 (dd, $J = 6.5, 8.7$ Hz, 1H), 2.98 (m, 1H), 2.87 (m, 1H), 1.82-1.62 (m, 4H), 1.48 (m, 2H), 1.24 (t, $J = 5.5$ Hz, 6H); ^{13}C NMR: (125.7 MHz, CDCl_3) δ 174.2, 171.4, 136.1, 128.5, 128.1, 127.9, 77.3, 77.0, 76.7, 67.9, 66.2, 41.6, 40.7, 39.9, 38.3, 32.4, 28.2, 25.3, 22.0, 21.9; HRMS (EI) calc'd for $[\text{C}_{19}\text{H}_{24}\text{O}_4\text{Na}]^+$ requires m/z 339.1567, found m/z 339.1562.

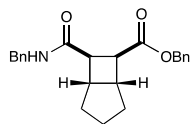
Benzyl 7-((tert-butylthio)carbonyl)bicyclo[3.2.0]heptane-6-carboxylate (Table 2-4, entry 5,



2-35): In a 1.5 dram vial was placed 51.2 mg (0.1023 mmol) of the **2-31** in 1.5 mL dichloromethane. The vial was sealed with a septum and flushed with a nitrogen atmosphere. 50 μL (0.33 mmol, 3.5 equiv) of DBU were added and

let stir for several minutes before addition of 0.150 mL (1.33 mmol, 13 equiv) *tert*-butylthiol. After 3.5 h, the reaction was concentrated *in vacuo* and purified by column chromatography (10:1 Hex:EtOAc) to afford 35.1 mg (0.101 mmol, 88% yield, >10:1 d.r.) of a clear oil. IR (thin film) 3629, 3093, 2262, 1634 cm^{-1} ; ^1H NMR: (500.2 MHz, CDCl_3) δ 7.33 (m, 5H), 5.12 (m, 2H), 3.66 (dd, $J = 10.1, 8.7$ Hz, 1H), 3.19 (dd, $J = 8.7, 6.3$ Hz, 1H), 2.99 (m, 1H), 2.86 (m, 1H), 1.78 (m, 4H), 1.47 (s, 9H), 1.44 (m, 2H); ^{13}C NMR: (125.7 MHz, CDCl_3) δ 198.1, 173.9, 136.1, 128.5, 128.1, 127.9, 66.2, 48.2, 47.6, 40.6, 40.6, 40.1, 32.2, 30.0, 27.3, 25.3; HRMS (EI) calc'd for $[\text{C}_{21}\text{H}_{24}\text{N}_2\text{O}_6+\text{H}]^+$ requires m/z 353.1860, found m/z 353.1851.

Benzyl 7-(benzylcarbamoyl)bicyclo[3.2.0]heptane-6-carboxylate (Table 2-4, entry 6, **2-36**):

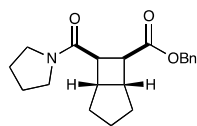


In a 1.5 dram vial was placed 47.0 mg (0.099 mmol) of **2-31** in 1.5 mL dichloromethane. The vial was sealed with a septum and flushed with a

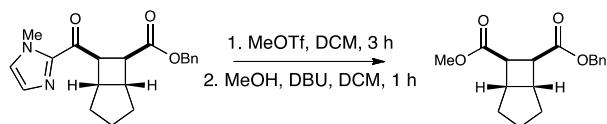
nitrogen atmosphere. 200 μL (1.83 mmol, 20 equiv) benzylamine were added. After 2 h, the solution was concentrated *in vacuo* and purified by chromatography on a silica column (5:1

Hex:EtOAc) to afford 33.3 mg of a colorless oil (0.916 mmol, >10:1 d.r.). IR (thin film) 3305, 2954, 1729, 1649 cm^{-1} ; ^1H NMR: (500.2 MHz, CDCl_3) δ 7.29 (m, 10H), 5.73 (t, $J = 5.6$ Hz, 1H), 5.11 (ABq, 2H), 4.43 (d, $J = 5.6$ Hz, 2H), 3.37 (t, $J = 9.8$ Hz, 1H), 3.17 (dd, $J = 8.4, 5.6$ Hz, 1H), 2.89 (m, 2H), 1.80 (m, 4H), 1.48 (m, 2H); ^{13}C NMR: (125.7 MHz, CDCl_3) δ 174.3, 170.7, 138.3, 135.9, 128.7, 128.5, 128.2, 128.0, 127.8, 127.5, 66.4, 43.5, 41.7, 41.0, 40.5, 38.1, 32.3, 27.9, 25.7; HRMS (EI) calc'd for $[\text{C}_{21}\text{H}_{24}\text{N}_2\text{O}_6+\text{H}]^+$ requires m/z 353.1860, found m/z 353.1851.

Benzyl 7-(pyrrolidine-1-carbonyl)bicyclo[3.2.0]heptane-6-carboxylate (Table 2-4, entry 7, **2-37**):



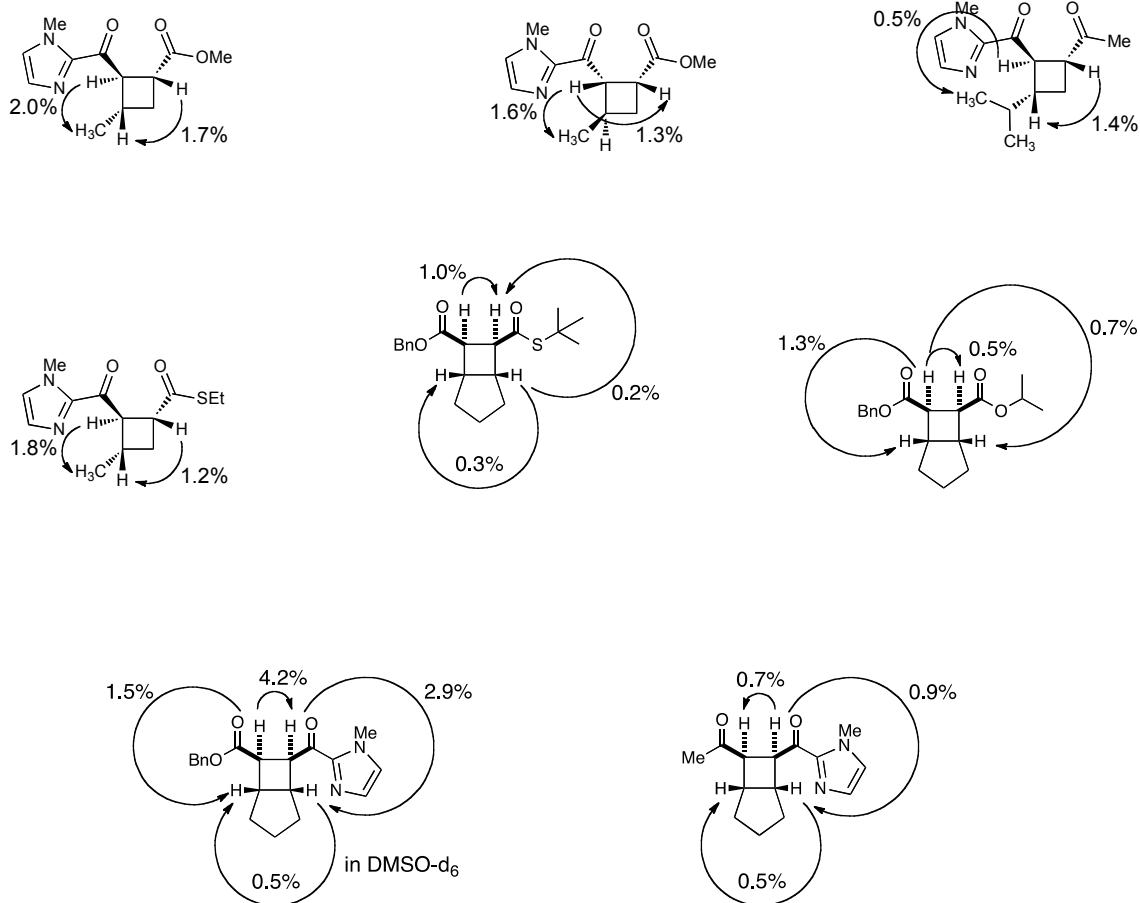
In an oven-dried 1.5 dram vial was placed 50.1 mg (0.099 mmol) of **2-31** in 1.5 mL dichloromethane. 100 μL (1.20 mmol, 12.0 equiv) distilled pyrrolidine were added. After 12 h, the solution was concentrated *in vacuo* and purified by column chromatography (1:1 Hex/EtOAc with 2% TEA) to afford 24 mg to afford (0.741 mmol, >10:1 d.r.) of a colorless oil. IR (thin film) 3629, 3093, 2262, 1634 cm^{-1} ; ^1H NMR: (500.2 MHz, CDCl_3) δ 7.35 (m, 5H), 5.12 (s, 2H), 3.56-3.42 (m, 3H), 3.38 (dd, $J = 6.8, 6.8$ Hz, 1H), 3.36 (dd, $J = 6.8, 6.8$ Hz, 1H), 3.22 (m, 1H), 2.94 (m, 1H), 2.86 (m, 1H), 1.97-1.73 (m, 7H), 1.45 (m, 3H); ^{13}C NMR: (125.7 MHz, CDCl_3) δ 175.0, 169.0, 136.2, 128.5, 128.4, 128.0, 128.0, 77.3, 77.0, 76.8, 66.2, 45.6, 45.5, 40.7, 40.5, 40.3, 37.4, 32.4, 28.2, 26.1, 25.4, 24.3; HRMS (EI) calc'd for $[\text{C}_{20}\text{H}_{24}\text{NO}_3+\text{H}]^+$ requires m/z 327.1829, found m/z 327.1833.



One-pot methylation-esterification procedure: An oven-dried Schlenk flask containing 99.8 mg (0.295 mmol) cyclobutane **2-16** and 1.5 mL dry dichloromethane (0.2 M) was stirred under N_2 before careful addition of freshly distilled MeOTf (40 μL , 0.341 mmol, 1.1 equiv). The flask was sealed, and the reaction was stirred at room temperature for 90 min. The volatiles were removed *in vacuo*, and the residue was dissolved in 1.5 mL dichloromethane. To this solution

were added 100 μL DBU (0.669 mmol, 2.3 equiv) and 500 μL (12.5 mmol, 44 equiv) freshly distilled methanol. The vessel was sealed and the reaction was stirred for 90 min under N_2 . The reaction was then concentrated and the crude residue loaded directly onto silica for purification by chromatography (4:1 Hex:EtOAc) to afford 49.5 mg of a colorless oil (0.1717 mmol, 58% yield).

2.5.5 Stereochemical Assignments by *nOe*



2.6 References

- ¹ Hansen, T. V.; Stenstrøm, Y. *Naturally Occurring Cyclobutanes*. In *Organic Synthesis: Theory and Applications*; Hudlicky, T., Ed.; Elsevier: Oxford, U.K., 2001; Vol. 5, pp 1–38. (b) Dembitsky, V. M. Bioactive cyclobutane-containing alkaloids. *J. Nat. Med.* **2008**, *62*, 1–33.
- ² Oppolzer, W. The intermolecular [2+2] photoaddition/cyclobutane-fragmentation sequence in organic synthesis. *Acc. Chem. Res.* **1982**, *15*, 135–141. (b) Winkler, J. D.; Bowen, C. M.; Liotta, F. [2+2] Photocycloaddition/fragmentation strategies for the synthesis of natural and unnatural products. *Chem. Rev.* **1995**, *95*, 2003–2020. (c) Lee-Ruff, E.; Mladenova, G. Enantiomerically pure cyclobutane derivatives and their use in organic synthesis. *Chem. Rev.* **2003**, *103*, 1449–1483. (d) Namyslo, J. C.; Kaufmann, D. E. The application of cyclobutane derivatives in organic synthesis. *Chem. Rev.* **2003**, *103*, 1485–1537.
- ³ For reviews of [2+2] enone photocycloadditions, see: (a) de Mayo, P. Photochemical syntheses. 37. Enone photoannulation. *Acc. Chem. Res.* **1971**, *4*, 41–47. (b) Baldwin, S. W. Synthetic aspects of 2+2 cycloadditions of α,β -unsaturated carbonyl compounds. *Org. Photochem.* **1981**, *5*, 123–225. (c) Crimmins, M. T. Synthetic applications of intramolecular enone-olefin photocycloadditions. *Chem. Rev.* **1988**, *88*, 1453–1473. (d) Demuth, M.; Mikhail, G. New developments in the field of photochemical syntheses. *Synthesis* **1989**, 145–162. (e) Schuster, D. I.; Lem, G.; Kaprinidis, N. A. New insights into an old mechanism: [2+2] photocycloaddition of enones to alkenes. *Chem. Rev.* **1993**, *93*, 3–22. (f) Iriondo-Alberdi, J.; Greaney, M. F. Bioactive cyclobutane-containing alkaloids *Eur. J. Org. Chem.* **2007**, 4801–4815. (g) Bach, T.; Hehn, J. P. Photochemical reactions as key steps in natural product syntheses. *Angew. Chem. Int. Ed.* **2011**, *50*, 1000–1045.
- ⁴ Smith, A. B., III; Sulikowski, G. A.; Sulikowski, M. M.; Fujimoto, K. Applications of an asymmetric [2+2]-photocycloaddition. Total synthesis of (–)-echinosporin. Construction of an advanced 11-deoxyprostaglandin intermediate. *J. Am. Chem. Soc.* **1992**, *114*, 2567–2576
- ⁵ (a) Dilling, W. L.; Tabor, T. E.; Boer, F. P.; North, P. P. Organic photochemistry. IX. The photocycloaddition of 2-cyclopentenone to *cis*- and *trans*-dichloroethylene. Evidence for initial attack at carbon-3 and rotational equilibration of the diradical intermediates. *J. Am. Chem. Soc.* **1970**, *92*(5), 1399–1400. (b) Morrison, H.; Rodriguez, O. Organic photochemistry. XXIX. Z/E photoisomerization of 3-methyl-3-penten-2-one. Evidence for nonradiative decay. *J. Photochem.* **1974**, *3*, 471–474.
- ⁶ Corey, E. J.; Bass, J. D.; LeMahieu, R.; Mitra, R. B. A study of the photochemical reactions of 2-cyclohexenones with substituted olefins. *J. Am. Chem. Soc.* **1964**, *86*, 5570–5583.
- ⁷ Roh, Y.; Jang, H.-Y.; Lynch, V.; Bauld, N. L.; Krische, M. J. Anion radical chain cycloaddition of tethered enones: Intramolecular cyclobutanation and Diels-Alder cycloaddition. *Org. Lett.* **2002**, *4*, 611–613.
- ⁸ For reviews on recent developments in transition metal photoredox catalysis in organic synthesis, see: (a) Zeitler, K. Photoredox catalysis with visible light. *Angew. Chem., Int. Ed.* **2009**, *48*, 9785–9789. (b) Yoon, T. P.; Ischay, M. A.; Du, J. Visible light photocatalysis as a greener approach to photochemical synthesis. *Nat. Chem.* **2010**, *2*, 527–532. (c) Narayanam, J. M. R.; Stephenson, C. R. J. Visible light photoredox catalysis: applications to organic synthesis.

Chem. Soc. Rev. **2011**, *40*, 102–113. (d) Teply, F. Photoredox catalysis by $[\text{Ru}(\text{bpy})_3]^{2+}$ to trigger transformations of organic molecules. Organic synthesis using visible-light photocatalysis and its 20th century roots. *Collect. Czech. Chem. Commun.* **2011**, *76*, 859–917.

⁹ Bard, A. J.; Faulkner, L. R. *Electrochemical Methods*, Wiley, New York, **1980**, pp. 500–511.

¹⁰ Ischay, M. A.; Anzovino, M. E.; Du, J.; Yoon, T. P. Efficient visible light photocatalysis of [2+2] enone cycloadditions. *J. Am. Chem. Soc.* **2008**, *130*, 12886–12887.

¹¹ Du, J.; Yoon, T. P. Crossed intermolecular [2+2] cycloadditions of acyclic enones via visible light photocatalysis. *J. Am. Chem. Soc.* **2009**, *131*, 14604–14605.

¹² Ischay, M. A.; Yoon, T. P. Accessing the synthetic chemistry of radical ions. *Eur. J. Org. Chem.* **2012**, 3359–3372.

¹³ House, H. O.; Huber, L. E.; Umen, M. J. Empirical rules for estimating the reduction potential of α,β -unsaturated carbonyl compounds. *J. Am. Chem. Soc.* **1972**, *94*, 8471–8475.

¹⁴ Facilitation of electrochemical reactions using a noncleavable redox-active group has been termed a “redox tag” strategy by Chiba. See: (a) Okada, Y.; Akaba, R.; Chiba, K. Electrocatalytic formal [2+2] cycloaddition reactions between anodically activated aliphatic enol ethers and unactivated olefins possessing an alkoxyphenyl group. *Org. Lett.* **2009**, *11*, 1033–1035. (b) Okada, Y.; Nishimoto, A.; Akaba, R.; Chiba, K. Electron-transfer-induced intermolecular [2+2] cycloaddition reactions based on the aromatic “redox tag” strategy. *J. Org. Chem.* **2011**, *76*, 3470–3476.

¹⁵ Similarly, facilitation of electrochemical reactions using a silyl or stannyl electrofugal group has been termed an “electroauxiliary” approach by Yoshida. See: (a) Yoshida, J.; Takada, K.; Ishichi, Y.; Isoe, S. Anodic cyclization of unsaturated α -stannyl ethers. Termination by bromide derived from dibromomethane. *J. Chem. Soc., Chem. Commun.* **1994**, 2361–2362. (b) Yoshida, J.; Nishiwaki, K. Redox selective reactions of organo-silicon and -tin compounds. *J. Chem. Soc., Dalton Trans.* **1998**, 2589–2596.

¹⁶ Evans, D. A.; Johnson, J. S. Catalytic enantioselective hetero Diels–Alder reactions of α,β -unsaturated acyl phosphonates with enol ethers. *J. Am. Chem. Soc.* **1998**, *120*, 4895–4896. (b) Evans, D. A.; Scheidt, K. A.; Fandrick, K. R.; Lam, H. W.; Wu., J. Enantioselective indole Friedel–Crafts alkylations catalyzed by bis(oxazoliny)pyridine-scandium(III) triflate complexes. *J. Am. Chem. Soc.* **2003**, *125*, 10780–10781. (c) Takenaka, N.; Abell, J. P.; Yamamoto, H. Asymmetric conjugate addition of silyl enol ethers catalyzed by tethered bis(8-quinolinato) aluminum complexes. *J. Am. Chem. Soc.* **2007**, *129*, 742–743. (d) Samanta, S.; Zhao, C.-G. Organocatalytic enantioselective synthesis of α -hydroxy phosphonates. *J. Am. Chem. Soc.* **2006**, *128*, 7442–7443. (e) Jiang, H.; Paixão, M. W.; Monge, D.; Jørgensen, K. A. Acyl phosphonates: good hydrogen bond acceptors and ester/amide equivalents in asymmetric organocatalysis. *J. Am. Chem. Soc.* **2010**, *132*, 2775–2783.

¹⁷ Lee, S. D.; Brook, M. A.; Chan, T. H. Conversion of primary amides into active acylating agents via acylpyrroles. *Tetrahedron Lett.* **1983**, *24*, 1569–1572. (b) Kinoshita, T.; Okada, S.; Park, S. R.; Matsunaga, S.; Shibasaki, M. Sequential Wittig olefination-catalytic asymmetric epoxidation with reuse of waste $\text{Ph}_3\text{P}(\text{O})$. *Angew. Chem., Int. Ed.* **2003**, *42*, 4680–4684. (c)

Shaghafi, M. B.; Kohn, B. L.; Jarvo, E. R. Palladium-catalyzed conjugate addition allylation reactions of α,β -unsaturated *N*-acylpyrroles. *Org. Lett.* **2008**, *10*, 4743–4746.

¹⁸ Sibi, M. P.; Shay, J. J.; Liu, M.; Jasperse, C. P. Organocatalysis in conjugate amine additions. Synthesis of β -amino acid derivatives. *J. Am. Chem. Soc.* **1998**, *120*, 6615–6616. (b) Itoh, K.; Kanemasa, S. Enantioselective Michael additions of nitromethane by a catalytic double activation method using chiral Lewis acid and achiral amine catalysis. *J. Am. Chem. Soc.* **2002**, *124*, 13394–13395. (c) Ishihara, K.; Fushimi, M. Design of a small-molecule catalyst using intramolecular cation- π interactions for enantioselective Diels–Alder and Mukaiyama–Michael reactions. *Org. Lett.* **2006**, *8*, 1921–1924. (d) Sibi, M. P.; Itoh, K. Organocatalysis in conjugate amine additions. Synthesis of β -amino acid derivatives. *J. Am. Chem. Soc.* **2007**, *129*, 8064–8065.

¹⁹ (a) Davies, D. H.; Haire, N. A.; Hall, J.; Smith, E. H. Synthesis of γ -lactones from intermediate 2-(γ -hydroxyacyl)imidazoles by *N*-methylation and base-catalyzed carbon-carbon bond cleavage. Application to the synthesis of (\pm)-cavernosine. *Tetrahedron* **1992**, *48*, 7839–7856. (b) Evans, D. A.; Song, H.-J.; Fandrick, K. R. Enantioselective nitrene cycloadditions of α,β -unsaturated 2-acyl imidazoles catalyzed by bis(oxazoliny)pyridine-cerium(IV) triflate complexes. *Org. Lett.* **2006**, *8*, 3351–3354. (c) Andrus, M. B.; Christiansen, M. A.; Hicken, E. J.; Gainer, M. J.; Bedke, D. K.; Harper, S. R.; Dodson, D. S.; Harris, D. T. Phase-transfer-catalyzed asymmetric acylimidazole alkylation. *Org. Lett.* **2007**, *9*, 4865–4868. (d) Evans, D. A.; Fandrick, K. R.; Song, H. J.; Scheidt, K. A.; Xu, R. Enantioselective Friedel–Crafts alkylations catalyzed by bis(oxazoliny)pyridine-scandium(III) triflate complexes. *J. Am. Chem. Soc.* **2007**, *129*, 10029–10041. (e) Trost, B. M.; Lehr, K.; Michaelis, D. J.; Xu, J.; Buckl, A. K. Palladium-catalyzed asymmetric allylic alkylation of 2-acylimidazoles as ester enolate equivalents. *J. Am. Chem. Soc.* **2010**, *132*, 8915–8917.

²⁰ Consistent with this observation, cyclic voltammetry revealed that the α,β -unsaturated 2-acylimidazole reduces at a significantly less negative peak potential than the other test substrates depicted in Table 2-1. See the Supporting Information for details of these electrochemical measurements.

²¹ The subsequent cleavage of the imidazolyl group could also be achieved without isolation of the acylimidazolium salt; however, we found that the yields of the cleavage products were somewhat lower when this one-pot protocol was utilized.

²² Evans, D. A.; Fandrick, K. R.; Song, H. J. Enantioselective Friedel–Crafts alkylations of α,β -unsaturated 2-acyl imidazoles catalyzed by bis(oxazoliny)pyridine-scandium(III) triflate complexes. *J. Am. Chem. Soc.* **2005**, *127*, 8942–8943.

²³ Chaumontet, M.; Retailleau, P.; Baudoin, O. Cycloadditions of 1,1-disubstituted benzocyclobutenes obtained by C(sp³)-H activation. *J. Org. Chem.* **2009**, *74*, 1774–1776.

²⁴ Giraud, F.; Guillon, R.; Loge, C.; Pagniez, F.; Picot, C.; Le Borgne, M.; Le Pape, P. Synthesis and structure-activity relationships of 2-phenyl-1-[(pyridinyl- and piperidinylmethyl)amino]-3-(1*H*-1,2,4-triazol-1-yl)propan-2-ols. *Bioorg. Med. Chem. Lett.* **2009**, *19*, 301–304.

-
- ²⁵ Tran, Y. S.; Kwon, O. An application of the phosphine-catalyzed [4+2] annulation in indole alkaloid synthesis: formal syntheses of (±)-alstonerine and (±)-macroline. *Org. Lett.* **2005**, *7*, 4289–4291.
- ²⁶ Xiao, Y.; Liu, P. IspH protein of the deoxyxylulose phosphate pathway: mechanistic studies with C1-deuterium-labeled substrate and fluorinated analogue. *Angew. Chem. Int. Ed.* **2004**, *47*, 9722–9725.
- ²⁷ Kuroda, H.; Hanaki, E.; Izawa, H.; Kano, M.; Itahashi, H. A convenient method for the preparation of α -vinylfurans by phosphine-initiated reactions of various substituted enynes bearing a carbonyl group with aldehydes. *Tetrahedron* **2004**, *60*, 1913–1920.
- ²⁸ Ando, K.; Tsuji, E.; Ando, Y.; Kunimoto, J.; Kobayashi, R.; Yokomizo, T.; Shimizu, T.; Yamashita, M.; Ohta, S.; Nabe, T.; Takeshi, K.; Kohno, S.; Ohisi, Y. Synthesis of 2-, 4- and 5-(2-alkylcarbamoyl-1-methylvinyl)-7-alkoxybenzo[b]furans and their leukotriene B4 receptor antagonistic activity. *Org. Biomol. Chem.* **2005**, *3*, 2129–2139.
- ²⁹ Blumberg, L. C.; Costa, B.; Goldstein, R. Chemoselective 1,3-dipolar cycloadditions of azomethine ylide with conjugated dienes. *Tetrahedron Lett.* **2011**, *52*, 872–874.

Chapter 3. Photogenerated Nitrenes for Intermolecular Olefin Aziridination

3.1 Introduction

Oxidative olefin functionalization provides a powerful means to construct carbon-carbon and carbon-heteroatom bonds in a wide variety of skeletal frameworks.¹ Within the context of carbon-nitrogen bond formation,² olefin aziridination installs a well-behaved carbon electrophile that serves as a versatile platform for the regio- and stereoselective synthesis of myriad architectures, including diamines,^{3a} amino alcohols,^{3b} β -amino acids,^{3c} aminosulfides,^{3d} and a plethora of nitrogenous heterocycles.^{3e-g} Such diverse reactivity primarily results from the significant ring strain (~27 kcal/mol) inherent to aziridines.⁴

Despite the vast utility of this strained heterocycle, efficient single-step olefin aziridination methods remain scarce, particularly in comparison to analogous methods for epoxidation. Deriving inspiration from oxo-group transfer chemistry to effect catalytic epoxidation, hypervalent iodonium ylides such as *N*-tosyliminoaryliodinane (PhI=NTs) were introduced as nitrene sources for imido group transfer reactions to carbon-hydrogen bonds and alkenes via catalysis by heme enzymes and biomimetic metalloporphyrins.⁵ These seminal publications began an entire field of study devoted to transition metal-catalyzed nitrene transfer via the putative intermediacy of metallonitrenes. The archetypal PhI=NTs ylide has been widely used in this field as an imido group transfer reagent and has typically proven uniquely competent as a nitrene source. Thus, the variety of aziridines accessible in a single synthetic step has long proven to be quite limited.

On a more practical level, many aziridination methods require a large excess of olefin relative to nitrene precursor, limiting the utility of aziridination reactions upon complex alkene substrates. For example, Fe(III) and Fe(IV) porphyrin complexes catalyze styrene aziridination with catalyst:ylide:styrene = 1:100:10000.⁶ Even the widely-utilized Cu-catalyzed aziridination developed by Evans requires a 5-fold excess of olefin relative to nitrene precursor.⁷ While select aziridination protocols reported by Du Bois,⁸ Lebel,⁹ and Zhang¹⁰ are able to achieve aziridination using the olefin as the limiting reagent, intermolecular aziridinations capable of this

at low catalyst loadings across both internal and terminal styrenyl and aliphatic olefins with no byproduct separation remain elusive. Indeed, most of the aforementioned methodologies employ $\text{PhI}=\text{NTs}$ and therefore necessarily generate stoichiometric iodobenzene as a byproduct, often complicating purification efforts. Finally, functional group compatibility was not thoroughly explored in many of these reports, and expanding the repertoire of substrates amenable to aziridination is highly desirable.

As discussed in Chapter 1, transition metal identity has profound implications on the relative stereochemistry of the product aziridine.¹¹ While all metallonitrenes are thought to have triplet ground states, the transition metal determines the rate at which ring-closure to aziridine occurs after the first C-N bond-forming event. If ring closure is fast relative to C-C bond rotation, the aziridination is stereospecific, even though the mechanism proceeds via a diradical intermediate. While this is the case for Rh and Ag, other transition metals including Cu, Fe, Mn, and Co give non-stereospecific addition. Thus, the complex nature of metal nitrene chemistry constitutes a drawback of this methodology.

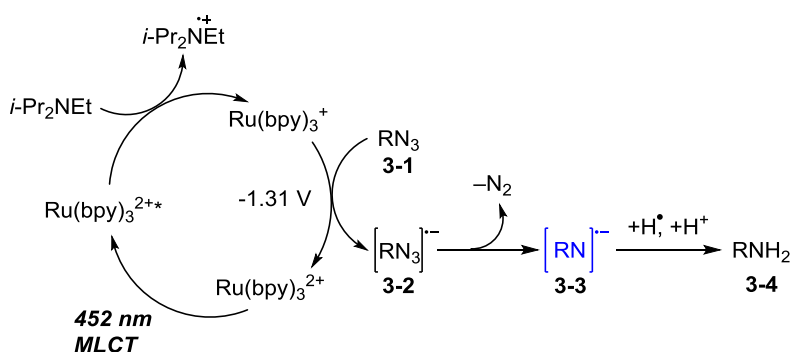
Arguably the most straightforward method for olefin aziridination involves the addition of a free nitrene. However, most methods for free nitrene formation and subsequent aziridination suffer from low yields of the desired aziridine and poor chemoselectivity due to competing hydrogen atom abstraction and C-H insertion pathways arising from multiple electronic states of the nitrene (Chapter 1). Being able to selectively generate a single nitrene species would alleviate complications arising from thermolysis, α -elimination, or direct photolysis of nitrene precursors.

3.2 System Design

Considering the significant limitations and mechanistic nuances of metal-catalyzed and photochemical methodologies for efficient, intermolecular olefin aziridination, we sought a fundamentally different approach. At the outset, we surmised that one electron reduction of

readily available organic azides would directly generate a nitrene radical anion. While never previously implicated as an intermediate in olefin aziridination, nitrene radical anions have been generated in the gas phase by dissociative electron attachment and are known to exhibit a reactivity profile similar to that of a free triplet nitrene, despite the extra electron occupancy.¹² Based on the work discussed in Chapter 2, it was hypothesized that room temperature, visible-light PET from a polypyridyl transition metal photosensitizer to an organic azide followed by extrusion of N₂ would be the ideal methodology by which to generate a nitrene radical anion. Subsequent trapping of the nitrene radical anion by an olefin would afford either the respective aziridine or the product of olefin hydroamination. Without multiple spin states available, the intrinsic reactivity of this relatively unexplored species could be studied within the context of oxidative olefin functionalization. We also considered that the breadth of nitrene precursors could be expanded significantly, as the additional electron present in nitrene radical anions is known to shut down the deleterious rearrangement pathways that plague aryl nitrenes, for example.

Scheme 3-1. Photochemical reduction of aryl azides by Ru(bpy)₃²⁺

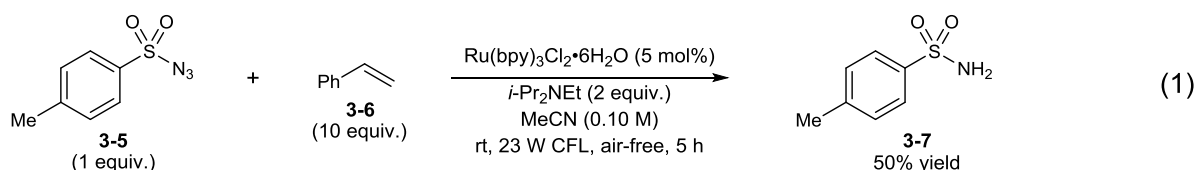


Lending credence to our proposal for nitrene radical anion generation was recent work by Liu and coworkers on the photochemical reduction of aryl azides by Ru(bpy)₃²⁺ (Scheme 3-1).¹³ In the presence of an electron donor, Ru(bpy)₃^{2+*} is reduced to Ru(bpy)₃⁺; one-electron reduction of an aryl azide (**3-1**) by Ru(bpy)₃⁺ gives an azido radical anion (**3-2**). Subsequent extrusion of molecular nitrogen affords a putative nitrene radical anion (**3-3**) that undergoes

reduction to the corresponding aniline (**3-4**) via protonation and hydrogen atom abstraction. While this report strengthened the validity of our experimental design and hypothesis, the nature of the reactive intermediate was never studied, and it was unclear if this proposed nitrene radical anion would undergo productive aziridination with styrenyl and aliphatic olefins.

3.3 Initial Results

To test the feasibility of atom transfer from a reduced organic azide to an olefin, reaction conditions similar to those developed for cyclobutanation of aryl enones (Chapter 2) were applied to a system containing tosyl azide (**3-5**) and styrene (**3-6**) (eq. 1). The major product of the reaction was reduction of tosyl azide to *p*-toluenesulfonamide (**3-7**) with the non-characterizable minor products (34%) presumably arising from reaction between the radical cation of diisopropylethylamine with the reduced azide intermediate. Since nitrene radical anions have both free radical and anionic character, formation of *p*-toluenesulfonamide was expected, especially when the precedent of Liu is considered. Additionally, it is well-established that reductive quenching of $\text{Ru}(\text{bpy})_3^{2+}$ by *N,N*-diisopropylethylamine affords an amine radical cation, the α -protons of which are approximately 20 $\text{p}K_a$ units more acidic than the parent tertiary amine.¹⁴ Facile deprotonation by tosyl nitrene radical anion affords an ethylimine that is speculated to undergo rapid decomposition.

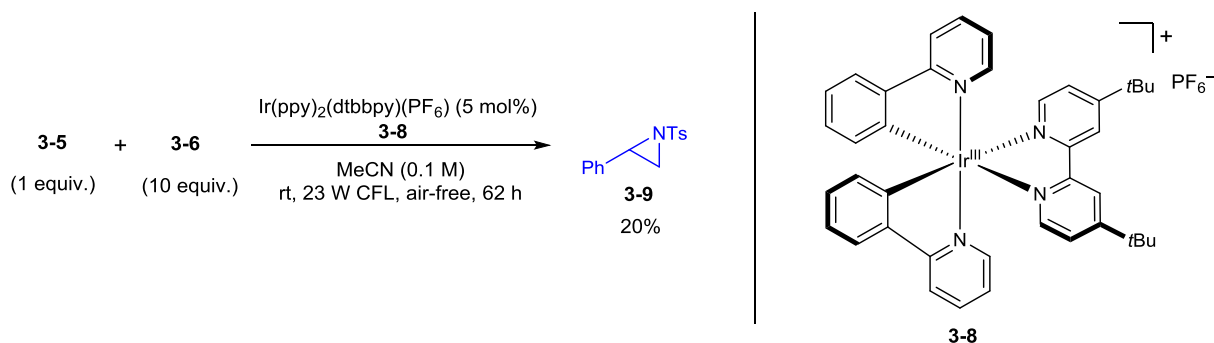


Control experiments revealed that both $\text{Ru}(\text{bpy})_3^{2+}$ and *i*-Pr₂NEt were required for the reduction of TsN_3 to TsNH_2 . Indeed, while electron transfer from $\text{Ru}(\text{bpy})_3^+$ ($E^\circ(\text{Ru}^{2+/+}) = -1.28 \text{ V vs. SCE}$)¹⁵ to **3-5** ($E^\circ(\text{TsN}_3/\text{TsN}^-) = -1.29 \text{ V}$)¹⁶ is isoergic, electron transfer from $\text{Ru}(\text{bpy})_3^{2+}$ ($E^\circ(\text{Ru}^{3+/2+}) = -0.81 \text{ V}$) to **3-5** is highly endergonic ($E^\circ_{\text{rxn}} = -0.48 \text{ V}$). In the

absence of styrene the same products in the same distribution were observed, indicating that styrene was not participating. A wide range of other acceptors, including 1-hexene, cyclohexene, methyl vinyl ketone, and methyl acrylate failed to undergo reaction, and the same products as above were obtained in all cases. Reductive quenchers lacking α -amino protons diminished sulfonamide formation, but no additional identifiable products were recovered from the crude reactions.

These data suggested that *i*-Pr₂NEt was directly responsible for undesired sulfonamide formation. Accordingly, when *i*-Pr₂NEt was omitted, very little (<5%) of **3-7** was formed. The lack of styrene aziridination was not surprising given that reduction of **3-5** by Ru(bpy)₃^{2+*} is endergonic. Therefore, a screen was initiated to identify a photocatalyst complex that could carry out reduction of **3-5** directly from the excited state. Gratifyingly, heteroleptic iridium complex **3-8** (ppy = 2-phenylpyridine, dtbbpy = 4,4'-di-*tert*-butyl-2,2'-dipyridyl)¹⁷ afforded aziridine **3-9** in 20% yield after 62 h (Scheme 3-2).

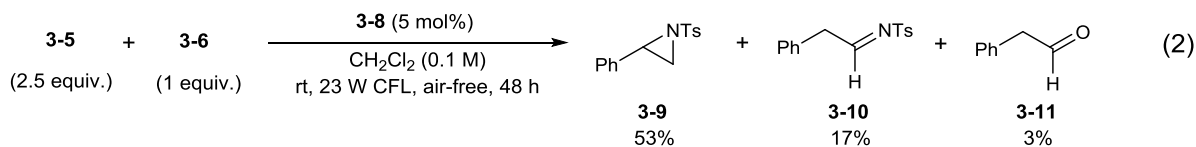
Scheme 3-2. Azide reduction with iridium complex **3-8** in the absence of reductive quencher



3.4 Optimization Studies

A brief solvent optimization found that replacement of MeCN with CH₂Cl₂ gave **3-9** in slightly higher yield (28%) after 62 h. It was postulated that the reaction could be accelerated by having a substantially higher concentration of putative nitrene radical anion relative to olefin. Indeed, using styrene (**3-6**) as the limiting reagent and employing 2.5 equiv of TsN₃ (**3-5**) relative to **3-6** afforded complete conversion of **3-6** in 48 h. Aziridine **3-9** was obtained in

modest yield (53%) along with remaining **3-6** (19%), aldimine **3-10**, and a very small amount of phenylacetaldehyde **3-11** (eq. 2).



Control experiments demonstrated that both light and photocatalyst were required to achieve azide consumption and, consequently, aziridination. This suggests that the transition metal catalyst is not simply acting as a Lewis acid to facilitate azide decomposition to the putative nitrene radical anion.¹⁸ A solvent screen showed that relatively nonpolar, chlorinated solvents were optimal, as CDCl₃, CH₂Cl₂ and 1,2-dichloroethane all afforded **3-9** in modest yields after 48 h. Catalyst loading was found to have a substantial effect on the rate of consumption of **3-6**. While 10 mol% of **3-8** gave the overall fastest consumption of **3-6** (9% remaining after 48 h) and highest yield of **3-9** (57%), it was decided that 2.5 mol% of **3-8** would be used due to the impracticability of employing such high loadings of the iridium catalyst.

Table 3-1. Concentration and scale-up studies

$$\begin{array}{c}
 \text{3-5} \quad + \quad \text{3-6} \\
 (2.5 \text{ equiv.}) \quad (1 \text{ equiv.})
 \end{array}
 \xrightarrow[\text{rt, 23 W CFL, air-free}]{\begin{array}{c} \text{3-8 (2.5 mol\%)} \\ \text{CH}_2\text{Cl}_2 \end{array}}
 \begin{array}{c}
 \text{Ph} \begin{array}{c} \diagup \text{NTs} \\ \diagdown \end{array} \\
 \text{3-9}
 \end{array}
 +
 \begin{array}{c}
 \text{Ph} \text{---} \text{CH} \text{---} \text{CH} \text{---} \text{NTs} \\
 \quad \quad \quad | \\
 \quad \quad \quad \text{H} \\
 \text{3-10}
 \end{array}$$

| entry | [3-6] (M) | 3-6 (mmol) | time (h) | conversion (3-6) | consumption (3-5) ^a | yield ^b 3-9 | yield 3-10 | mass balance |
|-------|-----------------------|----------------------|-------------|------------------------------|--|----------------------------------|----------------------|-----------------|
| 1 | 0.05 | 0.08 | 48 | 78% | 0.82 equiv. | 38% | 14% | 74% |
| 2 | 0.2 | 0.08 | 48 | 100% | 1.00 equiv. | 58% | 18% | 76% |
| 3 | 0.4 | 0.08 | 24 | 100% | 1.02 equiv. | 63% | 14% | 77% |
| 4 | 0.4 | 0.50 | 86 | 86% | 0.98 equiv. | 46% | 16% | 76% |

^aBased on 2.5 equiv. azide. ^bAll yields are ¹H NMR yields vs. 1,4-bis(trimethylsilyl)benzene as an internal standard

As expected for an intermolecular process, increasing the concentration of **3-6** from 0.1 M to 0.4 M led to a substantial decrease in the time required to reach complete conversion

of styrene (Table 3-1). Performing the reaction under aerobic conditions led to a substantially lower rate of azide consumption, poor yield of **3-9**, and low mass balance. This is likely due to competitive quenching of the catalyst excited state by O₂.

Attempts to scale the reaction to synthetically useful quantities were met with considerable difficulty. A reaction using 0.5 mmol of **3-6** required 86 h to achieve 86% conversion of **3-6**. Additionally, we observed significant erosion in mass balance if the latter reaction was allowed to proceed to full conversion of **3-6**. ¹H NMR analysis revealed that **3-10** was decomposing over the course of the reaction, thus identifying the confounding variable accounting for both yield of aziridination and modest mass balances.

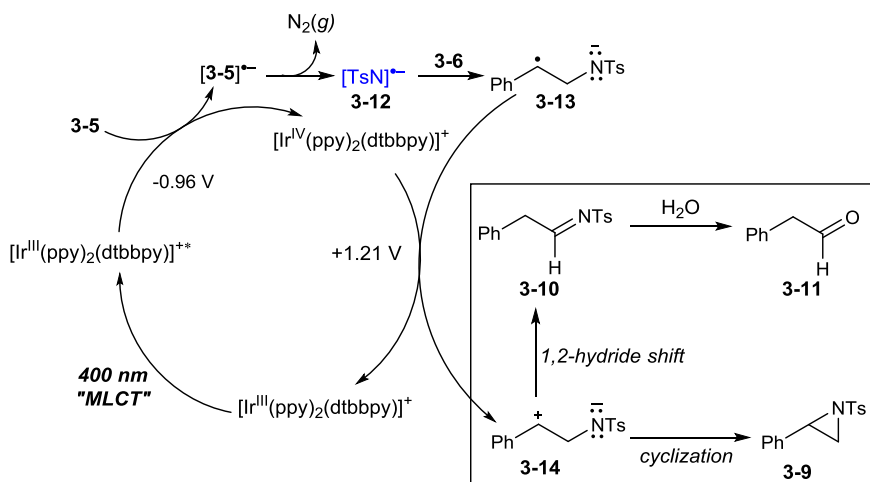
In an effort to ameliorate the sluggish reactivity, we hypothesized that addition of either Lewis or Brønsted acids would activate the parent azide toward photochemical degradation. This, in turn, should facilitate generation of the supposed nitrene radical anion intermediate. Screening a wide range of transition metal, lanthanide, and lanthanoid Lewis acids as well as an assortment of Brønsted acids with pK_a values ranging from -6 to 9 (DMSO) gave no improvement in the yield of aziridination. Addition of water (up to 10 equiv.) had no deleterious effect on the reaction. Given that the photocatalytic reactions studied here are proposed electron transfer processes in non-aqueous solutions, an electrolyte should have profound consequences on ion pairing, solution conductivity, reversibility of electron transfer, and thermodynamics of multielectron processes.¹⁹ Strongly- and weakly-coordinating tetrabutylammonium salts were investigated, but even at concentrations as high as 400 mM in electrolyte, no significant effects were observed.

3.5 Mechanistic Studies

3.5.1. Proposal for the Intermediacy of a Nitrene Radical Anion

A mechanism consistent with these preliminary results is shown in Scheme 3-3. Single electron reduction of **3-5** by $[\text{Ir}(\text{III})]^{+\bullet}$ forms an azide radical anion $[\mathbf{3-5}]^{\bullet-}$; these species are known to be highly unstable and undergo extrusion of molecular nitrogen to form nitrene radical anion **3-12**. Radical addition to **3-6** gives distonic radical anion **3-13** that undergoes facile oxidation by Ir(IV) to benzylic cation **3-14**, thus returning the photosensitizer to ground state Ir(III). At this point, ring closure furnishes aziridine **3-9**. However, a 1,2-hydride shift is postulated to give aldimine **3-10**, and hydrolysis of **3-10** by adventitious water leads to phenylacetaldehyde **3-11**.

Scheme 3-3. Proposed mechanism for photocatalyzed aziridination via a nitrene radical anion



A variety of experiments were designed to probe this mechanistic proposal. To begin, *para*-substituted arylsulfonyl azides were synthesized and submitted to the reaction conditions (Table 3-2). Surprisingly, the yield of aziridine was found to be lowest for the most electron deficient (**3-15** and **3-16**) and most electron rich (**3-19**) azides; decomposition of **3-15** was expected to lead to the most electrophilic, and thus the most reactive nitrene radical anion in the series with respect to olefin aziridination. Unexpectedly, the initial rates of formation of aziridine, aldimine, and aldehyde were found to be identical for **3-16** and **3-5**. However, as discussed in

Section 3.4, both the aldimine and aldehyde decompose over the course of the reaction. Additionally, we found the rate of aldimine decomposition to be fastest for aldimines synthesized from electron-deficient nitrene radical anion precursors (**3-15** and **3-16**). Indeed, when the reaction is allowed to proceed for an additional 24 h, complete disappearance of both aldimine and aldehyde is observed in all cases, while the yield of aziridine remains unchanged. We were very surprised to observe that octanesulfonyl azide **3-20** gave successful aziridination, as one electron reduction of **3-20** by the excited state of **3-8** $[\text{Ir}(\text{ppy})_2(\text{dtbbpy})]^{+*}$ ($E^\circ(\text{Ir}^{4+/3+*}) = -0.96 \text{ V}$) was determined to be highly endergonic ($E^\circ_{\text{rxn}} = -0.63 \text{ V}$).

Table 3-2. Survey of sulfonyl azides

Reaction scheme: $\text{R-SO}_2\text{N}_3 + \text{3-6} \xrightarrow[\text{rt, 23 W CFL, air-free, 48 h}]{\text{3-8 (2.5 mol \%), CH}_2\text{Cl}_2 (0.4 \text{ M})} \text{Ph-aziridine} + \text{Ph-aldimine} + \text{Ph-aldehyde}$

| entry | R | conversion (3-6) | conversion (azide) ^a | yield ^b aziridine | yield aldimine | yield aldehyde |
|-------|--|------------------------------|------------------------------------|---------------------------------|-------------------|-------------------|
| 1 | 3,5-(CF ₃) ₂ Ph (3-15) | 28% | 12% | 7% | — | — |
| 2 | 4-CF ₃ Ph (3-16) | 33% | 21% | 17% | — | — |
| 3 | 4-CIPh (3-17) | 71% | 29% | 31% | 7% | — |
| 4 | Ph (3-18) | 79% | 29% | 43% | 11% | — |
| 5 | 4-CH ₃ Ph (3-5) | 85% | 32% | 42% | 17% | — |
| 6 | 4-OMePh (3-19) | 83% | 14% | 20% | 8% | 8% |
| 7 | C ₈ H ₁₇ (3-20) | 35% | 28% | 20% | 8% | — |

^aBased on 2.5 equiv. azide; ^bAll yields are ¹H NMR yields vs. 1,4-bis(trimethylsilyl)benzene as a calibrated internal standard

To determine if the initial rate of azide decomposition varies among azides, time course studies were carried out for **3-16** and **3-5**. These data collected within the first 2 h of reaction showed a 3.6-fold higher rate of consumption of **3-16** ($8.38 \times 10^{-4} \text{ M}^{-1}\text{s}^{-1}$) relative to **3-6** ($2.30 \times 10^{-4} \text{ M}^{-1}\text{s}^{-1}$). Since the free energy change for electron transfer should be greater as inductive removal of electron density from the azido moiety increases, these data support a

more kinetically facile reduction of electron-deficient azides versus electron-rich azides. While the initial rate of consumption of **3-16** was higher than **3-5**, this rate dramatically decreased after 2 h, whereas the rate of consumption of **3-8** followed a much shallower trajectory. This suggested a mechanism involving catalyst decomposition. Indeed, monitoring the reaction by ^1H NMR spectroscopy revealed decomposition of $\text{Ir}(\text{ppy})_2(\text{dtbbpy})^+$ to multiple products that could not be isolated. Heteroleptic iridium complexes are known to be susceptible to radical addition on the ligand framework, affording photochemically inert complexes.²⁰

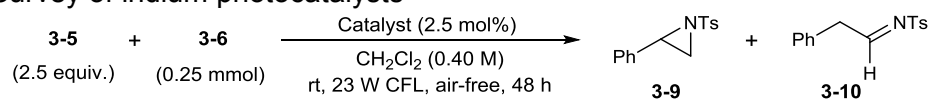
Table 3-3. Survey of olefins in photosensitized aziridination

| entry | R | conversion (olefin) | conversion (3-5) | yield aziridine | yield aldimine | yield aldehyde |
|-------|--|---------------------|---------------------------|-----------------|----------------|----------------|
| 1 | 4-CF ₃ Ph (3-21) | 76% | 0.73 equiv. | 41% | 3% | 7% |
| 2 | 4-ClPh (3-22) | 88% | 0.88 equiv. | 43% | 12% | 5% |
| 3 | Ph (3-6) | 85% | 0.79 equiv. | 42% | 17% | 0% |
| 4 | 4-CH ₃ Ph (3-23) | 77% | 0.77 equiv. | 34% | 19% | 0% |
| 5 | 4-OAcPh (3-24) | 58% | 0.70 equiv. | 34% | 12% | 0% |
| 6 | C ₆ H ₁₃ (3-25) | 85% | 0.79 equiv. | 42% | 8% | 11% |

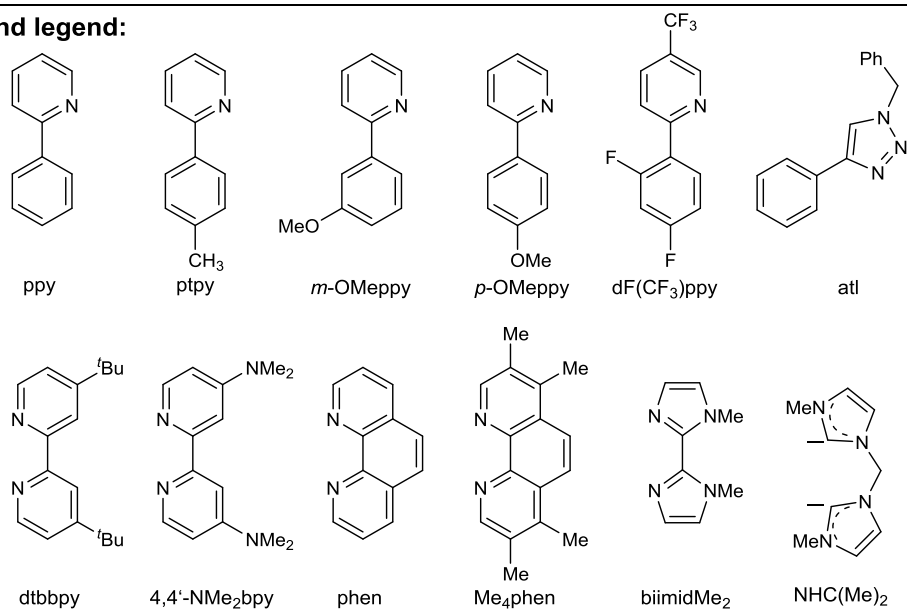
We also conducted a survey of alkenes (Table 3-3). It is evident from these data that the aziridination is essentially insensitive to the electronic nature of the styrene or aliphatic olefin. Given that the mechanistic proposal in Scheme 3-3 invokes the intermediacy of a benzylic radical and a benzylic cation, rate-determining nitrene radical anion addition would manifest in greater rates of aziridination for more electron-rich olefins. Indeed, increasing electron density at the benzylic position should stabilize an incipient cation or radical and thus lead to higher rates of reaction. However, this is not observed, as styrenyl olefin **3-21** and aliphatic olefin **3-25** give comparable reactivity. Therefore, radical addition to the olefin is likely not rate-determining.

One of the most intriguing aspects of the system is that aziridination proceeds despite a highly endergonic electron transfer from $[\text{Ir}(\text{ppy})_2(\text{dtbbpy})]^{+*}$ ($E^\circ(\text{Ir}^{4+/3+*}) = -0.96 \text{ V}$) to sulfonyl azides. For example, the Gibbs free energy of electron transfer to **3-5** ($E^\circ(\text{TsN}_3/\text{TsN}^-) = -1.29 \text{ V}$) is endergonic ($E^\circ_{\text{rxn}} = -0.33 \text{ V}$). This prompted an investigation into the electronic properties of the photocatalyst (Table 3-4). Specifically, we hypothesized that a more strongly-donating ligand set around Ir would lead to a more electron rich complex and thus faster azide reduction and more rapid aziridination. In accordance with crystal-field theory, the ligand-field splitting energy of $[\text{Ir}(\text{CAN})_2(\text{NAN})]^+$ catalysts (where CAN = cyclometalating ligand and NAN = neutral ligand), and consequently the reduction potentials of all the species in the catalytic cycle, can be tuned by varying substituents on the CAN ligands; the identity of the NAN ligand is critical to ensure redox reversibility, prevent self-quenching, and modulate both the excited state lifetime of the complex and quantum yield of phosphorescence.¹⁷

Thus, a variety of complexes were synthesized and submitted to the reaction conditions (Table 3-4). These data showed that the CAN and NAN ligands could not be tuned strictly independently. That is, the π -donor/acceptor and σ -donor/acceptor properties of the NAN ligand would have direct effects on the redox properties of the overall complex. For example, $[\text{Ir}(\text{ppy})_2(\text{Me}_4\text{phen})]^+$ exhibited nearly equivalent reactivity to the original $[\text{Ir}(\text{ppy})_2(\text{dtbbpy})]^+$ complex. This was surprising because Me_4phen is reported to increase the quantum yield of phosphorescence of the parent complex by a factor of two and increase the excited state lifetime by a factor of four. It is clear from these data that the most competent iridium complexes for this aziridination contain an electron neutral cyclometalating ligand (ppy or ptpy) and 4,4'-di-*tert*-butyl-2,2'-dipyridyl as the electron rich neutral ligand.

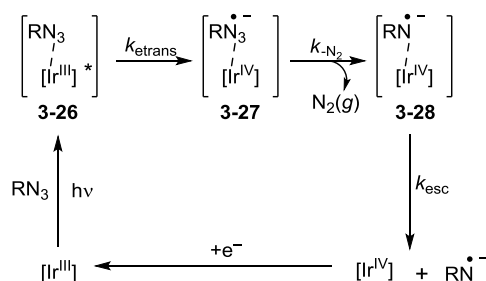
Table 3-4. Survey of iridium photocatalysts

| entry | catalyst complex | conversion (3-6) | conversion (3-5) ^a | yield ^b 3-9 | yield 3-10 |
|-------|---|------------------|-------------------------------|------------------------|------------|
| 1 | Ir(ppy) ₂ (dtbbpy)(PF ₆) | 85% | 0.79 equiv. | 42% | 17% |
| 2 | Ir(ppy) ₂ (phen)(PF ₆) | 72% | 0.62 equiv. | 33% | 7% |
| 3 | Ir(ppy) ₂ (Me ₄ phen)(PF ₆) | 86% | 0.86 equiv. | 40% | 10% |
| 4 | Ir(ppy) ₂ (biimidMe ₂)(PF ₆) | 17% | 0.10 equiv. | 0% | 0% |
| 5 | Ir(ppy) ₂ (NHCMe ₂)(PF ₆) | 12% | 0.09 equiv. | 3% | 0% |
| 6 | Ir(ppy) ₂ (4,4'-NMe ₂ bpy)(PF ₆) | 76% | 0.80 equiv. | 45% | 5% |
| 7 | Ir(ppy) ₃ | 26% | 0.13 equiv. | 4% | 0% |
| 8 | Ir(pty) ₂ (dtbbpy)(PF ₆) | 72% | 0.70 equiv. | 30% | 4% |
| 9 | Ir(pty) ₂ (phen)(PF ₆) | 63% | 0.61 equiv. | 30% | 9% |
| 10 | Ir(<i>p</i> -OMeppy) ₂ (dtbbpy)(PF ₆) | 59% | 0.40 equiv. | 24% | 7% |
| 11 | Ir(<i>m</i> -OMeppy) ₂ (dtbbpy)(PF ₆) | 14% | 0.20 equiv. | 6% | 0% |
| 12 | Ir(dF(CF ₃)ppy) ₂ (dtbbpy)(PF ₆) | 36% | 0.10 equiv. | 0% | 0% |
| 13 | Ir(atl) ₂ (dtbbpy)(PF ₆) | 74% | 0.77 equiv. | 45% | 11% |

Ligand legend:

This catalyst survey prompted an evaluation of the proposed mechanism. In particular, we considered a more detailed analysis of the sensitization events and electron transfer steps leading to formation of the putative nitrene radical anion. As shown in Scheme 3-4, photoexcitation of [Ir(III)] to give [Ir(III)]* results in the formation of encounter complex **3-26** between [Ir(III)]* and the azide. At this point, electron transfer (k_{etrans}) from [Ir(III)]* to the azide affords encounter complex **3-27** between [Ir(IV)] and an azide radical anion that rapidly decomposes to the nitrene radical anion ($k_{-\text{N}_2}$). The radical anion in encounter complex **3-28** can either donate an electron to [Ir(IV)] to regenerate the [Ir(III)] ground state or escape (k_{esc}) from the ion pair and become solvated.

Scheme 3-4. Sensitization and electron transfer steps in nitrene radical anion formation



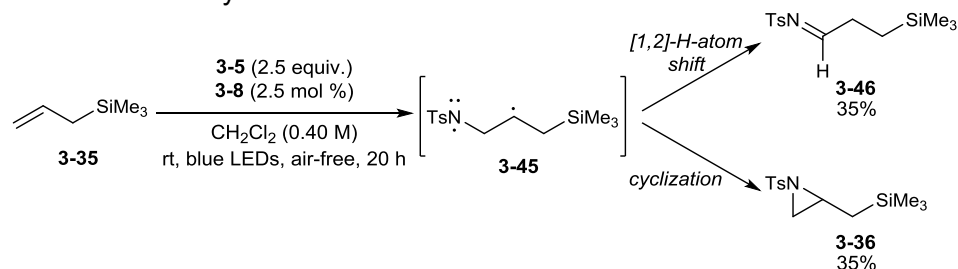
Given this analysis, we sought to determine if electron transfer or cage escape was rate determining. We predicted that if cage escape was rate-determining, increased solvent polarity should decrease ion pairing between the oxidized photocatalyst and the nitrene radical anion intermediate thus increasing the rate of cage escape and, in turn, increasing the rate of aziridination. In order to evaluate the widest scope of solvents, an iridium complex having the highly lipophilic, very weakly-coordinating tetrakis[(3,5-trifluoromethyl)phenyl]borate ($\text{BAr}_4^{\text{F}-}$) counteranion was synthesized. Unlike $\text{Ir}(\text{ppy})_2(\text{dtbbpy})(\text{PF}_6)$, $\text{Ir}(\text{ppy})_2(\text{dtbbpy})(\text{BAr}_4^{\text{F}-})$ was soluble in all organic solvents tested. This comprehensive solvent screen revealed no correlation between solvent dielectric and rate of aziridination. In fact, highly polar solvents, such as acetonitrile and DMF gave somewhat poorer reactivity. According to the argument presented above, this result is incongruent with rate-determining cage escape. Furthermore, the

mechanistic proposal in Scheme 3-3 invokes charged intermediates that should be stabilized in polar solvents; such a proposal is at odds with a near complete lack of dependence on solvent dielectric. These data, along with those presented in Tables 3-1 and 3-2 suggest that electron transfer from the photocatalyst to the azide may be rate determining.

3.5.2 Preliminary Exploration of Substrate Scope

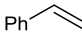
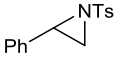
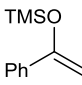
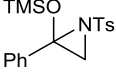
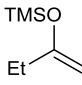
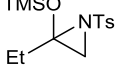
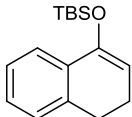
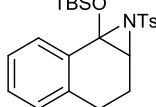
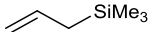
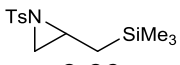
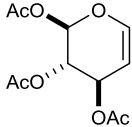
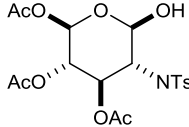
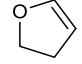
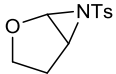
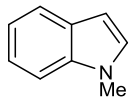
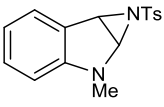
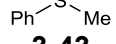
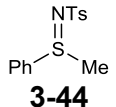
We hypothesized that a substrate scope study might allow us to gain further insight to the nature of the intermediate involved in aziridination. However, before exploring substrate scope, light source optimization studies were undertaken to ameliorate the sluggish reactivity observed. Gratifyingly, using monochromatic ($\lambda = 452$ nm) blue light-emitting diodes (LEDs)²¹ led to a nearly twofold increase in reactivity for aziridination of **3-6** (Table 3-5, entry 1).

Scheme 3-5. Aziridination of allylsilane **3-35**



Silyl ethers **3-29**, **3-31**, and **3-33** were tolerated, though the poor mass balance is due to decomposition of products **3-30**, **3-32**, and **3-34** to the corresponding α -amino acetophenones. Aziridination of allyltrimethylsilane **3-35** was successful, though a 1:1 mixture of **3-36** (35% yield) and aldimine **3-46** (35% yield) was obtained (Scheme 3-5). This is in contrast to the aziridination of 1-octene **3-25** (Table 3-4, entry 6), in which the ratio between aziridine and aldimine remained constant at 5:1 throughout the course of the reaction. This dramatic contrast can be understood by considering biradical intermediate **3-45**. Stabilization of the alkyl radical by the β -silyl group leads to long-lived intermediate **3-45** in which a 1,2-hydrogen atom shift is competitive with aziridination. Indeed, stabilization of alkyl radicals by the β -silicon effect is well-documented.²²

Table 3-5. Preliminary exploration of substrate scope^a

| entry ^a | substrate | product | time | yield ^b |
|--------------------|--|--|------|--------------------|
| 1 |  3-6 |  3-9 | 24 h | 61% ^c |
| 2 |  3-29 |  3-30 | 20 h | 51% ^c |
| 3 |  3-31 |  3-32 | 20 h | 22% |
| 4 |  3-33 |  3-34 | 20 h | 42% |
| 5 |  3-35 |  3-36 | 20 h | 35% |
| 6 |  3-37 |  3-38 | 45 h | 40% ^c |
| 7 ^d |  3-39 |  3-40 | 20 h | — |
| 8 ^d |  3-41 |  3-42 | 20 h | — |
| 9 |  3-43 |  3-44 | 20 h | 99% |

^aAll reactions were conducted using 0.25 mmol of substrate, 2.5 equiv. of **3-5**, and 2.5 mol% **3-8** in 0.63 mL of CH₂Cl₂ under air-free conditions ^bYields were obtained by ¹H NMR using trimethyl(phenyl)silane as an internal standard, unless otherwise specified. ^cIsolated yield, purification conditions not optimized. ^dNo aziridine was obtained in these experiments.

Tri-O-acetyl-D-glucal **3-37** underwent aziridination. However, the corresponding aziridine was readily hydrolysed on silica and resulted in formation of the corresponding amino alcohol (**3-38**) in moderate yield. Unfortunately, other electron-rich heterocycles such as **3-39** and **3-41** decomposed under the reaction conditions. Interestingly, thioanisole (**3-43**) afforded

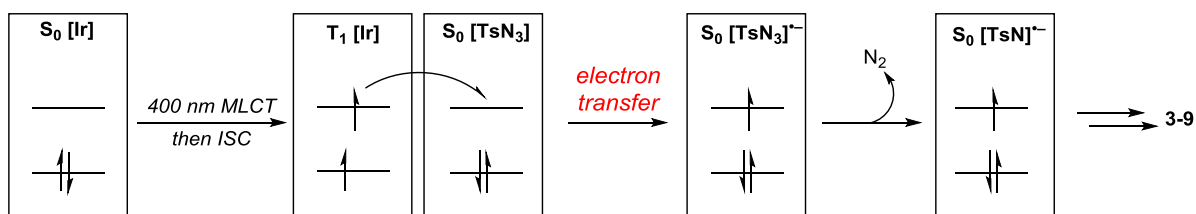
iminosulfide **3-44** instead of radical addition to the aromatic nucleus. This behavior is most consistent with the behavior of a nitrene.¹²

3.5.3 Proposal for the Intermediacy of a Free Nitrene via Energy Transfer

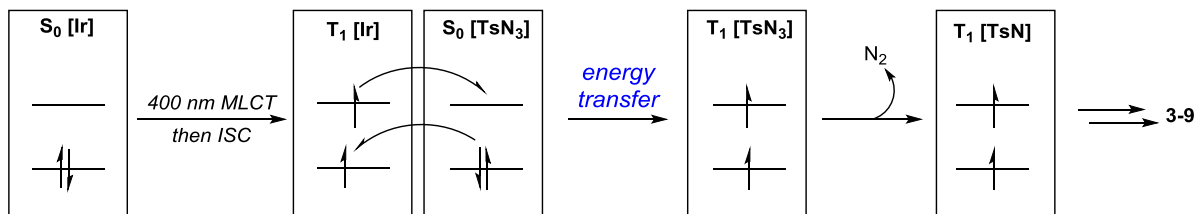
Multiple pieces of evidence shed doubt on our initial mechanistic proposal for electron transfer outlined in Scheme 3-3. As discussed above, the reaction is insensitive to solvent dielectric, an unexpected result for a reaction proceeding via a proposed series of charged intermediates. Further, the computed endothermicity of electron transfer between $[\text{Ir}(\text{III})]^{+*}$ and TsN_3 is sufficiently high to argue against the thermodynamic plausibility of this step. Even octanesulfonyl azide served as a competent nitrene precursor despite an electron transfer event computed to be endergonic by 630 mV. Finally, the interesting observation of iminosulfide formation instead of radical addition to the aromatic nucleus of thioanisole appears consistent with a nitrene intermediate.

Scheme 3-6. Electron transfer versus concerted electron exchange

Electron transfer mechanism:

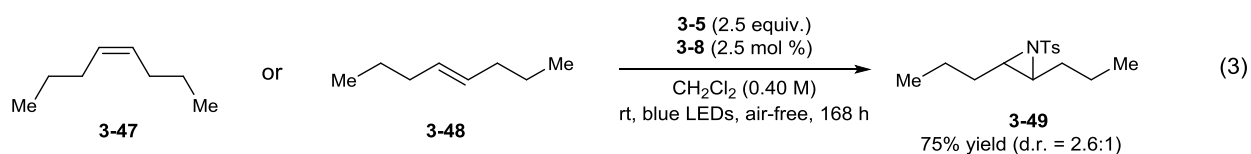


Energy transfer mechanism:

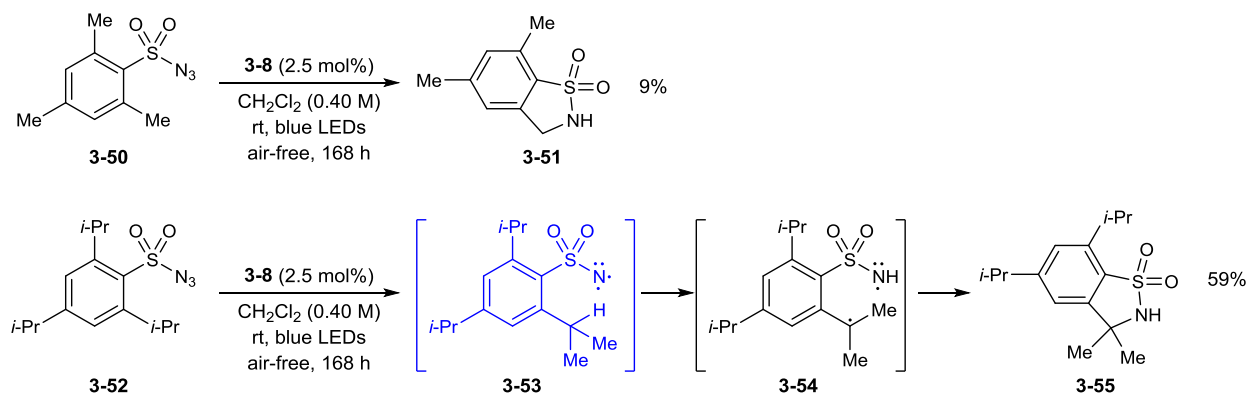


The requirement for both photocatalyst and light in order to affect aziridination (Section 3.4) necessitates a molecular orbital interaction between photocatalyst and azide. This frontier

orbital interaction can either lead to (a) full electron transfer (charge transfer) from photocatalyst to azide or (b) electron exchange (electronic energy transfer) between photocatalyst and azide (Scheme 3-6). Indeed, there is strong precedent for energy transfer from octahedrally saturated ruthenium complexes to organic substrates,²³ and heteroleptic iridium complexes are known to undergo energy transfer in bimetallic arrays with ruthenium polypyridyl complexes.²⁴ These studies led us to posit that iridium photocatalyst **3-8** could be acting as a triplet sensitizer of azide decomposition.^{25,26} That is, instead of electron *transfer* from the excited state of **3-8** (Scheme 3-6, top), a concerted electron *exchange* could occur between the excited state and azide (Scheme 3-6, bottom). This presumably would afford access to free triplet sulfonylnitrenes in a selective manner, thereby avoiding formation of the highly reactive singlet sulfonylnitrene state typically formed by classical photochemical methods.²⁷



To ascertain whether the putative nitrene intermediate was of singlet or triplet spin multiplicity, experiments probing the stereospecificity of aziridination were executed. Specifically, olefin aziridination proceeding via a singlet nitrene should afford stereospecific aziridination, whereas a triplet nitrene should undergo non-stereospecific aziridination.²⁸ In the event, *cis*-oct-4-ene (**3-47**) and *trans*-oct-4-ene (**3-48**) were independently subjected to photocatalyzed aziridination in the presence of azide **3-5** (eq. 3). After 7 days, both reactions afforded a 75% yield of aziridine **3-49** (d.r. = 2.6:1 *trans:cis*). Additionally, both olefins underwent gradual equilibration to a 4:1 mixture of *trans:cis*-oct-4-ene. This equilibration did not occur in the absence of TsN₃. While the involvement of a nitrene radical anion cannot be conclusively excluded by these data, the lack of stereospecificity provides evidence against formation of a singlet nitrene and appears to be most consistent with reaction of a triplet nitrene.

Scheme 3-7. Probing reactivity of the photogenerated intermediate


We surmised that corroborating evidence for the intermediacy of a sulfonyl nitrene could be obtained by investigating the decomposition of mesitylsulfonyl azide **3-50** and isopropylphenylsulfonyl azide **3-52** (Scheme 3-6). For instance, free triplet sulfonylnitrene intermediate **3-53** should afford benzosultam product **3-55** via hydrogen atom abstraction from the proximal isopropyl groups followed by radical rebound in species **3-54**. Indeed, exposure of **3-50** and **3-52** to the optimized reaction conditions for 7 days afforded benzosultams **3-51** and **3-55** in moderate yields. As discussed in Chapter 1, benzosultam product **3-55** is observed when the corresponding hypervalent iodonium ylide of **3-52** is reacted in the presence of either $\text{Rh}_2(\text{OAc})_4$ or porphyrin complexes of Fe or Mn; the resulting metallonitrenes are thought to exist as ground state triplets.²⁹ Thus, formation of benzosultam products in our chemistry appears consistent with a triplet nitrene. A singlet nitrene is unlikely because the photosensitizer is incapable of sensitization from the singlet excited state (S_1) due to very rapid (~ 100 fs) ISC to the first triplet excited state (T_1).³⁰ Furthermore, even the energy contained within the incident electromagnetic field (450 nm, 64 kcal/mol) is insufficient to access S_1 of a sulfonyl azide. However, it is important to note that these experiments do not rigorously exclude a nitrene radical anion intermediate.^{31,32}

3.6 Conclusions

We have successfully demonstrated photocatalytic aziridination of both aliphatic and styrenyl olefins in the presence of aromatic sulfonyl azides. Significantly, we discovered that the olefin could be used as the limiting reagent, an advantage over many metallonitrene-mediated aziridination protocols requiring vast excesses of olefin relative to nitrene precursor.

The data obtained in these studies demonstrate that a nitrogen-centered intermediate is generated under mild conditions from a precursor amenable to facile synthetic modification, thus allowing for a broad scope of aziridine products. This intermediate is generated in a selective manner, thus avoiding complexities arising from singlet and triplet manifolds typically observed in direct photolysis of organic azides. Decomposition of the sulfonyl azide precursor to the intermediate only affords dinitrogen as a byproduct, thereby avoiding formation of stoichiometric organic byproduct. Mechanistic analyses provided strong evidence that this intermediate is a free triplet nitrene, though a nitrene radical anion cannot explicitly be excluded. This discussion continues in Chapter 4, where further evidence is provided for a triplet sensitization mechanism.

3.7 References

¹ (a) Müller, P.; Fruit, C. Enantioselective catalytic aziridinations and asymmetric nitrene insertions into CH bonds. *Chem. Rev.* **2003**, *103*, 2905–2919. (b) Jacobsen, E. N. In *Comprehensive Asymmetric Catalysis*; Jacobsen, E. N., Pfaltz, A., Yamamoto, H., Eds.; Springer: Berlin, 1999; Vol. 2, p 607. (c) Pearson, W. H.; Lian, B. W.; Bergmeier, S. C. *Comprehensive Heterocyclic Chemistry, II*; Katritzky, A. R., Rens, C. W., Scriven, E. F. V., Eds.; Pergamon: New York, NY, 1996; Vol. 1A, pp 1–60.

² Padwa, A. In *Comprehensive Heterocyclic Chemistry III*, Vol. 1, Katritzky, A.R.; Ramsden, C.A.; Scriven, E. F. V.; Taylor, R. J. K., Eds.; Elsevier Academic Press: California, 2008; pp 1–105.

³ For selected examples, see: (a) Fukuta, V.; Mita, T.; Fukuda, N.; Kanai, M.; Shibasaki, M. De Novo synthesis of Tamiflu via a catalytic asymmetric ring-opening of *meso*-aziridines with TMSN₃. *J. Am. Chem. Soc.* **2006**, *128*, 6312–6313. (b) Xiong, C.; Wang, W.; Cai, C.; Hruby, V., J. Regioselective and stereoselective nucleophilic ring opening reactions of a phenyl-substituted aziridine: Enantioselective synthesis of β -substituted tryptophan, cysteine, and serine derivatives. *J. Org. Chem.* **2002**, *67*, 1399–1402. (c) Mita, T.; Fukimori, I.; Wada, R.; Wen, J.; Kanai, M.; Shibasaki, M. Catalytic enantioselective desymmetrization of *meso*-*N*-acylaziridines

with TMSCN. *J. Am. Chem. Soc.* **2005**, *127*, 11252–11253. (d) Li, B.-F.; Zhang, M.-J.; Hou, X.-L.; Dai, L.-X. A facile synthesis of enantiopure 2-aziridinesulfinimines and their highly diastereoselective reactions with phosphite anions. *J. Org. Chem.* **2002**, *67*, 2902–2906. (e) Pohlhaus, P. D.; Bowman, R. K.; Johnson, J. S. Lewis acid-promoted carbon-carbon bond cleavage of aziridines: divergent cycloaddition pathways of derived ylides. *J. Am. Chem. Soc.* **2004**, *126*, 2294–2295. (f) Baeg, J.-O.; Bensimon, C.; Alper, H. The first enantiospecific palladium-catalyzed cycloaddition of aziridines and heterocumulenes. Novel synthesis of chiral five-membered ring heterocycles. *J. Am. Chem. Soc.* **1995**, *117*, 4700–4701. (g) Trost, B. M.; Osipov, M.; Dong, G. Palladium-catalyzed dynamic kinetic transformations of vinyl aziridines with nitrogen heterocycles: rapid access to biologically active pyrroles and indoles. *J. Am. Chem. Soc.* **2010**, *132*, 15800–15807.

⁴ Bach, R. D.; Dmitrenko, O. Effect of geminal substitution on the strain energy of dioxiranes. Origin of the low ring strain of dimethyldioxirane. *J. Org. Chem.* **2002**, *67*, 3884–3896.

⁵ See Chapter 1 for a complete discussion. For seminal publications, see (a) Yamada, Y.; Yamamoto, T.; Okawara, M. Synthesis and reaction of new I–N ylide, N-tosyliminoiodinane. *Chem. Lett.* **1975**, 361–362. (b) Groves, J. T.; Nemo, T. E.; Myers, R. S. Hydroxylation and epoxidation catalyzed by iron-porphine complexes. Oxygen transfer from iodosylbenzene. *J. Am. Chem. Soc.* **1979**, *101*, 1032–1033. (c) Breslow, R.; Gellman, S. H. Tosylamidation of cyclohexane by a cytochrome P-450 model. *J. Chem. Soc., Chem. Commun.* **1982**, 1400–1401.

⁶ Simkhovich, L.; Gross, Z. Iron(IV) corroles are potent catalysts for aziridination of olefins by Chloramine-T. *Tetrahedron Lett.* **2001**, *42*, 8089–8092.

⁷ Evans, D. A.; Faul, M. M.; Bilodeau, M. T. Development of the copper-catalyzed olefin aziridination reaction. *J. Am. Chem. Soc.* **1994**, *116*, 2742–2753.

⁸ Guthikonda, K.; Du Bois, J. A unique and highly efficient method for catalytic olefin aziridination. *J. Am. Chem. Soc.* **2002**, *124*, 13672–13673.

⁹ Lebel, H.; Huard, K.; Lectard, S. N-tosyloxycarbamates as a source of metal nitrenes: rhodium-catalyzed C–H insertion and aziridination reactions. *J. Am. Chem. Soc.* **2005**, *127*, 14198–14199.

¹⁰ Gao, G.-Y.; Harden, J. D.; Zhang, X. P. Cobalt-catalyzed efficient aziridination of alkenes. *Org. Lett.* **2005**, *7*, 3191–3193.

¹¹ Maestre, L.; Sameera, W. M. C.; Mar Díaz-Requejo, M.; Maseras, F.; Pérez, P. J. A general mechanism for the copper- and silver-catalyzed olefin aziridination reactions: concomitant involvement of the singlet and triplet pathways. *J. Am. Chem. Soc.* **2013**, *135*, 1338–1348.

¹² (a) McDonald, R. N.; Chowdhury, A. K. Hypovalent radicals. 7. Gas-phase generation of phenylnitrene anion radical and its reaction with phenyl azide. *J. Am. Chem. Soc.* **1980**, *102*, 5118–5119. (b) Pellerite, M. J.; Brauman, J. I. Gas-phase ion-molecule reactions of phenylnitrene radical anion. *J. Am. Chem. Soc.* **1981**, *103*, 676–677.

¹³ Chen, Y.; Kamlet, A. S.; Steinman, J. B.; Liu, D. R. A biomolecule-compatible visible-light-induced azide reduction from a DNA-encoded reaction-discovery system. *Nat. Chem.* **2011**, *3*, 146–153.

¹⁴ Lewis, F. D.; Ho, T. I.; Simpson, J. T. Photochemical addition of tertiary amines to stilbene. Free-radical and electron-transfer mechanisms for amine oxidation. *J. Am. Chem. Soc.* **1982**, *104*, 1924–1929.

¹⁵ All reduction potentials reported in the text are versus saturated calomel electrode (SCE) in MeCN.

¹⁶ TsN₃ exhibits an irreversible cathodic wave at –1.29 V vs. SCE, and the true half-wave reduction potential is slightly more anodic than this value. Therefore, though this cannot be used to compute the thermodynamics of one electron transfer in the most rigorous sense, it is instructional for ascertaining the approximate magnitude of the change in free energy in this electron transfer.

¹⁷ (a) Lowry, M. S.; Hudson, W. R.; Pascal, R. A.; Bernhard, S. Accelerated luminophore discovery through combinatorial synthesis. *J. Am. Chem. Soc.* **2004**, *126*, 14129–14135. (b) Lowry, M. S.; Goldsmith, J. I.; Slinker, J. D.; Rohl, R.; Pascal, R. A.; Malliaras, G. G.; Bernhard, S. Single-layer electroluminescent devices and photoinduced hydrogen production from an ionic iridium(III) complex. *Chem. Mater.* **2005**, *17*, 5712–5719.

¹⁸ (a) Kwart, H.; Kahn, A. A. Copper-catalyzed decomposition of benzenesulfonyl azide in hydroxylic media. *J. Am. Chem. Soc.* **1967**, *89*, 1950–1951. (b) Kwart, H.; Kahn, A. A. Copper-catalyzed decomposition of benzenesulfonyl azide in cyclohexane solution. *J. Am. Chem. Soc.* **1967**, *89*, 1951–1953.

¹⁹ LeSuer, R. J.; Geiger, W. E. Improved electrochemistry in low-polarity media using tetrakis(pentafluorophenyl)-borate salts as supporting electrolytes. *Angew. Chem. Int. Ed.* **2000**, *39*, 248–250.

²⁰ (a) Flamigni, L.; Barbieri, A.; Sabatini, C.; Ventura, B.; Barigelletti, F. Photochemistry and photophysics of coordination compounds: iridium. *Top. Curr. Chem.* **2007**, *281*, 143–203. (b) Prier, C.K.; Rankic, D. A.; MacMillan, D. W. C. Visible light photoredox catalysis with transition metal complexes: applications in organic synthesis. *Chem. Rev.* **2013**, *113*, 5322–5363.

²¹ In contrast to a broadband light source, such as a 23 W CFL bulb, irradiation turned to the photocatalyst λ_{max} should result in higher quantum yields of phosphorescence.

²² Ibrahim, M. R.; Jorgensen, W. L. Ab initio investigations of the β -silicon effect on alkyl and cyclopropyl carbenium ions and radicals. *J. Am. Chem. Soc.* **1989**, *111*, 819–824.

²³ (a) Ikezawa, H.; Kutal, C.; Yasufuku, K.; Yamazaki, H. Direct and sensitized valence photoisomerization of a substituted norbornadiene. examination of the disparity between singlet- and triplet-state reactivities. *J. Am. Chem. Soc.* **1986**, *108*, 1589–1594. (b) Islangulov, R. R.; Castellano, F. N. Photochemical upconversion: anthracene dimerization sensitized to visible light by a Ru^{II} chromophore. *Angew. Chem. Int. Ed.* **2006**, *45*, 5957–5959.

²⁴ Ortmans, I.; Didier, P.; Kirsh-De Mesmaeker, A. New charge transfer luminescent polymetallic complexes of rhodium(III), iridium(III), and ruthenium(II) with the bridging ligand 1,4,5,8,9,12-hexatriphenylene. *Inorg. Chem.* **1995**, *34*, 3695–3704.

²⁵ In accord with this hypothesis, we recently reported that the same class of transition metal photocatalysts can also promote [2+2] cycloaddition reactions of styrenes (ref. a) and dienes (ref. b) via a complementary energy transfer process. See (a) Lu, Z.; Yoon, T. P. Visible light photocatalysis of [2+2] styrene cycloadditions by energy transfer. *Angew. Chem. Int. Ed.* **2012**, *51*, 10329–10332. (b) Hurlley, A. E.; Yoon, T. P. [2+2] cycloaddition of 1,3-dienes by visible light photocatalysis. *Angew. Chem. Int. Ed.* **2014**, *53*, 8991–8994.

²⁶ Xiao has also reported a photocatalytic [2+2] oxindole dimerization that they have suggested to occur via energy transfer: Zou, Y.-Q.; Duan, S.-W.; Meng, X.-G.; Hu, H.-Q.; Gao, S.; Chen, J. R.; Xiao, W. J. Visible light induced intermolecular [2+2]-cycloaddition reactions of 3-ylideneoxindoles through energy transfer pathway. *Tetrahedron* **2012**, *68*, 6914–6918.

²⁷ See Chapter 1, Section 1.2.5 for a complete discussion on the photochemistry of sulfonylnitrenes.

²⁸ (a) McConaghy, J. S., Jr.; Lwowski, W. Singlet and triplet nitrenes. I. Carboethoxynitrene generated by α -elimination. *J. Am. Chem. Soc.* **1967**, *89*, 2537–2364. (b) McConaghy, J. S., Jr.; Lwowski, W. Singlet and triplet nitrenes. II. Carboethoxynitrene generated from ethyl azidoformate. *J. Am. Chem. Soc.* **1967**, *89*, 4450–4456.

²⁹ (a) Breslow, R.; Gellman, S. H. Intramolecular nitrene C-H insertions mediated by transition-metal complexes as nitrogen analogues of cytochrome P-450 reactions. *J. Am. Chem. Soc.* **1983**, *105*, 6728–6729. (b) Svastits, E. W.; Dawson, J. H.; Breslow, R.; Gellman, S. H. Functionalized nitrogen atom transfer catalyzed by cytochrome P-450. *J. Am. Chem. Soc.* **1985**, *107*, 6427–6428.

³⁰ Kubicki, J.; Luk, H. L.; Zhang, Y.; Vyas, S.; Peng, H.-L.; Hadad, C. M.; Platz, M. S. Direct observation of a sulfonyl azide excited state and its decay processes by ultrafast time-resolved IR spectroscopy. *J. Am. Chem. Soc.* **2012**, *134*, 7036–7044.

³¹ Herbranson, D. E.; Hawley, M. D. Electrochemical reduction of *p*-nitrophenyl azide. Evidence consistent with the formation of *p*-nitrophenylnitrene anion radical as a short-lived intermediate. *J. Org. Chem.* **1990**, *55*, 4297–4303.

³² Murata, S.; Nakatsuji, R.; Tomioka, H. Mechanistic studies of pyrene-sensitized decomposition of *p*-butylphenyl azide: generation of nitrene radical anion through a sensitizer-mediated electron transfer from amines to the azide. *J. Chem. Soc. Perkin Trans. 2.* **1995**, 793–799.

Chapter 4. Visible-Light Sensitization of Vinyl Azides by Transition-Metal Photocatalysis

Portions of this work have previously been published:

Farney, E. P.; Yoon, T. P. Visible-light sensitization of vinyl azides by transition-metal photocatalysis. *Angew. Chem. Int. Ed.* **2014**, *53*, 793–797.

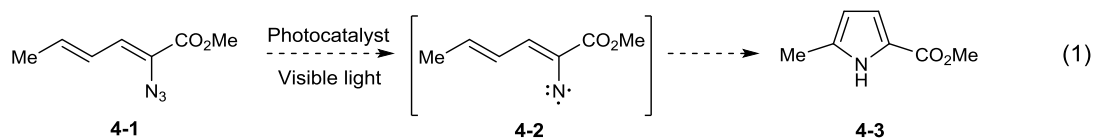
4.1 Introduction

The use of visible light activated transition metal complexes to catalyze synthetically useful reactions has received increasing attention over the past few years.¹ These new methods are attractive both because of the greater operational facility of photoreactions that can use visible light instead of high-energy UV light and because of the lower propensity of complex organic molecules to undergo photodecomposition under lower-energy visible light irradiation. Almost all of these powerful new reactions, both those developed in our laboratory and in others', have involved substrate activation steps that proceed by photoinduced electron transfer (PET) from polypyridyl ruthenium or iridium sensitizers.

The previous chapter described our discovery that visible-light induced photosensitization of aromatic sulfonyl azides in the presence of heteroleptic iridium complexes afforded efficient aziridination of styrenyl and aliphatic olefins. As discussed in Section 3.5, we obtained substantial evidence supporting the intermediacy of a free nitrene.^{2,3} We were particularly drawn to nitrenes due to their importance in a wide range of carbon–nitrogen bond-forming reactions, including several that produce synthetically useful heterocycles such as aziridines,⁴ indoles,⁵ and pyrroles.⁶ Traditional methods for accessing nitrenes rely on their photochemical generation from azides. This attractive strategy liberates only dinitrogen as a stoichiometric byproduct.⁷ However, the photolysis of azides with short-wavelength, high-energy UV light generally results in poor functional group tolerance and competitive photodecomposition processes that often diminish the overall yield of these reactions.⁸ Therefore, we were interested in further exploring visible light PET as a potentially generalizable method for selectively generating nitrenes and harnessing their reactivity under mild conditions.

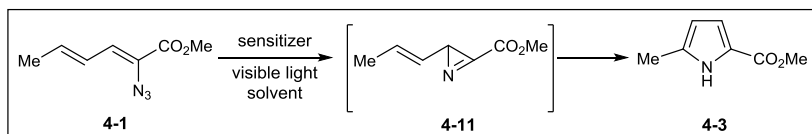
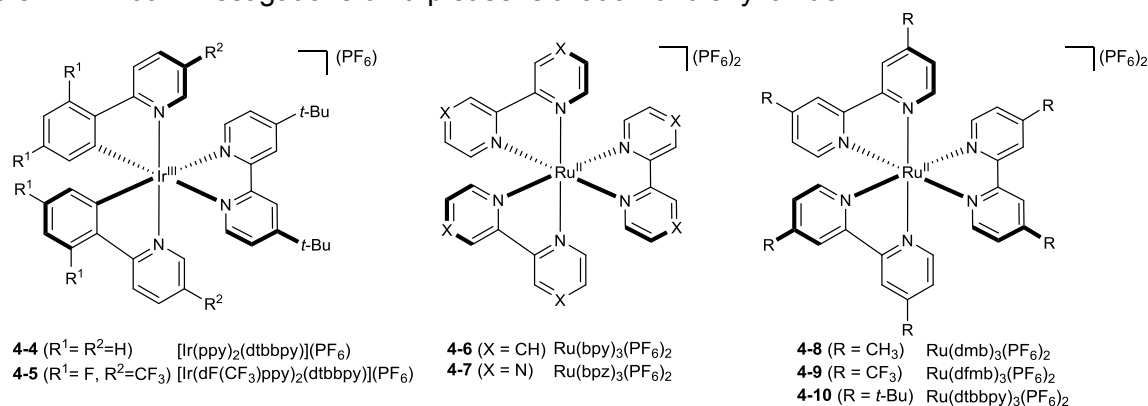
4.2 Reaction Design

As a test of our hypothesis regarding the role of the photocatalyst as a triplet sensitizer of azide decomposition (Chapter 3), we investigated the photocatalytic transformation of dienyl azides into pyrroles via a putative free triplet nitrene intermediate (eq. 1). Driver has reported that this overall transformation can be achieved by Lewis acid catalysis, although the method is limited to α -azidoesters and does not tolerate strongly Lewis basic substituents.⁹ The Lewis acid-catalyzed reaction was proposed to proceed via a chelate-controlled Schmidt-like cyclization that does not involve a discrete nitrene intermediate. This cyclization reaction thus offered an interesting, synthetically valuable benchmark to test our mechanistically distinct ideas about photocatalytic activation of azides.



Dienyl azide **4-1** is insufficiently electron-deficient to be easily reduced by either ruthenium or iridium photocatalysts. For example, reduction of **4-1** ($E^\circ(\text{RN}_3/\text{RN}^-) = -1.81$ V) by $[\text{Ir}(\text{ppy})_2(\text{dtbbpy})]^{+*}$ ($E^\circ(\text{Ir}^{4+/3+*}) = -0.96$ V)¹⁰ is endergonic by 850 mV. On the other hand, we calculated that the first electronically excited triplet state of **4-1** ($E_T = 45.4$ kcal/mol)¹¹ was energetically well poised for sensitization by the long-lived $[\text{Ir}(\text{ppy})_2(\text{dtbbpy})]^{+*}$ triplet state ($E_T = 50$ kcal/mol).¹⁰

Our initial experiments probing this hypothesis are outlined in Table 4-1. We began with conditions from the photocatalytic aziridination discussed in Chapter 3; MeCN was used in place of CH_2Cl_2 to ensure homogeneity of all sensitizers screened. In the event, irradiation of a degassed solution of **4-1** in MeCN with a blue LED light source in the presence of iridium photocatalysts **4-4** and **4-5** resulted in formation of the expected pyrrole **4-3** along with a non-isolable compound we assigned by ^1H NMR as *2H*-azirine **4-11**. Analogous azirines have been implicated as intermediates in the pyrolytic conversion of styrenyl azides to indoles.¹² It should

Table 4-1. Initial investigations on triplet sensitization of dienyl azide **4-1**

| entry ^a | sensitizer (loading) | solvent (concentration) | time | yield 2 (yield 4) ^b |
|--------------------|------------------------|---|-------|---|
| 1 | 4-4 (2.5 mol%) | MeCN (0.4 M) | 1.5 h | 11% (32%) |
| 2 | 4-5 (2.5 mol%) | MeCN (0.4 M) | 1.5 h | 9% (32%) |
| 3 | 4-6 (2.5 mol%) | MeCN (0.4 M) | 1.5 h | 12% (31%) |
| 4 | 4-7 (2.5 mol%) | MeCN (0.4 M) | 1.5 h | 9% (22%) |
| 5 | 4-8 (2.5 mol%) | MeCN (0.4 M) | 1.5 h | 21% (48%) |
| 6 | 4-9 (2.5 mol%) | MeCN (0.4 M) | 1.5 h | 17% (28%) |
| 7 | 4-10 (2.5 mol%) | MeCN (0.4 M) | 1.5 h | 25% (39%) |
| 8 | 4-10 (2.5 mol%) | DMSO (0.4 M) | 1.5 h | 22% (48%) |
| 9 | 4-10 (2.5 mol%) | acetone (0.4 M) | 1.5 h | 21% (41%) |
| 10 | 4-10 (2.5 mol%) | CH ₂ Cl ₂ (0.4 M) | 1.5 h | 28% (32%) |
| 11 | 4-10 (2.5 mol%) | CHCl ₃ (0.4 M) | 1.5 h | 30% (27%) |
| 12 | 4-10 (2.5 mol%) | CHCl ₃ (0.1 M) | 1.5 h | 34% (24%) |
| 13 | 4-10 (2.5 mol%) | CHCl ₃ (0.1 M) | 5 h | 94% (0%) |
| 14 | 4-10 (1 mol%) | CHCl ₃ (0.1 M) | 5 h | 91% (0%) |
| 15 | none | CHCl ₃ (0.1 M) | 5 h | 0% (0%) |
| 16 ^c | 4-10 (1 mol%) | CHCl ₃ (0.1 M) | 5 h | 0% (0%) |
| 17 ^d | 4-10 (1 mol%) | CHCl ₃ (0.1 M) | 5 h | 73% (12%) |
| 18 ^e | none | MeCN (0.1 M) | 5 h | 49% (0%) |

^aReactions conducted using 0.25 mmol of **4-1** under air-free conditions with irradiation from a blue LED strip unless otherwise noted. ^bYields determined by ¹H NMR analysis using an internal standard.

^cReaction conducted in the dark. ^dReaction irradiated with a 23 W compact fluorescent lightbulb.

^eReaction irradiated at 254 nm in a Rayonet reactor.

be noted that these reactions were stopped at partial conversions of **4-1** in order to accurately ascertain rates of conversion.

Given the low yields and sluggish reactivity using the iridium photosensitizers, a series of ruthenium polypyridyl photocatalysts (**4-6–4-10**) was surveyed. Despite the fact that the excited state reduction potentials of the photocatalysts assayed span almost a volt (-0.05 V and -0.94 V vs. SCE for **4-7** and **4-8**, respectively),¹³ similar levels of conversion to **4-3** were observed in each case after 90 min of irradiation (entries 3–7). This observation would be surprising for a mechanism involving photoinduced reduction of **4-1**. On the other hand, it is consistent with a triplet energy transfer process, as the excited state triplet energies of these five photocatalysts are quite similar (45–47 kcal/mol).¹⁴

We also studied solvent effects on the efficiency of the transformation (entries 7–11) and observed little dependence on solvent polarity, as reactions in chloroform ($\epsilon = 4.81$) and acetonitrile ($\epsilon = 36.6$) gave similar results. These data, too, support an energy transfer mechanism, as charged radical ion intermediates would be strongly destabilized in nonpolar media. We observed a modest increase in conversion upon decreasing the concentration of **4-1** (entry 12), and extending the reaction time to 5 h provided complete conversion to pyrrole **4-3** (entry 13), which confirmed that **4-11** is fully converted to **4-3** over the course of the reaction. Interestingly, we noted that the conversion of **4-11** to **4-3** proceeds in the absence of light, indicating that this transformation is a thermal process. Lowering the catalyst loading to 1 mol% had little effect on the yield of the reaction (entry 14), and under these optimized conditions, we observed that irradiation of **4-1** cleanly produced **4-3** in 91% yield after 5 h of irradiation.

Control experiments demonstrated that both photocatalyst and light are required for reaction of **4-1** (entries 15 and 16). On the other hand, the reaction can be conveniently conducted using a variety of visible light sources; while intense blue LED strips provided somewhat faster rates, reactions irradiated with household light bulbs nevertheless provide good yields (entry 17). Direct photoreactions of **4-1** using 254 nm UV light suffered from

significant photodecomposition, resulting in much lower yields and poor overall mass balance (entry 18), verifying our contention that the ability to use visible light in these reactions indeed provides a significant synthetic advantage.

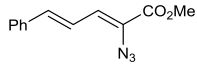
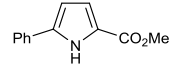
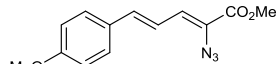
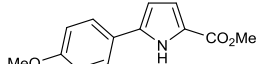
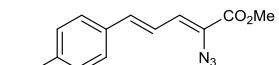
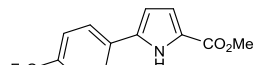
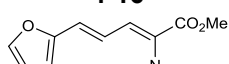
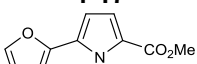
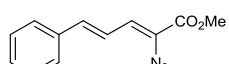
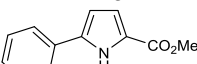
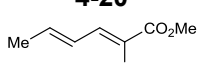
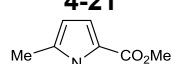
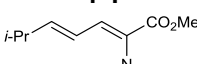
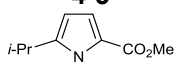
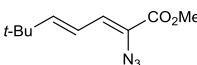
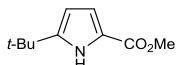
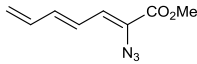
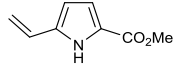
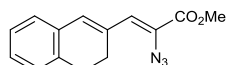
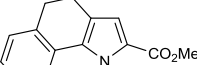
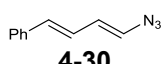
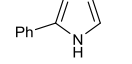
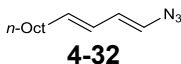
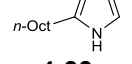
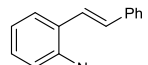
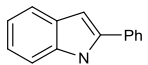
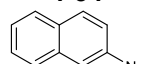
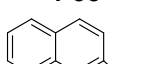
4.3 Results and Discussion

Table 4-2 summarizes our investigations into the scope of this transformation. Both electron-rich and electron-poor aryl substituents can be present on the dienyl unit, and the corresponding pyrroles can be isolated in nearly quantitative yields (entries 1–5). Although heterocyclic substituents are not well tolerated under Driver's Lewis acid-catalyzed process, these substrates were smoothly transformed to pyrroles **4-19** and **4-21** under our optimized conditions. As expected, aliphatic dienyl azides were compatible with the reaction conditions (entries 6–8). Vinyl substitution was also tolerated, affording **4-27** containing a versatile handle for further synthetic elaboration (entry 9). Tricyclic fused heterocycles were also accessible from γ -substituted azidoacrylates (entry 10).

Dienyl azides lacking an α -ester substituent are also readily transformed into pyrroles (entries 11–13). We found that this class of substrates does not react under the Lewis acid catalyzed conditions reported by Driver, even after prolonged reaction times, presumably due to the lack of the chelating moiety involved in the Schmidt-type activation of the azide. Conversely, 1-azido-4-phenylbutadiene **4-30** smoothly undergoes cyclization to afford pyrrole **4-31** in excellent yield after 4 h of irradiation.

Aliphatic dienyl azide **4-32** also underwent cyclization, although the conversion to pyrrole was modest after extended irradiation. We attribute the slow rate of reaction to the higher triplet energy of the less conjugated dienyl azide, computed to be 52 kcal/mol.¹¹ This value is somewhat higher than the triplet excited state of $\text{Ru}(\text{dtbbpy})_3^{2+*}$ ($E_T = 47$ kcal/mol),¹⁴ which would be consistent with inefficient triplet energy transfer. On the other hand, the $[\text{Ir}(\text{dF}(\text{CF}_3)\text{ppy})_2(\text{dtbbpy})]^+$ complex (**4-5**) we found to be optimal for visible light triplet

Table 4-2. Pyrrole synthesis substrate scope study

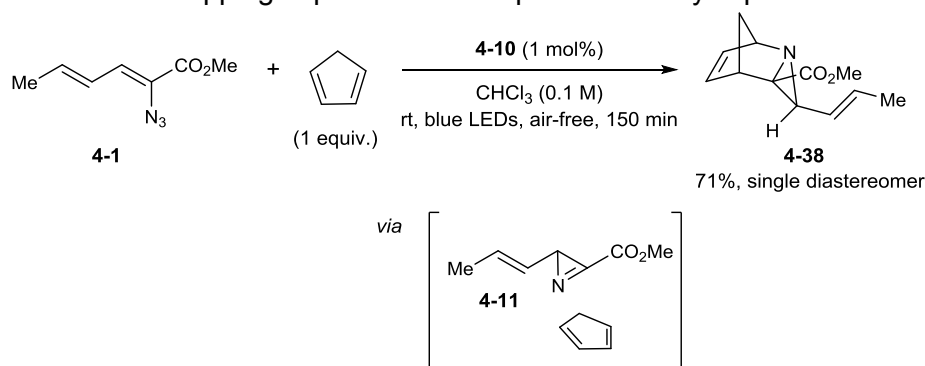
| entry ^a | substrate | product | time | yield |
|--------------------|--|---|-------|-------|
| 1 |  4-12 |  4-13 | 3 h | 99% |
| 2 |  4-14 |  4-15 | 4 h | 99% |
| 3 |  4-16 |  4-17 | 2.5 h | 95% |
| 4 |  4-18 |  4-19 | 4 h | 98% |
| 5 |  4-20 |  4-21 | 3 h | 86% |
| 6 |  4-1 |  4-3 | 8 h | 93% |
| 7 |  4-22 |  4-23 | 11 h | 89% |
| 8 |  4-24 |  4-25 | 14 h | 86% |
| 9 |  4-26 |  4-27 | 2 h | 89% |
| 10 |  4-28 |  4-29 | 4 h | 96% |
| 11 |  4-30 |  4-31 | 3 h | 92% |
| 12 |  4-32 |  4-33 | 36 h | 47% |
| 13 ^b |  4-34 |  4-35 | 12 h | 70% |
| 14 |  4-36 |  4-37 | 20 h | 75% |

^aData represent the averaged isolated yields from two reproducible experiments. ^bConducted using [Ir(dF(CF₃)ppy)₂(dtbbpy)](PF₆) **4-5** (1 mol%) as photocatalyst.

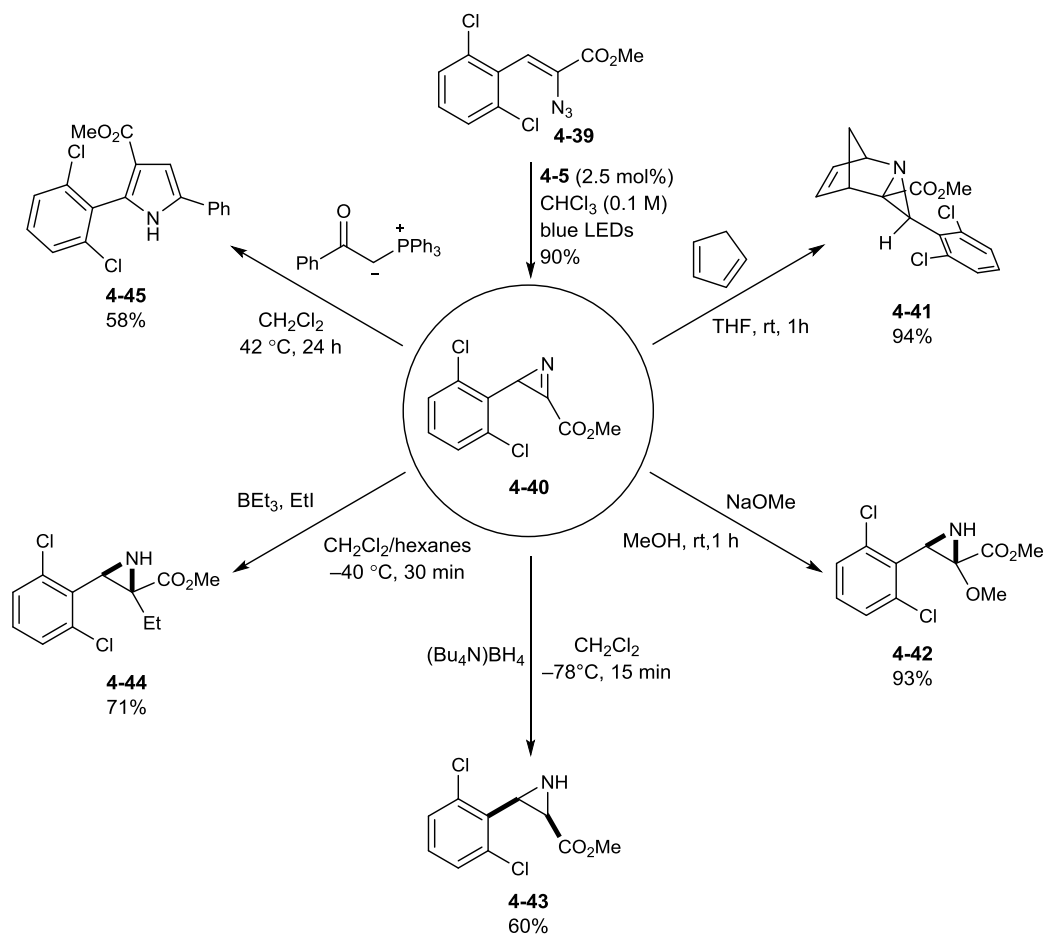
sensitization of styrenes^{2a} has a significantly higher-energy triplet state ($E_T = 61$ kcal/mol),¹⁰ and using this photocatalyst, we could isolate the cyclized pyrrole product in 70% yield after 12 h.

Furthermore, sensitization of aryl azides proceeded smoothly to afford indoles (entries 14–15). This is noteworthy because direct photolysis of aryl azides in solution at room temperature produces a singlet nitrene that typically undergoes rapid rearrangement to the corresponding non-isolable didehydroazepine.^{15,16} Indeed, direct irradiation of **4-36** at 350 nm resulted in complete consumption of the starting azide within 1 h but produced only 51% yield of indole **4-37** as a part of a complex, inseparable mixture.

Scheme 4-1. 2*H*-Azirine trapping experiment in the presence of cyclopentadiene



We were intrigued by the appearance of transitory intermediate **4-11** at partial conversions of dienyl azide **4-1**. We assigned the structure of this intermediate as azirine **4-11** based upon analogy to the photochemical production of azirines by UV irradiation of β -styrenyl azides.¹² The identity of **4-11** was confirmed by adding 1 equiv. of cyclopentadiene to a photocatalytic transformation of **4-1**, which produced the hetero-Diels–Alder cycloadduct expected from interception of the highly reactive C=N moiety in 71% isolated yield and as a single diastereomer. Notably, this trapping experiment, too, is markedly more efficient under photocatalytic conditions; the same experiment conducted by direct UV photolysis at 254 nm produced only 40% of the trapped hetero-Diels–Alder cycloadduct along with inseparable decomposition products.

Scheme 4-2. Isolation and manipulation of 2*H*-azirine **4-40**

The azirine can be produced in high yields in cases where subsequent ring expansion to the five-membered heterocycle is prohibited. For example, irradiation of the aryl-substituted vinyl azide **4-39** in the presence of photocatalyst **4-5** generated azirine **4-40** in 90% yield. While **4-11** is not amenable to isolation due to facile reactivity with molecular oxygen, **4-40** was obtained as a bench-stable white solid.

However, like **4-11**, most azirines are engaged in a wide range of transformations due to their high ring strain (~ 26 kcal/mol), a reactive π -bond, and their propensity to undergo ring cleavage. Indeed, cleavage of the weaker σ C-N bond can afford vinyl nitrenes, iminocarbenes, or nitrile ylides.¹⁷ As such, azirines can be used in the synthesis of myriad heterocyclic compounds. Hetero-Diels–Alder cycloaddition with cyclopentadiene to afford cycloadduct **4-41**

is rapid and high-yielding. To highlight the utility of azirines generated under photocatalyzed azide decomposition, we converted **4-40** to a variety of other aziridines by addition of nucleophiles and radicals to the C=N bond (**4-42**, **4-43** and **4-44**). Finally, we found that **4-40** can be easily converted to highly substituted pyrrole **4-45** by reaction with a stabilized phosphonium ylide.

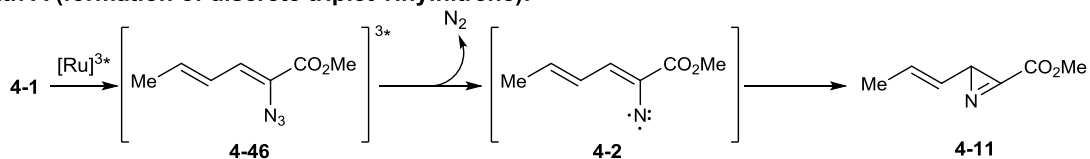
4.4 Mechanistic Studies and Considerations

4.4.1 Sensitization of Vinyl Azides

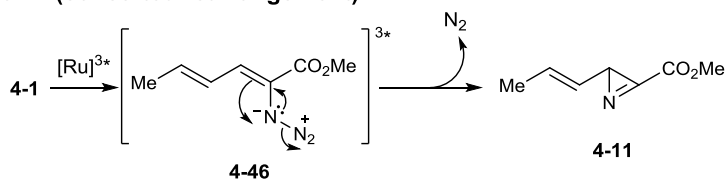
Having established a broad substrate scope for the visible light-mediated sensitization of azidoacrylates, we sought to further understand the mechanism by which the reaction proceeds. An important consideration is the observation of *2H*-azirine **4-11** by ^1H NMR spectroscopy, as this suggests the azirine is an intermediate in the formation of pyrrole **4-3**. The question of how azirine **4-11** is generated from the lowest triplet excited state of **4-1** presents two possibilities as shown in Scheme 4-3, namely Path A (extrusion of nitrogen to generate a triplet vinyl nitrene followed by cyclization) or Path B (concerted rearrangement with loss of nitrogen).

Scheme 4-3. Pathways for generation of azirine **4-11**

Path A (formation of discrete triplet vinyl nitrene):



Path B (concerted rearrangement):

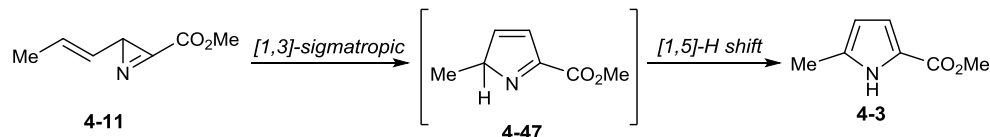


Early studies of L'abbé and Mathys provided support for concerted rearrangement to give **4-11**, though the authors noted that formation of a discrete triplet vinyl nitrene intermediate could not explicitly be excluded.¹² At the time of these studies, triplet vinyl nitrenes had never been observed, and thus concerted rearrangement was much more widely accepted. Recently,

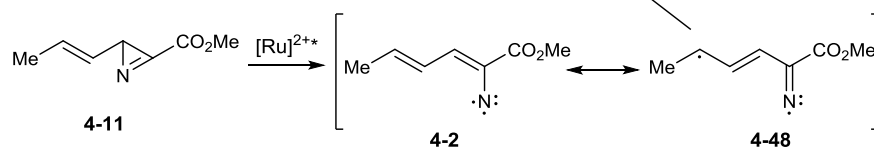
however, Gudmundsdottir provided solution phase IR, UV-Vis, and EPR data consistent with the existence of triplet vinyl nitrenes.^{18a} Subsequent studies demonstrated direct observation of triplet vinyl nitrenes in glassy matrices.^{18b} Given the confirmed existence of triplet vinyl nitrenes, it appears that both pathways in Scheme 4-3 are equally plausible.

Scheme 4-4. Pathways for conversion of azirine **4-11** to pyrrole **4-3**

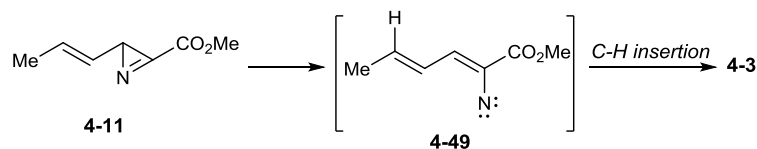
Path A (Initial sigmatropic rearrangement):



Path B (Initial iminyl biradical cyclization):



Path C (Singlet nitrene insertion):

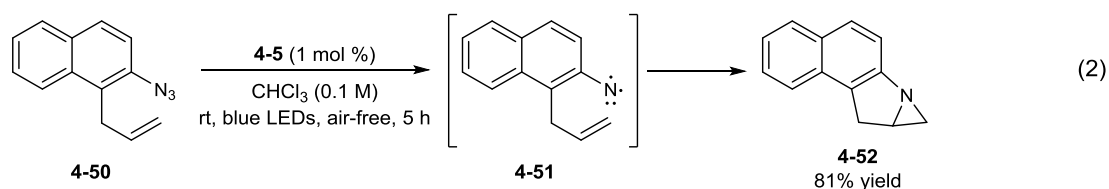


The transformation of azirine **4-11** to pyrrole **4-3** is also of interest. This could occur by suprafacial [1,3]-sigmatropic alkyl shift to give **4-47** followed by a [1,5]-hydrogen shift to afford pyrrole **4-3** (Path A). Alternatively, energy transfer from the ruthenium sensitizer to **4-11** could produce triplet nitrene **4-2**, a resonance structure of which is iminyl biradical **4-48** (Path B); radical cyclization of **4-48** would afford species **4-47**. Path B is effectively ruled out by the observation that conversion of **4-11** to **4-3** is a thermal process; ISC from singlet azirine **4-11** to triplet vinylnitrene **4-2** is thermally disallowed, as a spin flip would have to occur. Given that the conversion of **4-11** to **4-3** is a thermal process, Path C can be envisioned, wherein C-N bond cleavage of **4-11** produces singlet vinyl nitrene **4-49** followed by nitrene insertion into the δ C-H bond of the diene. This seems unlikely given that the ground state of vinylnitrenes is the triplet, with the first singlet state lying 15 kcal/mol higher in energy, a prohibitive energy barrier for a

room-temperature rearrangement. However, rigorous quantum mechanical calculations on *dienyl*nitrenes have not been performed, and these species have not been characterized. Thus Path C cannot be rigorously excluded based solely on analogy to vinylnitrenes. Even with these considerations, Path A appears most likely.

4.4.2 Sensitization of Aryl Azides

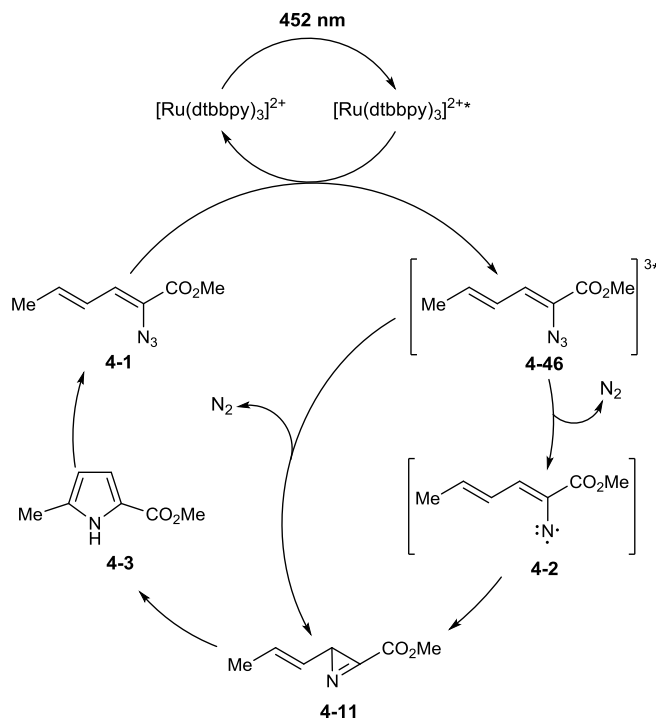
We surmised that an arylnitrene could be trapped in an intramolecular sense by photocatalytic activation of azidonaphthalene **4-50** (eq. 3). Unlike substrates **4-34** and **4-36**, **4-50** possesses a discontinuous π spin system between the naphthalene and allyl moieties, thereby precluding an electrocyclic mechanism by which rearrangement would follow sensitization. Therefore, observation of aziridine **4-52** necessarily demands a mechanism involving the intramolecular trapping of photogenerated triplet nitrene **4-51** by the pendant olefin. We calculated the triplet excited state energy of **4-50** to be 62.0 kcal/mol,¹¹ suggesting that **4-50** could be efficiently sensitized by iridium photocatalyst **4-5**. Indeed, visible light irradiation of **4-50** for 5 h in the presence of this Ir complex resulted in the clean production of aziridine **4-52**, thus providing substantive evidence for the intermediacy of a triplet nitrene and validating the hypotheses presented in this and the previous chapter.



Scheme 4-5 outlines our working mechanism for the photocatalytic generation of pyrrole **4-3**. Irradiation of $\text{Ru}(\text{dtbbpy})_3^{2+}$ with visible light at 452 nm produces its long-lived excited state; exergonic energy transfer to dienyl azide **4-1** produces excited triplet azide **4-46**. Azide **4-46** can either expel dinitrogen to afford azirine **4-11** directly or can expel dinitrogen to give free

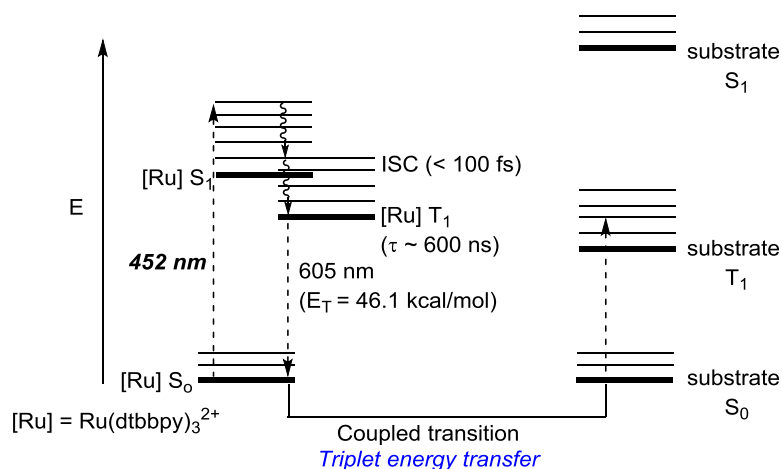
nitrene **4-2** that undergoes ISC to **4-11**. Slow but high-yielding rearrangement of **4-11** produces pyrrole **4-3**.

Scheme 4-5. Energy transfer mechanism from [Ru] sensitizer to azidoacrylates



4.4.3 Photophysical Considerations

Up to this point, triplet sensitization has been presented as a mechanism by which a photosensitizer with a given triplet state can, upon excitation, transfer its energy to a substrate having a triplet state of similar energy. However, this notion is not rigorously correct. As shown in the Jablonski diagram presented in Scheme 4-6, photocatalyst excitation occurs when light having energy equal to the S_0 - S_1 gap interacts with the photocatalyst.

Scheme 4-6. Jablonski diagram for triplet energy transfer

Specifically, the oscillating electromagnetic (EM) field of light is comprised of oscillating dipolar electric and magnetic force fields. When electrons in a molecule (a given photocatalyst, for this discussion) possess a resonance oscillation frequency (ν) that corresponds to a resonance oscillation frequency of an oscillating electric dipole (photon) in the electromagnetic field, the resonance condition ($E = h\nu$) for absorption is obeyed. This induces an exchange of energy from the electromagnetic field with the electrons of the photocatalyst, thus driving the electrons of the photocatalyst into oscillation and producing the first singlet excited state (S_1).¹⁹ Due to significant spin-orbit coupling resulting from the interaction between the d orbitals on Ru and the appropriate ligand π orbitals, intersystem crossing (ISC) is extremely rapid ($< 100 \text{ fs}$)²⁰ and produces the first triplet state in near quantitative quantum yield. In the absence of a quencher (dienyl azide substrate, in this case), radiative relaxation to the ground state (phosphorescence) will occur. However, in the presence of a quencher (dienyl azide) having a triplet state closely matched in energy to that of $[\text{Ru}]$, energy from the visible portion of the EM field is harnessed by the ruthenium photocatalyst and transferred to the quencher.

The photocatalyst is required because direct transfer of energy from the EM field to the dienyl azide is not possible due to the high-lying S_1 state (dienyl azide $\lambda_{\text{max}} = 291 \text{ nm}$). Furthermore, the $S_0 \rightarrow T_1$ transition is spin-forbidden by quantum mechanics, and thus the

extinction coefficient (ϵ_A) for this transition is small. This fact leads to an important conclusion regarding the mechanism for coupled transition. Indeed, one could imagine that emission of a photon from $[\text{Ru}] T_1$ could be used to directly excite the dienyl azide ($S_0 \rightarrow T_1$). However, this is effectively ruled out as a possible mechanism because of the direct proportionality between the spectral overlap integral and ϵ_A . Another potential mechanism for triplet-triplet energy transfer involves dipole-dipole energy transfer (Förster resonance energy transfer), in which the requisite resonance condition is achieved via through-space overlap of the dipolar electric fields of $[\text{Ru}]^{2+*}$ and the dienyl azide. This mechanism, too, is ruled out because $S_0 \rightarrow T_1$ transitions have very small oscillator strengths, and thus, very small transition dipoles. As such, dipolar coupling between $[\text{Ru}]^{2+*}$ and the dienyl azide will be weak.

Given the infeasibility of the aforementioned mechanisms operating via through-space interactions, a final mechanism for triplet-triplet energy transfer involves direct orbital overlap between $[\text{Ru}]^{2+*}$ and the dienyl azide. While it has been demonstrated in this and the previous chapter that full electron transfer (charge transfer) from sensitizer to substrate is not plausible, an induced electron *exchange* interaction between $[\text{Ru}]^{2+*}$ and the dienyl azide (Dexter energy transfer) appears completely feasible given the computational data for a close match between $[\text{Ru}]^{2+*} T_1$ and dienyl azide T_1 . This “close match” implies that the energies of the photosensitizer HOMO and LUMO as well as the energies of the substrate sensitizer HOMO and LUMO are of similar energy, a necessary requirement for exergonic electron exchange to occur.

4.5 Conclusions

We have demonstrated that photocatalytic activation of aryl and vinyl azides with visible light provides a convenient method to access the chemistry of nitrenes. Indeed, one of the most intriguing implications of these investigations is the possibility that visible light photocatalysis might provide a convenient method to access all of the diverse reactivity of free nitrenes under

exceptionally mild conditions. The ability to use low-energy visible light in this application minimizes complications arising from photodecomposition and thus provides uniformly higher yields than direct photoexcitation with UV light. In addition, the methodologies developed in this and the previous chapter allow for the efficient transfer of energy from the EM field of light to an organic substrate. This notion carries powerful implications for the re-investigation of transformations requiring UV-irradiation as well as the development of novel reactions for which redox operations are infeasible.

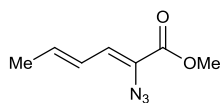
4.6 Experimental

4.6.1. General Information

Dichloromethane, tetrahydrofuran, diethyl ether, toluene, and acetonitrile were dried by passage through columns of activated alumina. HPLC grade CHCl_3 was washed with 1 M NaOH and deionized H_2O , passed through a column of activated, basic Brockmann I Al_2O_3 , and fractionally distilled from K_2CO_3 immediately prior to use. Irradiations were performed using a 1 W blue light-emitting diode (LED) strip ($\lambda = 465\text{--}470$ nm) purchased from Creative Lighting Solutions. Chromatography was performed with Purasil 60 Å silica gel (230–400 mesh). ^1H and ^{13}C NMR data for all previously uncharacterized compounds were obtained using Varian Inova-500 and Bruker-500 spectrometers and are referenced to TMS (0.00 ppm) or residual protio solvent signal. IR spectral data were obtained using a Bruker Vector 22 spectrometer (thin film on NaCl). Melting points were obtained using a Mel-Temp II (Laboratory Devices, Inc., USA) melting point apparatus. Mass spectrometry was performed with a Micromass LCT (electrospray ionization, time-of-flight analyzer or electron impact). These facilities are funded by the NSF (CHE-9974839, CHE-9304546) and the University of Wisconsin.

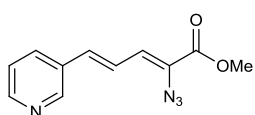
The catalyst complexes $[\text{Ir}(\text{dF}(\text{CF}_3)\text{ppy})_2(\text{dtbbpy})](\text{PF}_6)^{10}$ and $\text{Ru}(\text{dtbbpy})_3(\text{PF}_6)_2^{14}$ were prepared according to literature procedures. Compounds **4-12**, **4-14**, **4-16**, **4-18**, and **4-39** were prepared as described by Seeberger,²¹ and compound **4-34** was prepared according to a procedure reported by Driver.²² Compounds **4-41** and **4-44** were prepared according to Gilchrist²³ and Lemos,²⁴ respectively.

4.6.2. Synthesis of Cyclization Substrates



(2Z,4E)-Methyl 2-azidohexa-2,4-dienoate (4-1).

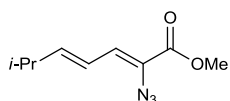
Prepared using a modification of the procedure reported by Driver.⁹ To a 100 mL round bottomed flask that had been flame-dried under high vacuum and purged with N₂ was added THF (14 mL) and hexamethyldisilazane (4.84 g, 30.0 mmol). The mixture was cooled to 0 °C after which *sec*-BuLi (24.0 mL of a 1.37 M solution in cyclohexane, 32.8 mmol) was added slowly. (Note: we found that use of *n*-BuLi led to formation of significant amounts of the butyl ester ((2Z,4E)-butyl 2-azidohexa-2,4-dienoate), and purification of the desired product away from the butyl ester derivative was very difficult). To ensure quantitative deprotonation, the reaction was stirred at 0 °C for an additional 10 min and thereafter cooled to –78 °C. After 10 min at –78 °C, a solution of freshly distilled crotonaldehyde (2.00 g, 28.5 mmol) in methyl azidoacetate (13.1 g, 114.1 mmol) was added dropwise over 1 h. Throughout the addition, a thick, dark sludge formed and continuous, vigorous stirring was required to achieve acceptable yields. Subsequently, the reaction was warmed to –10 °C and stirred until complete consumption of crotonaldehyde was observed (2 h). Thereafter, the mixture was warmed to rt and stirred for 2 h. At this time, the reaction was diluted with Et₂O (20 mL) and quenched via the slow addition of H₂O (20 mL). The organic layer was separated, and the aqueous layer was extracted with Et₂O (2 x 30 mL). The organic layers were combined and washed with H₂O (2 x 30 mL), brine (1 x 30 mL), dried over Na₂SO₄, filtered, and the volatiles were removed *in vacuo* to give a brown oil that was purified via flash column chromatography using a solvent gradient (99:1 to 24:1 hexanes:EtOAc) to afford the product (1.45 g, 8.66 mmol, 30% yield) as a pale yellow oil. Spectral data were in complete agreement with reported values.⁹



(2Z,4E)-Methyl 2-azido-5-(pyridin-3-yl)penta-2,4-dienoate (Table 4-2,

entry 5, 4-20). Prepared according to the procedure of Seeberger.²¹ A flame-dried 50 mL round bottomed flask under an atmosphere of N₂ was charged with *trans*-3-

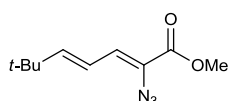
(3-pyridyl)acrolein (500 mg, 3.76 mmol), dry MeOH (5.3 mL), and methyl azidoacetate (1080 mg, 9.39 mmol). The solution was cooled to $-15\text{ }^{\circ}\text{C}$, and after 10 min, a solution of NaOMe (freshly prepared from 216 mg Na (9.39 mmol) in 5.3 mL MeOH) was added dropwise over 20 min. The reaction was stirred at $-15\text{ }^{\circ}\text{C}$ for an additional 90 min, then slowly warmed to $4\text{ }^{\circ}\text{C}$ and stirred for 12 h. Subsequently, the heterogeneous mixture was poured into ice-cold saturated aqueous NH_4Cl (15 mL). The resulting precipitate was isolated on a fritted funnel and washed with deionized H_2O until the filtrate came through clear. The beige solid was dissolved in CH_2Cl_2 and dried over Na_2SO_4 . The organic solution was filtered, and the volatiles were removed *in vacuo* to give a residue that was purified by flash column chromatography using a solvent gradient (1:1 to 1:2 hexanes:EtOAc) to afford the title compound (455 mg, 1.98 mmol, 52% yield) as a pale yellow solid (mp = $99.7\text{--}100.4\text{ }^{\circ}\text{C}$). IR (neat) 2115, 1705, 1598, 1438, 1374, 1248, 971 cm^{-1} . ^1H NMR: (500.2 MHz, CDCl_3) δ 8.66 (d, $J = 1.8\text{ Hz}$, 1H), 8.52 (dd, $J = 4.8, 1.6\text{ Hz}$, 1H), 7.82 (app dt, $J = 8.0, 1.8\text{ Hz}$, 1H), 7.29 (dd, $J = 8.1, 4.9\text{ Hz}$, 1H), 7.22 (dd, $J = 15.9, 11.2\text{ Hz}$, 1H), 6.78 (d, $J = 15.9\text{ Hz}$, 1H), 6.74 (dd, $J = 11.2, 0.9\text{ Hz}$, 1H), 3.89 (s, 3H); ^{13}C NMR: (125.8 MHz, CDCl_3) δ 163.4, 149.7, 149.2, 134.8, 133.1, 132.1, 126.7, 125.9, 124.1, 123.6, 52.8; HRMS (EI) calculated for $[\text{C}_{11}\text{H}_{10}\text{N}_4\text{O}_2]^+$ requires m/z 230.0804, found m/z 202.0737 ($[\text{M}-\text{N}_2]^+$, requires m/z 202.0742).



(2Z,4E)-Methyl 2-azido-6-methylhepta-2,4-dienoate (Table 4-2, entry 7, **4-**

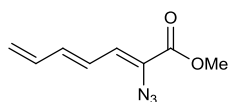
22). Prepared in a similar manner to (2Z,4E)-methyl 2-azidohexa-2,4-dienoate **1** using (*E*)-4-methylpent-2-enal (980 mg, 10.0 mmol),²⁵ methyl azidoacetate (4.60 g, 40.0 mmol), hexamethyldisilazane (1.69 g, 10.5 mmol), *sec*-BuLi (8.38 mL of a 1.37 M solution in cyclohexane, 11.5 mmol), and THF (5.0 mL). Purified via flash column chromatography using a solvent gradient (99:1 to 24:1 hexanes:EtOAc) to afford the product (683 mg, 3.50 mmol, 35% yield) as a pale yellow oil. IR (neat) 2122, 1714, 1673, 1374, 1271, 1231 cm^{-1} . ^1H NMR: (500.2 MHz, CDCl_3) δ 6.58 (d, $J = 11.0\text{ Hz}$, 1H), 6.39 (ddd, $J = 15.4, 11.2, 1.4\text{ Hz}$, 1H), 6.04 (ddd, $J =$

15.4, 6.8, 0.7 Hz, 1H), 3.84 (s, 3H), 2.44 (d of septets, $J = 6.8, 1.3$ Hz, 1H), 1.05 (d, $J = 6.8$ Hz, 6H); ^{13}C NMR: (125.8 MHz, CDCl_3) δ 162.8, 149.6, 127.0, 122.8, 120.4, 51.5, 30.8, 20.8; HRMS (EI) calculated for $[\text{C}_9\text{H}_{13}\text{N}_3\text{O}_2]^+$ requires m/z 195.1008, found m/z 167.0941 ($[\text{M}-\text{N}_2]^+$, requires m/z 167.0946).



(2Z,4E)-Methyl 2-azido-6,6-dimethylhepta-2,4-dienoate (Table 4-2, entry 8, **4-24**). Prepared in a similar manner to (2Z,4E)-methyl 2-azidohexa-2,4-

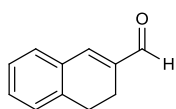
dienoate **1** using (*E*)-4,4-dimethylpent-2-enal (650 mg, 5.79 mmol),²⁵ ethyl azidoacetate (2.67 g, 23.2 mmol), hexamethyldisilazane (0.982 g, 6.08 mmol), *sec*-BuLi (4.86 mL of a 1.37 M solution in cyclohexane, 6.66 mmol), and THF (2.9 mL). Purified via flash column chromatography using a solvent gradient (99:1 to 24:1 hexanes:EtOAc) to afford the product (376 mg, 1.79 mmol, 31% yield) as a pale yellow oil. IR (neat) 2126, 1717, 1689, 1498, 1442, 1239 cm^{-1} . ^1H NMR: (500.2 MHz, CDCl_3) δ 6.59 (dd, $J = 11.0, 0.5$ Hz, 1H), 6.36 (dd, $J = 15.5, 10.9$ Hz, 1H), 6.07 (dd, $J = 15.5, 0.6$ Hz, 1H), 3.84 (s, 3H), 1.07 (s, 9H); ^{13}C NMR: (125.8 MHz, CDCl_3) δ 162.8, 153.4, 127.3, 122.9, 118.3, 51.5, 33.2, 28.1; HRMS (EI) calculated for $[\text{C}_{10}\text{H}_{15}\text{N}_3\text{O}_2]$ requires m/z 209.1164, found m/z 209.1159.



(2Z,4E)-Methyl 2-azidohepta-2,4,6-trienoate (Table 4-2, entry 9, **4-26**). A

flame-dried 50 mL round bottomed flask under an atmosphere of N_2 was charged with (*E*)-penta-2,4-dienal (600 mg, 7.31 mmol),²⁶ dry MeOH (10.3 mL), and methyl azidoacetate (2103 mg, 18.3 mmol). The solution was cooled to -15 $^\circ\text{C}$, and after 10 min, a solution of NaOMe (freshly prepared from 420 mg Na (18.3 mmol) in 10.3 mL MeOH) was added dropwise over 20 min. The reaction was stirred at -15 $^\circ\text{C}$ for an additional 90 min, then slowly warmed to 4 $^\circ\text{C}$ and stirred for 12 h. Subsequently, the heterogeneous mixture was poured into ice-cold saturated aqueous NH_4Cl (25 mL) and extracted with EtOAc (3 x 40 mL). The organic layer was dried over Na_2SO_4 , filtered, and the volatiles were removed *in vacuo*. The resulting residue was purified via flash column chromatography (99:1 hexanes:EtOAc) to

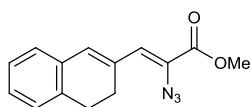
afford the trienyl azide (458 mg, 2.56 mmol, 35% yield) as a yellow oil that was used immediately. IR (neat) 2124, 1714, 1684, 1438, 1368, 1234 cm^{-1} . ^1H NMR: (499.8 MHz, C_6D_6) δ 6.56 (ddd, $J = 14.9, 11.4, 0.5$ Hz, 1H), 6.46 (d, $J = 11.4$ Hz, 1H), 6.19 (dtd, $J = 17.0, 10.8, 0.5$ Hz, 1H), 6.07 (ddd, $J = 14.7, 10.9, 0.5$ Hz, 1H), 5.07 (ddd, $J = 16.9, 1.4$ Hz, 1H), 4.99 (dd, $J = 10.8, 1.3$ Hz, 1H), 3.25 (s, 3H); ^{13}C NMR: (125.7 MHz, C_6D_6) δ 162.9, 139.3, 136.7, 126.6, 126.1, 125.9, 120.7, 51.7; HRMS (EI) calculated for $[\text{C}_8\text{H}_9\text{N}_3\text{O}_2]^+$ requires m/z 179.0695, found m/z 151.0628 ($[\text{M}-\text{N}_2]^+$, requires m/z 151.0633).



3,4-Dihydronaphthalene-2-carbaldehyde (4-53). Prepared according to the procedure of Mock and Tsou.²⁷ To a 250 mL round bottomed flask that had

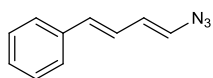
been flame-dried under high vacuum and purged with N_2 was added distilled triethyl orthoformate (6.72 g, 45.4 mmol), which was then cooled to -30 $^\circ\text{C}$. Subsequently, a solution of $\text{BF}_3 \cdot \text{Et}_2\text{O}$ (7.73 g, 54.5 mmol) in CH_2Cl_2 (23 mL) was added dropwise over 20 min. The resulting slurry was stirred at -30 $^\circ\text{C}$ for an additional 5 min then warmed to 0 $^\circ\text{C}$ for 15 min. The solution was thereafter cooled to -78 $^\circ\text{C}$ and α -tetralone (3.32 g, 22.7 mmol) was added dropwise over 5 min followed by dropwise addition of diisopropylethylamine (8.80 g, 68.1 mmol) over 30 min. The reaction was then warmed to -20 $^\circ\text{C}$ and stirred for 30 min and slowly warmed to -10 $^\circ\text{C}$ over 90 min. Thereafter, the reaction was poured into saturated aqueous NaHCO_3 (250 mL) and CH_2Cl_2 (150 mL) was added followed by vigorous stirring for 10 min. The resulting layers were separated, and the organic layer was washed with cold, 0.5 M H_2SO_4 (1 x 50 mL) and cold H_2O (1 x 50 mL) and dried over Na_2SO_4 . The organic layer was filtered, and the volatiles were removed *in vacuo* to afford a viscous, orange oil that was purified by Kugelrohr distillation (0.05 Torr, 200 $^\circ\text{C}$ glass oven temperature) to give 2-(diethoxymethyl)-3,4-dihydronaphthalen-1(2H)-one (5.24 g, 21.1 mmol, 93% yield) as a clear oil whose spectral data matched the reported literature values.²⁸ A dry 250 mL round bottomed flask equipped with an addition funnel was charged with 2-(diethoxymethyl)-3,4-dihydronaphthalen-1(2H)-one (3.20 g,

12.9 mmol) and EtOH (25 mL). The mixture was cooled to 0 °C, and then a solution of NaBH₄ (1.71 g, 45.1 mmol) in EtOH (55 mL) was added dropwise over 10 min. The reaction was heated to 80 °C and stirred for 30 min. Thereafter, the mixture was cooled to 0 °C and 6 M HCl was added dropwise over 20 min until H₂ evolution had ceased and the solution achieved a pH of 1. Subsequently, the reaction was heated to 80 °C and stirred for 4 h. At this time, the solution was cooled to rt and poured into brine (300 mL). EtOAc (150 mL) was added, and the organic layer was separated and washed with brine (1 x 50 mL), dried over Na₂SO₄, filtered, and the volatiles were removed *in vacuo* to afford a crude orange oil. Purification by flash-column chromatography on silica (9:1 hexanes:EtOAc) afforded the carbaldehyde (682 mg, 4.31 mmol, 33% yield over two steps) as a pale yellow oil. Spectral data were in complete agreement with previously reported values.²⁹



(Z)-Methyl 2-azido-3-(3,4-dihydronaphthalen-2-yl)acrylate (Table 4-2, entry 10, **4-28**). Prepared in a similar manner to (2*Z*,4*E*)-methyl 2-azido-5-

(pyridin-3-yl)penta-2,4-dienoate **4-20** using 3,4-dihydronaphthalene-2-carbaldehyde **4-53** (600 mg, 3.79 mmol), MeOH (5.3 mL), methyl azidoacetate (1091 mg, 9.49 mmol), and a solution of NaOMe (prepared from 218 mg Na (9.48 mmol) in 5.3 mL MeOH). The resulting residue was purified by flash-column chromatography using a solvent gradient (9:1 to 7:1 hexanes:EtOAc) to afford the title compound (534 mg, 2.09 mmol, 55% yield) as a pale yellow solid (mp = 62.6–64.0 °C). IR (neat) 2122, 1717, 1672, 1354, 1231 cm⁻¹. ¹H NMR: (499.8 MHz, CDCl₃) δ 7.14 (m, 4H), 6.88 (s, 1H), 6.66 (s, 1H), 3.88 (s, 3H), 2.85 (m, 2H), 2.80 (m, 2H); ¹³C NMR: (125.7 MHz, CDCl₃) δ 164.3, 136.0, 135.0, 134.8, 133.8, 128.5, 127.8, 127.4, 126.7, 123.9, 52.9, 27.9, 25.6; HRMS (EI) calculated for [C₁₄H₁₃N₃O₂]⁺ requires *m/z* 255.1003, found *m/z* 255.1002.

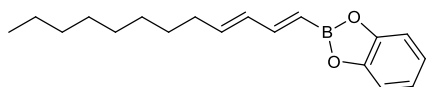


((1*E*,3*E*)-4-azidobuta-1,3-dien-1-yl)benzene (Table 4-2, entry 11, **4-30**).

Prepared according to the procedure of Guo.³⁰ A 25 mL round bottomed flask was charged with anhydrous CuSO₄ (42.5 mg, 0.267 mmol) and sodium azide (208 mg, 3.19

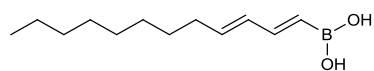
mmol). Then MeOH (8.0 mL) was added followed immediately by ((1*E*,3*E*)-4-phenylbuta-1,3-dien-1-yl)boronic acid (463 mg, 2.66 mmol).³¹ The heterogeneous brown solution was vigorously stirred open to the atmosphere for 18 h. Thereafter, the volatiles were removed *in vacuo*, and the crude residue was dissolved in CH₂Cl₂ and filtered through a pad of silica (1:1 hexanes:EtOAc). The volatiles were removed *in vacuo* to give a dark yellow oil that was purified via flash column chromatography on silica (20:1 hexanes:EtOAc) to afford the product (163 mg, 0.95 mmol, 36% yield) as a pale yellow solid (mp = 51.4–53.1 °C). IR (neat) 2102, 1346, 1264, 976, 907 cm⁻¹. ¹H NMR: (500.2 MHz, CDCl₃) δ 7.41–7.36 (m, 2H), 7.35–7.29 (m, 2H), 7.26–7.20 (m, 1H), 6.70 (ddd, *J* = 15.4, 10.9, 0.6 Hz, 1H), 6.49 (dd, *J* = 15.6, 0.7 Hz, 1H), 6.25 (dd, *J* = 13.3, 0.7 Hz, 1H), 6.12 (ddd, *J* = 13.2, 10.8, 0.8 Hz, 1H); ¹³C NMR: (125.8 MHz, CDCl₃) δ 137.1, 131.5, 129.1, 128.7, 127.5, 126.1, 124.9, 120.7; HRMS (EI) calculated for [C₁₀H₉N₃]⁺ requires *m/z* 171.0796, found *m/z* 143.0730 ([M-N₂]⁺, requires *m/z* 143.0735).

2-((1*E*,3*E*)-Dodeca-1,3-dien-1-yl)benzo[*d*][1,3,2]dioxaborole (4-54). To a 25 mL round



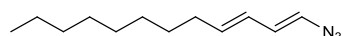
bottomed flask with a stir bar that had been flame-dried under high vacuum and purged with N₂ was added (*E*)-dodec-3-en-1-yne (1.39 g, 8.46 mmol).^{32,33} To the stirred compound was added freshly distilled catecholborane³⁴ (1.02 g, 8.46 mmol) over 5 min. Thereafter, the reaction was heated to 70 °C and stirred for 3 h, resulting in the formation of a dark brown oil. After cooling the mixture to rt, the crude oil was purified by Kugelrohr distillation at 0.05 Torr (impurity collected at 50–80 °C, product distilled at 132 °C) to afford the title compound (1.74 g, 6.12 mmol, 72% yield) as a clear oil. IR (neat) 2937, 2856, 2379, 2345, 1649, 1455, 1136, 1002 cm⁻¹. ¹H NMR: (500.2 MHz, CDCl₃) δ 7.34 (dd, *J* = 17.7, 10.4 Hz, 1H), 7.21 (app dd, *J* = 5.8, 3.3 Hz, 2H), 7.07 (app dd, *J* = 5.8, 3.3 Hz, 2H), 6.26 (dd, *J* = 15.2, 10.5 Hz, 1H), 6.06 (dt, *J* = 14.7, 7.1 Hz, 1H), 5.75 (d, *J* = 17.7 Hz, 1H), 2.17 (dt, *J* = 7.9, 7.7 Hz, 2H), 1.44 (tt, *J* = 7.9, 7.6 Hz, 2H), 1.29 (m, 10H), 0.89 (t, *J* = 6.8 Hz, 3H); ¹³C NMR: (125.8 MHz, CDCl₃) δ 152.9, 148.3, 142.0, 132.1, 122.5, 112.2,

32.8, 31.8, 29.4, 29.2, 29.2, 28.9, 22.7, 14.1; HRMS (EI) calculated for $[C_{18}H_{25}BO_2]^+$ requires m/z 284.1948, found m/z 284.1979.



(1E,3E)-Dodeca-1,3-dien-1-ylboronic acid (4-55). A 50 mL round bottomed flask was charged with 2-((1E,3E)-dodeca-1,3-

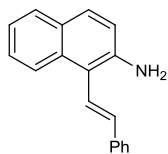
dien-1-yl)benzo[d][1,3,2]dioxaborole **4-54** (1.74 g, 6.12 mmol). Cold H₂O (29.2 mL) was added over 5 min, and the resulting heterogeneous mixture was vigorously stirred at rt for 2 h. The white precipitate that formed was isolated on a 15 mL medium fritted glass funnel, washed with copious H₂O, and air-dried for 15 min to afford the title compound (1.10 g, 5.25 mmol, 86% yield) as a white solid (mp = 88.3–90.2 °C). IR (neat) 2927, 2853, 2360, 2344, 1648, 1455, 1136, 1001 cm⁻¹. ¹H NMR: (500.2 MHz, (CD₃)₂CO) δ 6.95 (dd, *J* = 17.6, 10.3 Hz, 1H), 6.66 (s, 2H), 6.13 (ddd, *J* = 15.1, 10.3, 0.7 Hz, 1H), 5.84 (dt, *J* = 14.7, 7.2 Hz, 1H), 5.44 (d, *J* = 17.6 Hz, 1H), 2.11 (dtd, *J* = 7.7, 7.3, 1.1 Hz, 2H), 1.41 (tt, *J* = 7.9, 7.5 Hz, 2H), 1.30 (m, 10H), 0.88 (t, *J* = 6.9 Hz, 3H); ¹³C NMR: (125.8 MHz, (CD₃)₂CO) δ 149.3, 139.3, 134.6, 34.1, 33.5, 30.8, 30.7, 24.2, 15.2; HRMS (EI) calculated for $[C_{12}H_{23}BO_2]^+$ requires m/z 210.1791, found m/z 210.1779.



(1E,3E)-1-Azidododeca-1,3-diene (Table 4-2, entries 12-13, **4-32**).

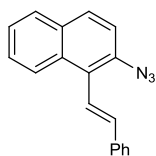
A 25 mL round bottomed flask was charged with anhydrous CuSO₄ (76.6 mg, 0.480 mmol) and sodium azide (374 mg, 5.76 mmol). Then MeOH (14.4 mL) was added followed immediately by (1E,3E)-dodeca-1,3-dien-1-ylboronic acid **4-55** (1009 mg, 4.80 mmol). The heterogeneous brown solution was stirred vigorously open to the atmosphere for 12 h. Thereafter, the volatiles were removed *in vacuo* and the crude residue was dissolved in CH₂Cl₂ and filtered through a pad of silica (1:1 hexanes:EtOAc). The volatiles were removed *in vacuo* and the residue was purified via flash column chromatography on silica (hexanes) to afford the title compound (318 mg, 1.53 mmol, 32% yield) as a pale yellow oil. IR (neat) 2102, 1651, 1611, 1457, 972 cm⁻¹. ¹H NMR: (499.8 MHz, C₆D₆) δ 5.85 (dd, *J* = 13.2, 11.0 Hz, 1H), 5.75 (dtd, *J* = 15.0, 10.8, 1.3 Hz, 1H), 5.45 (d, *J* = 13.2 Hz, 1H), 5.39 (dt, *J* = 14.6, 7.1 Hz, 1H), 1.96 (dtd, *J* = 7.9, 7.3, 1.3 Hz,

2H), 1.27 (m, 12H), 0.91 (t, $J = 6.9$ Hz, 3H); ^{13}C NMR: (125.7 MHz, C_6D_6) δ 133.9, 126.7, 126.4, 120.6, 32.8, 32.0, 29.6, 29.4, 29.3, 22.8, 14.1; HRMS (EI) calculated for $[\text{C}_{12}\text{H}_{21}\text{N}_3]^+$ requires m/z 207.1735, found m/z 179.1669 ($[\text{M}-\text{N}_2]^+$, requires m/z 179.1674).



(E)-1-Styrylnaphthalen-2-amine (4-56). To a 100 mL round bottomed flask was added 1-bromonaphthalen-2-amine (500 mg, 2.25 mmol),³⁵ *trans*-2-phenylvinylboronic acid (500 mg, 3.38 mmol), K_2CO_3 (1245 mg, 9.01 mmol), and

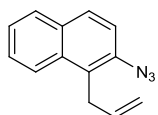
$\text{Pd}(\text{PPh}_3)_4$ (260 mg, 0.225 mmol). The system was equipped with a reflux condenser, evacuated, and purged with N_2 before adding toluene (23 mL), EtOH (9 mL), and H_2O (4.5 mL). The reaction was heated to 100 °C and refluxed for 72 h. Thereafter, the reaction was cooled to rt and diluted with H_2O (30 mL) and CH_2Cl_2 (30 mL). The organic layer was separated, and the aqueous layer was extracted with CH_2Cl_2 (2 x 30 mL). The combined organic layers were washed with H_2O (1 x 30 mL) and brine (1 x 30 mL), dried over Na_2SO_4 , filtered, and concentrated *in vacuo*. The crude residue was purified via flash column chromatography on silica using a solvent gradient (20:1 to 10:1 hexanes:EtOAc) to afford the title compound (359 mg, 1.46 mmol, 65% yield) as a bright yellow solid (mp = 74.9–76.5 °C). IR (neat) 3448, 3377, 3055, 3023, 2361, 2339, 1618, 1512, 1394, 1280, 1146 cm^{-1} . ^1H NMR: (500.0 MHz, CDCl_3) δ 7.92 (d, $J = 8.6$ Hz, 1H), 7.71 (d, $J = 8.0$ Hz, 1H), 7.62 (d, $J = 8.6$ Hz, 1H), 7.60 (m, 2H), 7.40 (m, 4H), 7.32 (tt, $J = 7.2, 1.2$ Hz, 1H), 7.25 (td, $J = 8.1, 1.2$ Hz, 1H), 7.00 (d, $J = 8.8$ Hz, 1H), 6.97 (d, $J = 16.8$ Hz, 1H), 4.13 (s, 2H); ^{13}C NMR: (125.7 MHz, CDCl_3) δ 141.5, 137.4, 135.2, 133.2, 128.8, 128.7, 128.3, 128.2, 127.8, 126.5, 126.3, 123.7, 123.4, 122.4, 118.4, 115.3; HRMS (EI) calculated for $[\text{C}_{18}\text{H}_{16}\text{N}_3]^+$ requires m/z 246.1278, found m/z 246.1282.



(E)-2-Azido-1-styrylnaphthalene (Table 4-2, entry 14, **4-34**). To a 100 mL round bottomed flask was added (*E*)-1-styrylnaphthalen-2-amine (**4-56**) (200 mg, 0.815 mmol) followed by H_2O (4.5 mL) and glacial AcOH (4.5 mL). The heterogeneous

mixture was cooled to 0 °C and allowed to stir for 10 min before adding NaNO_2 (78.8 mg, 1.14

mmol) in a single portion. The resulting dark orange mixture was stirred at 0 °C for 1 h. Subsequently, NaN₃ (79.4 mg, 1.22 mmol) was added portionwise over 3 min and the resulting yellow solution was warmed to rt and stirred for 45 min. The reaction was diluted with H₂O (30 mL) and Et₂O (30 mL) and transferred to a 250 mL Erlenmeyer flask with a large stir bar. The solution was vigorously stirred while solid Na₂CO₃ was added until pH ~ 7. The organic layer was separated and the aqueous layer was extracted with Et₂O (2 x 30 mL). The organic layers were combined and washed with H₂O (2 x 20 mL) and brine (1 x 20 mL) before being dried over Na₂SO₄. The volatiles were removed *in vacuo* and the residue was purified via flash column chromatography on silica using a solvent gradient (50:1 to 25:1 hexanes:EtOAc) to afford the title compound (139 mg, 0.512 mmol, 63% yield) as an off-white solid (mp = 95.5–96.1 °C). IR (thin film) 3081, 3061, 2953, 2327, 2111, 2051, 1640, 1619, 1598, 1299 cm⁻¹. ¹H NMR: (500.0 MHz, CDCl₃) δ 8.21 (d, *J* = 8.7 Hz, 1H), 7.83 (d, *J* = 7.8 Hz, 1H), 7.82 (d, *J* = 8.7 Hz, 1H), 7.60 (d, *J* = 7.5 Hz, 2H), 7.51 (td, *J* = 6.9, 1.3 Hz, 1H), 7.43 (m, 4H), 7.37 (d, *J* = 8.8 Hz, 1H), 7.31 (tt, *J* = 7.1, 1.3 Hz, 1H), 7.04 (d, *J* = 16.8 Hz, 1H); ¹³C NMR: (125.7 MHz, CDCl₃) δ 137.3, 136.4, 134.3, 132.5, 131.3, 129.1, 128.8, 128.5, 128.0, 127.1, 126.6, 125.3, 125.2, 125.1, 121.9, 117.2, HRMS (EI) calculated for [C₁₈H₁₃N₃]⁺ requires *m/z* 271.1109, found *m/z* 243.1044 ([M-N₂]⁺, requires *m/z* 243.1043).



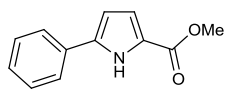
1-Allyl-2-azidonaphthalene (Table 4-2, entry 15, **4-36**). To a flame-dried 25 mL round bottomed flask was added 1-bromonaphthalen-2-amine (290 mg, 1.31 mmol).³⁵ The flask was equipped with a reflux condenser and the system was evacuated and purged with N₂ before adding DMF (3.3 mL), allyltributylstannane (519 mg, 1.56 mmol), and Pd(PPh₃)₄ (151 mg, 0.131 mmol). The mixture was heated to 85 °C and stirred for 40 h. Thereafter, the reaction was cooled to rt and diluted with H₂O (5 mL) and Et₂O (10 mL). The organic layer was separated, and the aqueous layer was extracted with Et₂O (4 x 5 mL). The combined organic layers were washed with H₂O (4 x 5 mL) and subsequently dried over

Na₂SO₄. The volatiles were removed *in vacuo* and the residue was purified via flash column chromatography on silica (9:1 hexanes:EtOAc) to afford 1-allylnaphthalen-2-amine (176 mg, 0.960 mmol, 73% yield) as a pale yellow oil. To a 100 mL round bottomed flask was added 1-allylnaphthalen-2-amine (171 mg, 0.933 mmol) followed by H₂O (5.2 mL) and glacial AcOH (5.2 mL). The heterogeneous mixture was cooled to 0 °C and allowed to stir for 10 min before adding NaNO₂ (90.1 mg, 1.31 mmol) in a single portion. The resulting dark orange mixture was stirred at 0 °C for 1 h. Subsequently, NaN₃ (91 mg, 1.40 mmol) was added portionwise over 3 min and the resulting yellow solution was warmed to rt and stirred for 1 h. The reaction was diluted with H₂O (30 mL) and Et₂O (30 mL) and transferred to a 250 mL Erlenmeyer flask with a large stir bar. The solution was vigorously stirred while solid Na₂CO₃ was added until pH ~ 7. The organic layer was separated and the aqueous layer was extracted with Et₂O (2 x 30 mL). The organic layers were combined and washed with H₂O (2 x 20 mL) and brine (1 x 20 mL) before being dried over Na₂SO₄. The volatiles were removed *in vacuo* and the residue was purified via flash column chromatography on silica (50:1 hexanes:EtOAc) to afford the title compound (151 mg, 0.722 mmol, 77% yield) as a pale yellow oil. IR (thin film) 3081, 3061, 2953, 2327, 2111, 2051, 1640, 1619, 1598, 1299 cm⁻¹. ¹H NMR: (500.0 MHz, CDCl₃) δ 7.94 (d, *J* = 8.6 Hz, 1H), 7.81 (m, 2H), 7.52 (td, *J* = 6.8, 1.2 Hz, 1H), 7.43 (t, *J* = 7.8 Hz, 1H), 7.35 (d, *J* = 8.7 Hz, 1H), 6.00 (ddt, *J* = 17.3, 10.6, 6.2 Hz, 1H), 5.02 (dd, *J* = 10.3, 1.6 Hz, 1H), 4.96 (dd, *J* = 17.3, 1.6 Hz, 1H), 3.82 (d, *J* = 6.0 Hz, 2H); ¹³C NMR: (125.7 MHz, CDCl₃) δ 135.9, 134.6, 132.9, 131.2, 128.7, 128.7, 127.0, 125.2, 125.0, 124.2, 116.9, 115.7, 30.7, HRMS (EI) calculated for [C₁₃H₁₁N₃]⁺ requires *m/z* 209.0948, found *m/z* 209.0944.

4.6.3. Cyclizations of Vinyl and Aryl Azides

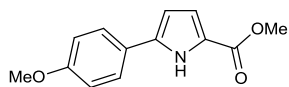
General procedure for visible light sensitization of azides: To an oven-dried 25 mL Schlenk tube with a stir bar was added the azide (0.75 mmol, 1 equiv.), Ru(dtbbpy)₃(PF₆)₂ or [Ir(dF(CF₃)ppy)₂(dtbbpy)](PF₆) (0.0075 mmol, 0.01 equiv.), and freshly distilled CHCl₃ (7.5 mL,

0.1 M). The solution was submitted to three freeze-pump-thaw cycles, purged with N₂, and irradiated at rt with a 1 W blue light-emitting diode (LED) strip ($\lambda = 465\text{--}470$ nm). Upon completion of the reaction, the mixture was concentrated *in vacuo*, and the crude residue was purified by flash column chromatography to afford the pure pyrrole.



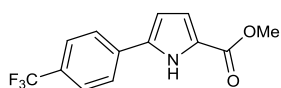
Methyl 5-phenyl-1H-pyrrole-2-carboxylate (Table 4-2, entry 1, **4-13**).

Experiment 1: Prepared according to the General Procedure using 172 mg (0.75 mmol) of (2Z,4E)-methyl 2-azido-5-phenylpenta-2,4-dienoate **4-12**,⁹ 9.0 mg (0.0075 mmol) of Ru(dtbbpy)₃(PF₆)₂, 7.5 mL of chloroform, and an irradiation time of 3 h. Purified by flash column chromatography on silica using a solvent gradient (7:1 to 5:1 hexanes:EtOAc) to afford 148 mg (0.74 mmol, 98% yield) of the pyrrole as a white solid. Experiment 2: 172 mg (0.75 mmol) of dienyl azide, 9.2 mg (0.0077 mmol) of Ru(dtbbpy)₃(PF₆)₂, and 7.5 mL of chloroform. Isolated 150 mg (0.75 mmol, 99% yield). All spectral data were in complete agreement with previously reported values.⁹



Methyl 5-(4-methoxyphenyl)-1H-pyrrole-2-carboxylate (Table 4-2, entry 2, **4-15**). Experiment 1: Prepared according to the General

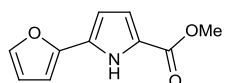
Procedure using 195 mg (0.75 mmol) of (2Z,4E)-methyl 2-azido-5-(4-methoxyphenyl)penta-2,4-dienoate **4-14**,⁹ 9.1 mg (0.0076 mmol) of Ru(dtbbpy)₃(PF₆)₂, 7.5 mL of chloroform, and an irradiation time of 4 h. Purified by flash column chromatography on silica using a solvent gradient (4:1 to 3:1 hexanes:EtOAc) to afford 171 mg (0.74 mmol, 98% yield) of the pyrrole as a white solid. Experiment 2: 194 mg (0.75 mmol) of dienyl azide, 9.0 mg (0.0075 mmol) of Ru(dtbbpy)₃(PF₆)₂, and 7.5 mL of chloroform. Isolated 172 mg (0.74 mmol, 99% yield). All spectral data were in complete agreement with previously reported values.⁹



Methyl 5-(4-(trifluoromethyl)phenyl)-1H-pyrrole-2-carboxylate (Table 4-2, entry 3, **4-17**). Experiment 1: Prepared according to the

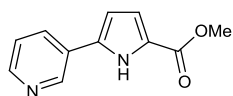
General Procedure using 224 mg (0.75 mmol) of (2Z,4E)-methyl 2-azido-5-(4-

(trifluoromethyl)phenyl)penta-2,4-dienoate **4-16**,⁹ 9.0 mg (0.0075 mmol) of Ru(dtbbpy)₃(PF₆)₂, 7.5 mL of chloroform, and an irradiation time of 2.5 h. Purified by flash column chromatography on silica using a solvent gradient (8:1 to 6:1 hexanes:EtOAc) to afford 194 mg (0.72 mmol, 96% yield) of the pyrrole as a white solid. Experiment 2: 223 mg (0.75 mmol) of dienyl azide, 9.1 mg (0.0076 mmol) of Ru(dtbbpy)₃(PF₆)₂, and 7.5 mL of chloroform. Isolated 190 mg (0.71 mmol, 95% yield). All spectral data were in complete agreement with previously reported values.⁹



Methyl 5-(furan-2-yl)-1H-pyrrole-2-carboxylate (Table 4-2, entry 4, **4-19**).

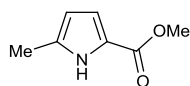
Experiment 1: Prepared according to the General Procedure using 164 mg (0.75 mmol) of (2Z,4E)-methyl 2-azido-5-(furan-2-yl)penta-2,4-dienoate **4-18**,⁹ 9.1 mg (0.0076 mmol) of Ru(dtbbpy)₃(PF₆)₂, 7.5 mL of chloroform, and an irradiation time of 4 h. Purified by flash column chromatography on silica using a solvent gradient (4:1 to 3:1 hexanes:EtOAc) to afford 142 mg (0.74 mmol, 99% yield) of the pyrrole as a white solid. Experiment 2: 164 mg (0.75 mmol) of dienyl azide, 9.0 mg (0.0075 mmol) of Ru(dtbbpy)₃(PF₆)₂, and 7.5 mL of chloroform. Isolated 138 mg (0.72 mmol, 96% yield). All spectral data were in complete agreement with previously reported values.⁹



Methyl 5-(pyridin-3-yl)-1H-pyrrole-2-carboxylate (Table 4-2, entry 5, **4-21**).

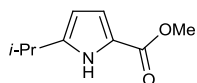
Experiment 1: Prepared according to the General Procedure using 173 mg (0.75 mmol) of (2Z,4E)-methyl 2-azido-5-(pyridin-3-yl)penta-2,4-dienoate **4-20**, 9.2 mg (0.0077 mmol) of Ru(dtbbpy)₃(PF₆)₂, 7.5 mL of chloroform, and an irradiation time of 3 h. Purified by flash column chromatography on silica using a solvent gradient (1:1 to 1:2 hexanes:EtOAc) to afford 132 mg (0.65 mmol, 87% yield) of the pyrrole as a white solid (mp = 147.9–149.4 °C). Experiment 2: 173 mg (0.75 mmol) of dienyl azide, 9.0 mg (0.0075 mmol) of Ru(dtbbpy)₃(PF₆)₂, and 7.5 mL of chloroform. Isolated 132 mg (0.65 mmol, 86% yield). IR (neat) 3321, 2952, 1689, 1645, 1436, 1283, 1156 cm⁻¹. ¹H NMR: (500.2 MHz, CDCl₃) δ 9.96 (m, 1H), 8.93 (dd, *J* = 2.2, 0.7 Hz, 1H), 8.55 (dd, *J* = 4.8, 1.8 Hz, 1H), 7.89 (app dtd, *J* = 8.0, 2.2, 1.7

Hz, 1H), 7.34 (ddd, $J = 8.0, 4.9, 0.7$ Hz, 1H), 6.99 (dd, $J = 3.9, 2.5$ Hz, 1H), 6.60 (dd, $J = 3.8, 2.7$ Hz, 1H), 3.90 (s, 3H); ^{13}C NMR: (125.8 MHz, CDCl_3) δ 161.8, 148.6, 146.4, 133.7, 132.0, 127.5, 124.1, 123.6, 117.0, 108.9, 51.8; HRMS (EI) calculated for $[\text{C}_{11}\text{H}_{10}\text{N}_2\text{O}_2]^+$ requires m/z 202.0742, found m/z 202.0740.



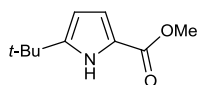
Methyl 5-methyl-1H-pyrrole-2-carboxylate (Table 4-2, entry 6, **4-3**).

Experiment 1: Prepared according to the General Procedure using 126 mg (0.75 mmol) of (2Z,4E)-methyl 2-azidohexa-2,4-dienoate **4-1**, 9.0 mg (0.0075 mmol) of $\text{Ru}(\text{dtbbpy})_3(\text{PF}_6)_2$, 7.5 mL of chloroform, and an irradiation time of 8 h. Purified by flash column chromatography on silica using a solvent gradient (9:1 to 7:1 hexanes:EtOAc) to afford 96 mg (0.69 mmol, 92% yield) of the pyrrole as a white solid. Experiment 2: 126 mg (0.75 mmol) of dienyl azide, 9.0 mg (0.0075 mmol) of $\text{Ru}(\text{dtbbpy})_3(\text{PF}_6)_2$, and 7.5 mL of chloroform. Isolated 99 mg (0.71 mmol, 95% yield). All spectral data were in complete agreement with previously reported values.^{9,36}



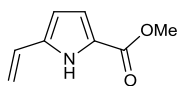
Methyl 5-isopropyl-1H-pyrrole-2-carboxylate (Table 4-2, entry 7, **4-23**).

Experiment 1: Prepared according to the General Procedure using 146 mg (0.75 mmol) of (2Z,4E)-methyl 2-azido-6-methylhepta-2,4-dienoate **4-21**, 9.0 mg (0.0075 mmol) of $\text{Ru}(\text{dtbbpy})_3(\text{PF}_6)_2$, 7.5 mL of chloroform, and an irradiation time of 11 h. Purified by flash column chromatography on silica using a solvent gradient (9:1 to 7:1 hexanes:EtOAc) to afford 111 mg (0.66 mmol, 89% yield) of the pyrrole as a white solid (mp = 59.8–61.8 °C). Experiment 2: 147 mg (0.75 mmol) of dienyl azide, 9.0 mg (0.0075 mmol) of $\text{Ru}(\text{dtbbpy})_3(\text{PF}_6)_2$, and 7.5 mL of chloroform. Isolated 112 mg (0.67 mmol, 89% yield). IR (neat) 3311, 2956, 1682, 1496, 1221, 1158 cm^{-1} . ^1H NMR: (500.2 MHz, CDCl_3) δ 9.10 (br s, 1H), 6.83 (dd, $J = 3.6, 2.5$ Hz, 1H), 5.98 (m, 1H), 3.83 (s, 3H), 2.96 (septet, $J = 6.8$ Hz, 1H), 1.28 (d, $J = 6.8$ Hz, 6H); ^{13}C NMR: (125.8 MHz, CDCl_3) δ 161.9, 144.8, 120.8, 115.9, 106.1, 51.3, 27.4, 22.3; HRMS (EI) calculated for $[\text{C}_9\text{H}_{13}\text{NO}_2]^+$ requires m/z 167.0946, found m/z 167.0938.



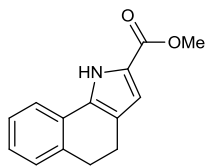
Methyl 5-(tert-butyl)-1H-pyrrole-2-carboxylate (Table 4-2, entry 8, **4-25**).

Experiment 1: Prepared according to the General Procedure using 157 mg (0.75 mmol) of (2Z,4E)-methyl 2-azido-6,6-dimethylhepta-2,4-dienoate **4-24**, 9.0 mg (0.0075 mmol) of Ru(dtbbpy)₃(PF₆)₂, 7.5 mL of chloroform, and an irradiation time of 14 h. Purified by flash column chromatography on silica using a solvent gradient (9:1 to 7:1 hexanes:EtOAc) to afford 115 mg (0.63 mmol, 85% yield) of the pyrrole as a white solid (mp = 125.0–126.8 °C). Experiment 2: 157 mg (0.75 mmol) of dienyl azide, 9.0 mg (0.0075 mmol) of Ru(dtbbpy)₃(PF₆)₂, and 7.5 mL of chloroform. Isolated 119 mg (0.66 mmol, 88% yield). IR (neat) 3333, 2952, 1689, 1492, 1274, 1171 cm⁻¹. ¹H NMR: (500.2 MHz, CDCl₃) δ 8.98 (br s, 1H), 6.82 (dd, *J* = 3.7, 2.5 Hz, 1H), 6.00 (dd, *J* = 3.7, 2.7 Hz, 1H), 3.83 (s, 3H), 1.32 (s, 9H); ¹³C NMR: (125.8 MHz, CDCl₃) δ 161.9, 147.8, 120.8, 115.7, 105.7, 51.4, 31.8, 30.3; HRMS (EI) calculated for [C₁₀H₁₅NO₂]⁺ requires *m/z* 181.1103, found *m/z* 181.1100.

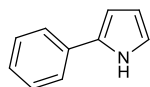


Methyl 5-vinyl-1H-pyrrole-2-carboxylate (Table 4-2, entry 9, **4-27**).

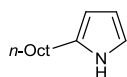
Experiment 1: Prepared according to the General Procedure using 134 mg (0.75 mmol) of (2Z,4E)-methyl 2-azidohepta-2,4,6-trienoate **4-26**, 9.1 mg (0.0076 mmol) of Ru(dtbbpy)₃(PF₆)₂, 7.5 mL of chloroform, and an irradiation time of 2 h. Purified by flash column chromatography on silica using a solvent gradient (8:1 to 7:1 hexanes:EtOAc) to afford 99 mg (0.65 mmol, 87% yield) of the pyrrole as a white solid (mp = 100.3–101.4 °C). Experiment 2: 134 mg (0.75 mmol) of dienyl azide, 9.1 mg (0.0076 mmol) of Ru(dtbbpy)₃(PF₆)₂, and 7.5 mL of chloroform. Isolated 102 mg (0.67 mmol, 90% yield). IR (neat) 3285, 1682, 1483, 1439, 1331, 1257, 1149, 1052 cm⁻¹. ¹H NMR: (500.2 MHz, CDCl₃) δ 9.26 (m, 1H), 6.86 (dd, *J* = 3.8, 2.4 Hz, 1H), 6.55 (dd, *J* = 17.8, 11.2 Hz, 1H), 6.27 (dd, *J* = 3.7, 2.7 Hz, 1H), 5.57 (d, *J* = 17.9 Hz, 1H), 5.22 (d, *J* = 11.4 Hz, 1H), 3.86 (s, 1H); ¹³C NMR: (125.8 MHz, CDCl₃) δ 161.6, 135.3, 126.3, 122.5, 116.3, 113.1, 109.7, 51.5; HRMS (EI) calculated for [C₈H₉NO₂]⁺ requires *m/z* 151.0633, found *m/z* 151.0628.



Methyl 4,5-dihydro-1H-benzo[g]indole-2-carboxylate (Table 4-2, entry 10, **4-29**). Experiment 1: Prepared according to the General Procedure using 191 mg (0.75 mmol) of (*Z*)-methyl 2-azido-3-(3,4-dihydronaphthalen-2-yl)acrylate **4-28**, 9.1 mg (0.0076 mmol) of Ru(dtbbpy)₃(PF₆)₂, 7.5 mL of chloroform, and an irradiation time of 4 h. Purified by flash column chromatography on silica using a solvent gradient (6:1 to 4:1 hexanes:EtOAc) to afford 164 mg (0.72 mmol, 96% yield) of the pyrrole as a white solid (mp = 145.3–147.0 °C). Experiment 2: 191 mg (0.75 mmol) of dienyl azide, 9.0 mg (0.0075 mmol) of Ru(dtbbpy)₃(PF₆)₂, and 7.5 mL of chloroform. Isolated 165 mg (0.73 mmol, 97% yield). IR (neat) 3303, 2844, 1686, 1448, 1300, 766 cm⁻¹. ¹H NMR: (499.8 MHz, CDCl₃) δ 9.75 (br s, 1H), 7.47 (m, 1H), 7.19 (m, 3H), 6.78 (d, *J* = 2.2 Hz, 1H), 3.90 (s, 3H), 2.94 (t, *J* = 7.1 Hz, 1H), 2.75 (t, *J* = 7.1 Hz, 1H); ¹³C NMR: (125.7 MHz, CDCl₃) δ 162.2, 136.4, 133.0, 128.6, 128.1, 127.0, 126.7, 121.9, 121.8, 120.4, 114.4, 51.7, 29.8, 21.5; HRMS (EI) calculated for [C₁₄H₁₃NO₂]⁺ requires *m/z* 227.0946, found *m/z* 227.0950.

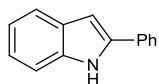


2-Phenyl-1H-pyrrole (Table 4-2, entry 11, **4-31**). Experiment 1: Prepared according to the General Procedure using 129 mg (0.75 mmol) of ((1*E*,3*E*)-4-azidobuta-1,3-dien-1-yl)benzene **4-30**, 9.1 mg (0.0076 mmol) of Ru(dtbbpy)₃(PF₆)₂, 7.5 mL of chloroform, and an irradiation time of 3 h. Purified by flash column chromatography on silica using a solvent gradient (7:1 to 6:1 hexanes:EtOAc) to afford 100 mg (0.70 mmol, 93% yield) of the pyrrole as a white solid. Experiment 2: 128 mg (0.75 mmol) of dienyl azide, 9.0 mg (0.0075 mmol) of Ru(dtbbpy)₃(PF₆)₂, and 7.5 mL of chloroform. Isolated 97 mg (0.68 mmol, 90% yield). All spectral data were in complete agreement with a sample of commercially available material.



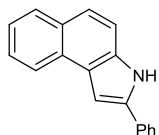
2-Octyl-1H-pyrrole (Table 4-2, entries 12-13, **4-33**). Experiment 1: Prepared according to the General Procedure using 156 mg (0.75 mmol) of (1*E*,3*E*)-1-azidododeca-1,3-diene **4-32**, 9.0 mg (0.0075 mmol) of Ru(dtbbpy)₃(PF₆)₂, 7.5 mL of chloroform, and an irradiation time of 36 h. Purified by flash column chromatography on silica using a

solvent gradient (10:1 to 8:1 hexanes:EtOAc) to afford 61 mg (0.34 mmol, 45% yield) of the pyrrole as a clear oil that turned yellow upon standing. Experiment 2: 156 mg (0.75 mmol) of dienyl azide, 9.2 mg (0.0077 mmol) of Ru(dtbbpy)₃(PF₆)₂, and 7.5 mL of chloroform. Isolated 66 mg (0.37 mmol, 49% yield). Experiment 3: Prepared according to the General Procedure using 156 mg (0.75 mmol) of (1*E*,3*E*)-1-azidododeca-1,3-diene **4-32**, 8.4 mg (0.0075 mmol) of [Ir(dF(CF₃)ppy)₂(dtbbpy)](PF₆), 7.5 mL of chloroform, and an irradiation time of 12 h. Purified by flash column chromatography on silica using a solvent gradient (10:1 to 8:1 hexanes:EtOAc) to afford 91 mg (0.51 mmol, 68% yield) of the pyrrole. Experiment 4: 156 mg (0.75 mmol) of dienyl azide, 8.3 mg (0.0074 mmol) of [Ir(dF(CF₃)ppy)₂(dtbbpy)](PF₆), and 7.5 mL of chloroform. Isolated 95 mg (0.53 mmol, 71% yield). IR (neat) 3383, 2952, 2931, 2856, 1567, 1467, 1093 cm⁻¹. ¹H NMR: (500.2 MHz, CDCl₃) δ 7.89 (br s, 1H), 6.66 (dd, *J* = 2.7, 1.6 Hz, 1H), 6.13 (app dt, *J* = 3.0, 2.6 Hz, 1H), 5.91 (m, 1H), 2.59 (m, 2H), 1.62 (tt, *J* = 7.9, 6.7 Hz, 2H), 1.30 (m, 10H), 0.88 (t, *J* = 6.7 Hz, 3H); ¹³C NMR: (125.7 MHz, CDCl₃) δ 133.0, 116.0, 108.3, 104.9, 32.0, 29.8, 29.5, 29.5, 29.3, 27.8, 22.8, 14.2; HRMS (EI) calculated for [C₁₂H₂₁N]⁺ requires *m/z* 179.1674, found *m/z* 179.1669.



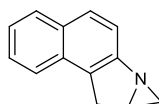
2-Phenyl-1*H*-indole (Table 4-2, entry 14, **4-35**). Experiment 1: Prepared according to the General Procedure using 166 mg (0.75 mmol) of (*E*)-1-azido-2-

styrylbenzene **4-34**, 9.0 mg (0.0075 mmol) of Ru(dtbbpy)₃(PF₆)₂, 7.5 mL of chloroform, and an irradiation time of 20 h. Purified by flash column chromatography on silica (20:1 hexanes:EtOAc) to afford 107 mg (0.55 mmol, 74% yield) of the pyrrole as a white solid. Experiment 2: 166 mg (0.75 mmol) of dienyl azide, 9.0 mg (0.0075 mmol) of Ru(dtbbpy)₃(PF₆)₂, and 7.5 mL of chloroform. Isolated 110 mg (0.57 mmol, 76% yield). All spectral data were in complete agreement with previously reported values.²



2-Phenyl-3H-benzo[e]indole (Table 4-2, entry 15, **4-37**). Experiment 1:

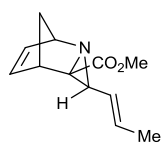
Prepared according to the General Procedure using 204 mg (0.75 mmol) of (*E*)-2-azido-1-styrylnaphthalene **4-36**, 9.1 mg (0.0076 mmol) of Ru(dtbbpy)₃(PF₆)₂, 7.5 mL of chloroform, and an irradiation time of 6 h. Purified by flash column chromatography on silica (9:1 hexanes:EtOAc) to afford 169 mg (0.69 mmol, 93% yield) of the pyrrole as a white solid (mp = 136.6–137.1 °C). Experiment 2: 204 mg (0.75 mmol) of dienyl azide, 9.0 mg (0.0075 mmol) of Ru(dtbbpy)₃(PF₆)₂, and 7.5 mL of chloroform. Isolated 167 mg (0.69 mmol, 92% yield). IR (neat) 3427, 3048, 1621, 1603, 1484, 1455, 1333, 1181, 1026 cm⁻¹. ¹H NMR: (500.0 MHz, CDCl₃) δ 8.65 (br s, 1H), 8.27 (d, *J* = 8.1 Hz, 1H), 7.90 (d, *J* = 8.1 Hz, 1H), 7.72 (m, 2H), 7.61 (d, *J* = 8.8 Hz, 1H), 7.56 (m, 2H), 7.47 (m, 2H), 7.43 (td, *J* = 6.9, 1.0 Hz, 1H), 7.38 (d, *J* = 1.9 Hz, 1H), 7.32 (tt, *J* = 7.2, 1.2 Hz, 1H); ¹³C NMR: (125.7 MHz, CDCl₃) δ 136.1, 133.2, 132.5, 129.4, 129.1, 128.6, 128.1, 127.4, 125.9, 124.9, 124.3, 123.6, 123.4, 123.0, 112.5, 99.3; HRMS (EI) calculated for [C₁₈H₁₄N]⁺ requires *m/z* 244.1121, found *m/z* 244.1116.



8a,9-Dihydro-8H-azirino[1,2-a]benzo[e]indole (**4-56**). Prepared according to

the General Procedure using 103 mg (0.49 mmol) of 1-allyl-2-azidonaphthalene (**4-54**), 5.5 mg (0.0049 mmol) of [Ir(dF(CF₃)ppy)₂(dtbbpy)](PF₆), 4.9 mL of chloroform, and an irradiation time of 5 h. Purified by flash column chromatography on silica (3:2 hexanes:EtOAc) to afford 71 mg (0.39 mmol, 81% yield) of the aziridine as an off-white solid (mp = 78.4–80.8 °C). IR (neat) 3060, 3024, 2988, 2904, 2850, 1625, 1586, 1517, 1460, 1257, 1157 cm⁻¹. ¹H NMR: (500.0 MHz, CDCl₃) δ 7.84 (d, *J* = 8.3 Hz, 1H), 7.68 (d, *J* = 8.7 Hz, 1H), 7.64 (d, *J* = 8.4 Hz, 1H), 7.49 (d, *J* = 8.6 Hz, 1H), 7.47 (m, 1H), 7.39 (m, 1H), 3.69 (d, *J* = 16.8 Hz, 1H), 3.56 (dd, *J* = 16.8, 7.4 Hz, 1H), 3.18 (m, 1H), 2.46 (d, *J* = 5.3 Hz, 1H), 1.41 (d, *J* = 3.9 Hz, 1H); ¹³C NMR: (125.7 MHz, CDCl₃) δ 155.7, 131.5, 131.3, 130.0, 128.6, 128.0, 126.3, 124.4, 123.5, 119.5, 41.2, 39.4, 31.7; HRMS (EI) calculated for [C₁₃H₁₁N]⁺ requires *m/z* 181.0886, found *m/z* 181.0884.

4.6.4. *n*Oe Studies and Manipulation of the Azirine Intermediate



Methyl 3-((*E*)-prop-1-en-1-yl)-2-azatricyclo[3.2.1.0^{2,4}]oct-6-ene-4-carboxylate

(4-38). To an oven-dried 25 mL Schlenk tube with a stir bar was added 41.8 mg

(0.25 mmol) of (2*Z*,4*E*)-methyl 2-azidohepta-2,4-dienoate **4-1**, 16.5 mg (0.25

mmol) of freshly cracked cyclopentadiene, 3.0 mg (0.0025 mmol) of Ru(dtbbpy)₃(PF₆)₂, and 2.5

mL of CH₃CN. The solution was submitted to three freeze-pump-thaw cycles, purged with N₂,

and irradiated at rt with a 1 W blue light-emitting diode (LED) strip (λ = 465–470 nm) for 150

min. Thereafter, the reaction was diluted with 1:1 hexanes:EtOAc (1 mL) and eluted through a

short silica plug. The volatiles were removed *in vacuo*, and the residue was purified via flash

column chromatography on silica (3:2 hexanes:EtOAc) to afford the title compound (36.1 mg,

0.176 mmol, 71% yield) as a clear oil. IR (neat) 3060, 3024, 2988, 2904, 2850, 1625, 1586,

1517, 1460, 1257, 1157 cm⁻¹. ¹H NMR: (500.0 MHz, CDCl₃) δ 6.19 (dd, *J* = 5.4, 2.4 Hz, 1H),

5.73 (m, 1H), 5.72 (dq, *J* = 16.0, 6.6 Hz, 1H), 5.47 (ddq, *J* = 16.0, 8.0, 1.6 Hz, 1H), 4.20 (s, 1H),

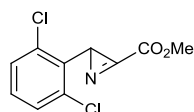
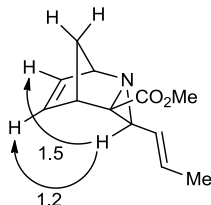
3.78 (s, 3H), 3.53 (s, 1H), 2.09 (d, *J* = 8.1 Hz, 1H), 2.02 (dt, *J* = 8.1, 1.8 Hz, 1H), 1.69 (d, *J* = 8.1

Hz, 1H), 1.67 (dd, *J* = 6.6, 1.5 Hz, 1H); ¹³C NMR: (125.7 MHz, CDCl₃) δ 172.3, 132.6, 130.4,

128.6, 126.3, 66.8, 58.9, 54.6, 52.4, 49.6, 47.4, 18.0; HRMS (EI) calculated for [C₁₂H₁₆NO₂]⁺

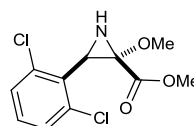
requires *m/z* 206.1176, found *m/z* 206.1173.

The relative stereochemistry of **4-38** was determined using NOESY1D spectra – Varian's standard NOESY1D Chempack sequence was used with a typical setup as follows: mix=0.7 x T₁(shortest) ~ 1 s, d1=3 x T₁(longest) ~ 12 s, nt=16, ss=-2, selective pulse using a seduce shape. The numbers shown are % enhancements measured as ratios of integrals, normalized by number of protons involved, of the enhanced to selected protons.



Methyl 2-(2,6-dichlorophenyl)-2H-azirine-3-carboxylate (4-40). Prepared

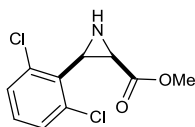
according to the General Procedure using 204 mg (0.75 mmol) of vinyl azide **4-39**, 8.4 mg (0.0049 mmol) of $[\text{Ir}(\text{dF}(\text{CF}_3)\text{ppy})_2(\text{dtbbpy})](\text{PF}_6)$, 7.5 mL of chloroform, and an irradiation time of 8 h. Thereafter, the volatiles were removed *in vacuo* and the resulting residue was recrystallized from benzene/hexanes to afford 165 mg (0.68 mmol, 90% yield) of the azirine as an off-white solid. All spectral data were in complete agreement with previously reported values.^{5c}



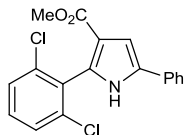
Methyl 3-(2,6-dichlorophenyl)-2-methoxyaziridine-2-carboxylate (4-42).

To a flame-dried 12 mL vial was added a solution of NaOMe (freshly prepared from 5.7 mg Na (0.25 mmol) in 1.23 mL MeOH). The solution was cooled to 0 °C and then THF (1.23 mL) was added. The solution was stirred for 5 min before adding methyl 2-(2,6-dichlorophenyl)-2H-azirine-3-carboxylate **4-40** (30 mg, 0.123 mmol) in a single portion. The reaction immediately turned light yellow and was stirred for 10 min, at which time TLC analysis indicated complete consumption of the azirine. The reaction was quenched with H₂O (5 mL) and extracted into EtOAc (2 x 25 mL). The organic layers were combined and washed with brine (1 x 25 mL), dried over Na₂SO₄, filtered, and concentrated *in vacuo* to give a clear residue that was purified via flash column chromatography using a solvent gradient (4:1 to 2:1 hexanes:EtOAc) to afford the title product (31 mg, 0.11 mmol, 91% yield) as a clear oil as a single diastereomer. IR (neat) 3277, 1740, 1533, 1121, 777 cm⁻¹. ¹H NMR: (500.0 MHz, CDCl₃) δ 7.29 (d, *J* = 8.0 Hz, 2H), 7.17 (t, *J* = 8.0 Hz, 1H), 3.71 (s, 3H), 3.57 (s, 3H) 3.47 (d, *J* = 9.8 Hz, 1H), 2.61 (d, *J* = 9.7 Hz, 1H); ¹³C NMR: (125.7 MHz, CDCl₃) δ 169.6, 135.6, 130.8, 129.5,

128.5, 73.9, 54.8, 53.3, 46.8; HRMS (EI) calculated for $[C_{11}H_{12}Cl_2NO_3]^+$ requires m/z 276.0189, found m/z 276.0194.



Methyl 3-(2,6-dichlorophenyl)aziridine-2-carboxylate (4-43). To a flame-dried 24 mL vial was added methyl 2-(2,6-dichlorophenyl)-2*H*-aziridine-3-carboxylate **4-40** (120 mg, 0.492 mmol). The system was evacuated and purged with N_2 three times before adding CH_2Cl_2 (4.9 mL). The homogenous solution was cooled to -78 °C and subsequently a solution of Bu_4NBH_4 (127 mg, 0.492 mmol) in CH_2Cl_2 (4.9 mL) was added dropwise over 5 min. The reaction was stirred for an additional 30 min, after which 1H NMR showed no remaining azirine. The reaction was warmed to 0 °C and H_2O (5 mL) was added to quench the reaction. The organic layer was separated and further extracted with H_2O (2 x 5 mL), washed with brine (1 x 5 mL), dried over Na_2SO_4 , filtered, and the volatiles were removed *in vacuo* to afford 198 mg of a viscous yellow oil. The residue was dissolved in CH_2Cl_2 (2 mL) and eluted through a short plug of silica gel (4:1 hexanes:EtOAc). The volatiles were removed *in vacuo* and the resulting residue was purified via flash column chromatography on silica (5:1 hexanes:EtOAc) to afford the title compound (72 mg, 0.293 mmol, 58% yield) as a clear oil as a single diastereomer. IR (neat) 3282, 1723, 1546, 1132, 798 cm^{-1} . 1H NMR: (500.0 MHz, $CDCl_3$) δ 7.29 (d, $J = 8.0$ Hz, 2H), 7.17 (t, $J = 8.0$ Hz, 1H), 3.65 (s, 3H), 3.27 (br s, 1H), 3.10 (br s, 1H), 2.02 (br s, 1H); ^{13}C NMR: (125.7 MHz, $CDCl_3$) δ 171.1, 136.0, 131.5, 129.4, 128.4, 52.6, 39.1, 36.9; HRMS (EI) calculated for $[C_{10}H_9Cl_2NO_2]^+$ requires m/z 245.0010, found m/z 245.0008. The relative stereochemistry was determined by performing a D_2O shake – the broad singlets at δ 3.27 and δ 3.10 resolved to δ 3.27 (dd, $J = 9.6, 5.8$ Hz, 1H), 3.10 (dd, $J = 7.8, 5.8$ Hz, 1H). The $^3J = 5.8$ Hz coupling is consistent with a *cis* relationship of the aziridine ring protons.



Methyl 2-(2,6-dichlorophenyl)-5-phenyl-1H-pyrrole-3-carboxylate (4-45). To

a flame-dried 12 mL vial under N_2 was added methyl 2-(2,6-dichlorophenyl)-2H-azirine-3-carboxylate **4-40** (100 mg, 0.41 mmol) and 1-phenyl-2-(triphenylphosphanylidene)-ethanone (156 mg, 0.41 mmol) followed by CH_2Cl_2 (2.0 mL). The reaction was stirred at rt for 24 h after which the mixture was directly purified via flash column chromatography using a solvent gradient (5:1 to 2:1 hexanes:EtOAc) to afford the title product (82 mg, 0.24 mmol, 58% yield) as a white solid (mp = 161.6–163.1 °C). IR (neat) 3319, 2962, 1689, 1645, 1436, 1137 cm^{-1} . 1H NMR: (500.0 MHz, $CDCl_3$) δ 8.54 (br s, 1H), 7.53 (d, J = 7.3 Hz, 2H), 7.42 (m, 4H), 7.30 (m, 2H), 7.04 (d, J = 3.0 Hz, 1H), 3.71 (s, 3H); ^{13}C NMR: (125.7 MHz, $CDCl_3$) δ 164.4, 136.6, 132.6, 131.4, 131.1, 131.0, 130.6, 129.1, 127.9, 127.3, 124.1, 116.3, 107.4, 51.2; HRMS (EI) calculated for $[C_{18}H_{14}Cl_2NO_2]^+$ requires m/z 346.0397, found m/z 346.0409.

4.7 References

¹ (a) Narayanam, J. M. R.; Tucker, J. W.; Stephenson, C. R. J. Electron-transfer photoredox catalysis: Development of a tin-free reductive dehalogenation reaction. *J. Am. Chem. Soc.* **2009**, *131*, 8756–8757; (b) Nagib, D. A.; MacMillan, D. W. C. Trifluoromethylation of arenes and heteroarenes by means of photoredox catalysis. *Nature* **2011**, *480*, 224–228; (c) DiRocco, D. A.; Rovis, T. Catalytic asymmetric α -acylation of tertiary amines mediated by a dual catalysis mode: N-heterocyclic carbene and photoredox catalysis. *J. Am. Chem. Soc.* **2012**, *134*, 8094–8097; (d) Kalyani, D.; McMurtrey, K. B.; Neufeldt, S. R.; Sanford, M. S. Room-temperature C-H arylation: merger of Pd-catalyzed C-H functionalization and visible-light photocatalysis. *J. Am. Chem. Soc.* **2011**, *133*, 18566–18569; (e) Maity, S.; Zhu, M.; Shinabery, R. S.; Zheng, N. Intermolecular [3+2] cycloaddition of cyclopropylamines with olefins by visible-light photocatalysis. *Angew. Chem.* **2012**, *124*, 226–230; *Angew. Chem. Int. Ed.* **2012**, *51*, 222–226.

² In accord with this hypothesis, we recently reported that the same class of transition metal photocatalysts can also promote [2+2] cycloaddition reactions of (a) styrenes (b) dienes via a complementary energy transfer process. See (a) Lu, Z.; Yoon, T. P. Visible light photocatalysis of [2+2] styrene cycloadditions by energy transfer. *Angew. Chem. Int. Ed.* **2012**, *51*, 10329–10332. (b) Hurlley, A. E.; Yoon, T. P. [2+2] cycloaddition of 1,3-dienes by visible light photocatalysis. *Angew. Chem. Int. Ed.* **2014**, *53*, 8991–8994.

³ Xiao has also reported a photocatalytic [2+2] oxindole dimerization that they have suggested to occur via energy transfer: Zou, Y.-Q.; Duan, S.-W.; Meng, X.-G.; Hu, H.-Q.; Gao, S.; Chen, J. R.; Xiao, W. J. Visible light induced intermolecular [2+2]-cycloaddition reactions of 3-ylideneoxindoles through energy transfer pathway. *Tetrahedron* **2012**, *68*, 6914–6918.

⁴ (a) Nicholas, P. P. Thermolysis of ethyl azidoformate in 2,3-dimethyl-2-butene. Example of a simple olefin giving a dominant 1,2,3- Δ^2 -triazoline intermediate. *J. Org. Chem.* **1975**, *40*, 3396–3398; (b) Li, Z.; Quan, R. W.; Jacobsen, E. N. Mechanism of the (diimine)copper-catalyzed asymmetric aziridination of alkenes. Nitrene transfer via ligand-accelerated catalysis. *J. Am. Chem. Soc.* **1995**, *117*, 5889–5890; (c) Bergmeier, S. C.; Stanchina, D. M. Acylnitrene route to vicinal amino alcohols. Application to the synthesis of (–)-bestatin and analogues. *J. Org. Chem.* **1999**, *64*, 2852–2859.

⁵ (a) Hemetsberger, H.; Knittel, D.; Weidmann, H. Enazide, 3. Mitt.: Thermolyse von α -azidozimestern; synthese von indolderivaten. *Monatsh. Chem.* **1970**, *101*, 161–165; (b) Knittel, D. Verbesserte synthese von α -azidozimtsäure-estern und 2H-azirinen. *Synthesis* **1985**, 186–188; (c) Henn, L.; Hickey, D. M. B.; Moody, C. J.; Rees, C. W. Formation of indoles, isoquinolines, and other fused pyridine from azidoacrylates. *J. Chem. Soc. Perkin Trans. 1* **1984**, 2189–2196; (d) Tichenor, M. S.; Trzupsek, J. D.; Kastrinsky, D. B.; Shiga, F.; Hwang, I.; Boger, D. L. Asymmetric total synthesis of (+)- and *ent*(–)-Yatakemycin and duocarmycin SA: evaluation of Yatekemycin key partial structure and its unnatural enantiomer. *J. Am. Chem. Soc.* **2006**, *128*, 15683–15696; (e) Stokes, B. J.; Dong, H.; Leslie, B. E.; Pumphrey, A. L.; Driver, T. G. Intramolecular C-H amination reactions: exploitation of the Rh₂(II)-catalyzed decomposition of azidoacrylates. *J. Am. Chem. Soc.* **2007**, *129*, 7500–7501.

⁶ (a) Hemetsberger, H.; Spira, I.; Schoenfelder, W. *J. Chem. Res. Synop.* **1977**, 247–249; (b) C. J. Moody, G. J. Warrelow, Vinyl azides in heterocyclic synthesis. Part 10. Synthesis of the isoindolobenzazepine alkaloid lennoxamine. *J. Chem. Soc. Perkin Trans. 1* **1990**, 2929–2936.

⁷ *Azides and Nitrenes, Reactivity and Utility*; E. F. V. Scriven, Ed.; Academic: New York, **1984**, pp. 205–246.

⁸ (a) Lwowski, W.; Mattingly, T. W. The decomposition of ethyl azidoformate in cyclohexene and in cyclohexane. *J. Am. Chem. Soc.* **1964**, *87*, 1947–1958; (b) Lewis, F. D.; Saunders, W. H. Sensitized photolysis of organic azides. Possible case of nonclassical energy transfer. *J. Am. Chem. Soc.* **1968**, *90*, 7033–7038; (c) Marcinek, A.; Leyva, E.; Whitt, D.; Platz, M. S. Evidence for stepwise nitrogen extrusion and ring expansion upon photolysis of phenyl azide. *J. Am. Chem. Soc.* **1993**, *115*, 8609–8612; (d) Borden, W. T.; Gritsan, N. P.; Hadad, C. M.; Karney, W. L.; Kemnitz, C. R.; Platz, M. S. The interplay of theory and experiment in the study of phenylnitrene. *Acc. Chem. Res.* **2000**, *33*, 765–771; (e) Singh, P. N. D.; Mandel, S. M.; Sankaranarayanan, J.; Muthukrishnan, S.; Chang, M.; Robinson, R. M.; Lahti, P. M.; Ault, B. S.; Gudmundsdóttir, A. D. Selective formation of triplet alkyl nitrenes from photolysis of β -azido-propiophenone and their reactivity. *J. Am. Chem. Soc.* **2007**, *129*, 16263–16272.

⁹ Dong, H.; Shen, M.; Redford, J.; Stokes, B. J.; Pumphrey, A. L.; Driver, T. G. Transition metal-catalyzed synthesis of pyrroles from dienyl azides. *Org. Lett.* **2007**, *9*, 5191–5194.

¹⁰ Lowry, M.S.; Goldsmith, J.I.; Slinker, J.D.; Rohl, R.; Pascal, R.A.; Malliaras, G.G.; Bernhard, S. Single-layer electroluminescent devices and photoinduced hydrogen production from an ionic iridium(III) complex. *Chem. Mater.* **2005**, *17*, 5712–5719. Note: the value for the 4+/3+*

reduction potential of $[\text{Ir}(\text{dF}(\text{CF}_3)\text{ppy})_2(\text{dtbbpy})]^{+*}$ is misreported; we measured this value to be ($E^\circ(\text{Ir}^{4+/3+*}) = -0.89$ V vs. SCE in MeCN).

¹¹ Theoretical calculations on azides **4-1**, **4-32**, and **4-50** were performed using the Gaussian 09 software package. Geometrical optimization of the dienyl azide was carried out at the B3LYP/6-31G(d) level of theory prior to performing excited state calculations at the same level of theory.

¹² (a) L'abbé, G.; Mathys, G. Mechanism of the thermal decomposition of vinyl azides. *J. Org. Chem.* **1974**, *39*, 1778–1779; (b) Isomura, K.; Ayabe, G.-I.; Hatano, S.; Taniguchi, H. Evidence for vinyl nitrene intermediates in the thermal rearrangement of 2*H*-azirines into indoles. *J. Chem. Soc. Chem. Commun.* **1980**, 1252–1253.

¹³ The excited state redox potentials were obtained under the assumption that the Helmholtz free energy change for the transition from the ground state to the ³MLCT state can be approximated by the corresponding minimum-to-minimum energy difference (2.00–2.04 eV for the complexes studied). See Navon, G.; Sutin, N. Mechanism of the Quenching of the Phosphorescence of Tris(2,2'-bipyridine)ruthenium(II) by Some Cobalt(III) and Ruthenium(III) Complexes. *Inorg. Chem.* **1974**, *13*, 2159–2164.

¹⁴ (a) Bernhard, S.; Barron, J.A.; Houston, P.L.; Abruna, H.D.; Ruglovsky, J.L.; Gao, X.; Malliaras, G.G. Electroluminescence in ruthenium(II) complexes. *J. Am. Chem. Soc.* **2002**, *124*, 13624–13628. (b) Rillema, D.P.; Allen, G.; Meyer, T.J.; Conrad, D. Redox properties of ruthenium(II) tris chelate complexes containing the ligands 2,2'-bipyrazine, 2,2'-bipyridine, and 2,2'-bipyrimidine. *Inorg. Chem.* **1983**, *22*, 1617–1622.

¹⁵ Murata, S.; Nakatsuki, R.; Tomioka, H. Mechanistic studies of pyrene-sensitized decomposition of *p*-butylphenyl azide: generation of nitrene radical anion through a sensitizer-mediated electron transfer from amines to the azide. *J. Chem. Soc. Perkin Trans 2*, **1995**, 793–799.

¹⁶ Due to the open-shell electronic configuration of this excited singlet, intersystem crossing to the ground state triplet at room temperature in fluid solution is slow and has not been observed. See (a) Borden, W.T.; Gritsan, N.P.; Hadad, C.M.; Karney, W.L.; Kemnitz, C.R.; Platz, M.S. The interplay of theory and experiment in the study of phenylnitrene. *Acc. Chem. Res.* **2000**, *33*, 765–771. (b) Burdzinski, G.; Hackett, J.C.; Wang, J.; Gustafson, T.L.; Hadad, C.M.; Platz, M.S. Early events in the photochemistry of aryl azides from femtosecond UV/Vis spectroscopy and quantum chemical calculations. *J. Am. Chem. Soc.* **2006**, *128*, 13402–13411.

¹⁷ (a) Nair, V. Azirines. In *Small Ring Heterocycles Part 1: Aziridines, Azirines, Thiiranes, Thiirenes*; Hassner, A., Ed.; John Wiley and Sons: New York, 1983; pp 215-332. (b) Palacios, F.; de Retana, A. M. O.; de Marigorta, E. M.; de los Santos, J. M. *Eur. J. Org. Chem.* **2001**, 2401–2414.

¹⁸ (a) Rajam, S.; Murthy, R. S.; Jadhav, A. V.; Li, Q.; Keller, C.; Carra, C.; Pace, T. C. S.; Bohne, C.; Ault, B. S.; Gudmundsdóttir, A. D. Photolysis of (3-methyl-2*H*-azirin-2-yl)-phenylmethanone: direct detection of a triplet vinylnitrene intermediate. *J. Org. Chem.* **2011**, *76*, 9934–9945. (b) Sarkar, S. K.; Sawai, A.; Kanahara, K.; Wentrup, C.; Abe, M.; Gudmundsdóttir, A. D. Direct detection of a triplet vinylnitrene, 1,4-naphthoquinone-2-yl nitrene, in solution and cryogenic matrices. *J. Am. Chem. Soc.* **2015**, *137*, 4207–4214.

- ¹⁹ Turro, N.J.; Ramamurthy, V.; Scaiano, J.C. In "Modern molecular photochemistry of organic molecules", University Science Books, Sausalito, CA, 2010, pp. 169–196.
- ²⁰ (a) Damrauer, N. H.; Cerullo, G.; Yeh, A.; Boussie, T. R.; Shank, C. V.; McCusker, J. K. Femtosecond dynamics of excited-state evolution in [Ru(bpy)₃]²⁺. *Science* **1997**, *275*, 54–57.
(b) Yeh, A.; Shank, C. V.; McCusker, J. K. Ultrafast electron localization dynamics following photo-induced charge transfer. *Science* **2000**, *289*, 935–938.
- ²¹ O'Brien, A.G.; Levesque, F.; Seeberger, P.H. Continuous flow thermolysis of azidoacrylates for the synthesis of heterocycles and pharmaceutical intermediates. *Chem. Commun.* **2011**, *47*, 2688–2690.
- ²² Shen, M.; Leslie, B.E.; Driver, T.G. Dirhodium(II)-catalyzed intramolecular C-H amination of aryl azides. *Angew. Chem. Int. Ed.* **2008**, *47*, 5056–5059.
- ²³ Alves, M.J.; Gilchrist, T.L. Methyl 2-aryl-2H-azirine-3-carboxylates as dienophiles. *J. Chem. Soc. Perkin Trans 1* **1998**, 299–303.
- ²⁴ Alves, M.J.; Fortes, G.; Guimaraes, E.; Lemos, A. Intermolecular alkyl radical addition to methyl 2-(2,6-dichlorophenyl)-2H-azirine-3-carboxylate. *Synlett* **2003**, 1403–1406.
- ²⁵ Piers, E.; Jung, G.L.; Ruediger, E.H. Synthesis of functionalized bicyclo[3.2.1]octa-2,6-dienes by thermal rearrangement of substituted 6-exo-(1-alkenyl)bicyclo[3.1.0]hex-2-ene systems. *Can. J. Chem.* **1987**, *65*, 670–682.
- ²⁶ Milton-Fry, M.J.; Cullen, A.J.; Sammakia, T. The total synthesis of the oxopolyene macrolide RK-397. *Angew. Chem. Int. Ed.* **2007**, *46*(7), 1066–1070.
- ²⁷ Mock, W. L.; Tsou, H.-R. Procedure for diethoxymethylation of ketones. *J. Org. Chem.* **1981**, *46*, 2557–2561.
- ²⁸ Dasgupta, R.; Ghatak, R. A simple synthesis of α,β -unsaturated aldehydes by 1,3-carbonyl transposition through one carbon homologation. *Tetrahedron Lett.* **1985**, *26*(12), 1581–1584.
- ²⁹ Thota, N.; Reddy, M. V.; Kumar, A.; Khan, I. A.; Sangwan, P. L.; Kalia, N. P.; Koul, J. L.; Koul, S. Substituted dihydronaphthalenes as efflux pump inhibitors of *Staphylococcus aureus*. *Eur. J. Med. Chem.* **2010**, *45*, 3607–3616.
- ³⁰ Tao, G. -Z.; Cui, X.; Li, J.; Liu, A. -X.; Liu, L.; Guo, Q. -X. Copper-catalyzed synthesis of aryl azides and 1-aryl-1,2,3-triazoles from boronic acids. *Tetrahedron Lett.* **2007**, *48*, 3525–3529.
- ³¹ Torrado, A.; López, S.; Alvarez, R.; de Lera, A. R. General synthesis of retinoids and arotinoids via palladium-catalyzed cross-coupling of boronic acids with electrophiles. *Synthesis* **1995**, 285–293.
- ³² Peterson, M. A.; Polt, R. E-1-lithio-1-alkenes in hydrocarbon solvent. *Synth. Commun.* **1992**, *22*(3), 477–480.

³³ Negishi, E.; Kitora, M.; Xu, C. Direct synthesis of terminal alkynes via Pd-catalyzed cross coupling of aryl and alkenyl halides with ethynylmetals containing Zn, Mg, and Sn. Critical comparison of counteractions. *J. Org. Chem.* **1997**, *62*(25), 8957–8960.

³⁴ Brown, H. C.; Gupta, S. K. Catecholborane (1,3,2-benzodioxaborole) as a new, general monohydroboration reagent for alkynes. Convenient synthesis of alkeneboronic esters and acids from alkynes via hydroboration. *J. Am. Chem. Soc.* **1972**, *94*, 4370–4371.

³⁵ Couzijn, E. P. A.; van den Engel, D. W. F.; Slootweg, J. C.; de Kanter, F. J. J.; Ehlers, A. W.; Schakel, M.; Lammertsma, K. Configurationally rigid pentaorganosilicates. *J. Am. Chem. Soc.* **2002**, *131*, 3741–3751.

³⁶ Yoshida, M.; Uchiyama, K.; Narasaka, K. Synthesis of dihydropyrroles and tetrahydropyridines by the cyclization of *O*-methylsulfonyloximes having an active methine group. *Heterocycles* **2000**, *52*, 681–691.

**Chapter 5. Towards a Photocatalytic Enantioselective Radical Cation Diels–Alder
Cycloaddition**

5.1 Introduction

Despite increasing efforts in recent years, new methods for the enantioselective formation of chiral compounds by photochemical methods remain scarce. One common explanation for the dearth of successful methods is that the high energy content (80–120 kcal/mol) of a photoactivated substrate gives rise to rapid radiative and non-radiative relaxation pathways as well as low activation barriers for subsequent transformations. In addition, our group and Bach's have emphasized the need to outcompete the occurrence of any racemic background reactivity. Thus, photocatalytic stereocontrol is an inherently challenging problem for which there is no general solution.

The most frequently employed method to achieve catalytic enantioselective photochemical reactions in solution involves exciplex formation using a selectively excited chiral sensitizer.¹ However, our group, among others, has demonstrated that visible light induced electron transfer can be employed to achieve a diverse range of bond forming events. Given that these electron transfer reactions proceed via the intermediacy of radical ions, the challenge of effecting enantiofacial discrimination in these reactions involves the differentiation of enantiotopic faces of a radical ion in diastereomeric transition states. Herein we present previously unexplored concepts for imparting stereochemical control upon reactions involving radical cation chemistry.

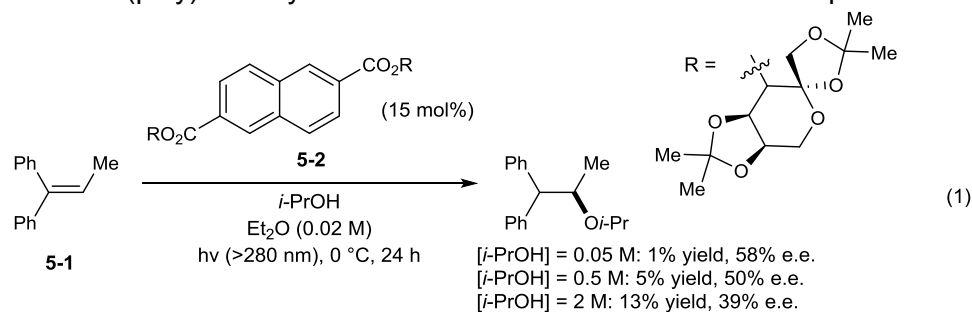
The reemergence of radical chemistry in the synthetic literature coincides with the improved control over chemo-, regio-, and stereoselectivity in such transformations.² While early approaches to enantioselective radical reactions relied upon a covalently bound chiral auxiliary-radical pair to control the configuration of a newly-formed stereogenic center,³ a number of recent investigations have obviated the need for enantiofacial control via chiral auxiliaries. First, facial discrimination can occur when a Lewis acid coordinated to a chiral ligand set chelates a substrate.⁴ Our group has demonstrated this strategy within the context of a photocatalytic [2+2] radical anion cycloaddition, in which a two-catalyst system consisting of

$\text{Ru}(\text{bpy})_3^{2+}$ and a chiral Lewis acid cocatalyst promotes a highly stereoselective cycloaddition.⁵ Alternatively, it is possible to differentiate the enantiotopic faces of a prochiral radical with chiral reagents, such as chiral hydrogen-atom donors.⁶ However, chiral templates based upon purely noncovalent interactions that achieve comparable levels of stereocontrol have only lately been established. In recent studies, Bach and co-workers were able to demonstrate that a chiral hydrogen-bonding template induced high levels of enantioselectivity in radical reactions.⁷

These former studies prompted our continued investigations pertaining to the control of absolute stereochemistry in bimolecular reactions of radical ion intermediates. In particular, we wondered if we might be able to develop a general approach for asymmetric induction in reactions of radical cation intermediates, which cannot coordinate readily to an electrophilic chiral Lewis acid. Transformations involving these highly electrophilic species have thus far failed to succumb to classical paradigms of asymmetric induction.

The only reported reaction proceeding via a putative radical cation intermediate for which modest levels of enantioinduction (up to 58%) were achieved is the chiral arene(poly)carboxylate-sensitized anti-Markovnikov addition of alcohol nucleophiles to 1,1-diphenylpropene (Scheme 5-1).^{8a} A detailed mechanistic analysis revealed that enantioselectivity is imparted by the relative stability of diastereomeric exciplexes formed from the ground state of electron rich alkene **5-1** and the excited state of naphthalene sensitizer **5-2**.^{8b} Specifically, it was found that the combination of nonpolar solvents and polar chiral saccharide moieties covalently bound to the sensitizer facilitates electron transfer from **5-1** to give a chiral radical ion pair between the radical cation of **5-1** and reduced **5-2**. The dissociation energy of this chiral ion pair, however, is prohibitively high due to low bulk solvent polarity, and hence the chiral information is effectively transferred from the sensitizer to substrate within the proposed confined radical ion pair.

Scheme 5-1. Arene(poly)carboxylate-sensitized addition of alcohol nucleophiles



While this strategy provided the first example of moderate levels of absolute stereochemical control in reactions proceeding via a putative radical cation intermediate, the requirement for a large excess of the polar nucleophile (*i*-PrOH) revealed a dramatic tradeoff between chemical and optical yield as [*i*-PrOH] was increased. A common occurrence in asymmetric photochemical reactions proceeding via electron transfer, this trend was previously observed by Schuster in the context of Diels–Alder reactions sensitized by axially chiral dicyanonaphthalene frameworks.^{1d,9} This is a potentially powerful strategy to induce asymmetrical facial bias in radical ion reactions as well as reactions resulting in significant charge polarization prior to nucleophilic attack. However, generalization of these studies is challenging, as exciplex formation cannot easily be predicted *a priori* and is often sensitive to small structural perturbations.

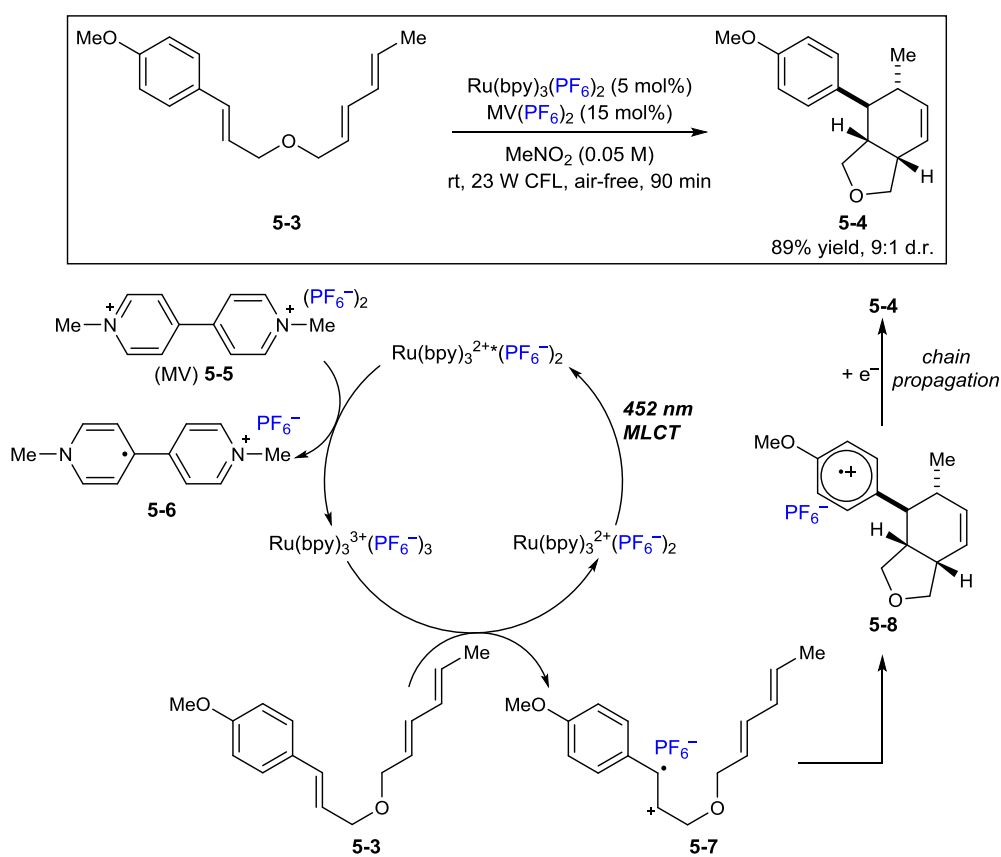
5.2 System Design: First-Generation Approach

We sought a fundamentally different strategy for achieving asymmetric induction in radical cation reactions. Based on recent work in our research group, we hypothesized that photoinduced electron transfer from an electron rich styrene to a ruthenium bipyridyl complex containing a chiral counteranion would afford a chiral ion pair. Indeed, maintaining charge neutrality requires that the radical cation be counterbalanced by an opposing negative charge, namely the counteranion introduced with the ruthenium complex. Based on the studies of Inoue

and Schuster, interception of this chiral ion pair with a diene was expected to afford enantioenriched cycloadduct.

Our photocatalyzed radical cation Diels–Alder cycloaddition chemistry offered an ideal platform to test this hypothesis (Scheme 5-2).¹⁰ The proposed mechanism begins with excitation of $\text{Ru}(\text{bpy})_3^{2+}$ and metal-to-ligand charge transfer (MLCT) to give the mildly reducing triplet $\text{Ru}(\text{bpy})_3^{2+*}$. In the presence of methyl viologen (MV) **5-5** oxidative quenching occurs to afford a strongly oxidizing $\text{Ru}(\text{bpy})_3^{3+}$ species. Thereafter, one-electron oxidation of electron-rich tethered styrenyl substrate **5-3** ($E_{\text{ox}} = +1.22 \text{ V}$)¹¹ affords delocalized radical cation **5-7**. Subsequent intramolecular cycloaddition proceeds to furnish **5-8** that suffers reduction via chain propagation to yield **5-4**.

Scheme 5-2. Mechanistic proposal for a photocatalyzed radical cation Diels–Alder cycloaddition



Radical cation **5-7** exists as an ion pair with the only counterbalancing negative charge in solution: that (PF_6^-) which is introduced with the photocatalyst and methyl viologen. It follows that a decrease in solvent dielectric should result in a substantial increase in Coulombic attraction between **5-7** and PF_6^- . If the energy of this attraction is greater than the thermal energy available to separate the charges, **5-7** and PF_6^- will form a strong ion pair (a contact ion pair).¹² It seemed plausible that a chiral counteranion might afford transfer of stereochemical information within this contact ion pair.

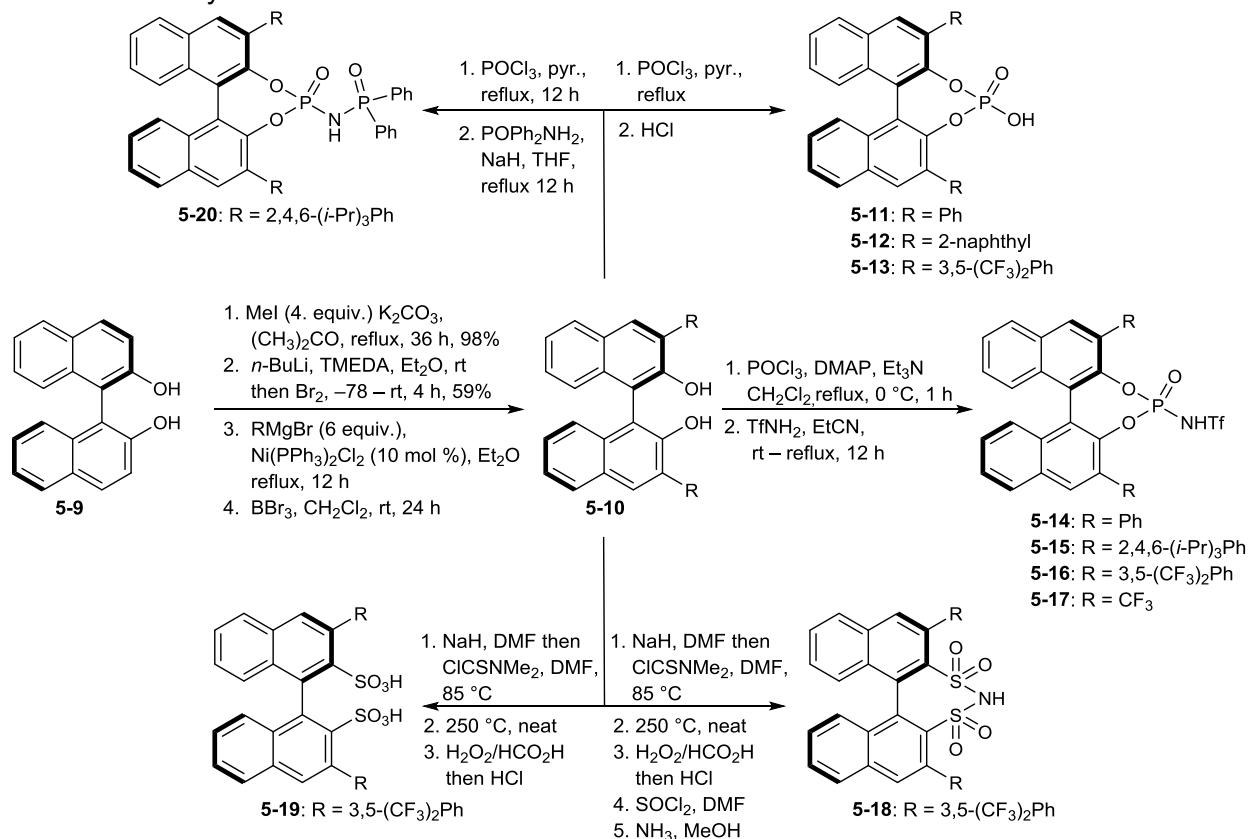
5.3 Results and Discussion: First-Generation Approach

To begin study of the reaction depicted in Scheme 5-2 a variety of $\text{Ru}(\text{bpy})_3^{2+}(\text{X}^*)_2$ and $\text{MV}(\text{X}^*)_2$ complexes were synthesized, where X^* denotes a chiral counteranion. As to the identity of X^* , we elected to study chiral conjugate bases derived from 1,1'-binaphthyl-2,2'-diol (BINOL, **5-9**) monophosphoric acids **5-11** (Scheme 5-3).¹³ The chiral ion pairs between chiral phosphate anions and prochiral cations, including iminium ions,¹⁴ metal ions,¹⁵ and carbocations,¹⁶ have led to the development of highly enantioselective transformations. Additionally, BINOL derivatives are amenable to facile synthesis.¹⁷

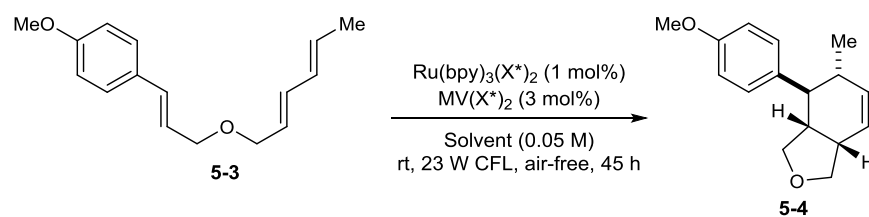
A library of BINOL derivatives (Scheme 5-3) was prepared from common precursor **5-10** according to known methods, and the resulting acids were converted to their respective ammonium phosphate or silver (I) phosphate salts.^{17,18,19} Subsequently, conditions for counteranion metathesis with $\text{Ru}(\text{bpy})_3\text{Cl}_2$ and MVCl_2 were realized by heating the complexes in MeOH followed by chromatography on neutral Al_2O_3 . However, when the resulting chiral $\text{Ru}(\text{bpy})_3(\text{X}^*)_2$ and $\text{MV}(\text{X}^*)_2$ complexes were evaluated in the intramolecular radical cation Diels-Alder reaction, inconsistent and irreproducible reactivity was observed. Hypothesizing incomplete salt metathesis or photodecomposition arising from residual silver salts, the BINOL derivatives were prepared as their sodium salts. The resulting $\text{Ru}(\text{bpy})_3(\text{X}^*)_2$ and $\text{MV}(\text{X}^*)_2$ complexes were also further purified by diffusion recrystallization. With this more rigorous

methodology, all synthesized $\text{Ru}(\text{bpy})_3(\text{X}^*)_2$ and $\text{MV}(\text{X}^*)_2$ species exhibited the expected stoichiometry for 1:2 complexes and gave reproducible reactivity.

Scheme 5-3. Synthesis of substituted BINOL **5-10** and derivatization



These newly synthesized complexes were evaluated in the intramolecular Diels-Alder reaction (Table 5-1). To begin, a nonpolar solvent screen was undertaken with $\text{Ru}(\text{bpy})_3(\text{X}^*)_2$ and $\text{MV}(\text{X}^*)_2$ complexes containing chiral phosphate counteranions **5-11**[−], **5-12**[−], and **5-13**[−]. However, it was discovered that these complexes afforded < 5% conversion of **5-3** in solvents with a lower dielectric constant than acetone ($\epsilon = 21.0$). In contrast, all of the other $\text{Ru}(\text{bpy})_3(\text{X}^*)_2$ and $\text{MV}(\text{X}^*)_2$ complexes gave moderate reactivity in CH₂Cl₂ and CHCl₃. Reactions carried out in other common nonpolar organic solvents (PhCH₃, Et₂O, THF, PhCF₃) gave essentially no conversion of **5-3**, likely due to poor solubility of the $\text{Ru}(\text{bpy})_3(\text{X}^*)_2$ and $\text{MV}(\text{X}^*)_2$ complexes in these solvents.

Table 5-1. Chiral catalyst and oxidative quencher screen^a

| entry | X* | pK _a (HX*) ^e | solvent | yield 5-4 ^b | d.r. 5-4 ^b | e.e. (major) ^c | remaining 5-3 ^b |
|-------|--------------------------|------------------------------------|---------------------------------|-------------------------------|------------------------------|---------------------------|-----------------------------------|
| 1 | 5-11 ⁻ | 3.86 | MeNO ₂ | 15% | 3:1 | 26% | 68% |
| 2 | 5-11 ⁻ | | CH ₂ Cl ₂ | < 5% | — | — | — |
| 3 | 5-12 ⁻ | 3.77 | MeNO ₂ | 13% | 3:1 | 35% | 75% |
| 4 | 5-13 ⁻ | 2.63 | MeNO ₂ | < 5% | — | — | — |
| 5 | 5-14 ⁻ | — | MeNO ₂ | 64% | 7:1 | 10% | 0% |
| 6 | 5-14 ⁻ | | CH ₂ Cl ₂ | 12% | 3.5:1 | 27% | 62% |
| 7 | 5-14 ⁻ | 3.34 | CHCl ₃ | < 5% | — | — | 85% |
| 8 | 5-15 ⁻ | | CH ₂ Cl ₂ | 11% | 2:1 | 22% | 37% |
| 9 | 5-15 ⁻ | — | CHCl ₃ | 6% | 5:1 | — | 27% |
| 10 | 5-16 ⁻ | | CH ₂ Cl ₂ | 32% | 5:1 | 17% | 35% |
| 11 | 5-16 ⁻ | — | CHCl ₃ | 8% | 5:1 | 28% | 55% |
| 12 | 5-17 ⁻ | | CH ₂ Cl ₂ | 16% | 4.3:1 | 8% | 21% |
| 13 | 5-17 ⁻ | 1.74 | CHCl ₃ | < 5% | — | — | 36% |
| 14 | 5-18 ⁻ | | CH ₂ Cl ₂ | 12% | 1.2:1 | — | 73% |
| 15 | 5-18 ⁻ | — | CHCl ₃ | 9% | 1.5:1 | — | 70% |
| 16 | 5-20 ⁻ | | MeNO ₂ | 11% | 2.5:1 | 9% | 45% |

^aTo an oven-dried 25-mL Schlenk tube with a magnetic stirrer was added Ru(bpy)₃(X*)₂ and MV(X*)₂ followed by a stock solution of **5-3** (0.05 mmol) and trimethyl(phenyl)silane internal standard (0.05 mmol) in dry solvent (0.05 M). The solution was submitted to 3 freeze-pump-thaw cycles, purged with N₂ and irradiated at room temperature with a 23 W (1380 lumens) compact fluorescent bulb for 45 h.

^bSubsequently, an aliquot was collected for ¹H NMR analysis to determine yield **5-4**, d.r. **5-4** and remaining **5-3**, and the reaction was thereafter diluted with EtOAc and passed through a silica plug eluting with EtOAc. Volatiles were removed *in vacuo* and the crude mixture was submitted to silica gel chromatography to obtain a purified mixture of diastereomers. ^cDetermined by SFC analysis on Daicel OD-H chiral stationary phase eluting with MeOH (6%, isocratic, 3 mL/min total flow rate). ^dReactions affording low conversion of **5-3** to **5-4** precluded further analysis, and these results are denoted with a “—”. ^epK_a values (± 0.08) are reported for the conjugate acids of X* in DMSO solvent; unreported data is denoted with a “—”.²⁰

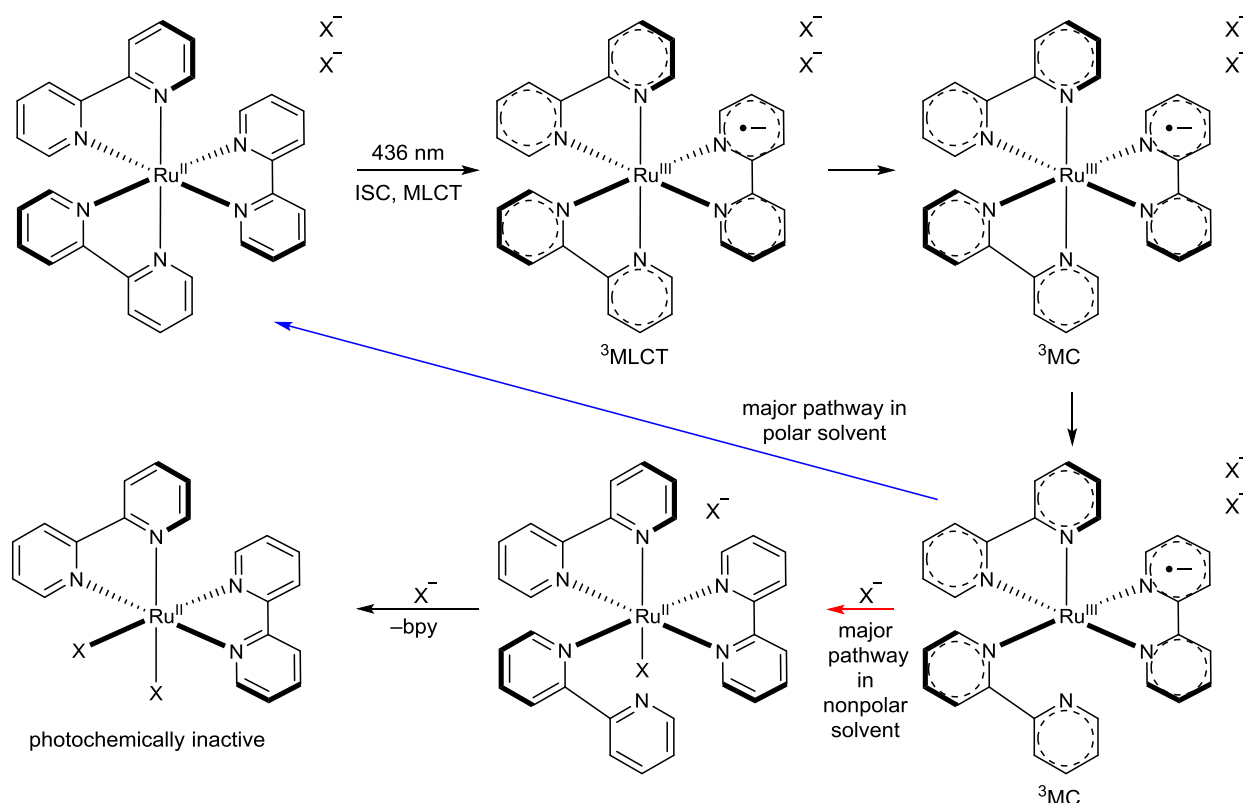
We were pleased to observe enantioselectivity with all of the complexes studied, thus providing proof-of-principle for our original hypotheses. Interestingly, **5-11⁻** and **5-12⁻** gave moderate enantioselectivity in MeNO₂. This was unexpected because the high dielectric constant of MeNO₂ could preclude tight ion pair formation and thus disrupt effective transmission of stereochemical information from the chiral phosphate anion. Furthermore, the sluggish reactivity observed with complexes containing **5-11⁻**, **5-12⁻**, and **5-13⁻** (entries 1–4) led us to consider the implications of ion pairing on reactivity. As the counteranion Lewis basicity is decreased, the resulting radical cation-counteranion pair becomes less stabilized. To a first approximation, this decreased thermodynamic stability of the ion pair might lead to a decrease in the free energy required to overcome the activation barrier for the first bond forming event (Scheme 5-2, **5-7** → **5-8**). Therefore, we hypothesized that BINOL counteranions exhibiting lower Lewis basicity than phosphate should lead to substantially increased reactivity.

Indeed, complexes containing less basic *N*-triflyl-phosphoramidate (**5-14⁻**, **5-15⁻**, **5-16⁻**, **5-17⁻**) (entries 5–13) gave significantly improved reactivity compared to the phosphate counteranions (compare entries 1 and 5). To see if this reactivity trend was general, bis-sulfonamide (**5-18⁻**) and bis-sulfonic acid (**5-19⁻**) complexes were prepared and screened. However, **5-18⁻** (entries 14 and 15) afforded lower reactivity compared to the *N*-triflyl-phosphoramidates, and complexes containing **5-19⁻** rapidly decomposed under the photocatalysis conditions. In an attempt to leverage the optical yields observed with phosphate counteranions (entries 1 and 3) and the reactivity observed with less coordinating *N*-triflyl-phosphoramidates (entries 5 and 10), Ru(bpy)₃(X^{*})₂ and MV(X^{*})₂ complexes containing *N*-phosphinyl phosphoramidate **5-20** were prepared. However, these complexes gave poor reactivity.

This final result led to a study of catalyst integrity throughout the photoreaction. Hypothesizing that rapid catalyst death could be contributing to the sluggish reactivity observed with all of the complexes studied in Table 5-1, an experiment was carried out at high catalyst loadings (5 mol% Ru(bpy)₃(**5-11⁻**)₂ and 15 mol% MV(**5-11⁻**)₂). Indeed, ¹H NMR analysis

revealed disappearance of bpy ligand protons throughout the reaction in tandem with multiple new resonances. Attempts at isolation of these new species were unsuccessful, even at larger reaction scales. However, a literature search uncovered several reports documenting a decomposition mode of polypyridyl Ru(II) complexes in low dielectric solvents (Scheme 5-4).^{21,22} This decomposition pathway, known as photoanation, occurs when a polypyridyl Ru(II) complex containing a Lewis basic counteranion in its second coordination sphere is irradiated. For example, upon dissolution in CH₂Cl₂ with irradiation at 436 nm, Gleria and co-workers discovered that [Ru(bpy)₃]²⁺(2Cl⁻) underwent rapid transformation to Ru(bpy)₂Cl₂.

Scheme 5-4. Photoanation chemistry of polypyridyl Ru(II) complexes in nonpolar solvents



At this point, a critical analysis of our first-generation approach was necessary. Most significantly, enantioenriched cycloadduct was obtained in many of the reactions studied, validating the hypothesis that a chiral counteranion can control the stereochemistry of radical cation reactions. Many elements of this approach, however, conspired against its success. To

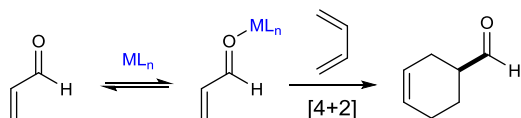
begin, low reactivity and moderate mass balance was observed for all complexes studied. While photoanation is undoubtedly responsible for attenuated reactivity, it is highly likely that the counteranion is non-innocent and substantially affects the rate of chain propagation as well as the electrochemical potentials of the photocatalyst (see Chapter 6). In terms of counteranion basicity, Table 5-1 lists known dissociation constants for the parent acids, where it can be observed that the pK_a values for all the scaffolds investigated span a narrow range (1.7–3.9). This current limitation in the field of chiral Brønsted acid catalysis thereby precluded a thorough study of the relationship between counteranion Lewis basicity and enantioinduction in our system. Finally, preparation of the small library of $Ru(bpy)_3(X^*)_2$ and $MV(X^*)_2$ complexes proved tedious and non-amenable to rapid screening.

5.4 Second-Generation Approach

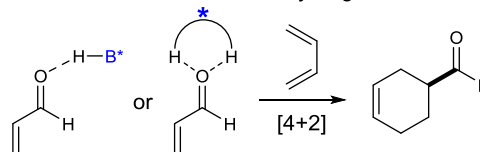
The preceding analysis of our first-generation approach to an enantioselective transformation proceeding via a putative radical cation led to a broader survey of methods by which to induce asymmetry in reactions involving substantial charge polarization. Indeed, given the discussion in Section 5.2, the Diels–Alder reaction appeared to be an ideal model system upon which to base this analysis (Scheme 5-5).

Scheme 5-5. Mechanistic constructs for enantioselective Diels–Alder reactions

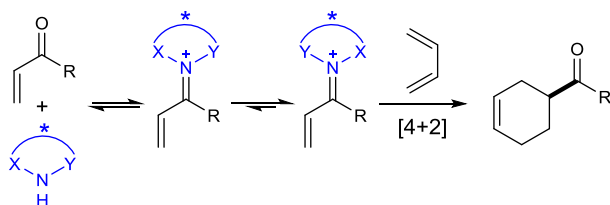
Chiral Lewis acid catalysis



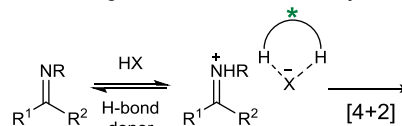
Chiral Brønsted acid or double hydrogen-bond catalysis



Chiral imidazolidinone organocatalyst approach



Anion-binding/anion-abstraction catalysis

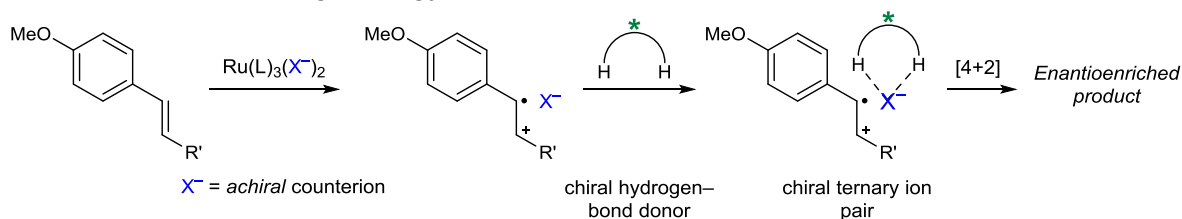


- Allows non-covalent catalysis of reactions proceeding via charged intermediates

Perhaps the most widely employed method to achieve facial discrimination in traditional Diels–Alder chemistry is chiral Lewis acid complexation to electron-deficient carbonyl compounds.²³ This complexation lowers the dienophile LUMO energy, thus facilitating cycloaddition. Chiral Brønsted acid catalysis²⁴ follows similar logic but relies on moderate (4–15 kcal/mol, 1.5–2.2 Å) electrostatic interactions to achieve control over absolute stereochemistry. The chiral imidazolidinone organocatalyst approach pioneered by MacMillan^{25a} replaces lone pair coordination with selective π -bond formation, resulting in a highly directional mode of asymmetric induction, opening the possibility of utilizing ketone-derived dienophiles. However, the method is somewhat limited by pronounced steric effects due to covalent bonding.^{25b}

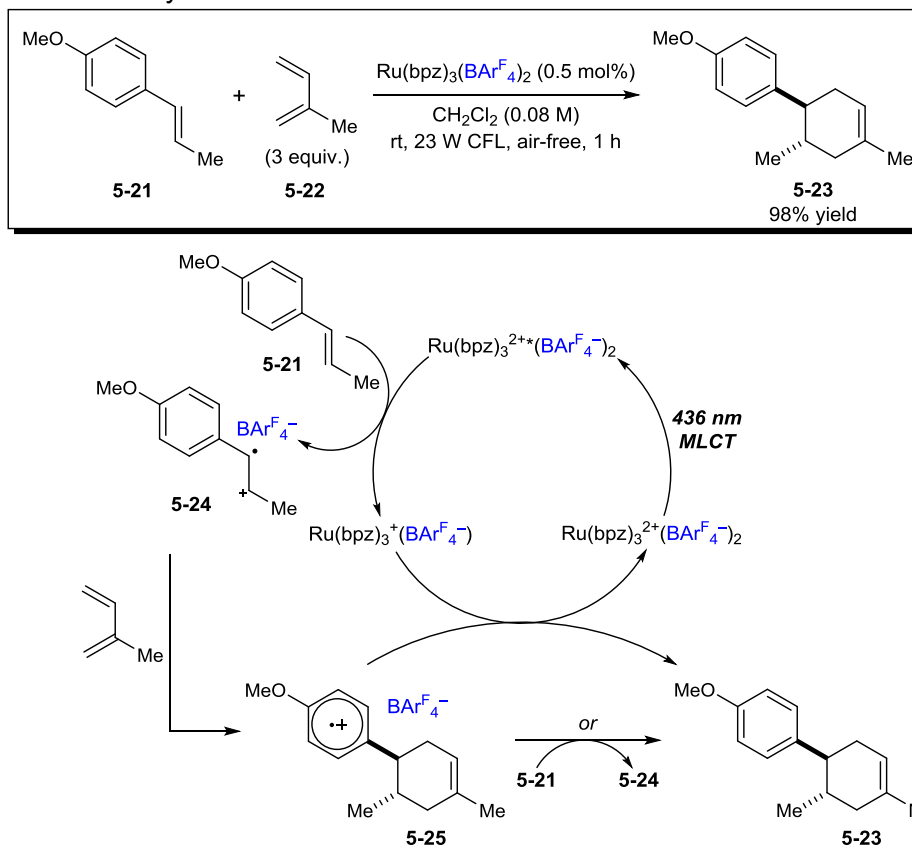
Anion-binding catalysis offers a fundamentally different paradigm for asymmetric induction. Deriving inspiration from the fields of anion recognition²⁶ and enzymology²⁷, this mode of catalysis utilizes chiral hydrogen bond-assisted heterolysis of polar C-X bonds (anion-abstraction), the result of which is liberation of a reactive cationic species with simultaneous formation of a chiral ion pair.^{28,29} Alternatively, the chiral hydrogen bond donor can directly control the reactivity and facial bias of ion-paired intermediates (anion-binding, Scheme 5-5). Unlike the previously discussed methods, ion-pairing allows for non-covalent catalysis of reactions proceeding via charged intermediates. Through this analysis, we hypothesized that reactions of radical cation intermediates might succumb to enantiodiscrimination utilizing ion-pairing catalysis in the presence of a chiral hydrogen-bond donor (Scheme 5-6).

Scheme 5-6. Anion-binding strategy applied to a radical cation intermediate



To begin these investigations, we elected to pursue the *intermolecular* variant of our first-generation approach due to the poor mass balances often observed at long reaction times with tethered styrenyl substrates such as **5-3** (Table 5-1). Additionally, the reaction shown in Scheme 5-7 generates a single diastereomer, thus avoiding issues pertaining to isomer separation and analysis.

Scheme 5-7. Photocatalyzed intermolecular radical cation Diels–Alder reaction



Scheme 5-7 depicts our current mechanistic understanding of the photocatalyzed intermolecular radical cation Diels–Alder reaction,^{10b} with particular emphasis on ion-paired intermediates. In a similar fashion to Scheme 5-2, a sufficiently electron rich substrate, such as anethole **5-21** undergoes oxidative quenching ($E^\circ(\text{R}/\text{R}^{*\cdot}) = +1.13 \text{ V}$)¹¹ with the highly oxidizing triplet $\text{Ru}(\text{bpz})_3^{2+*}$ to form ion-paired intermediate **5-24**. Reaction with isoprene (**5-22**) in a formal Diels–Alder reaction occurs to afford **5-25**. Reduction by $\text{Ru}(\text{bpz})_3^+$ or chain propagation furnishes cycloadduct **5-23**. While our initial publication used oxygen as a terminal oxidant to

turn over $\text{Ru}(\text{bpz})_3^+$, we found that omitting oxygen gave only a moderate decrease in reaction efficiency, thereby underscoring the feasibility of product formation by chain propagation. Indeed, as in the first-generation approach, preliminary experiments (Section 5.5) revealed that omission of oxygen led to significantly higher mass balances, likely due to the absence of non-productive reactivity from superoxide radical anion ($\text{O}_2^{\cdot-}$) formation.

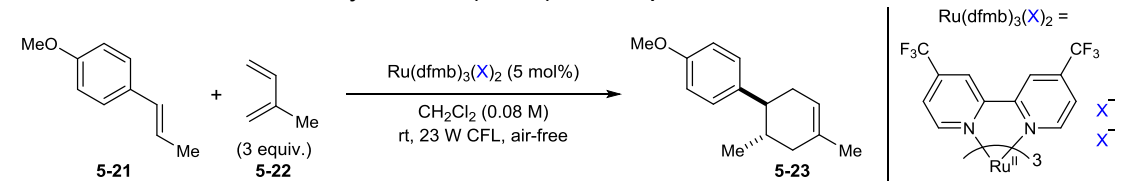
5.5 Results and Discussion: Second-Generation Approach

With a model system identified, we wished to investigate a possible correlation between counteranion basicity and reaction rate in a series of nonpolar ($\epsilon < 12$) solvents. However, experience in our laboratory has shown that $\text{Ru}(\text{bpz})_3^{2+}$ complexes not containing the $\text{BAr}^{\text{F}}_4^-$ counteranion are insoluble in solvents less polar than acetone. Therefore, in order to continue investigations, the catalyst $\text{Ru}(\text{dfmb})_3^{2+}$ (dfmb = 4,4'-bis(trifluoromethyl)-2,2'-bipyridine) was prepared (Table 5-2).³⁰ While this species was found to have a less oxidizing triplet excited state ($E^\circ(\text{Ru}^{2+*/+}) = +1.16$ V) than $\text{Ru}(\text{bpz})_3^{2+}$ ($E^\circ(\text{Ru}^{2+*/+}) = +1.35$ V), $\text{Ru}(\text{dfmb})_3(\text{BAr}^{\text{F}}_4)_2$ **5-26** afforded comparable reactivity to $\text{Ru}(\text{bpz})_3(\text{BAr}^{\text{F}}_4)_2$.¹⁰ Additionally, with the exception of complex **5-27**, all other complexes shown in Table 5-2 were soluble in nonpolar solvents such as CH_2Cl_2 and CHCl_3 , thereby enabling comprehensive investigations.

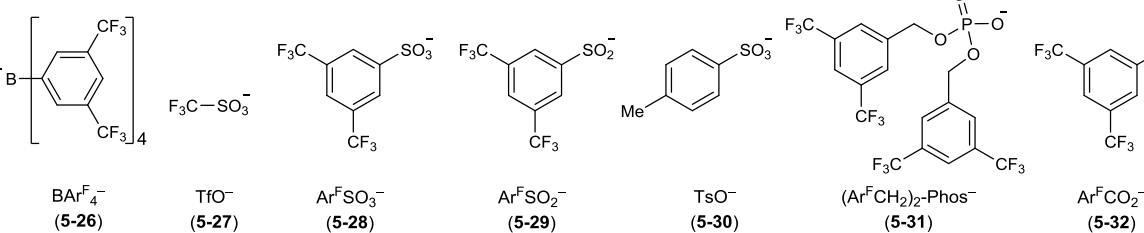
Electron-poor ureas can hydrogen-bond to a variety of anions, including phosphates, sulfates, and benzoates.³¹ Thus, we synthesized a variety of complexes bearing counteranions with the potential to undergo hydrogen-bonding to ureas and thioureas. Indeed, a strong correlation between counteranion basicity and reactivity was quickly established; Table 5-2 displays these results in order of increasing Lewis basicity ($\text{Ar}^{\text{F}} = 3,5\text{-bis(trifluoromethyl)phenyl}$). Complexes **5-26** and **5-27** containing the weakly-coordinating $\text{BAr}^{\text{F}}_4^-$ and TfO^- counteranions, respectively, demonstrated far more rapid conversion to cycloadduct than complexes containing aryl sulfonate (**5-28** and **5-30**), aryl sulfinate (**5-29**), benzyl phosphate (**5-31**) or aryl carboxylate (**5-32**) anions. Notably, the acidity

of the parent acids span more than 23 pK_a units (–15 [TfOH] to 8.5 [est., Ar^F-CO₂H]), thus highlighting a potential advantage of this second-generation approach.

Table 5-2. Counteranion survey with Ru(dfmb)₃²⁺ complexes^a



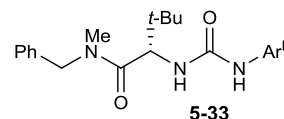
X =



| entry | [Ru] | time | yield ^b 5-23 | remaining ^b 5-21 |
|-------|-------------|--------|--------------------------------|------------------------------------|
| 1 | 5-26 | 20 min | 98% | — |
| 2 | 5-27 | 24 h | 55% | 37% |
| 3 | 5-28 | 24 h | 14% | 80% |
| 4 | 5-29 | 24 h | 7% | 83% |
| 5 | 5-30 | 24 h | 2% | 95% |
| 6 | 5-31 | 24 h | 0% | 100% |
| 7 | 5-32 | 24 h | 0% | 100% |

^aTo an oven-dried 25-mL Schlenk tube with a magnetic stirrer was added [Ru] followed by a stock solution of **5-21** (0.061 mmol), **5-22** (0.18 mmol), and trimethyl(phenyl)silane internal standard (0.061 mmol) in dry CH₂Cl₂ (0.08 M). The solution was submitted to 3 freeze-pump-thaw cycles, purged with N₂, and irradiated at room temperature with a 23 W CFL. ^bSubsequently, an aliquot was collected for ¹H NMR analysis to determine yield **5-23** and remaining **5-21**.

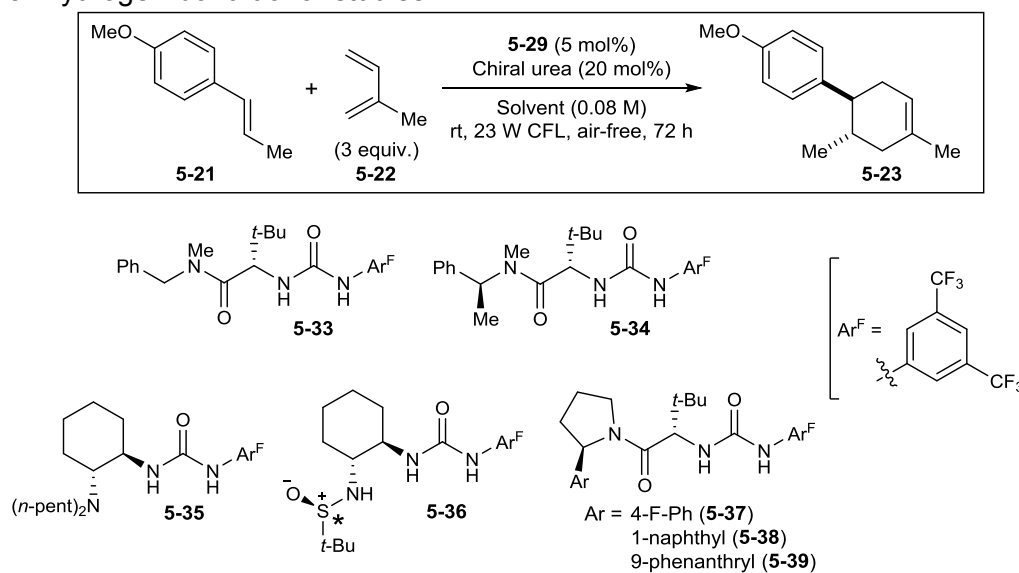
We wished to determine if the presence of a hydrogen-bond donor would accelerate catalysis beyond that of the background reactivity just established. In the event, chiral urea **5-33** was synthesized and evaluated with complexes **5-28** and **5-29** under the conditions described in Table 5-2.



After 24 h, we were delighted to observe that the reaction containing **5-29** and **5-33** exhibited a threefold increase in rate over background; a twofold increase was observed with **5-28** and **5-33**. Therefore, **5-29** was used for further studies.

5.5.1 Jacobsen-Type Ureas as H-Bond Donors

Given the substantial increase over background activity observed with **5-33**, a small library of chiral ureas originally developed by Jacobsen³² was synthesized and submitted to the optimized reaction conditions (Table 5-3). While **5-34** gave similar reactivity to **5-33**, no enantioinduction was observed. Diaminocyclohexyl urea **5-35** and sulfinamides (*R*)- and (*S*)-**5-36**^{32c} derived from Ellman's auxiliary inhibited reactivity, likely due to photoanation resulting from the high Lewis basicity of the tertiary amine and sulfinamide nitrogen, respectively. However, ureas containing an α -aryl pyrrolidine moiety (**5-37**, **5-38**, **5-39**)^{32d,e} afforded modest enantioselectivity (entries 6–12), thus providing proof-of-principle for this mode of enantioinduction. A brief solvent screen with **5-38** uncovered that use of nonpolar aromatic solvents (entries 10–11) affords significantly improved asymmetric induction. Given the increase in enantioselectivity observed upon exchanging the 4-F-phenyl nucleus of **5-37** with a naphthyl moiety, it appeared reasonable to propose a positive relation between quadrupole moment or polarizability of the aryl substituent and enantioselectivity. Indeed, Jacobsen has observed this trend in an α -aryl pyrrolidine urea-catalyzed electrocyclization cascade proceeding via an iminium ion.^{32e} Therefore, **5-39** was synthesized to test this hypothesis, but no increase in enantioinduction was observed.

Table 5-3. Hydrogen-bond donor studies^a

| entry | chiral urea | solvent | yield ^b 5-23 | e.e. ^c | remaining ^b 5-21 |
|-------|---------------------------|---------------------------------|--------------------------------|-------------------|------------------------------------|
| 1 | 5-33 | CH ₂ Cl ₂ | 24% | 0% | 61% |
| 2 | 5-34 | CH ₂ Cl ₂ | 23% | 0% | 72% |
| 3 | 5-35 | CH ₂ Cl ₂ | 0% | — | 96% |
| 4 | (<i>R</i>)- 5-36 | CH ₂ Cl ₂ | 10% | 0% | 80% |
| 5 | (<i>S</i>)- 5-36 | CH ₂ Cl ₂ | 11% | 0% | 77% |
| 6 | 5-37 | CH ₂ Cl ₂ | 23% | 4% | 65% |
| 7 | 5-38 | CH ₂ Cl ₂ | 23% | 9% | 70% |
| 8 | 5-38 | CHCl ₃ | 5% | 11% | 85% |
| 9 | 5-38 | THF | 3% | 17% | 96% |
| 10 | 5-38 | PhCF ₃ | 11% | 21% | 81% |
| 11 | 5-38 | PhCH ₃ | 5% | 29% | 89% |
| 12 | 5-39 | CH ₂ Cl ₂ | 18% | 9% | 76% |

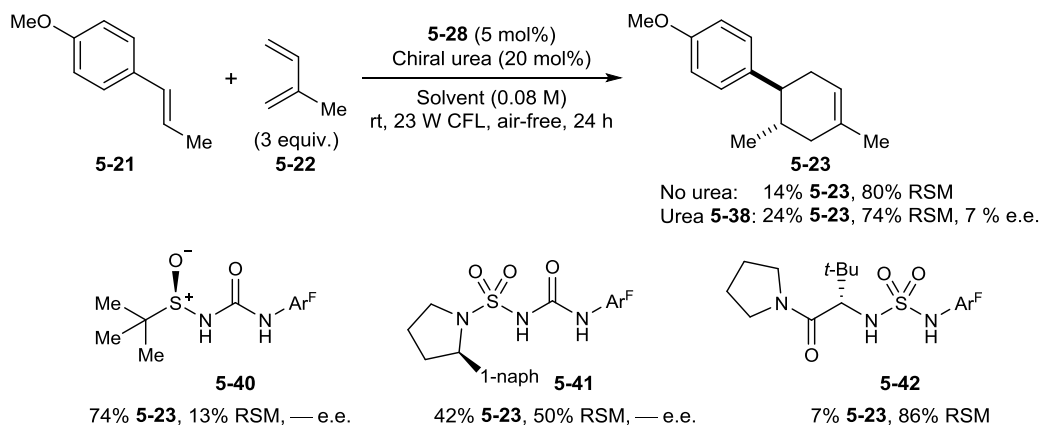
^{a,b}See Table 5-2. After 72 h, diluted with 25:1 hexanes:EtOAc and purified on silica gel using this eluent.

^cSample was dissolved in 6:1 hexanes:*i*-PrOH (2 mL) and e.e. was determined by HPLC analysis on Daicel OJ-H chiral stationary phase eluting with 99:1 hexanes:*i*-PrOH (isocratic, 1 mL/min flow rate, 278 nm; enantiomers had retention times of 5.4 and 5.9 min, residual **5-21** had a retention time of 15.8 min).

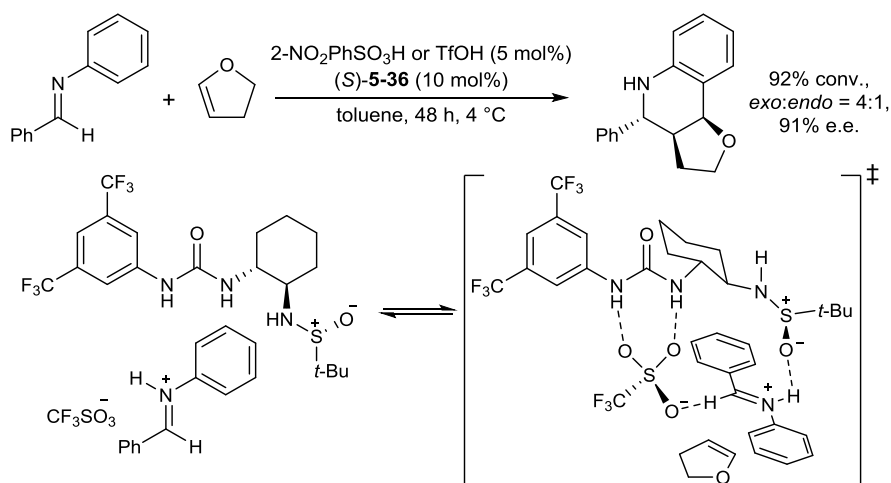
The results in Table 5-3 demonstrate a tradeoff between chemical and optical yield (entries 7–11). While this trend was expected from the studies presented by Inoue and Schuster,^{8b,9c} we came to realize an important facet of our methodology: counteranion basicity can easily be modulated via electronic modification to the counteranion itself or by electrostatic perturbation using a hydrogen-bond donor. It follows that the strongest perturbation should occur in the presence of a potent hydrogen-bond donor, that is, a species having substantially acidic H-X bonds. Given that thiourea is substantially more acidic ($pK_a = 21.0$) than urea ($pK_a = 26.9$),³³ an obvious experiment entailed replacing the urea functionality of **5-38** with a thiourea. However, the thiourea analogue completely inhibited the radical cation cyclization.³⁴ Furthermore, Schreiner's thiourea $((Ar^F NH)_2 CS)^{28b}$ neither inhibited nor accelerated reactivity above background. Given these data, thioureas were not investigated further, despite enhanced H-bond donation.

5.5.2 Diaminocyclohexyl Ureas: Impetus and Structure-Activity Relationships

The results with Schreiner's thiourea in tandem with the hypothesis of a correlation between reaction rate and hydrogen-bond donor ability lead to the search for non-oxidizable H-bond donors possessing acidic H-X bonds. Given the greater reactivity observed with sulfonate catalyst **5-28** compared to sulfinate catalyst **5-29** (Table 5-2), we opted to employ **5-28** for the remainder of our studies. Recent investigations by Ellman demonstrated that replacement of the methinyl-peptide residue in **5-38** with a sulfinamide or sulfonamide affords a substantial increase in urethane proton acidity.³⁵ In accordance with these observations, sulfinamido urea **5-40** and sulfamoyl urea **5-41** were prepared (Scheme 5-8). Gratifyingly, **5-40** and **5-41** accelerated the rate of Diels-Alder cycloaddition by 7-fold and 4-fold above background, respectively, thus verifying our hypothesis. Given the latter result, we surmised that replacement of the urethane carbonyl with a sulfoxide would dramatically alter reactivity, but sulfuric diamide **5-42** inhibited reactivity.

Scheme 5-8. Survey of sulfonamide, sulfonamide, and sulfamoyl ureas


The substantial increase in catalysis observed with sulfinamide urea **5-40** prompted a search for H-bond donors having a high affinity for sulfonates. Recent investigations by Jacobsen and co-workers on aryl sulfonate- and trifluoromethylsulfonate-catalyzed [4+2] cycloadditions between *N*-aryl imines and electron-rich olefins (Povarov reaction, Scheme 5-9) demonstrated high enantioinduction in the presence of sulfinamido urea (**S**)-**5-36** (Table 5-3).³⁶ Surprisingly, measurable binding between weakly basic triflate and (**S**)-**5-36** was observed ($K = 9000 \pm 2000 \text{ M}^{-1}$).

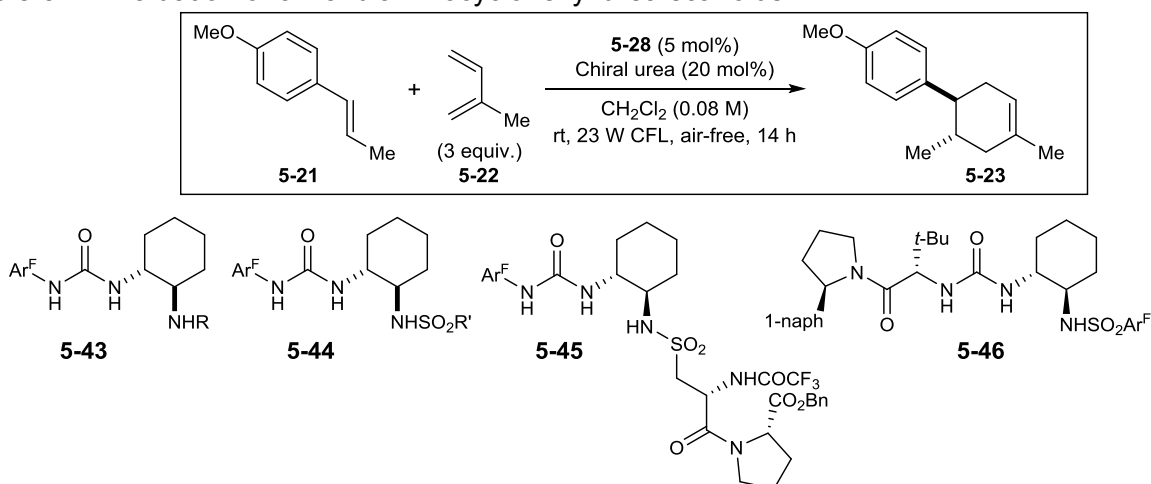
Scheme 5-9. Asymmetric induction for an intermolecular, sulfonate-catalyzed Povarov reaction


Interestingly, preliminary experiments revealed that (**S**)-**5-36** inhibited our radical cation Diels-Alder cycloaddition (Table 5-3, entry 5). Considering the high Lewis basicity ($pK_a \sim 22$) of the sulfinamide nitrogen, photoanation is almost certainly operative, and further analysis of this

reaction by ^1H NMR spectroscopy revealed that, indeed, ~50% of photocatalyst **5-28** had decomposed within 8 h of reaction. Nevertheless, we felt that the diaminocyclohexyl scaffold could serve as a highly modular platform and were inspired by the work of Sakakura and Ishihara³⁷ on increasingly potent H-bond donors derived from this framework.

In the event, a small library of chiral diaminocyclohexyl ureas was prepared and screened under the standard reaction conditions (Table 5-4). In general, ureas containing a Lewis basic nitrogen atom (**5-43a**, **5-36**) gave poor reactivity. However, by rendering this nitrogen atom increasingly less basic, reactivity dramatically improved (entries 3–5). Indeed, **5-43d** gave the largest increase over background reactivity observed to that point. Various BINOL and TADDOL frameworks (not shown) were appended to the **5-45** scaffold, but low reactivity and no significant enantioselectivity was observed. By replacing the amide or sulfonamide functionality in the **5-43** series with a sulfonamide, reactivity improved further (entries 6–11), and the reaction containing **5-44e** reached completion in 8 h. This represents an approximate 20-fold increase above racemic background.

Given the promising results with **5-44c**, a variety of chiral amines, chiral amino acids, and chiral cystic acids (e.g. **5-45**) were synthesized and appended to the chiral framework of **5-44**. In general, all of these hydrogen bond donors afforded 30–35% yield of **5-23** with e.e. values between 1–5% (entry 11). Replacing the chiral diaminocyclohexyl backbone of **5-44e** with (1*R*,2*R*)-bisphenylethylenediamine or (1*R*,2*R*)-bis(1-naphthyl)ethylenediamine gave no measureable improvement in e.e. Replacement of the 3,5-bis(trifluoromethyl)phenyl (Ar^{F}) moiety bonded to the urea with a phenyl group or a tosylate lead to a dramatic loss in reactivity. Finally, fusing the peptidomimetic scaffold of urea **5-38** with the diaminocyclohexylsulfonamide fragment of **5-44e** gave urea **5-46**. However, as shown in entry 12, a urea bonded to an electron-deficient aromatic nucleus appears necessary for competent reactivity.

Table 5-4. Evaluation of chiral diaminocyclohexyl urea scaffolds^a

| entry | chiral urea | R or R' | yield ^b 5-23 | e.e. ^c | remaining ^b 5-21 |
|-------|---|---------------------------------------|--------------------------------|-------------------|------------------------------------|
| 1 | 5-43a | COMe | — | — | 100% |
| 2 | (<i>R</i>) or (<i>S</i>)- 5-36 | SO <i>t</i> -Bu | 8% | -2% | 92% |
| 3 | 5-43b | CO(Ar ^F) | 35% | 3% | 57% |
| 4 | 5-43c | CONH(Ar ^F) | 63% | 4% | 26% |
| 5 | 5-43d | COCF ₃ | 82% | 1% | 14% |
| 6 | 5-44a | 2,4,6-(<i>i</i> -Pr) ₃ Ph | 26% | -3% | 71% |
| 7 | 5-44b | NH(<i>n</i> -octyl) | 37% | -2% | 55% |
| 8 | 5-44c | <i>n</i> -octyl | 55% | -2% | 42% |
| 9 | 5-44d | Ph | 87% | -3% | 9% |
| 10 | 5-44e | Ar ^F | 93% | -6% | — |
| 11 | 5-45 | — | 35% | -4% | 56% |
| 12 | 5-46 | — | 12% | -1% | 88% |

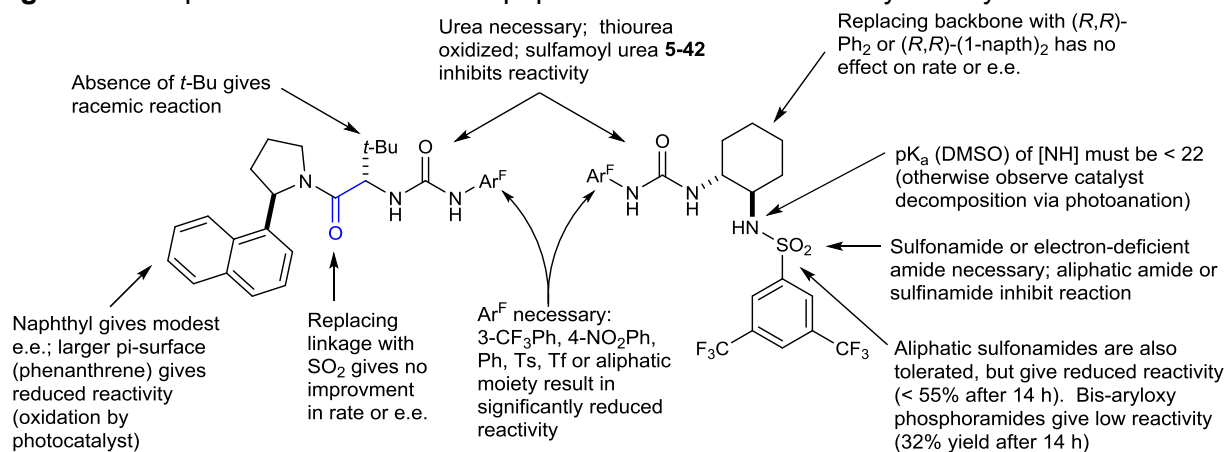
^{a,b,c}See Tables 5-2, 5-3 for complete experimental and analytical details; reactions stopped after 14 h of irradiation.

Overall, this study uncovered a variety of highly competent H-bond donors. Indeed, when compared to the Jacobsen-type ureas screened in Table 5-3, our novel H-bond donors provided dramatically improved reactivity. However, very low optical yields were observed for

all of these diaminocyclohexyl urea structures, and attempts to introduce further elements of chirality gave no improvements in stereochemical induction.

To this point, the only substrate investigated has been *trans*-anethole (**5-21**). This flat styrene derivative is relatively devoid of functionality. Hence, achieving non-covalent enantiodiscrimination is likely relying upon the large quadrupole moment of an aromatic nucleus (naphthalene, phenanthrene) on the chiral hydrogen bond donor (**5-38**, **5-39**) to electrostatically interact with one face of the transient radical cation intermediate derived from oxidation of **5-21**. We hypothesized that introduction of Lewis basic functionality on the substrate would facilitate a second mode of interaction with a chiral hydrogen bond donor. Further, we stipulated that introducing an acidic H–X bond on the substrate would create hydrogen-bonding interactions with the counteranion of the photocatalyst. These two distinct approaches were executed in a substrate engineering campaign (see Table S5-1, p. xx). However, though several intriguing results emerged, no improvements in enantioselectivity were observed.

Figure 5-1. Expanded SAR studies for peptidomimetic and diaminocyclohexyl urea scaffolds



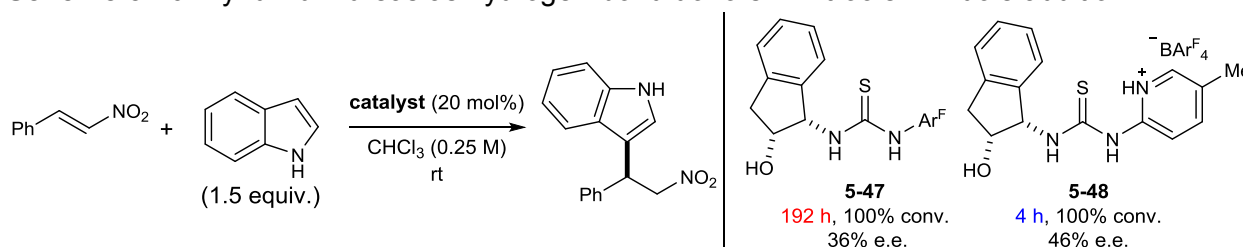
As exemplified by the structure-activity relationship (SAR) studies shown in Figure 5-1, small perturbations on the two major scaffolds investigated thus far often resulted in dramatically reduced catalysis. Wishing to further investigate the Jacobsen-type peptidomimetic framework due to promising levels of enantioinduction (Table 5-3) we realized that the most

significant factor limiting derivatization is the requirement for the Ar^F moiety directly bonded to the urea.

5.5.3 Pyridinium and Quinolinium Ureas H-Bond Donors

This latter realization was also made by Seidel and co-workers and prompted design of new H-bond catalysts (Scheme 5-10) in which the Ar^F substituent (as in **5-47**) was replaced with a protonated pyridine (as in **5-48**) or quinoline nucleus.³⁸ In accordance with their hypothesis, these pyridinium and quinolinium H-bond donors were substantially more active.

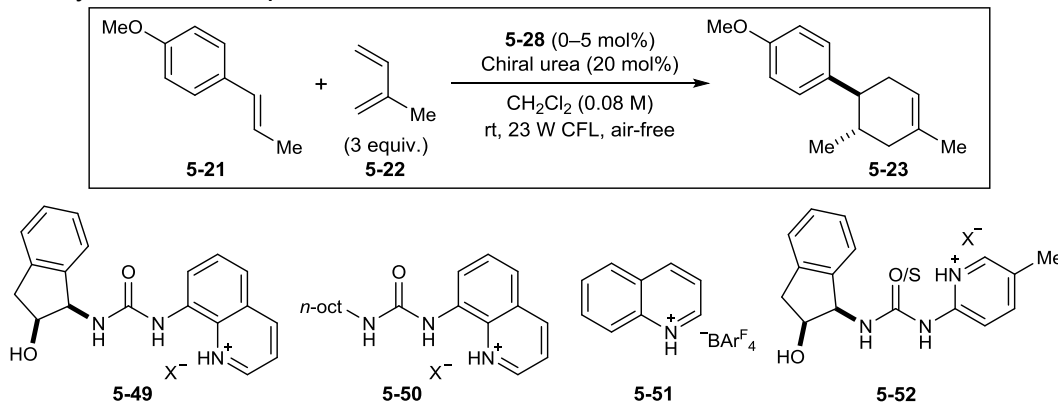
Scheme 5-10. Pyridinium ureas as hydrogen-bond donors in nitroolefin/indole addition



Surmising that this novel design principle could guide efforts in development of new Jacobsen-type peptidomimetic scaffolds for our radical cation Diels-Alder cycloaddition, a variety of pyridinium and quinolinium ureas were synthesized and submitted to the standard reaction conditions (Table 5-5). We were pleased to observe that the presence of quinolinium urea **5-49a** gave very rapid reactivity, with the cycloaddition reaching full conversion in 30 min (entry 1), nearly a 20-fold increase over urea **5-44e** (Table 5-4). Based on extensive work from Fukuzumi³⁹ and recent reports from Nicewicz⁴⁰ on acridinium-sensitized additions to alkenes, it was hypothesized that the quinolinium urea might be acting as a photoinduced electron transfer (PET) sensitizer. Indeed, the first singlet excited state (S₁) of quinolinium salts is known to be a powerful one-electron oxidant ($E_{\text{red}}(\text{S}_1) = +2.4 - +2.8 \text{ V vs. SCE}$).³⁹ In accord with these data, omission of photocatalyst **5-28** (entry 2) gave full conversion of **5-21**.⁴¹ Given this result, we surmised that the quinolinium urea could potentially play two roles: that of a PET sensitizer and that of a chiral hydrogen-bond donor. However, screening various chiral scaffolds based on

5-49a did not improve stereinduction, and enantioselectivity with **5-49a** did not improve at lower temperatures.

Table 5-5. Pyridinium and quinolinium ureas as H-bond donors and PET sensitizers



| entry | 5-28 | chiral urea | X ⁻ | time | yield ^b 5-23 | e.e. ^c | remaining ^b 5-21 |
|-------|-------------|------------------|--|--------|-----------------------------------|-------------------|---------------------------------------|
| 1 | 5 mol% | 5-49a | BAr ^F ₄ ⁻ | 30 min | 87% | 4% | — |
| 2 | — | 5-49a | BAr ^F ₄ ⁻ | 30 min | 87% | 6% | — |
| 3 | — | 5-49b | Ar ^F SO ₃ ⁻ | 24 h | — | — | 99% |
| 4 | — | 5-50 | BAr ^F ₄ ⁻ | 30 min | 50% | — | 37% |
| 5 | — | 5-51 | BAr ^F ₄ ⁻ | 30 min | 98% | — | — |
| 6 | — | 5-52a (O) | BAr ^F ₄ ⁻ | 30 min | 45% | 3% | 51% |
| 7 | — | 5-52a (S) | BAr ^F ₄ ⁻ | 30 min | 58% | 4% | 38% |
| 8 | — | 5-52b (S) | TfO ⁻ | 24 h | 3% | — | 97% |
| 9 | — | 5-52c (S) | Ar ^F SO ₃ ⁻ | 24 h | — | — | 99% |
| 10 | 5 mol% | 5-52c (S) | Ar ^F SO ₃ ⁻ | 24 h | — | — | 90% |
| 11 | 5 mol% | 5-52d (O) | Ar ^F SO ₃ ⁻ | 14 h | 7% | — | 88% |

^{a,b,c}See Tables 5-2, 5-3 for complete experimental and analytical details.

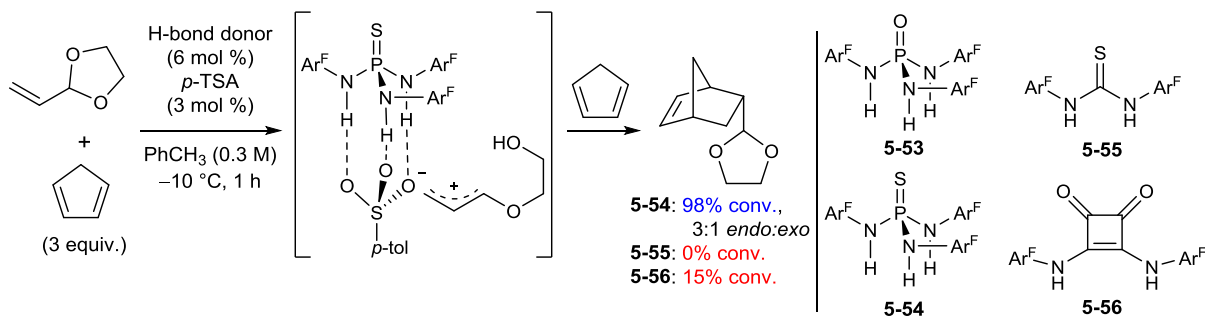
Perhaps most curious was a pronounced counteranion effect; indeed, when BAr^F₄⁻ was exchanged for Ar^FSO₃⁻, no catalysis was observed (entry 3). Surprisingly, pyridinium ureas and thioureas **5-52** were competent PET sensitizers when the BAr^F₄⁻ counteranion was employed (entries 6–11),⁴² though here too we observed a counteranion effect. The lack of catalysis with **5-52c (S)** lead to the hypothesis that this structure might be an ideal, potent H-bond donor.

Therefore, we introduced **5-52c (S)** to the standard reaction conditions with photocatalyst **5-28** but only observed inhibition of reactivity (entry 10). Suspecting thiourea oxidation, the corresponding urea was submitted, but inhibition was once again observed (entry 11), likely due to the basic hydroxyl group on the chiral aminoindanol scaffold.

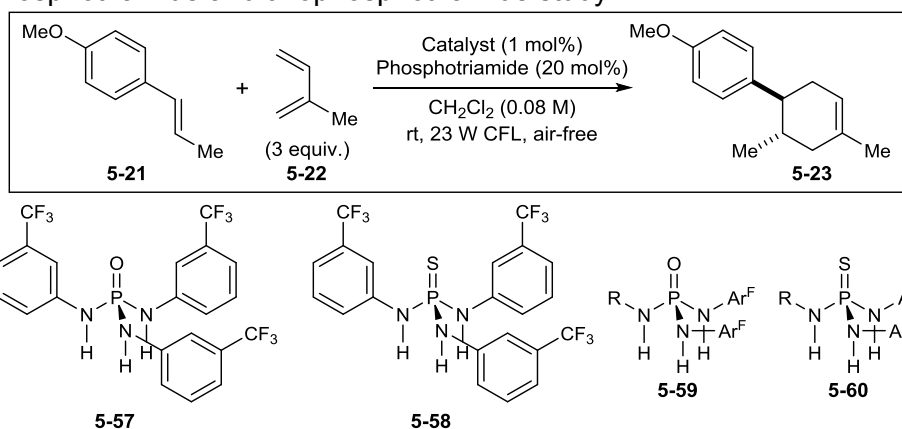
While this line of inquiry was stymied by irreproducible data, low levels of stereoinduction, and a pronounced counteranion effect, these results along with those in Table 5-2 ultimately inspired the studies performed in Chapter 6. At this time, we were lead back to the hypothesis outlined in Section 5.5.2: design of an H-bond donor framework that would effectively bind the tetrahedral sulfonate anion in catalyst **5-28** would be ideal for achieving rapid catalysis. Furthermore, we desired that this scaffold be amenable to introduction of chirality at a late stage in its synthesis, thus opening the door to rapid, facile diversification.

5.5.4 C₃-Symmetric Phosphotriamides and Synthesis of Non-Symmetric Derivatives for Introduction of Chirality

We initiated a literature search for an H-bond donor with high affinity for the tetrahedral sulfonate anion in catalyst **5-28**. Originally investigated⁴³ as neutral alternatives to acidic pyridinium and guanidinium H-bond catalysts, phosphotriamide **5-53** and thiophosphotriamide **5-54** (Scheme 5-11) were shown by Gale and co-workers⁴⁴ to have high affinity ($K_a > 10^4 \text{ M}^{-1}$) for sulfate (SO_4^{2-}). A recent comparison between **5-53**, Schreiner's thiourea **5-55**, and squaramide **5-56** in Gassman's⁴⁵ Brønsted-acid promoted ionic Diels–Alder cycloaddition (Scheme 5-11) revealed pronounced rate acceleration in the presence of the thiophosphotriamide.⁴⁶

Scheme 5-11. Phosphotriamides as sulfonate anion-binding scaffolds in an ionic cycloaddition


Given the proposed mode of anion binding and the acceleration in catalysis in systems containing sulfonate anions, we hypothesized that **5-53** and **5-54** would effectively bind the *p*-toluenesulfonate anion of catalyst **5-30** and afford significant rate increases over the Jacobsen-type ureas in our radical cation Diels–Alder system. To our great delight, **5-53** and **5-54** demonstrated a far superior reactivity profile compared to all other H-bond donors studied to this point (Table 5-6). Indeed, when **5-54** was added to a reaction containing the *p*-toluenesulfonate anion of catalyst **5-30**, a massive increase in reactivity was observed (entries 1–2), in agreement with the results in Scheme 5-11. A similar increase was noted in the presence of catalyst **5-28** (entries 3–5), and the greater acidity of the N–H protons in **5-54** relative to **5-53** led to faster catalysis. Unfortunately, after screening many C₃-symmetric phosphotriamides and thiophosphotriamides (not shown), it became quickly apparent that small electronic perturbations gave far less active hydrogen-bond donors.

Table 5-6. Phosphotriamide and thiophosphotriamide study

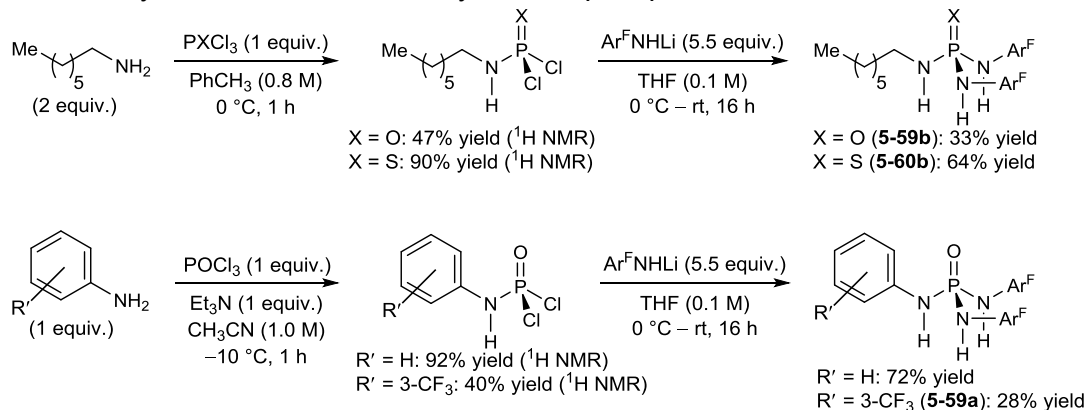
| entry | catalyst | phosphotriamide | R | time | yield ^b 5-23 | remaining ^b 5-21 |
|-------|-------------|-----------------|-------------------------------------|--------|--------------------------------|------------------------------------|
| 1 | 5-30 | — | — | 20 h | 2% | 93% |
| 2 | 5-30 | 5-54 | — | 20 h | 95% | 2% |
| 3 | 5-28 | — | — | 20 h | 15% | 80% |
| 4 | 5-28 | 5-53 | — | 90 min | 73% | 22% |
| 5 | 5-28 | 5-54 | — | 90 min | 93% | 3% |
| 6 | 5-28 | 5-57 | — | 20 h | 18% | 78% |
| 7 | 5-28 | 5-58 | — | 20 h | 13% | 81% |
| 8 | 5-28 | 5-59a | 3-CF ₃ Ph | 20 h | 81% | 13% |
| 9 | 5-28 | 5-59b | <i>n</i> -octyl | 20 h | 13% | 86% |
| 10 | 5-28 | 5-60a | 3-CF ₃ Ph | 20 h | 9% | 88% |
| 11 | 5-28 | 5-60b | <i>n</i> -octyl | 20 h | 17% | 75% |
| 12 | 5-28 | 5-60c | –CH ₂ CO ₂ Et | 20 h | 13% | 85% |

^{a,b}See Tables 5-2, 5-3 for complete experimental and analytical details.

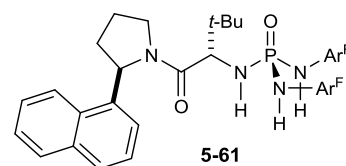
As in previous studies, here too we observed a strong relationship between reaction rate and highly electron deficient aryl groups appended to the hydrogen-bonding nucleus. However, there was no obvious method by which the C₃-symmetric Ar^F frameworks of **5-53** and **5-54** could be rendered chiral. This led us to hypothesize that synthesis of non-symmetric phosphotriamide architectures containing two Ar^F moieties (**5-59** and **5-60**) might allow for large electronic variations in the remaining position (R). Such frameworks had never previously been

synthesized, and thus, novel routes to these scaffolds were developed. After substantial optimization, we arrived at the methods shown in Scheme 5-12.

Scheme 5-12. Syntheses of novel, non-symmetric phosphotriamides



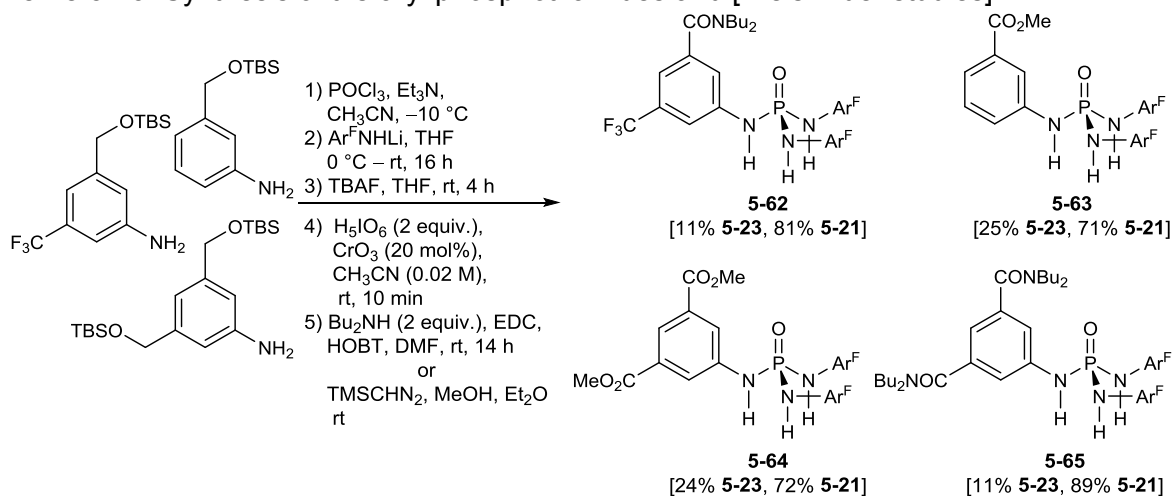
Several unexpected results were obtained when these scaffolds were employed (Table 5-6). When a *single* trifluoromethyl group from the corresponding C₃-symmetric phosphotriamide **5-53** was omitted to give **5-59a**, a substantial decrease in catalysis occurred (compare entries 4 and 8). Even more drastic was the inhibition of reactivity observed with **5-60a** (compare entries 3, 5, and 10). Unfortunately, alkyl groups (**5-62b** and **5-63b**) dramatically slowed reactivity (entries 9, 11). We hypothesize this is, in part, due to photoanation resulting from substantially increased nitrogen basicity. Surmising that the presence of an α -ester moiety would (a) significantly increase N-H acidity⁴⁷ and (b) provide a model system for peptidomimetic hybrid **5-61**, **5-60c** was synthesized. The resulting scaffold afforded no increase in the rate of catalysis (entry 12), thereby obviating preparation of **5-61** and its congeners. Taken together, the data in Table 5-6 demonstrate a very promising class of H-bond donors that exhibit pronounced sensitivity to electronic effects.



Given the requirement for a phosphotriamide possessing two Ar^F aniline moieties in conjunction with a third electron-deficient aniline, derivatives based on these criteria were synthesized (Scheme 5-13). Due to inefficient phosphoramidic dichloride formation when employing electron-deficient anilines (Scheme 5-12, R' = CF₃) a new route had to be devised.

In the event, *meta*-substituted TBS-protected anilines were subjected to the phosphotriamide synthesis outlined in Scheme 5-13. Subsequent deprotection followed by an optimized Cr(VI)-catalyzed oxidation protocol afforded a series of *meta*-benzoic acids that we imagined could serve as a branching point for the facile union of myriad chiral moieties with the phosphotriamide scaffold. The *meta*-benzoic acids were either submitted to amidation or esterification to yield analogues **5-62**, **5-63**, **5-64**, and **5-65**.

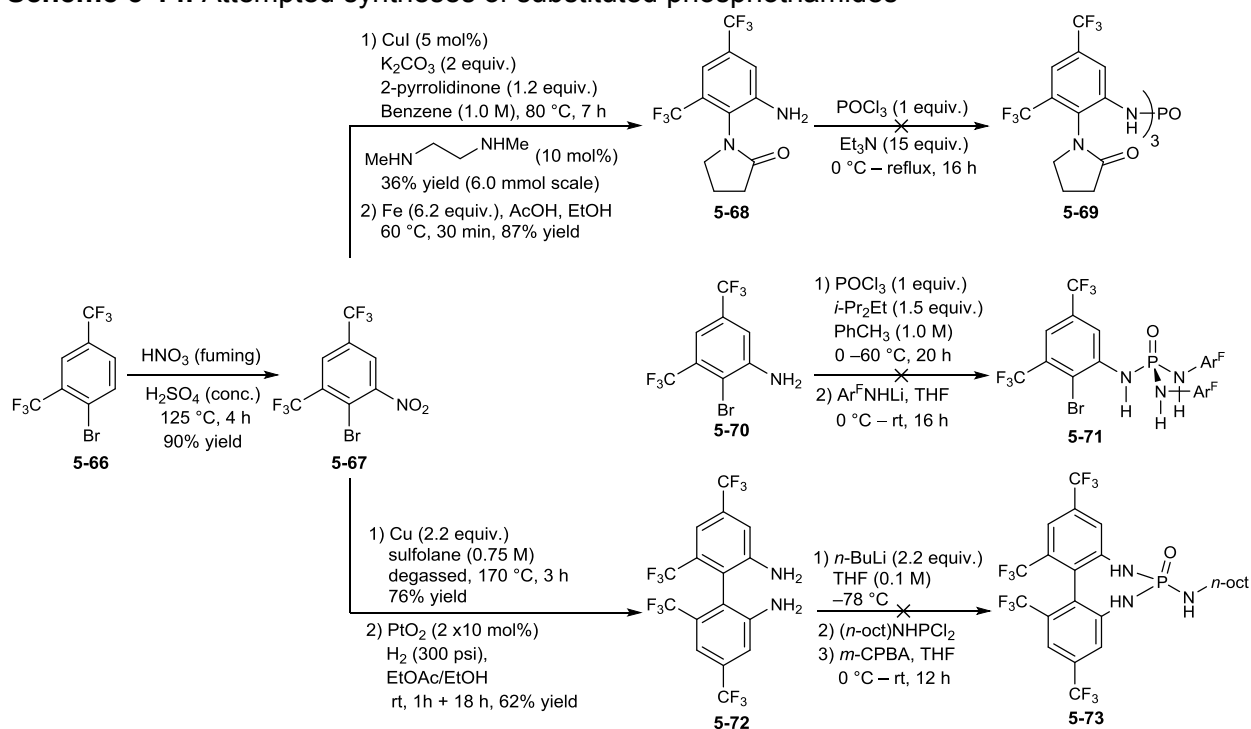
Scheme 5-13. Synthesis of tris-aryl phosphotriamides and [Diels-Alder studies]



As denoted by the bracketed results in Scheme 5-13, only **5-63** and **5-64** afforded increases over background catalysis in the radical cation Diels–Alder when submitted to the conditions in Table 5-6 for 20 h. While photoanation may be occurring in the presence of **5-62** and **5-65** as a result of the weakly nucleophilic amide nitrogen atoms, the low reactivity obtained with **5-64** was surprising, given the similar σ_{m} values for CF_3 and CO_2Me .⁴⁸

The pronounced electronic sensitivity led us to conclude that only an Ar^{F} -aniline or functionalized Ar^{F} -aniline moiety would be tolerated as the third substituent. We hypothesized that functionalization of the Ar^{F} moiety could be realized according to the chemistry outlined in Scheme 5-14.

Scheme 5-14. Attempted syntheses of substituted phosphotriamides



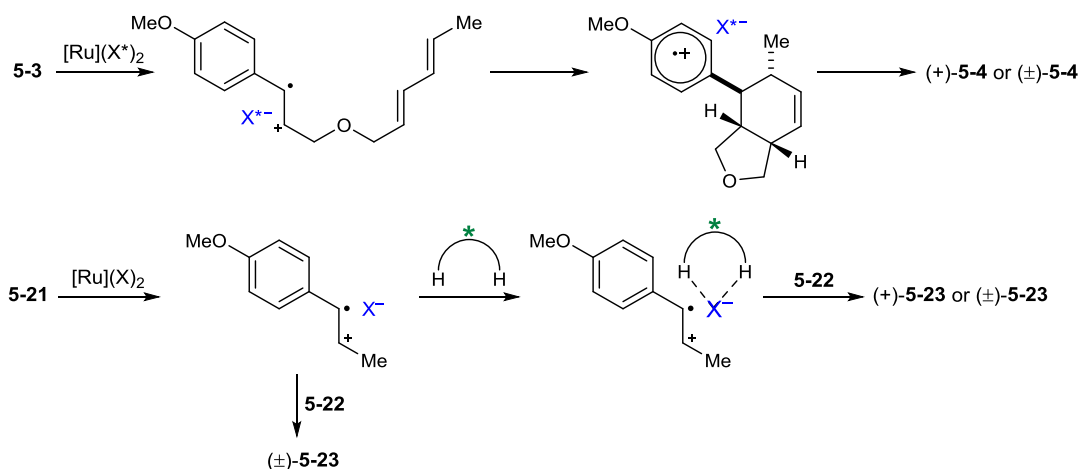
Nitration of 2,4-bis(trifluoromethyl)bromobenzene **5-66** afforded the highly substituted precursor **5-67** that served as a versatile intermediate. Buchwald amidation⁴⁹ was complicated by extensive hydrodehalogenation, a well-known deleterious side-reaction when employing electron-deficient substrates. Gratifyingly, after optimization, conditions were discovered to affect this coupling in moderate yield followed by reduction to afford **5-68**. When submitted to phosphotriamide formation no product was observed. We surmised that issues with this step could be avoided by installing the pyrrolidinone after phosphotriamide synthesis (**5-71**). However, **5-70** was recalcitrant to formation of the corresponding phosphoramidic dichloride under our optimized conditions. While thermal energy greatly increased the rate of consumption of **5-70**, the prolonged heating required to achieve complete conversion appeared to decompose any dichloride that formed.

Finally, we were intrigued by the possibility of stereochemical information relay from an axially chiral backbone, such as enantiopure TF-BIPHAM **5-72**.⁵⁰ Double deprotonation of **5-72** followed by treatment with a phosphoryl dichloride and subsequent oxidation should afford **5-73**.

We hypothesized that intramolecular capture of the phosphoramidyl monochloride intermediate from the first P-N bond forming event would be significantly more efficient than our protocol for intermolecular reaction with 2 equivalents of $\text{Ar}^{\text{F}}\text{NHLi}$ (Scheme 5-14). Racemic material was prepared from **5-67** via Cu-mediated oxidative coupling followed by high pressure reduction with H_2 on Adam's catalyst. Employing the procedure for phosphoramidate synthesis from BINAM-type ligands reported by Denmark and co-workers,⁵¹ we were unable to synthesize **5-73**. Other approaches also were unsuccessful, likely due to the poor nucleophilicity of the BIPHAM ligand. Unfortunately, the series of studies in Scheme 5-14 was stymied by the highly electron-deficient nature of the requisite aniline precursors. Indeed, we are unaware of any reports in which such electron-deficient aniline-based ligands undergo successful P-N bond formation, an apparent current limitation in the field of organophosphorus chemistry.

5.6 Concluding Remarks and Future Directions

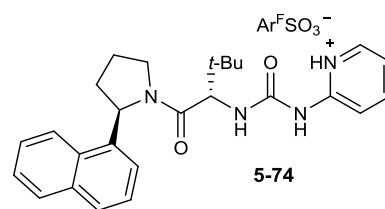
We remain intrigued by the transition state organization required to achieve high levels of enantioselectivity (Scheme 5-15). As the counteranion X^- is rendered less basic, the radical cation-anion pair is rendered less stable, and thus more reactive. However, a reduction in basicity directly correlates with a reduction in electrostatic attraction between the radical cation and X^- , and thus less effective relay of stereochemical information in the enantiodetermining step. These notions were borne out particularly well in the intermolecular system. That is, the putative ternary ion pair must assemble and have sufficient lifetime for participation in a bimolecular collision with a diene in order to obtain efficient stereochemical relay. Indeed, reaction from the chiral ternary ion pair competes with reaction from the prochiral binary ion pair. Contrastingly, in our first generation approach every radical cation-chiral phosphate ion pair formed, even those in chain propagation steps, must necessarily be a chiral ion pair. However, we believe that either approach has the potential to be a novel design strategy for achieving asymmetry in reactions proceeding via radical ion chain propagation.

Scheme 5-15. Comparison between first- and second-generation approaches

A closely related, more nuanced issue centers upon the mode in which the radical cation is generated. In the vast majority of reports regarding anion-pairing catalysis, the chiral hydrogen-bond donor induces substrate ionization to a reactive intermediate (anion-abstraction catalysis). In our system, the chiral hydrogen-bond donor does not induce radical cation formation, but instead must diffuse from the bulk solution and bind to the photocatalyst counteranion if enantiodiscrimination is to be achieved (anion-binding catalysis). This distinction between anion-abstraction and anion-binding catalysis may have profound ramifications for asymmetric induction, especially if cycloaddition can occur without *complete* ionization to the radical cation-anion pair. Assuming nearly diffusion-controlled cycloaddition after radical cation formation (achievable by tethering the diene to the species undergoing ionization) we postulate that a system in which a chiral H-bond donor induces ionization to the putative radical cation may give superior asymmetric induction.

A major advantage of our second-generation approach is the modularity and facile synthesis of chiral H-bond donors. However, the field of chiral anion-binding catalysis is just beginning, and thus, the diversity of scaffolds is currently quite

limited. Ureas and thiourea structures have dominated the field, but our studies clearly



demonstrate the need for novel structures. Encouraged by the very promising results obtained with pyridinium ureas and phosphotriamides, we propose that future studies further investigate scaffolds such as those in Scheme 5-14 as well as species similar to **5-74**. Due to the presence of the Lewis basic sulfonate, this pyridinium urea cannot act as a PET sensitizer but remains a potent H-bond donor.

One of the most pervasive empirical issues surrounding our two approaches is photocatalyst decomposition via photoanation. To the best of our knowledge, this pathway is unavoidable when homoleptic polypyridyl Ru(II) compounds are irradiated in nonpolar solvent in the presence of Lewis basic anions and/or nucleophiles. However, heteroleptic polypyridyl Ru(II) complexes are known to be significantly less prone to photoanation, and may prove particularly advantageous in future experiments.

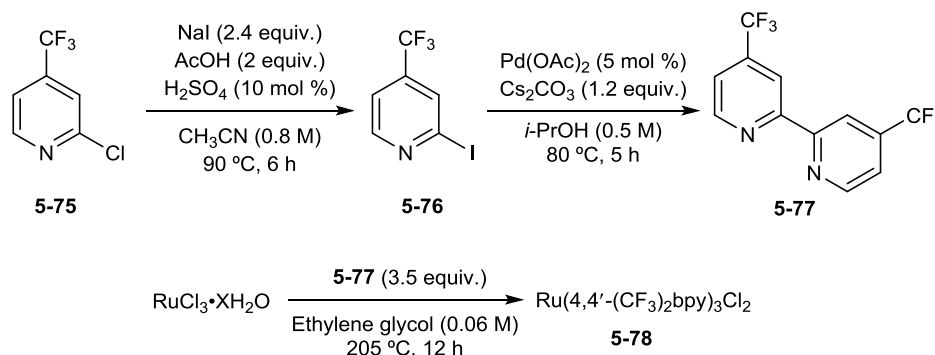
In closing, we have developed novel modes for achieving asymmetric induction in reactions of radical cation intermediates. Indeed, proof-of-concept and strong support for our hypotheses was observed in both our first- and second-generation systems. The asymmetric induction we have attempted to achieve, however, is entirely reliant upon strictly non-covalent, electrostatic interactions. Compared to either covalent catalysis or Lewis-acid catalysis, both of which induce enantioselectivity through strongly distance-dependent steric destabilization of all but the dominant pathway,⁵² the interactions inherent to ion-pairing and hydrogen-bonding are far weaker, less distance dependent, and less directional. In fact, given that the level of transition structure organization necessary for high stereoinduction is often achieved through highly directional catalyst–substrate interactions,²⁹ ion-pairing represents perhaps the least directional strategy currently known for achieving asymmetric catalysis. This also makes ion-pairing both a powerful approach to the challenge of stereoinduction and a strategy that we hope to further exploit in future investigations.

5.7 Experimental

5.7.1 General Information

Dichloromethane, tetrahydrofuran, diethyl ether, toluene, and acetonitrile (HPLC grade solvents) were dried by passage through columns of activated alumina. Ethylene glycol (Aldrich) was used as received. Water was purified by a Milli-Q system (Millipore Corporation) to achieve a resistivity of $18.2 \text{ M}\Omega \text{ cm}^{-1}$ at $25 \text{ }^\circ\text{C}$. Chromatography was performed with Purasil 60 Å silica gel (230–400 mesh) or with neutral alumina (Aldrich product # 11028). High vacuum refers to a reduced pressure that was measured to be 60 mTorr using a McLeod gauge. Anethole (**5-21**) was purified by chromatography on silica gel (hexanes: EtOAc = 20:1) and was subsequently submitted to fractional distillation under high vacuum at $95 \text{ }^\circ\text{C}$. Purified anethole was stored at room temperature in a vial wrapped in aluminum foil. Isoprene (**5-22**) was fractionally distilled from CaH_2 under N_2 at 45°C and stored at $5 \text{ }^\circ\text{C}$. ^1H , ^{13}C , ^{19}F , ^{31}P , and ^{11}B NMR data for all previously uncharacterized compounds were obtained using Bruker Avance III 400 MHz and Bruker Avance III 500 MHz spectrometers and are referenced to TMS (0.00 ppm) or residual protio solvent signal. The NMR facilities are supported by the NSF (CHE-1048642, CHE-9208463, S10 RR08389-01), the University of Wisconsin, and a generous gift from Paul J. Bender.

5.7.2 Synthesis of Polypyridyl Ru(II) Complexes



2-iodo-4-(trifluoromethyl)pyridine (5-76). A 250 mL round-bottom flask with a magnetic stirrer was charged with 2-chloro-4-(trifluoromethyl)pyridine **5-75** (Oakwood Chemical) (8.00 g, 44.1 mmol, 5.67 mL, 1 equiv.), NaI (15.8 g, 106 mmol, 2.4 equiv.), glacial AcOH (5.04 mL, 88.1 mmol, 2 equiv.), and CH₃CN (55 mL, 0.8 M). To the resulting faint yellow solution was added conc. H₂SO₄ (239 μL, 4.41 mmol, 0.1 equiv.) in a single portion, and the reaction turned bright red. The reaction was equipped with a water-cooled condenser before being placed in a 90 °C oil bath for 6 h. After the allotted time had elapsed, the resulting brown reaction was allowed to cool to rt, and the solvent was removed *in vacuo*. To the remaining residue was added H₂O (75 mL) and, with rapid stirring, solid NaHCO₃ until the reaction mixture reached pH = 7. The aqueous mixture was transferred to a separatory funnel and extracted with CH₂Cl₂ (3 x 100 mL). Residual iodine was removed by washing the combined organic phases with a saturated solution of sodium bisulfite (2 x 75 mL). The organic layer was washed with brine (1 x 50 mL), dried over Na₂SO₄, filtered, and the solvent was removed *in vacuo* to afford a yellow oil that was purified via flash column chromatography on silica (hexanes:EtOAc = 20:1) to afford 8.25 g (30.2 mmol, 69% yield) of **5-76** as a clear oil. ¹H NMR (500.0 MHz, CDCl₃) δ 8.57 (d, *J* = 5.1 Hz, 1H), 7.96 (s, 1H), 7.49 (d, *J* = 5.1 Hz, 2H); ¹³C NMR (125.7 MHz, CDCl₃) δ 151.6, 139.5 (q, *J*_{C-F} = 34.3 Hz), 130.7 (q, *J*_{C-F} = 3.6 Hz), 121.6 (q, *J*_{C-F} = 273.3 Hz), 118.5 (q, *J*_{C-F} = 3.6 Hz), 118.0. These data are consistent with previously reported values.⁵³ Note: proper storage of the

iodopyridine must be considered if not used immediately. To increase the shelf life of this reagent, store in a cool, dark place.

4,4'-bis(trifluoromethyl)-2,2'-bipyridine (5-77). A 250 mL round-bottom flask with a magnetic stirrer was charged with Pd(OAc)₂ (339 mg, 1.51 mmol, 0.05 equiv.) and Cs₂CO₃ (11.8 g, 36.3 mmol, 1.2 equiv.). The flask was equipped with a water-cooled condenser and was purged with N₂. Subsequently, a solution of **5-76** (8.25 g, 30.2 mmol, 1 equiv.) in *i*-PrOH (60 mL, 0.5 M) was added. The reaction was heated to an oil bath temperature of 80 °C under N₂ for 5 h. After the allotted time had elapsed, the reaction was allowed to cool to room temperature and was filtered through a pad of Celite. The filter cake was washed with CH₂Cl₂ (3 x 50 mL), and the volatiles were removed *in vacuo* to afford a brown solid. Insoluble impurities were removed by washing the brown solid with CH₂Cl₂, filtering, and removing CH₂Cl₂ *in vacuo*. The crude product was purified via flash column chromatography on silica (hexanes:EtOAc = 10:1) to afford 2.46 g (8.41 mmol, 56% yield) of **5-77** as a bright yellow solid. ¹H NMR (500.0 MHz, CDCl₃) δ 8.89 (d, *J* = 5.0 Hz, 2H), 8.73 (s, 2H), 7.59 (d, *J* = 5.0 Hz, 2H); ¹³C NMR (125.7 MHz, CDCl₃) δ 156.1, 150.3, 139.6 (q, *J*_{C-F} = 34.3 Hz), 122.8 (q, *J*_{C-F} = 273.3 Hz), 119.9 (q, *J*_{C-F} = 3.6 Hz), 117.2 (q, *J*_{C-F} = 3.6 Hz). These data are consistent with previously reported values.⁵⁴

Ru(dfmb)₃Cl₂ (5-78). A 100 mL round-bottom flask with a magnetic stirrer was charged with RuCl₃•XH₂O (Strem Chemicals) (379 mg, 1.83 mmol, 1 equiv.) and **5-77** (1.87 g, 6.40 mmol, 3.5 equiv.). The flask was equipped with a water-cooled condenser and was purged with N₂. Subsequently, ethylene glycol (30 mL, 0.06 M) was added and the reaction was heated to an oil bath temperature of 205 °C under N₂ for 12 h. The resulting dark red/black mixture was allowed to cool to rt. The crude reaction was added dropwise to a rapidly stirred mixture of Et₂O/acetone (1:1, 250 mL) over 15 min. The resulting homogeneous mixture was transferred to a dropping funnel and added slowly to a rapidly stirred solution of Et₂O (1.4 L) over 1 h. A red solid crashed out of solution during the addition and was isolated via slow filtration on a medium

porosity fritted funnel. The solid was washed with Et₂O (2 x 30 mL), then passed through the fritted funnel with CH₃CN. The volatiles were removed and the solid was dried under high vacuum. Thereafter, the dry solid was dissolved in CH₃OH (100 mL) and added dropwise to a rapidly stirred solution of Et₂O (350 mL) over 45 min. A red solid precipitated throughout the addition and was isolated on a fritted funnel and washed with Et₂O (2 x 30 mL). The purified solid was dried under high vacuum at 70 °C for 2 h to afford 1.40 g (1.38 mmol, 76% yield) of **5-78** as a red solid. ¹H NMR (500.0 MHz, CD₃OD) δ 9.40 (s, 6H), 8.15 (d, *J* = 5.9 Hz, 6H), 7.87 (dd, *J* = 5.9, 1.6 Hz, 6H); ¹³C NMR (125.7 MHz, CD₃OD) δ 159.1, 155.0, 141.1 (q, *J*_{C-F} = 35.8 Hz), 125.6 (q, *J*_{C-F} = 3.3 Hz), 123.5 (q, *J*_{C-F} = 274.6 Hz), 123.3 (q, *J*_{C-F} = 3.3 Hz); ¹⁹F NMR (376.5 MHz, CD₃OD) δ -66.1.

Ru(dfmb)₃(BAr^F₄)₂ (5-26). A 25 mL round-bottom flask with a magnetic stirrer was charged with **5-78** (100 mg, 0.0987 mmol, 1 equiv.) and H₂O (4.2 mL, 0.02 M). To this solution was added a solution of NaBAr^F₄ (Alfa Aesar) (179 mg, 0.202 mmol, 2.05 equiv.) in CH₃OH (1.4 mL, 0.07 M). An orange precipitate immediately formed, and the solution became difficult to stir. Additional H₂O (2 mL) was added, stirring was continued for 10 min, and the orange solid was isolated on a fritted funnel, washed with H₂O (2 x 3 mL), and dried. The dried solid was dissolved in acetone/CH₂Cl₂ (1:1, ~5 mL) and purified via gravity elution through a column of neutral Al₂O₃ using CH₂Cl₂ as the eluent. The first band that eluted was determined to be the desired product, so these fractions were pooled, the volatiles were removed *in vacuo*, and the resulting solid was dried under high vacuum. This residue was dissolved in a minimum volume of CH₂Cl₂ (5 mL) and passed through a 0.2 μm Whatman PTFE filter to remove residual NaBAr^F₄. To the filtrate was slowly added hexanes (30 mL) and an orange solid precipitated. The solid was isolated on a fritted funnel and dried under high vacuum to afford 220 mg (0.0819 mmol, 83% yield) of **5-26** as a reddish/orange solid. ¹H NMR (500.0 MHz, CD₃OD) δ 9.41 (s, 6H), 8.14 (d, *J* = 5.9 Hz, 6H), 7.86 (dd, *J* = 5.9, 1.6 Hz, 6H), 7.60 (m, 24H); ¹³C NMR (125.7 MHz, CD₃OD) δ

162.9 (q, $J_{C-B} = 49.7$ Hz), 159.2, 154.8, 141.4 (q, $J_{C-F} = 35.9$ Hz), 135.8, 130.4 (qq, $J_{C-F} = 31.6$, 3.1 Hz), 125.7 (q, $J_{C-F} = 271.6$ Hz), 125.5 (q, $J_{C-F} = 3.5$ Hz), 124.1 (q, $J_{C-F} = 273.8$ Hz), 123.3 (q, $J_{C-F} = 3.2$ Hz), 118.5 (m); ^{19}F NMR (376.5 MHz, CD_3OD) δ -64.3, -66.2; ^{11}B NMR (160.5 MHz, CD_3OD) δ -6.77.

Sodium 3,5-bis(trifluoromethyl)benzenesulfonate ($\text{Ar}^{\text{F}}\text{SO}_3\text{Na}$) (5-79). A 25 mL round-bottom flask with a magnetic stirrer was charged with 3,5-bis(trifluoromethyl)benzenesulfonyl chloride (Matrix Scientific) (3.35 g, 10.70 mmol) and H_2O (12 mL, 0.9 M). A reflux condenser was attached, and the heterogeneous reaction was heated to an oil bath temperature of 107 °C and stirred for 3 h. Thereafter, the reaction was briefly cooled and a distillation head was attached. The residual H_2O and dissolved HCl (g) was distilled off and the resulting pale yellow solid remaining in the distillation flask was dried *in vacuo*. This solid was dissolved in H_2O (10 mL) and 4 M NaOH was added to the resulting homogeneous solution to achieve $\text{pH} = 7$. Throughout this process, a white solid precipitated from solution and was isolated. Two successive recrystallizations from boiling H_2O (~10 mL) followed by drying under high vacuum in a desiccator over P_2O_5 for 12 h provided 2.47 g (7.81 mmol, 73% yield) of **5-79** as colorless needles. ^1H NMR (500.0 MHz, CD_3OD) δ 8.34 (s, 2H), 8.06 (s, 1H), ^{13}C NMR (125.7 MHz, CD_3OD) δ 149.6, 133.0 (q, $J_{C-F} = 33.8$ Hz), 127.7 (q, $J_{C-F} = 3.5$ Hz), 124.8 (septet, $J_{C-F} = 3.8$ Hz), 124.6 (q, $J_{C-F} = 272.4$ Hz); ^{19}F NMR (376.5 MHz, CD_3OD) δ -64.5.

$\text{Ru}(\text{dfmb})_3(\text{Ar}^{\text{F}}\text{SO}_3)_2$ (5-28). A 50 mL round-bottom flask with a magnetic stirrer was charged with **5-78** (450 mg, 0.444 mmol, 1 equiv.), **5-79** (393 mg, 1.24 mmol, 2.8 equiv.) and MeOH (22 mL, 0.02 M). A reflux condenser was attached, and the reaction was heated to an oil bath temperature of 75 °C and stirred for 90 min. After cooling to room temperature, MeOH was removed *in vacuo* to afford a red residue that was dissolved in acetone/ CH_2Cl_2 (1:1, ~8 mL) and subsequently purified via gravity elution through a column of neutral Al_2O_3 using acetone/ CH_2Cl_2

(1:1) as the eluent. The first band that eluted was determined to be the desired product, so these fractions were pooled, and the volatiles were removed *in vacuo*. The product was dissolved in a minimum volume of EtOAc and passed through a 0.2 μm Whatman PTFE filter to remove residual **5-78** and **5-79**. The filtrate was layered with hexanes and left to crystallize at 5 °C. The red needles that formed were isolated, washed with hexanes, and dried under high vacuum at 100 °C for 3 h to obtain 593 mg (0.379 mmol, 85% yield) of **5-28** as a reddish/orange solid. ^1H NMR (500.0 MHz, CD_3OD) δ 9.36 (s, 6H), 8.23 (s, 4H), 8.15 (d, $J = 5.9$ Hz, 6H), 8.05 (s, 2H), 7.87 (d, $J = 5.9$ Hz, 6H); ^{13}C NMR (125.7 MHz, CD_3OD) δ 159.3, 155.1, 149.7, 141.5 (q, $J_{\text{C-F}} = 35.5$ Hz), 133.0 (q, $J_{\text{C-F}} = 33.6$ Hz), 127.6 (q, $J_{\text{C-F}} = 3.6$ Hz), 125.7 (m), 124.8 (m), 124.7 (q, $J = 277.7$ Hz), 123.9 (q, $J_{\text{C-F}} = 273.2$ Hz), 123.4 (q, $J = 3.6$ Hz); ^{19}F NMR (376.5 MHz, CD_3OD) δ -64.5, -66.1.

Sodium 3,5-bis(trifluoromethyl)benzenesulfinate ($\text{Ar}^{\text{F}}\text{SO}_2\text{Na}$) (5-80). A 100 mL round-bottom flask with a magnetic stirrer was charged with 3,5-bis(trifluoromethyl)benzenesulfonyl chloride (Matrix Scientific) (2.00 g, 6.40 mmol, 1 equiv.) and H_2O (19 mL, 0.33 M). To the heterogeneous mixture was added Na_2SO_3 (1.29 g, 10.2 mmol, 1.6 equiv.) and NaHCO_3 (0.860 g, 10.2 mmol, 1.6 equiv.). A reflux condenser was attached, and the reaction was heated to an oil bath temperature of 107 °C and stirred for 3 h. Thereafter, the reaction was cooled to room temperature and H_2O was removed *in vacuo*. To the resulting off-white solid was added EtOH (20 mL) and the heterogeneous suspension was heated to a boil and filtered. The filter was rinsed with EtOH (2 x 10 mL) and the EtOH was removed *in vacuo* to afford a white powder. Recrystallization from H_2O provided 1.36 g (4.54 mmol, 71% yield) of **5-80** as colorless needles. ^1H NMR (500.0 MHz, CD_3OD) δ 8.20 (s, 2H), 7.97 (s, 1H); ^{13}C NMR (125.7 MHz, CD_3OD) δ 161.4, 133.0 (q, $J_{\text{C-F}} = 33.4$ Hz), 126.4 (q, $J_{\text{C-F}} = 3.5$ Hz), 124.9 (q, $J_{\text{C-F}} = 272.4$ Hz), 124.0 (septet, $J_{\text{C-F}} = 3.8$ Hz); ^{19}F NMR (376.5 MHz, CD_3OD) δ -64.3.

Ru(dfmb)₃(Ar^FSO₂)₂ (5-29). Prepared according to the procedure outlined for **5-28** using **5-78** (126 mg, 0.124 mmol, 1 equiv.), **5-80** (86.5 mg, 0.274 mmol, 2.2 equiv.) and MeOH (6.2 mL, 0.02 M). Obtained 151 mg (0.0986 mmol, 78% yield) of **5-29** as a reddish/orange solid. ¹H NMR (500.0 MHz, CD₃OD) δ 9.36 (s, 6H), 8.24 (s, 4H), 8.15 (d, *J* = 5.9 Hz, 6H), 8.05 (s, 2H), 7.87 (d, *J* = 5.9 Hz, 6H); ¹³C NMR (125.7 MHz, CD₃OD) δ 159.3, 155.1, 149.7, 141.5 (q, *J*_{C-F} = 35.5 Hz), 133.0 (q, *J*_{C-F} = 33.6 Hz), 127.6 (q, *J*_{C-F} = 3.6 Hz), 125.7 (m), 124.8 (m), 124.7 (q, *J* = 277.7 Hz), 123.9 (q, *J*_{C-F} = 273.2 Hz), 123.4 (q, *J* = 3.6 Hz); ¹⁹F NMR (376.5 MHz, CD₃OD) δ -64.5, -66.1.

Ru(dfmb)₃(OTs)₂ (5-30). Prepared according to the procedure outlined for **5-28** using **5-78** (80.5 mg, 0.0795 mmol, 1 equiv.), *p*-toluenesulfonic acid sodium salt (43.2 mg, 0.222 mmol, 2.8 equiv.) and MeOH (4.0 mL, 0.02 M). Obtained 77.1 mg (0.0584 mmol, 73% yield) of **5-30** as a reddish/orange solid. ¹H NMR (500.0 MHz, CD₃OD) δ 9.39 (s, 6H), 8.15 (d, *J* = 5.9 Hz, 6H), 7.86 (d, *J* = 5.9 Hz, 6H), 7.69 (d, *J* = 8.1 Hz, 4H), 7.23 (d, *J* = 8.1 Hz, 4H), 2.37 (s, 6H); ¹³C NMR (125.7 MHz, CD₃OD) δ 159.3, 155.1, 143.8, 141.8, 141.5 (q, *J*_{C-F} = 35.4 Hz), 129.9, 127.0, 125.7 (q, *J*_{C-F} = 3.4 Hz), 123.9 (q, *J*_{C-F} = 272.7 Hz), 123.4 (q, *J*_{C-F} = 3.4 Hz), 21.4; ¹⁹F NMR (376.5 MHz, CD₃OD) δ -66.1.

Ru(dfmb)₃(PF₆)₂ (5-81). To a 25 mL round bottom flask with a magnetic stirrer was charged **5-78** (261 mg, 0.258 mmol, 1 equiv.) and H₂O (13 mL, 0.02 M). To the resulting dark red solution was added ammonium hexafluorophosphate (88.2 mg, 0.541 mmol, 2.1 equiv.). A reddish/orange solid immediately precipitated and stirring was continued for 10 min before the solid was isolated on a fritted funnel, washed with H₂O (2 x 3 mL), and dried. Recrystallization from an acetone/Et₂O bilayer provided 252 mg (0.199 mmol, 77% yield) of **5-81** as a reddish/orange solid. ¹H NMR (500.0 MHz, (CD₃)₂SO) δ 9.57 (s, 6H), 8.03 (d, *J* = 6.0 Hz, 6H), 7.88 (dd, *J* = 6.0, 1.4 Hz, 6H); ¹³C NMR (125.7 MHz, (CD₃)₂SO) δ 157.4, 153.8, 137.9 (q, *J*_{C-F} =

34.7 Hz), 124.0 (q, $J_{C-F} = 3.4$ Hz), 122.5 (q, $J_{C-F} = 273.4$ Hz), 121.9 (q, $J_{C-F} = 3.4$ Hz); ^{19}F NMR (376.5 MHz, $(\text{CD}_3)_2\text{SO}$) δ -63.0, -70.1 (d, $J_{F-P} = 711.2$ Hz); ^{31}P NMR (162.0 MHz, $(\text{CD}_3)_2\text{SO}$) δ -144.2 (septet, $J_{P-F} = 711.5$ Hz).

Table S5-1. Substrate survey in the radical cation Diels-Alder cycloaddition

| <p>5-44e</p> | <p>5-38</p> | <p>5-82</p> |
|---|--|---|
| <p>5-44e, 14 h, 93% yield, -6.0% e.e., 0% RSM 5-38, 24 h, 24% yield, 6.6% e.e., 74% RSM 5-82, 14 h, 7% yield, -10.4% e.e., 93% RSM</p> | <p>5-44e, 20 h, 70% yield, 0.6% e.e., 0% RSM 5-38, 20 h, 14% yield, -10.1% e.e., 83% RSM 5-82, 20 h, 15% yield, -6.8% e.e., 74% RSM</p> | <p>5-44e, 20 h, 99% yield, -0.2% e.e., 0% RSM 5-38, 20 h, 13% yield, -7.8% e.e., 83% RSM</p> |
| <p>5-44e, 20 h, 28% yield, 3.8% e.e., 72% RSM 5-38, 20 h, 7% yield, -6.8% e.e., 86% RSM</p> | <p>5-44e, 20 h, 94% yield, 3.2% e.e., 0% RSM 5-38, 20 h, 17% yield, 6.0% e.e., 80% RSM</p> | <p>5-44e, 20 h, 45% yield, 2.0% e.e., 51% RSM 5-38, 20 h, 4% yield, -11.4% e.e., 80% RSM</p> |
| <p>5-44e, 20 h, 57% yield, -0.4% e.e., 5% RSM 5-38, 45 h, 2% yield, ND e.e., 26% RSM 5-82, 45 h, 1% yield, ND e.e., 11% RSM</p> | <p>5-44e, 20 h, 17% yield, 2.4% e.e., 70% RSM 5-38, 20 h, 1% yield, ND e.e., 90% RSM</p> | <p>5-44e, 20 h, 7% yield, -15.2% e.e., 82% RSM 5-38, 45 h, 3% yield, 5.4% e.e., 85% RSM 5-82, 45 h, 3% yield, -10.8% e.e., 85% RSM</p> |
| <p>5-44e, 45 h, 27% yield, 0.3% e.e., 56% RSM 5-38, 45 h, 2% yield, -0.4 e.e., 81% RSM</p> | <p>1% yield, 91% RSM No chiral H-bond donor</p> | <p>1% yield, 97% RSM No chiral H-bond donor</p> |
| <p>8% yield, 67% RSM No chiral H-bond donor</p> | <p>0% yield, 100% RSM No chiral H-bond donor</p> | <p>0% yield, 100% RSM No chiral H-bond donor</p> |

5.8 References

¹ (a) Hammond, G. S.; Cole, R. S. Asymmetric induction during energy transfer. *J. Am. Chem. Soc.* **1965**, *87*, 3256–3257. (b) Hoshi, N.; Furukawa, Y.; Hagiwara, H.; Uda, H.; Sato, K. Enantiomer differentiation in the photoinduced 1,5-phenyl shift of 3-methyl-2(3*H*)-oxepinone utilizing chiral sensitizers. *Chem. Lett.* **1980**, *9*, 47–50. (c) Inoue, Y.; Yokoyama, T.; Yamasaki, N.; Tai, A. An optical yield that increases with temperature in a photochemically induced enantiomeric isomerization. *Nature* **1989**, *341*, 225–226. (d) Kim, J. -I.; Schuster, G. B. Enantioselective catalysis of the triplex Diels-Alder reaction: A study of scope and mechanism. *J. Am. Chem. Soc.* **1992**, *114*, 9309–9317.

² (a) Radicals in Organic Synthesis (Eds.: Renaud, P.; Sibi, M. P.), Wiley-VCH, Weinheim, 2001. (b) Curran, D. P.; Porter, N. A.; Giese, B. In *Stereochemistry of Radical Reactions*, VCH, Weinheim, 1996.

³ (a) Tolbert, L. M.; Ali, M. B. High optical yields in a photochemical cycloaddition. Lack of cooperativity as a clue to mechanism. *J. Am. Chem. Soc.* **1982**, *104*, 1742–1744. (b) Yamamoto, Y.; Onuki, S.; Yumoto, M.; Asao, N. Zinc chloride as a radical initiator as well as a chelating agent. *J. Am. Chem. Soc.* **1994**, *116*, 421–422. (c) Sibi, M. P.; Jasperse, C. P.; Ji, J. Lewis acid-mediated intermolecular β -selective radical additions to *N*-enoyloxazolidinones. *J. Am. Chem. Soc.* **1995**, *117*, 10779–10780. (d) Molander, G. A.; McWilliams, J. C.; Noll, B. C. Remote stereochemical control of both reacting centers in ketyl-olefin radical cyclizations: involvement of a samarium tridentate ligate. *J. Am. Chem. Soc.* **1997**, *119*, 1265–1276.

⁴ For seminal reports on diastereoselective Lewis-acid catalysis of radical reactions see: (a) Guindon, Y.; Lavallee, J.-F.; Llinas-Brunet, M.; Horner, G.; Rancourt, J. Stereoselective chelation-controlled reduction of α -iodo- β -alkoxy esters under radical conditions. *J. Am. Chem. Soc.* **1991**, *113*, 9701–9702. (b) Toru, T.; Watanabe, Y.; Tsusaka, M.; Ueno, Y. High β -stereoselectivity in asymmetric radical addition to α -sulfinylcyclopentenones. *J. Am. Chem. Soc.* **1993**, *115*, 10464–10465. For early reports on enantioselective reactions with chiral Lewis acids see: (c) Murakata, M.; Tsutsui, H.; Hoshino, O. Enantioselective radical-mediated reduction of α -iodolactone using tributyltin hydride in the presence of a chiral amine and Lewis acid. *J. Chem. Soc. Chem. Commun.* **1995**, *4*, 481. (d) Wu, J. H.; Radinov, R.; Porter, N.A. Enantioselective free radical carbon-carbon bond forming reactions: chiral Lewis acid promoted acyclic additions. *J. Am. Chem. Soc.* **1995**, *117*, 11029.

⁵ Du, J.; Skubi, K. L.; Schultz, D. M.; Yoon, T. P. A dual-catalysis approach to enantioselective [2+2] photocycloadditions using visible light. *Science* **2014**, *344*, 392–396.

⁶ (a) Gielen, M.; Tondeur, Y. *J. Organomet. Chem.* **1977**, *127*, C75. (b) Nanni, D.; Curran, D. P. Synthesis and some reactions of the first chiral tin hydride containing a C_2 -symmetric binaphthyl substituent. *Tetrahedron: Asymmetry* **1996**, *7*, 2417–2422. (c) Blumenstein, M.; Schwarzkopf, K.; Metzger, J. O. Enantioselective hydrogen transfer from a chiral tin hydride to a prochiral carbon-centered radical. *Angew. Chem. Int. Ed.* **1997**, *36*, 235–236.

⁷ (a) Aechtner, T.; Dressel, M.; Bach, T. Hydrogen bond mediated enantioselectivity of radical reactions. *Angew. Chem. Int. Ed.* **2004**, *43*, 5849–5851.

⁸ (a) Inoue, Y.; Okano, T.; Yamasaki, N.; Tai, A. First photosensitized enantiodifferentiating polar addition: anti-Markovnikov methanol addition to 1,1-diphenylpropene. *J. Chem. Soc. Chem. Commun.* **1993**, *8*, 718–720. (b) Asaoka, S.; Wada, T.; Inoue, Y. Microenvironmental polarity control of electron-transfer photochirgenesis. Enantiodifferentiating polar addition of 1,1-diphenyl-1-alkenes photosensitized by saccharide naphthalenecarboxylates. *J. Am. Chem. Soc.* **2003**, *125*, 3008–3027.

⁹ While radical ions were observed in polar media, in which full electron transfer was shown to be operative and feasible, the investigators demonstrate significant (~40%) exciplex polarization in nonpolar solvents and provide evidence conclusively arguing against electron transfer: (a) Calhoun, G. C.; Schuster, G. B. Radical cation and triplex Diels-Alder reactions of 1,3-cyclohexadiene. *J. Am. Chem. Soc.* **1984**, *106*, 6870–6871. (b) Calhoun, G. C.; Schuster, G. B. The triplex Diels-Alder reaction of indene and cyclic dienes. *J. Am. Chem. Soc.* **1986**, *108*, 8021–8027. (c) Kim, J. -I.; Schuster, G. B. Enantioselective catalysis of the triplex Diels-Alder reaction: addition of *trans*- β -methylstyrene to 1,3-cyclohexadiene photosensitized with (–)-1,1'-bis(2,4-dicyanonaphthalene). *J. Am. Chem. Soc.* **1990**, *112*, 9635–9637.

¹⁰ (a) Lin, S.; Padilla, C. E.; Ischay, M. A.; Yoon, T. P. Visible light photocatalysis of intramolecular radical cation Diels-Alder cycloadditions. *Tetrahedron Lett.* **2012**, *53*, 3073–3076. (b) Lin, S.; Ischay, M. A.; Fry, C. G.; Yoon, T. P. Radical cation Diels-Alder cycloadditions by visible light photocatalysis. *J. Am. Chem. Soc.* **2011**, *133*, 13950–13953

¹¹ This was found to be an irreversible one-electron oxidation, so the potential is reported vs. SCE in CH₃CN at a scan rate of 100 mV/sec.

¹² (a) Bjerrum, N.; Dan. K. *Videsk. Selesk. Math.-Fys. Medd.* **1926**, *7*, 3. (b) Szwarc, M. *Acc. Chem. Res.* **1969**, *2*, 87–96. (c) Anslyn, E. V.; Dougherty, D. A. In *Modern Physical Organic Chemistry*, University Science Books, Sausalito, 2006, p. 164. (c) Marcus, Y.; Hefter, G. Ion pairing. *Chem. Rev.* **2006**, *106*, 4585–4621.

¹³ Brunel, J. M. BINOL: a versatile chiral reagent. *Chem. Rev.* **2005**, *105*, 857–897.

¹⁴ (a) Mayer, S.; List, B. Asymmetric counteranion-directed catalysis. *Angew. Chem, Int. Ed.* **2006**, *45*, 4193. (b) Li, C.; Wang, C.; Villa-Marcos, B.; Xiao, J. Chiral counteranion-aided asymmetric hydrogenation of acyclic imines. *J. Am. Chem. Soc.* **2008**, *130*, 14450–14451.

¹⁵ (a) O’Konnell, M. J. In *Catalytic Asymmetric Synthesis*, 2nd ed.; Ojima, I., Ed.; Wiley-VCH: New York, 2000; Chapter 10, p. 727. (b) Hamilton, G. L.; Kang, E. J.; Mba, M.; Toste, F. D. A powerful chiral counterion strategy for asymmetric transition metal catalysis. *Science* **2007**, *317*, 496–499. (c) Mukherjee, S.; List, B. Chiral counteranions in asymmetric transition-metal catalysis: highly enantioselective Pd/Brønsted acid-catalyzed direct α -allylation of aldehydes. *J. Am. Chem. Soc.* **2007**, *129*, 11336.

¹⁶ (a) Enders, D.; Narine, A. A.; Toulgoat, F.; Bisschops, T. Asymmetric Brønsted acid catalyzed isoindoline synthesis: enhancement of enantiomeric ratio by stereoablative kinetic resolution. *Angew. Chem. Int. Ed.* **2008**, *47*, 5661–5665. (b) Rueping, M.; Uria, U.; Lin, M.-Y.; Atodiresei, I. Chiral organic contact ion pairs in metal-free catalytic asymmetric allylic substitutions. *J. Am. Chem. Soc.* **2011**, *133*, 3732–3735.

¹⁷ (a) Schanz, H.-J.; Linseis, M. A.; Gillheany, D. G. Improved resolution methods for (*R,R*)- and (*S,S*)-cyclohexane-1,2-diamine and (*R*)- and (*S*)-BINOL. *Tetrahedron Asymmetry* **2003**, *14*, 2763–2769. (b) Wipf, P.; Jung, J.-K. Formal total synthesis of (+)-diepoxin σ . *J. Org. Chem.* **2000**, *65*, 6319–6337.

¹⁸ For the preparation of phosphoric acids (**5-11** – **5-13**), see: (a) Yamanaka, M.; Itoh, J.; Fuchibe, K.; Akiyama, T. Chiral Brønsted acid catalyzed enantioselective Mannich-type reaction. *J. Am. Chem. Soc.* **2007**, *129*, 6756–6764. For the preparation of *N*-triflyl phosphoramides (**5-14** – **5-16**), see: (b) Nakashima, D.; Yamamoto, H. Design of chiral *N*-triflyl phosphoramide as a strong chiral Brønsted acid and its application to asymmetric Diels-Alder reaction. *J. Am. Chem. Soc.* **2006**, *128*, 9626–9627. For the preparation of *N*-triflyl phosphoramide **5-17**, see (c) Wu, T. B.; Shen, L.; Chong, J. M. Asymmetric allylboration of aldehydes and ketones using 3,3'-disubstitutedbinaphthol-modified boronates. *Org. Lett.* **2004**, *6*, 2701–2704. For the preparation of disulfonamide **5-18** and bis-sulfonic acid **5-19**, see (d) García-García, P.; Lay, F.; Garcia-Garcia, P.; Rabalakos, C.; List, B. A powerful chiral counteranion motif for asymmetric catalysis. *Angew. Chem. Int. Ed.* **2009**, *48*, 4363–4366. For the preparation of *N*-phosphinyl phosphoramide **5-20**, see (e) Vellalath, S.; Čorić, I.; List, B. *N*-phosphinyl phosphoramide – a chiral Brønsted acid motif for the direct asymmetric N,O-acetalization of aldehydes. *Angew. Chem. Int. Ed.* **2010**, *49*, 9749–9752.

¹⁹ For the preparation of silver (I) phosphate salts (NH₄CO₃ was used in place of Ag₂CO₃ for the preparation of ammonium phosphate salts), see Aikawa, K.; Kojima, M.; Mikami, K. Axial chirality control of gold(biphep) complexes by chiral anions: application to asymmetric catalysis. *Angew. Chem. Int. Ed.* **2009**, *48*, 6073–6077.

²⁰ Christ, P.; Lindsay, A. G.; Vormittag, S. S.; Neudorfl, J.-M.; Berkessel, A.; O'Donoghue, A. C. pK_a values of chiral Brønsted acid catalysts: phosphoric acids/amides, sulfonyl/sulfonyl imides, and perfluorinated TADDOLs (TEFDDOLs). *Chem. Eur. J.* **2011**, *17*, 8524–8528.

²¹ (a) Gleria, M.; Minto, F.; Beggiato, G.; Bortolus, P. Photochemistry of tris(2,2'-bipyridine)ruthenium(II) in chlorinated solvents. *J. Chem. Soc. Chem. Commun.* **1978**, 285. (b) Hoggard, P. E.; Porter, G. B. Photoanation of the tris(2,2'-bipyridine)ruthenium(II) cation by thiocyanate. *J. Am. Chem. Soc.* **1978**, *100*, 1457–1463. (c) Jones, R. F.; Cole-Hamilton, D. J. The substitutional photochemistry of tris(bipyridyl)-ruthenium(II)chloride. *Inorg. Chim. Acta.* **1981**, L3–L5. (d) Khan, M. M. T.; Bhardwaj, R. C.; Bhardwaj, C. Ruthenium(II)-bipyrimidine complexes: characterization, spectroscopy and photoanation studies. *Polyhedron* **1990**, *9*, 1243–1248.

²² Juris, A.; Balzani, V. Ru(II) polypyridine complexes: photophysics, photochemistry, electrochemistry, and chemiluminescence. *Coord. Chem. Rev.* **1988**, *84*, 85–277.

²³ (a) Yates, P.; Eaton, P. Acceleration of the Diels-Alder reaction by aluminium chloride. *J. Am. Chem. Soc.* **1960**, *82*, 4436–4437. (b) Hashimono, S.-I.; Komeshima, N.; Koga, K. Asymmetric Diels-Alder reaction catalyzed by chiral alkoxyaluminium dichloride. *J. Chem. Soc. Chem. Commun.* **1979**, 437–438. (c) Evans, D. A.; Johnson, J. S.; Olhava, E. J. Enantioselective synthesis of dihydropyrans. Catalysis of hetero Diels–Alder reactions by bis(oxazoline) copper(II) complexes. *J. Am. Chem. Soc.* **2000**, *122*, 1635–1649.

²⁴ (a) Wasserman, A. Homogeneous catalysis of diene syntheses. A new type of third-order reaction. *J. Chem. Soc.* **1942**, 618–621. (b) Huang, Y.; Unni, A. K.; Thadani, A. N.; Rawal, V. H.

Hydrogen bonding: single enantiomers from a chiral-alcohol catalyst. *Nature* **2003**, *424*, 146. (c) Thadani, A. N.; Stankovic, A. R.; Rawal, V. H. Enantioselective Diels-Alder reactions catalyzed by hydrogen bonding. *Proc. Natl. Acad. Sci. U.S.A.* **2004**, *101*, 5846–5850.

²⁵ (a) Ahrendt, K. A.; Borths, C. J.; Macmillan, D. W. C. New strategies for organic synthesis: the first highly enantioselective organocatalytic Diels-Alder reaction. *J. Am. Chem. Soc.* **2000**, *122*, 4243–4244. (b) Mangion, I. K.; Northrup, A. B.; MacMillan, D. W. C. Importance of iminium geometry control in enamine catalysis: identification of a new catalyst architecture for aldehyde-aldehyde couplings. *Angew. Chem. Int. Ed.* **2004**, *43*, 6722–6724.

²⁶ For seminal early publications in the area of anion-binding by organic moieties, see (a) Park, C.H.; Simmons, H. E. Macrobicyclic amines. III. Encapsulation of halide ions by *in,in*-1,(*k*+2)-diazabicyclo[*k,l,m*]alkane-ammonium ions. *J. Am. Chem. Soc.* **1968**, *90*, 2431. (b) Fan, E.; Vanarman, S. A.; Kincaid, S.; Hamilton, A. D. Molecular recognition: hydrogen-bonding receptors that function in highly competitive solvents. *J. Am. Chem. Soc.* **1993**, *115*, 369–370.

²⁷ (a) Breslow, R. Centenary lecture. Biomimetic chemistry. *Chem. Soc. Rev.* **1972**, *1*(4), 553–580. (b) Tramantano, A.; Janda, K.D.; Schultz, P. G. Catalytic antibodies. *Science* **1986**, *234*, 1566–1570. (c) Pollack, S. J.; Jacobs, J. W.; Schultz, P. G. Selective chemical catalysis by an antibody. *Science* **1986**, *234*, 1570–1573.

²⁸ (a) Schreiner, P. R.; Wittkopp, A. H-bonding additives act like Lewis acid catalysts. *Org. Lett.* **2002**, *4*, 217–220. (b) Wittkopp, A.; Schreiner, P. R. Metal-free, noncovalent catalysis of Diels-Alder reactions by *neutral* hydrogen bond donors in organic solvents and in water. *Chem. Eur. J.* **2003**, *9*, 407–414.

²⁹ Brak, K.; Jacobsen, E. N. Asymmetric ion-pairing catalysis. *Angew. Chem. Int. Ed.* **2013**, *52*, 534–561.

³⁰ (a) Furue, M.; Maruyama, K.; Oguni, T.; Naiki, M.; Kamachi, M. Trifluoromethyl-substituted 2,2'-bipyridine ligands. Synthetic control of excited-state properties of ruthenium(II) tris-chelate complexes. *Inorg. Chem.* **1992**, *31*, 3792–3795. (b) McFarland, S. A.; Lee, F. S.; Cheng, K. A. W. Y.; Cozens, F. L.; Schepp, N. P. Picosecond dynamics of nonthermalized excited states in tris(2,2'-bipyridine)ruthenium(II) derivatives elucidated by high energy excitation. *J. Am. Chem. Soc.* **2005**, *127*, 7065–7070.

³¹ a) Etter, M. C.; Panunto, T. W. 1,3-bis(*m*-nitrophenyl)urea: an exceptionally good complexing agent for proton acceptors. *J. Am. Chem. Soc.* **1988**, *110*, 5896–5897; b) Etter, M. C.; Urbańczyk-Lipkowska, Z.; Zia-Ebrahimi, M.; Panunto, T. W. Hydrogen bond directed cocrystallization and molecular recognition properties of diarylureas. *J. Am. Chem. Soc.* **1990**, *112*, 8415–8426.

³² (a) Sigman, M. S.; Jacobsen, E. N. Schiff base catalysts for the asymmetric Strecker reaction identified and optimized from parallel synthetic libraries. *J. Am. Chem. Soc.* **1998**, *120*, 4901–4902. (b) Yoon, T. P.; Jacobsen, E. N. Highly enantioselective thiourea-catalyzed nitro-Mannich reactions. *Angew. Chem. Int. Ed.* **2005**, *44*, 466–468. (c) Tan, K. L.; Jacobsen, E. N. Indium-mediated asymmetric allylation of acylhydrazones using a chiral urea catalyst. *Angew. Chem. Int. Ed.* **2007**, *46*, 1315–1317. (d) Reisman, S. E.; Doyle, A. G.; Jacobsen, E. N. Enantioselective thiourea-catalyzed additions to oxocarbenium ions. *J. Am. Chem. Soc.* **2008**,

130, 7198–7199. (e) Knowles, R. R.; Lin, S.; Jacobsen, E. N. Enantioselective thiourea-catalyzed cationic polycyclizations. *J. Am. Chem. Soc.* **2010**, *132*, 5030–5032.

³³ Values in DMSO. See: Bordwell, F. G.; Algrim, D. J.; Harrelson, J. A., Jr. The relative ease of removing a proton, a hydrogen atom, or an electron from carboxamides versus thiocarboxamides. *J. Am. Chem. Soc.* **1988**, *110*, 5903–5904.

³⁴ Suspecting competitive excited state quenching of photocatalyst **5-29** by the sulfur nucleus of the thiourea, electrochemical analysis was performed. These data demonstrated the plausibility of slightly endergonic electron transfer from the sulfur nucleus of the thiourea ($E^\circ(\text{R/R}^+) = +1.29 \text{ V}$)¹¹ to the excited state of **5-29**.

³⁵ (a) Robak, M. T.; Trincado, M.; Ellman, J. A. Enantioselective aza-Henry reaction with an *N*-sulfinyl urea organocatalyst. *J. Am. Chem. Soc.* **2007**, *129*, 15110–15111. (b) Kimmel, K. L.; Robak, M. T.; Ellman, J. A. Enantioselective addition of thioacetic acid to nitroalkenes via *N*-sulfinyl urea organocatalysis. *J. Am. Chem. Soc.* **2009**, *131*, 8754–8756.

³⁶ Xu, H.; Zuend, S. J.; Woll, M. G.; Tao, Y.; Jacobsen, E. N. Asymmetric cooperative catalysis of strong Brønsted acid-promoted reactions using chiral ureas. *Science* **2010**, *327*, 986–990.

³⁷ Ogura, Y.; Akakura, M.; Sakakura, A.; Ishihara, K. Enantioselective cycloethoxycarbonylation of isatins promoted by a Lewis base- Brønsted acid cooperative catalyst. *Angew. Chem. Int. Ed.* **2013**, *52*, 8299–8303.

³⁸ Ganesh, M.; Seidel, D. Catalytic enantioselective additions of indoles to nitroalkenes. *J. Am. Chem. Soc.* **2008**, *130*, 16464–16465.

³⁹ (a) Ohkubo, K.; Suga, K.; Morikawa, K.; Fukuzumi, S. Selective oxygenation of ring-substituted toluenes with electron-donating and –withdrawing substituents by molecular oxygen via photoinduced electron transfer. *J. Am. Chem. Soc.* **2003**, *125*, 12850–12859. (b) Ohkubo, K.; Kobayashi, T.; Fukuzumi, S. Direct oxygenation of benzene to phenol using quinolinium ions as homogeneous photocatalysts. *Angew. Chem. Int. Ed.* **2011**, *50*, 8652–8655.

⁴⁰ (a) Hamilton, D. S.; Nicewicz, D. A. Direct catalytic anti-Markovnikov hydroetherification of alkenols. *J. Am. Chem. Soc.* **2012**, *134*, 18577–18530. (b) Perkowski, A. J.; Nicewicz, D. A. Direct catalytic anti-Markovnikov addition of carboxylic acids to alkenes. *J. Am. Chem. Soc.* **2013**, *135*, 10334–10337.

⁴¹ The magnitude of this result was not reproducible. Subsequent runs gave 20–30% lower conversions at the same time point. The pyridinium and quinolinium salts are hygroscopic; pre-drying the salts by dissolution in CH_2Cl_2 followed by stirring over freshly flame-dried MgSO_4 for 1 h under N_2 and subsequent removal of CH_2Cl_2 in an air-free environment immediately before experimental runs improved reproducibility. Further, storing the dried salts at -30°C in a glovebox helped to avoid decomposition over long periods of storage.

⁴² To a first approximation, this was an entirely unexpected result, as UV-Vis analysis ($1.6 \times 10^{-4} \text{ M}$) of pyridinium $\text{BAR}_4^{\text{F}^-}$ showed $\lambda_{\text{max}} = 315 \text{ nm}$ and **5-52a (S)** showed $\lambda_{\text{max}} = 312 \text{ nm}$. These maxima are both well outside the visible spectrum. However, at catalytically relevant concentrations ($1.6 \times 10^{-2} \text{ M}$, 20 mol%) absorbance at 400 nm was very low, but non-negligible (0.185 AU for **5-52a (S)**, 0.075 AU for **5-52b (S)**, and 0.060 AU for **5-52c (S)**).

-
- ⁴³ Rodriguez, A. A.; Yoo, H.; Ziller, J. W.; Shea, K. J. New architectures in hydrogen bond catalysis. *Tetrahedron Lett.* **2009**, *50*, 6830–6833.
- ⁴⁴ Cranwell, P. B.; Hiscock, J. R.; Haynes, C. J. E.; Light, M. E.; Wells, N. J.; Gale, P. A. Anion recognition and transport properties of sulfamide-, phosphoric triamide- and thiophosphoric triamide-based receptors. *Chem. Commun.* **2013**, *49*, 874–876.
- ⁴⁵ Gassman, P. G.; Singleton, D. A.; Wilwerding, J. J.; Chavan, S. P. Acrolein acetals as allyl cation precursors in the ionic Diels–Alder reaction. *J. Am. Chem. Soc.* **1987**, *109*, 2182–2184.
- ⁴⁶ Borovika, A.; Tang, P.-I.; Klapman, S.; Nagorny, P. Thiophosphotriamide-based cooperative catalysts for Brønsted acid promoted ion Diels–Alder reactions. *Angew. Chem. Int. Ed.* **2013**, *52*, 13424–13428.
- ⁴⁷ Lukesh, J. C., III; Palte, M. J.; Raines, R. T. A potent, versatile disulfide-reducing agent from aspartic acid. *J. Am. Chem. Soc.* **2012**, *134*, 4057–4059.
- ⁴⁸ However, it should be noted that a confounding variable in these studies is the heterogeneous nature of reactions containing **5-63**, **5-64**, and **5-65**. Furthermore, though thiophosphotriamide derivatives tended to exhibit superior solubility profiles, competitive sulfur oxidation inhibited reactivity.
- ⁴⁹ Klapars, A.; Huang, X.; Buchwald, S. L. A general and efficient copper catalyst for the amidation of aryl halides. *J. Am. Chem. Soc.* **2002**, *124*, 7421–7428.
- ⁵⁰ Wang, C.-J.; Gao, F.; Liang, G. Axial 4,4',6,6'-tetrakis-trifluoromethyl-biphenyl-2,2'-diamine (TF-BIPHAM): resolution and applications in asymmetric hydrogenation. *Org. Lett.* **2008**, *10*, 4711–4714.
- ⁵¹ Denmark, S. E.; Winter, S. B. D.; Su, X.; Wong, K.-T. Chemistry of trichlorosilyl enolates. 1. New reagents for catalytic, asymmetric aldol additions. *J. Am. Chem. Soc.* **1996**, *118*, 7404–7405.
- ⁵² Zuend, S. J.; Jacobsen, E. N. Mechanism of amido-thiourea catalyzed enantioselective imine hydrocyanation: transition state stabilization via multiple non-covalent interactions. *J. Am. Chem. Soc.* **2009**, *131*, 15358–15374.
- ⁵³ Schlosser, M.; Marull, M. The direct metalation and subsequent functionalization of trifluoromethyl-substituted pyridines and quinolones. *Eur. J. Org. Chem.* **2003**, 1569–1575.
- ⁵⁴ Schultz, D. M.; Sawicki, J. W.; Yoon, T.P. An improved procedure for the preparation of Ru(bpz)₃(PF₆)₂ via a high-yielding synthesis of 2,2'-bipyrazine. *Beilstein J. Org. Chem.* **2015**, *11*, 61–65.

**Chapter 6. Counteranion Effects on the Properties of Polypyridyl Ru(II)
Complexes**

6.1 Introduction

The photochemistry of tris-chelated polypyridyl Ru(II) complexes has been the subject of intense investigation for many decades.¹ Visible light induced excitation of the $[\text{Ru}(\text{L})_3]^{2+}$ singlet ground state followed by rapid intersystem crossing affords a long-lived, redox active metal-to-ligand charge transfer (MLCT) triplet excited state $[\text{Ru}(\text{L})_3]^{2+*}$ that is a potent source of electrochemical potential.² Taking advantage of the rich bimolecular quenching events made possible by the slow, radiationless decay of this MLCT excited state, our group,³ among others,⁴ has recently demonstrated that a variety of polypyridyl Ru(II) complexes catalyze a broad array of carbon–carbon and carbon–heteroatom bond forming reactions mediated by reactive open-shell radicals.

While the photophysical properties of these homoleptic sensitizers have been intensively studied in polar solvents such as water ($\epsilon = 78$) and acetonitrile ($\epsilon = 37.1$), their use in nonpolar organic solvents ($\epsilon < 20$) has received far less attention, primarily because reports of utilizing these photoinduced electron transfer sensitizers in synthetic organic chemistry were scarce before 2008. Empirically, however, the most commonly utilized ruthenium sensitizers exhibit sparing solubility in the solvents typically employed in synthetic applications due to their charge and to the presence of hydrophilic inorganic counteranions (Cl^- , PF_6^- , ClO_4^- , BF_4^-). This issue was certainly not localized to inorganic sensitizers, and research programs were launched in an attempt to identify counteranions that would enable study of naked cationic metal complexes in nonpolar organic solvents.⁵ Indeed, this locus of research in tandem with the advent of weakly-coordinating, lipophilic counteranions such as $\text{BAr}_4^{\text{F}-}$ was critical in answering fundamental questions regarding the reactivity, coordination geometries, and solution-phase behaviour of myriad transition metal, lanthanide, and lanthanoid complexes.⁶

Counteranion identity, however, had never been observed to modulate the chemical properties of polypyridyl ruthenium sensitizers, and as such, the aforementioned advances were

not deemed to be critical for eliciting desired reactivity from these photocatalyst complexes. Indeed, there was no reason to posit otherwise – the importance of ion-pairing is diminished in the high dielectric solvents inherent to the majority of investigations in the field of inorganic photochemistry.

6.2 Results and Discussion

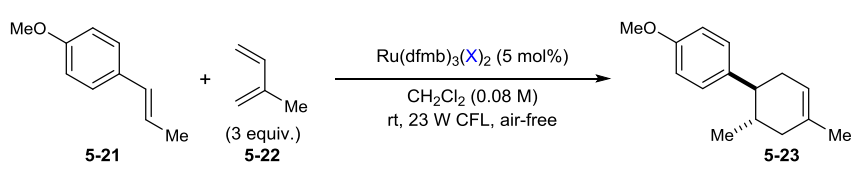
6.2.1 Photophysical Studies and the Kinetics of Excited State Quenching

In the course of investigating radical cation Diels-Alder cycloadditions promoted by visible light irradiation of $[\text{Ru}(\text{bpy})_3]^{2+}$ derivatives⁷ (Chapter 5), we were surprised to observe a dramatic dependence of the reaction rate on the identity of the photocatalyst counteranion. When mixtures of anethole (**5-21**) and isoprene (**5-22**) in CH_2Cl_2 ($\epsilon = 8.93$) were exposed to a series of $[\text{Ru}(\text{dfmb})_3](\text{X})_2$ complexes under anaerobic conditions, a decrease in cycloaddition to afford **5-23** occurred as the Lewis basicity of the counteranion X^- was increased (Table 5-2, Table 6-1). Thus, complex **5-26** containing a weakly coordinating counteranion such as $\text{BAr}_4^{\text{F}-}$ afforded rapid conversion to the cycloadduct, whereas complexes **5-28**, **5-29**, and **5-30** containing significantly more coordinating sulfonate and sulfinate counteranions gave sluggish conversion. To the best of our knowledge, this represents the first study revealing a strong correlation between photocatalyst counteranion and reaction rate in an organic transformation.

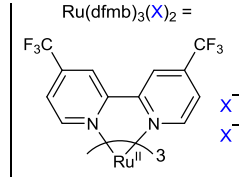
Given the nonpolar nature of CH_2Cl_2 , it appears reasonable to expect that tight ion pairing between the cationic $\text{Ru}(\text{dfmb})_3^{2+}$ and X^- may have a significant influence on the luminescence properties of $\text{Ru}(\text{dfmb})_3^{2+}$. Indeed, recent investigations have implicated formation of tight or contact ion pairs in perturbing the absorption spectra of polypyridyl Ru(II) complexes as well as the excited state lifetimes and the quantum yields of photoluminescence.⁸ Furthermore, Schuster⁹ and Tatikolov¹⁰ observed marked changes in the inherent electronic

structure and photophysical properties of cationic cyanines as the result of electrostatic interactions in both penetrated and solvent separated ion pairs.

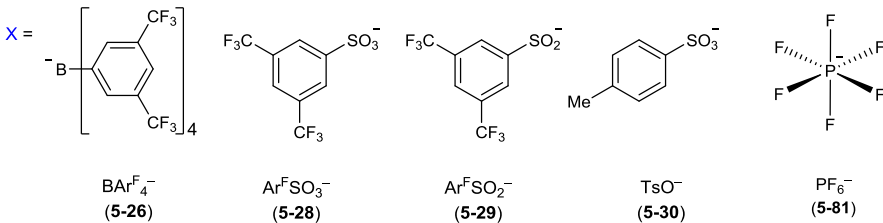
Table 6-1. Counteranion survey with Ru(dfmb)₃²⁺ complexes^a



Ru(dfmb)₃(X)₂ =



X =

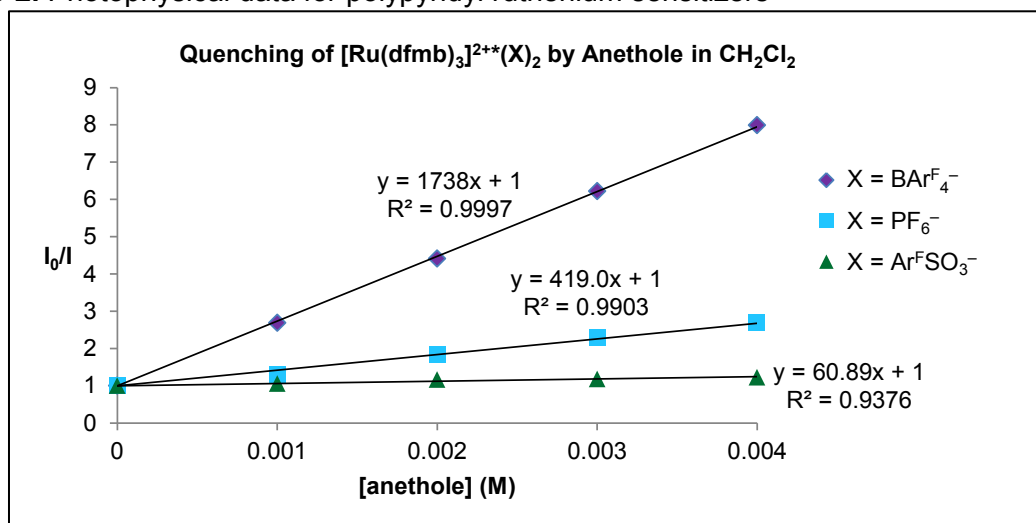


| entry | [Ru] | time | yield ^b 5-23 | remaining ^b 5-21 |
|-------|-------------|--------|--------------------------------|------------------------------------|
| 1 | 5-26 | 20 min | 98% | — |
| 2 | 5-28 | 20 h | 15% | 80% |
| 3 | 5-29 | 20 h | 10% | 85% |
| 4 | 5-30 | 20 h | 2% | 95% |

^aTo an oven-dried 25-mL Schlenk tube with a magnetic stirrer was added [Ru] followed by a stock solution of **5-21** (0.061 mmol), **5-22** (0.18 mmol), and trimethyl(phenyl)silane internal standard (0.061 mmol) in dry CH₂Cl₂ (0.08 M). The solution was submitted to 3 freeze-pump-thaw cycles, purged with N₂, and irradiated at room temperature with a 23 W CFL. ^bSubsequently, an aliquot was collected for ¹H NMR analysis to determine yield **5-23** and remaining **5-21**.

We surmised that the photocatalyst counteranion could be responsible for modulating any of three key properties relevant to product formation: (a) the ground state (S₀) luminescence and electrochemical properties,¹¹ (b) the excited triplet state (T₁) phosphorescence and kinetics of quenching by anethole, and/or (c) the chain length in radical cation propagation.

To begin, we examined the absorption properties of complexes **5-26**, **5-28**, and [Ru(dfmb)₃](PF₆)₂ (**5-81**) in CH₂Cl₂ (Table 6-2, column 3).¹² Electronic absorption data collected by UV-vis analysis showed a MLCT transition near 458 nm for all three complexes (Section 6.4.3). The same experiments conducted in MeCN gave common absorption maxima at 458 nm. Thus, the S₀→S₁ transition is minimally perturbed by counteranion identity.¹³

Table 6-2. Photophysical data for polypyridyl ruthenium sensitizers

| entry | {Ru} | λ_{abs} (nm) | λ_{em} (nm) | K_{SV} (M ⁻¹) | τ (ns) | $k_{\text{q}}^{\text{obs}}$ (M ⁻¹ s ⁻¹) |
|-------|-------------|-----------------------------|----------------------------|------------------------------------|-------------|--|
| 1 | 5-26 | 453 | 573 | 1738 | 520 | 3.34×10^9 |
| 2 | 5-81 | 458 | 605 | 419.0 | 856 | 4.89×10^8 |
| 3 | 5-28 | 458 | 618 | 60.89 | 948 | 6.42×10^7 |

Steady-state room temperature photoluminescence spectra of the complexes were collected in CH₂Cl₂ by irradiating samples at the MLCT peak wavelength and monitoring phosphorescence intensity (Section 6.4.3). We observed large bathochromic shifts of the characteristic CT emission band near 600 nm (Table 6-2, column 4) and increased photoluminescence intensity as the Lewis basicity of the counteranion was increased. These observations indicate that the counteranion has a significant effect on the electronic nature of Ru(dfmb)₃²⁺. Though the precise reasons behind the decrease in photoluminescence intensity remain unclear at this time, Meyer has observed that a decrease in integrated steady state photoluminescence is fundamentally related to changes in the radiative and nonradiative rate constants for excited state decay.^{8b} Studies carried out in MeCN, in contrast, revealed no bathochromic shift in the CT emission band at 608 nm and identical photoluminescence intensities. Thus this effect on the photophysical properties of the MLCT state emerge only in nonpolar organic solvents such as CH₂Cl₂.

Subsequently, the phosphorescence quenching of $\text{Ru}(\text{dfmb})_3^{2+*}$ by anethole was studied (Table 6-2) and was found to obey ($R^2 > 0.93$ for all cases) Stern-Volmer kinetics for dynamic quenching (eq 1):

$$\frac{I_0}{I} = 1 + K_{SV}[\text{anethole}] = 1 + k_q^{\text{obs}}\tau[\text{anethole}] \quad (1)$$

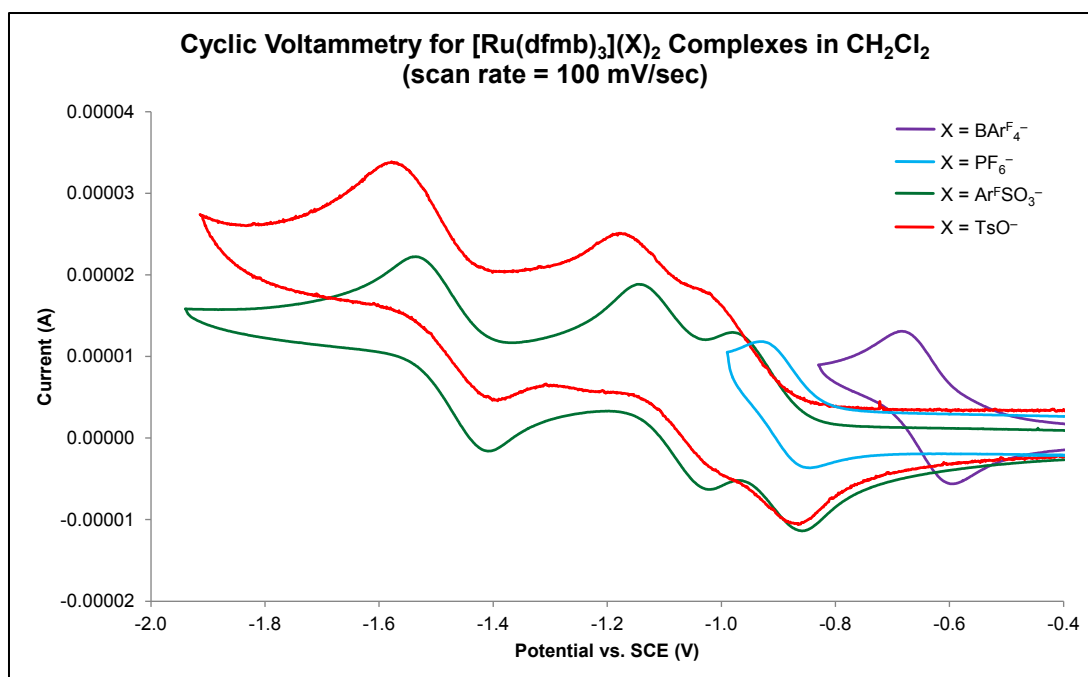
where I_0 and I represent the photoluminescence intensity in the absence and presence of anethole quencher, respectively, k_q^{obs} is the empirically-determined rate at which anethole quenches the photocatalyst excited state, and τ is the excited state lifetime. The Stern-Volmer constant (K_{SV}) for each complex was determined from the slope of the appropriate linear regression, and we observed a marked, 30-fold change in K_{SV} between **5-26** and **5-28**. Since K_{SV} is the product of k_q and τ , we independently measured τ and found relatively small differences for complexes **5-26**, **5-28**, and **5-81**. These measurements, however, enabled us to calculate k_q for each of the complexes, which was found to vary 50-fold between **5-26** and **5-28**. Therefore, we conclude that the photocatalyst counteranion dramatically alters the rate at which $\text{Ru}(\text{dfmb})_3^{2+*}$ is quenched by anethole.

6.2.2 Electrochemical Studies

Given the differences observed in the phosphorescence data, it seemed plausible that excited state redox potentials could be affected by counteranion identity. In accord with this hypothesis, the electrochemical properties of **5-26**, **5-28**, **5-30**, and **5-81** were investigated by obtaining a series of cyclic voltammograms in CH_2Cl_2 using $\text{Bu}_4\text{N}^+\text{X}^-$ salts as supporting electrolytes, with X^- corresponding to the respective photocatalyst counteranion. As shown in Table 6-3, lowering counteranion Lewis basicity resulted in significant anodic shifts of $\text{Ru}^{2+/+}$ ground state potentials. Using these potentials and the assumption that the Helmholtz free energy change for the $\text{S}_0 \rightarrow \text{T}_1$ transition can be approximated by the corresponding minimum-to-minimum energy difference ($E_{0,0}$),¹⁴ the catalytically-relevant first triplet excited state redox

potentials ($\text{Ru}^{2+*/+}$) were computed and were found to span a range of 480 mV.¹⁴ Of all the counteranions examined, BARF_4^- clearly has the largest influence on redox potential. However, the reasons for the substantial potential difference between BARF_4^- and the other counteranions, especially PF_6^- , are currently not understood.

Table 6-3. Electrochemical data in CH_2Cl_2 and the dependence on counteranion

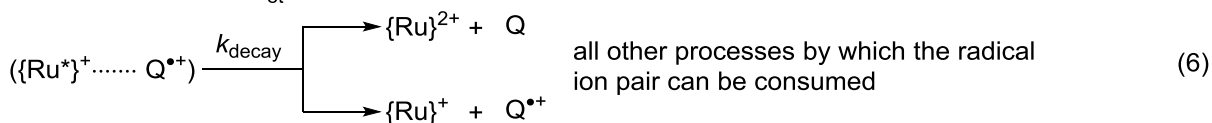
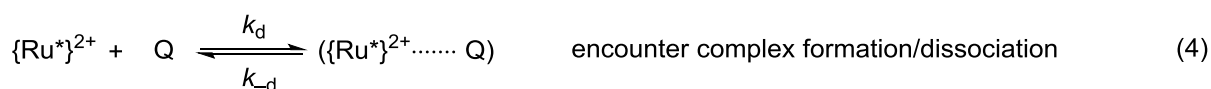


| entry | {Ru} | $E_{0,0}$ (eV) | $\text{Ru}^{2+/+}$ (V) | $\text{Ru}^{2+*/+}$ (V) | $\text{Ru}^{+/0}$ (V) | $\text{Ru}^{0/-}$ (V) |
|-------|-------------|----------------|------------------------|-------------------------|-----------------------|-----------------------|
| 1 | 5-26 | 2.17 | -0.65 | +1.52 | — | — |
| 2 | 5-81 | 2.05 | -0.89 | +1.16 | — | — |
| 3 | 5-28 | 2.01 | -0.93 | +1.08 | -1.09 | -1.48 |
| 4 | 5-30 | 1.99 | -0.95 | +1.04 | -1.10 | -1.49 |

The same experiments conducted in MeCN revealed minimal differences in redox potential between the four photocatalyst complexes (Section 6.4.4). This observation was consistent with the expected result, given that the high polarity of MeCN relative to CH_2Cl_2 precludes ion-pairing.

6.2.3 Free Energy of Electron Transfer and the Kinetics of Excited State Quenching

The photoluminescence and electrochemical data just presented led to the following question: why does the sensitizer counteranion modulate the rate (k_q) at which the excited state is quenched by anethole (Table 6-2, column 7)? To gain insight into this matter, we began by considering the following scheme for phosphorescence quenching by adiabatic outer sphere electron transfer (eqs 2–6):



where Q (quencher) represents anethole, {Ru} represents $\text{Ru}(\text{dfmb})_3^{2+}$ (counteranion omitted for clarity), and the various rate constants are as defined. The rate of non-radiative decay of the photocatalyst excited state can be expressed as follows (eq. 7):

$$\frac{d[\{\text{Ru}^*\}^{2+}]}{dt} = -k_q[\{\text{Ru}^*\}^{2+}][\text{Q}] = k_d[(\{\text{Ru}^*\}^{2+} \cdots \cdots \text{Q})] - k_d[\{\text{Ru}^*\}^{2+}][\text{Q}] \quad (7)$$

where k_q is the effective second-order rate constant for non-radiative excited state decay. Using the steady-state approximation (that is, $[(\{\text{Ru}^*\}^{2+} \cdots \cdots \text{Q})] = [(\{\text{Ru}^*\}^+ \cdots \cdots \text{Q}^{\bullet+})] = 0$), the semiempirical Rehm–Weller formula¹⁵ relating k_q to the free energy of reaction can be derived (eq. 8) with the respective variables defined (eq. 9–11):

$$k_q = \left(\frac{k_d}{1 + \frac{k_{-d}}{k_{et}} + \frac{k_{-d}}{k_{decay}} \left(\frac{1}{K_{et}} \right)} \right) \quad (8)$$

$$k_{-d} = \frac{k_d}{\Delta V_d} \quad (9)$$

$$K_{et} = \frac{k_{et}}{k_{-et}} = e^{\frac{-\Delta G^{\circ}_{et}}{RT}} \quad (10)$$

$$k_{et} = Z \left(e^{\frac{-\Delta G^{\ddagger}_{et}}{RT}} \right) \quad (11)$$

where ΔV_d is the encounter volume and Z is a frequency factor related to the reciprocal dielectric relaxation time of the solvent. Combining eqs. 10 and 11 with eq. 8, we obtain eq. 12 with the respective variables defined (eqs. 13–14):

$$k_q = \left(\frac{k_d}{1 + \frac{k_{-d}}{Z} \left(e^{\frac{\Delta G^{\ddagger}_{et}}{RT}} \right) + \frac{k_{-d}}{k_{decay}} \left(e^{\frac{\Delta G^{\circ}_{et}}{RT}} \right)} \right) \quad (12)$$

$$\Delta G^{\circ}_{et}(a) = N_A \left\{ e[E^{\circ}(Q^{*+}/Q) - E^{\circ}(Ru^{2+*}/+)] - \frac{e^2}{4\pi\epsilon_0\epsilon_r a} \right\} - \Delta E_{0,0} \quad (13)$$

$$\Delta G^{\ddagger}_{et} = \Delta G^{\ddagger}_{et}(0) \left(1 + \frac{\Delta G^{\circ}_{et}}{4\Delta G^{\ddagger}_{et}(0)} \right)^2 \quad (14)$$

where ΔG°_{et} is the Gibbs free energy (units: J mol⁻¹) of photoinduced direct electron transfer (no exciplex formation) from the excited state {Ru*}²⁺, N_A is Avogadro's number (6.022 × 10²³ mol⁻¹), e is the elementary charge (1.602 × 10⁻¹⁹ C), $E^{\circ}(Q^{*+}/Q)$ is the oxidation potential of anethole (1.13 V vs. SCE), $E^{\circ}(Ru^{2+*}/+)$ is the reduction potential of the Ru^{2+*/+} couple (units: V), ϵ_0 is vacuum permittivity (8.854 × 10⁻¹² C² J⁻¹ m⁻¹), ϵ_r is the dielectric constant of the medium (8.93 for CH₂Cl₂), a is the distance of the charged species after electron transfer (units: m), $\Delta E_{0,0}$ is the vertical excitation energy of {Ru} (units: J mol⁻¹), ΔG^{\ddagger}_{et} is the activation free energy, and $\Delta G^{\ddagger}_{et}(0)$ is the activation free enthalpy when $\Delta G^{\circ}_{et} = 0$. We favor the Marcus quadratic equation (eq. 14) over the empirically-derived relation for ΔG^{\ddagger}_{et} obtained by Rehm and Weller, as their relation generally tends to underestimate k_q for highly exergonic electron transfers and overestimate k_q for less exergonic and endergonic electron transfers. However, we

acknowledge the argument presented by Schuster that if $|\Delta G_{et}^{\circ}| \gg \Delta G_{et}^{\ddagger}(0)$, it is more favorable, from an empirical standpoint, to use the Rehm–Weller relation or the hyperbolic Marcus relation empirically derived by Agmon and Levine.¹⁶

Examining the variables in eqs. 12–14 within the context of sensitizer counteranion revealed some interesting observations. To begin, we considered eq. 13, where $E^{\circ}(\text{Ru}^{2+*/+})$ and $\Delta E_{0,0}$ are both strongly dependent upon counteranion identity in nonpolar solvent, as demonstrated by the results in Tables 6-2 and 6-3. To ascertain the magnitude of the relationship between counteranion identity and the driving force for electron transfer, ΔG_{et}° (assuming $a = 5 \times 10^{-10}$ m (5 Å)) was computed (Table 6-4, column 3) for the reaction between anethole and photocatalysts **5-26**, **5-28**, and **5-81**. The data demonstrate that changing the counteranion from $\text{BAr}_4^{\text{F}-}$ to ArSO_3^- decreases the thermodynamic driving force for photoinduced electron transfer by 13.8 kcal mol⁻¹.

Table 6-4. Empirical and computed thermochemical and kinetic data for excited state quenching

| entry | {Ru} | ΔG_{et}° (kcal mol ⁻¹) | ΔG_{et}^{\ddagger} (kcal mol ⁻¹) | k_q^{obs} (M ⁻¹ s ⁻¹) | k_q^{calc} (M ⁻¹ s ⁻¹) |
|-------|-------------|---|--|---|--|
| 1 | 5-26 | -66.2 | 2.85 | 3.34×10^9 | 4.07×10^9 |
| 2 | 5-81 | -55.2 | 4.18 | 4.89×10^8 | 2.76×10^8 |
| 3 | 5-28 | -52.4 | 4.77 | 6.42×10^7 | 1.03×10^8 |

Subsequently, we wished to determine the validity of our proposed mathematical model relating k_q and ΔG_{et}° . Given the very large negative ΔG_{et}° values, it was suspected that our model might place these electron transfer events in the Marcus inverted region; obviously, these electron transfer events are not in the inverted region because k_q^{obs} decreases as ΔG_{et}° becomes more positive. Thus, we wished to see if it were possible to fit our empirical data to eq. 12. It has been established that for the reactions of a given donor (anethole) with a series of related acceptors (polypyridyl ruthenium photocatalysts), k_d , k_{-d} , Z , and k_{decay} can be considered constant.¹⁶ Indeed, we postulate counteranion identity has no effect on any variable in the

Smoluchowski equation for k_d ,¹⁷ nor does counteranion change k_d , Z , or k_{decay} . Values for k_d and k_d/k_{decay} were taken as: $k_d = 8 \times 10^9 \text{ M}^{-1}\text{s}^{-1}$ and $k_d/k_{\text{decay}} = 7$.¹⁸

In the event, eq. 14 was inserted into eq. 12, and the experimental data was fit by plotting $\log(k_q^{\text{obs}})$ versus $\Delta G^{\circ}_{\text{et}}$. A nonlinear optimization protocol (SSE = 0.111) afforded values for $k_d/Z = 2.42 \times 10^{-2}$ and $\Delta G^{\ddagger}_{\text{et}}(0) = 23.8 \text{ kcal mol}^{-1}$, both of which appear reasonable given the results of Haim.¹⁸ Utilizing these values, the rate of excited state quenching by anethole was calculated to give k_q^{calc} values (Table 6-4) that were in reasonable agreement with empirically-determined k_q^{obs} values from the Stern-Volmer studies in Table 6-2. Indeed, our proposed model places these electron transfer events well outside the Marcus inverted region and accounts for the decreasing rate of excited state quenching as the exergonicity of electron transfer is decreased in tandem with an increase in counteranion Lewis basicity. We recognize the small size of this data set and propose quenching studies on catalysts **5-30**, **5-31**, and **5-32** (see Table 5-2), all of which contain counteranions of considerably greater basicity than those studied in Table 6-2. Hypothetically, the values of k_q obtained from these data ($k_q(\mathbf{5-30}) > k_q(\mathbf{5-31}) > k_q(\mathbf{5-32})$) would correlate well with increasingly positive values of $\Delta G^{\circ}_{\text{et}}$ ($\Delta G^{\circ}_{\text{et}}(\mathbf{5-30}) < \Delta G^{\circ}_{\text{et}}(\mathbf{5-31}) < \Delta G^{\circ}_{\text{et}}(\mathbf{5-32})$), thereby considerably expanding the data set and improving our model.

6.2.4 Counteranion Effects on Chain Propagation

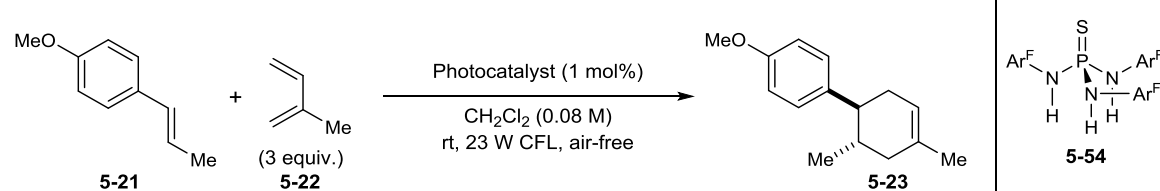
An important implication of these results is that the counteranion is responsible for greatly modulating both the ground and excited state photocatalyst properties in a nonpolar organic solvent. In fact, the ability to alter these properties via facile salt metathesis can be viewed as a strategy for reaction optimization. Traditional methods for fundamentally altering the properties of polypyridyl [Ru] complexes rely on de novo synthesis via pyrolysis of Ru(III) and an appropriate ligand under reducing conditions.¹⁹ Furthermore, direct manipulation of

quenching kinetics via facile anion metathesis of the corresponding ground state polypyridyl {Ru} complex may allow precise control of electron transfer events in complex transformations.

Up to this point, however, a correlation between counteranion identity and chain length of the charge-carrying radical cation has not been considered. Indeed, while quenching of T_1 may be responsible for the vast rate differences observed in Table 6-1, chain length could conceivably be affected by counteranion basicity. This conclusion led us to consider the relative energies of the ion pairs formed upon one-electron oxidation of anethole by $\text{Ru}(\text{dfmb})_3^{2+*}$. Lower energy, more stable, and thus less reactive ion pairs between the radical cation of anethole and the counteranion of the photocatalyst are expected when the counteranion has greater Lewis basicity.²⁰ Modulating this Lewis basicity changes the dynamic dipolar charge distribution between radical cation and anion and thus changes the inherent reactivity of the ion pair. Furthermore, the short lifetime of a high energy ion-paired intermediate precludes deleterious off-cycle termination and/or back electron transfer steps that decrease the overall efficiency of the transformation.

Specifically, we surmised that if excited state quenching was rate-determining, attenuating counteranion basicity in complexes **5-28** and **5-30** via addition of an exogenous hydrogen-bond donor (Chapter 5) would increase k_q and lead to an increase in the rate of radical cation Diels-Alder cycloaddition. However, if chain propagation is principally responsible for dictating reactivity, a difference in chain length commensurate with the difference in rates of cycloaddition would be observed.

In the event, C_3 -symmetric thiophosphotriamide **5-54** was subjected to the standard conditions (Table 6-5). To our delight, the reaction containing photocatalyst **5-28** and phosphotriamide **5-54** was complete in 2 h in nearly quantitative yield. The reaction containing photocatalyst **5-30** and **5-54** reached nearly quantitative yield in same time it took to attain 5% conversion in the absence of **5-54**. No background reactivity was observed in the absence of **5-28** or **5-30**.

Table 6-5. Quantum yield and chain length determinations^a


| entry ^a | {Ru} ^b | [5-54] (M) | quantum yield (Φ) | fraction of photons quenched by 5-21 | chain length |
|--------------------|-------------------|----------------------|--------------------------|---|--------------|
| 1 | 5-26 | — | 22.0 | 0.99 | 22.0 |
| 2 | 5-28 | — | 0.59 | 0.83 | 0.71 |
| 3 | 5-28 | 1.6×10^{-2} | 7.4 | 0.91 | 8.0 |

^aData collected at $\lambda = 436$ nm with a Hitachi F-4500 spectrofluorometer using degassed samples and is the average of two reproducible experimental runs. ^b 8.0×10^{-4} M.

To ascertain the precise role of hydrogen-bond donor **5-54**, quenching kinetics were carried out for complex **5-28** in the presence of **5-54**. The Stern-Volmer quenching constant was found to be 133.4 M^{-1} . While this represents a twofold increase over the value of K_{SV} for **5-28** in the absence of **5-54** (Table 2, entry 3), this increase does not correlate with the dramatically enhanced reactivity observed in the presence of **5-54**. Thus, it can be concluded that the rate-determining step of the radical cation Diels-Alder catalysed by **5-28** does not involve excited state quenching by anethole. However, the presence of **5-54** increased the chain length by a factor of 12. Therefore, we propose that **5-54** exerts its largest influence on chain propagation and this is what accounts for the dramatic difference in reactivity observed in the presence of **5-54**.

6.3 Conclusions

We have demonstrated that counteranion identity profoundly affects the nature of both ground and excited state properties of polypyridyl Ru(II) complexes in nonpolar organic solvent. Indeed, the use of photocatalyst counteranion to independently tune excited state properties represents a new reaction development paradigm for controlling kinetics of electron transfer in

the context of organic photoredox catalysis. Furthermore, we discovered that attenuating counteranion basicity using a hydrogen-bond donor led to a dramatic increase in the chain length for radical cation propagation.

6.4 Experimental

6.4.1 General Information

Dichloromethane, tetrahydrofuran, diethyl ether, toluene, and acetonitrile (HPLC grade solvents) were dried by passage through columns of activated alumina. Ethylene glycol (Aldrich) was used as received. Water was purified by a Milli-Q system (Millipore Corporation) to achieve a resistivity of $18.2 \text{ M}\Omega \text{ cm}^{-1}$ at $25 \text{ }^\circ\text{C}$. Chromatography was performed with Purasil 60 Å silica gel (230–400 mesh) or with neutral alumina (Aldrich product # 11028). High vacuum refers to a reduced pressure that was measured to be 60 mTorr using a McLeod gauge. Anethole was purified by chromatography on silica gel (hexanes: EtOAc = 20:1) and was subsequently submitted to fractional distillation under high vacuum at $95 \text{ }^\circ\text{C}$. Purified anethole was stored at room temperature in a vial wrapped in aluminum foil. Isoprene was fractionally distilled from CaH_2 under N_2 at $45 \text{ }^\circ\text{C}$ and stored at $5 \text{ }^\circ\text{C}$. ^1H , ^{13}C , ^{19}F , ^{31}P , and ^{11}B NMR data for all previously uncharacterized compounds were obtained using Bruker Avance III 400 MHz and Bruker Avance III 500 MHz spectrometers and are referenced to TMS (0.00 ppm) or residual protio solvent signal. The NMR facilities are supported by the NSF (CHE-1048642, CHE-9208463, S10 RR08389-01), the University of Wisconsin, and a generous gift from Paul J. Bender.

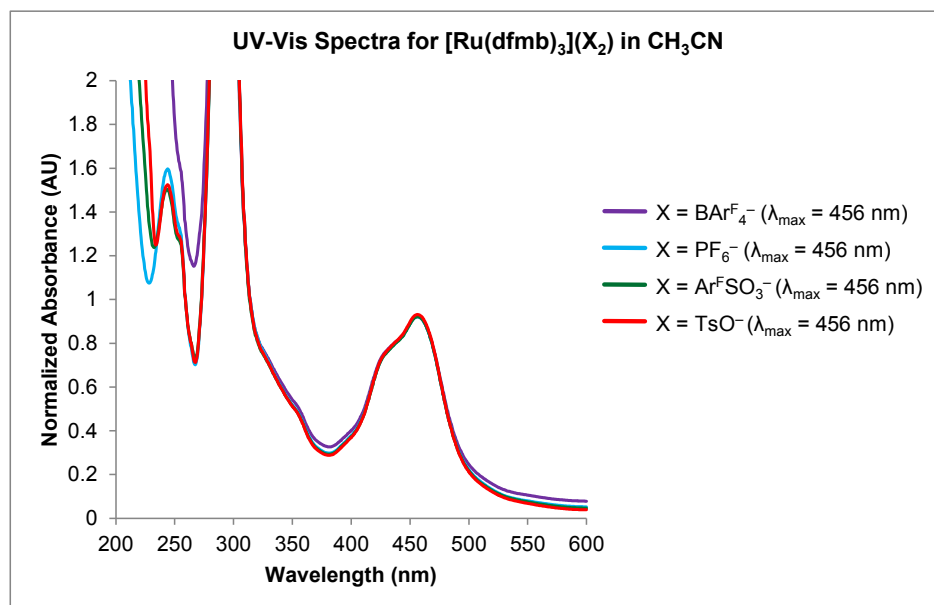
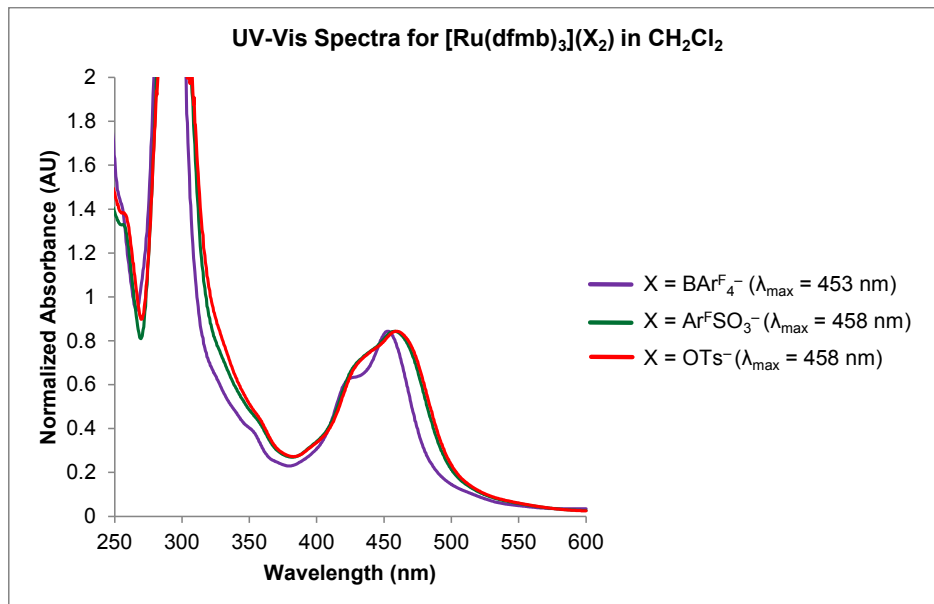
6.4.2 Radical Cation Diels–Alder Cycloadditions

General procedure for experiments in Table 6-1: A stock solution of anethole **5-21** (54.6 mg, 55.3 μ L, 0.368 mmol), isoprene **5-22** (75.3 mg, 111 μ L, 1.11 mmol), and trimethyl(phenyl)silane internal standard (55.4 mg, 63.4 μ L, 0.368 mmol) in dry CH_2Cl_2 (4.38 mL) was prepared. 810 μ L aliquots of this stock solution were added to oven-dried 25 mL Schlenk tubes containing the appropriate ruthenium photocatalyst (6.14×10^{-4} mmol, 1 mol%). This afforded reaction mixtures containing **5-21** (9.1 mg, 0.0614 mmol, 1 equiv.), **5-22** (12.5 mg, 0.184 mmol, 3 equiv.), trimethyl(phenyl)silane internal standard (9.2 mg, 0.0614 mmol, 1 equiv.) in CH_2Cl_2 (0.77 mL, 0.08 M). A stir bar was added to each reaction, and the solutions were submitted to three freeze-pump-thaw cycles, purged with N_2 , and irradiated at room temperature using a 23 W compact fluorescent light (CFL) bulb. The yield of cycloadduct **5-23** and remaining **5-21** were determined by ^1H NMR analysis of the unpurified reaction mixtures. ^1H NMR analysis of **5-23** was consistent with previously reported values.^{7a}

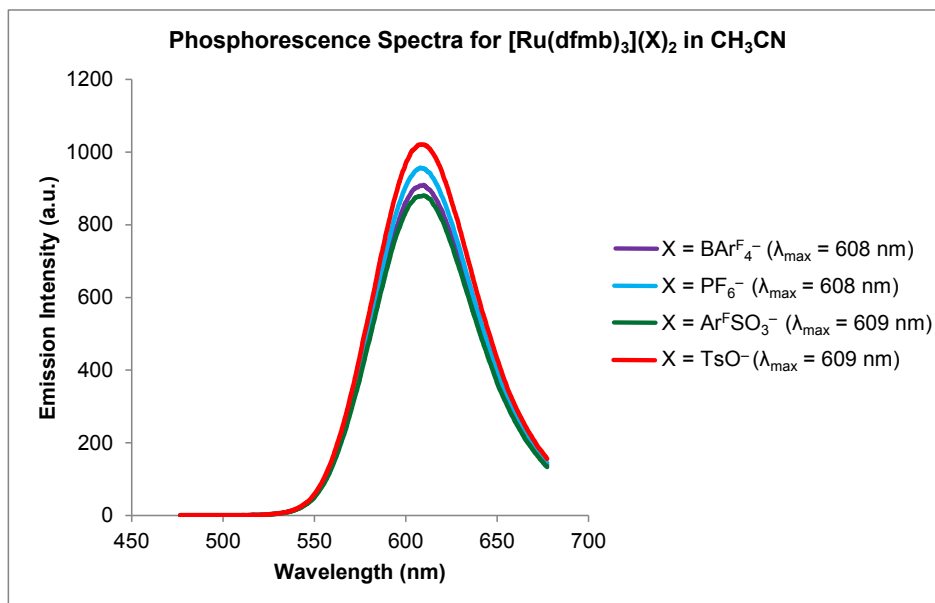
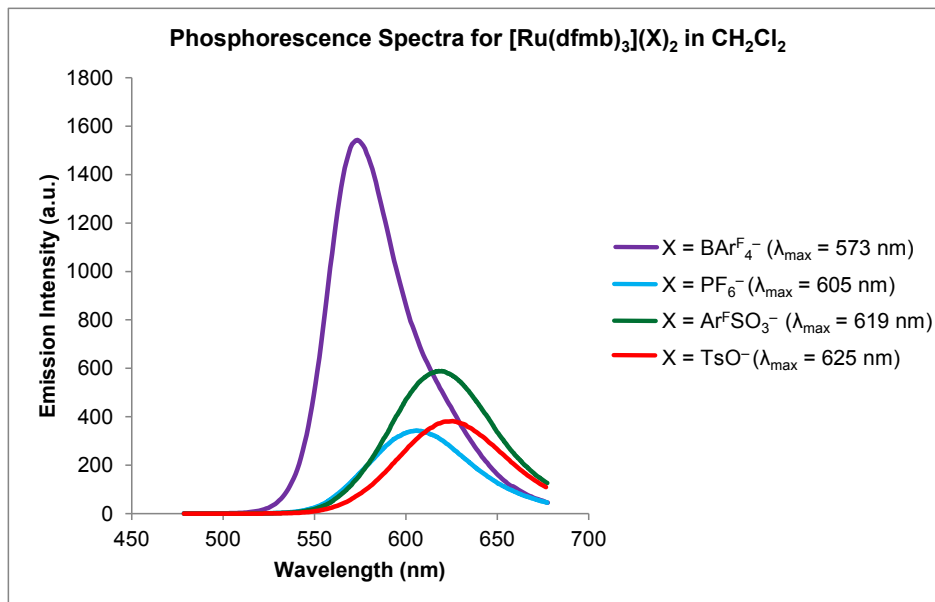
General procedure for experiments in Table 6-5: A stock solution of **5-21**, **5-22**, and trimethyl(phenyl)silane internal standard in dry CH_2Cl_2 was added to oven-dried 25 mL Schlenk tubes containing the appropriate ruthenium photocatalyst (6.14×10^{-4} mmol, 1 mol%) and thiophosphotriamide **5-54** (9.2 mg, 0.0123 mmol, 20 mol%)²¹. A stir bar was added to each reaction, and the solutions were submitted to three freeze-pump-thaw cycles, purged with N_2 , and irradiated at room temperature using a 23 W compact fluorescent light (CFL) bulb.

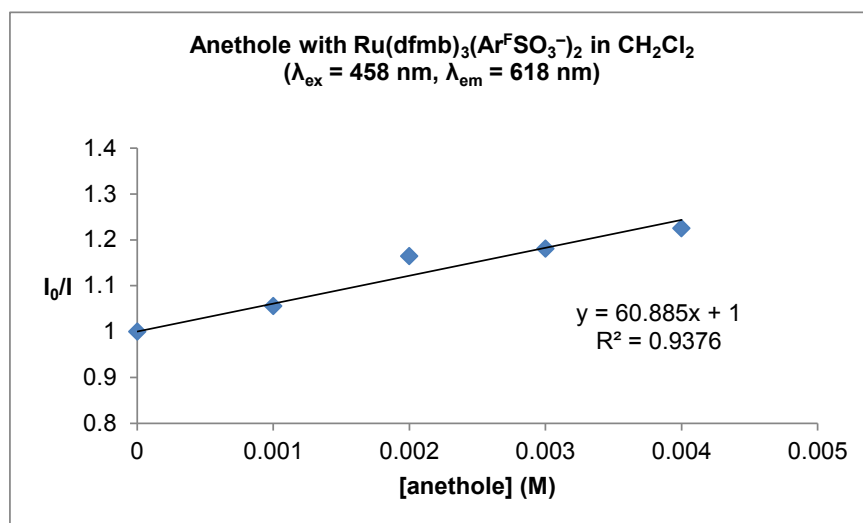
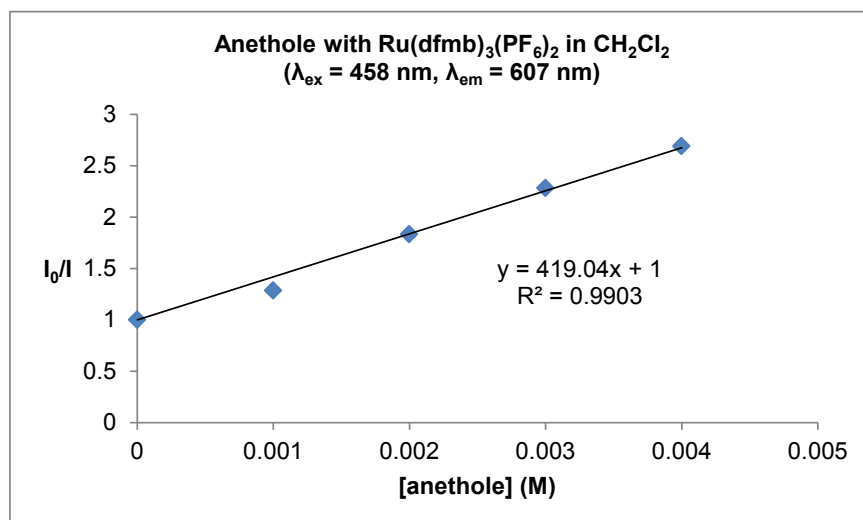
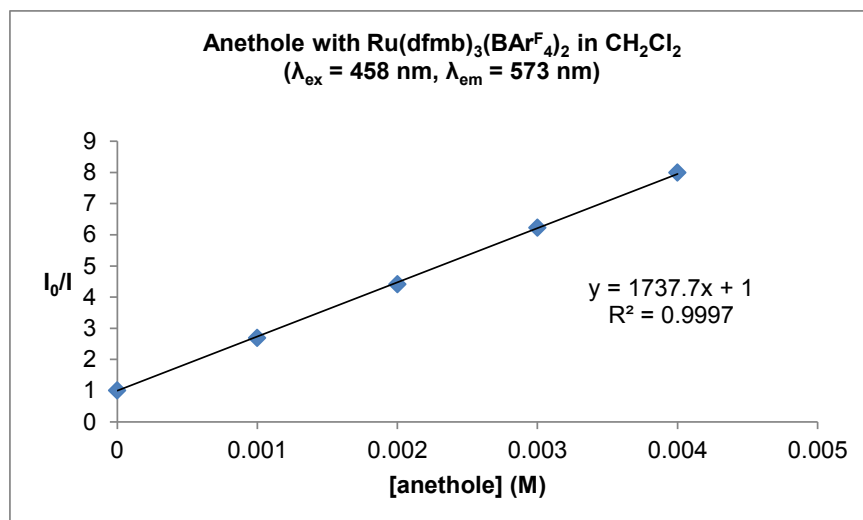
6.4.3 UV-Vis, Phosphorescence Spectra, and Chain Length Measurements

Solution spectra were measured in CH_2Cl_2 or acetonitrile at a ruthenium photocatalyst concentration of 3.9×10^{-5} M. UV-vis absorption spectra were recorded at room temperature using a Cary 50 diode-array spectrophotometer over a scan range of 600 nm \rightarrow 200 nm at a scan rate of 300 nm/min.

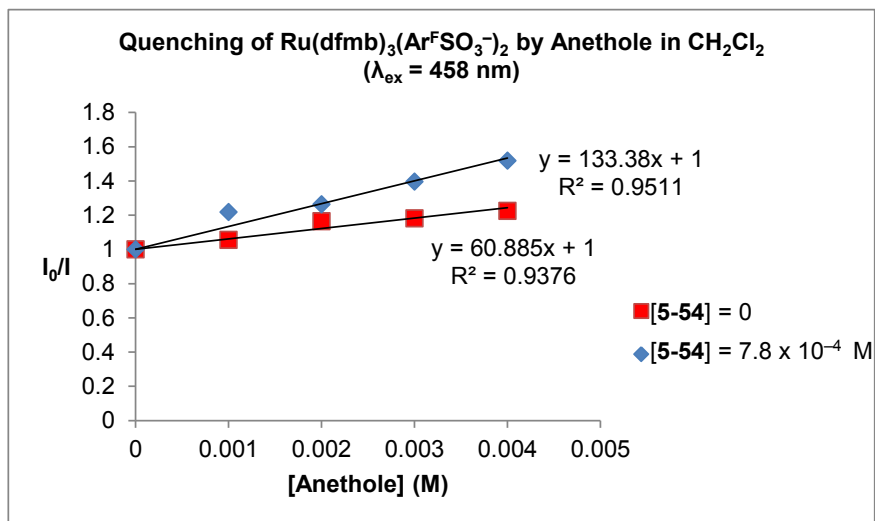


Steady-state photoluminescence spectra were obtained at room temperature using a Hitachi F4500 fluorescence spectrophotometer with a scan range of 478 nm→678 nm at a scan rate of 240 nm/min. Solution spectra were measured in CH₂Cl₂ or acetonitrile at a ruthenium photocatalyst [Ru] concentration of 3.9×10^{-5} M. The following sample preparation procedure was carried out in the dark. Samples were degassed by three freeze-pump-thaw cycles and subsequently transferred to fluorescence cuvettes that had been purged with N₂ for 30 min. The excitation wavelength for photoluminescence measurements was determined by the peak MLCT wavelength of the appropriate ruthenium photocatalyst acquired by UV-vis spectroscopy. All photoluminescence spectra were acquired normal to the incident beam. Excited state quenching kinetics experiments were carried out as follows: the luminescence intensity of a 3.9×10^{-5} M solution of [Ru] in CH₂Cl₂ was measured. Subsequently, aliquots of a 1.6×10^{-2} M stock solution of anethole quencher in CH₂Cl₂ were added to 2.0 mL of 7.8×10^{-5} M solutions of [Ru] in CH₂Cl₂. The final solution volume was adjusted to 4.0 mL via dilution with CH₂Cl₂. Samples were degassed as described above, and the luminescence intensities were determined. The ratio of unquenched to quenched intensity was plotted against [anethole], and it was found that samples obeyed ($R^2 > 0.93$) Stern-Volmer kinetics.

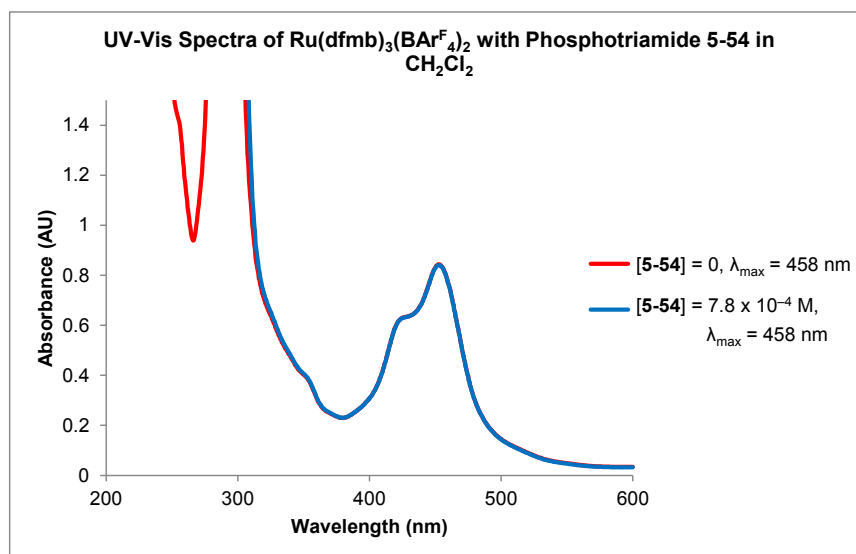


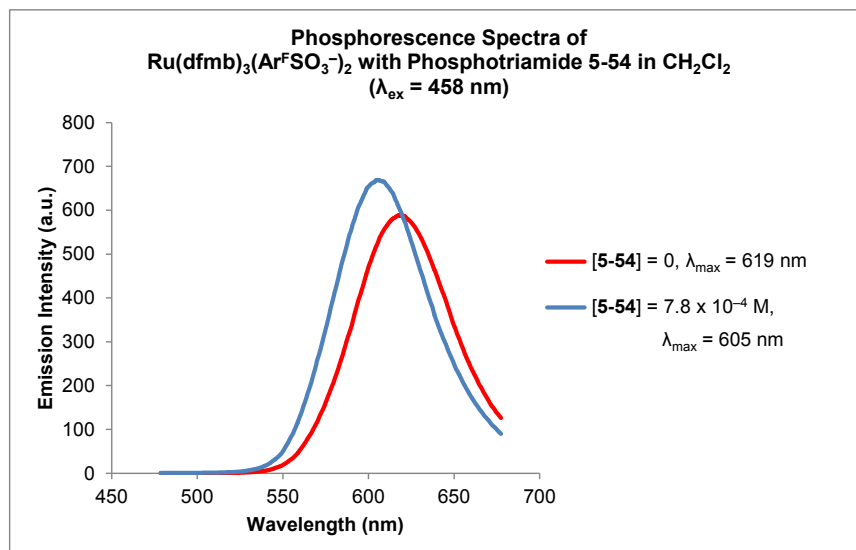
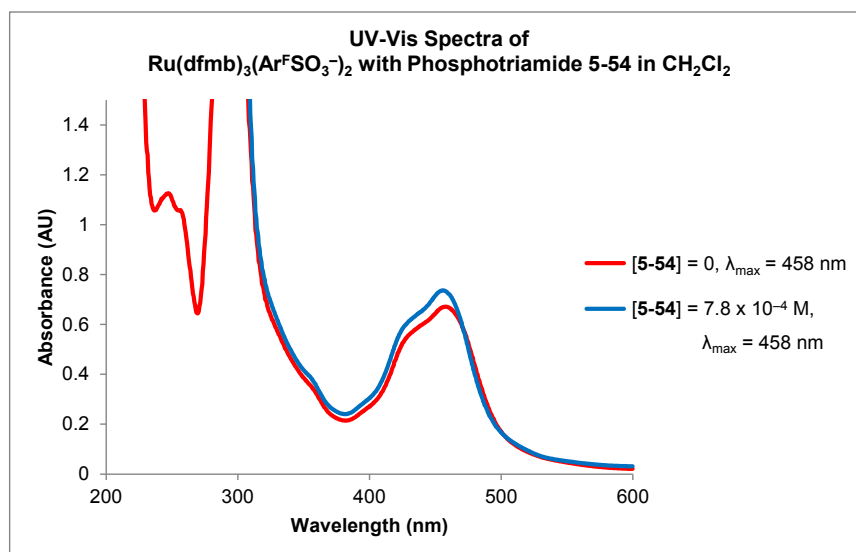
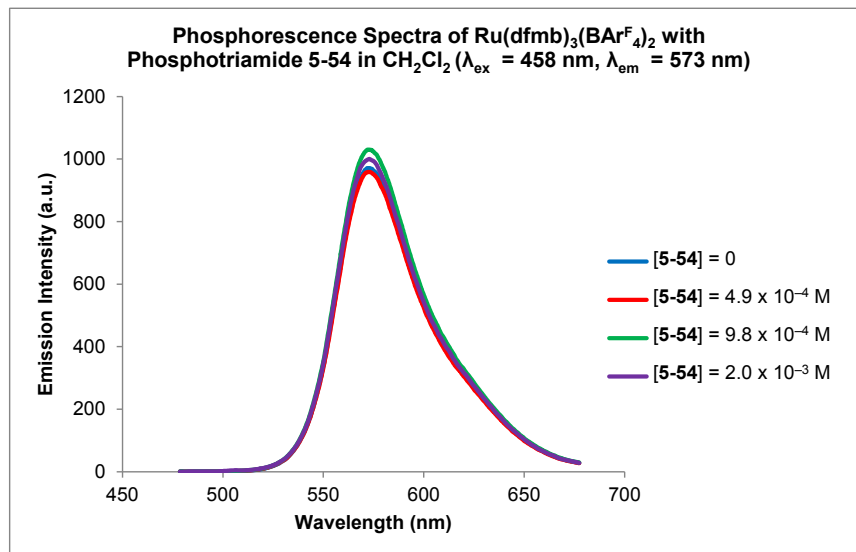
Luminescence Quenching Data Using Anethole as the Excited State Quencher

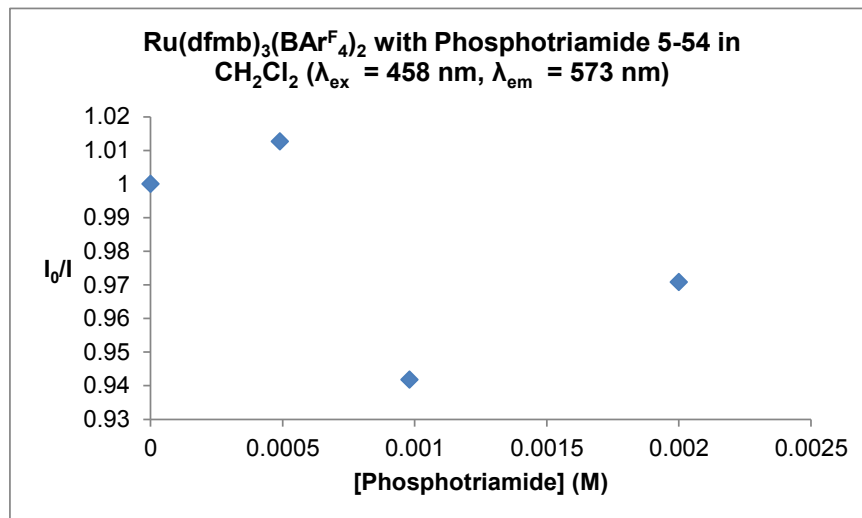
Luminescence Quenching Data Using Anethole as the Excited State Quencher in the Presence of thiophosphotriamide



To ascertain whether thiophosphotriamide hydrogen-bond donor **5-54** was changing the photophysical properties of the ruthenium complexes, a series of UV-vis and luminescence spectra were collected. In addition, **5-54** was employed as a potential quencher in an excited state kinetics study similar to those performed with anethole. No correlation was observed between added **5-54** and the ratio of unquenched to quenched intensity, indicating a lack of excited state quenching by **5-54**.







Chain lengths of radical cation Diels-Alder cycloadditions were determined as follows. The quantum yields (Φ) for the respective reactions were determined by the method outlined by Cismesia and Yoon.²² To ascertain chain length, the following formula was employed:

$$\text{chain length} = \frac{\Phi(\tau^{-1} + k_{q,\text{anethole}}[\text{anethole}] + k_{q,\text{isoprene}}[\text{isoprene}] + k_{q,[2+2]}[2 + 2])}{k_{q,\text{anethole}}[\text{anethole}]}$$

where τ is the excited state lifetime of the respective photocatalyst ($\tau^{-1} = k_r + k_{nr}$), $k_{q,\text{anethole}}$, $k_{q,\text{isoprene}}$, and $k_{q,[2+2]}$ are the rates of excited state quenching by the designated species, and [anethole], [isoprene], and [2+2] are the concentrations of the designated species. The [2+2] product results from homodimerization of anethole and forms in very small amounts (~2%) at low conversions of anethole. Furthermore, the rate of excited state quenching by isoprene was very small. Therefore, the final two terms in the numerator were determined to be negligible, and thus were ignored. Using this formula, chain lengths were determined for radical cation Diels-Alder cycloadditions.

Sample preparation for excited state lifetime measurements was as follows: a 3.9×10^{-5} M solution of the respective ruthenium photosensitizer in CH_2Cl_2 was degassed by 3 freeze-pump-thaw cycles and transferred to a N_2 -purged cuvette using standard Schlenk technique. Lifetime measurements were collected by the frequency-domain method with an ISS K2 multifrequency cross-correlation phase and modulation fluorometer. The excitation source

was intensity modulated through varying MHz frequencies at the sample's absorption maximum, producing shifts in the intensity and phase of fluorescence emission. Comparison to a standard (in this case fluorescein and glycogen) allows lifetime determination. Data was analyzed in Vinci (ISS).

6.4.4 Cyclic Voltammetry Experiments

Cyclic voltammetry was performed on a BASi EC Epsilon potentiostat connected to a BASi C3 cell stand and analyzed on a PC using Epsilon software. A three electrode setup was employed: Pt wire counter electrode, glassy carbon working electrode, and a Ag/AgNO₃ (0.01 M AgNO₃, 0.1 M Bu₄NPF₆ in CH₃CN) quasi reference electrode containing a polished silver wire immersed in the electrolyte solution. The entire assembly of this electrode was contained in a glass body, the tip of which consisted of a Vycor plug. The electrolyte solution in the electrode was replaced daily to ensure the Vycor plug was free of contaminants. With this setup, Fc/Fc⁺ (0.1 M Bu₄NPF₆ in CH₃CN) was measured to be 0.093 V vs. Ag/AgNO₃. A typical experiment was performed as follows: dry solvent and Bu₄NX electrolyte (0.1 M) (for example, Bu₄NBAr^F₄ was used in the analysis of Ru(dfmb)₃(BAr^F₄)₂) were introduced to the cell, the solution was sparged with dry N₂ with stirring for 5 min, and subsequently a voltammogram was recorded to establish background. Thereafter, the appropriate ruthenium catalyst complex (0.001 M) was introduced under N₂ and a second spectrum was collected. Finally, ferrocene internal standard (~0.001 M) was added, and a final voltammogram was collected. After referencing to ferrocene, voltammograms were referenced to SCE by adding 0.30 V to all potentials. Stirring was performed prior to each run to ensure exposure of electrodes to fresh analyte. The scan rate was 100 mV/sec. Between each catalyst complex analyzed, the glassy carbon working electrode was polished on Al₂O₃, sonicated in ultrapure H₂O, and washed in the organic solvent used for analysis.

For experiments performed in CH_2Cl_2 , the working and reference electrodes were placed as close as possible without touching to minimize Ohmic drop in the poorly conductive, highly resistive CH_2Cl_2 solvent. IR compensation experiments were performed in CH_2Cl_2 in the presence of an appropriate Bu_4NX electrolyte.²³ The uncompensated resistance was found to vary slightly with Bu_4NX electrolyte, and was typically between 550–850 Ohm. However, when IR compensation was applied, the half-wave potentials of both ferrocene and the catalyst redox couple of interest showed minimal (< 30 mV) shifts, and due to distortions sometimes introduced into the data by using IR compensation, compensation was not employed. It should be noted that all redox couples in CH_2Cl_2 exhibited quasi-reversible behavior, with $90 \text{ mV} < \Delta E_p < 180 \text{ mV}$ (peak separation increased with increasing Lewis basicity of X^- in supporting electrolyte and catalyst complex) and $1.1 < i_{pc}/i_{pa} < 1.4$. Redox couples in CH_3CN exhibited reversible, Nernstian behavior.

Preparation of supporting electrolytes

Tetrabutylammonium tetrakis-(3,5-bis(trifluoromethyl)phenyl)borate ($\text{Bu}_4\text{NBAR}^{\text{F}_4}$) (6-1). To a 25 mL round-bottom flask with a stir bar was added $\text{NaBAR}^{\text{F}_4}$ (1.33 g, 1.53 mmol, 1 equiv.) and distilled acetone (5.0 mL, 0.3 M). The solution was stirred until homogeneous, and subsequently, a solution of tetrabutylammonium chloride (426 mg, 1.53 mmol, 1 equiv.) in acetone (1.2 mL) was added. NaCl immediately precipitated from solution. The reaction was stirred for an additional 15 min before being filtered through a 0.2 μM Whatman filter. Acetone was removed *in vacuo* and the resulting viscous oil was dried under high vacuum for 1 h. Thereafter, the oil was dissolved in CH_2Cl_2 (10 mL), filtered, and CH_2Cl_2 was removed *in vacuo*. The oil was again dried on high vacuum and crystallization was induced by cooling to $-78 \text{ }^\circ\text{C}$ and allowing slow warming to room temperature under high vacuum. The resulting white solid was dried to constant mass to obtain 1.68 g (1.52 mmol, 99% yield) of a white, hygroscopic

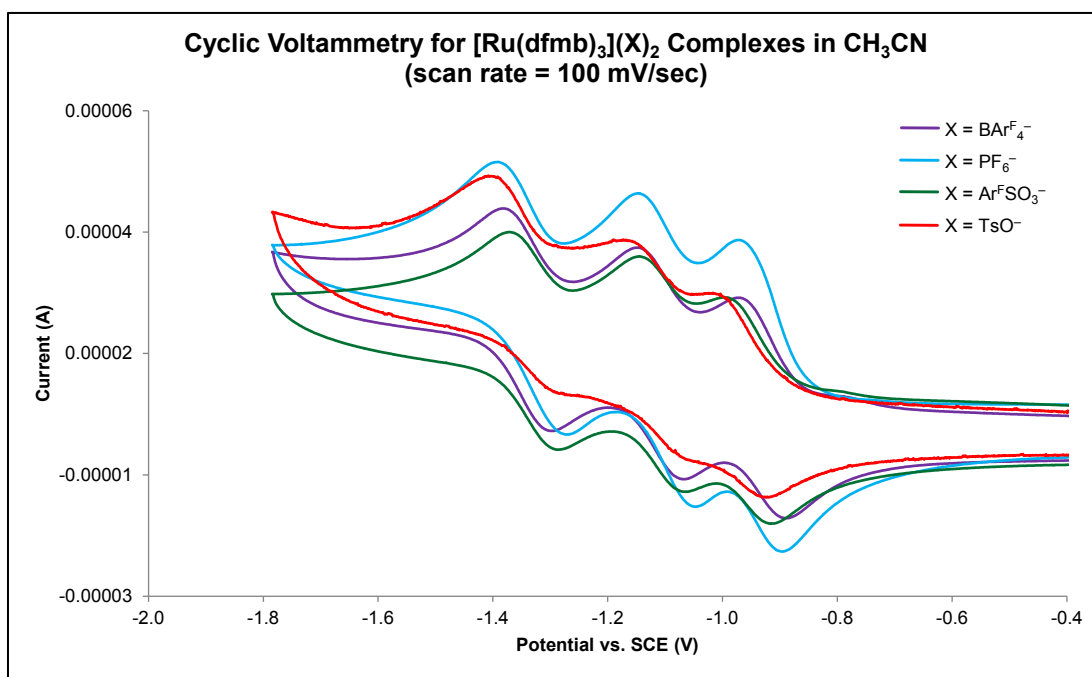
solid. ^1H NMR (500.0 MHz, CDCl_3) δ 7.69 (s, 8H), 7.53 (s, 4H), 2.99 (m, 8H), 1.53 (m, 8H), 1.33 (dq, $J = 14.8, 7.2$ Hz, 8H), 0.93 (t, $J = 7.2$ Hz, 12H); ^{13}C NMR (125.7 MHz, CDCl_3) δ 161.7 (q, $J_{\text{C-F}} = 49.6$ Hz), 134.8, 128.8 (qq, $J_{\text{C-F}} = 31.6, 3.1$ Hz), 124.5 (q, $J_{\text{C-F}} = 271.6$ Hz), 117.4 (m), 58.9, 23.6, 19.5, 13.1; ^{19}F NMR (376.5 MHz, CDCl_3) δ -62.4

Tetrabutylammonium 3,5-bis(trifluoromethyl)benzenesulfonate (6-2). A 100 mL round-bottom flask with a magnetic stirrer was charged with 3,5-bis(trifluoromethyl)benzenesulfonyl chloride (Matrix Scientific) (1.99 g, 6.35 mmol) and H_2O (15 mL, 0.4 M). A reflux condenser was attached, and the heterogeneous reaction was heated to an oil bath temperature of 107 °C and stirred for 3 h. Thereafter, the reaction was briefly cooled and a distillation head was attached. The residual H_2O and dissolved HCl (*g*) was distilled off and the resulting pale yellow solid remaining in the distillation flask was dried *in vacuo*. This solid was dissolved in H_2O (4 mL, 1.6 M) and a 1.0 M solution of tetrabutylammonium hydroxide in MeOH was added to achieve pH = 7. Subsequently, H_2O and MeOH were removed *in vacuo*, the residue obtained was dried on high vacuum and thereafter was dissolved in CH_2Cl_2 and filtered to remove insoluble solids. Recrystallization from H_2O followed by drying under high vacuum provided 2.06 g (3.85 mmol, 61% yield) of **6-2** as colorless needles. ^1H NMR (500.0 MHz, CDCl_3) δ 8.40 (s, 2H), 7.81 (s, 1H), 3.30 (m, 8H), 1.65 (m, 8H), 1.42 (dq, $J = 14.8, 7.2$ Hz, 8H), 0.99 (t, $J = 7.2$ Hz, 12H); ^{13}C NMR (125.7 MHz, CDCl_3) δ 149.4, 131.2 (q, $J_{\text{C-F}} = 33.4$ Hz), 126.8 (q, $J_{\text{C-F}} = 3.5$ Hz), 123.0 (q, $J_{\text{C-F}} = 272.4$ Hz), 122.5 (septet, $J_{\text{C-F}} = 3.8$ Hz), 58.8, 23.9, 19.7, 13.5; ^{19}F NMR (376.5 MHz, CDCl_3) δ -62.8.

Tetrabutylammonium *p*-toluenesulfonate (6-3). A 25 mL round-bottom flask with a magnetic stirrer was charged with *p*-toluenesulfonic acid monohydrate (1.00 g, 5.26 mmol) and H_2O (3 mL, 1.8 M). A 1.0 M solution of tetrabutylammonium hydroxide in MeOH was added over 5 min

to achieve pH = 7 (5.2 mL added). The exothermic reaction was allowed to stir for 15 min, and subsequently, H₂O and MeOH were removed *in vacuo*. The residue obtained was dissolved in CH₂Cl₂, transferred to a separatory funnel, separated from residual H₂O, and filtered to remove insoluble solids. Removal of CH₂Cl₂ *in vacuo* followed by recrystallization from H₂O and drying under high vacuum provided 1.38 g (3.85 mmol, 63% yield) of **6-3** as colorless needles. Spectral data were consistent with previously reported values.²⁴

Table S6-1. Electrochemical data in CH₃CN and the dependence on counteranion



| entry | {Ru} | $E_{0,0}$ (eV) | $\text{Ru}^{2+/+}$ (V) | $\text{Ru}^{2+*/+}$ (V) | $\text{Ru}^{+/0}$ (V) | $\text{Ru}^{0/-}$ (V) |
|-------|-------------|----------------|------------------------|-------------------------|-----------------------|-----------------------|
| 1 | 5-26 | 2.04 | -0.93 | +1.11 | -1.11 | -1.35 |
| 2 | 5-81 | 2.04 | -0.93 | +1.11 | -1.10 | -1.35 |
| 3 | 5-28 | 2.04 | -0.95 | +1.09 | -1.11 | -1.34 |
| 4 | 5-30 | 2.04 | -0.98 | +1.06 | -1.11 | -1.35 |

6.5 References

¹ Paris, J. P.; Brandt, W. W. Charge transfer luminescence of a ruthenium(II) chelate. *J. Am. Chem. Soc.* **1959**, *81*, 5001–5002.

² For general reviews on the photophysics of polypyridyl Ru(II) complexes, see (a) Kalayanasundaram, K. Photophysics, photochemistry, and solar energy conversion with tris(bipyridyl)ruthenium(II) and its analogues. *Coord. Chem. Rev.* **1982**, *46*, 159–244. (b) Juris, A.; Balzani, V.; Barigelletti, V.; Campagna, S.; Belser P.; Von Zelewsky, A. Ru(II) polypyridine complexes: photophysics, photochemistry, electrochemistry, and chemiluminescence. *Coord. Chem. Rev.* **1988**, *84*, 85–277.

³ (a) Du, J.; Skubi, K. L.; Schultz, D. M.; Yoon, T. P. A dual-catalysis approach to enantioselective [2+2] photocycloadditions using visible light. *Science* **2014**, *344*, 392–396. (b) Blum, T.; Zhu, Y.; Nordeen, S. A.; Yoon, T. P. Photocatalytic synthesis of dihydrobenzofurans by oxidative [2+2] cycloaddition of phenols. *Angew. Chem. Int. Ed.* **2014**, *53*, 11056–11059. (c) Tyson, E. L.; Niemeyer, Z. L.; Yoon, T. P. Redox mediators in visible light photocatalysis: photocatalytic radical thiol-ene additions. *J. Org. Chem.* **2014**, *79*, 1427–1436.

⁴ (a) Wallentin, C. J.; Nguyen, J. D.; Finkbeiner, P.; Stephenson, C. R. J. Visible light-mediated atom transfer radical addition via oxidative and reductive quenching of photocatalysts. *J. Am. Chem. Soc.* **2012**, *134*, 8875–8884. (b) Zho, Z.; Ahneman, D. T.; Terrett, J. A.; Doyle, A. G.; MacMillan, D. W. C. Merging photoredox with nickel catalysis: coupling of α -carboxyl sp^3 -carbons with aryl halides. *Science* **2014**, *345*, 437–440. (c) Ye, Y.; Sanford, M. S. Merging visible-light photocatalysis and transition-metal catalysis in the copper-catalyzed trifluoromethylation of boronic acids with CF_3I . *J. Am. Chem. Soc.* **2012**, *134*, 9034–9037. (d) Schnermann, M. J.; Overman, L. E. A concise synthesis of (–)-aplyviolene facilitated by a strategic tertiary radical conjugate addition. *Angew. Chem. Int. Ed.* **2012**, *51*, 9576–9580. (e) Tarantino, K. T.; Liu, P.; Knowles, R. R. Catalytic ketyl-olefin cyclizations enabled by proton-coupled electron transfer. *J. Am. Chem. Soc.* **2013**, *135*, 10022–10025.

⁵ (a) Strauss, S. H. The search for larger and more weakly coordinating anions. *Chem. Rev.* **1993**, *93*, 927–942. (b) Diaz-Torres, R.; Alvarez, S. Coordinating ability of anions and solvents towards transition metals and lanthanides. *Dalton Trans.* **2011**, *40*, 10742–10750. (c) Krossing, I.; Raabe, I. Noncoordinating anions—fact or fiction? A survey of likely candidates. *Angew. Chem. Int. Ed.* **2004**, *43*, 2067–2090.

⁶ (a) Kobayashi, H.; Sonoda, A.; Iwamoto, H.; Yoshimura, M. Tetrakis[3,5-di(*F*-methyl)phenyl]borate as the first efficient negatively charged phase transfer catalyst. Kinetic evidences. *Chem. Lett.* **1981**, *10*(5), 579–580. (b) Yakelis, N. A.; Bergman, R. G. Safe preparation and purification of sodium tetrakis[(3,5-trifluoromethyl)phenyl]borate ($NaBARF_{24}$): reliable and sensitive analysis of water in solutions of fluorinated tetraarylborates. *Organometallics* **2005**, *24*, 3579–3581.

⁷ (a) Lin, S.; Ischay, M. A.; Fry, C. G.; Yoon, T. P. Radical cation Diels-Alder cycloadditions by visible light photocatalysis. *J. Am. Chem. Soc.* **2011**, *133*, 13950–13953. (b) Lin, S.; Padilla, C. E.; Ischay, M. A.; Yoon, T. P. Visible light photocatalysis of intramolecular radical cation Diels-Alder cycloadditions. *Tetrahedron Lett.* **2012**, *53*, 3073–3076.

⁸ (a) Farnum, B. H.; Jou J. J.; Meyer, G. J. Visible light generation of I-I bonds by Ru-tris(diimine) excited states. *Proc. Natl. Acad. Sci. U.S.A.* **2012**, *109*, 15628-15633. (b) Ward, W. M.; Farnum, B. H.; Siegler, M.; Meyer, G. J. Chloride ion-pairing with Ru(II) polypyridyl compounds in dichloromethane. *J. Phys. Chem. A.* **2013**, *117*, 8883-8894.

⁹ (a) Chatterjee, S.; Davis, P. D.; Gottschalk, P.; Kurz, M.E.; Sauerwein, B.; Yang X.; Schuster, G. B. Photochemistry of carbocyanine alkyltriphenylborate salts: intra-ion-pair electron transfer and the chemistry of boranyl radicals. *J. Am. Chem. Soc.* **1990**, *112*, 6329-6338; (b) Yang, X.; Zaitsev, A.; Sauerwein, B.; Murphy, S.; Schuster, G. B. Penetrated ion pairs: photochemistry of cyanine dyes within organic borates. *J. Am. Chem. Soc.* **1992**, *114*, 793-794; (c) Tolmachev, A. I.; Zaitsev, A. K.; Koska, N.; Schuster, G. B. Counter-ion effects in cationic dyes: photophysics and photochemistry of a macrocyclic dimer of dimethylindocarbocyanine. *J. Photochem. Photobiol. A: Chem.* **1994**, *77*, 237-242.

¹⁰ (a) Tatikolov, A. S.; Shvedova, L. A.; Derevyanko, N. A.; Ischenko, A. A.; Kuzmin, V. A. The influence of counterion on photochemistry of cationic indopolycarbocyanine dyes in ion pairs. *Chem. Phys. Lett.*, 1992, **190**, 291; (b) Tatikolov, A. S.; Dzhulibekov, Kh. S.; Shvedova, L. A.; Kuzmin, V. A.; Ishchenko, A. A. Influence of "inert" counterions on the photochemistry of some cationic polymethine dyes. *J. Phys. Chem.* **1995**, *99*, 6525-6529.

¹¹ (a) Crutchley, R. J.; Lever, A. B. P.; Poggi, A. Bis(bipyrazine)ruthenium(II) complexes: characterization, spectroscopy, and electrochemistry. *Inorg. Chem.* **1983**, *22*, 2647-2650. (b) Yeomans, B. D.; Keslo, L. S.; Tregloan, P. A. Keene, F. R. Redox characteristics and anion association behavior of stereoisomeric forms of mono- and oligonuclear metal complexes using high pressure electrochemistry. *Eur. J. Inorg. Chem.* **2001**, 239-246.

¹² [Ru(dfmb)₃](PF₆)₂ was studied as a sensitizer in the series of experiments carried out in Table 6-1. However, the poor solubility of this complex in CH₂Cl₂ precluded any meaningful conclusions to be drawn regarding its ability to catalyze the radical cation Diels-Alder reaction.

¹³ These studies were somewhat hindered by the absorption of the anions themselves which prevented an examination of the π-π* transition at 280 nm and weak, formally spin-forbidden transitions in the near-UV.

¹⁴ The scan range for [Ru(dfmb)₃](BAR^F₄)₂ was deliberately limited to -0.84 V vs. SCE due to irreversible behavior observed for this complex on the return scan from -2.0 V vs. SCE.

¹⁵ Rehm, D.; Weller, A. Kinetics of fluorescence quenching by electron and H-atom transfer. *Isr. J. Chem.* **1970**, *8*, 259-271.

¹⁶ Scandola, F.; Balzani, V.; Schuster, G. B. Free-energy relationships for reversible and irreversible electron-transfer processes. *J. Am. Chem. Soc.* **1981**, *103*, 2519-2523.

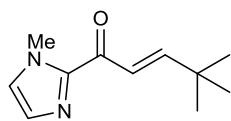
¹⁷ Rau, H.; Frank, R.; Greiner, G. Rate dependence of electron transfer on donor-acceptor separation and on free enthalpy change. The Ru(bpy)₃²⁺/Viologen²⁺ system. *J. Phys. Chem.* **1986**, *90*, 2476-2481.

¹⁸ Fürholz, U.; Haim, A. Kinetics and mechanism of the reactions of mononuclear and binuclear ruthenium(II) ammine complexes with peroxydisulfate. *Inorg. Chem.* **1987**, *26*, 3243-3248.

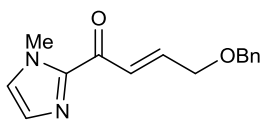
-
- ¹⁹ Mabrouk, P. A.; Wrighton, M. S. Resonance raman spectroscopy of the lowest excited state of derivatives of tris(2,2'-bipyridine)ruthenium(II): substituent effects on electron localization in mixed-ligand complexes. *Inorg. Chem.* **1986**, *25*, 526–531.
- ²⁰ Marcus, Y.; Hefter, G. Ion pairing. *Chem. Rev.* **2006**, *106*, 4585–4621.
- ²¹ Cranwell, P. B.; Hiscock, J. R.; Haynes, C. J. E.; Light, M. E.; Wells, N. J.; Gale, P. A. Anion recognition and transport properties of sulfamide-, phosphoric triamide- and thiophosphoric triamide-based receptors. *Chem. Commun.* **2013**, *49*, 874–876.
- ²² Cismesia, M. E.; Yoon, T. P. *Manuscript submitted*.
- ²³ Bond, A. M.; Oldham, K. B.; Snook, G. A. Use of the ferrocene oxidation process to provide both reference electrode potential calibration and a simple measurement (via semiintegration) of the uncompensated resistance in cyclic voltammetric studies in high-resistance organic solvents. *Anal. Chem.* **2000**, *72*, 3492–3496.
- ²⁴ Kohno, Y.; Arai, H.; Saita, S.; Ohno, H. Material design of ionic liquids to show temperature-sensitive LCST-type phase transition after mixing with water. *Aust. J. Chem.* **2011**, *64*, 1560–1567.

Appendix. NMR Spectra for New Compounds

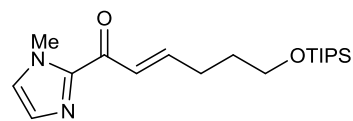
A.1 List of Compounds for Chapter 2



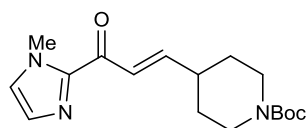
2-21



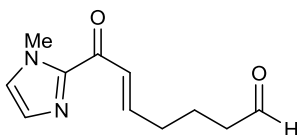
2-22



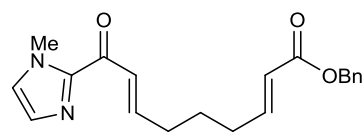
2-23



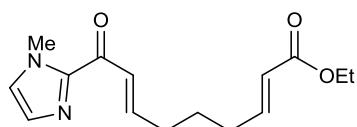
2-24



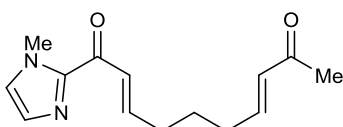
2-25



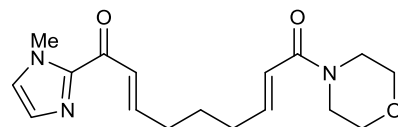
2-26



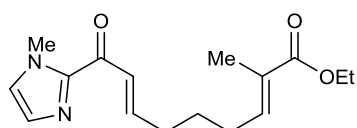
2-27



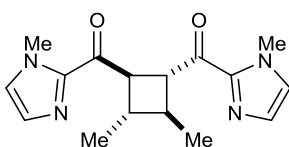
2-28



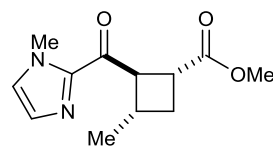
2-29



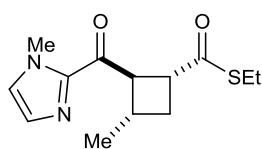
2-30



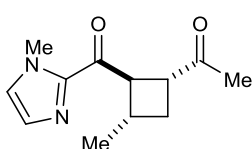
2-7



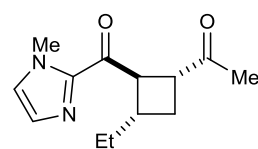
2-6



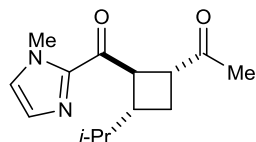
2-8



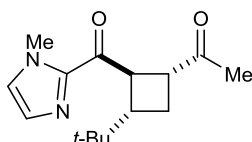
2-9



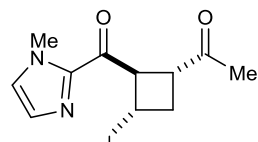
2-10



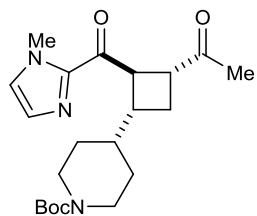
2-11



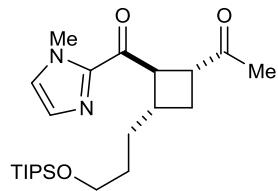
2-12



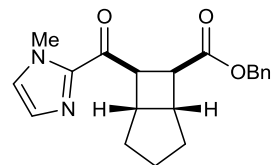
2-13



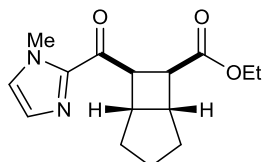
2-14



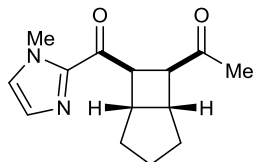
2-15



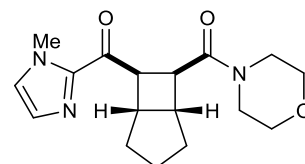
2-16



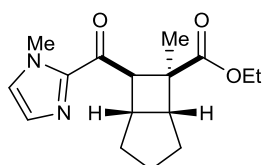
2-17



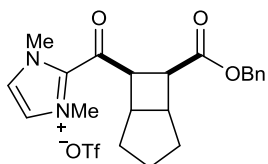
2-18



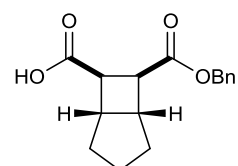
2-19



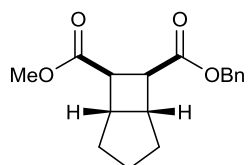
2-20



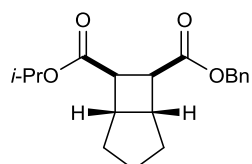
2-31



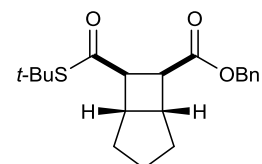
2-32



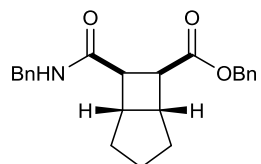
2-33



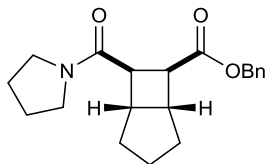
2-34



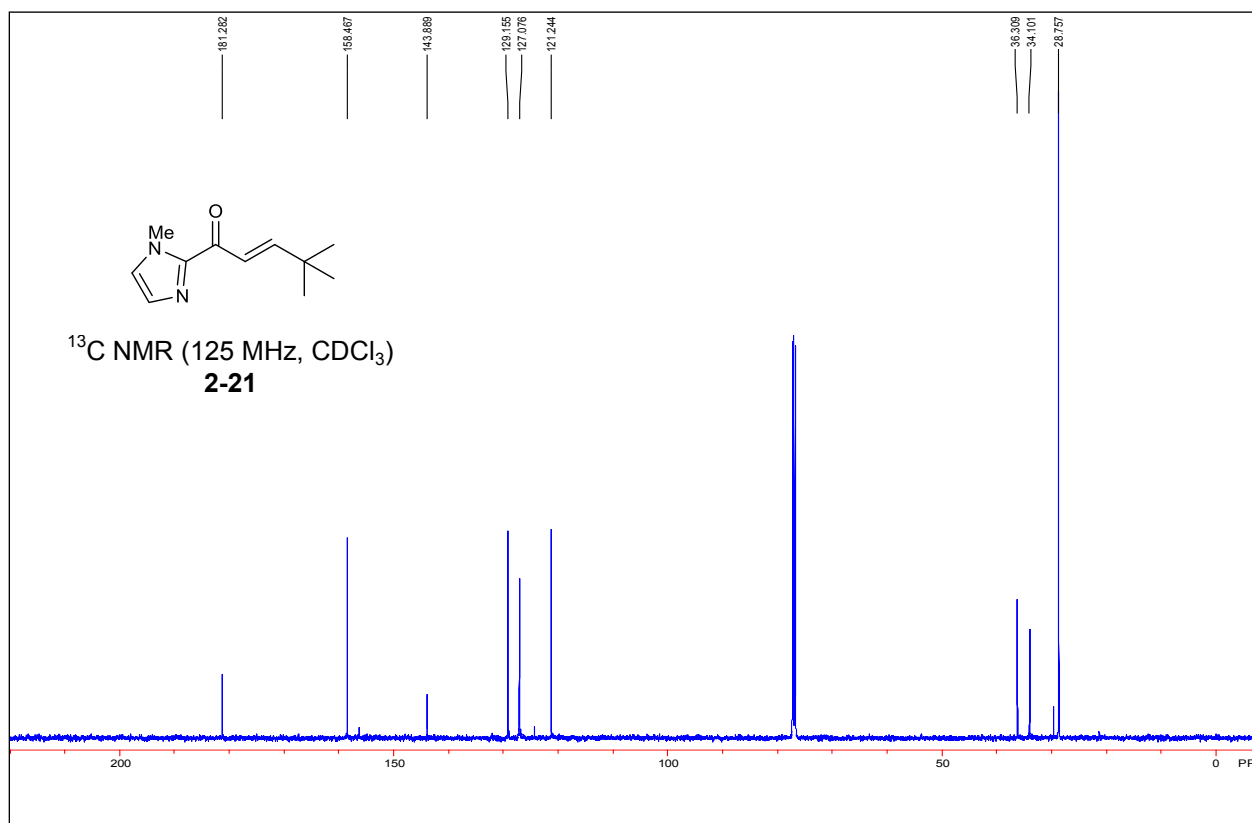
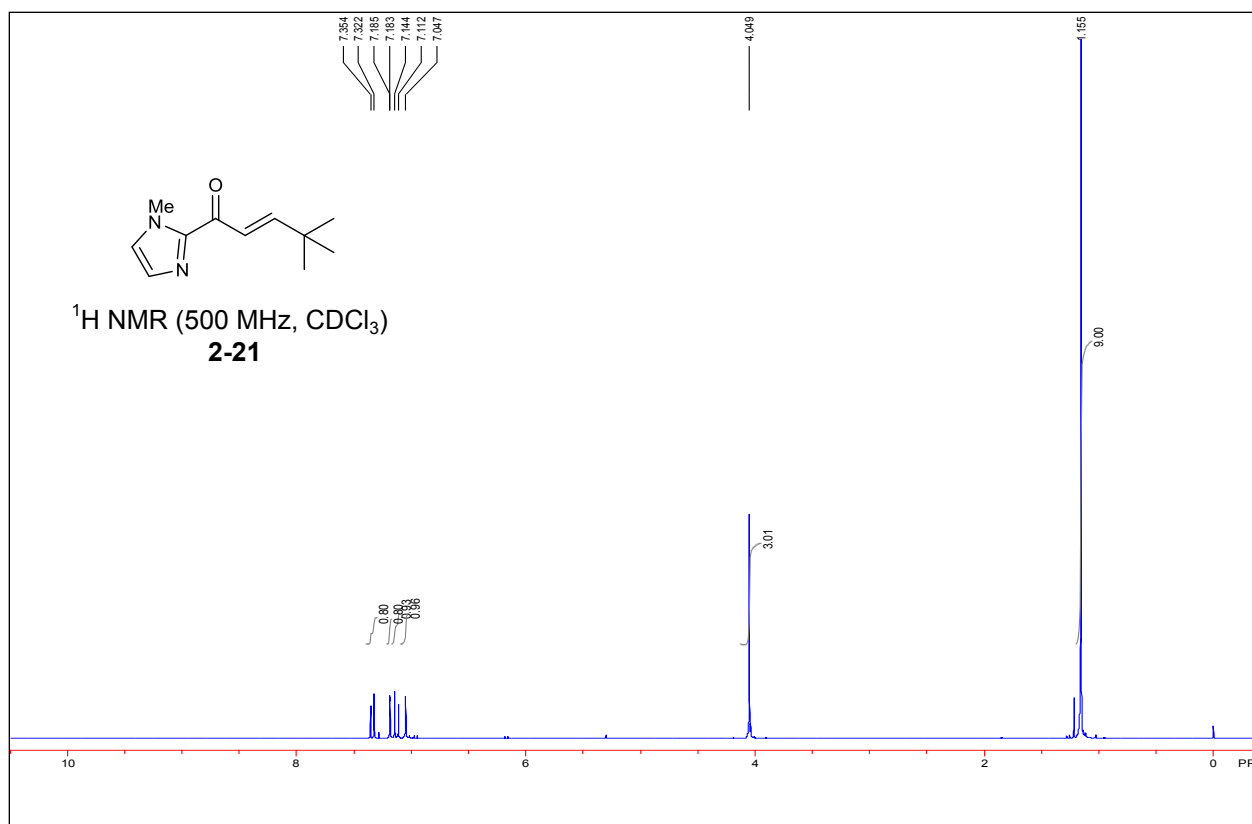
2-35

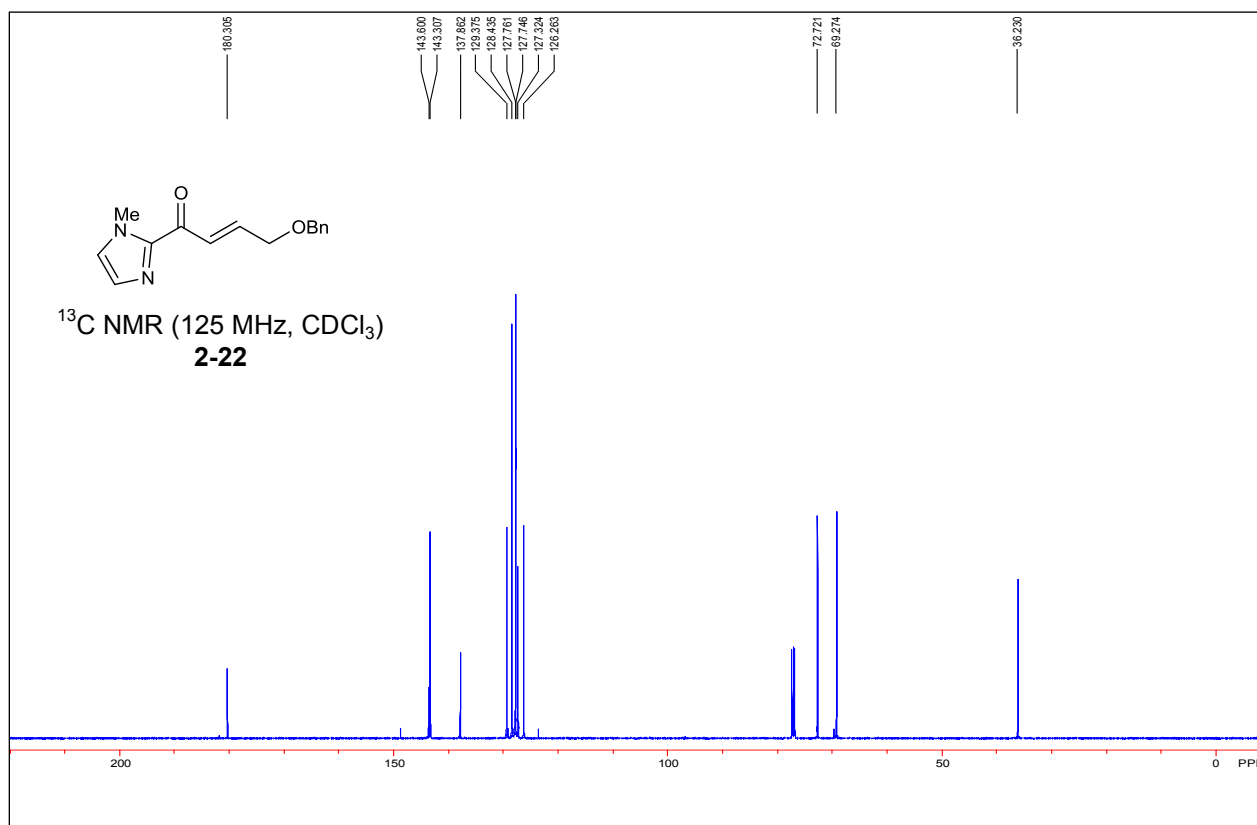
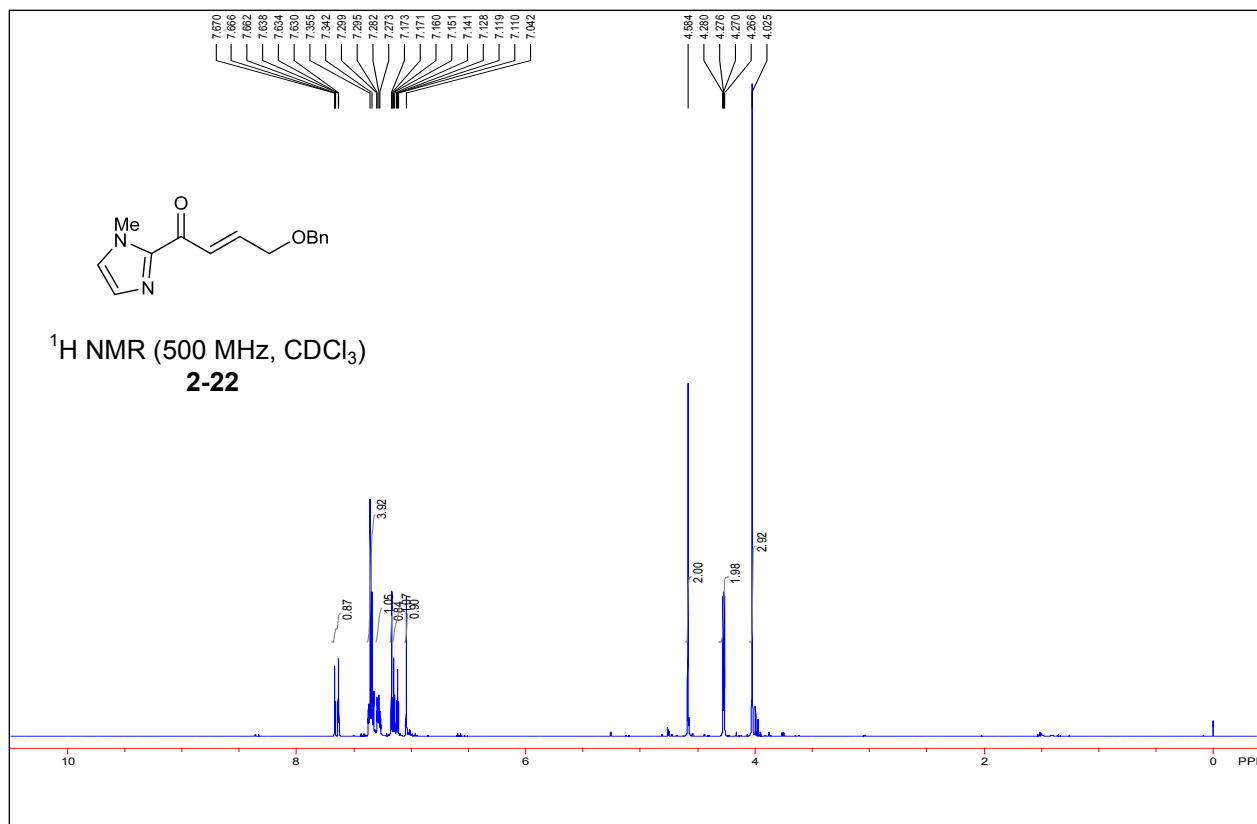


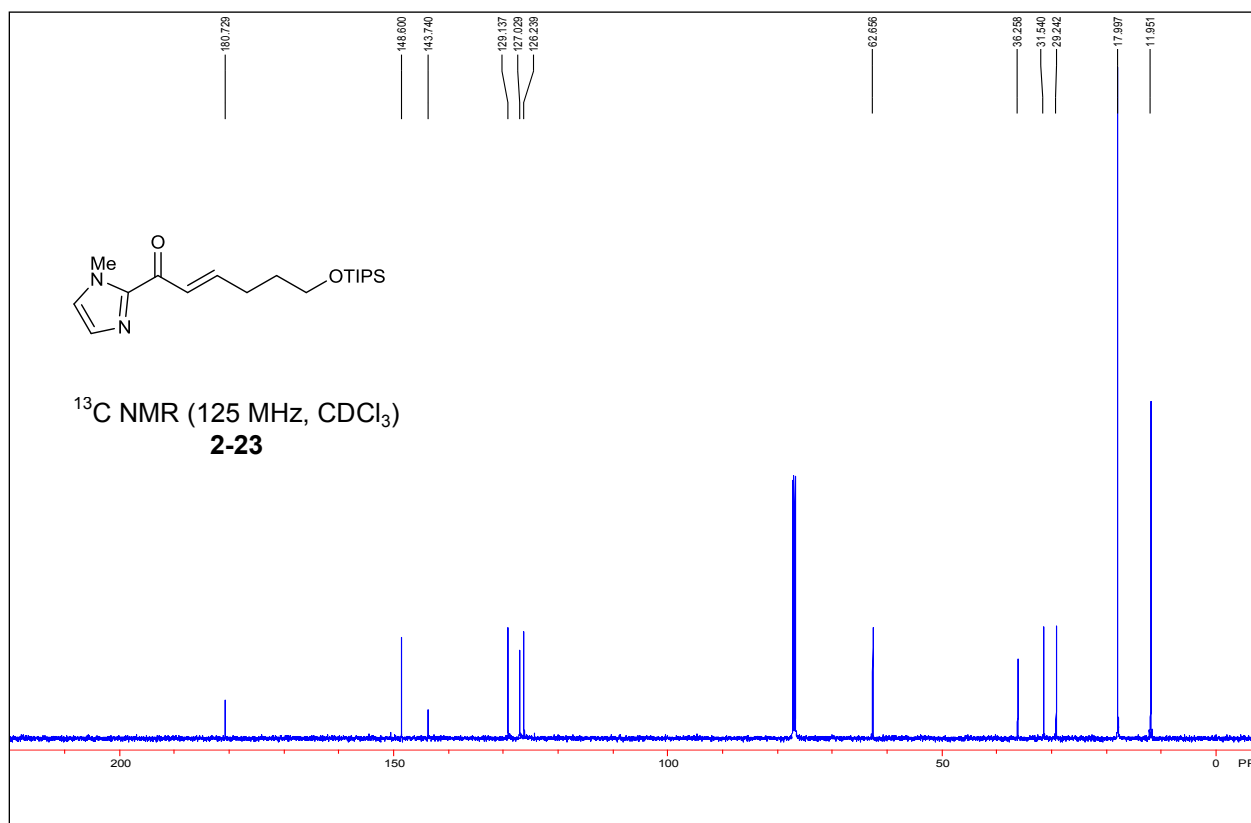
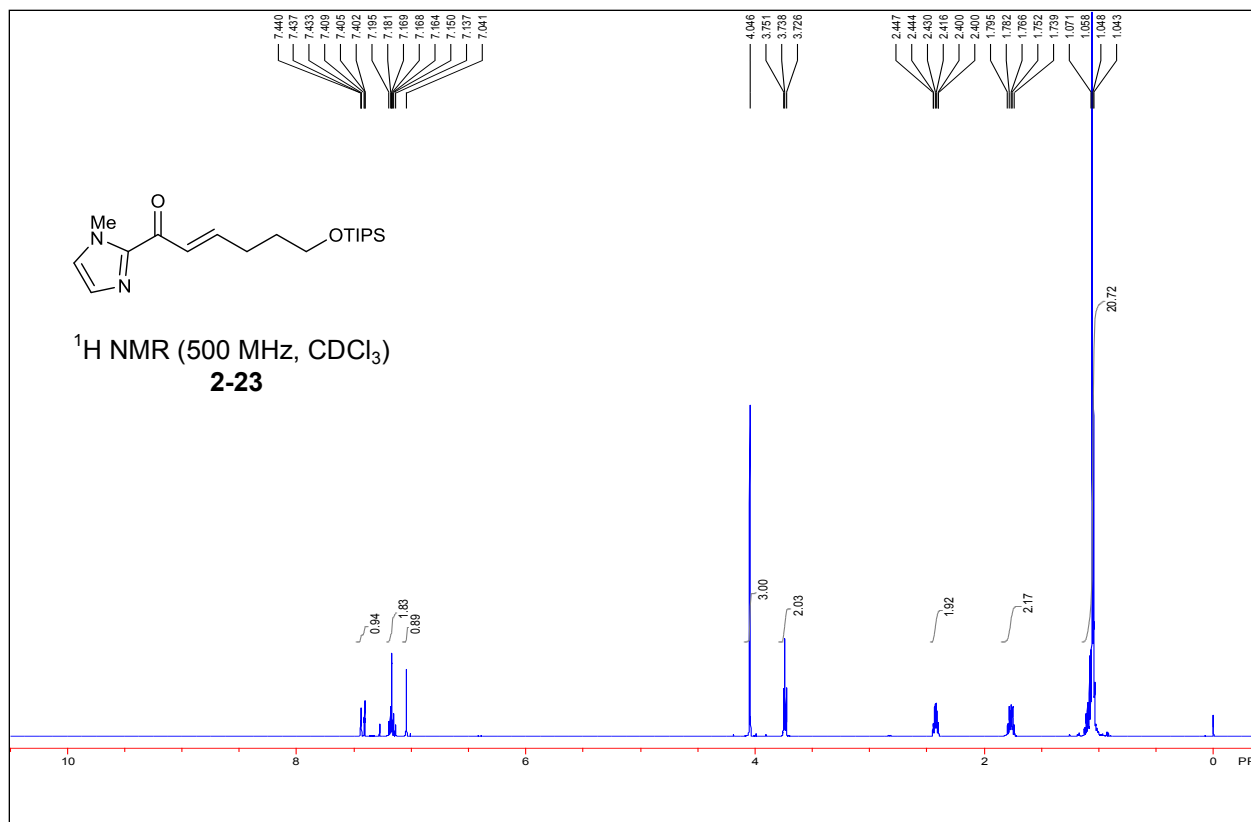
2-36

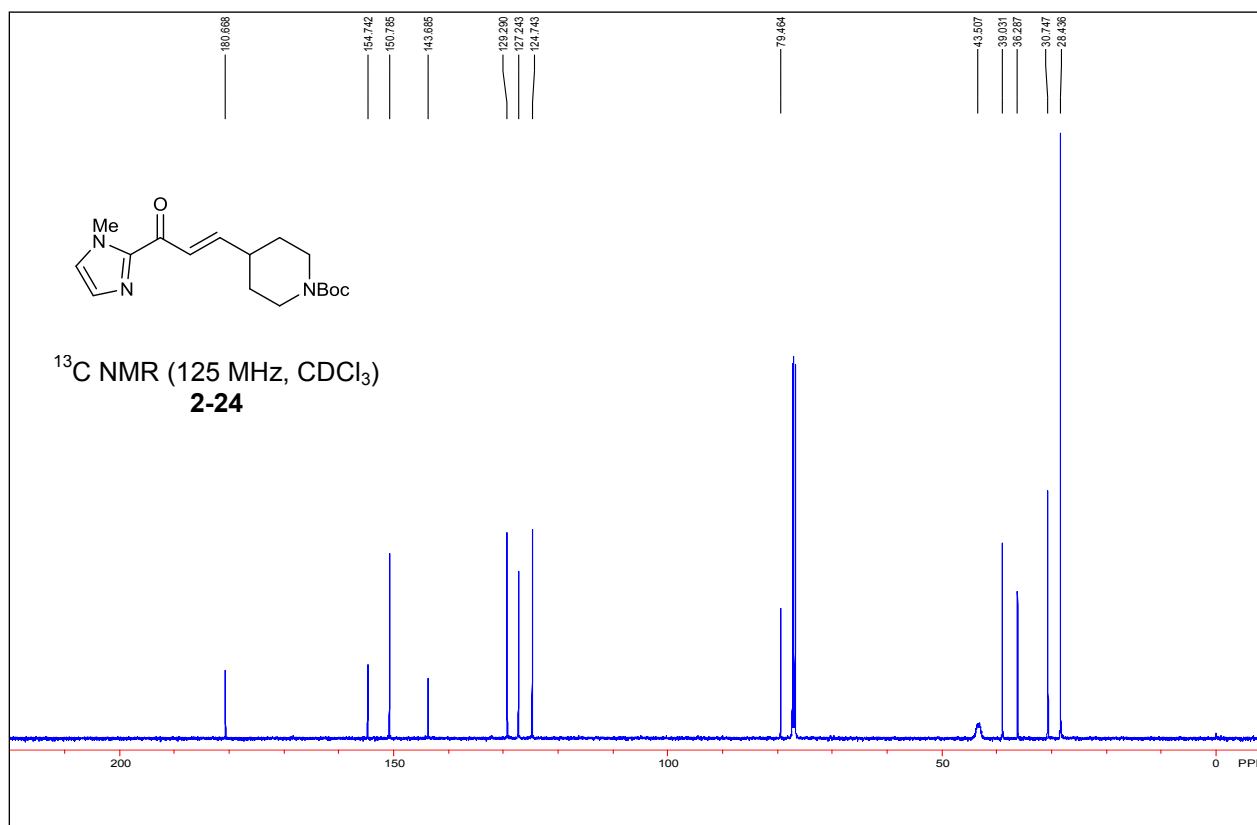
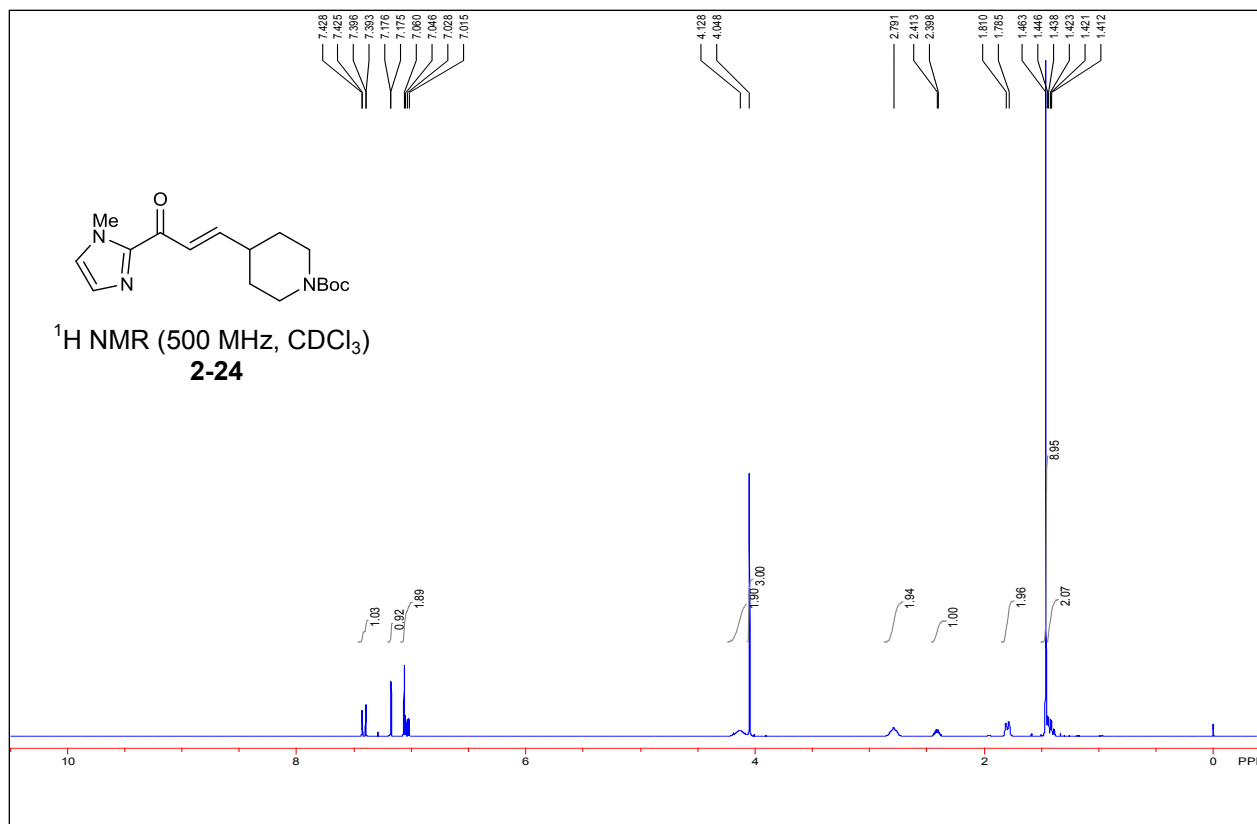


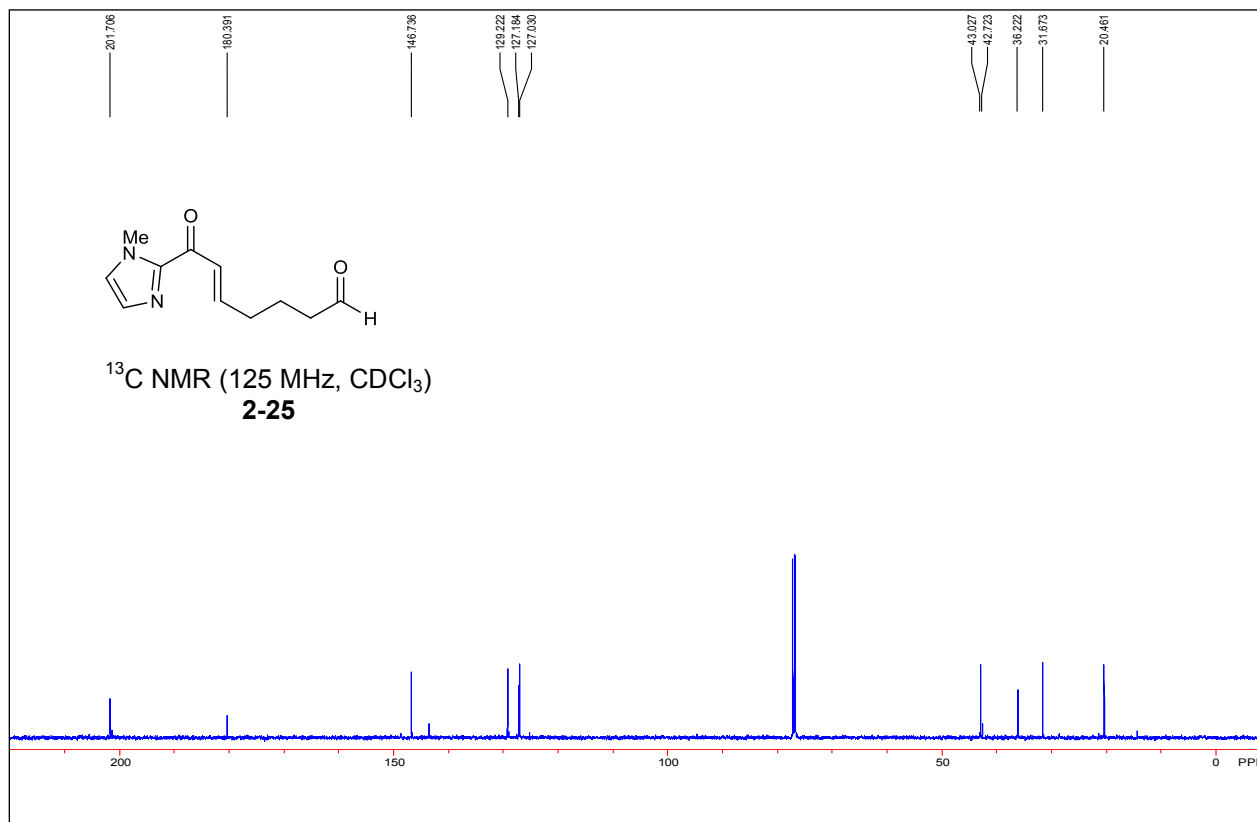
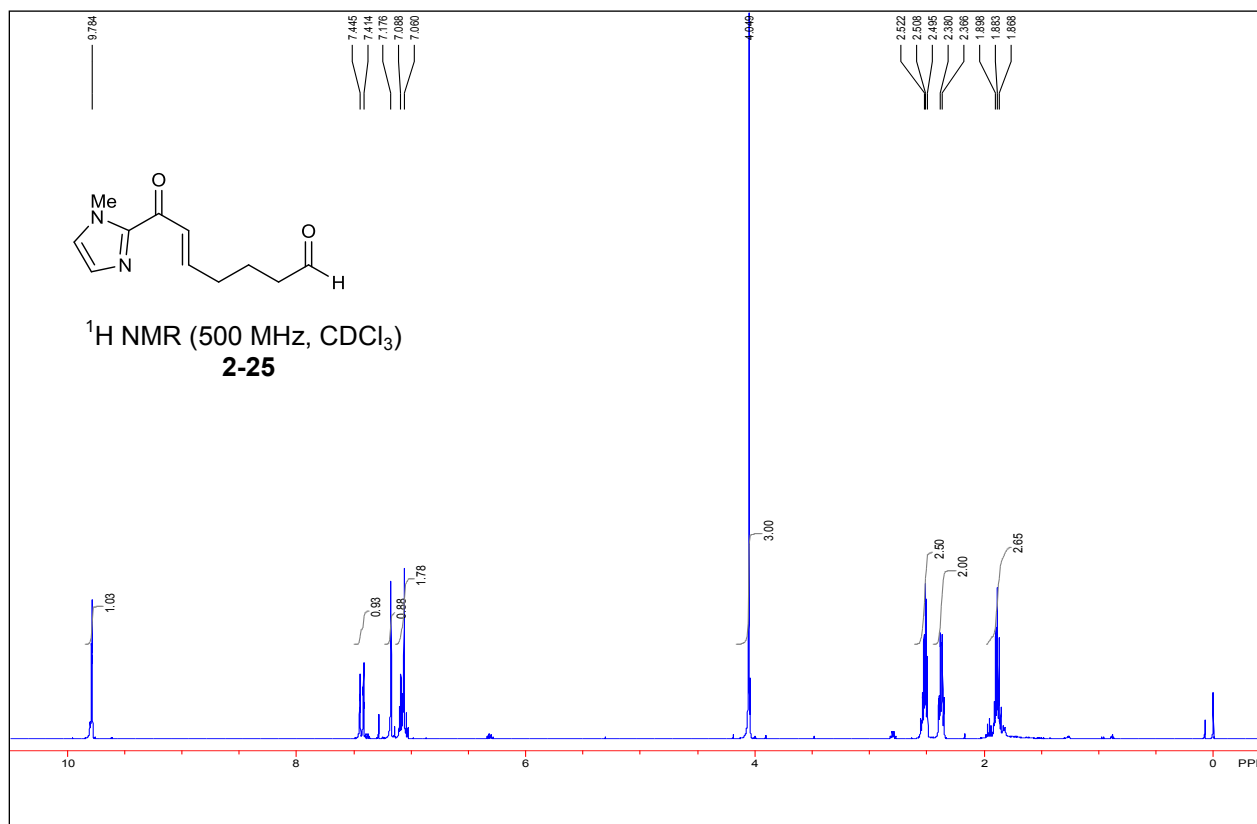
2-37

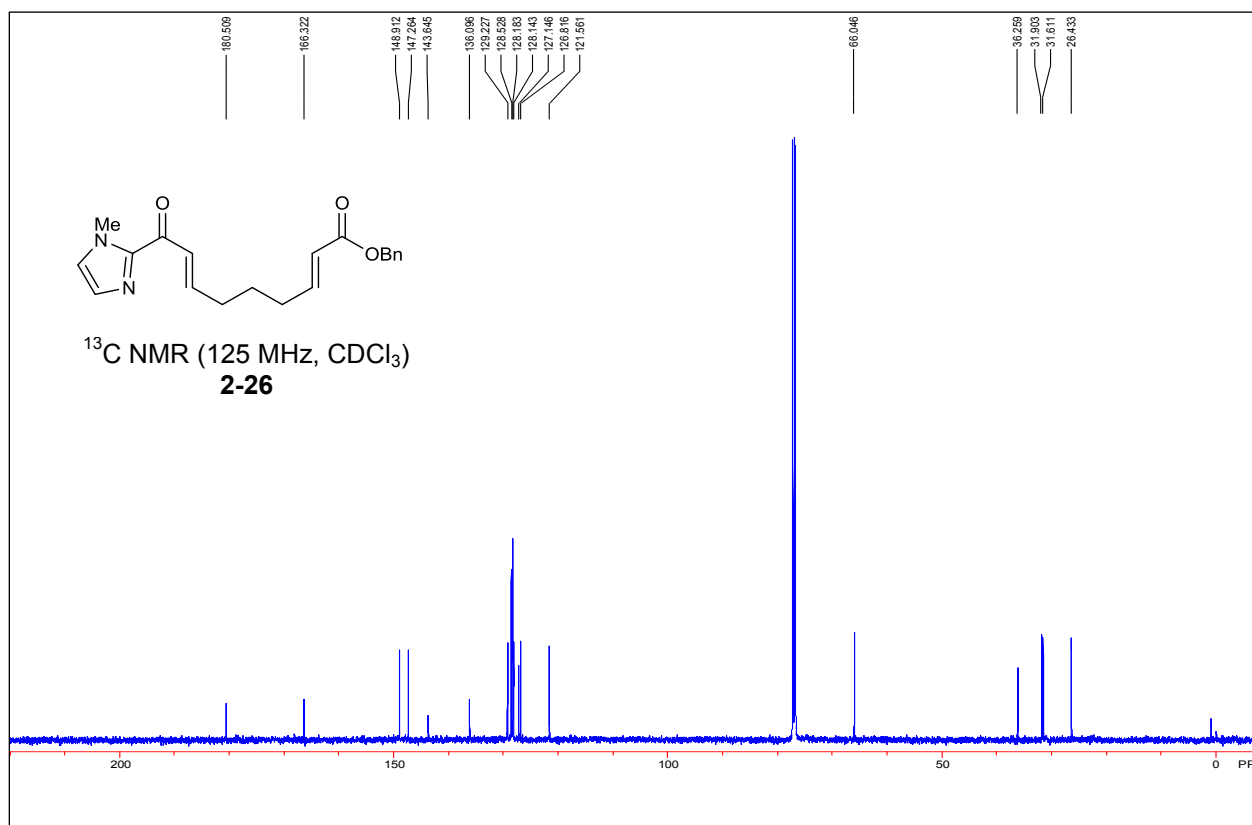
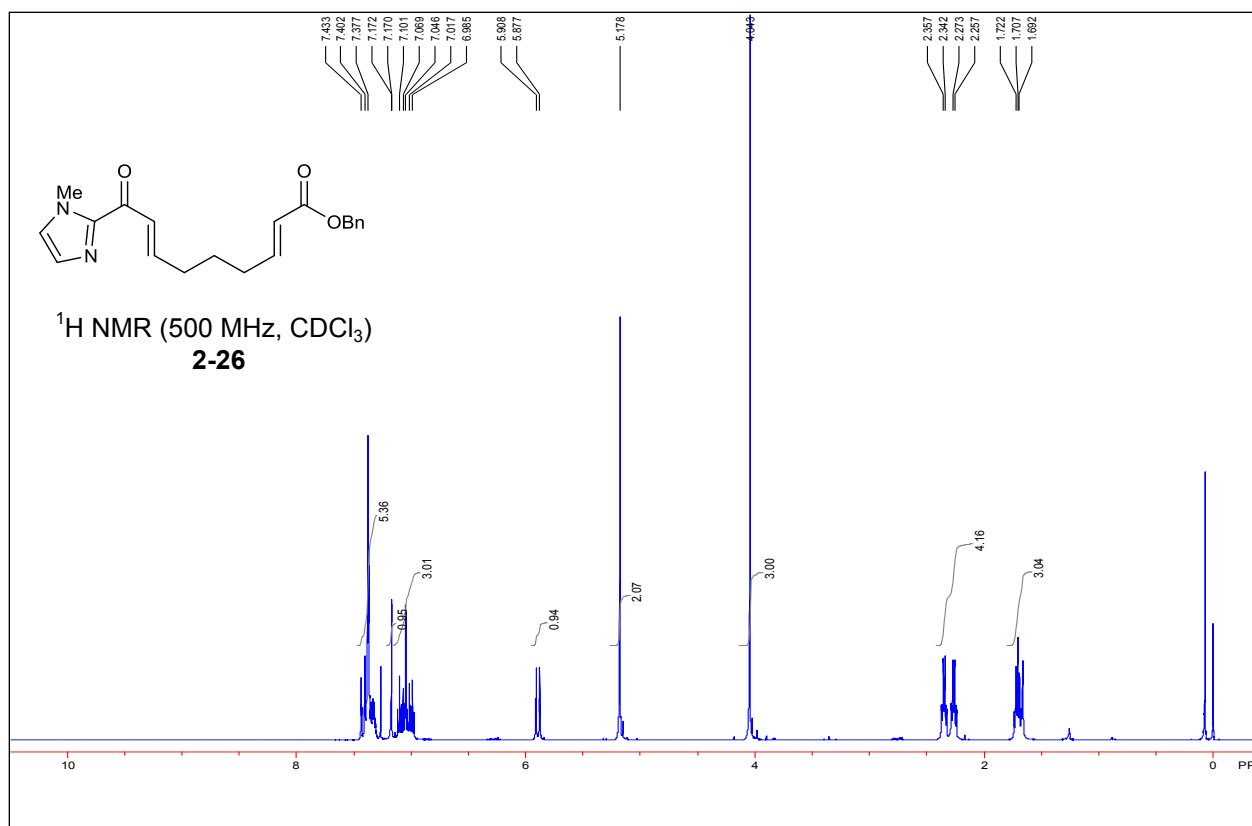


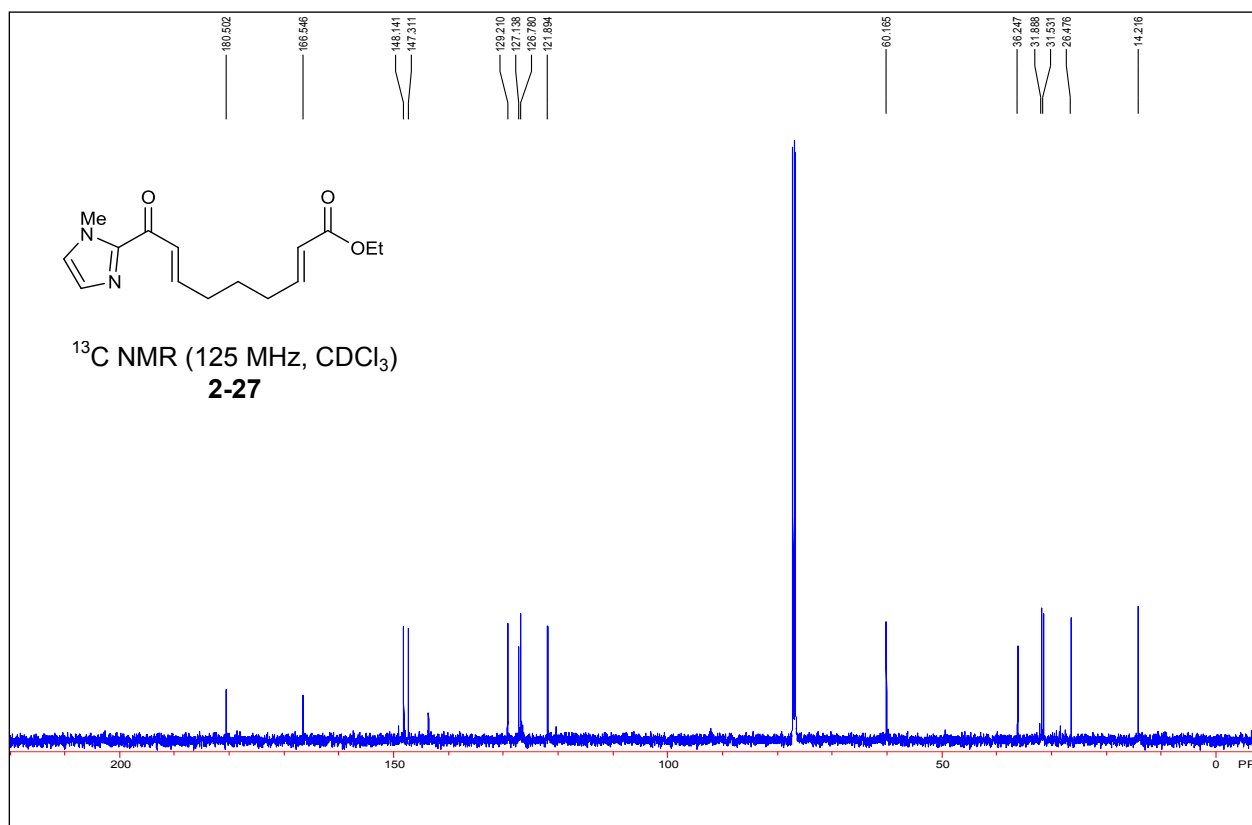
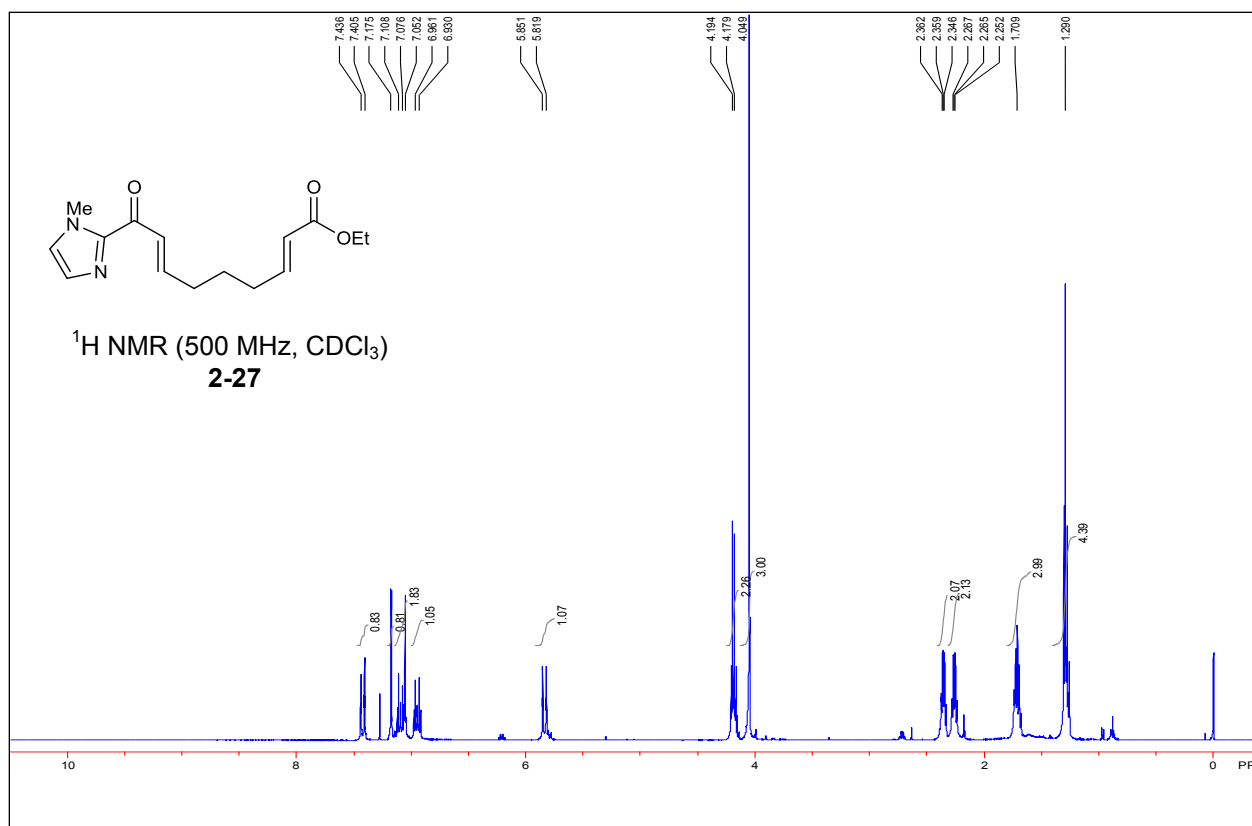


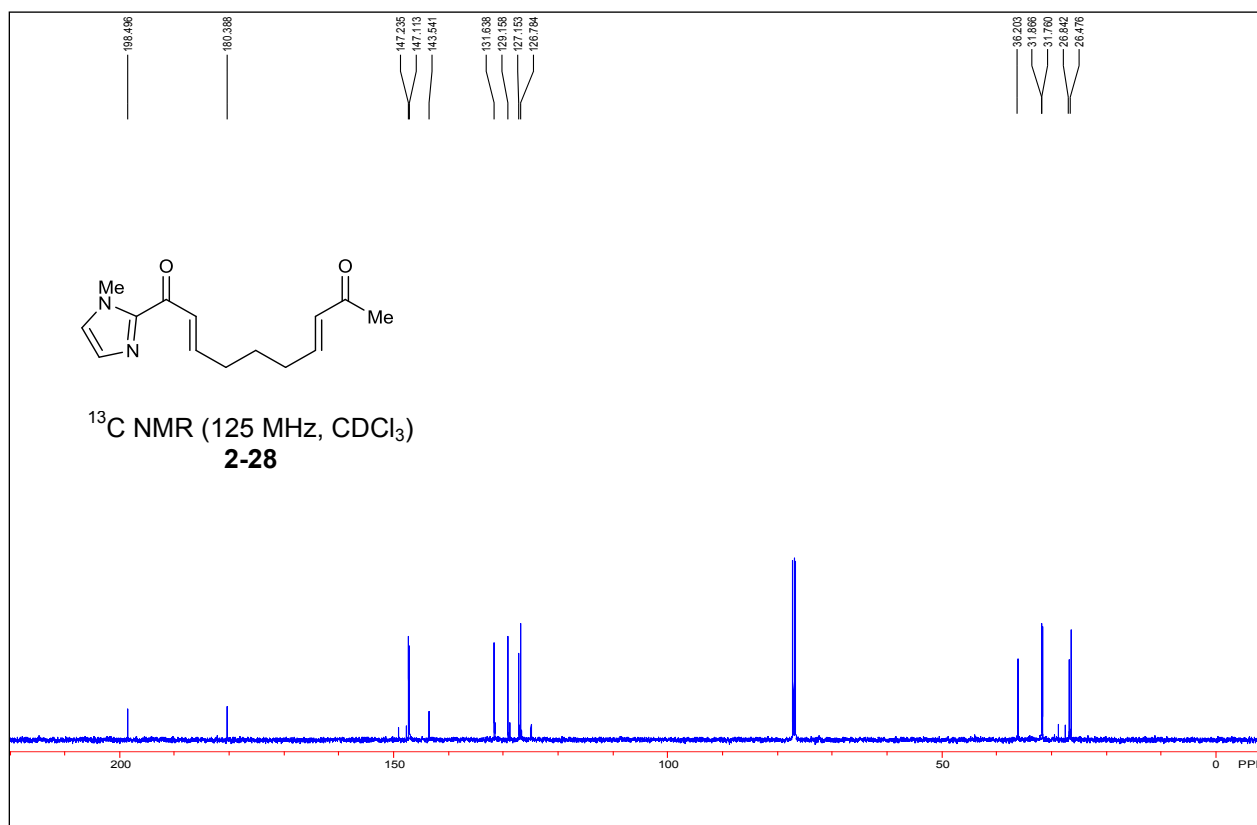
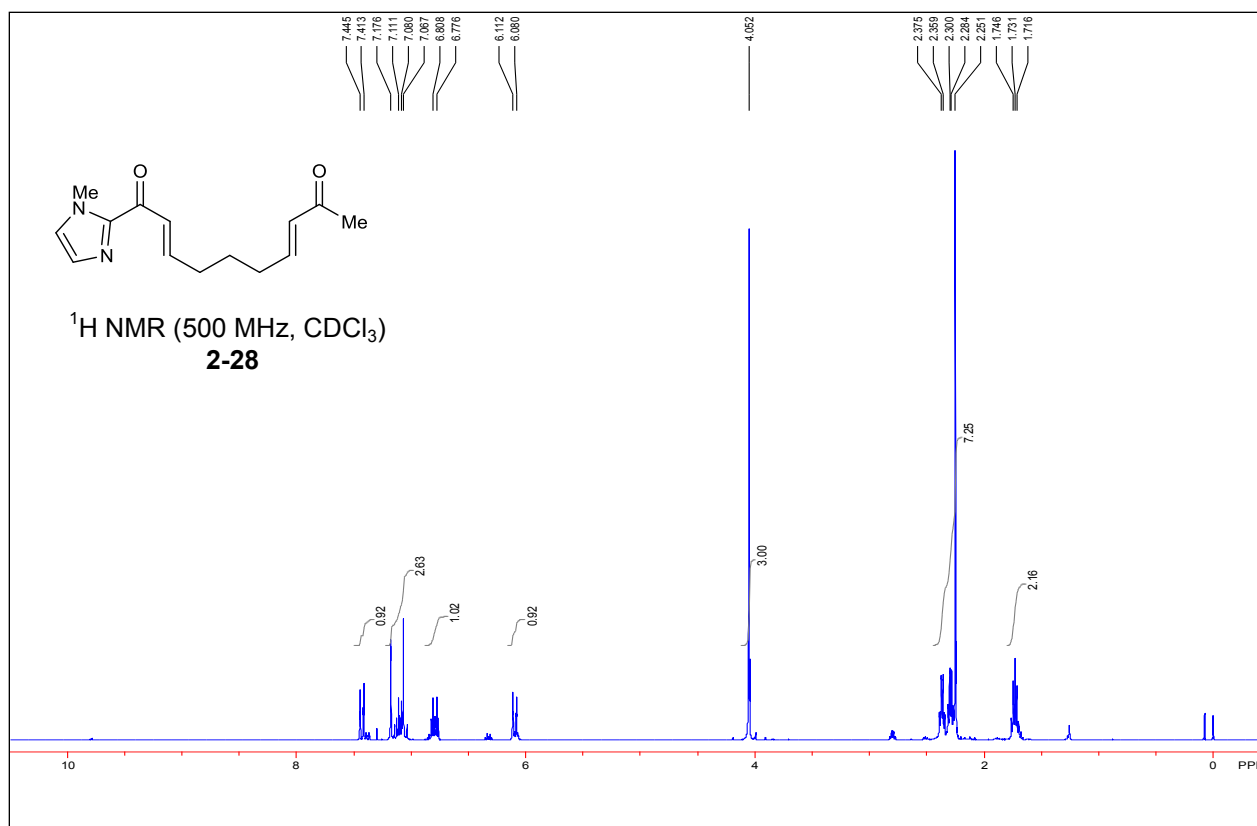


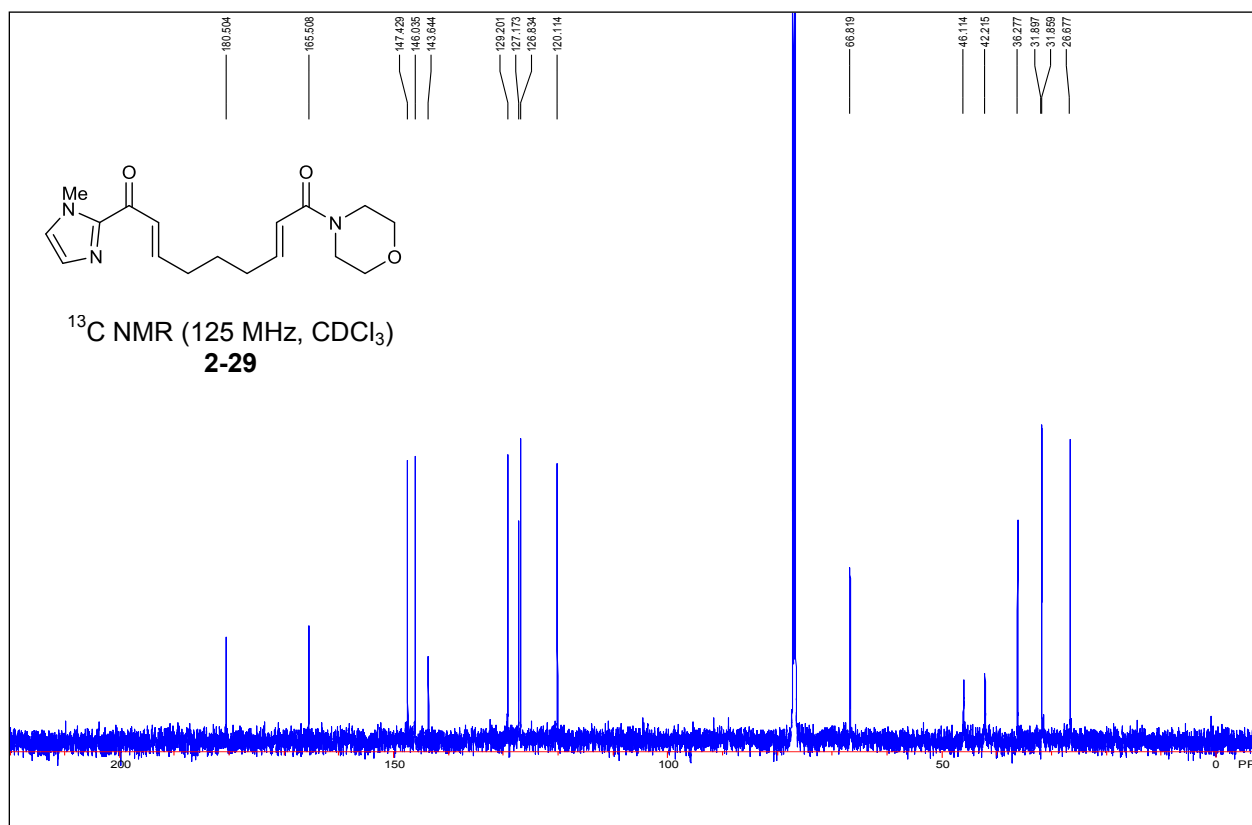
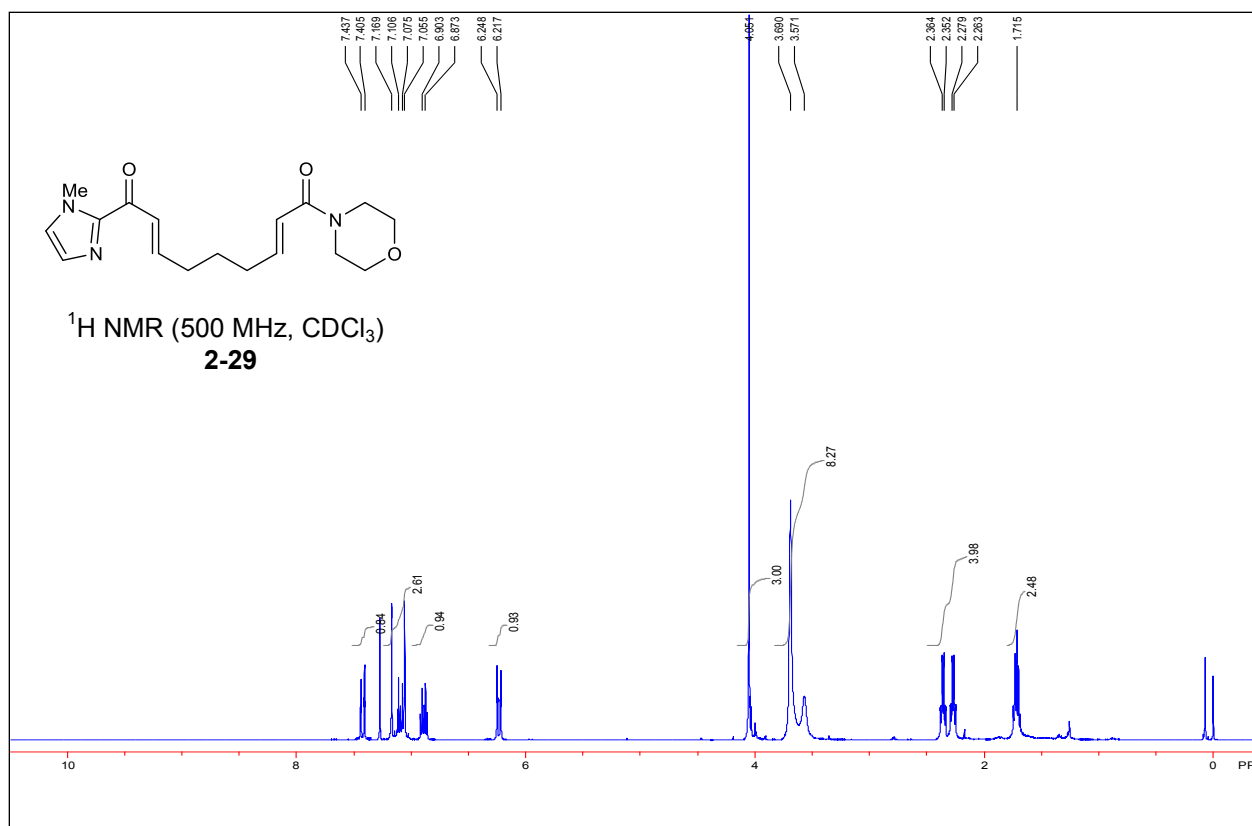


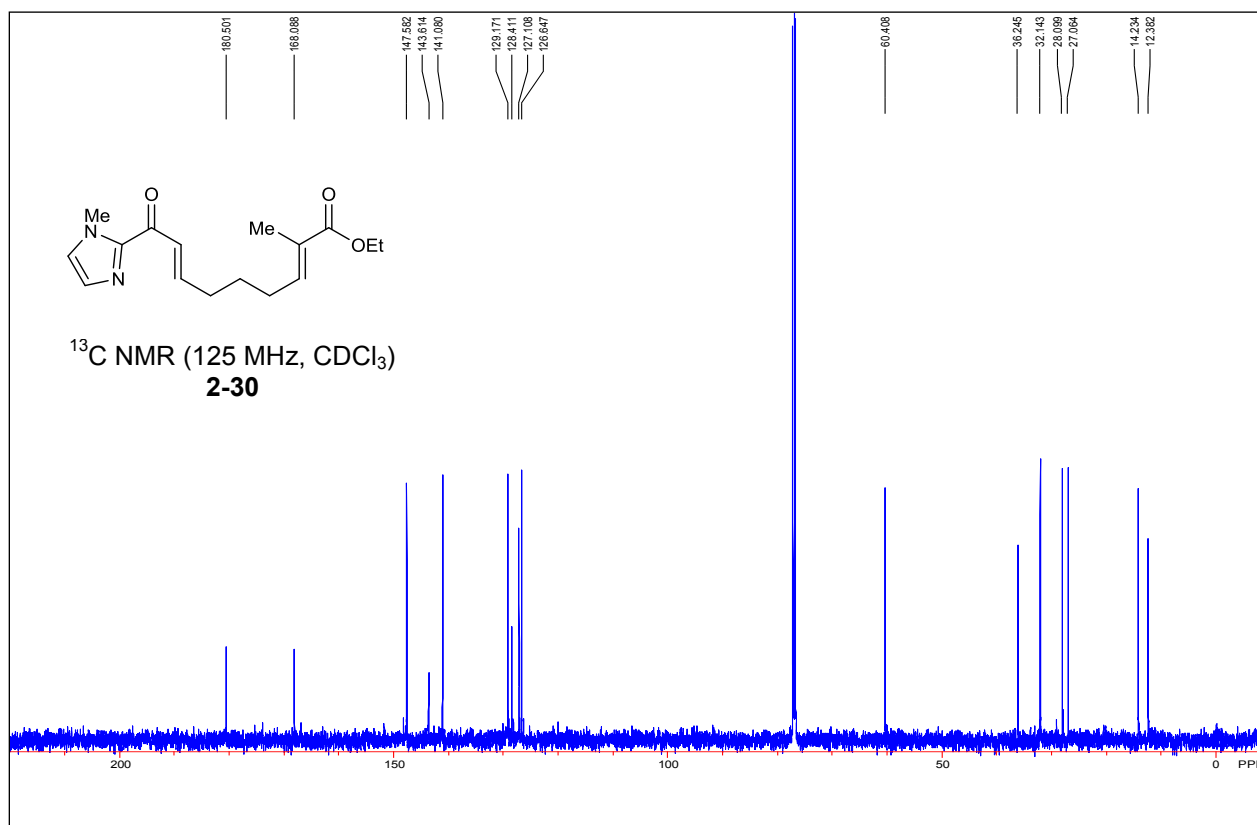
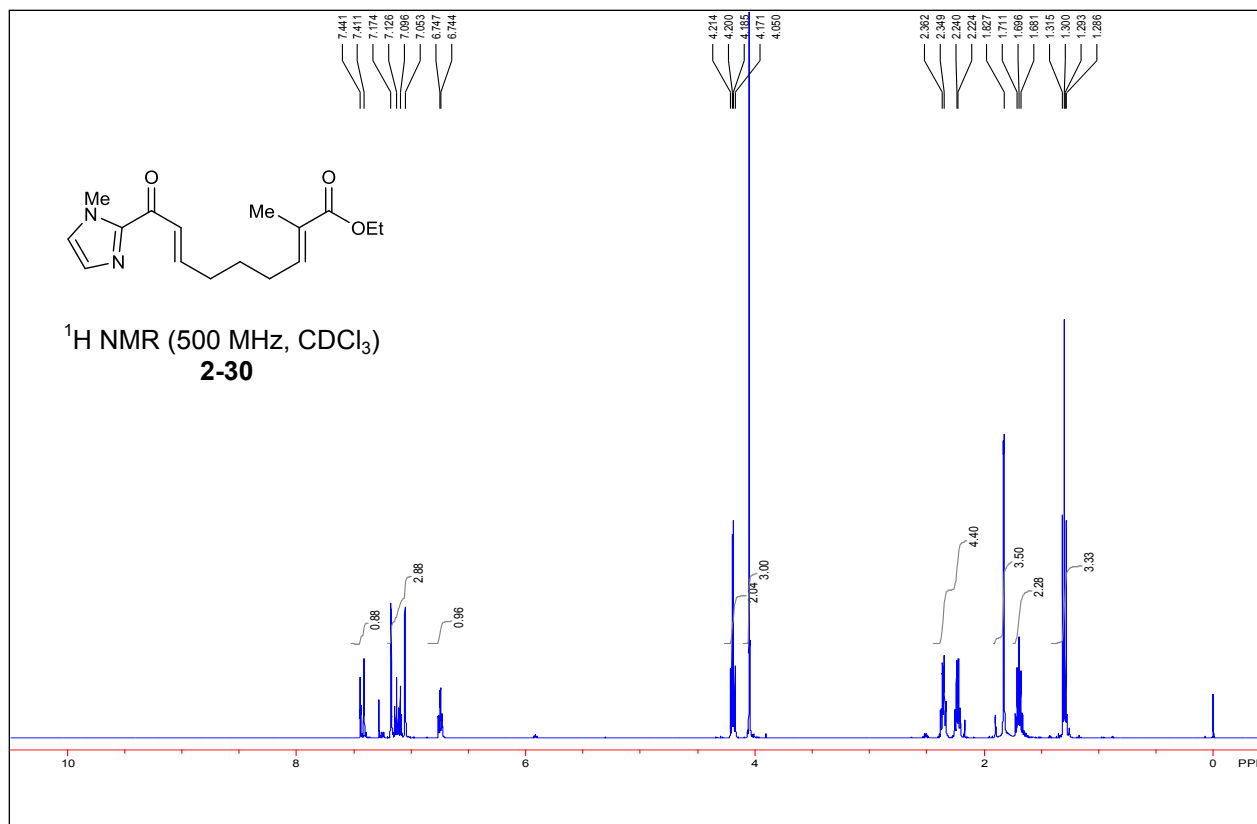


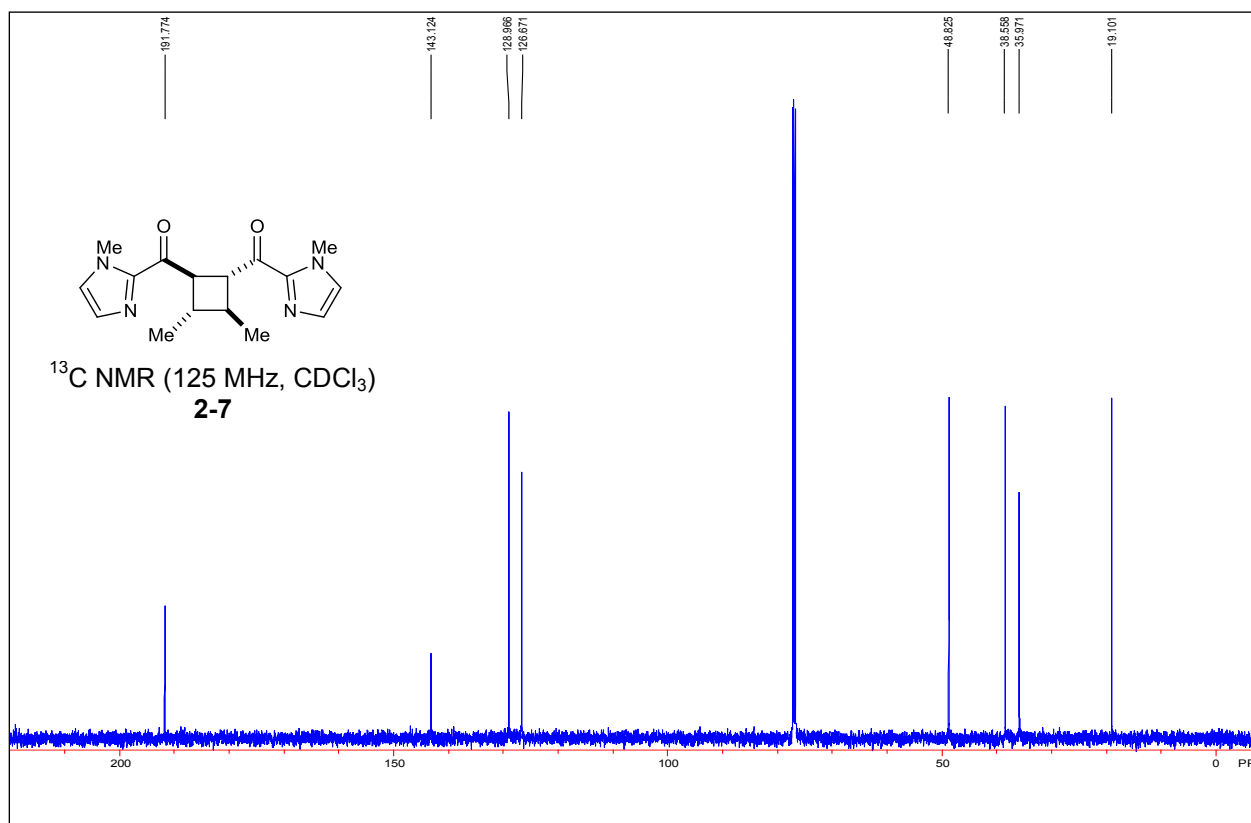
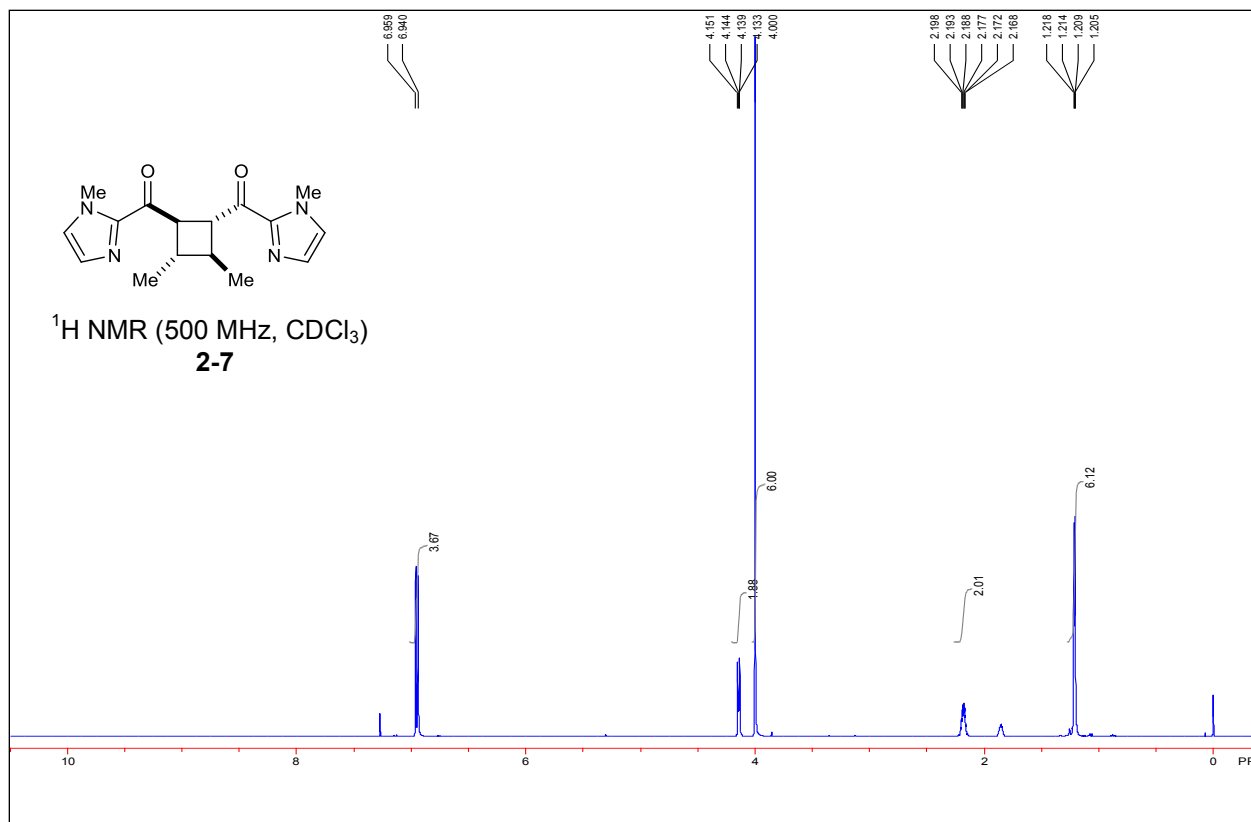


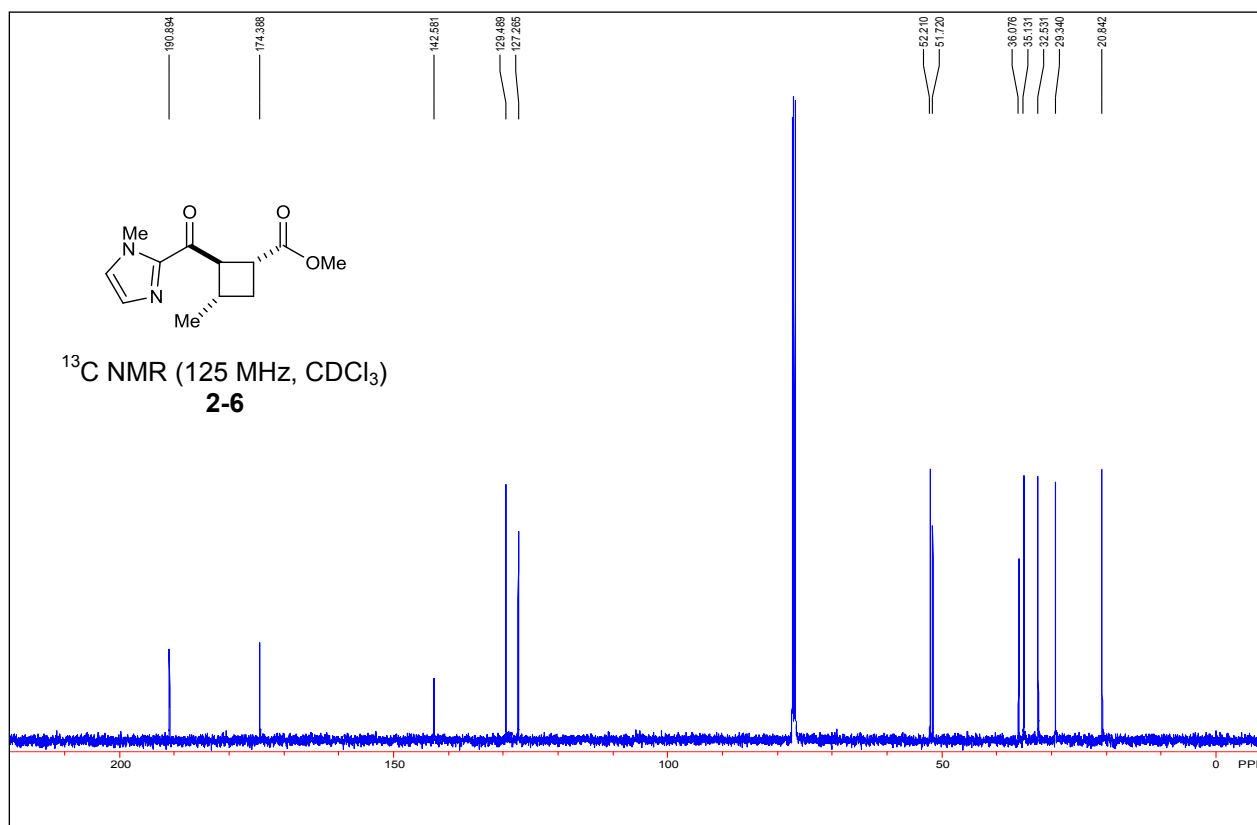
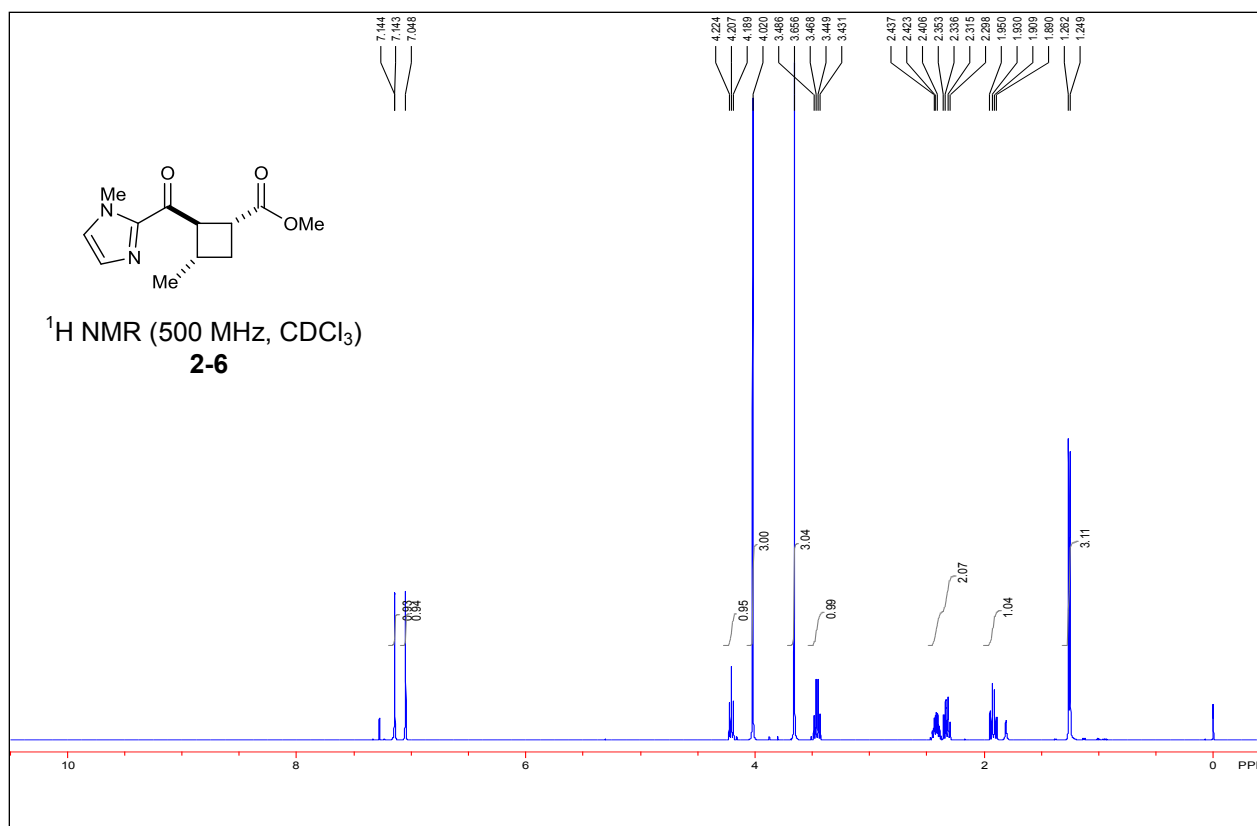


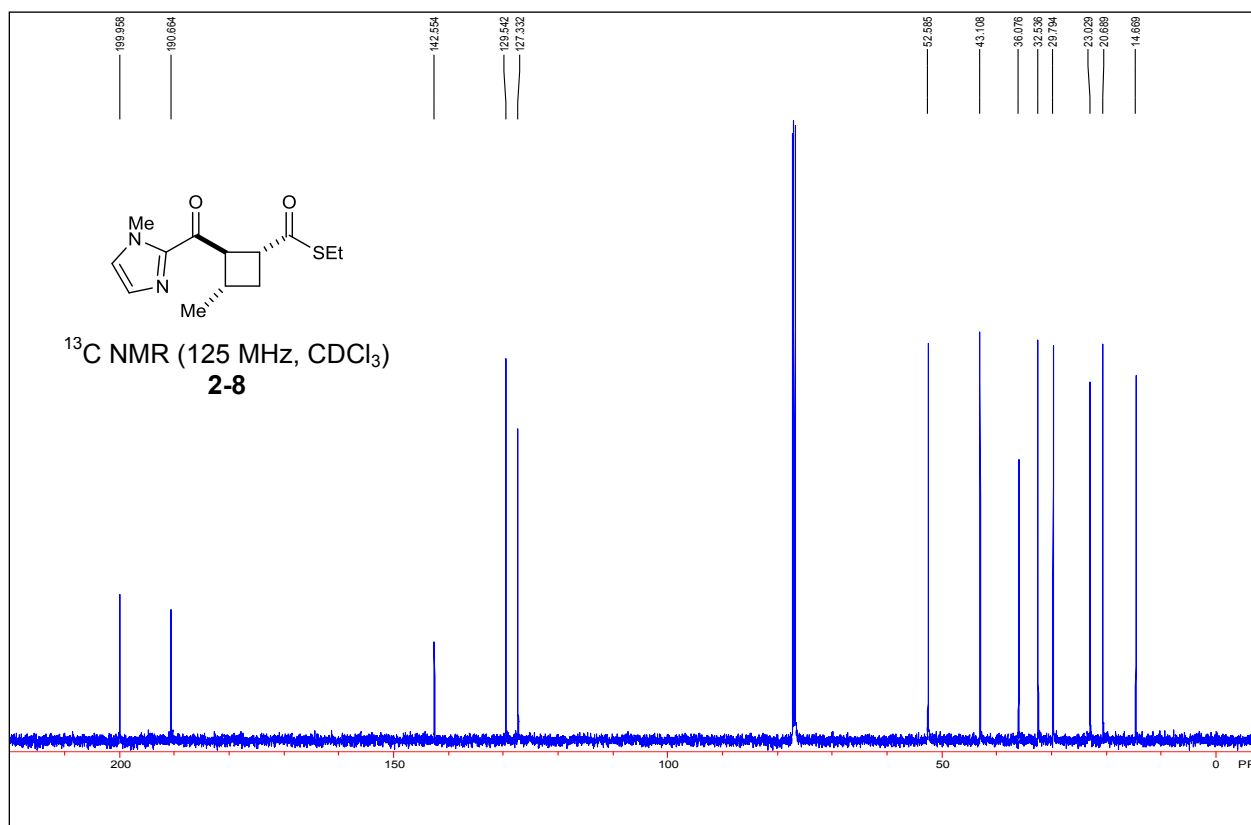
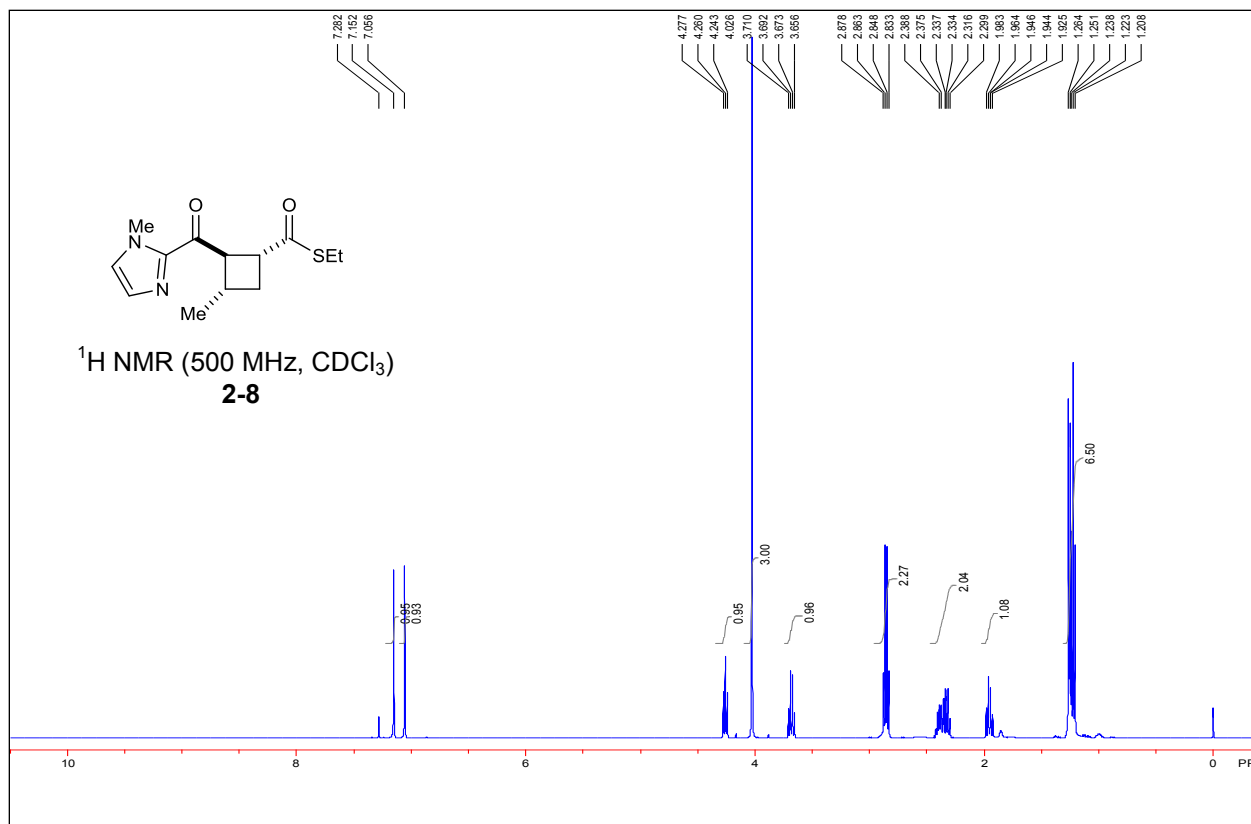


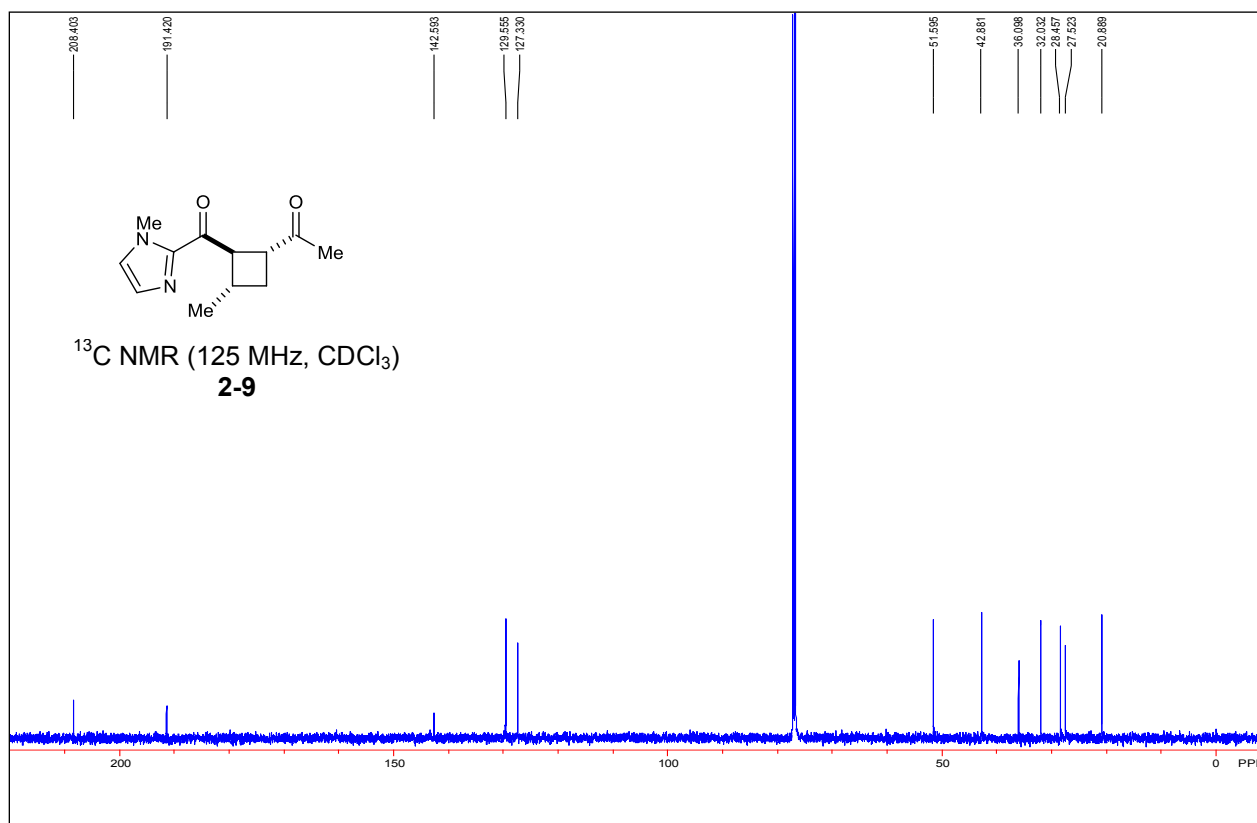
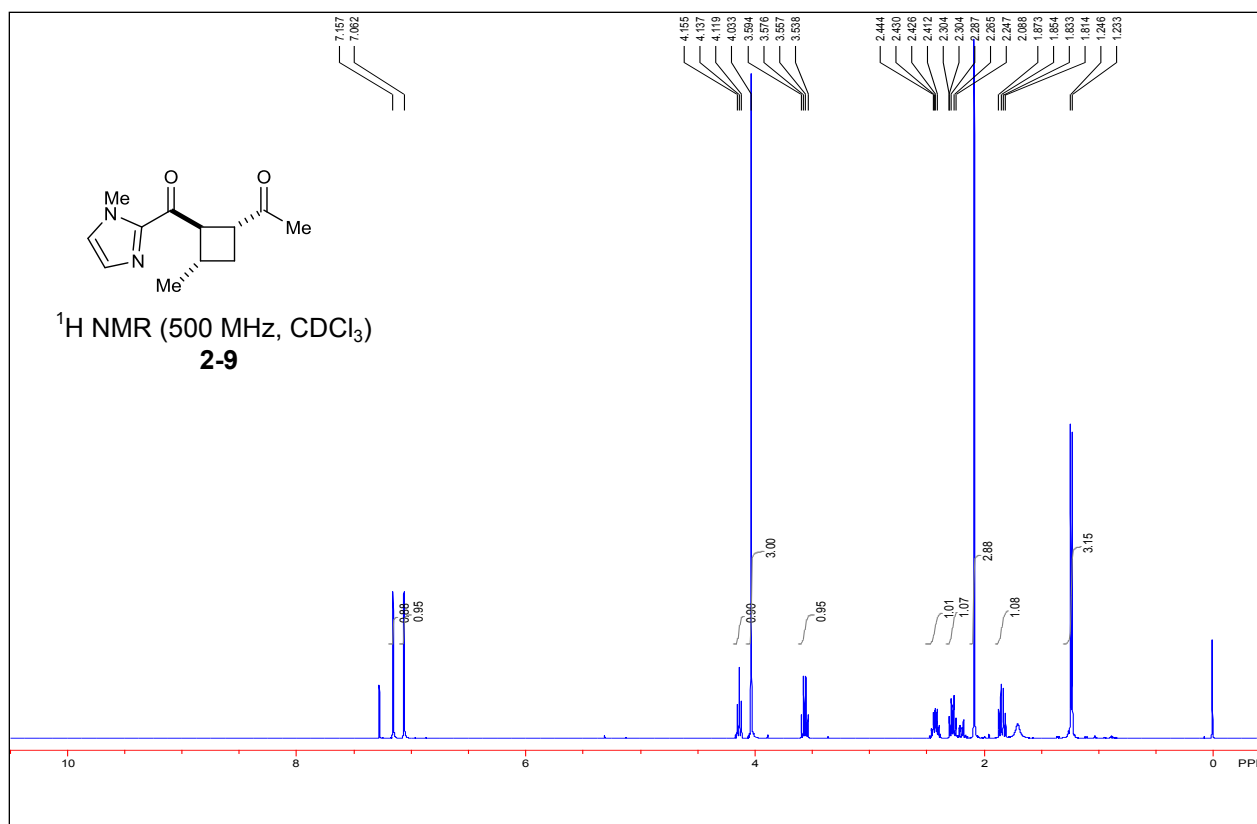


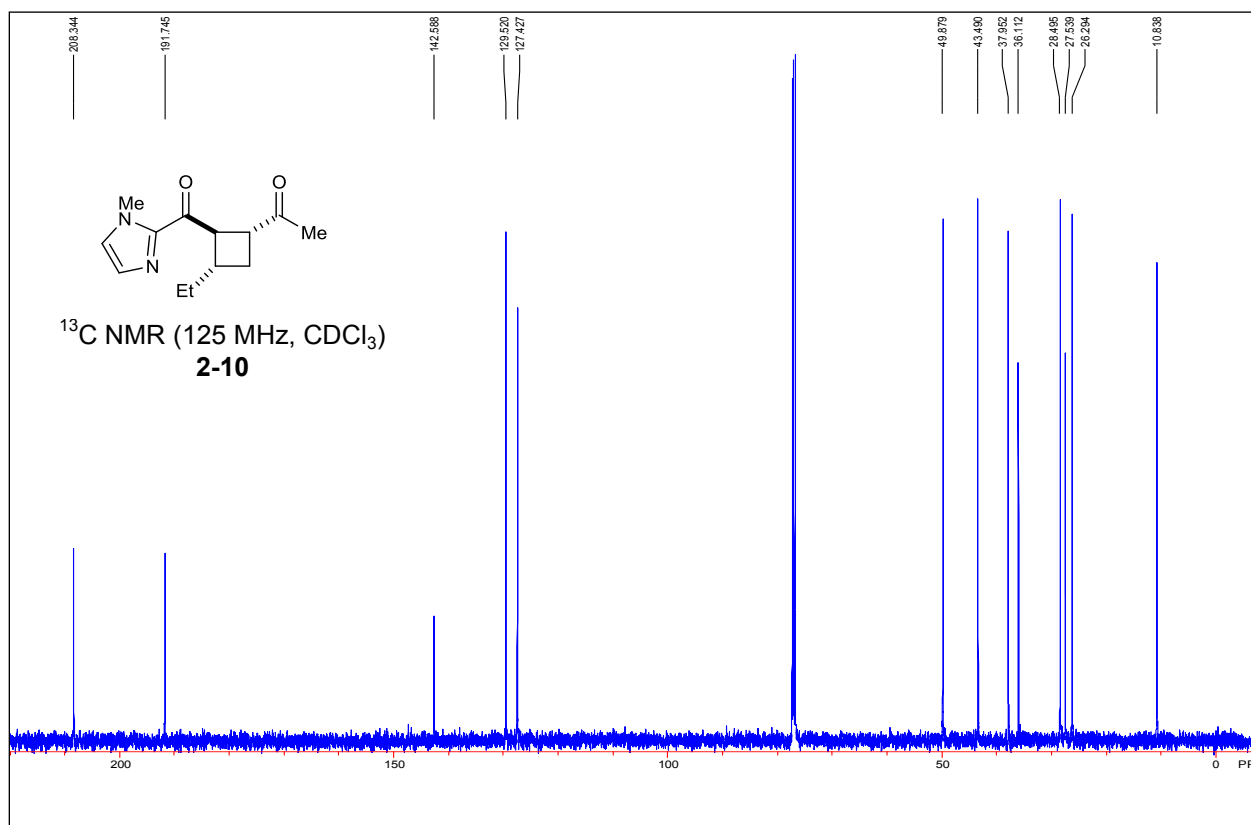
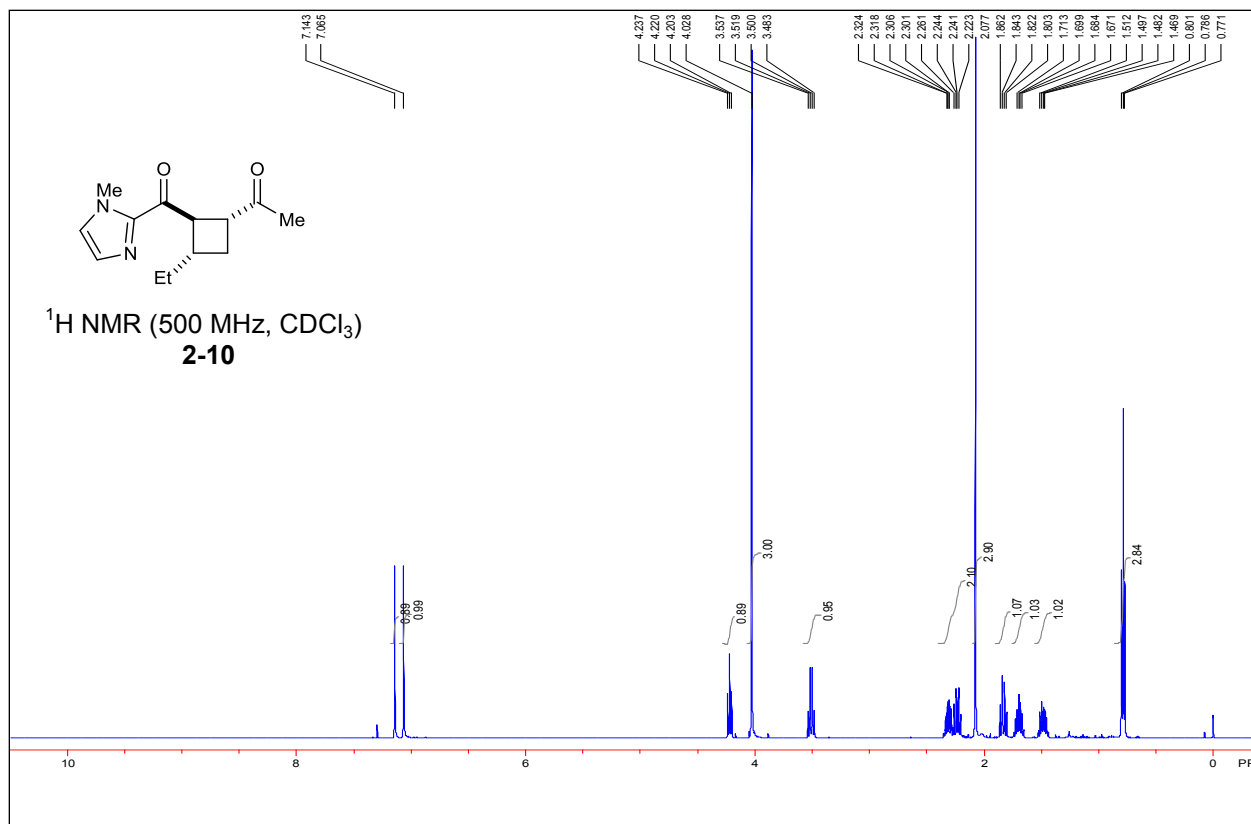


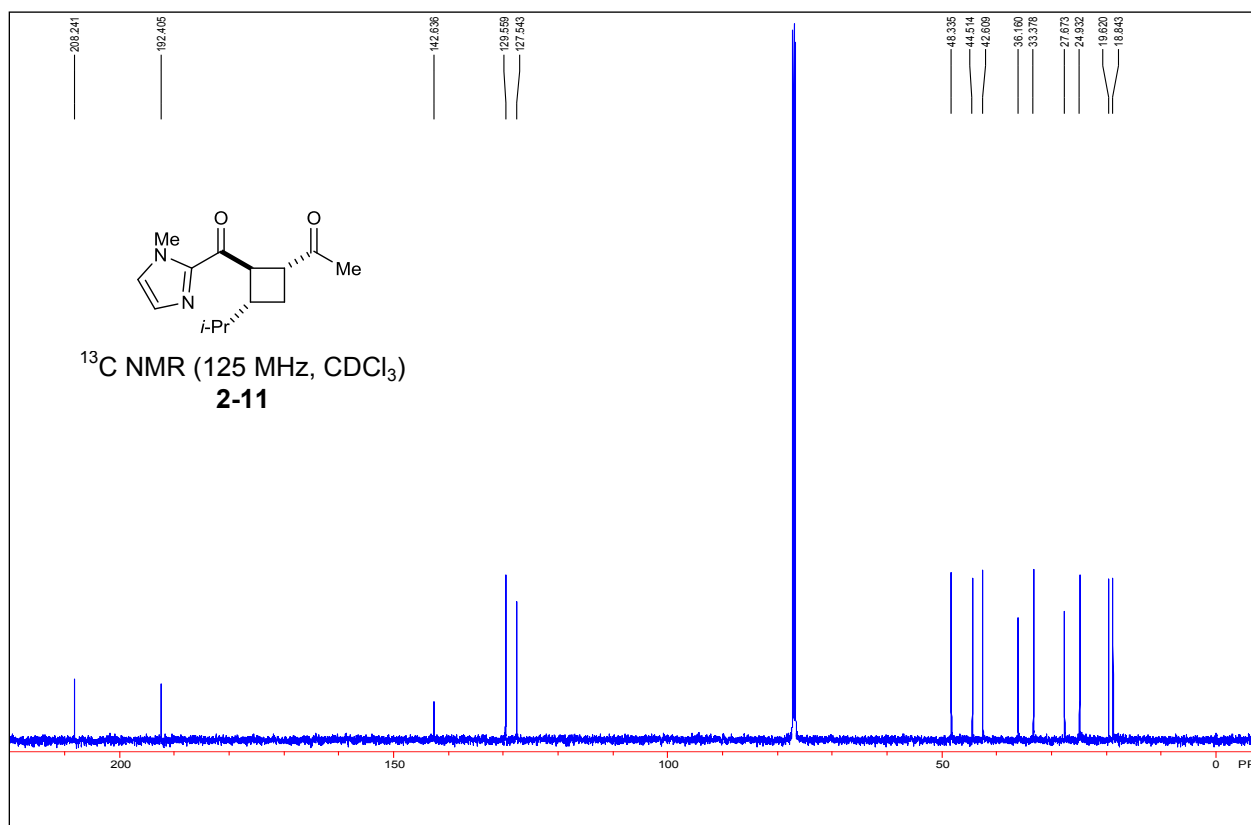
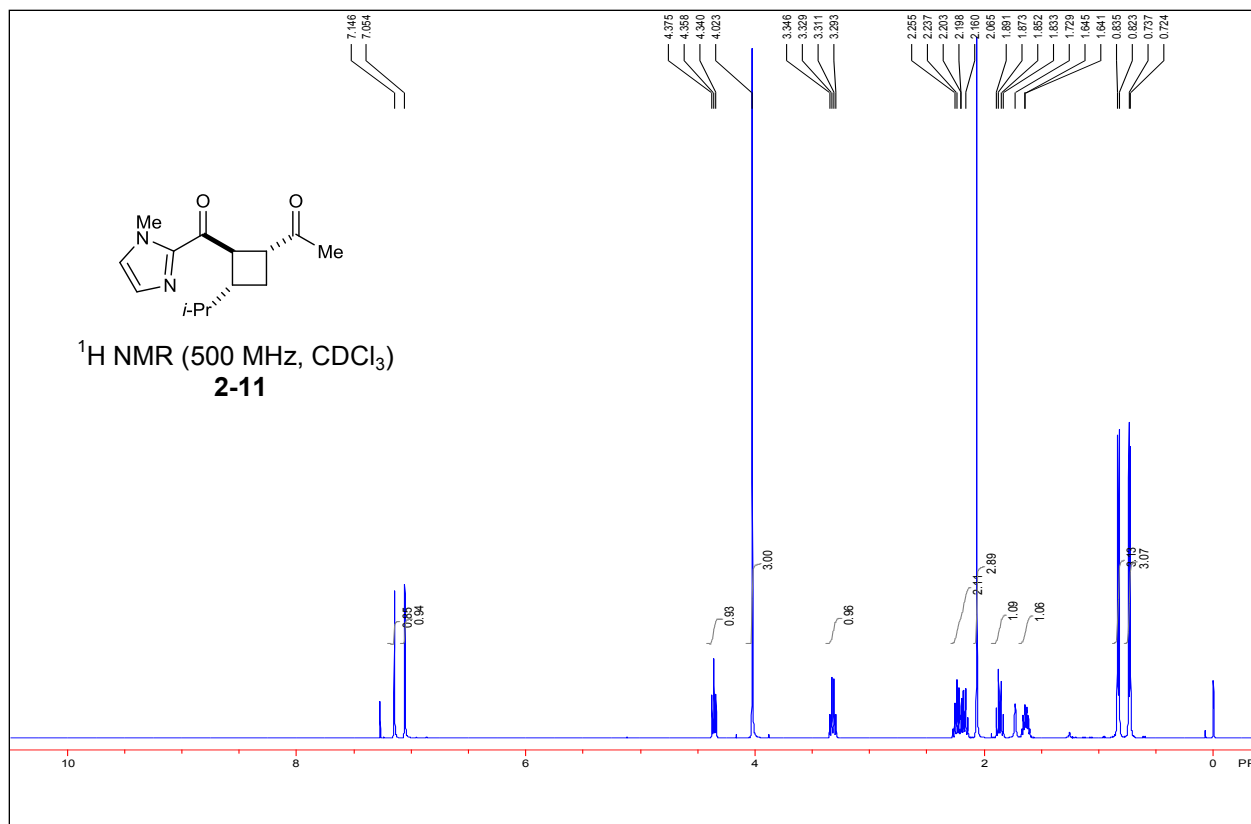


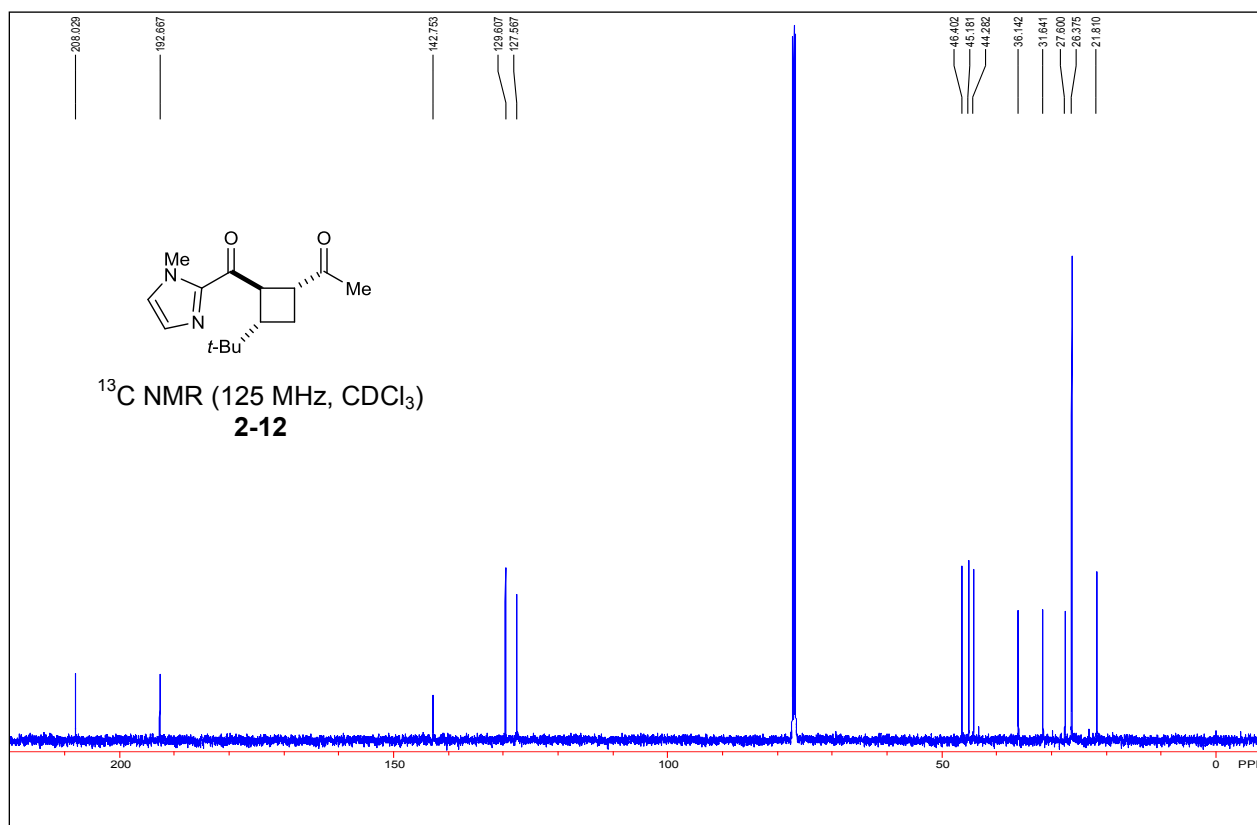
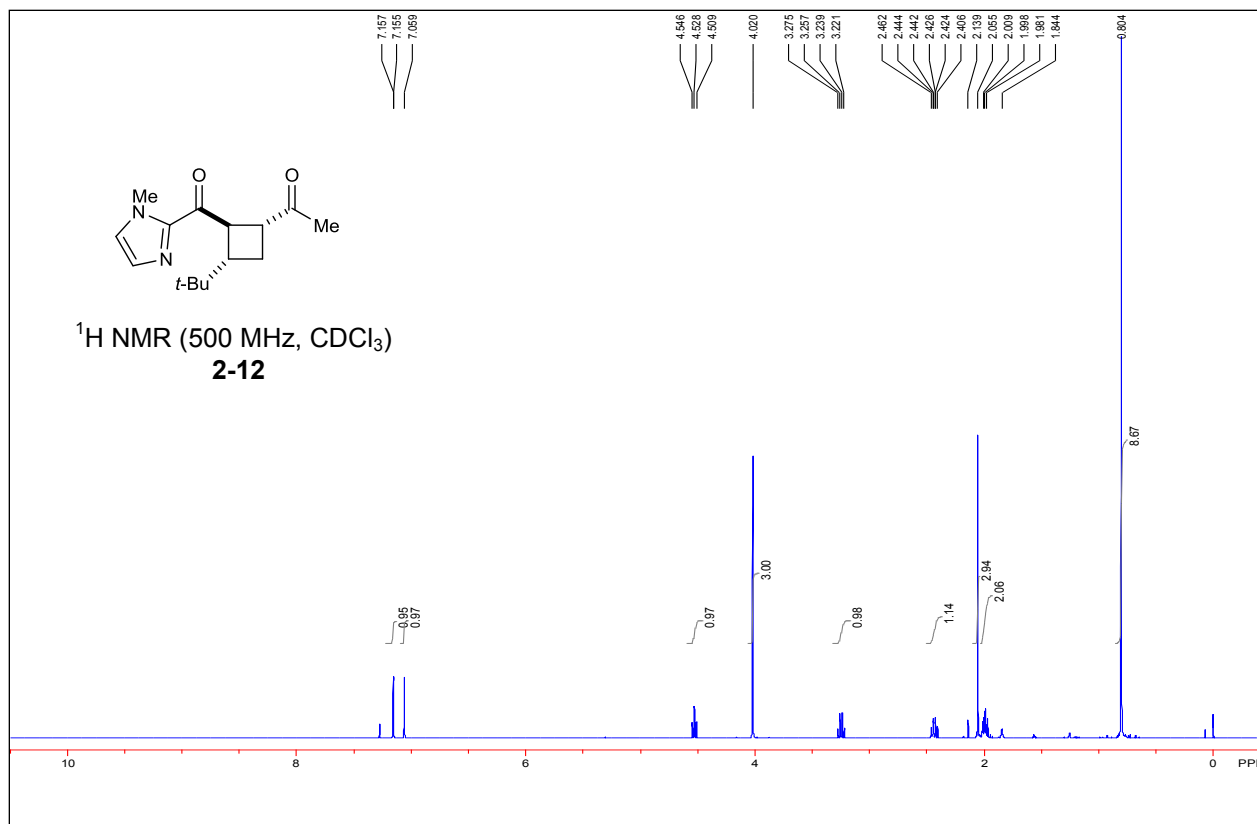


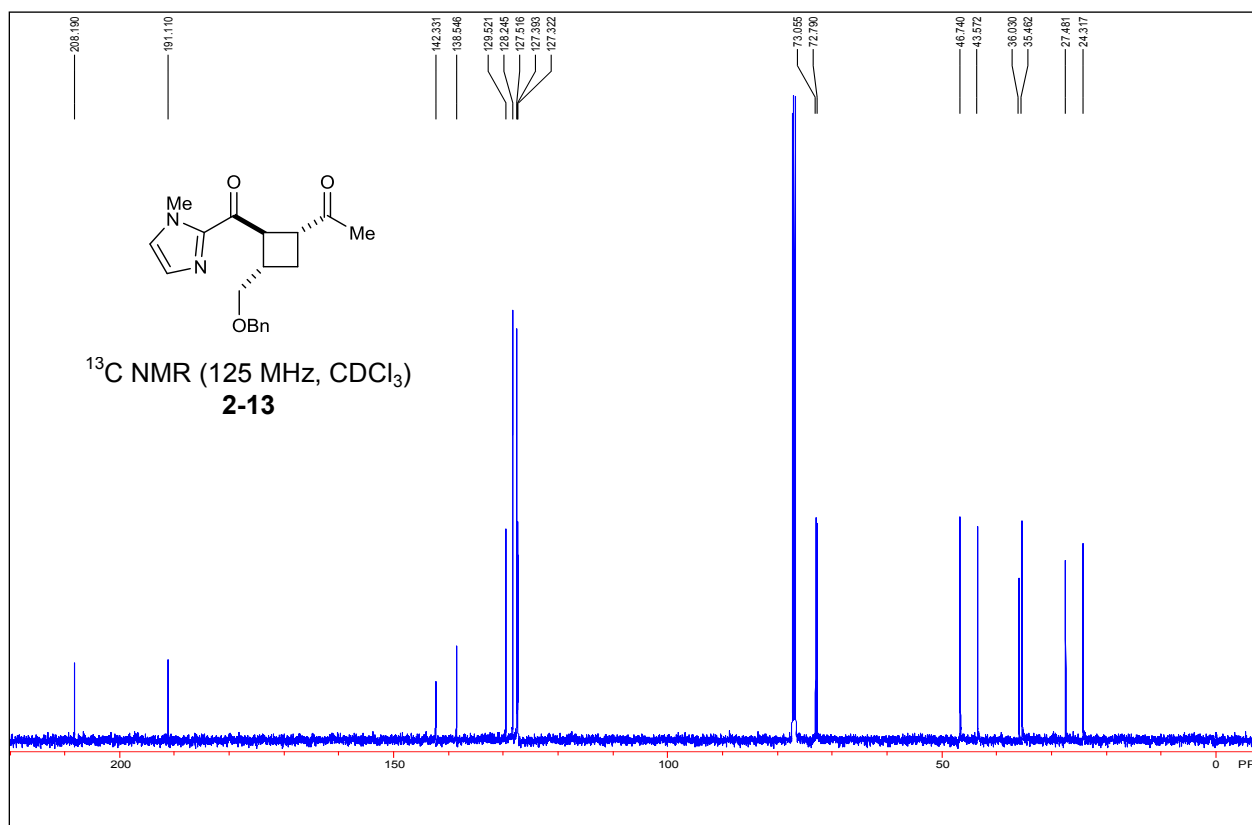
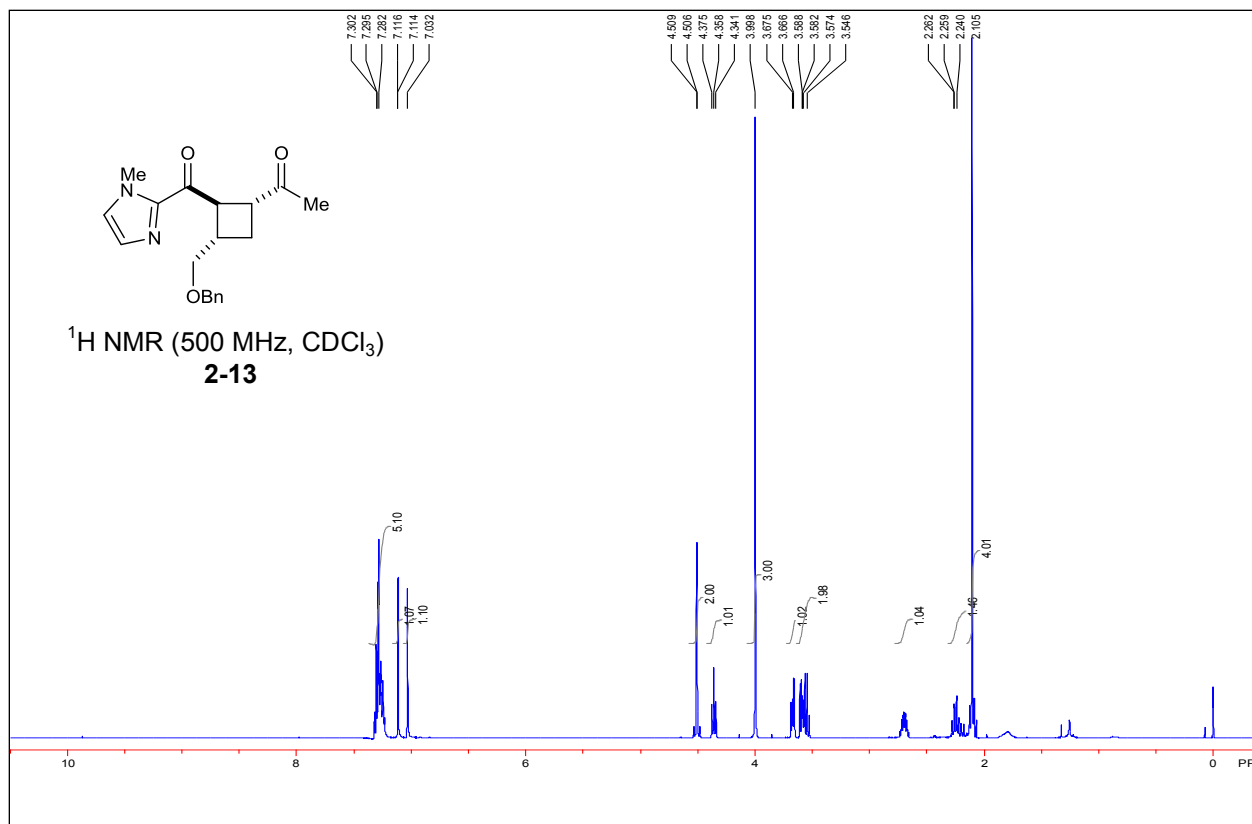


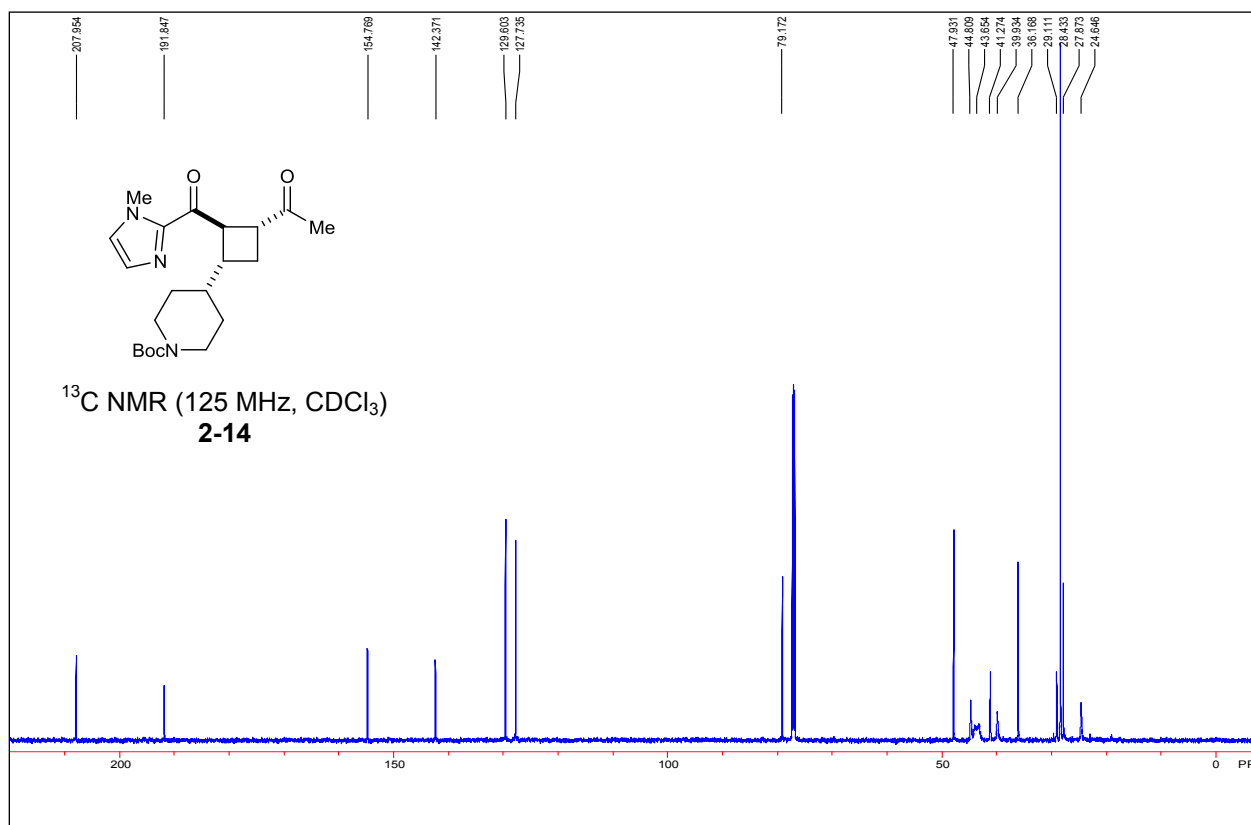
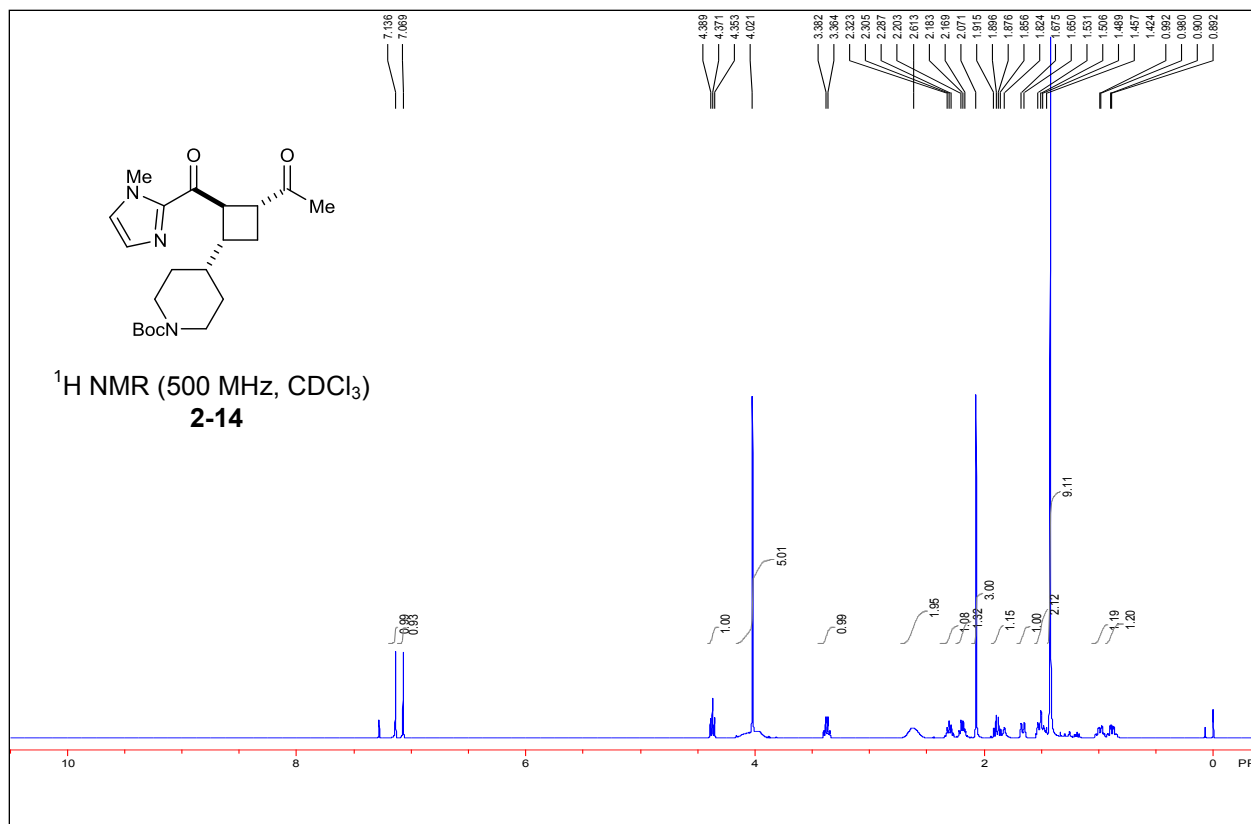


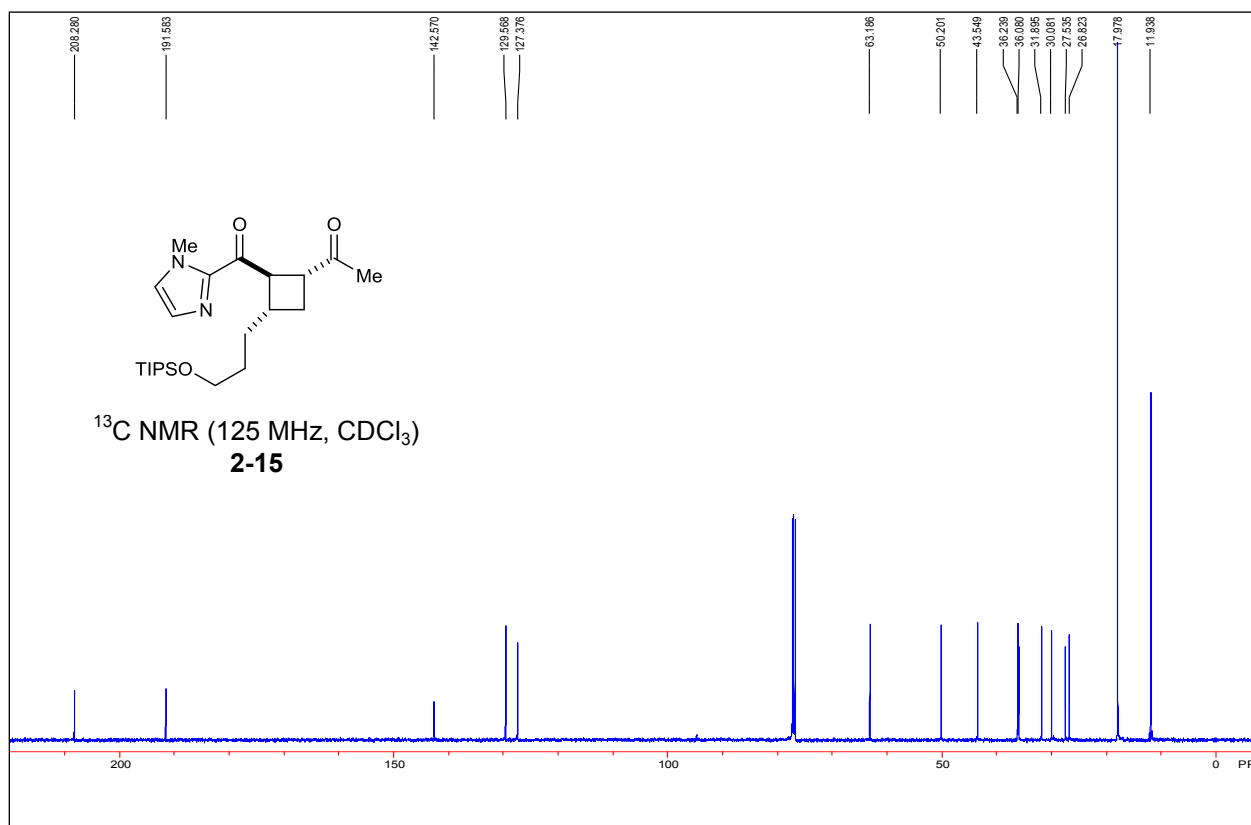
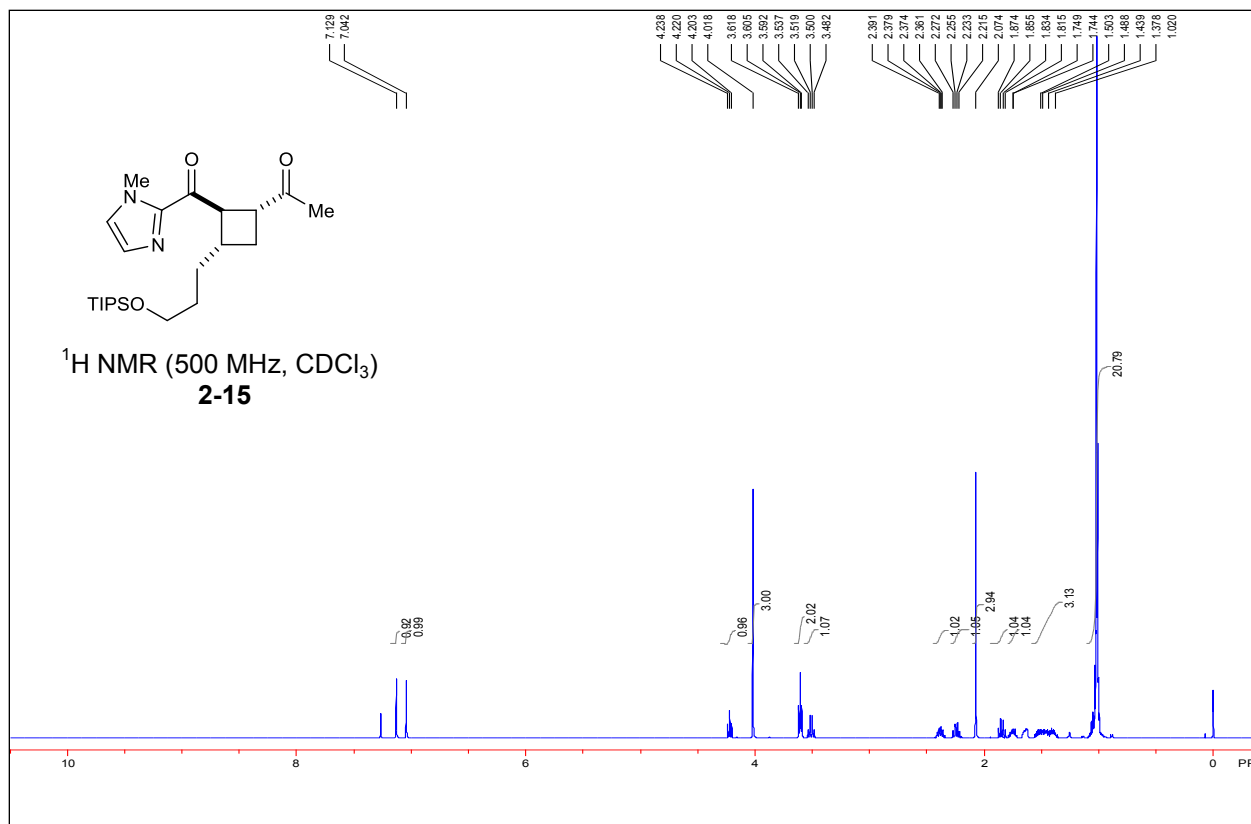


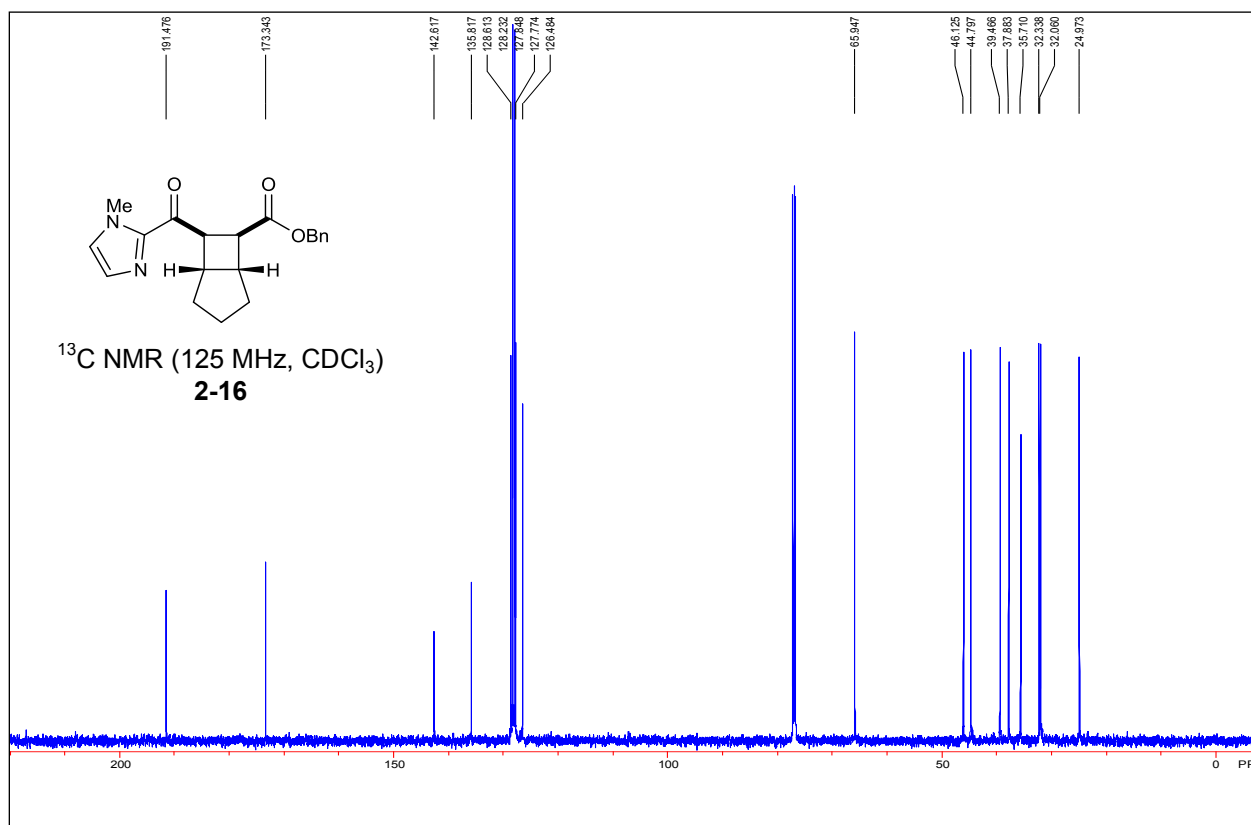
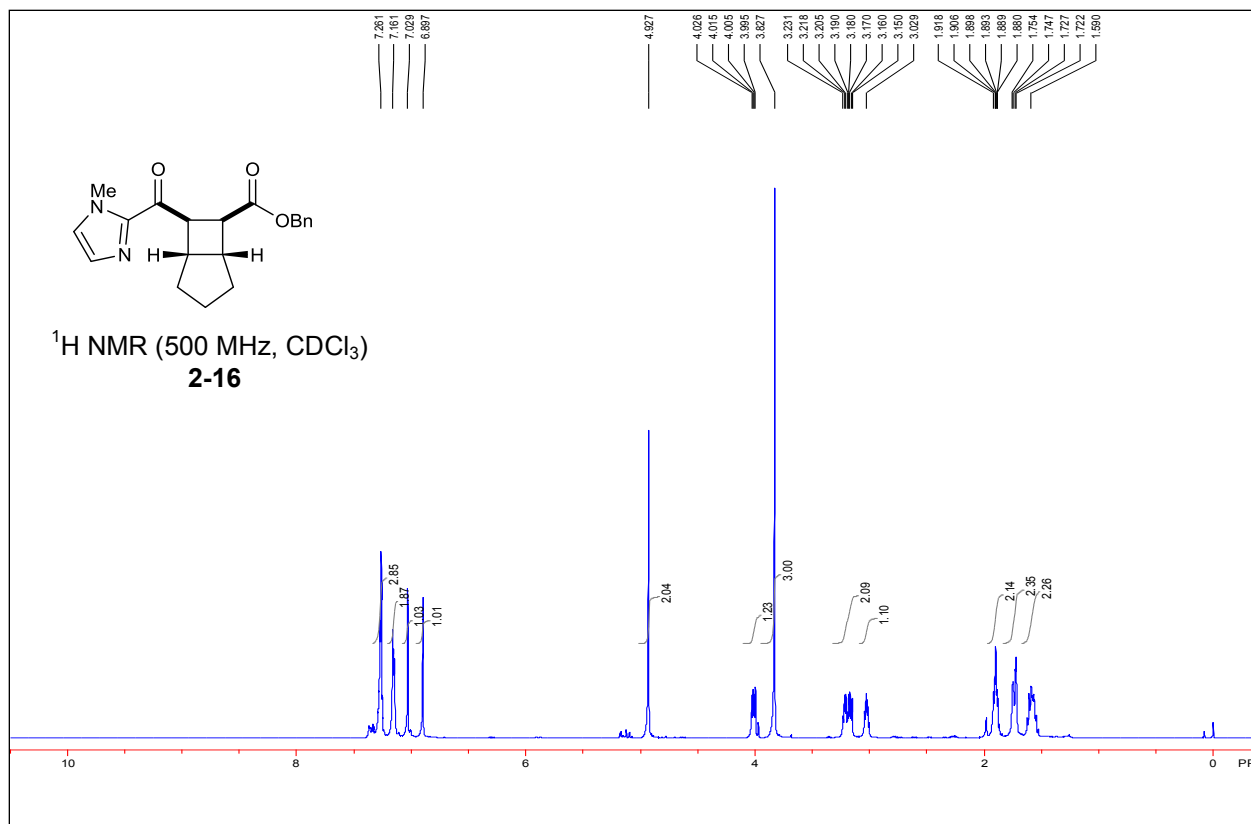


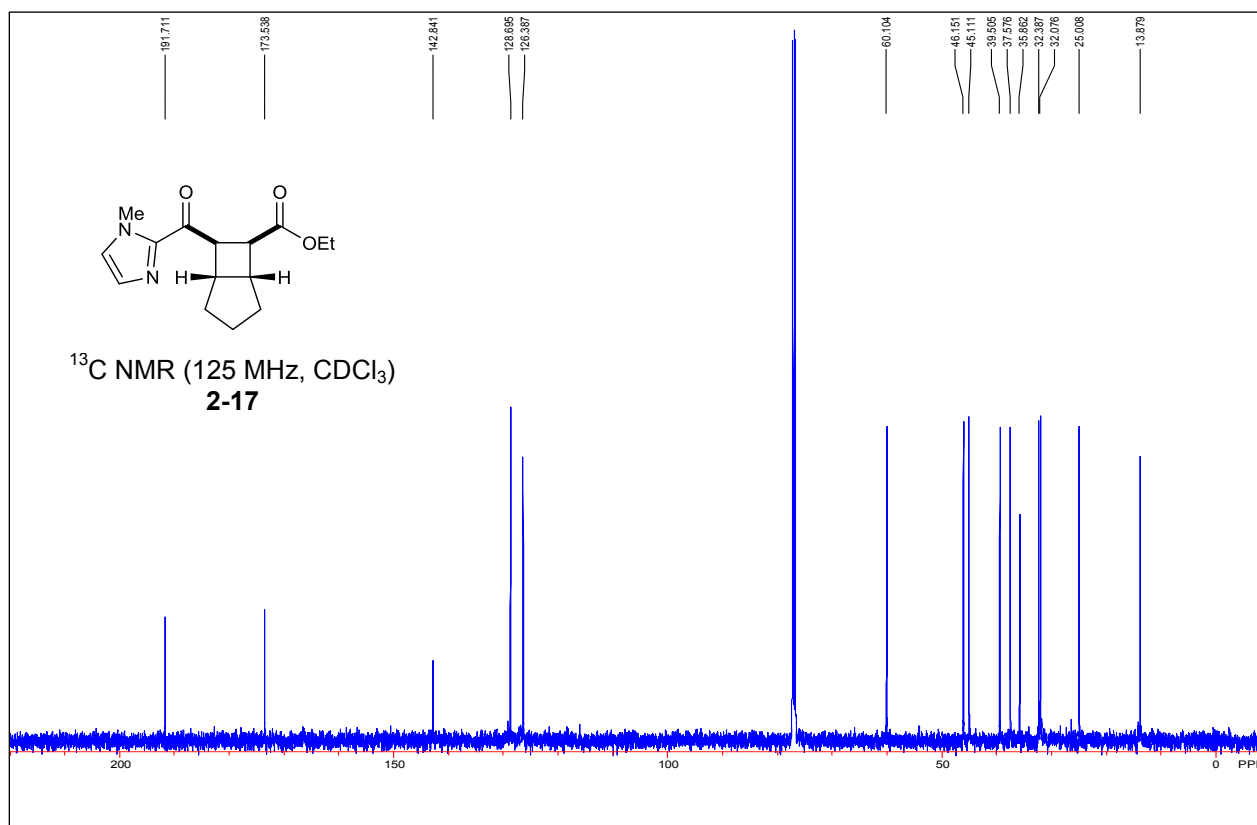
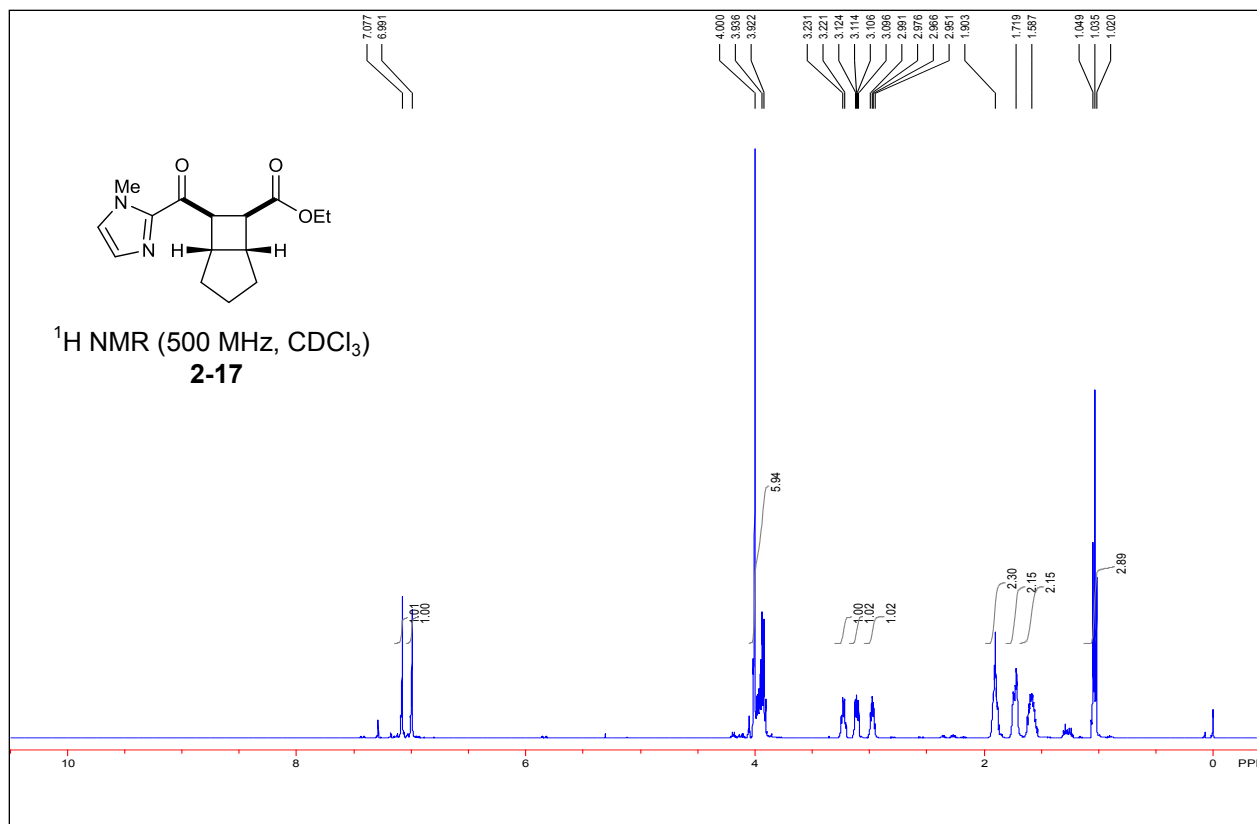


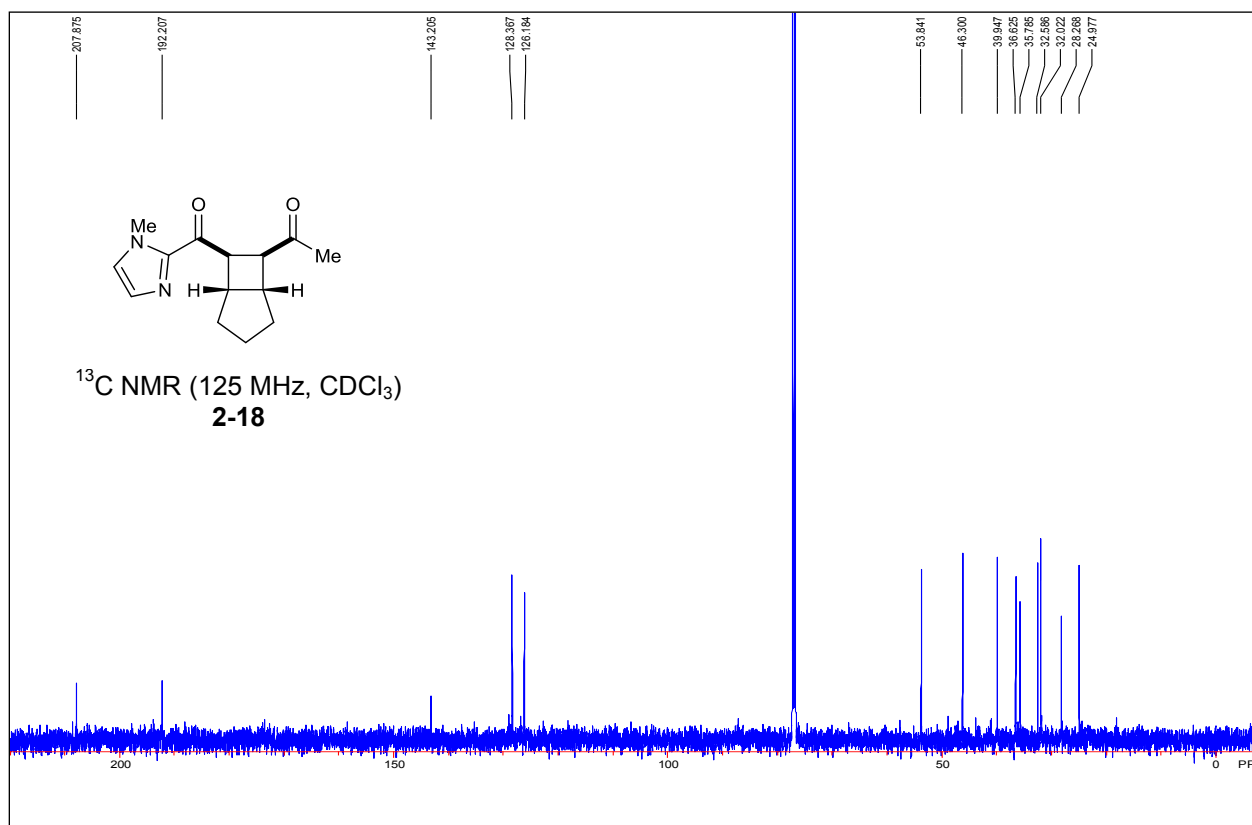
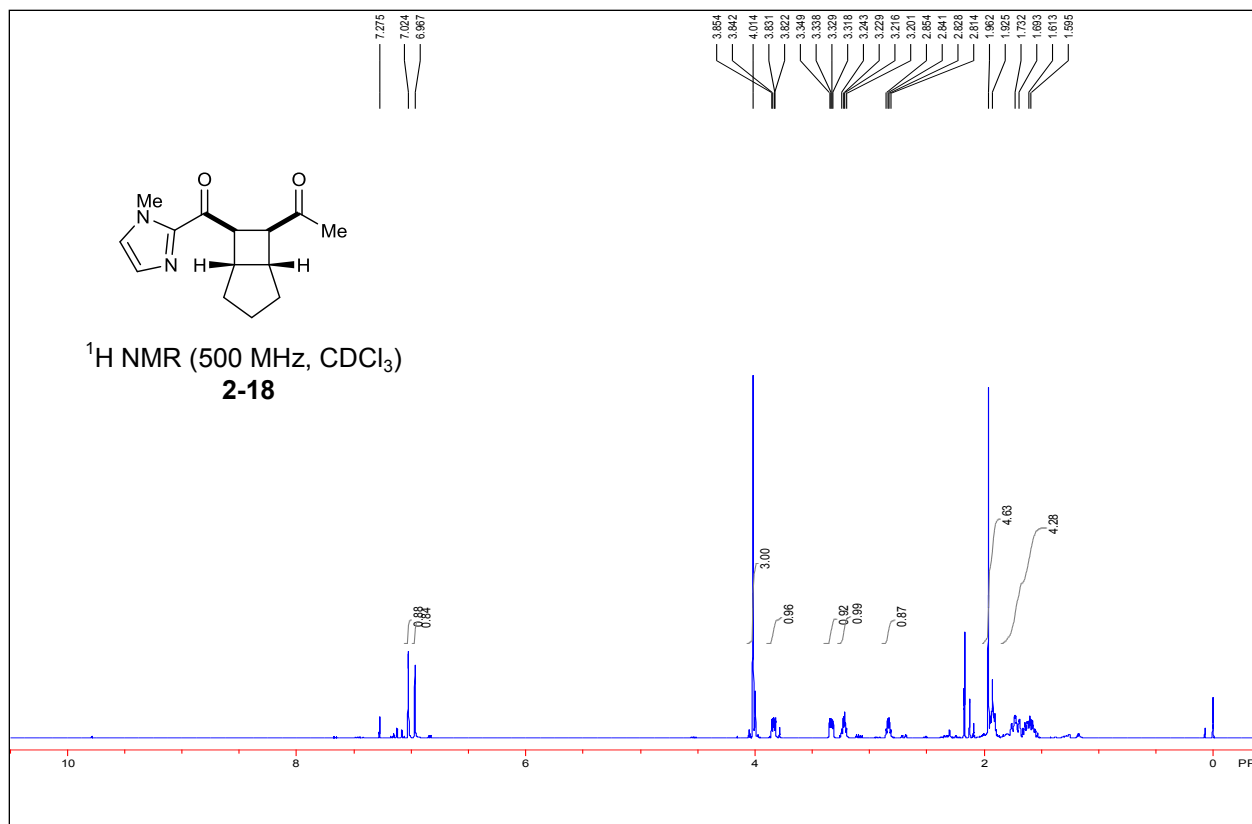


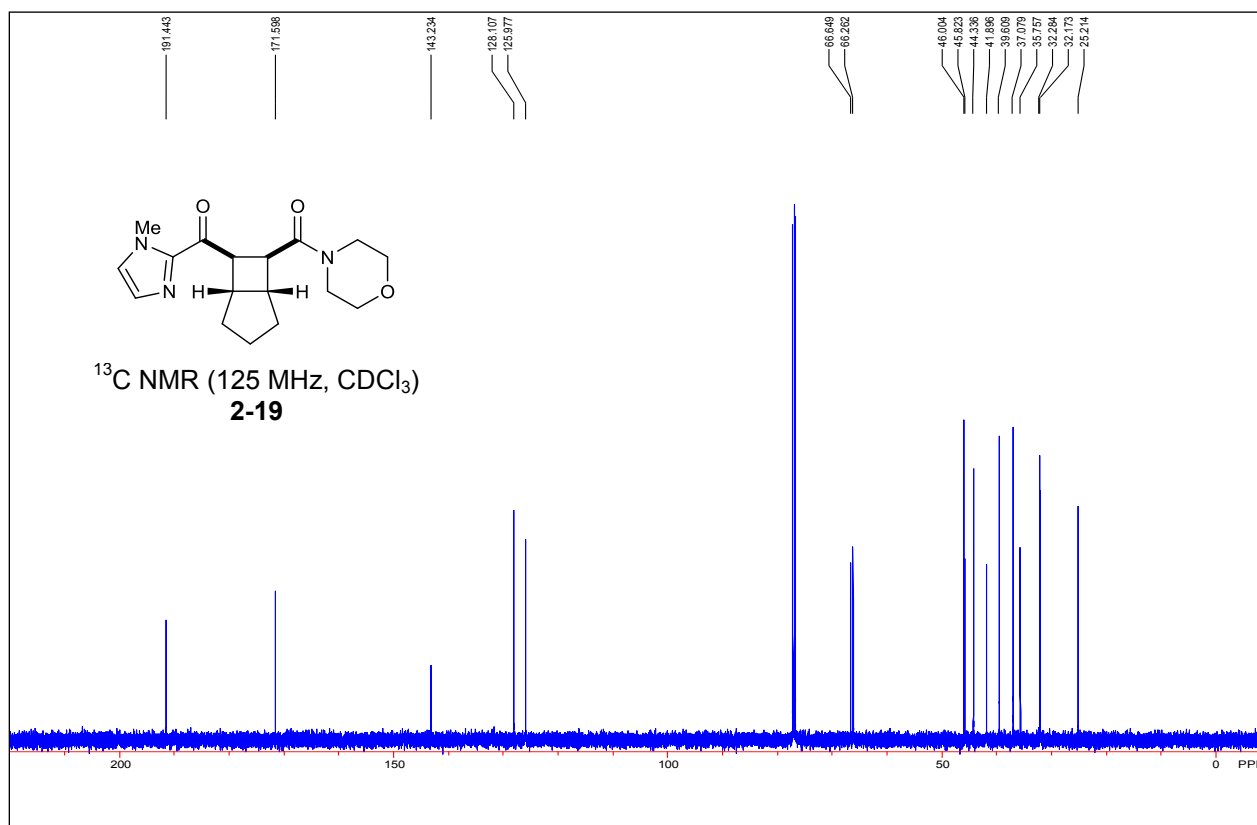
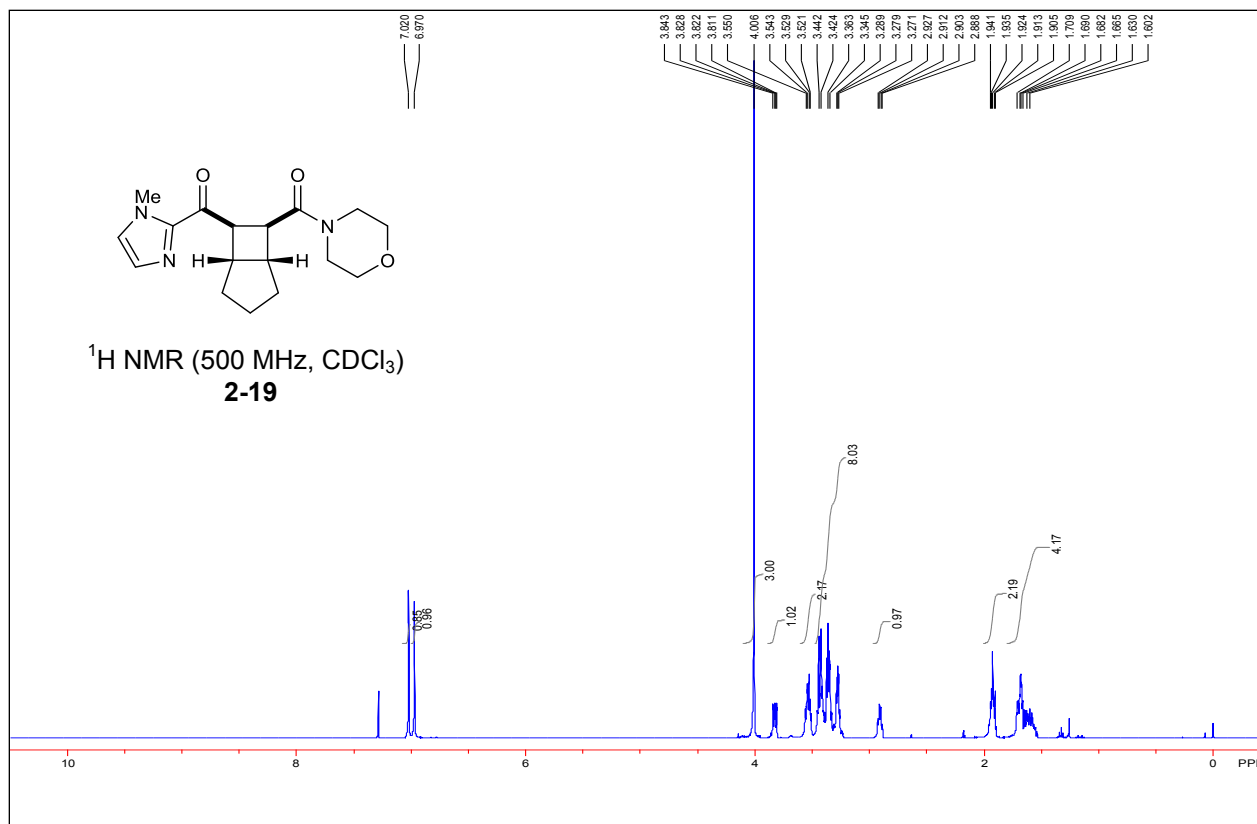


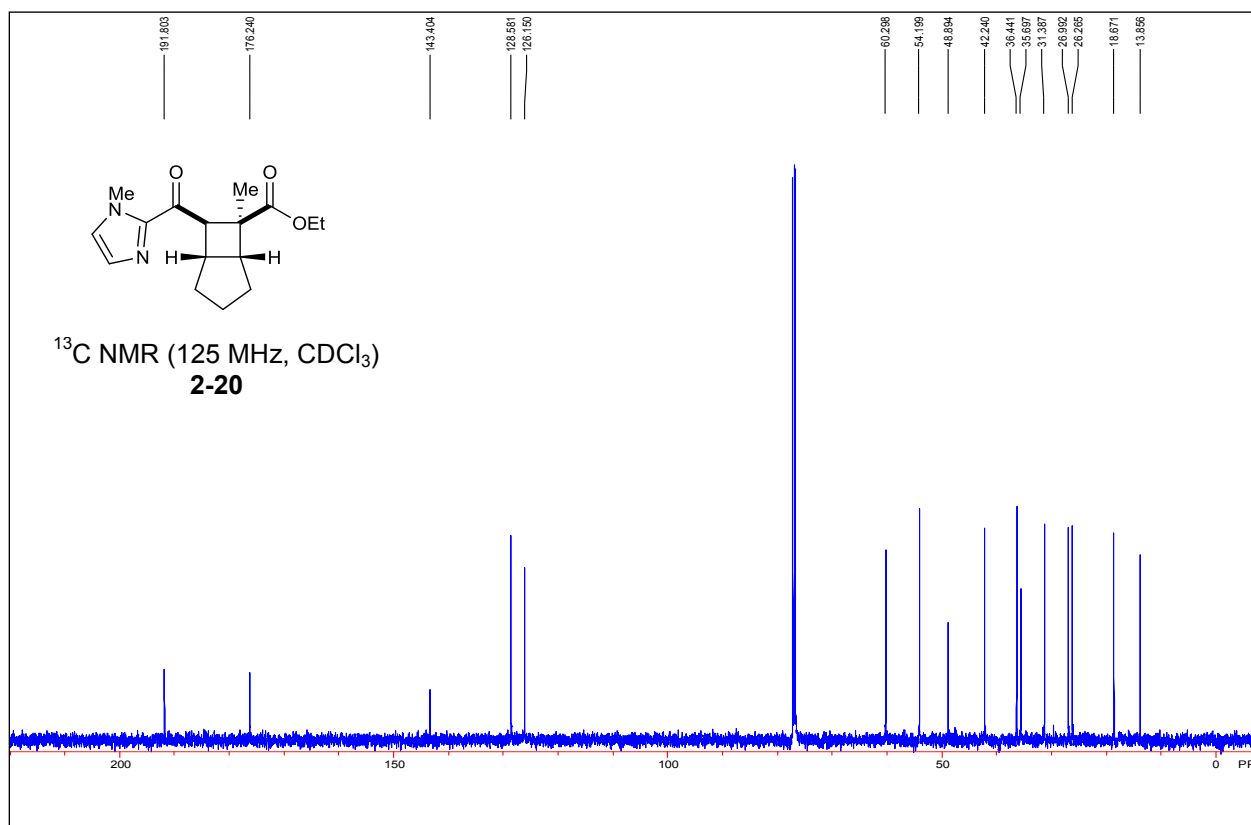
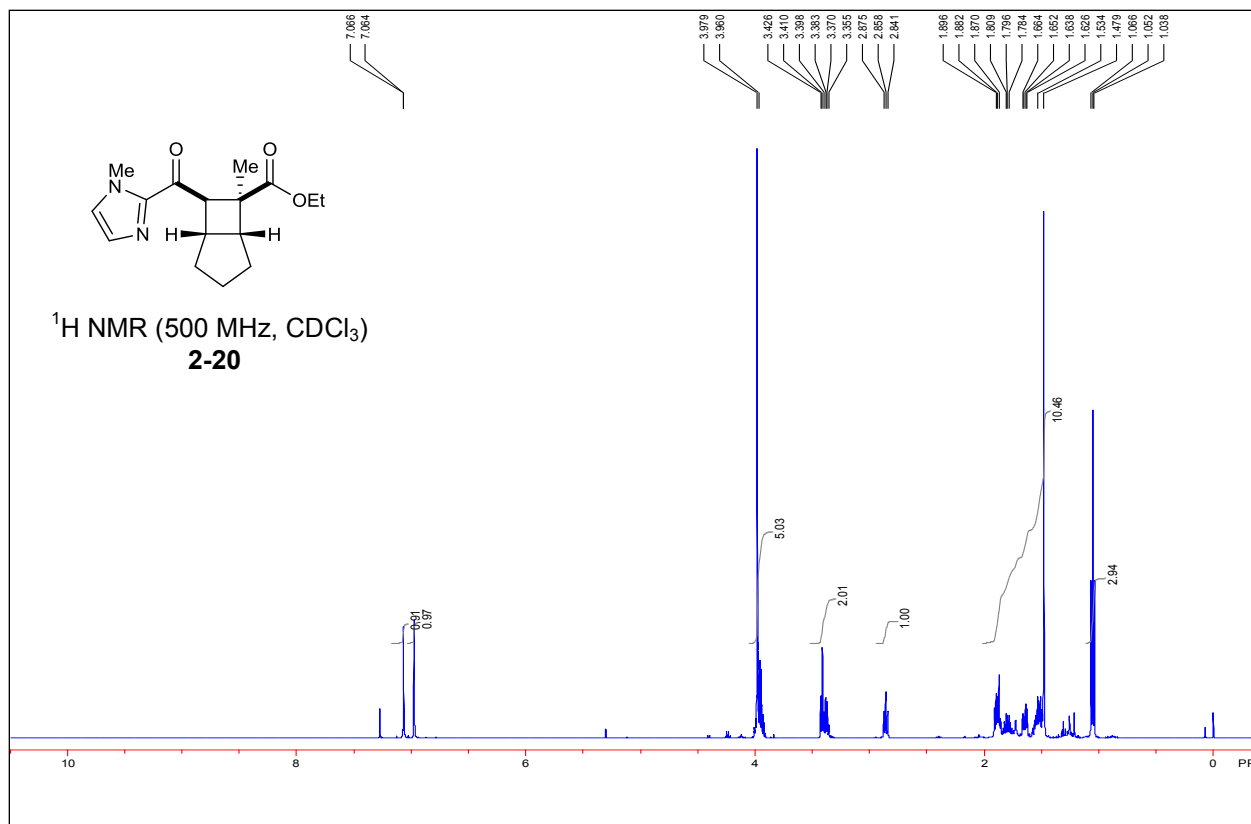


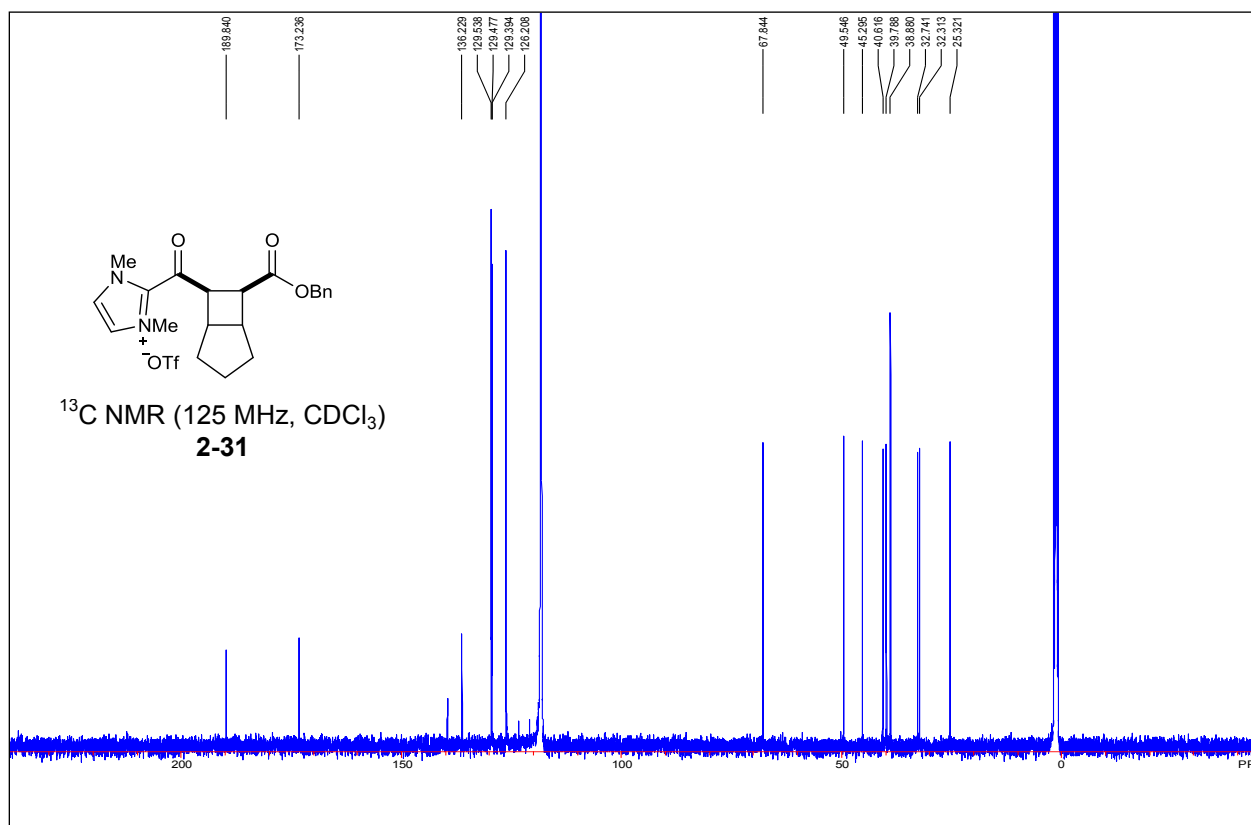
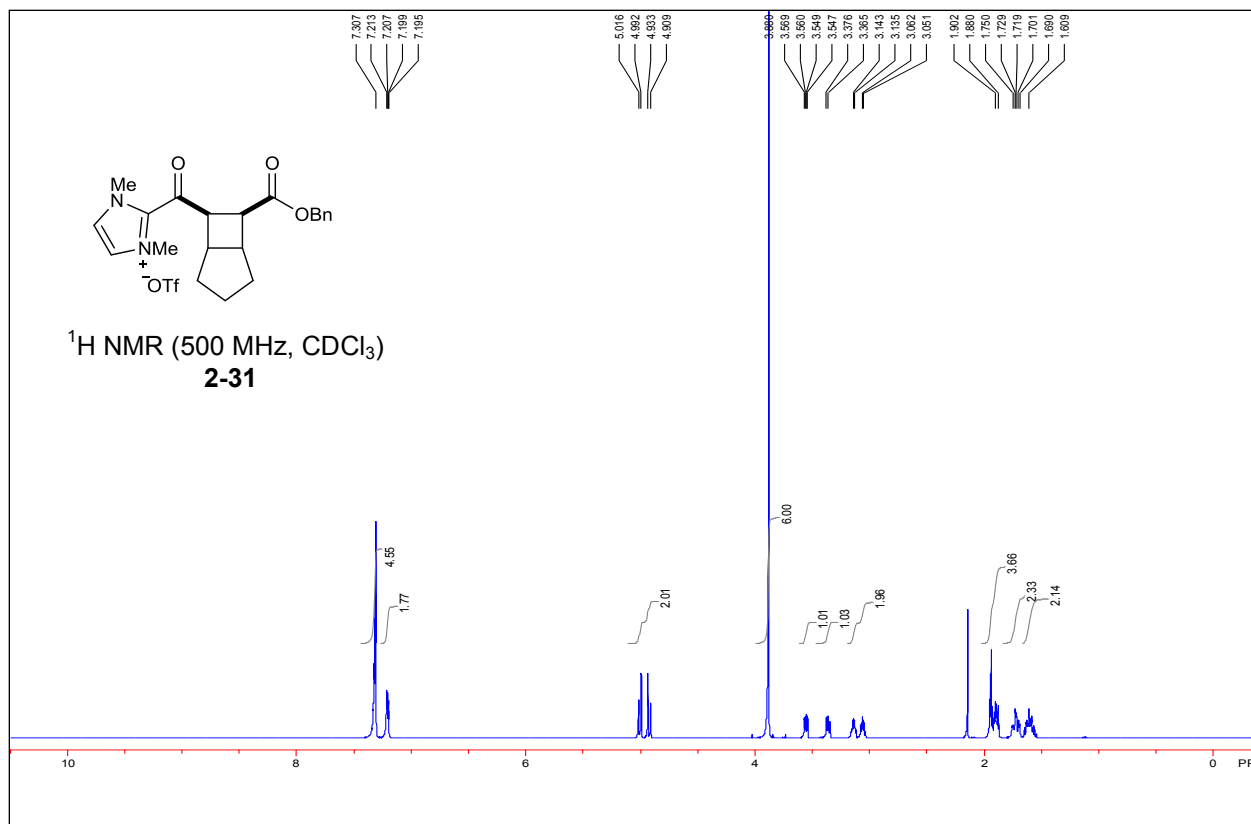


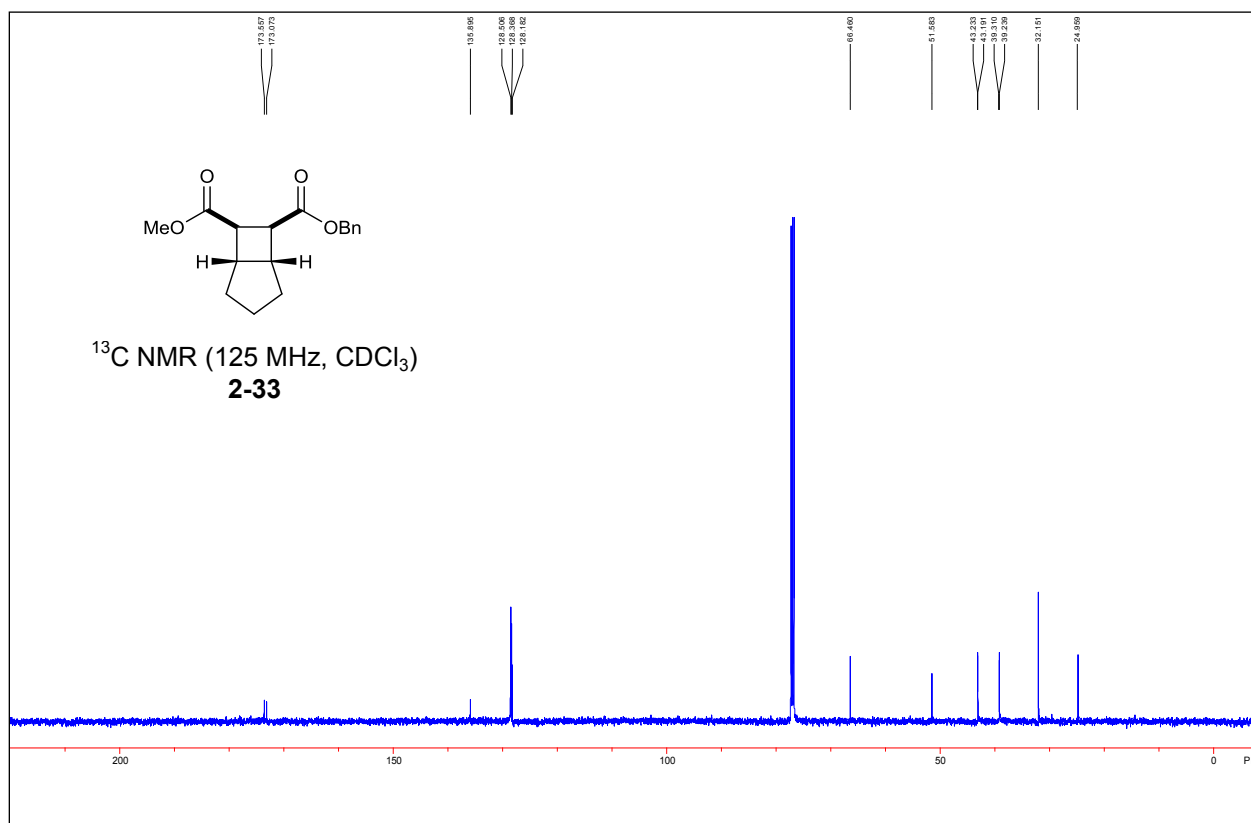
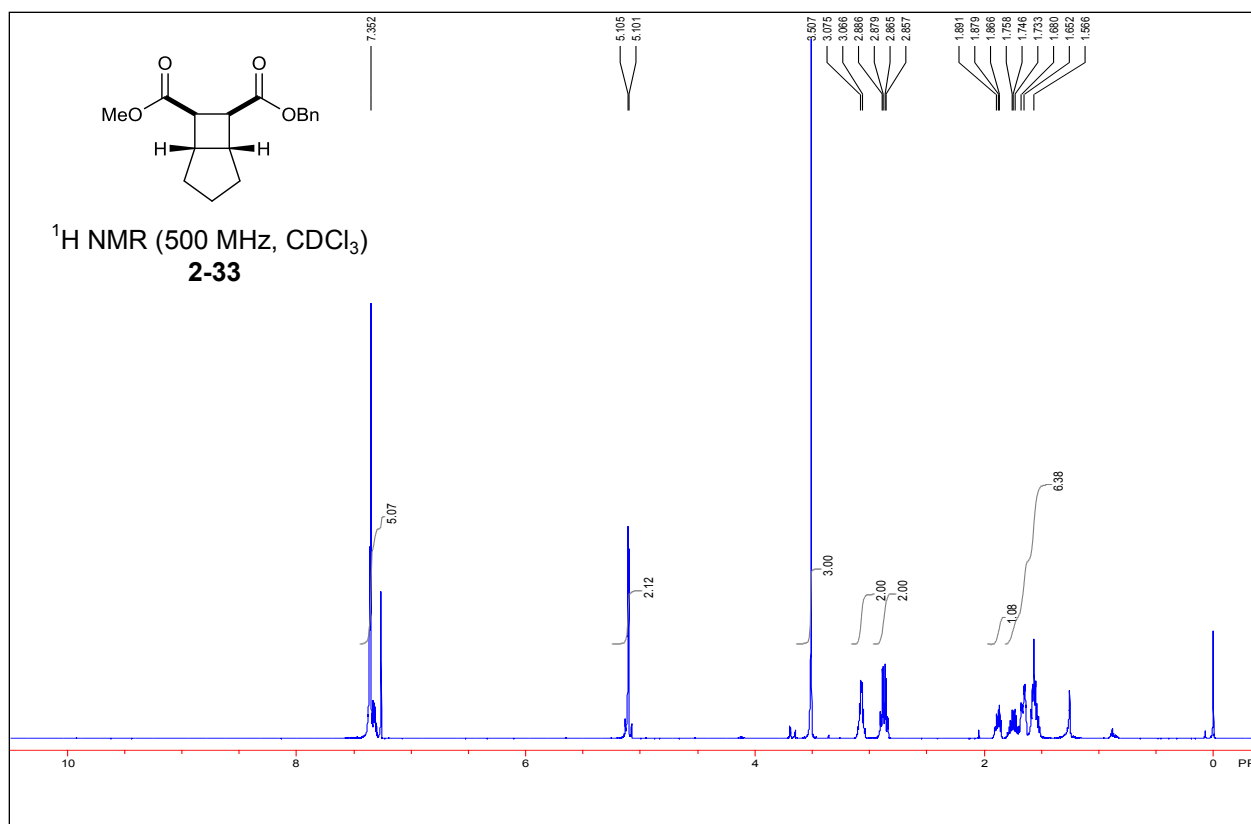


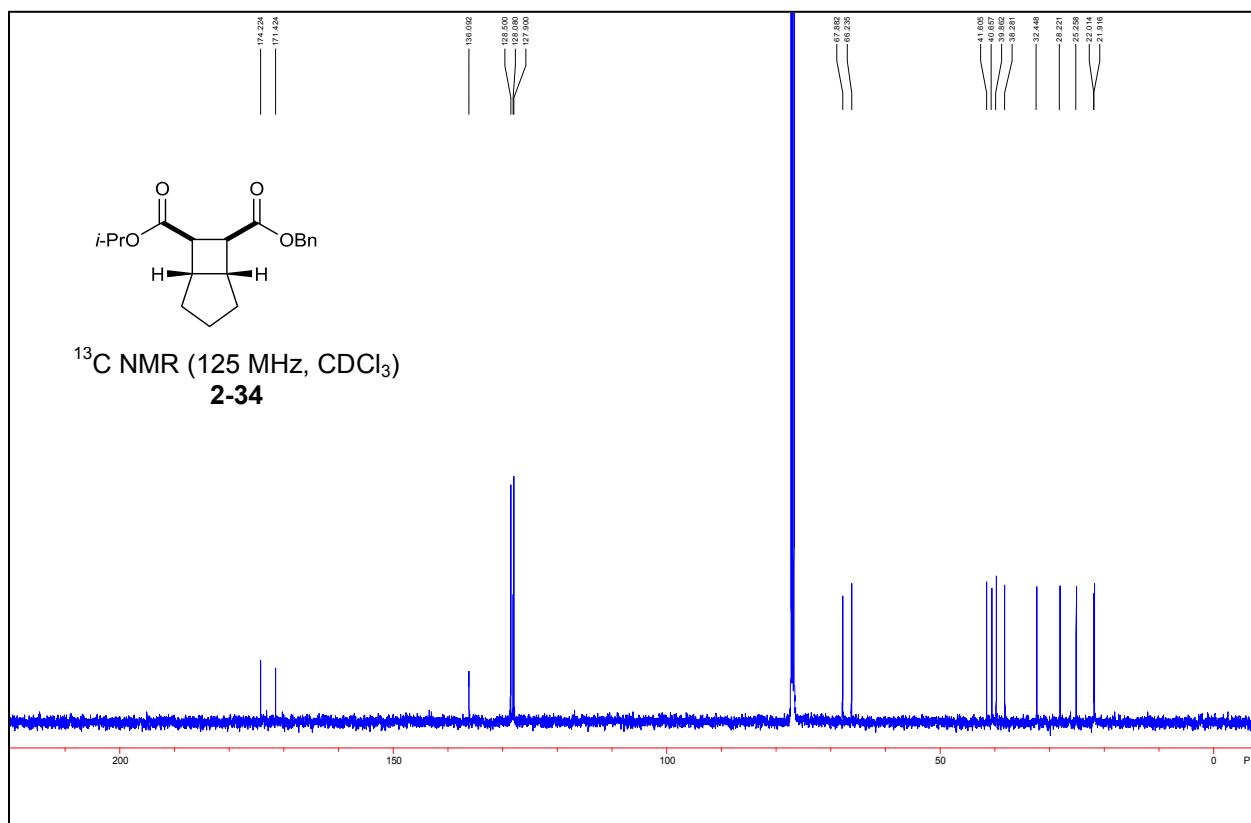
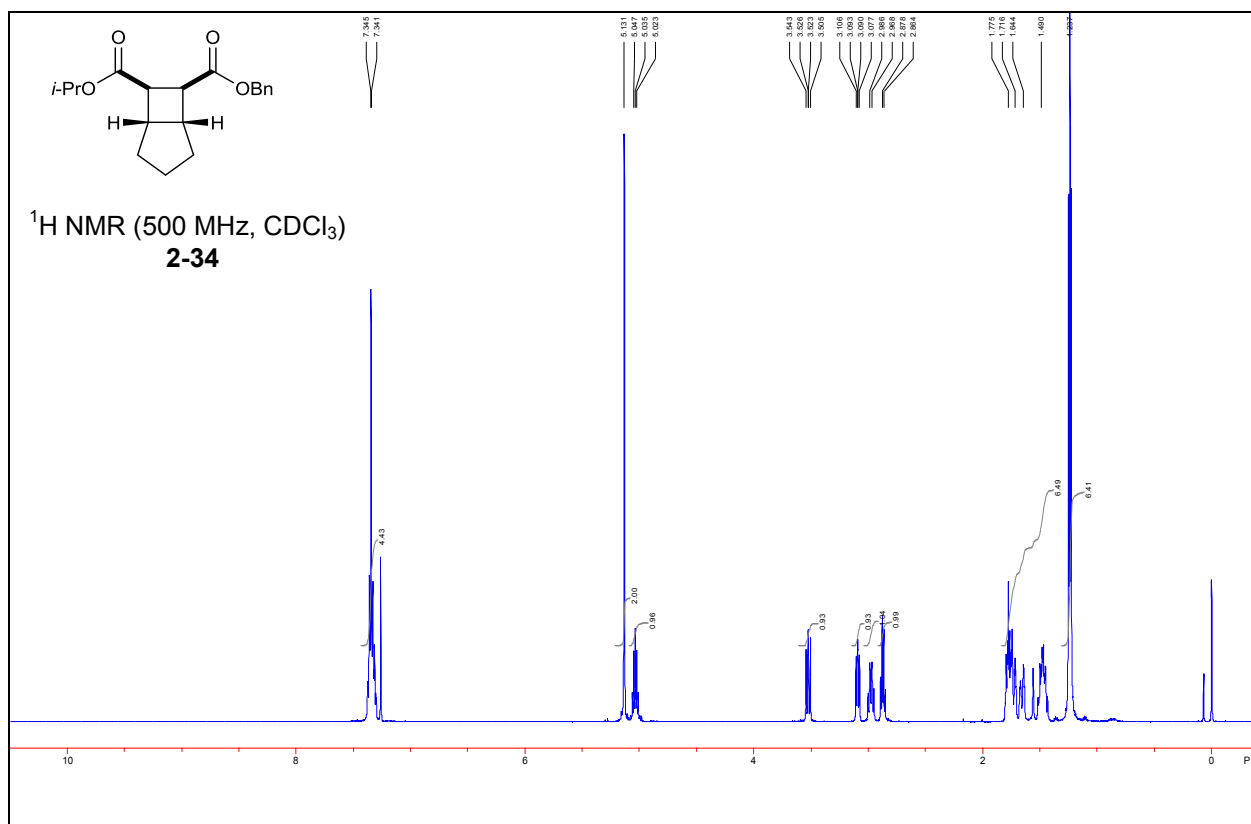


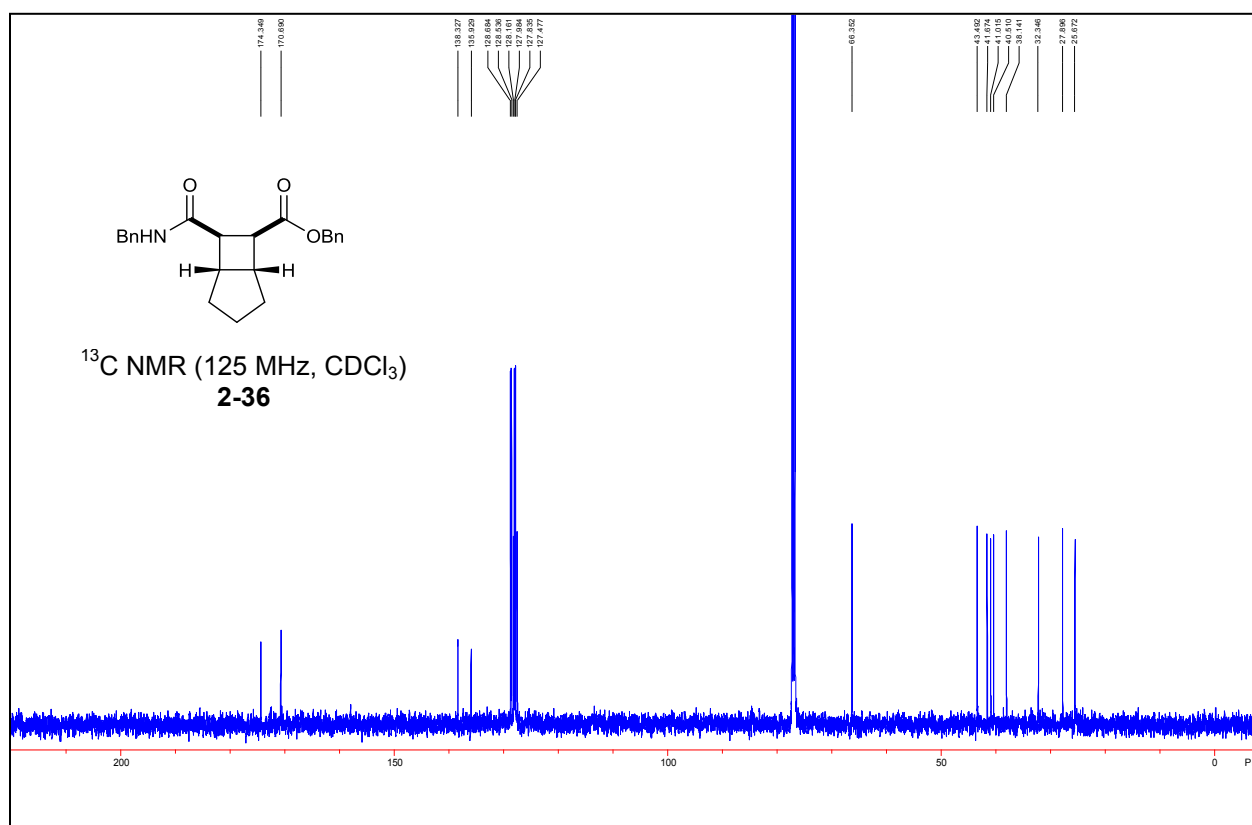
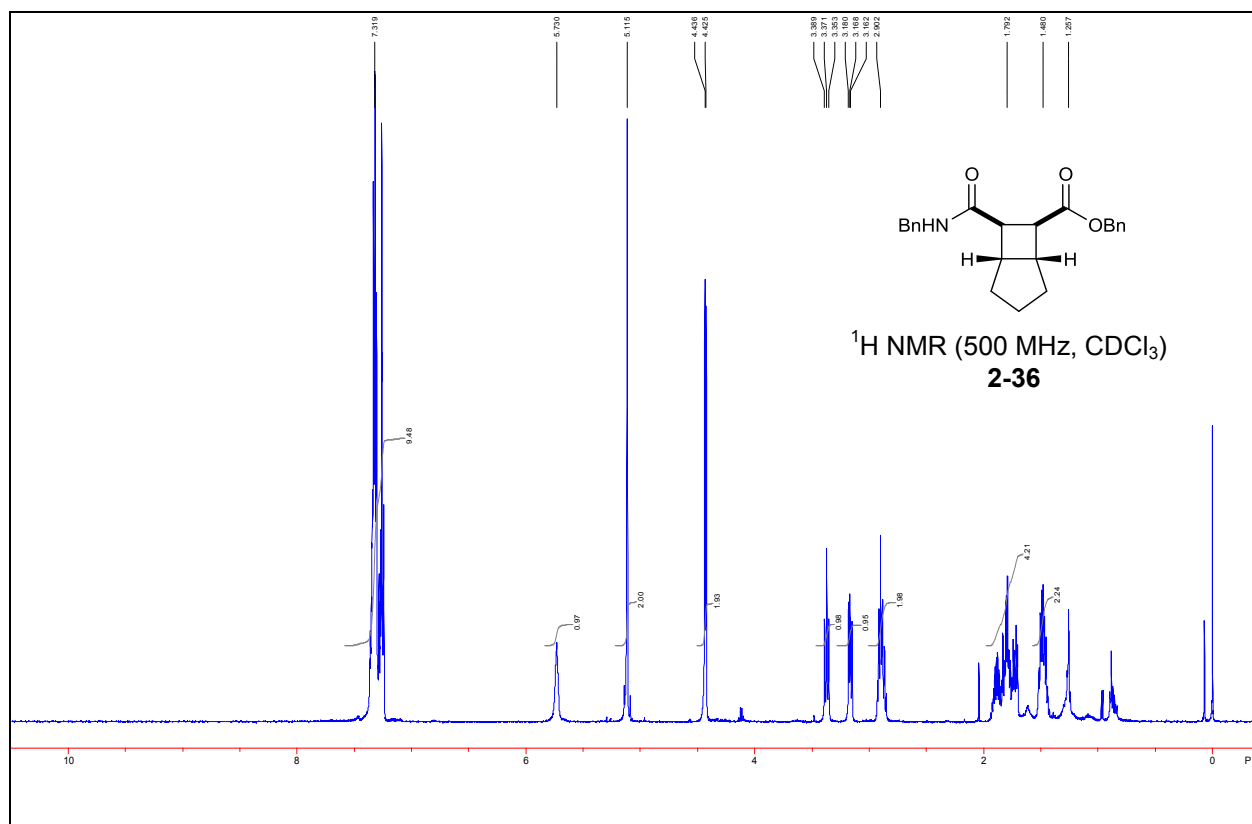


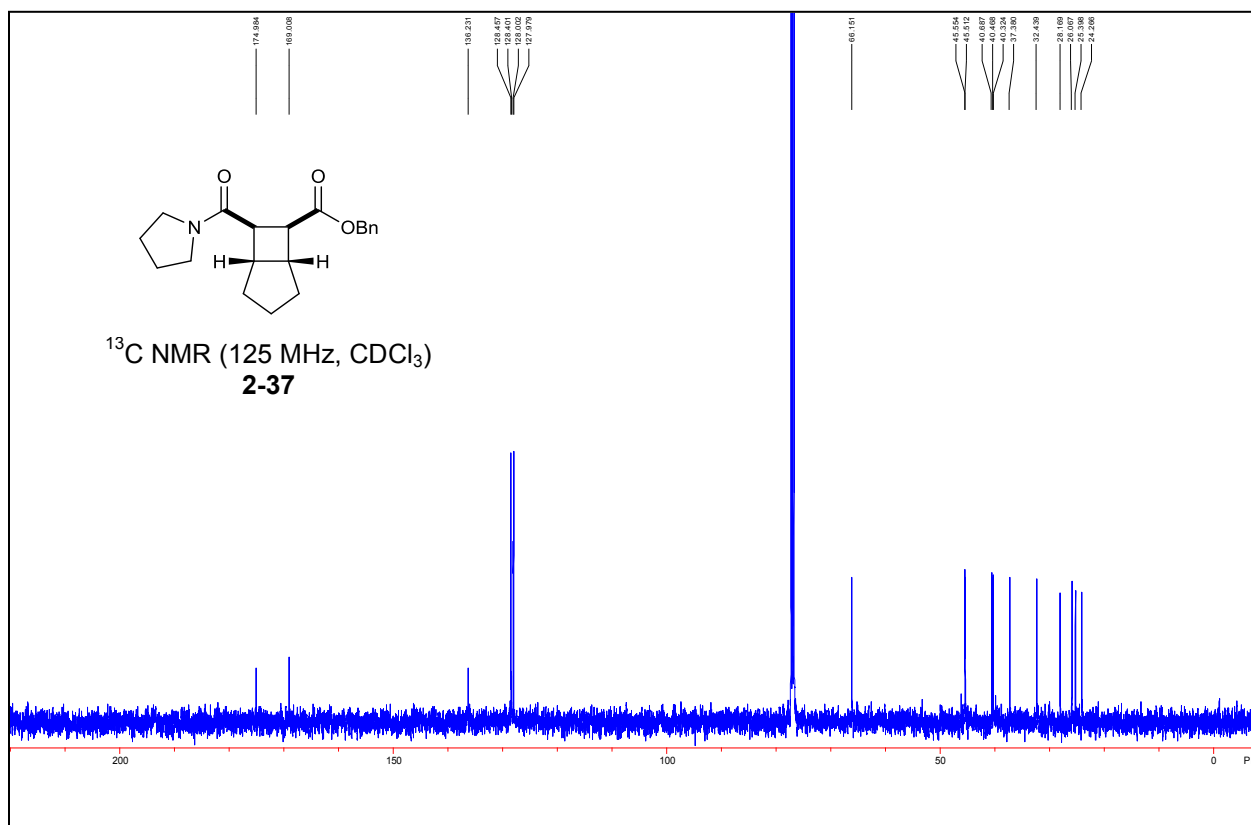
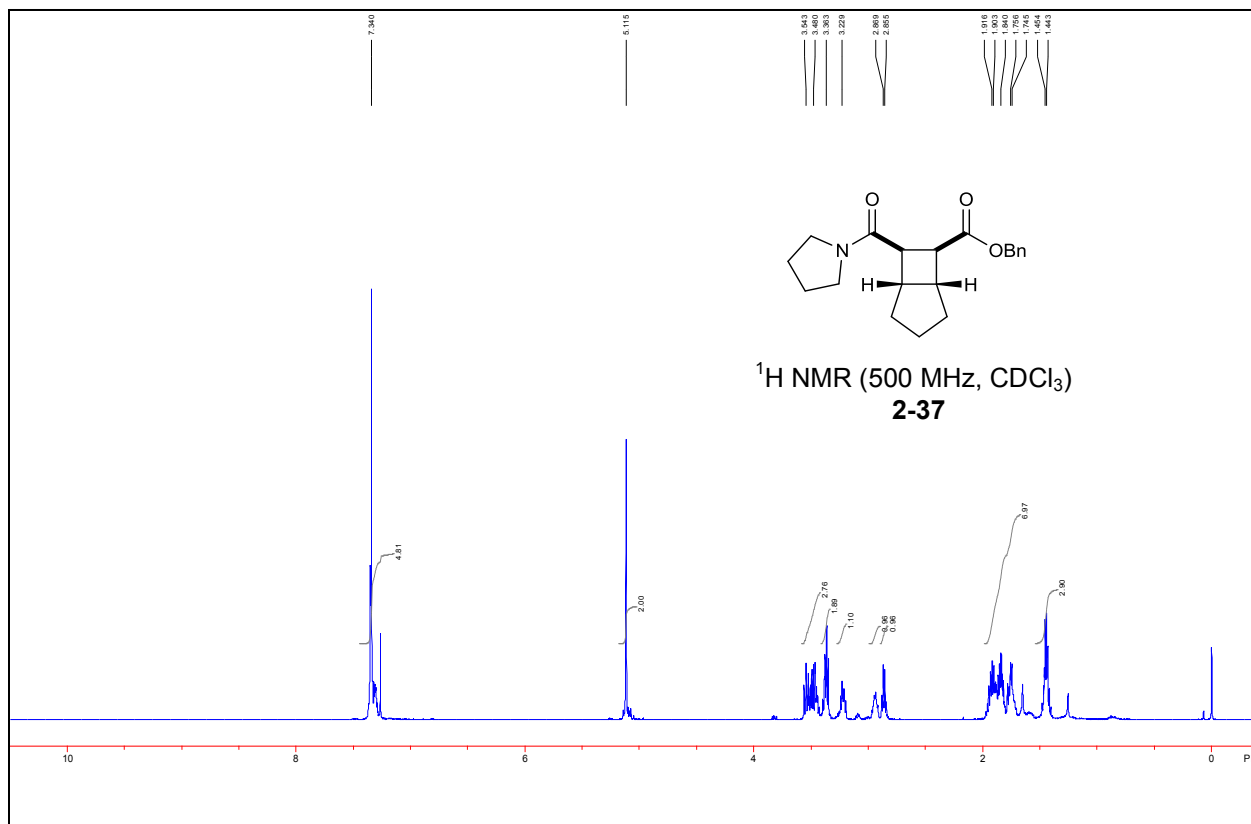




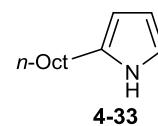
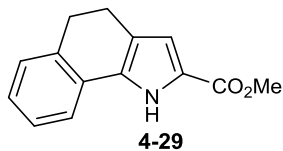
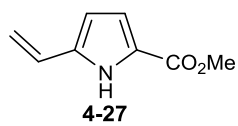
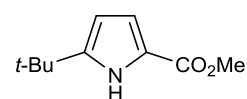
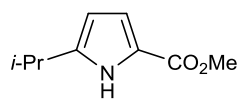
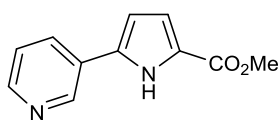
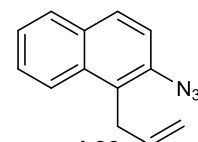
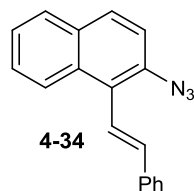
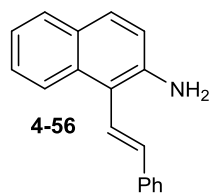
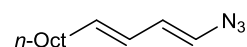
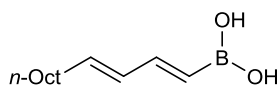
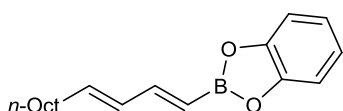
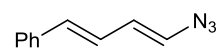
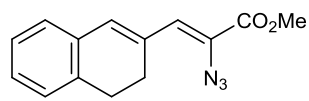
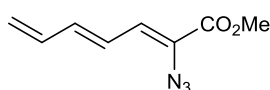
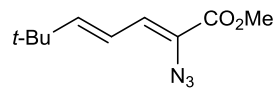
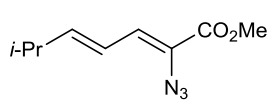
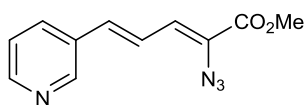


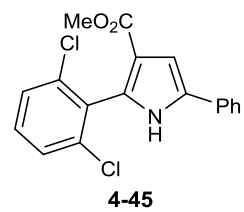
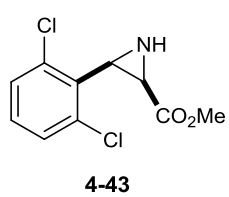
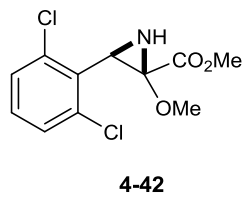
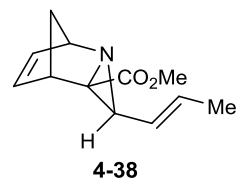
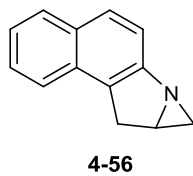
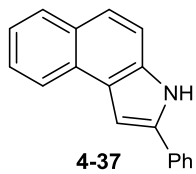


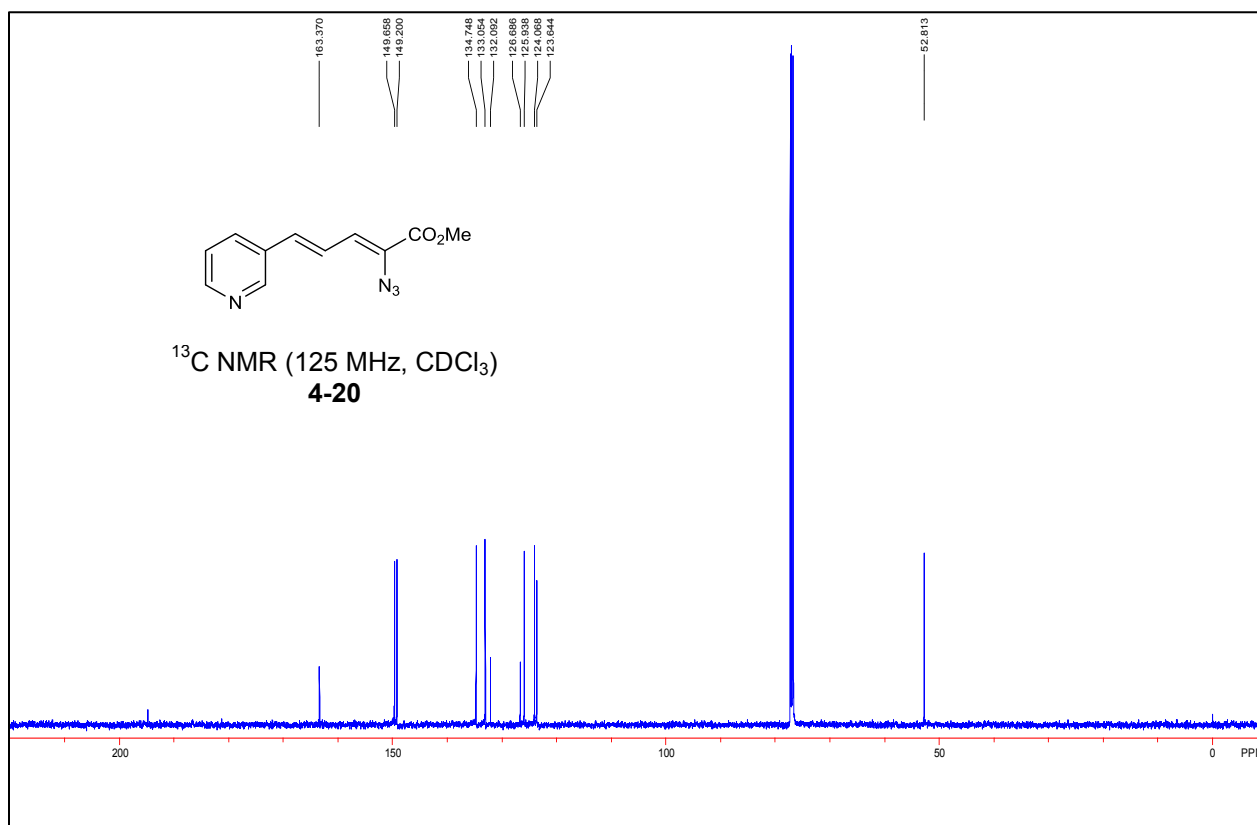
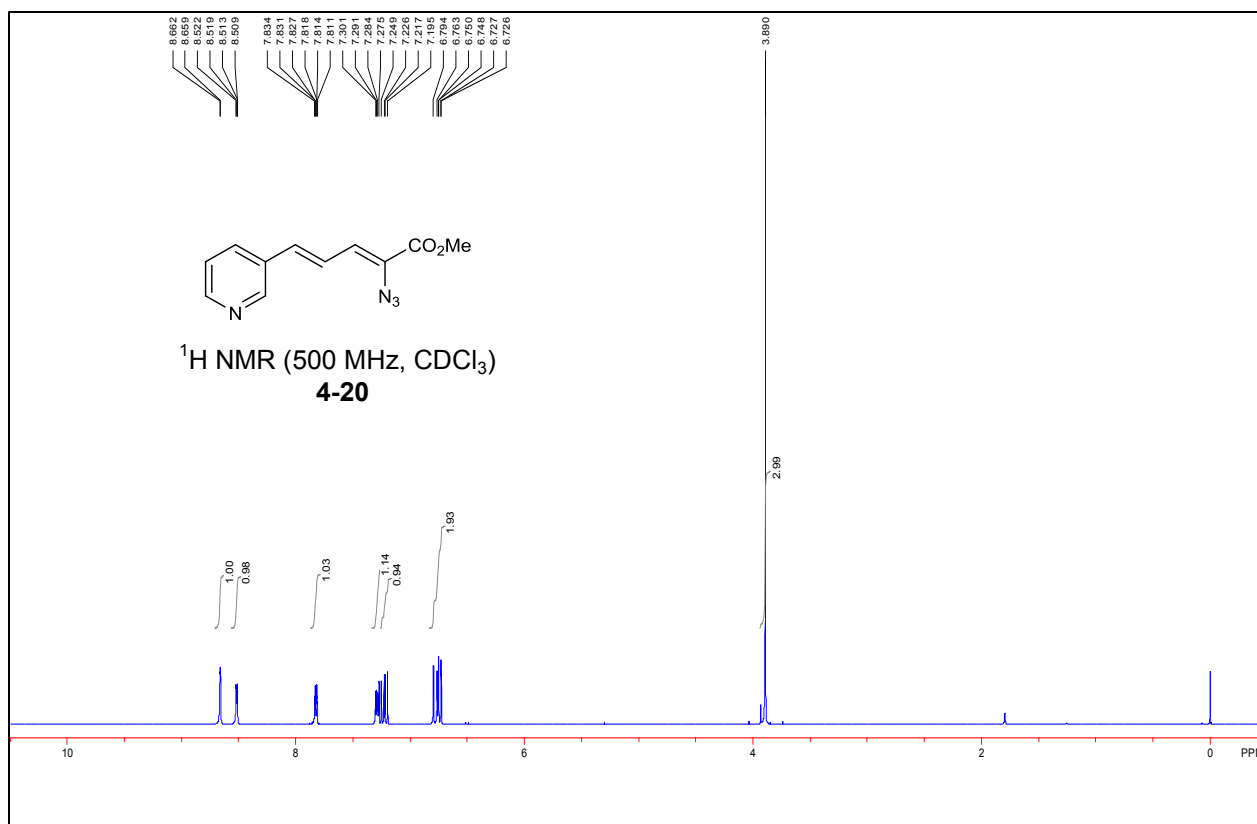


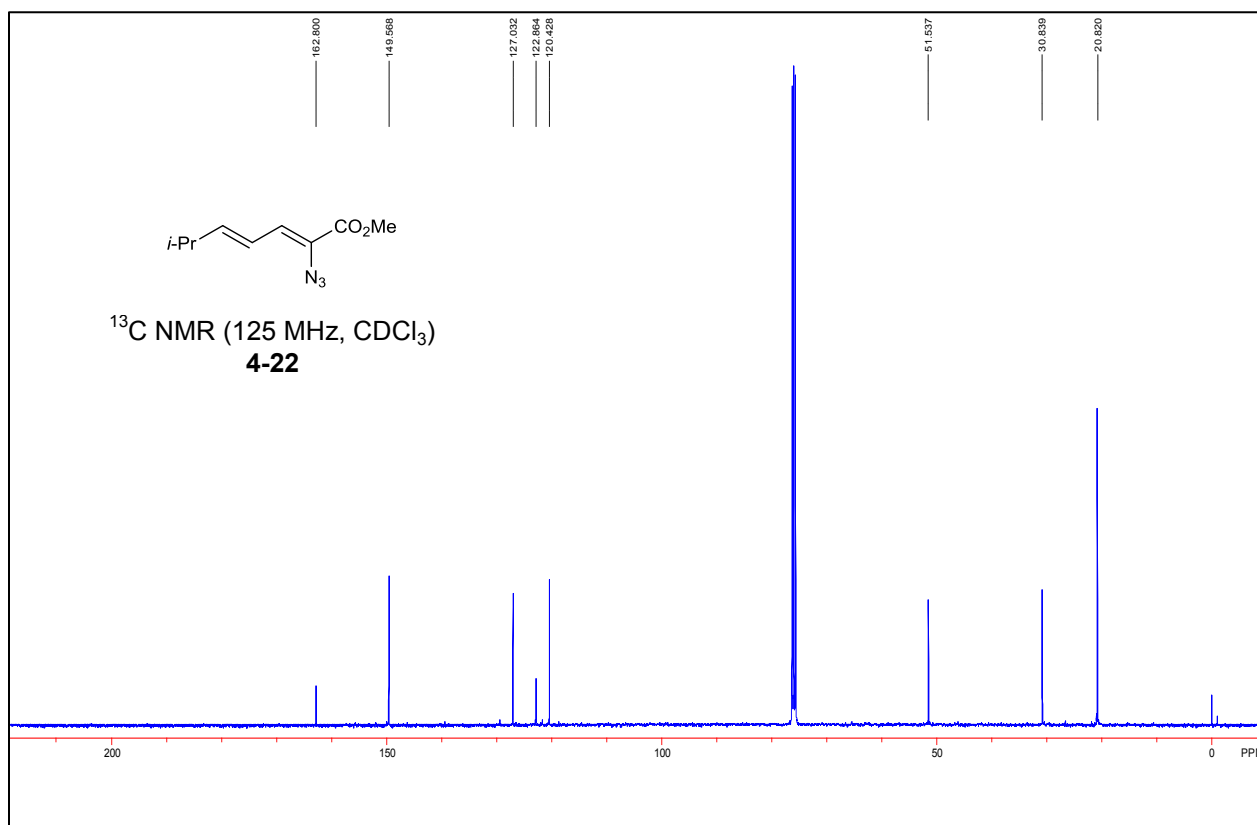
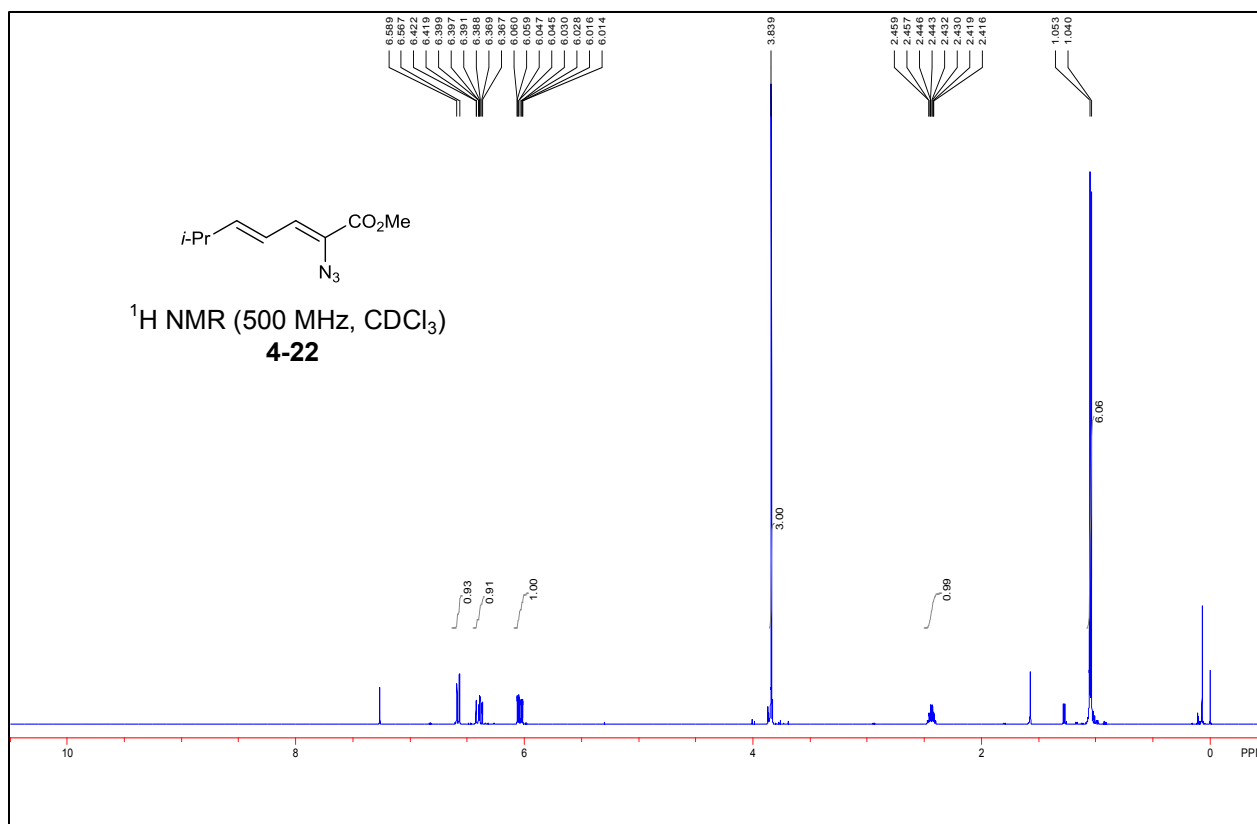


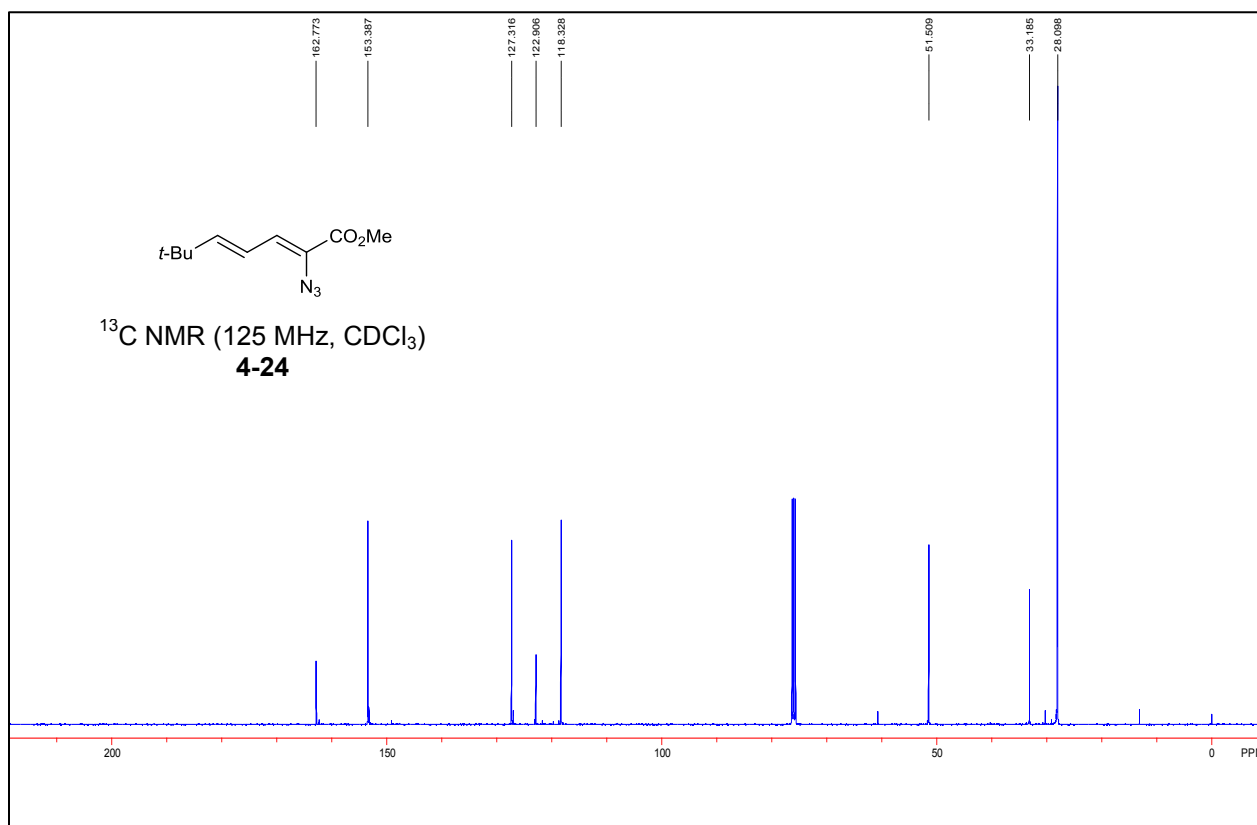
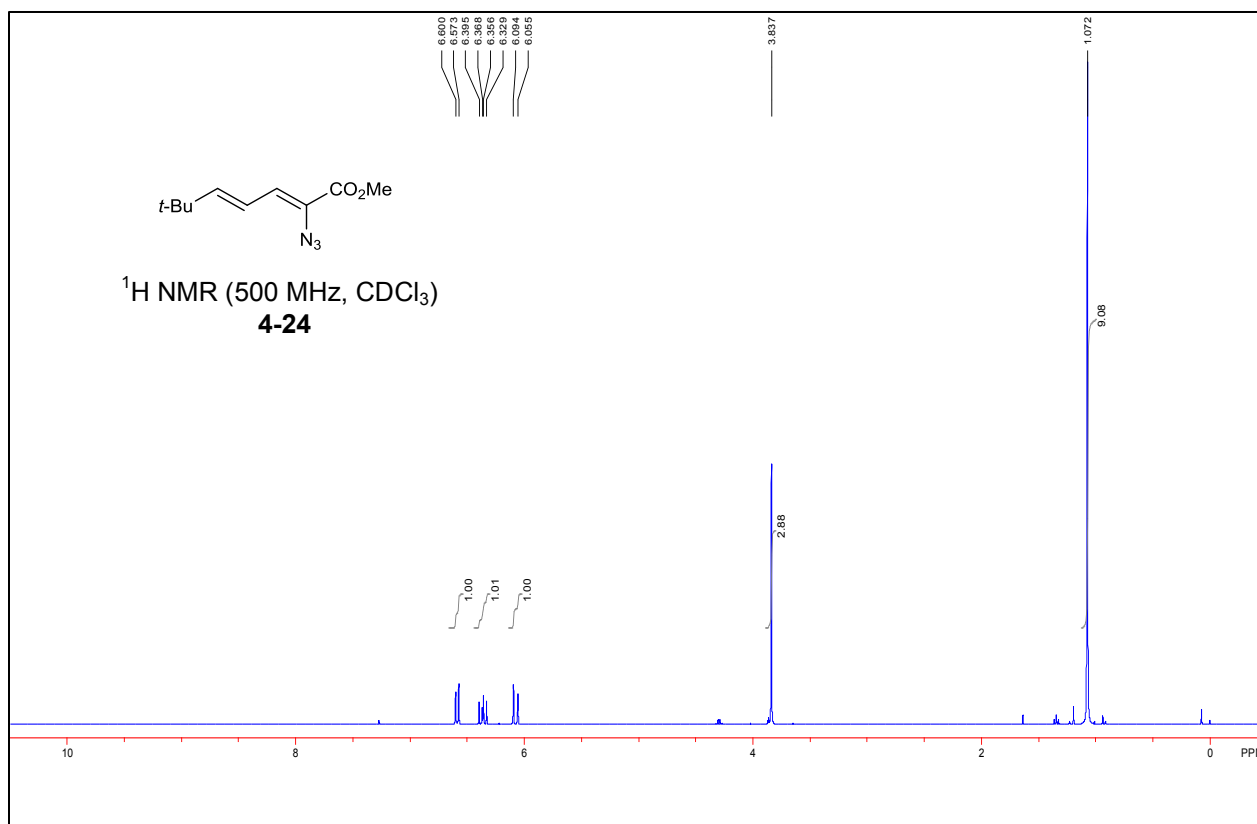
A.2 List of Compounds for Chapter 4

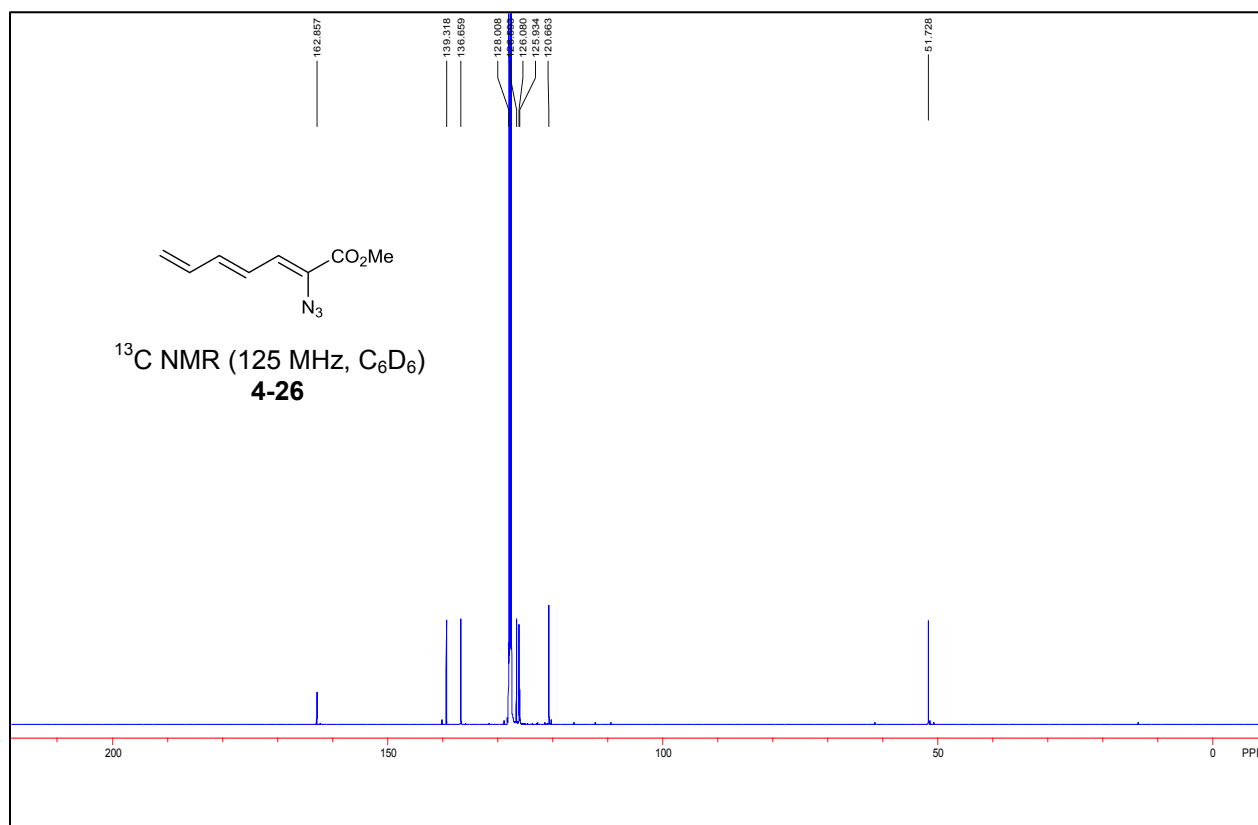
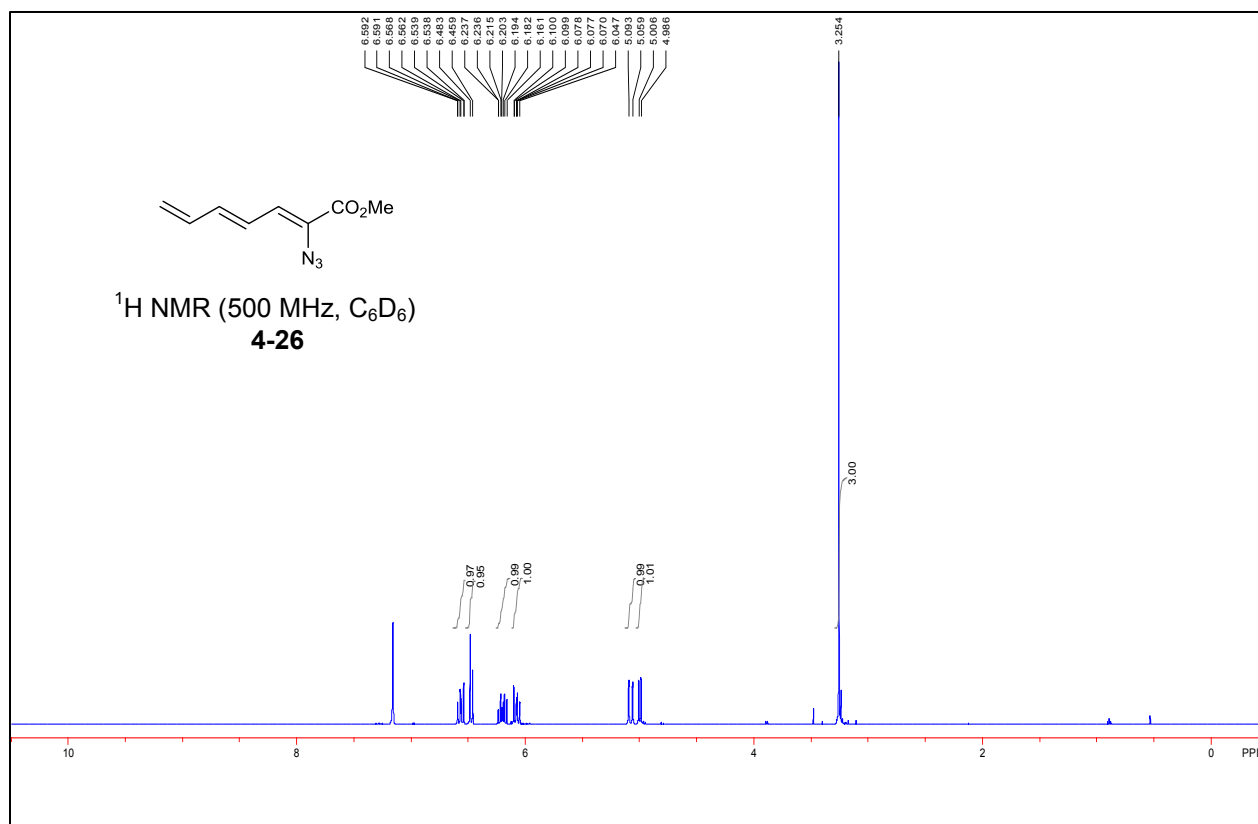


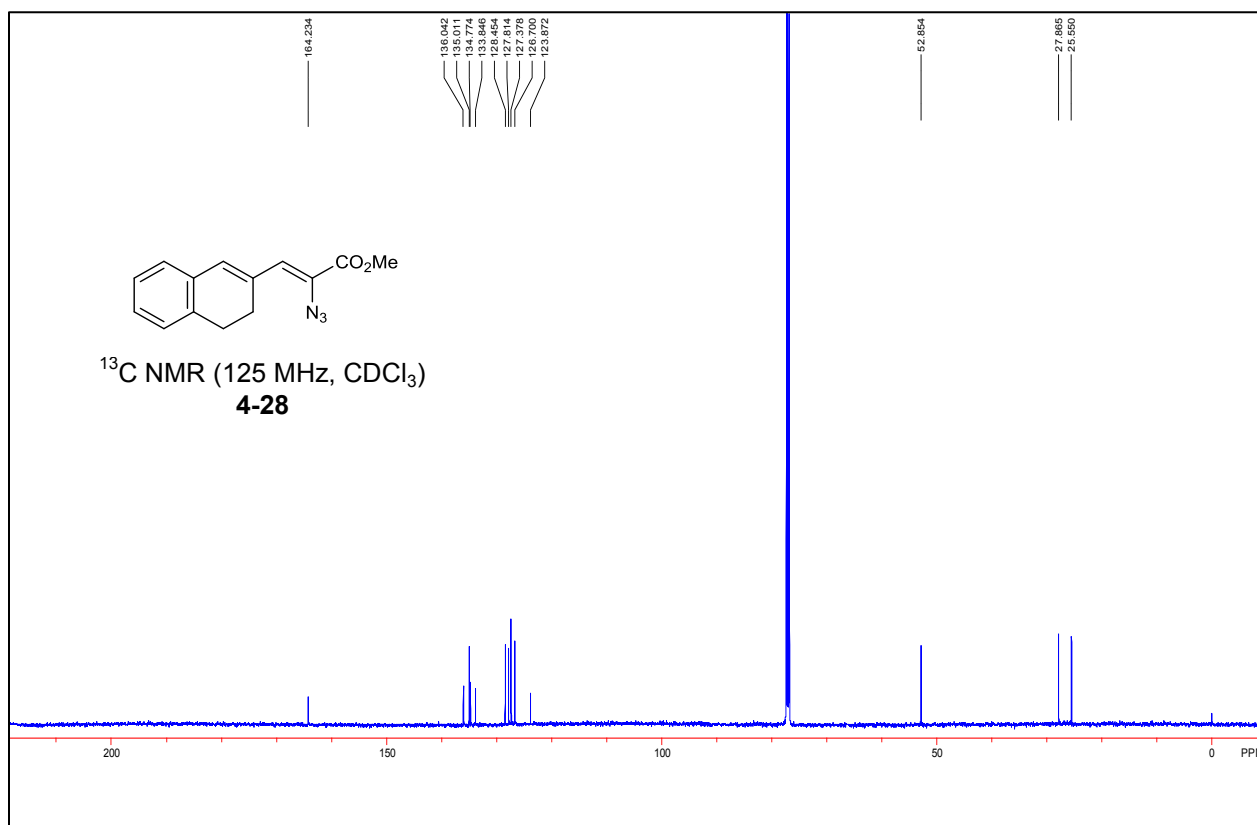
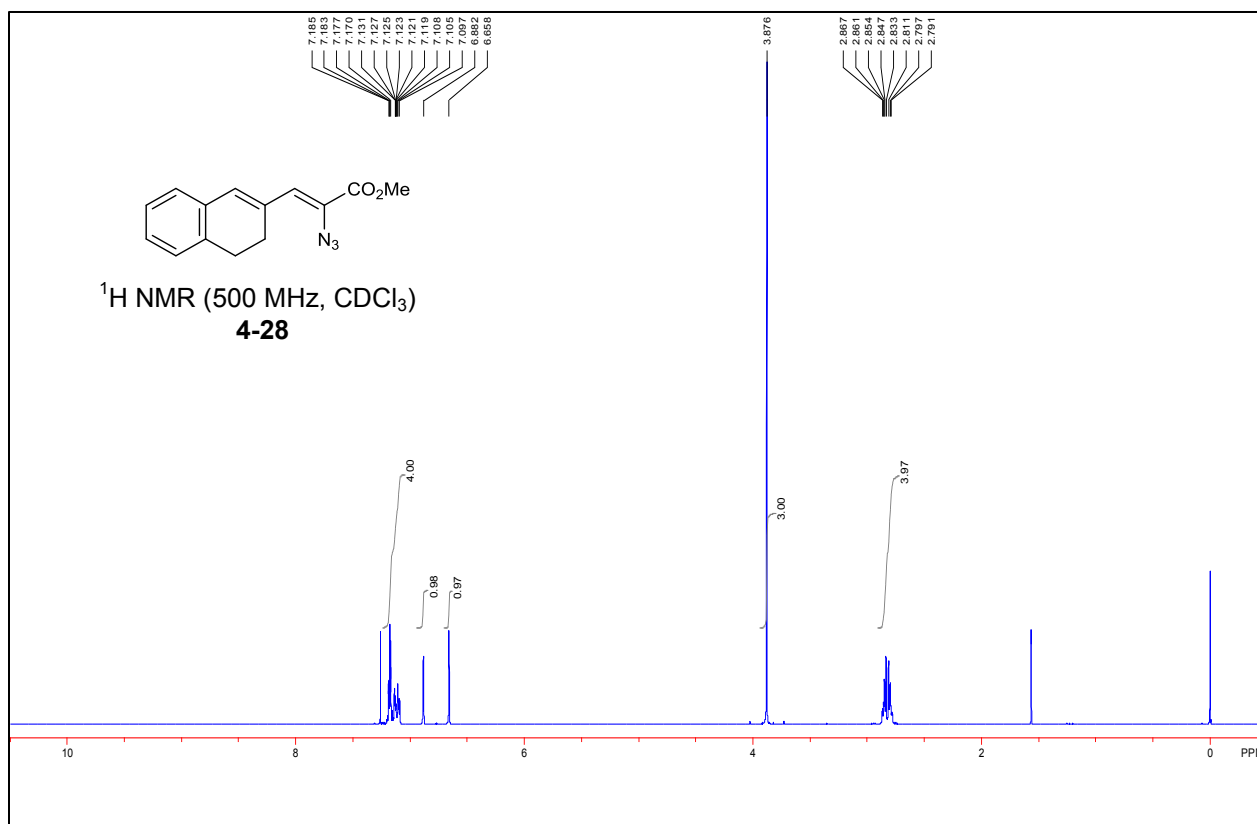


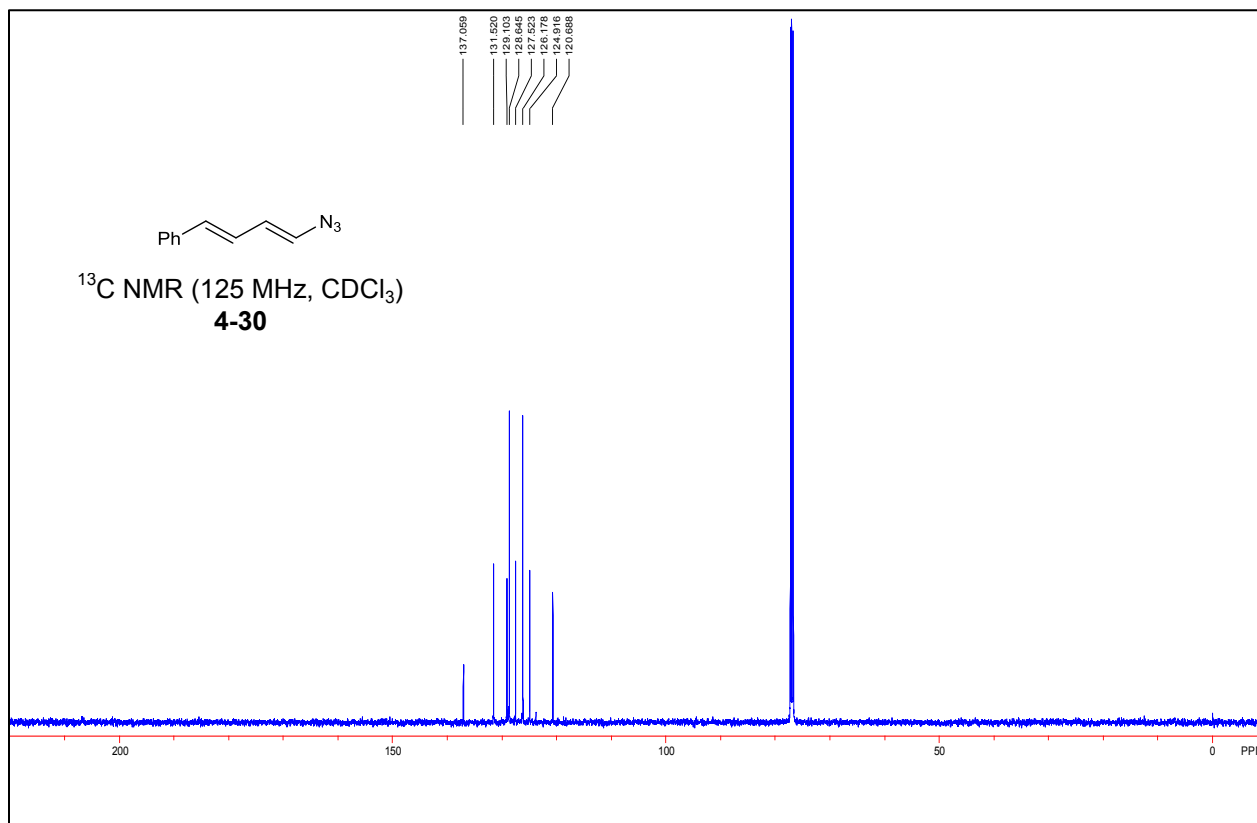
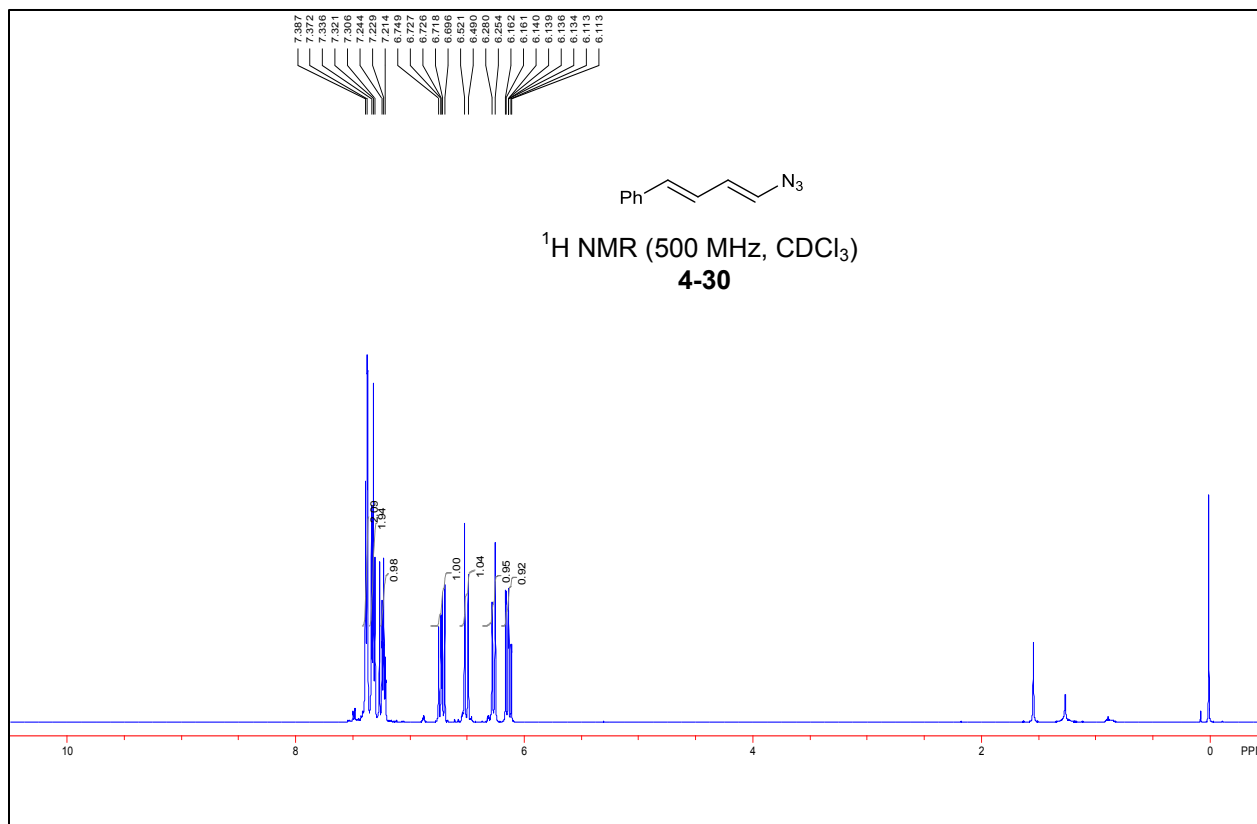


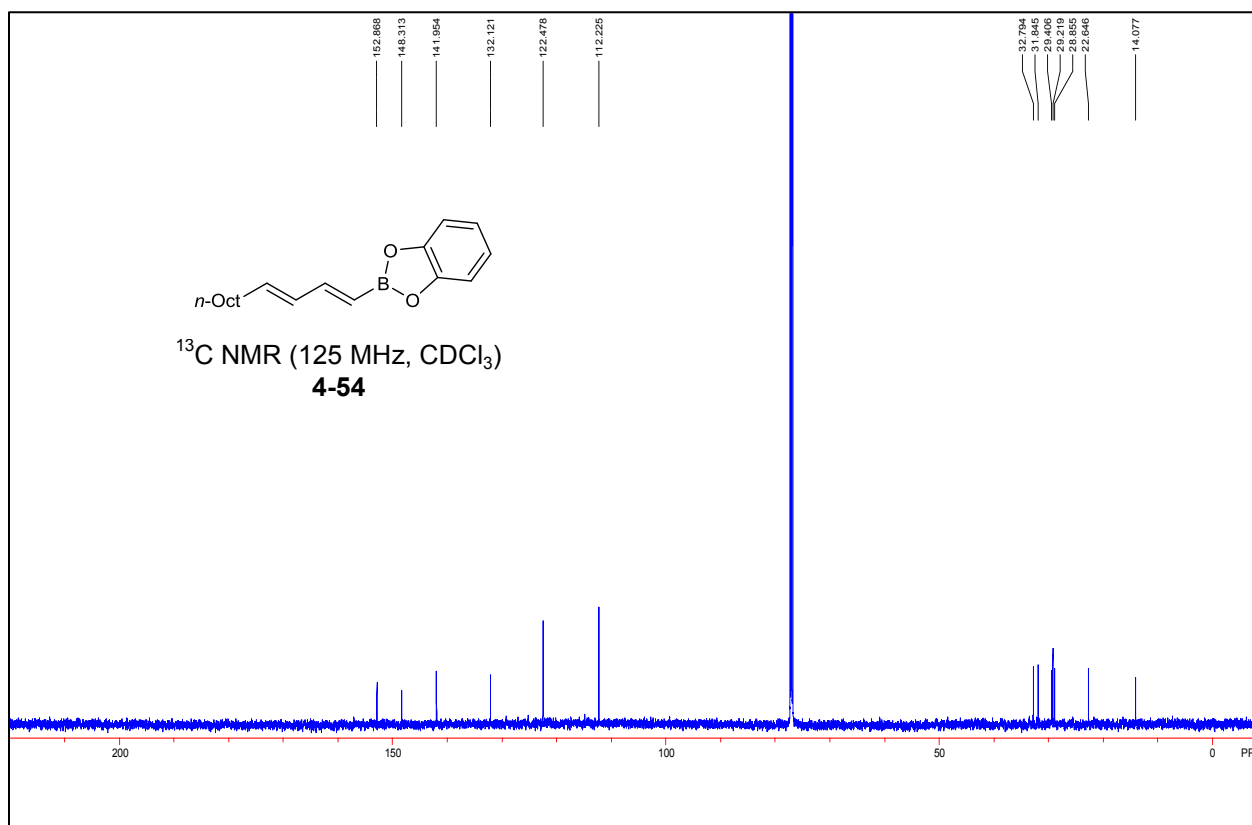
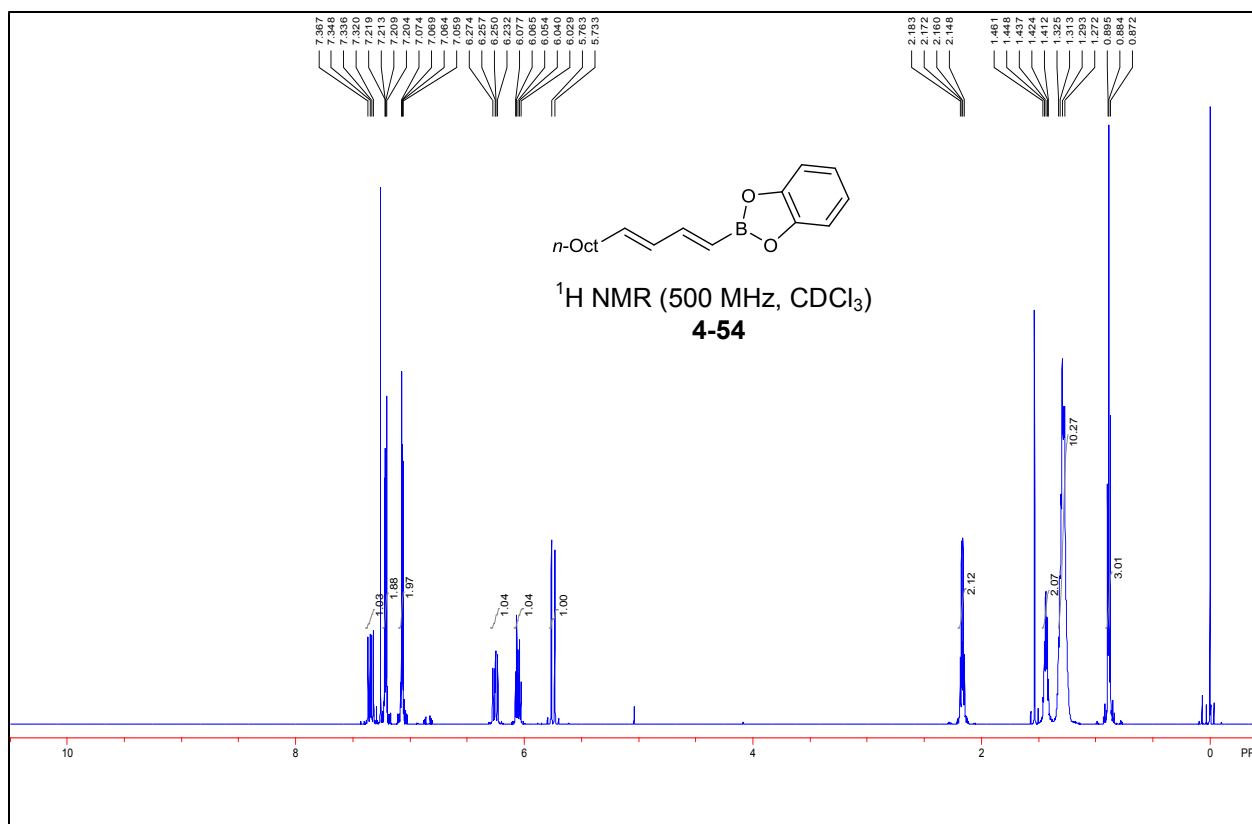


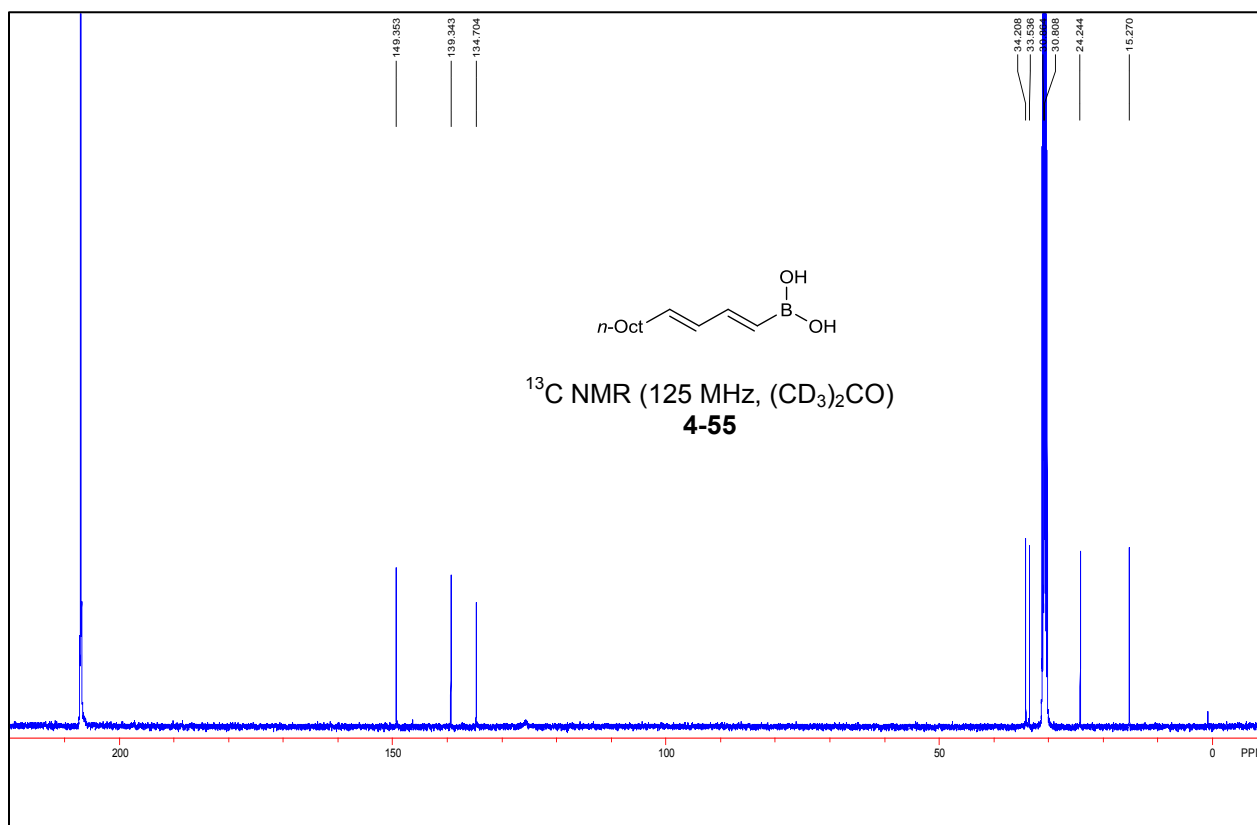
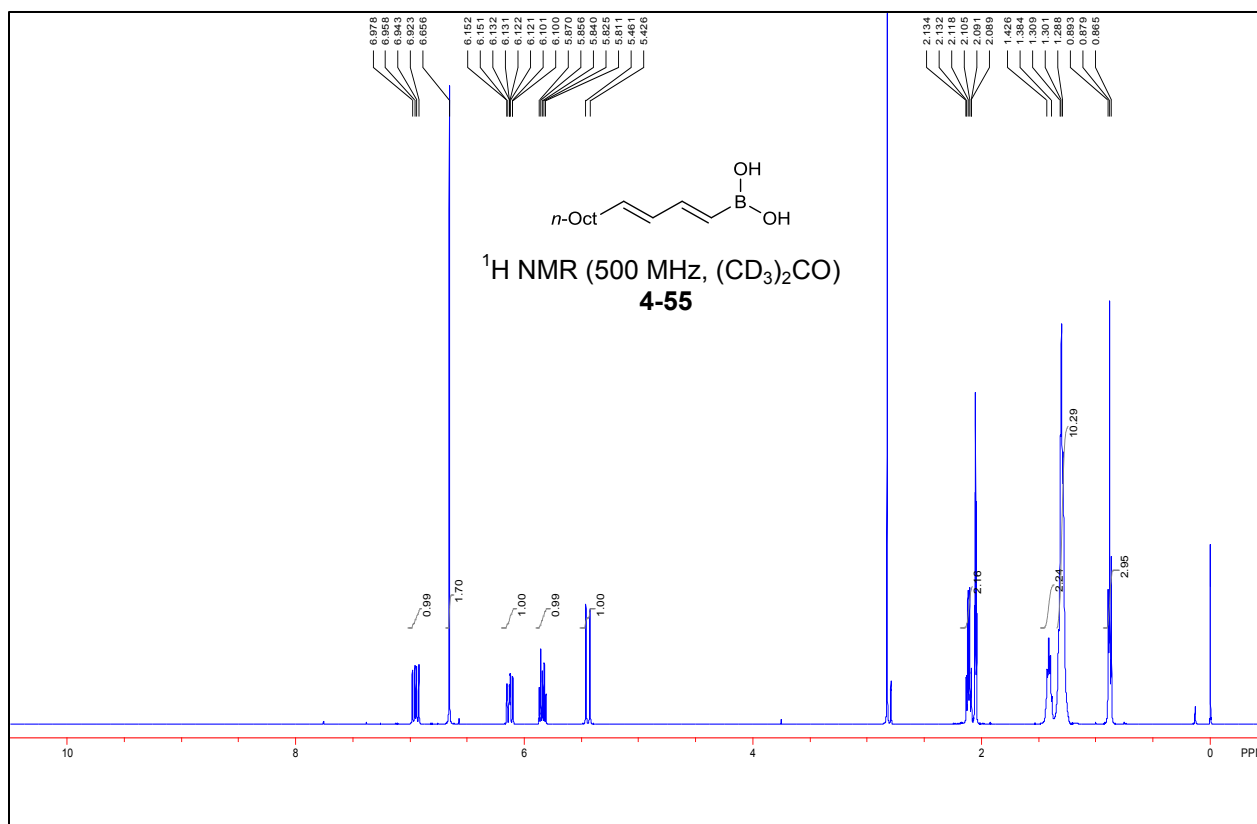


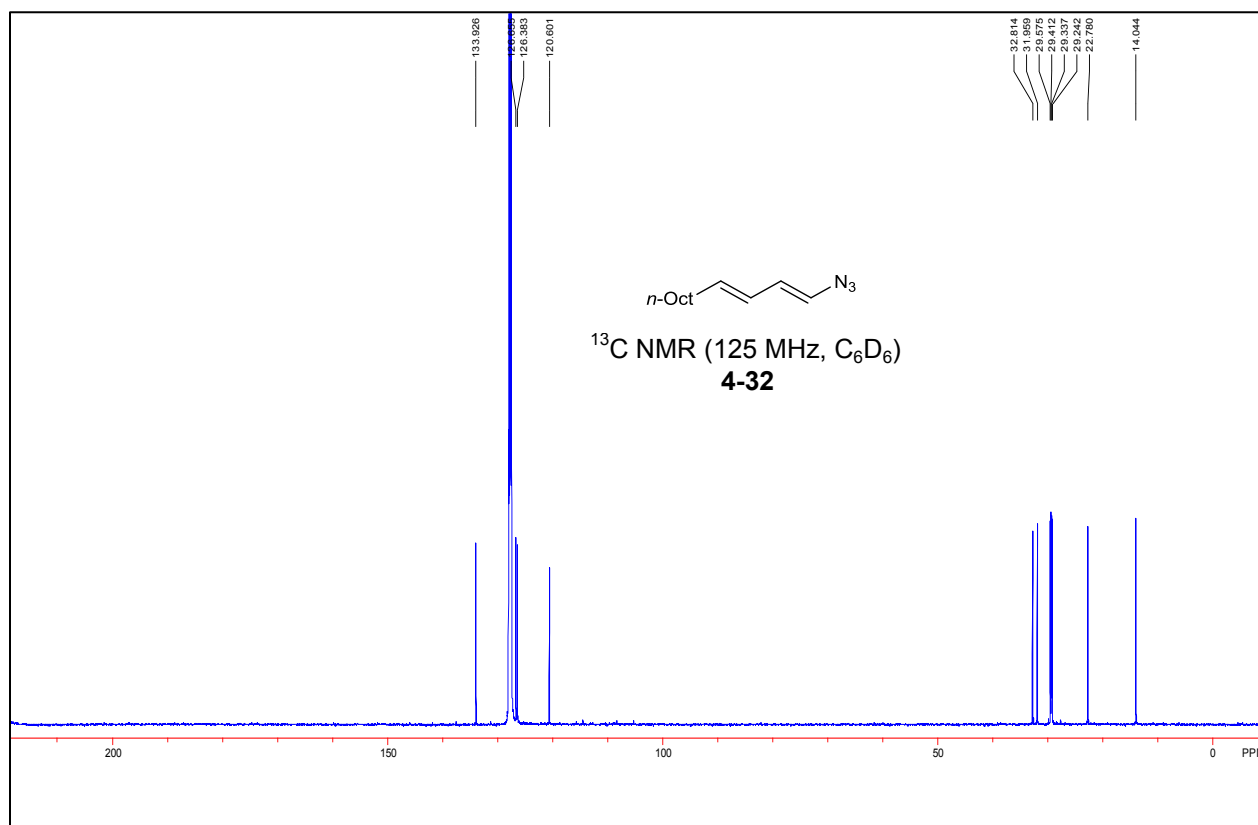
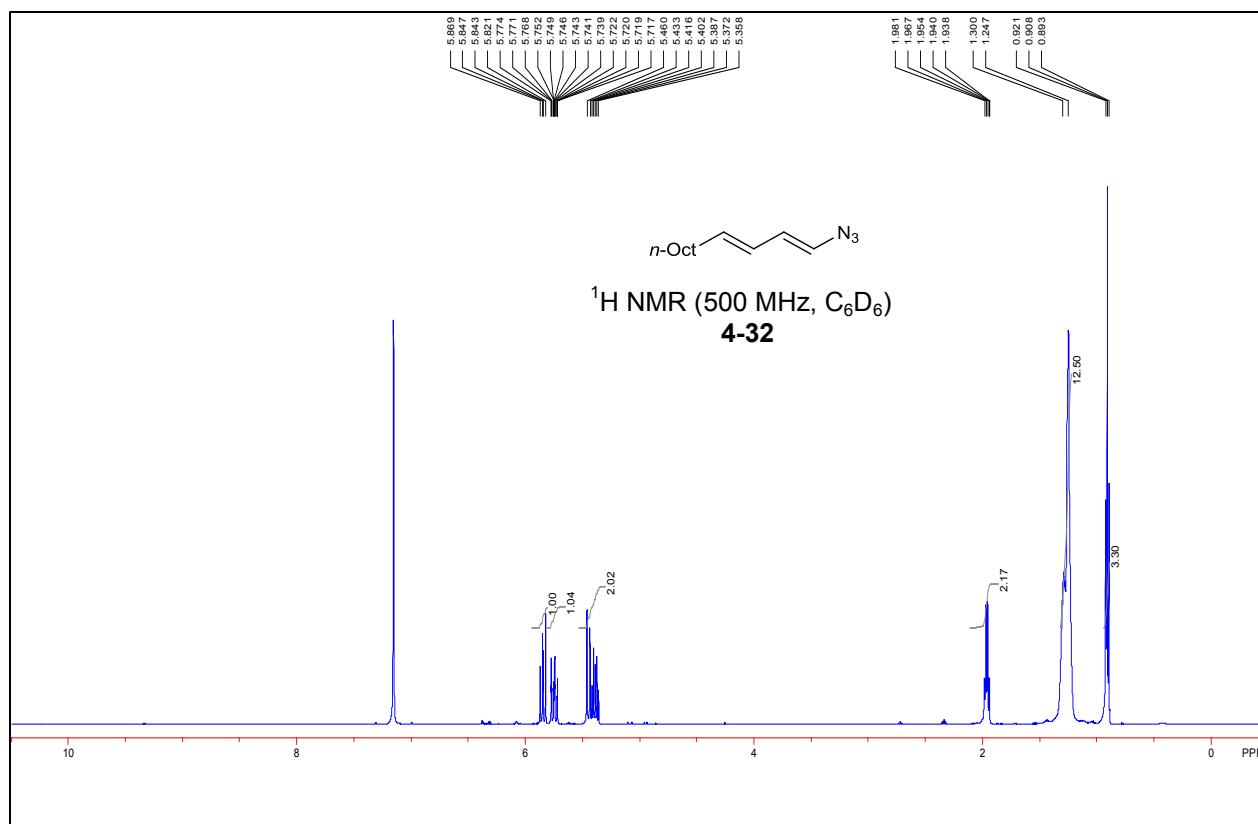


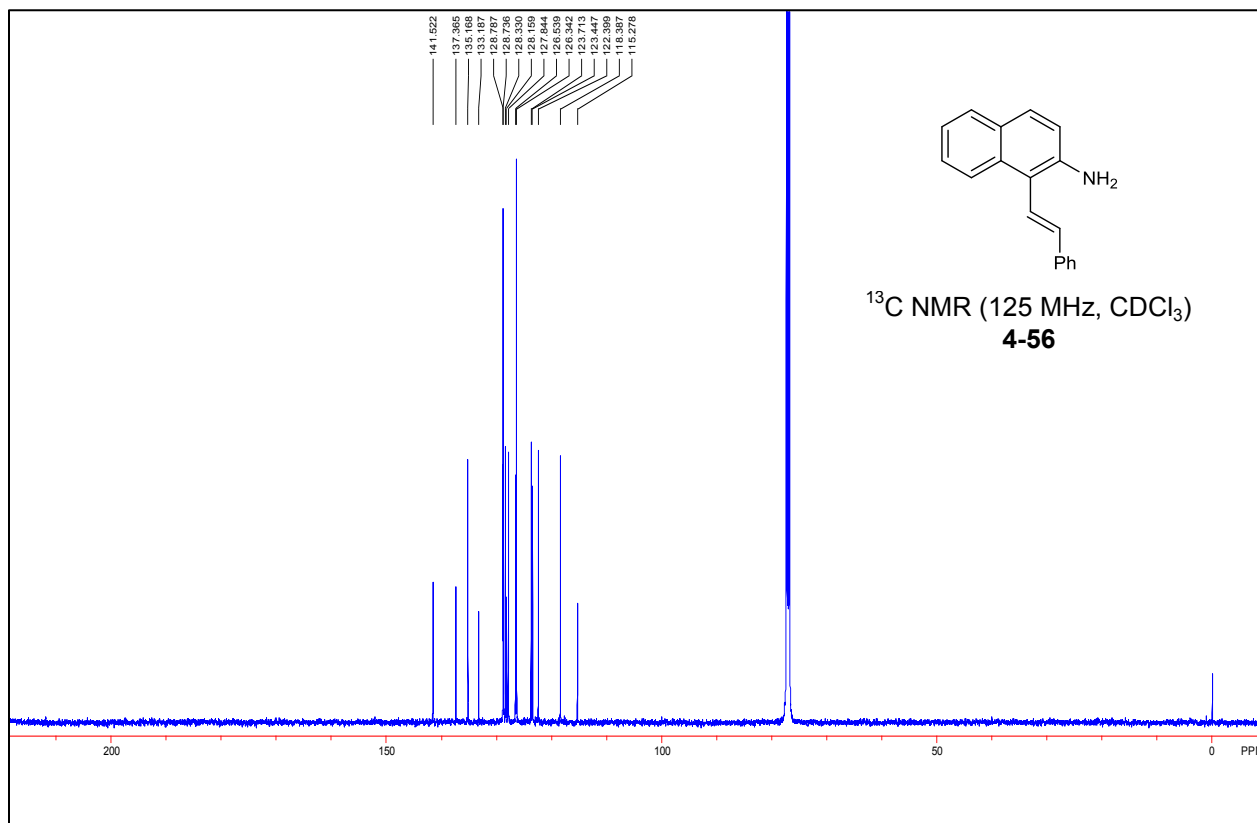
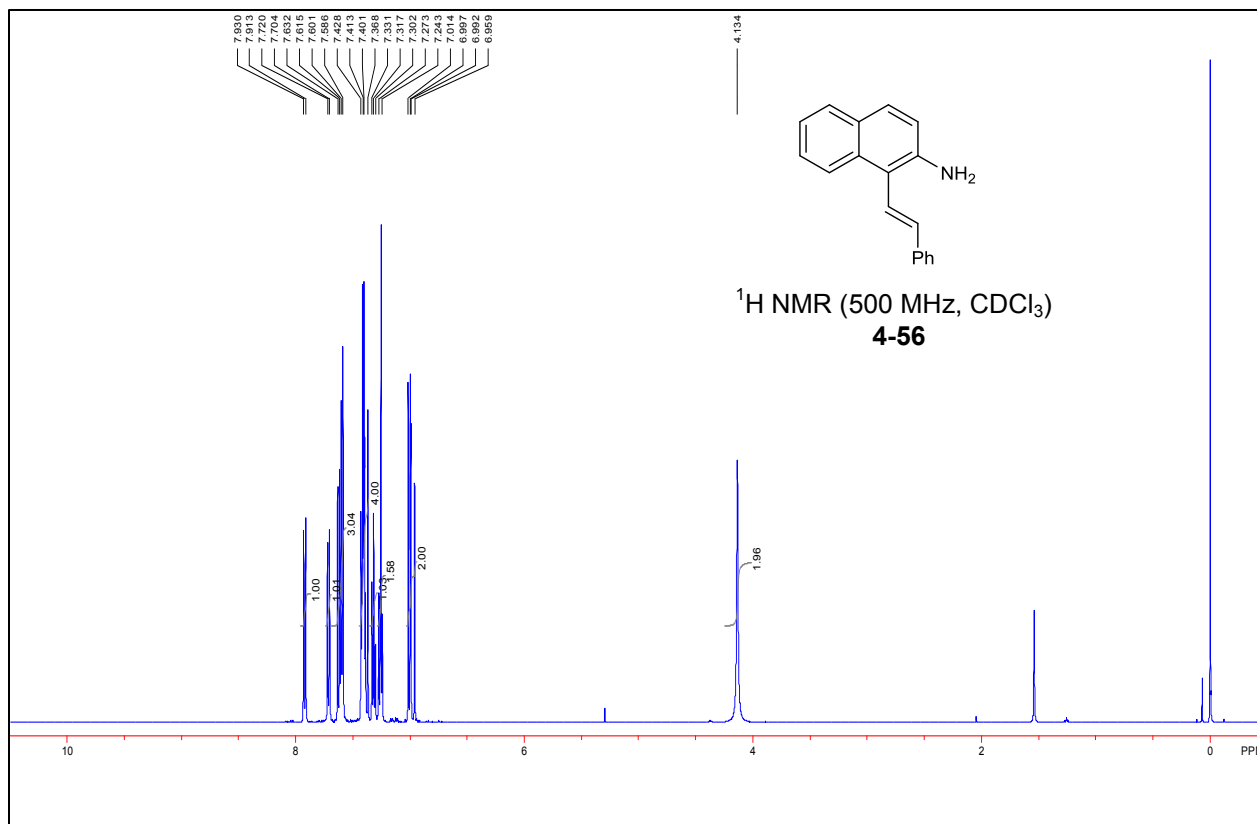


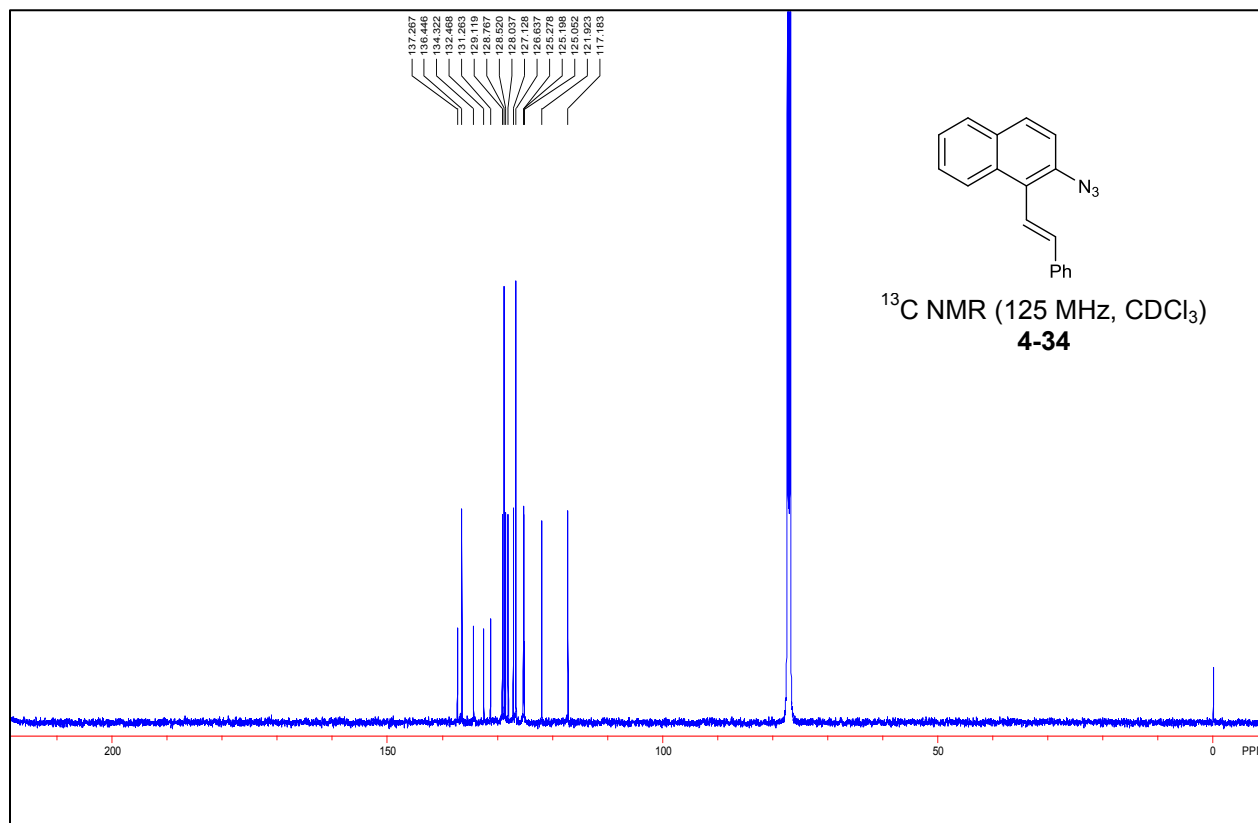
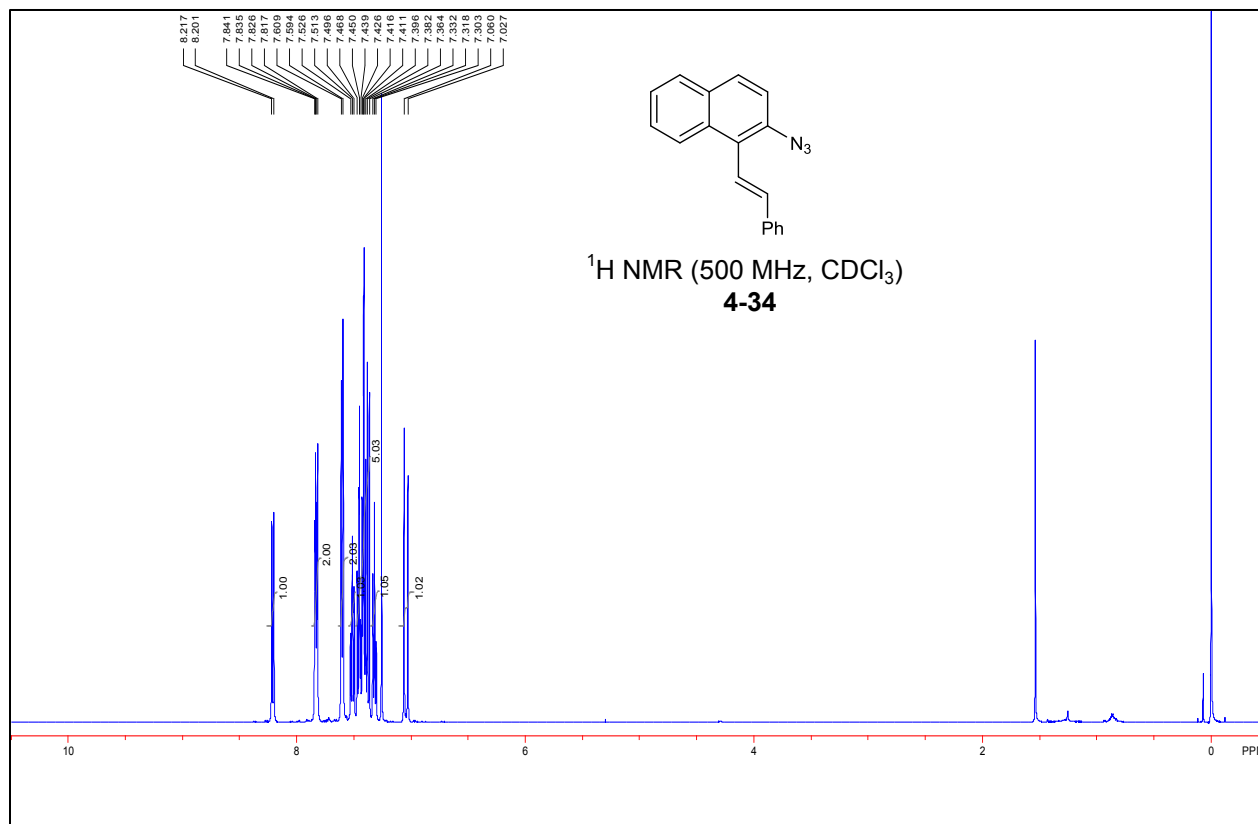


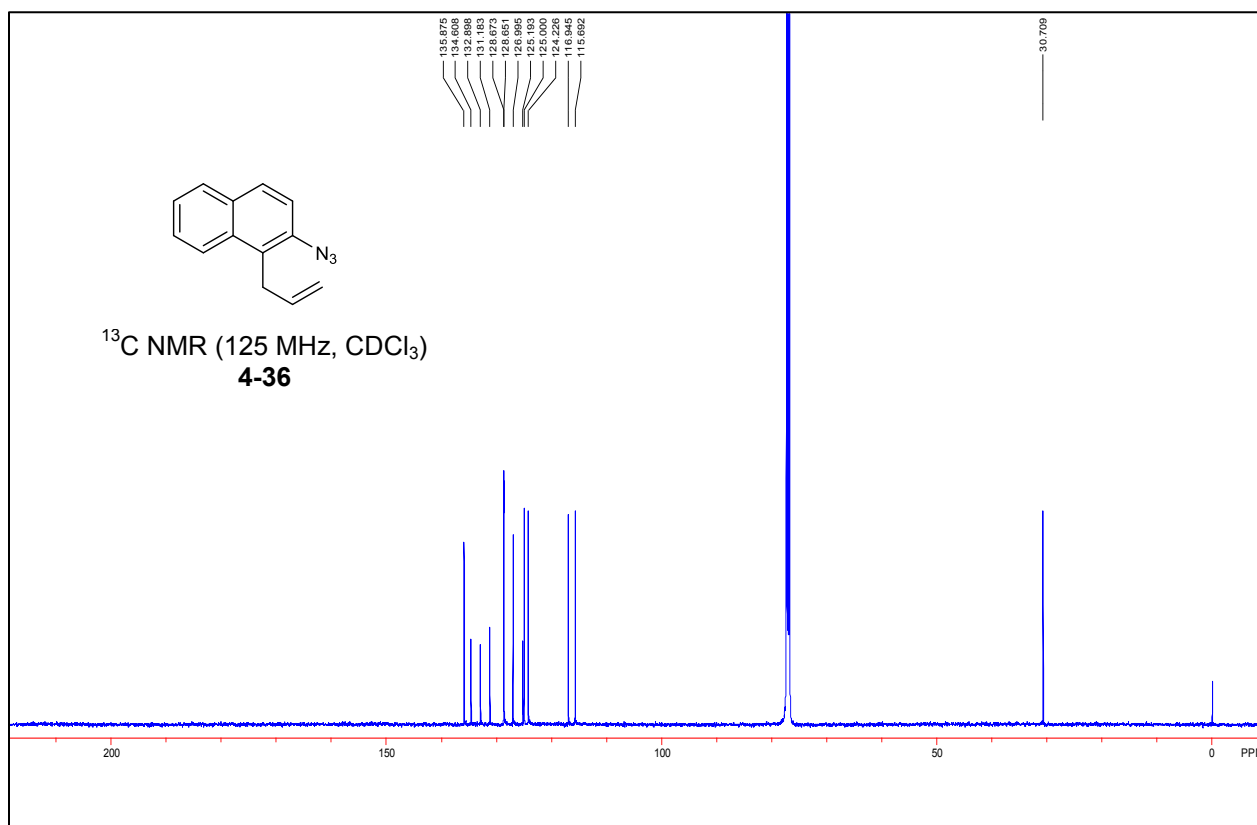
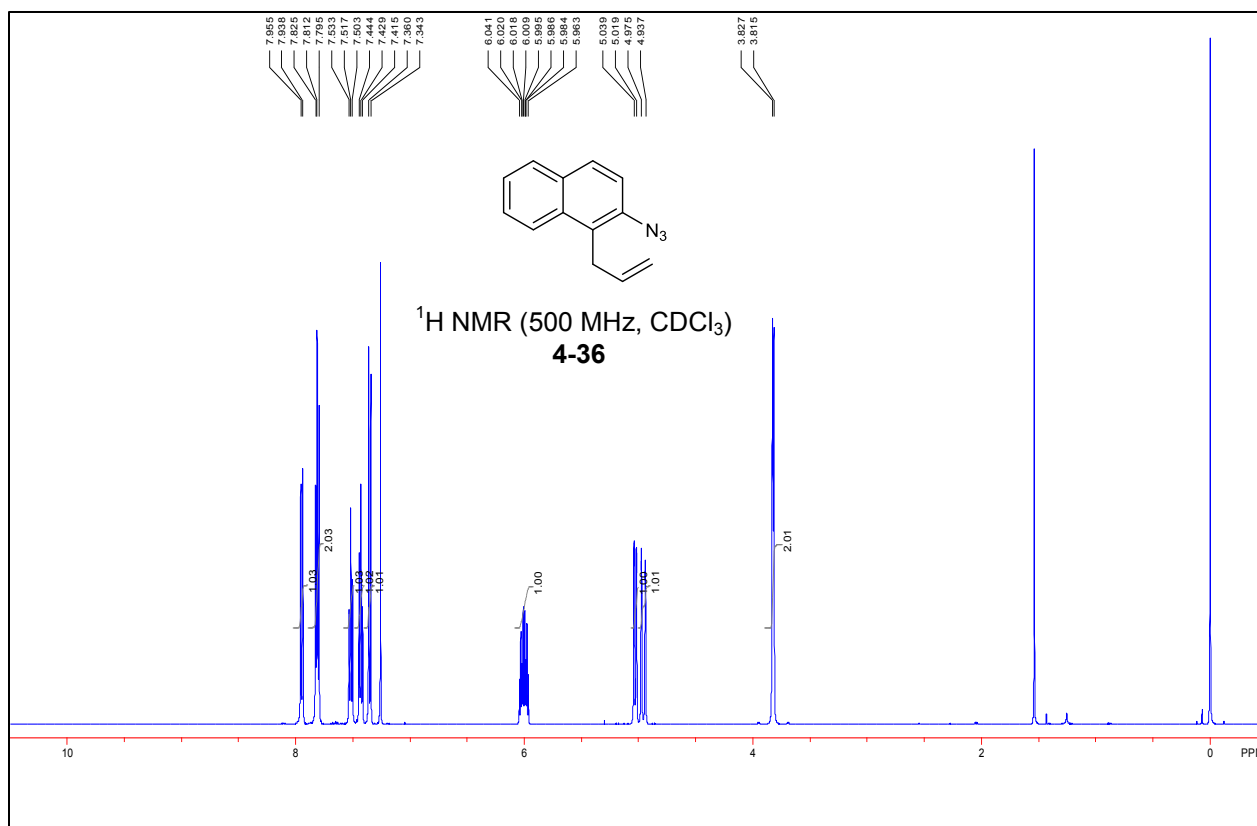


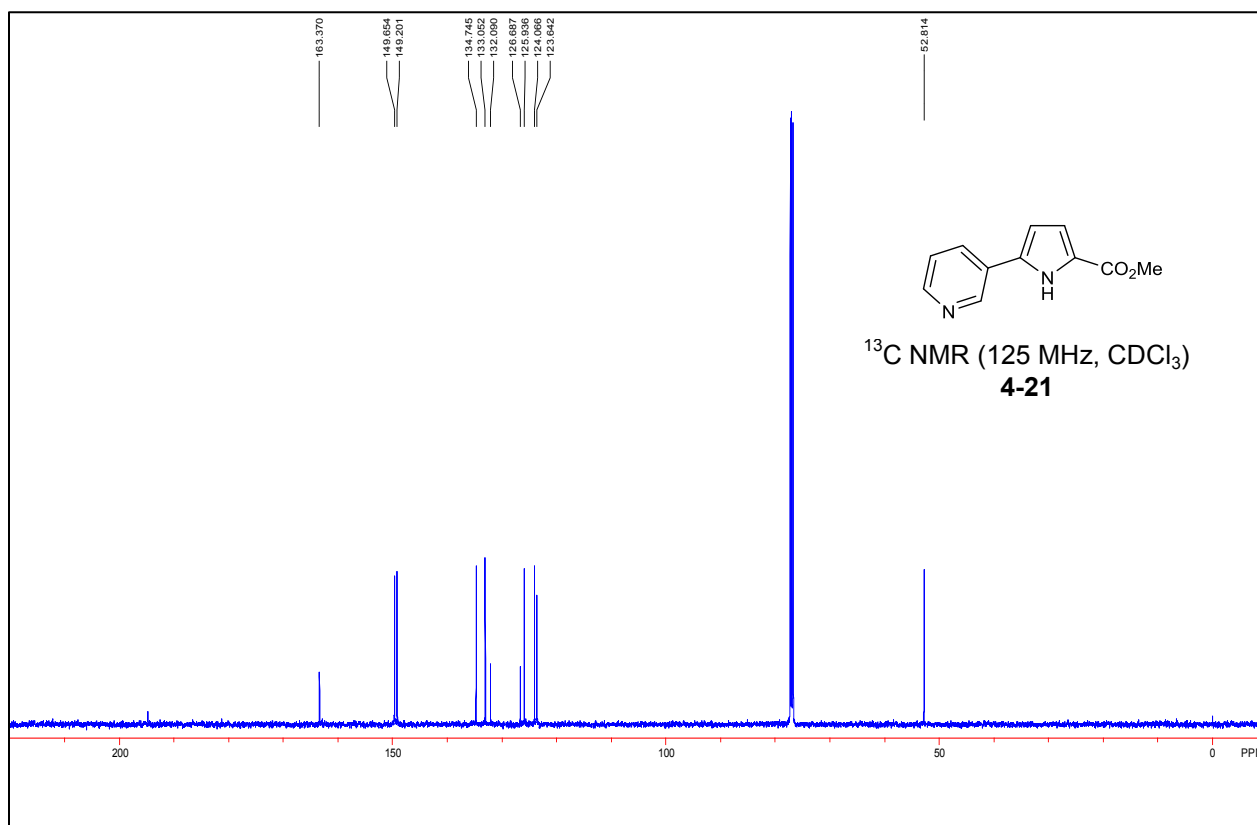
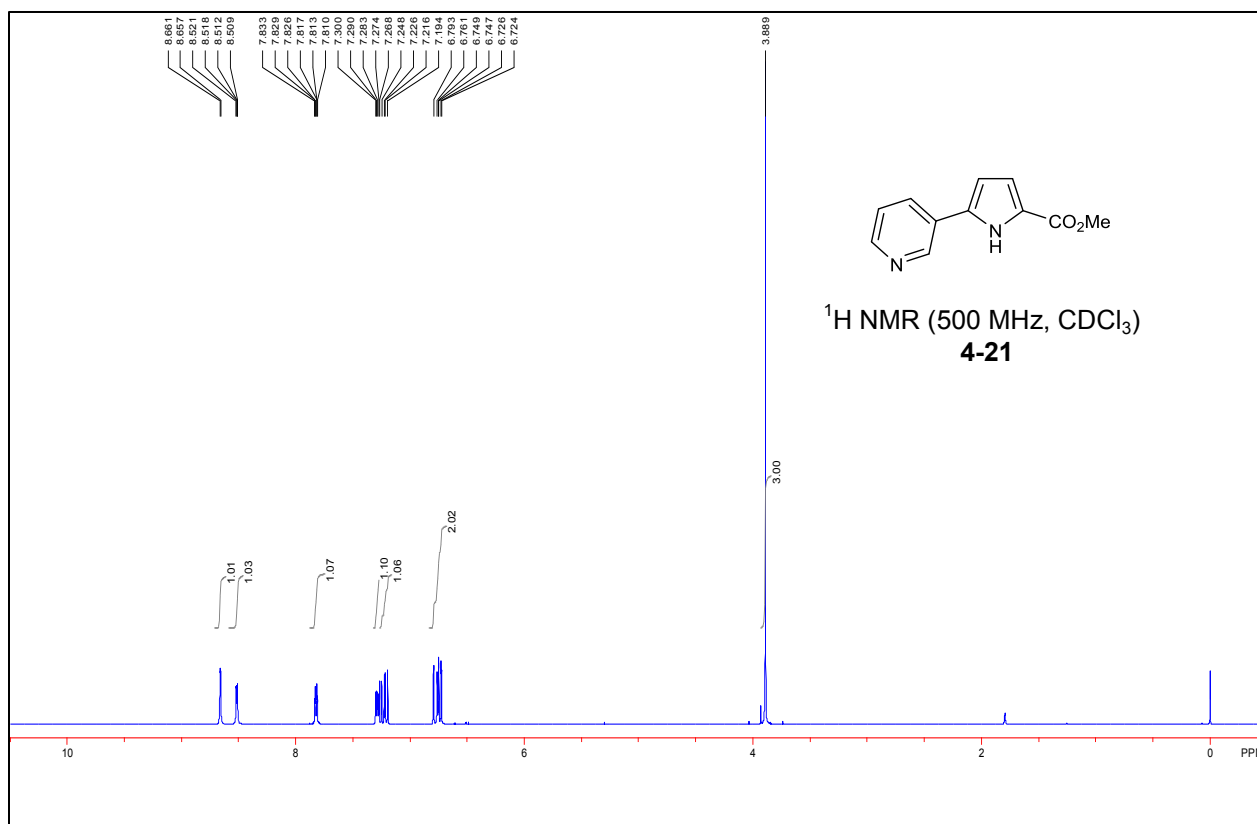


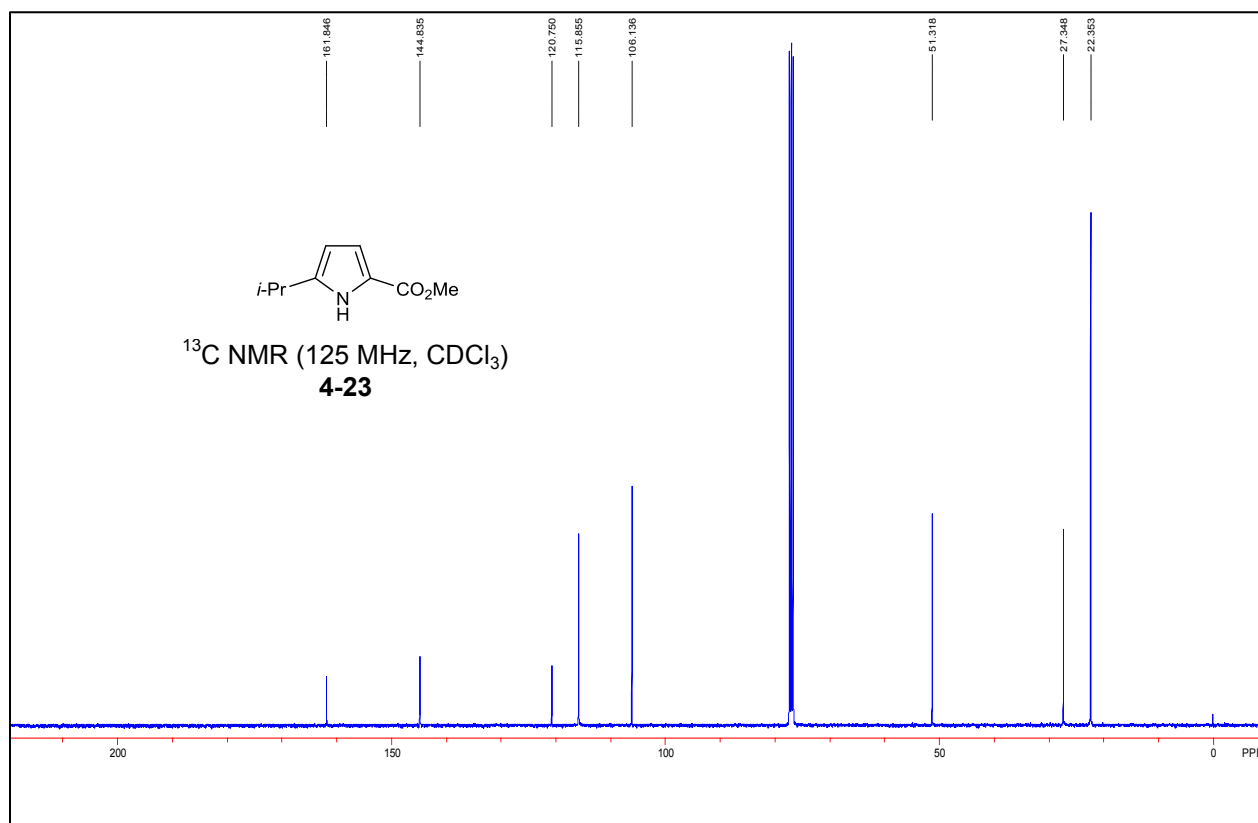
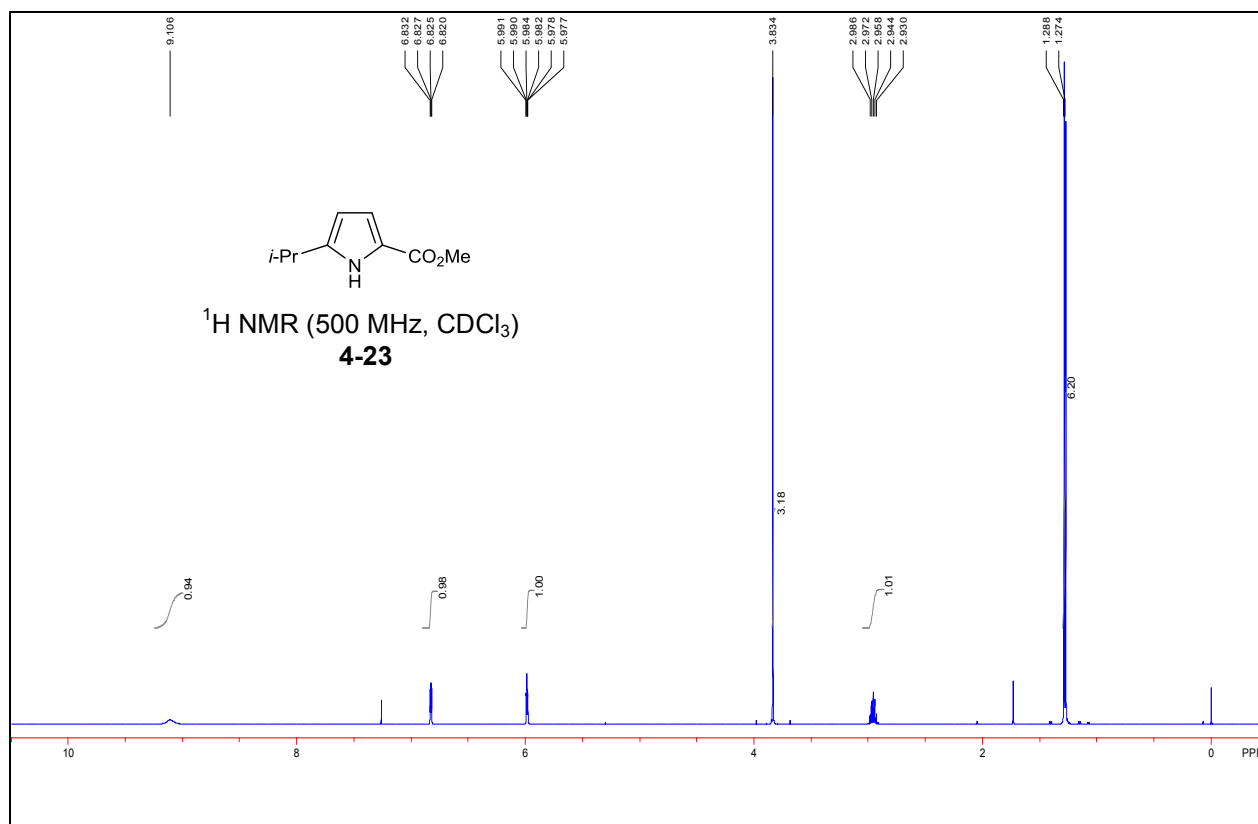


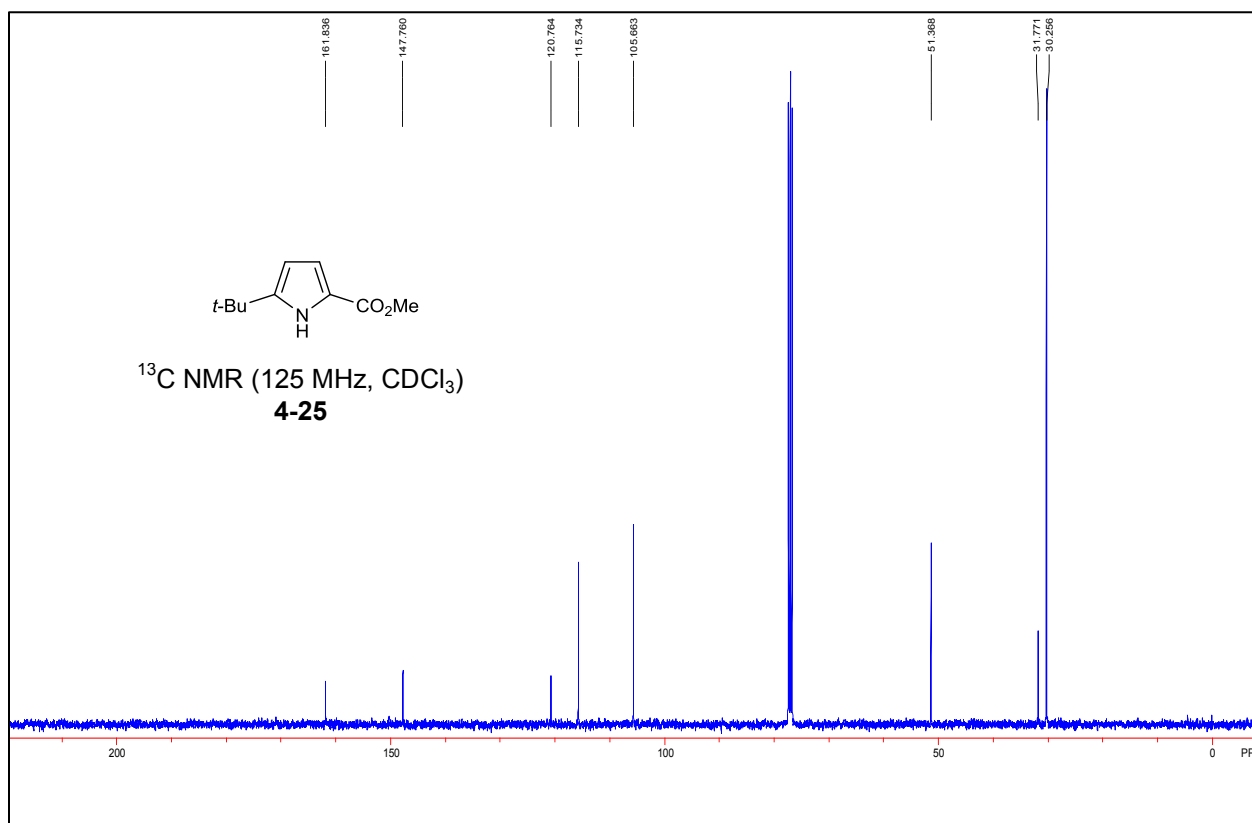
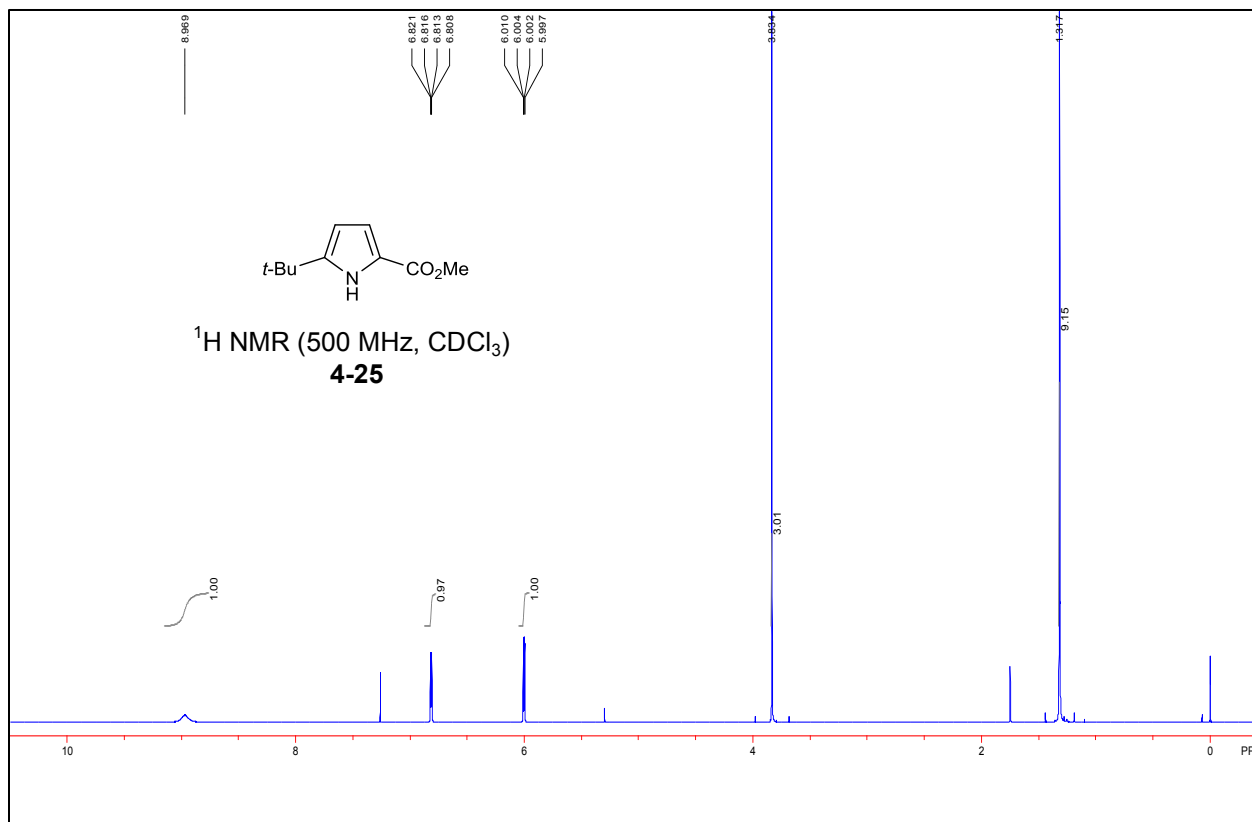


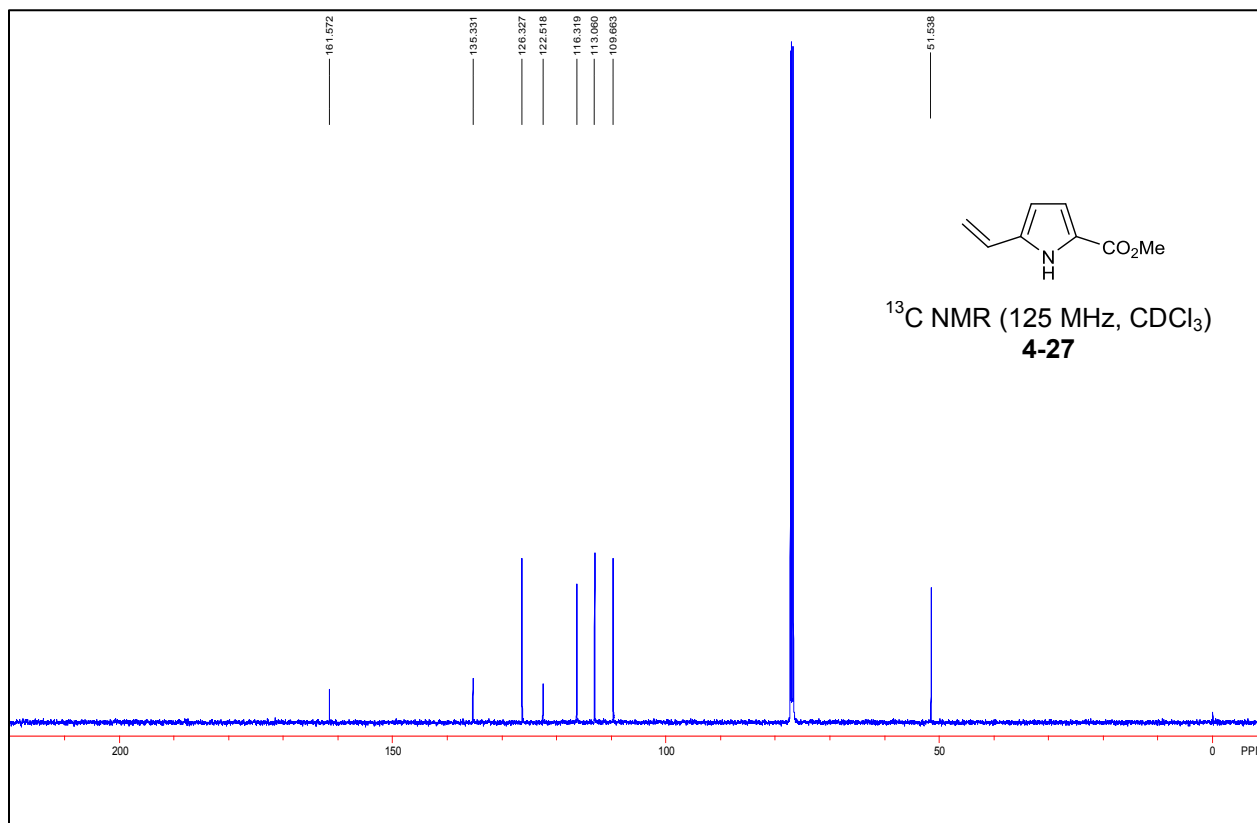
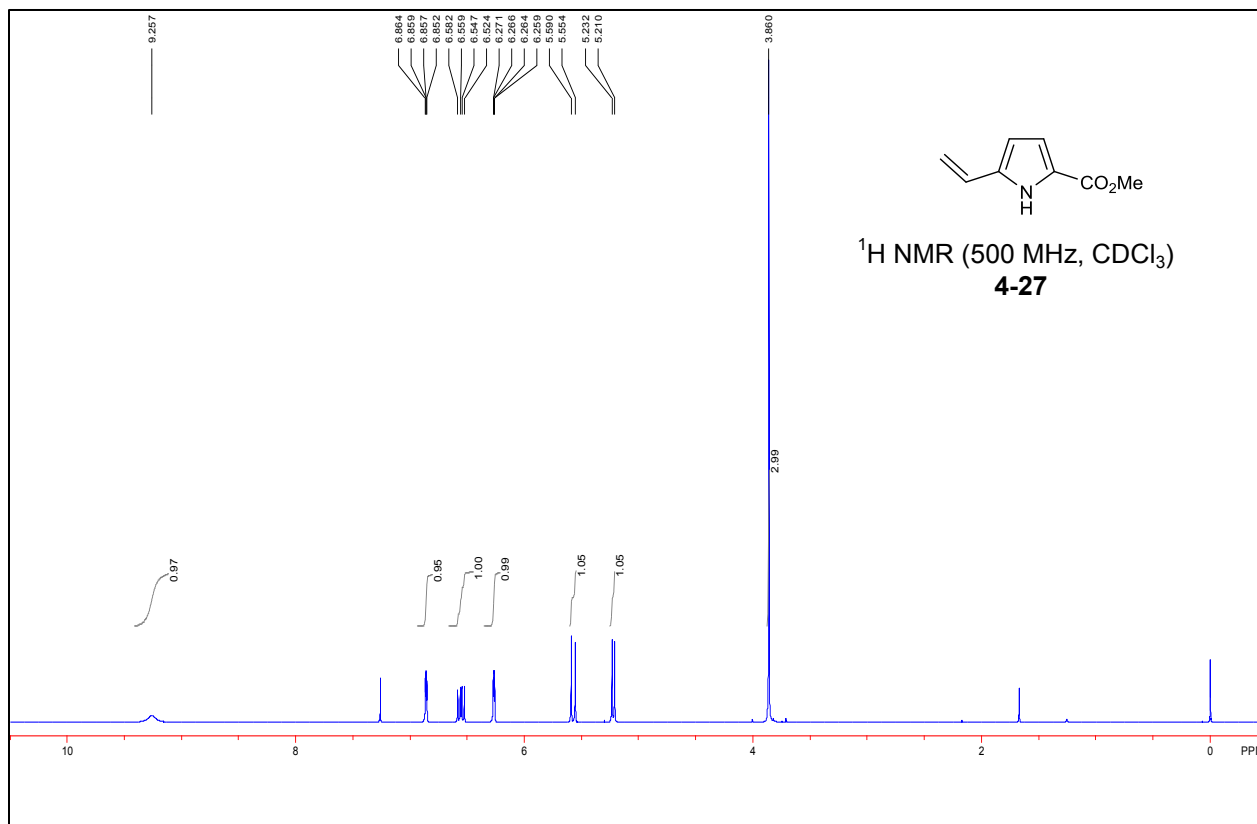


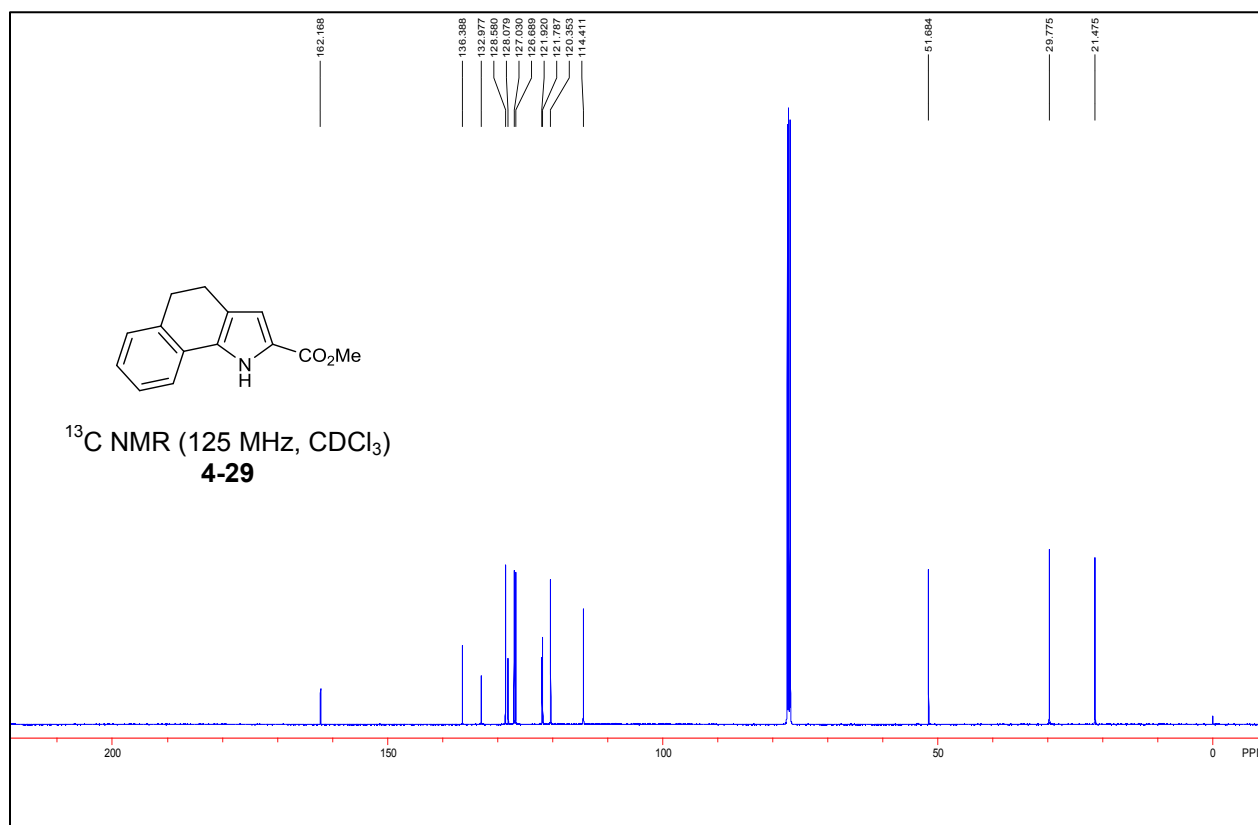
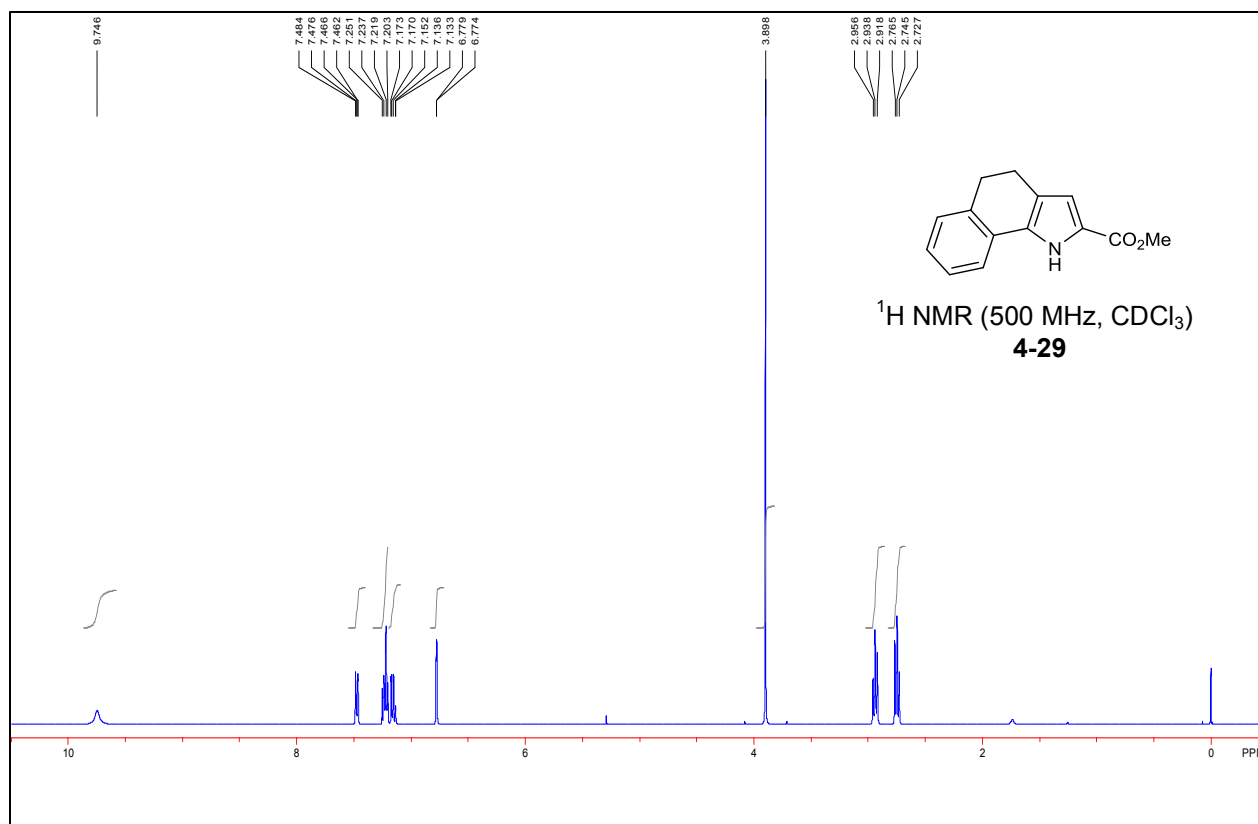


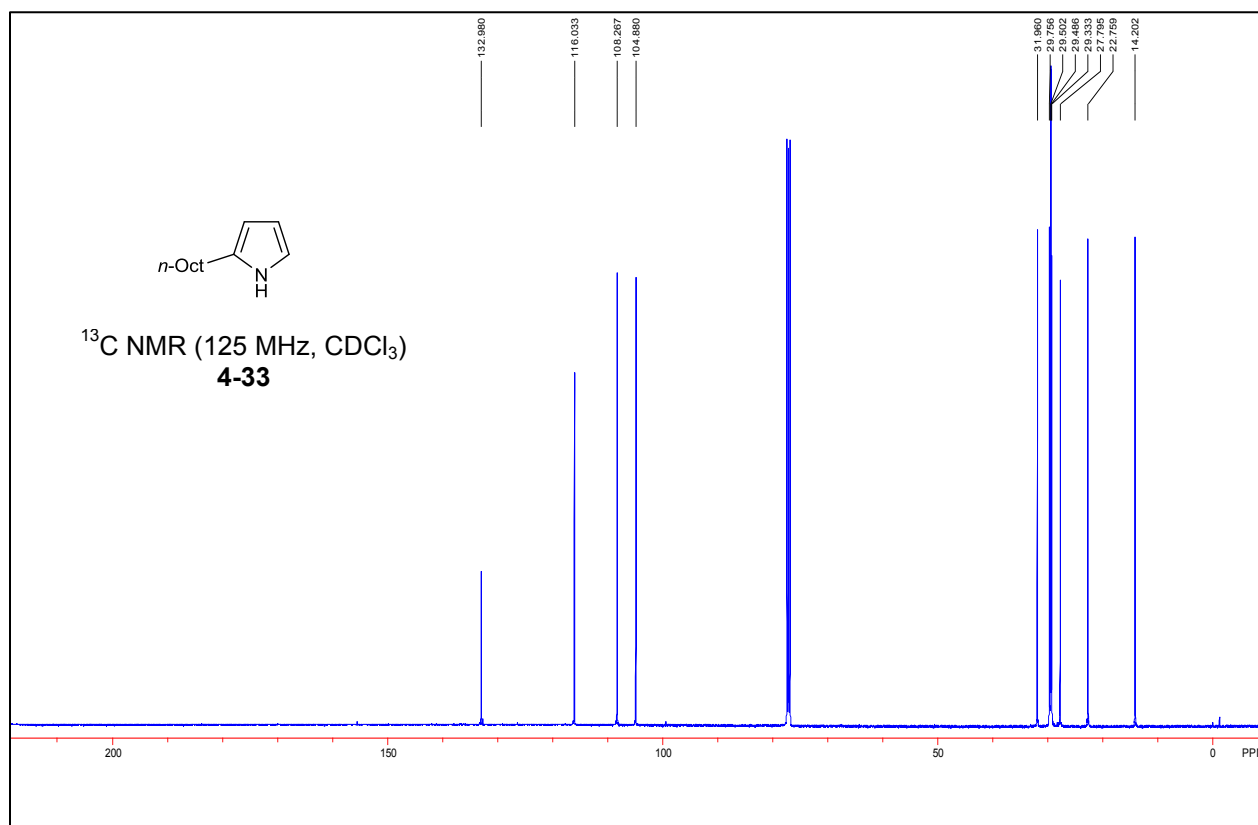
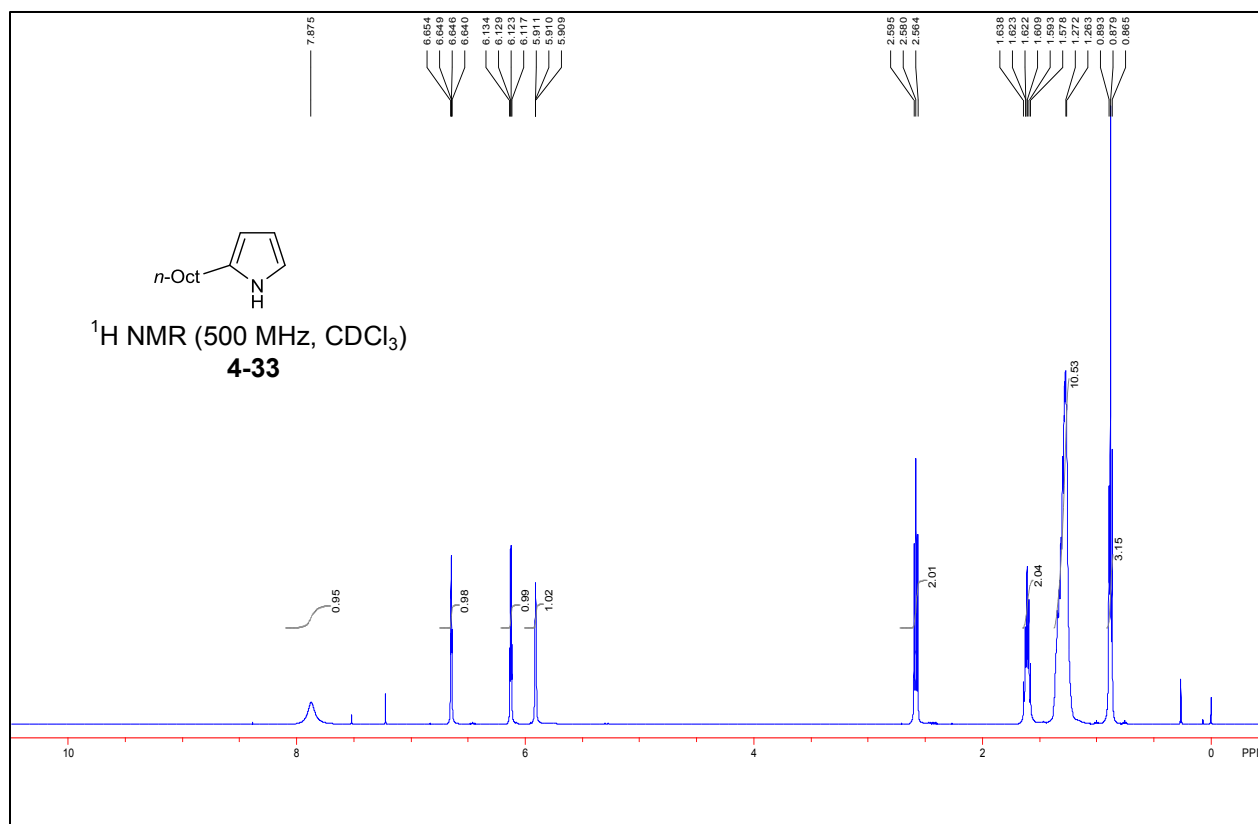


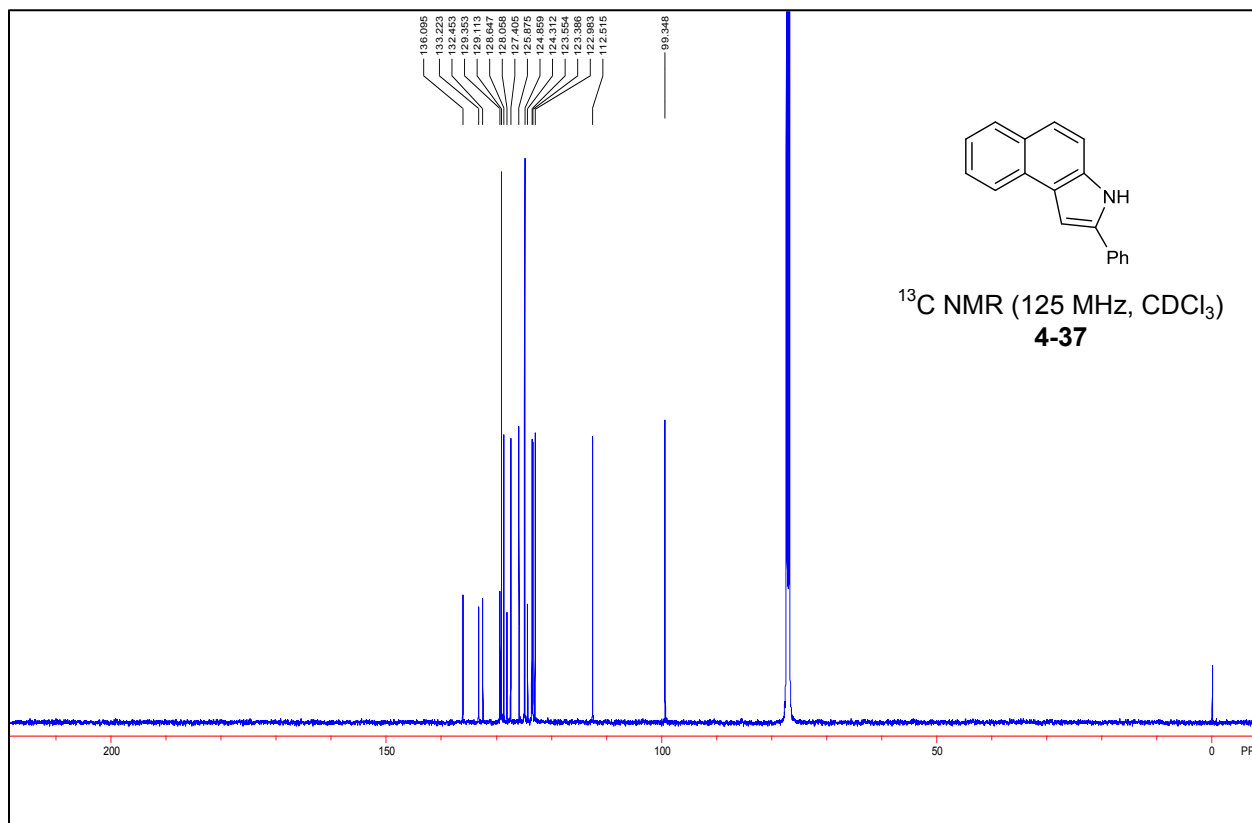
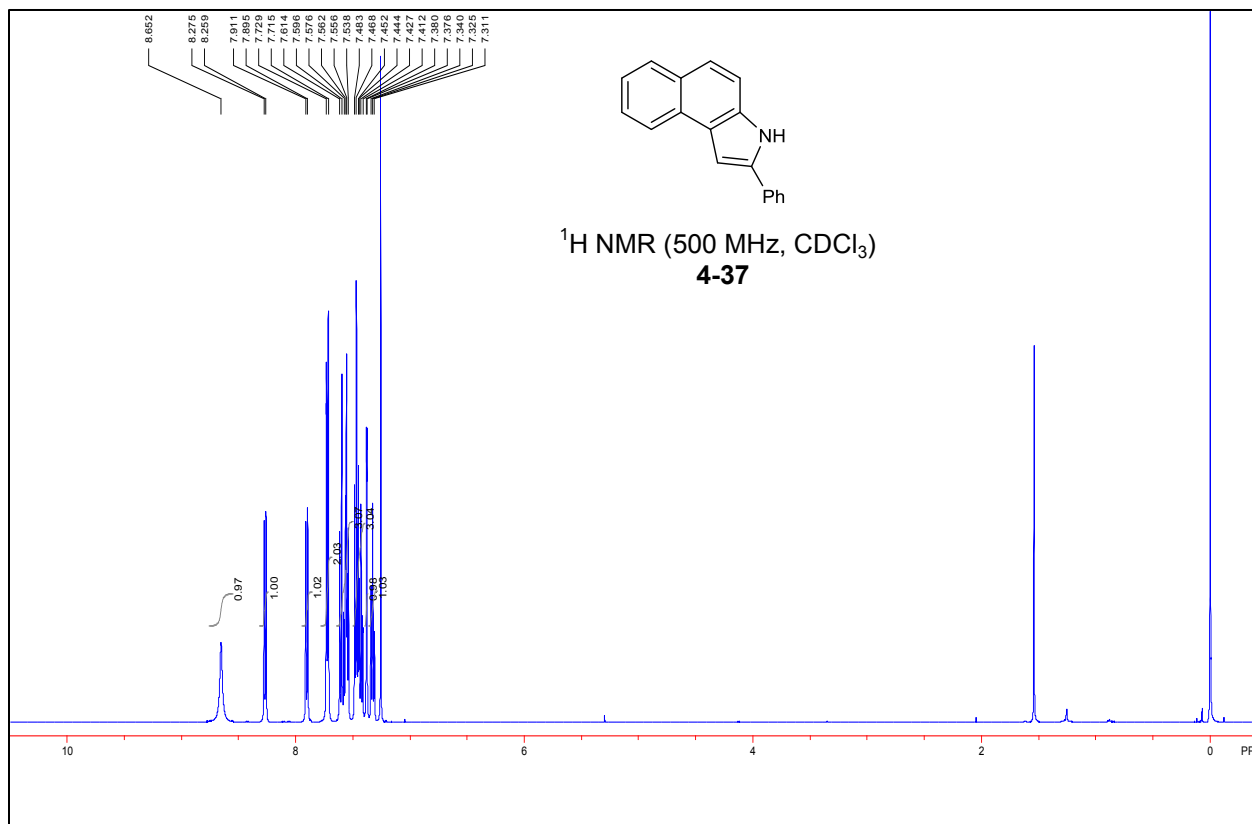


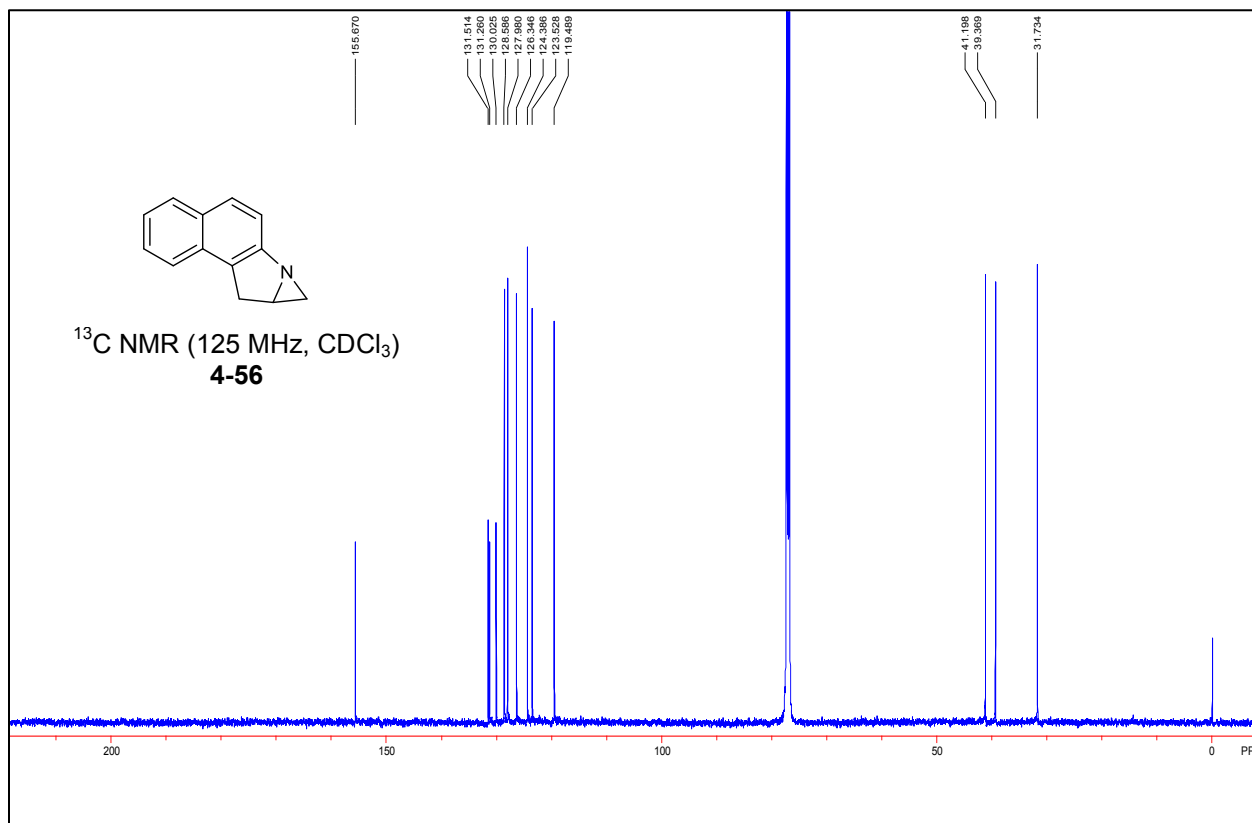
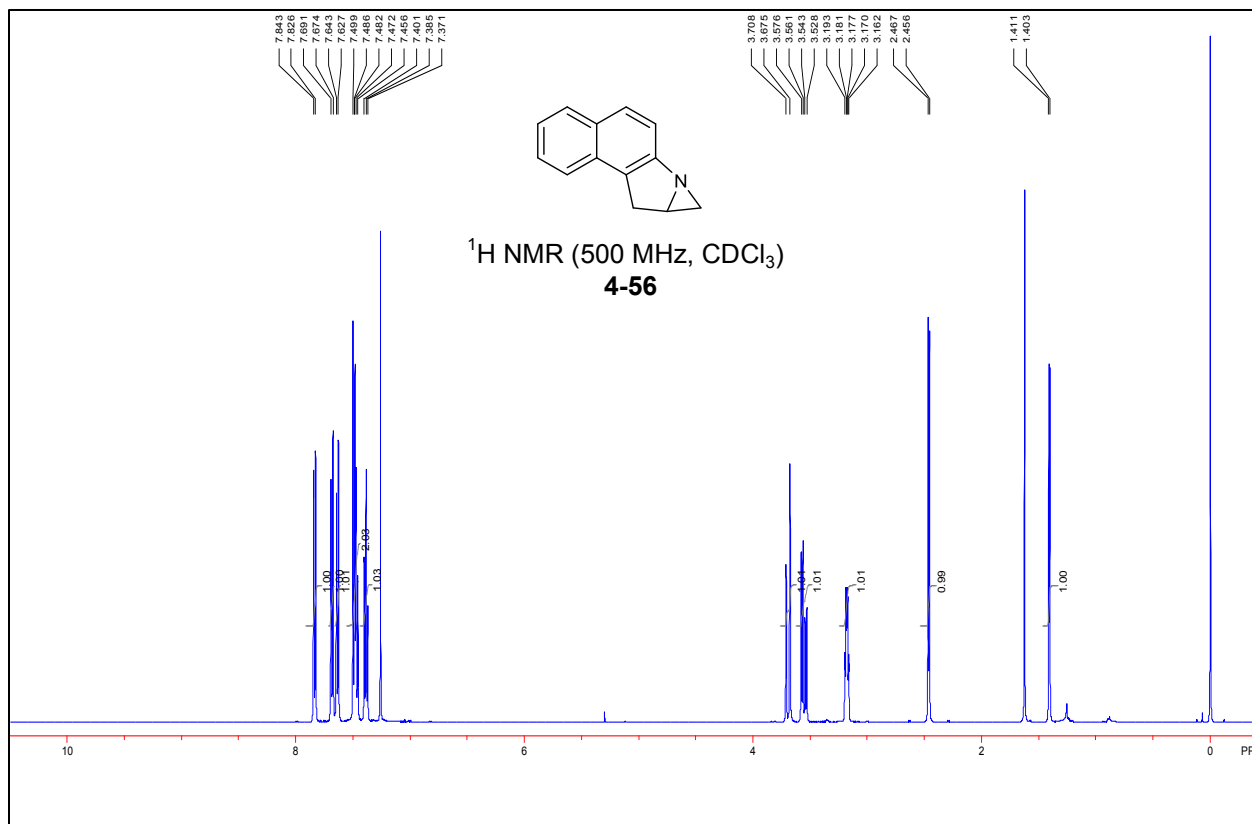


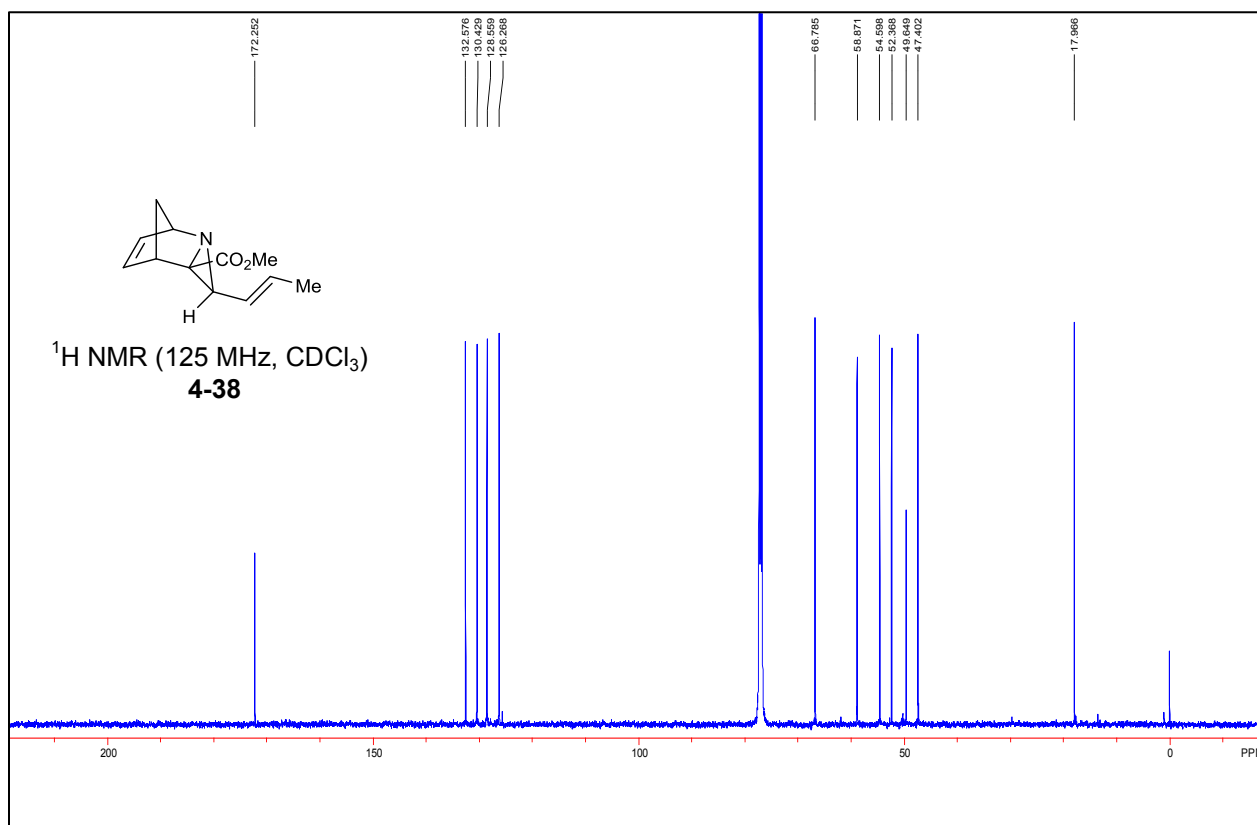
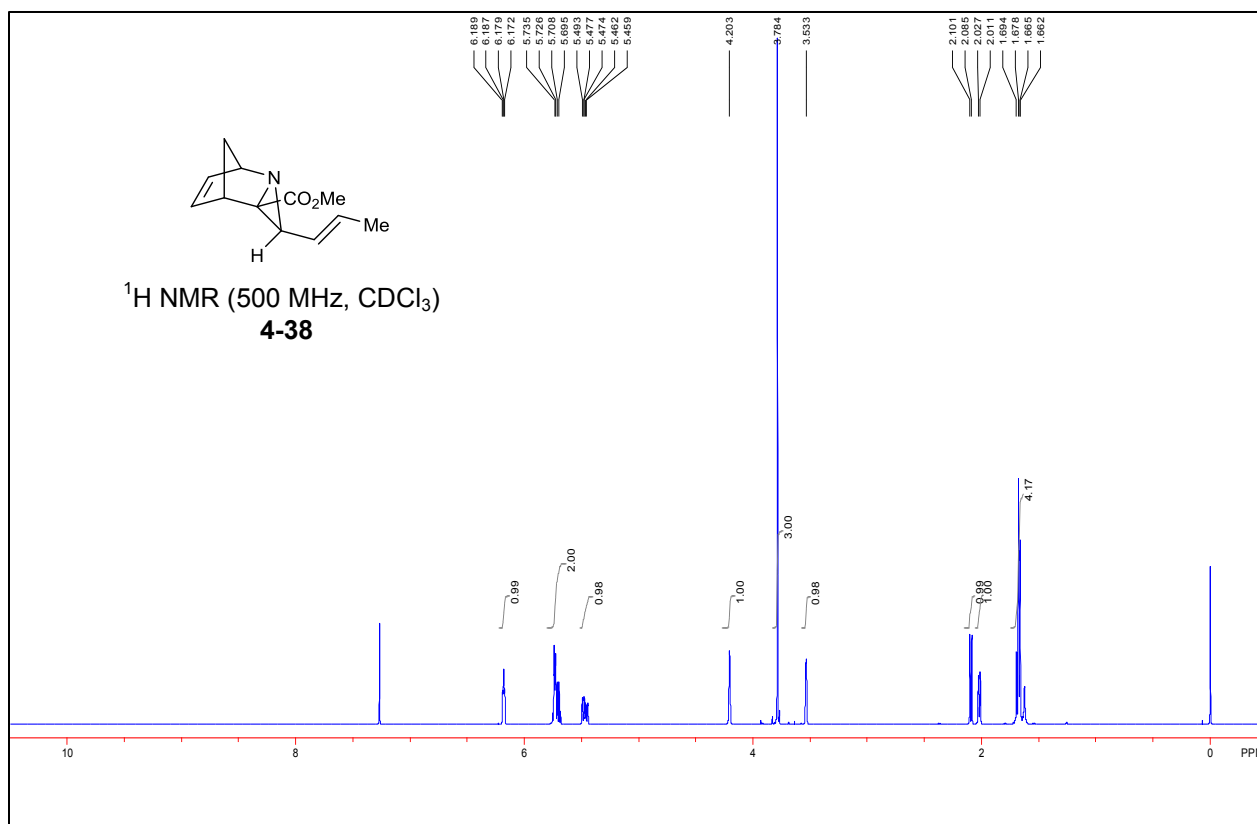


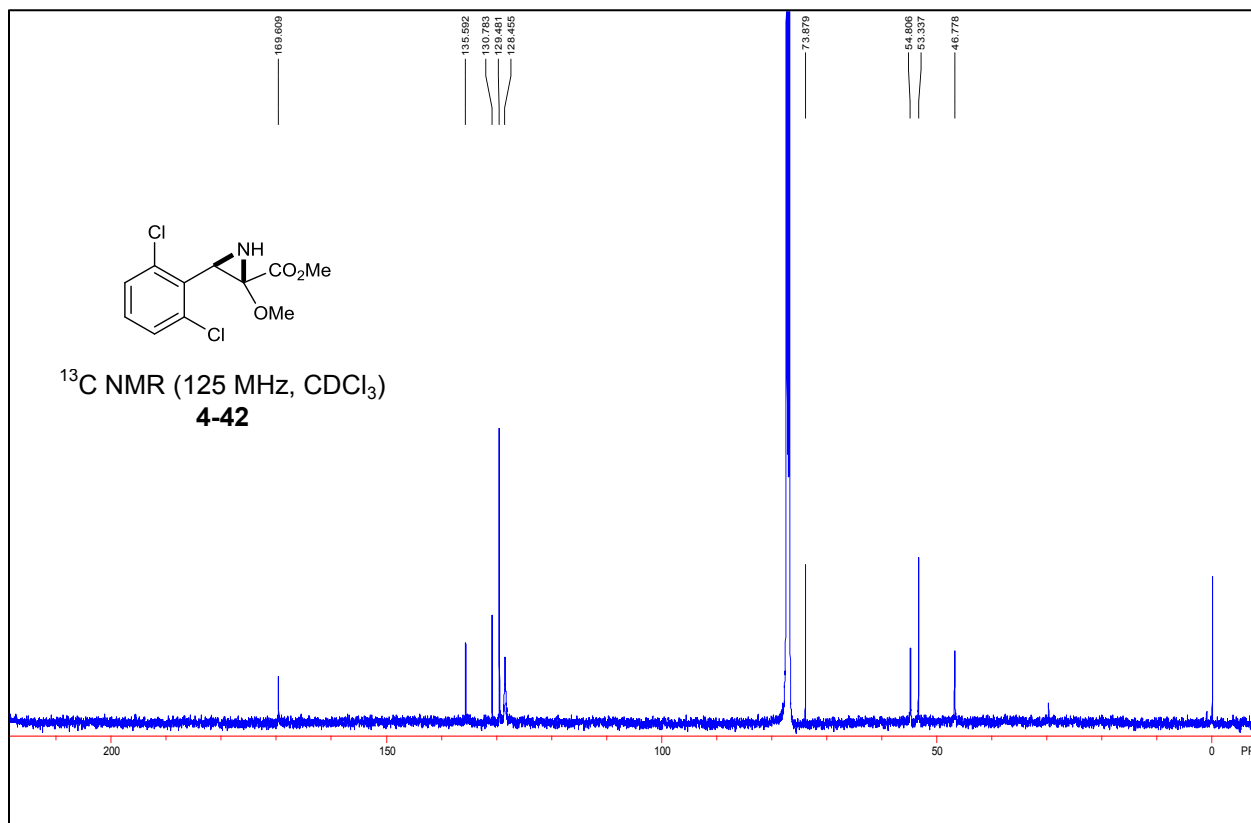
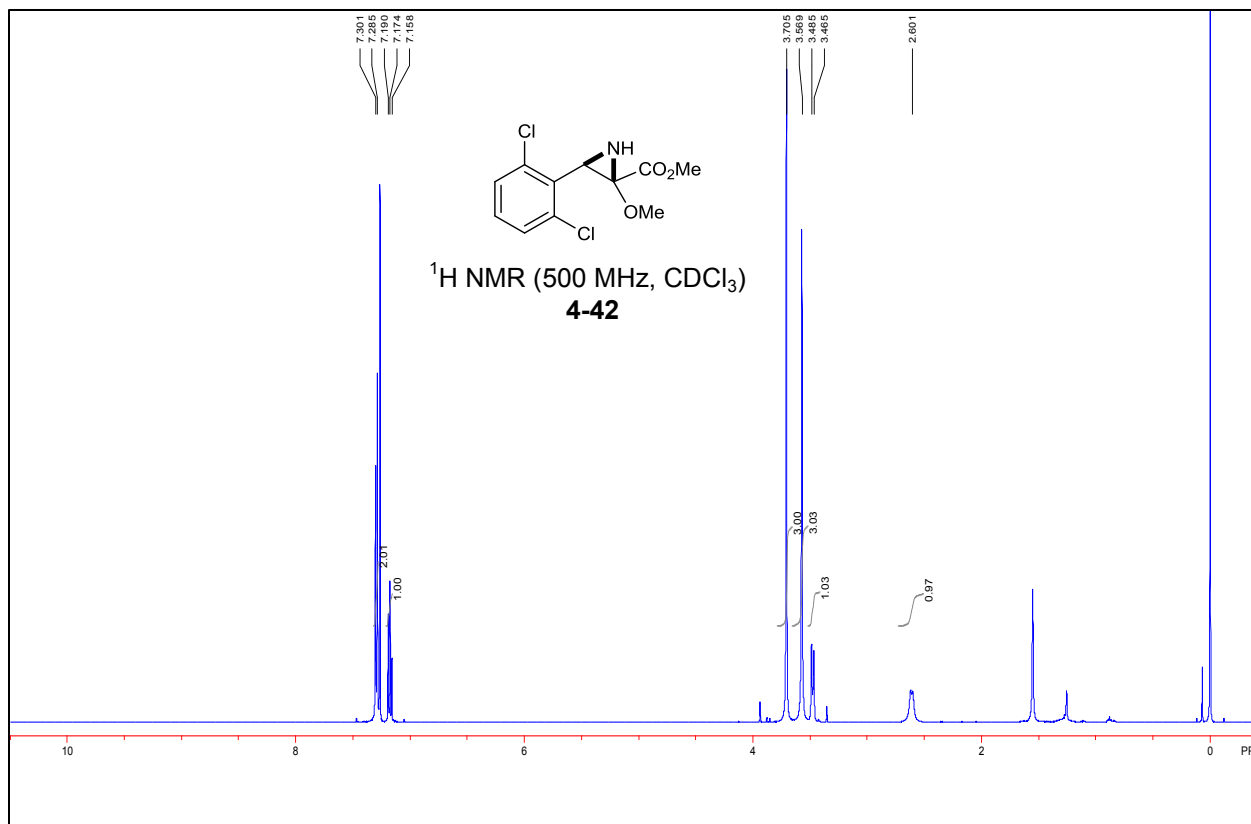


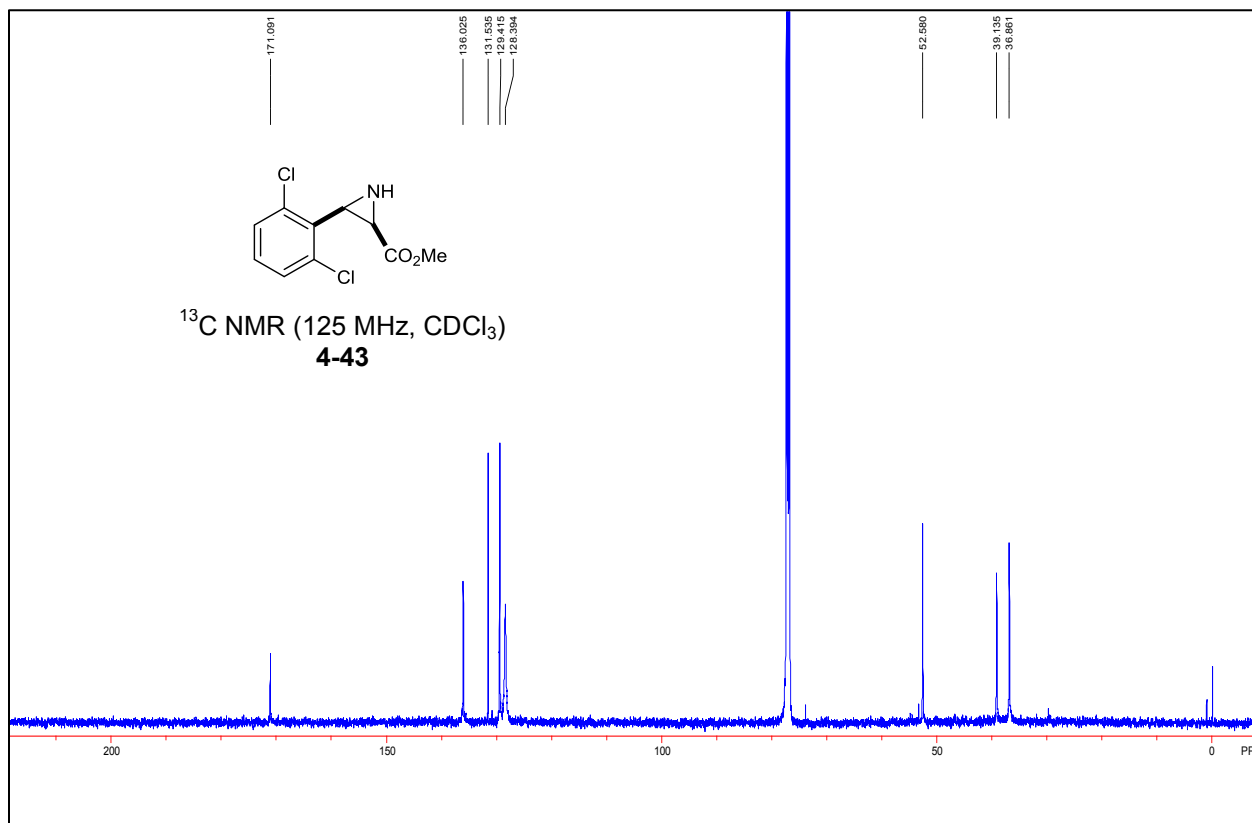
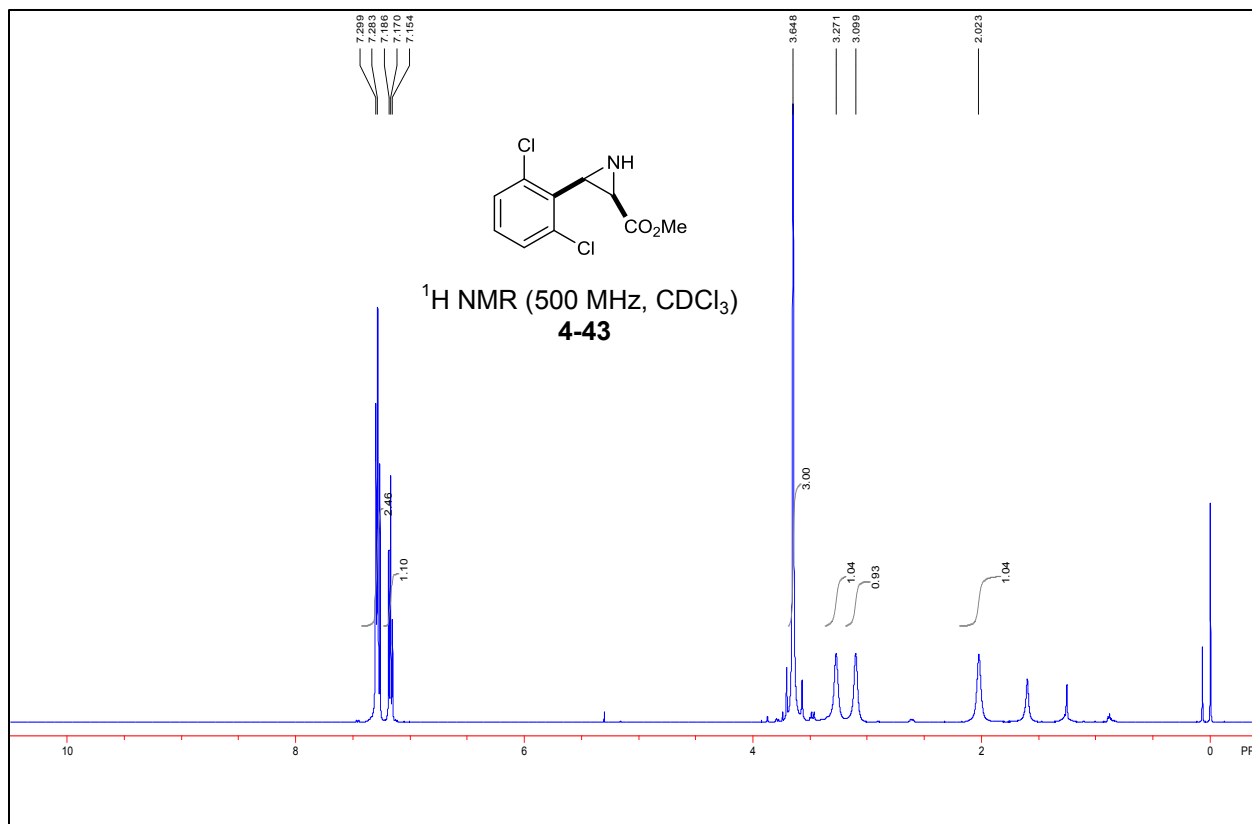


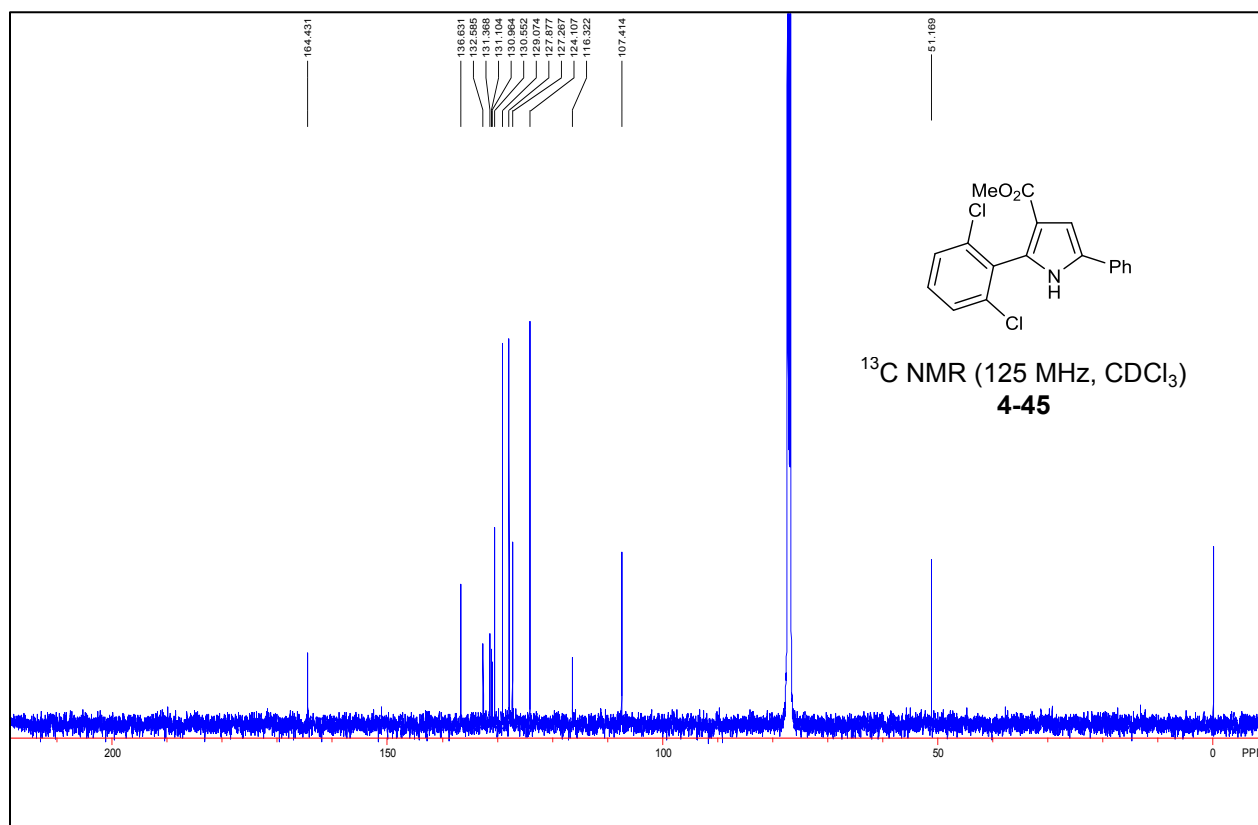
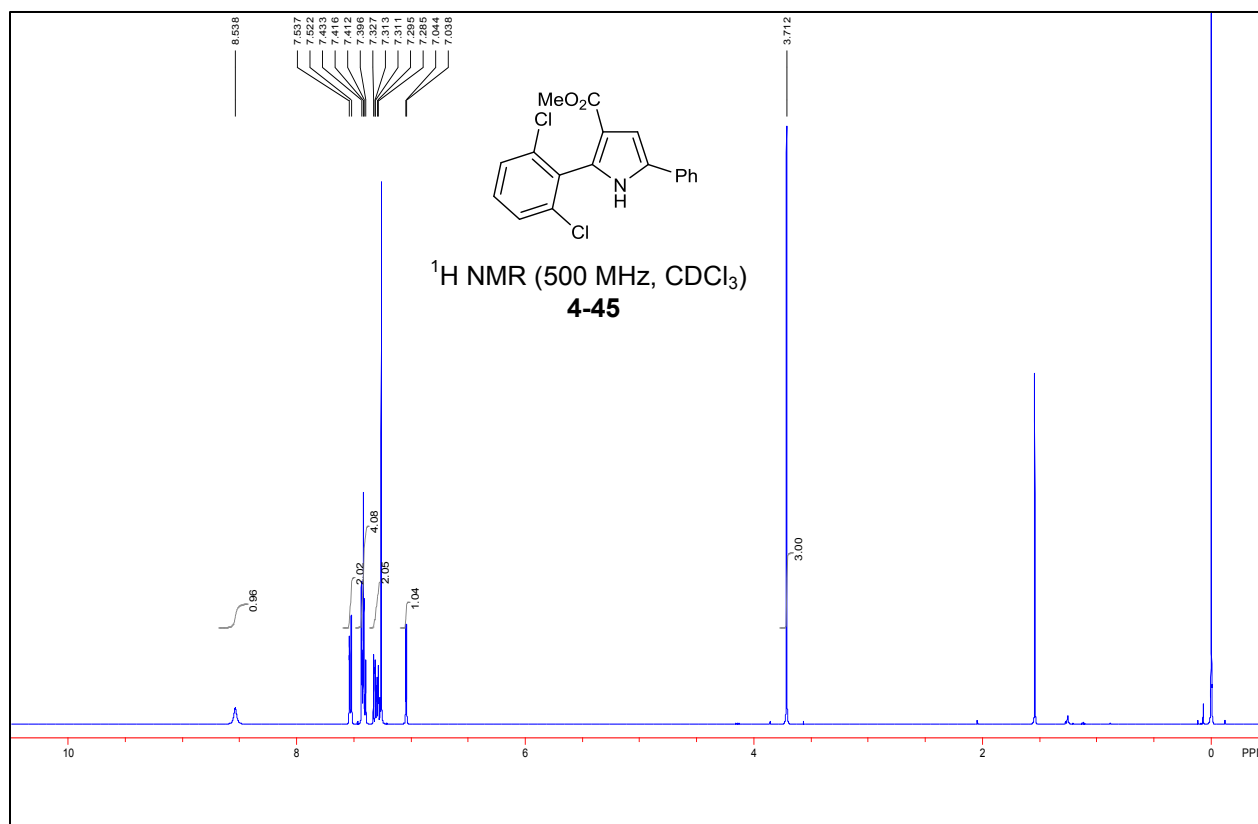




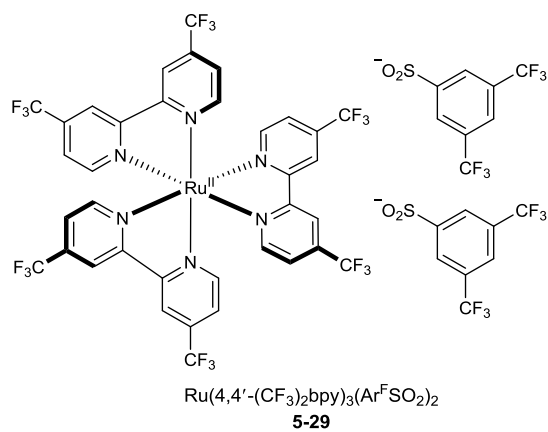
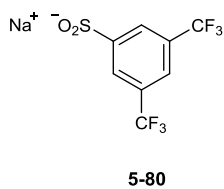
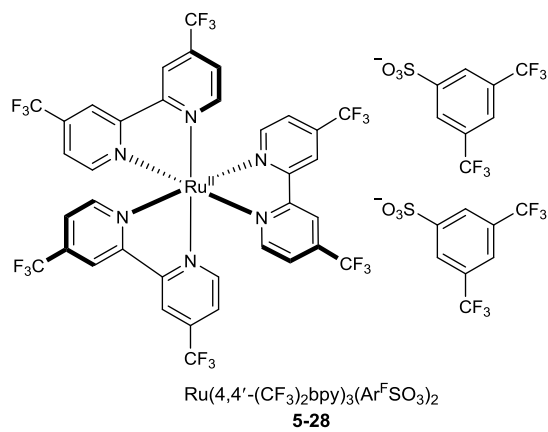
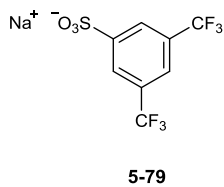
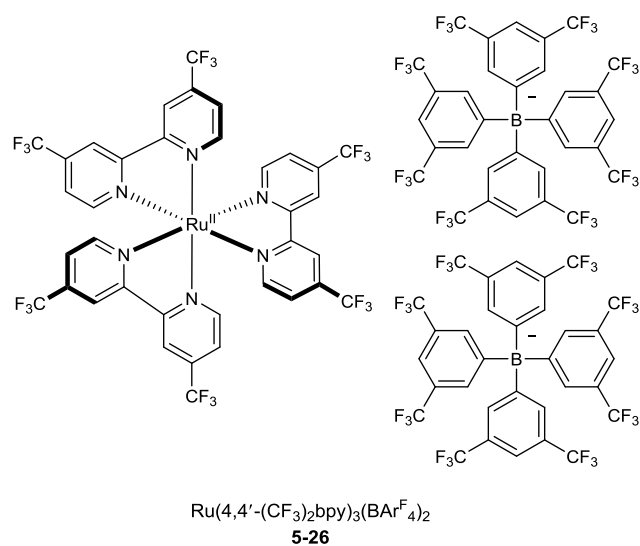
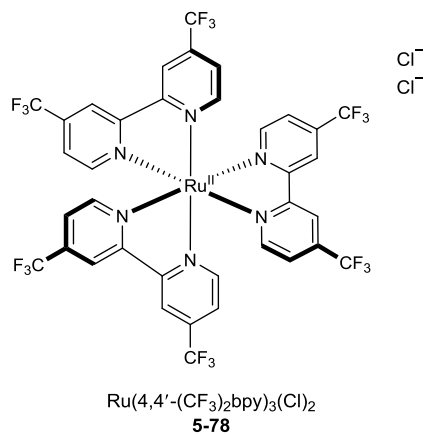


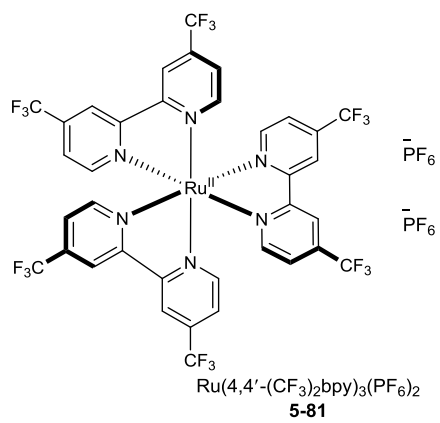
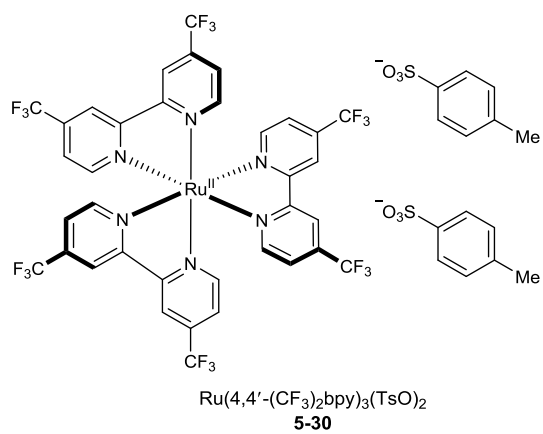


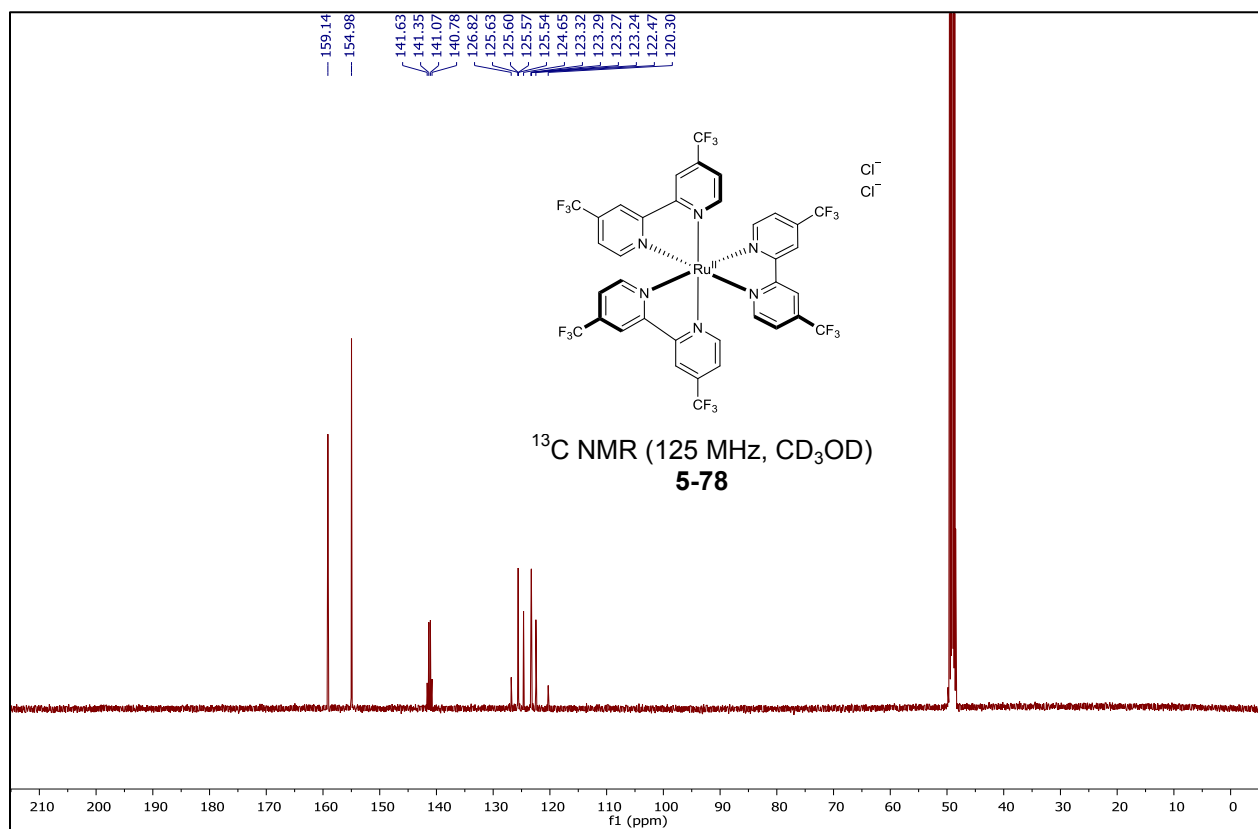
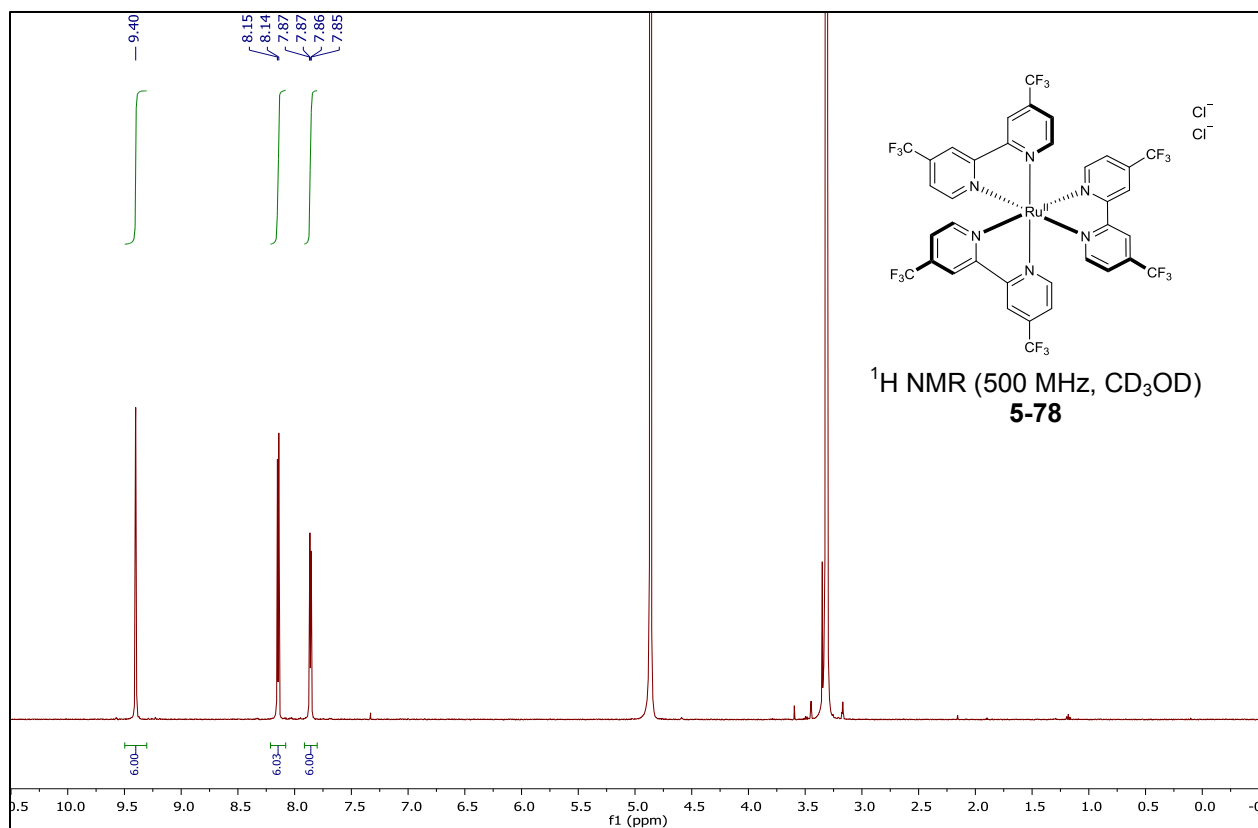


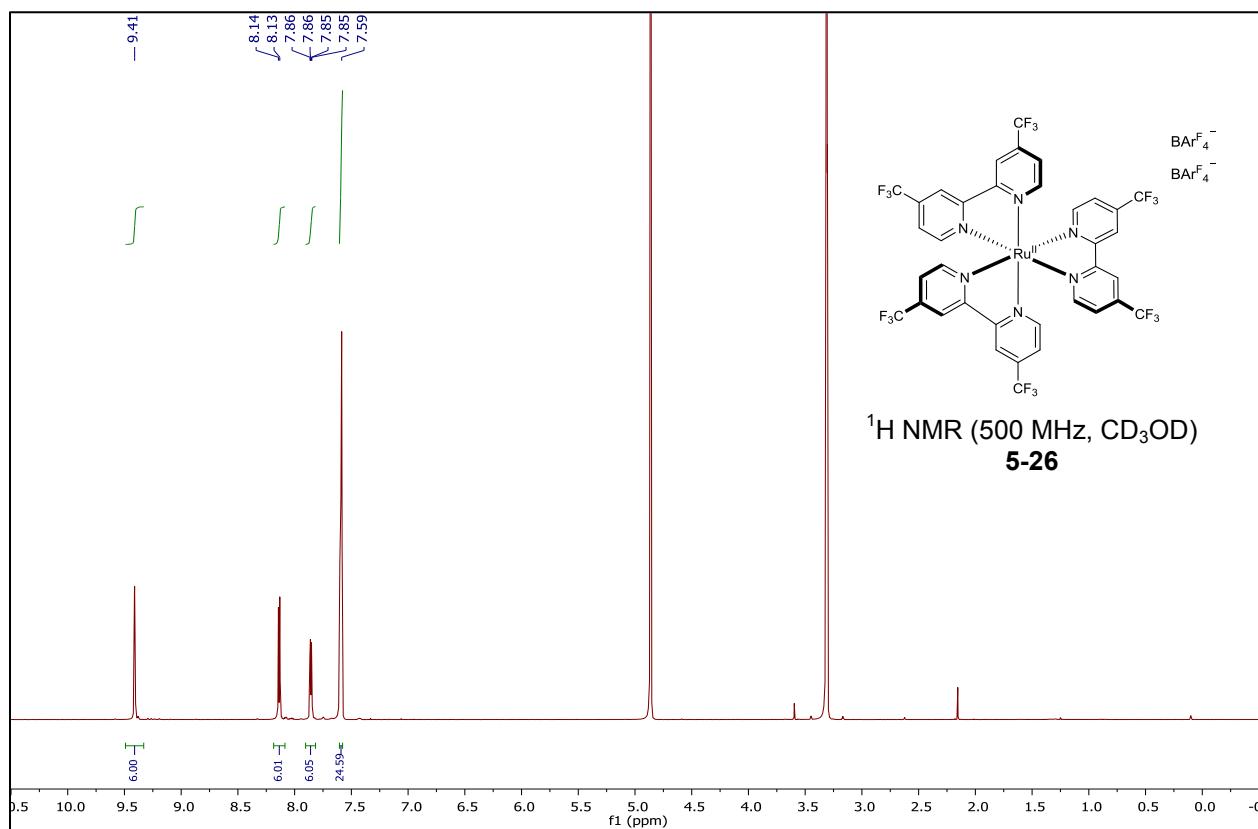
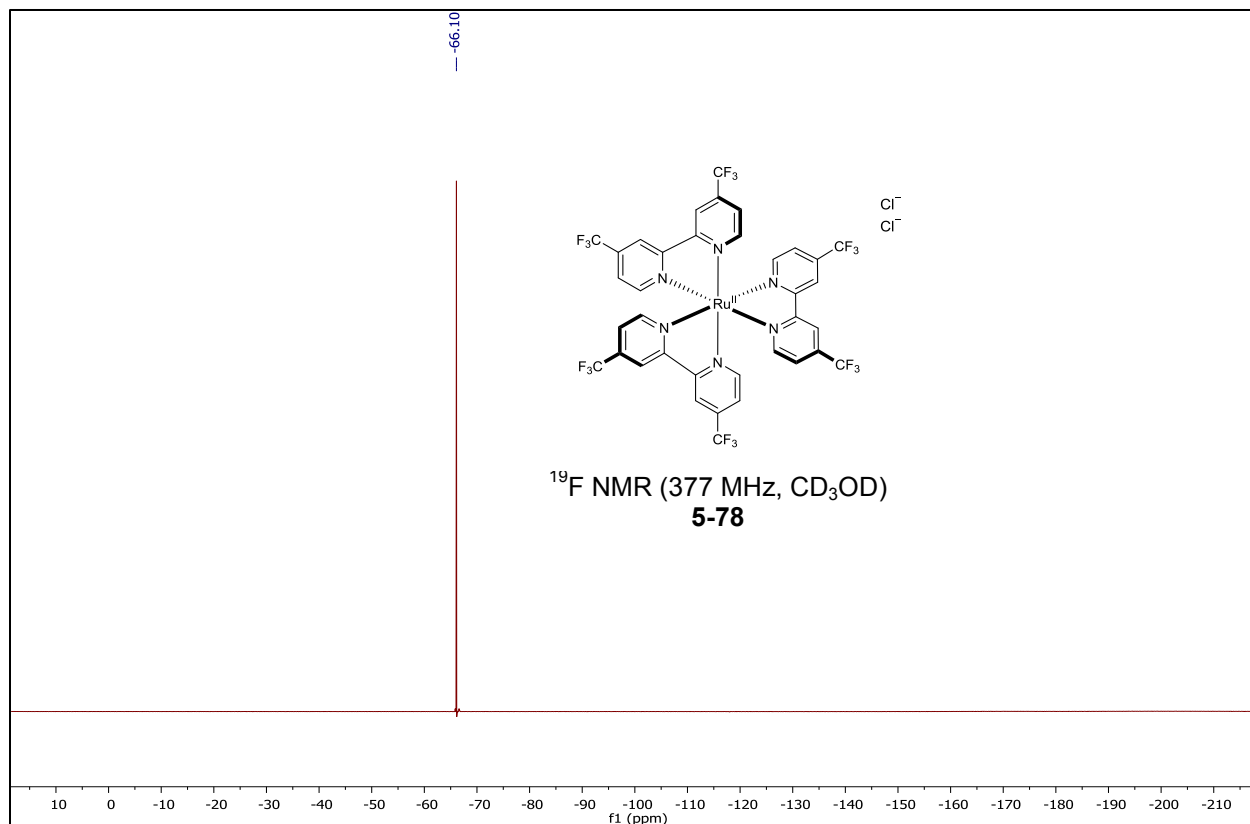


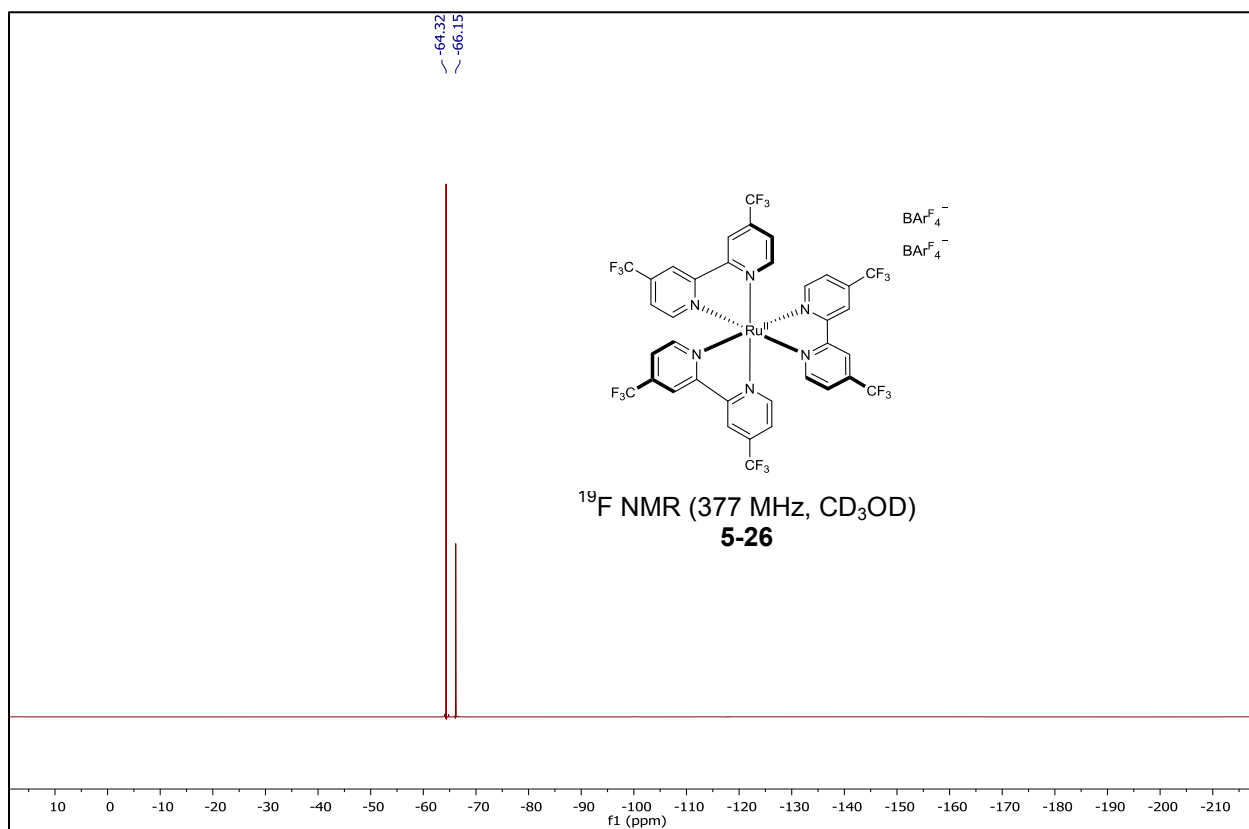
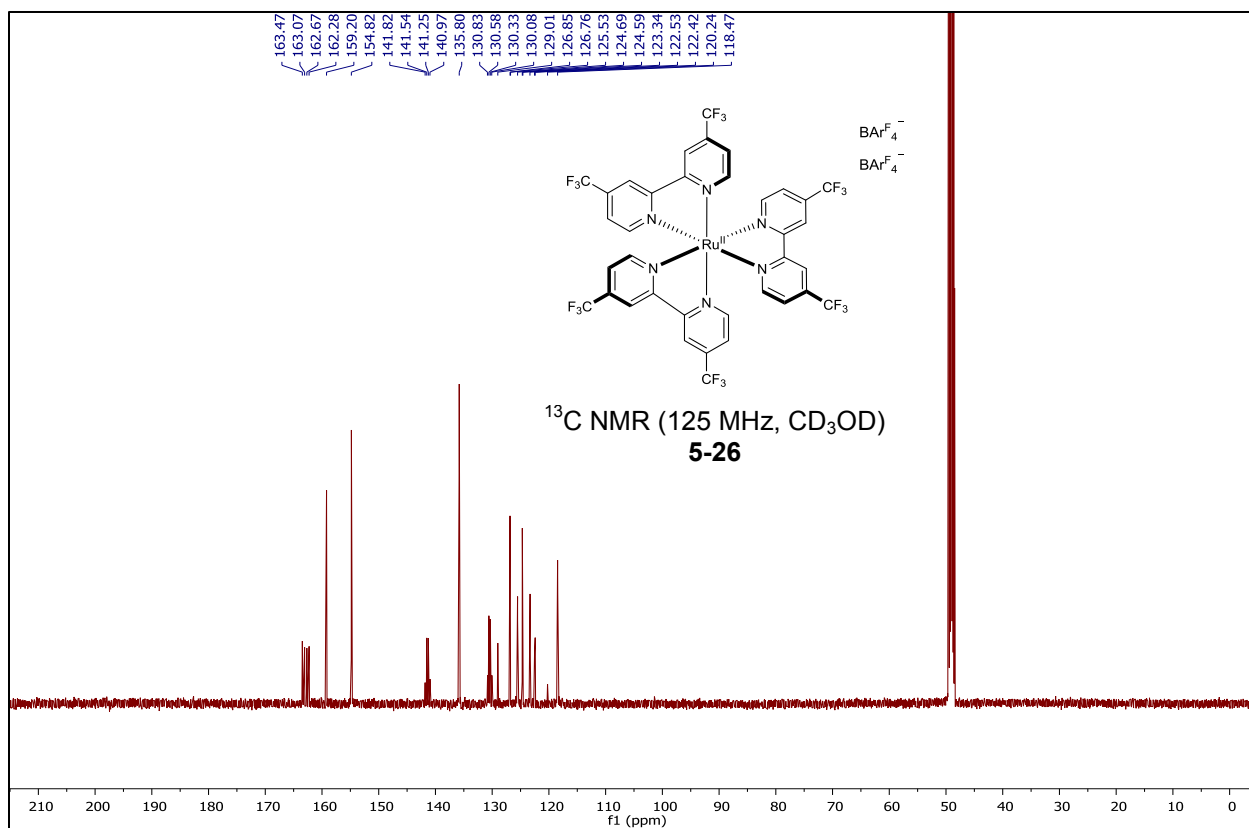
A.3 List of Compounds for Chapter 5

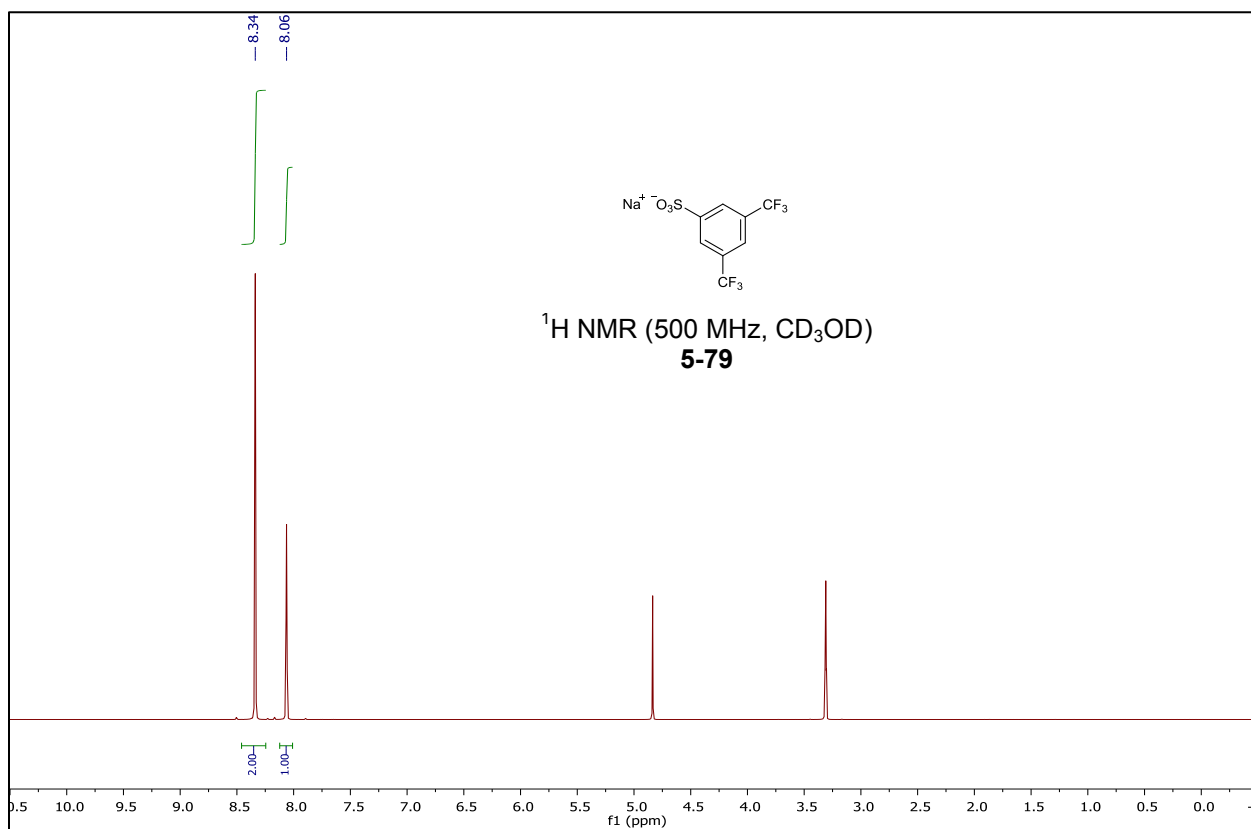
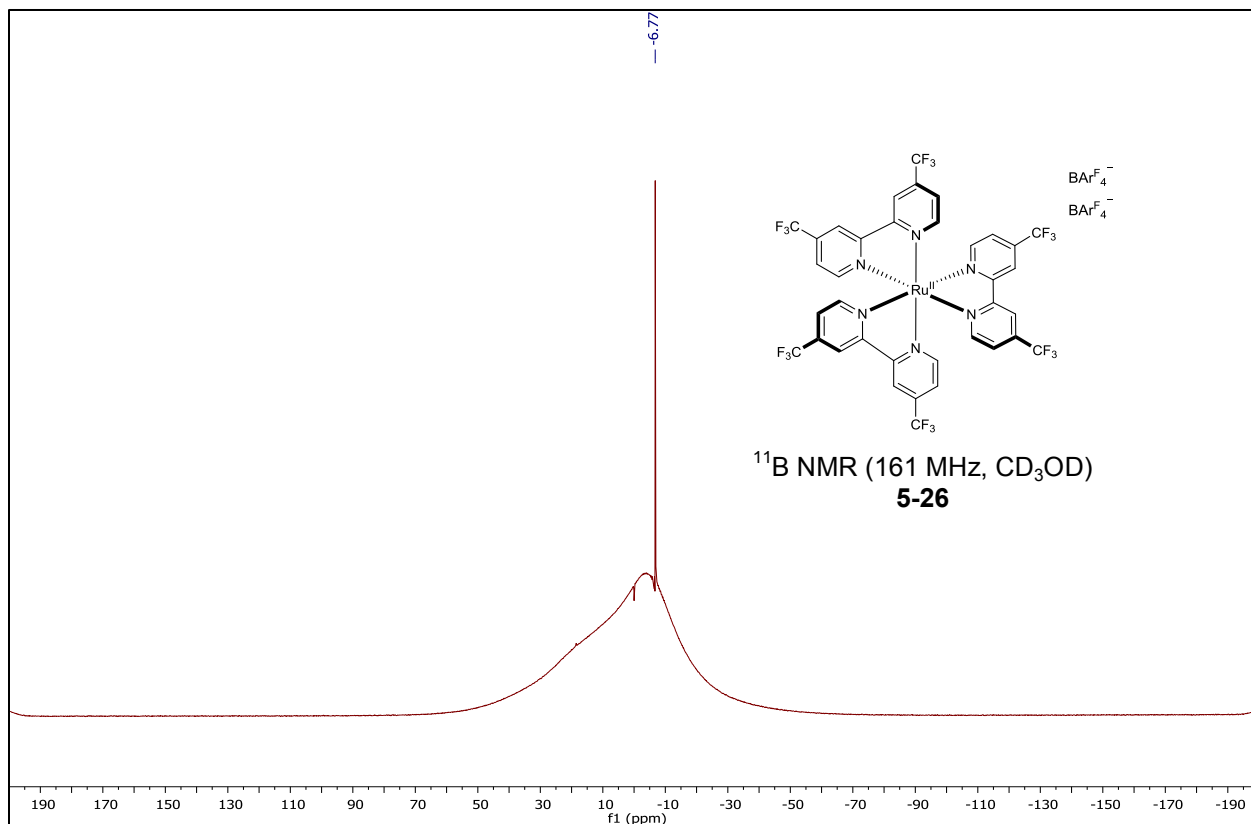


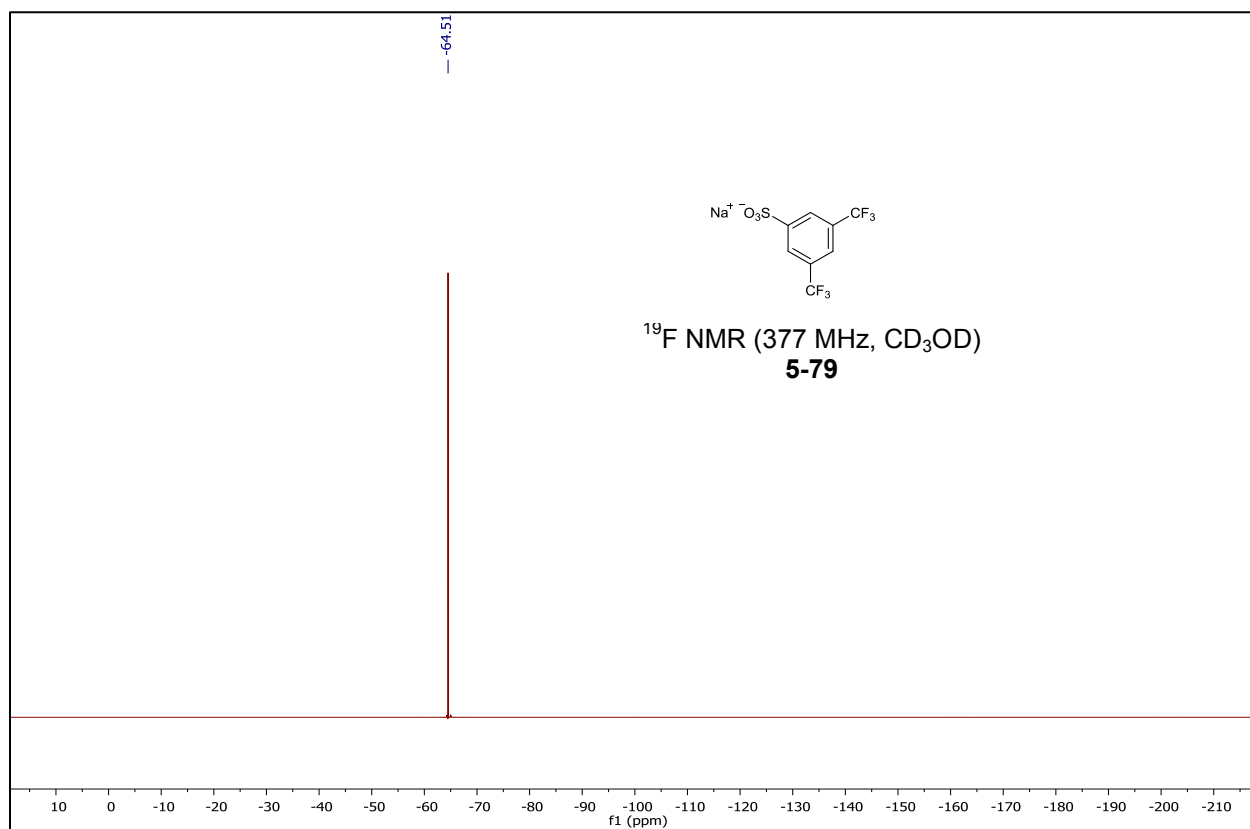
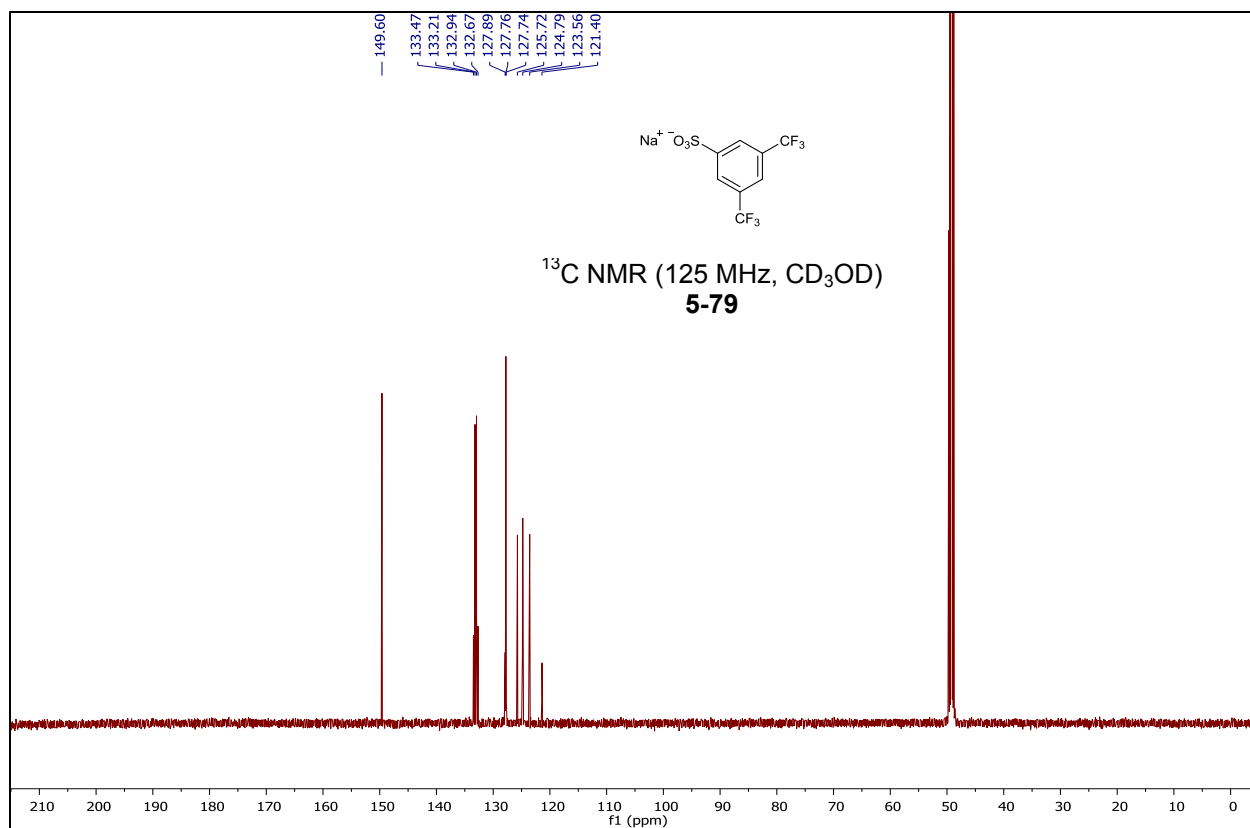


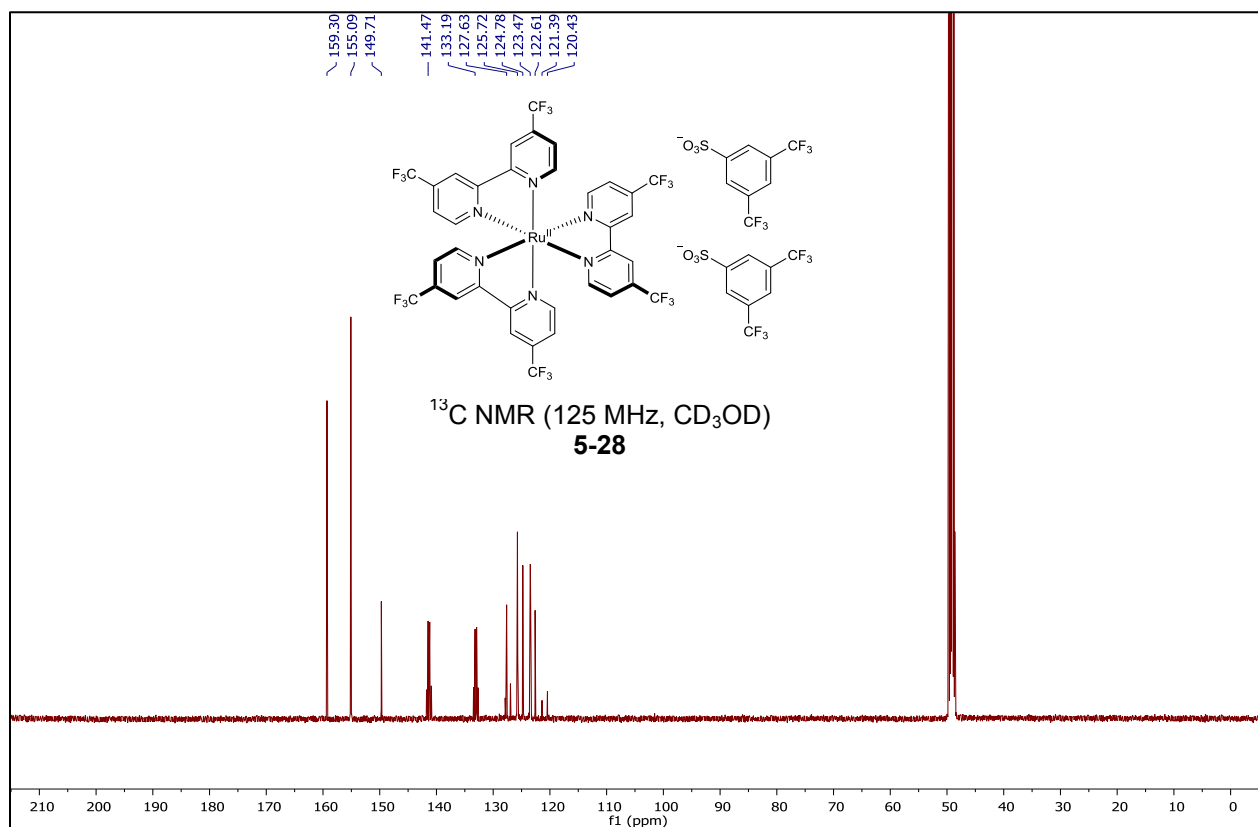
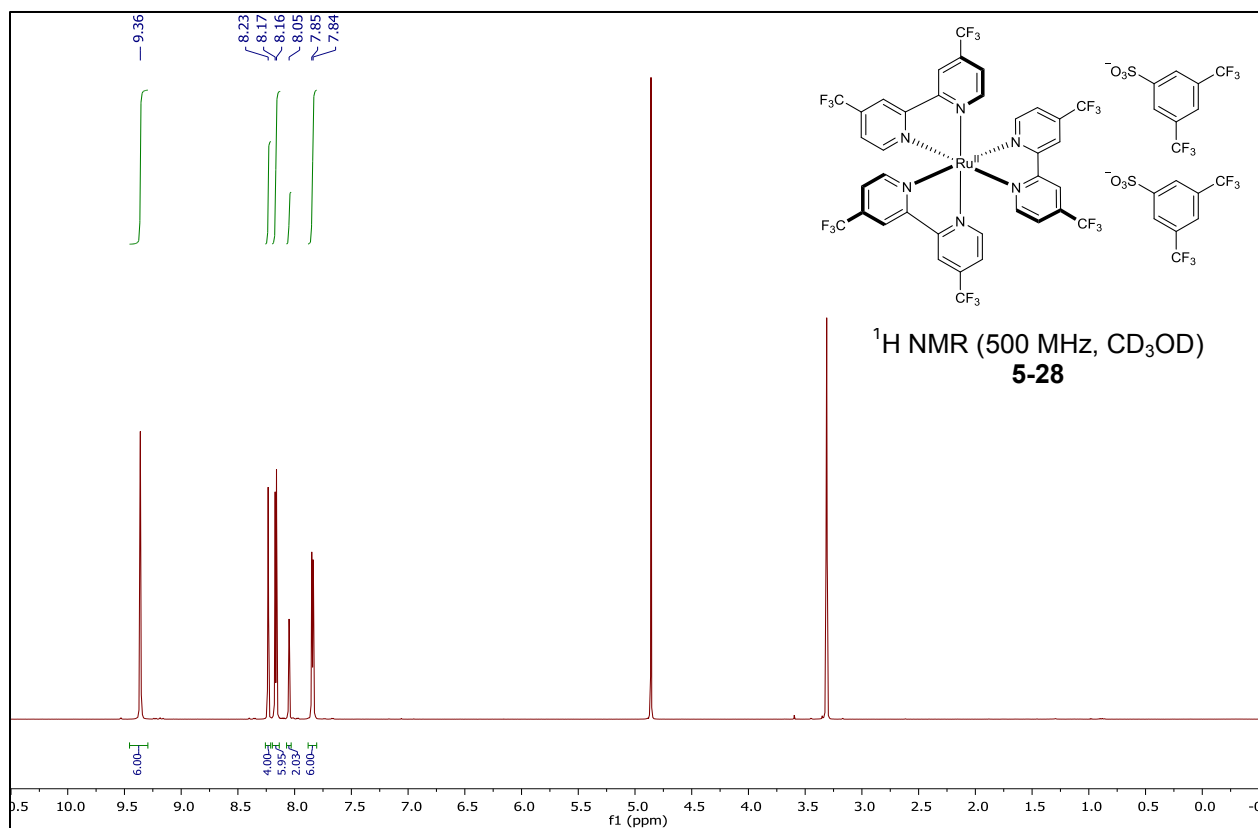


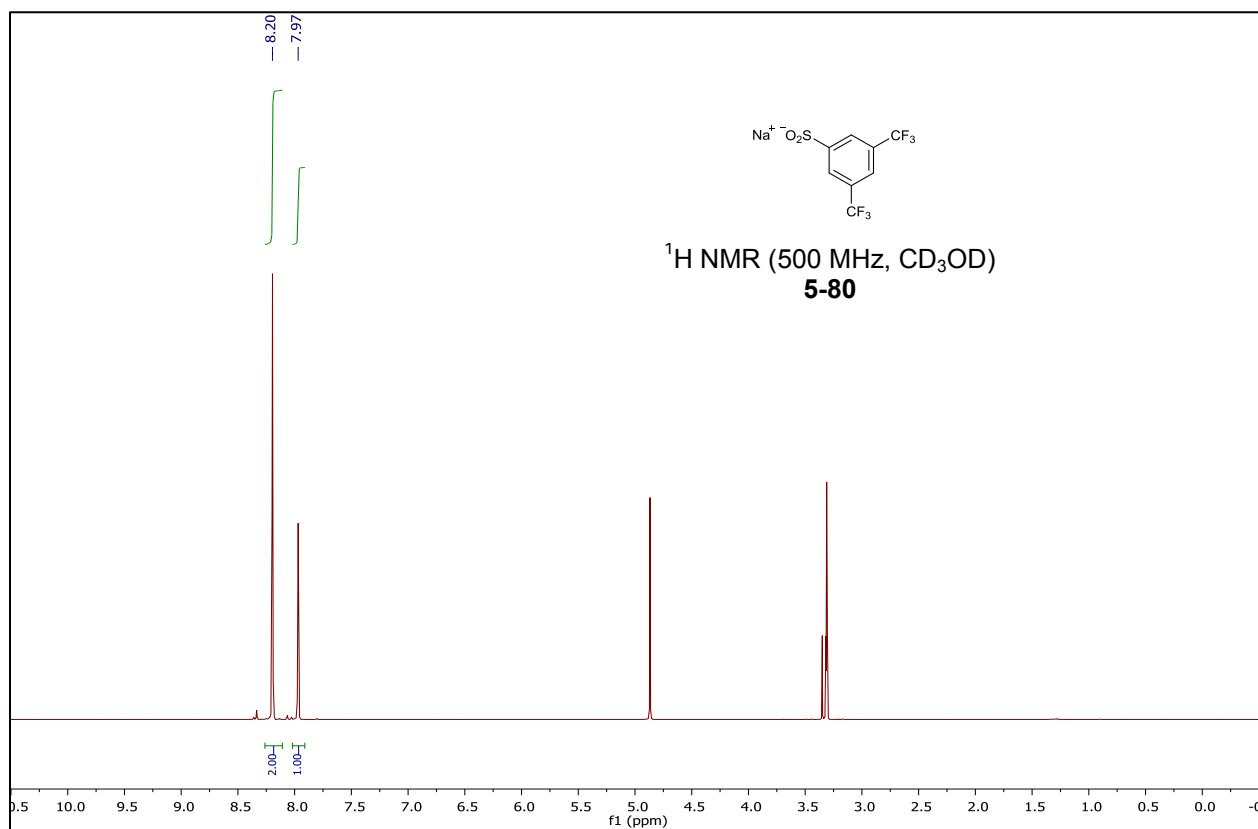
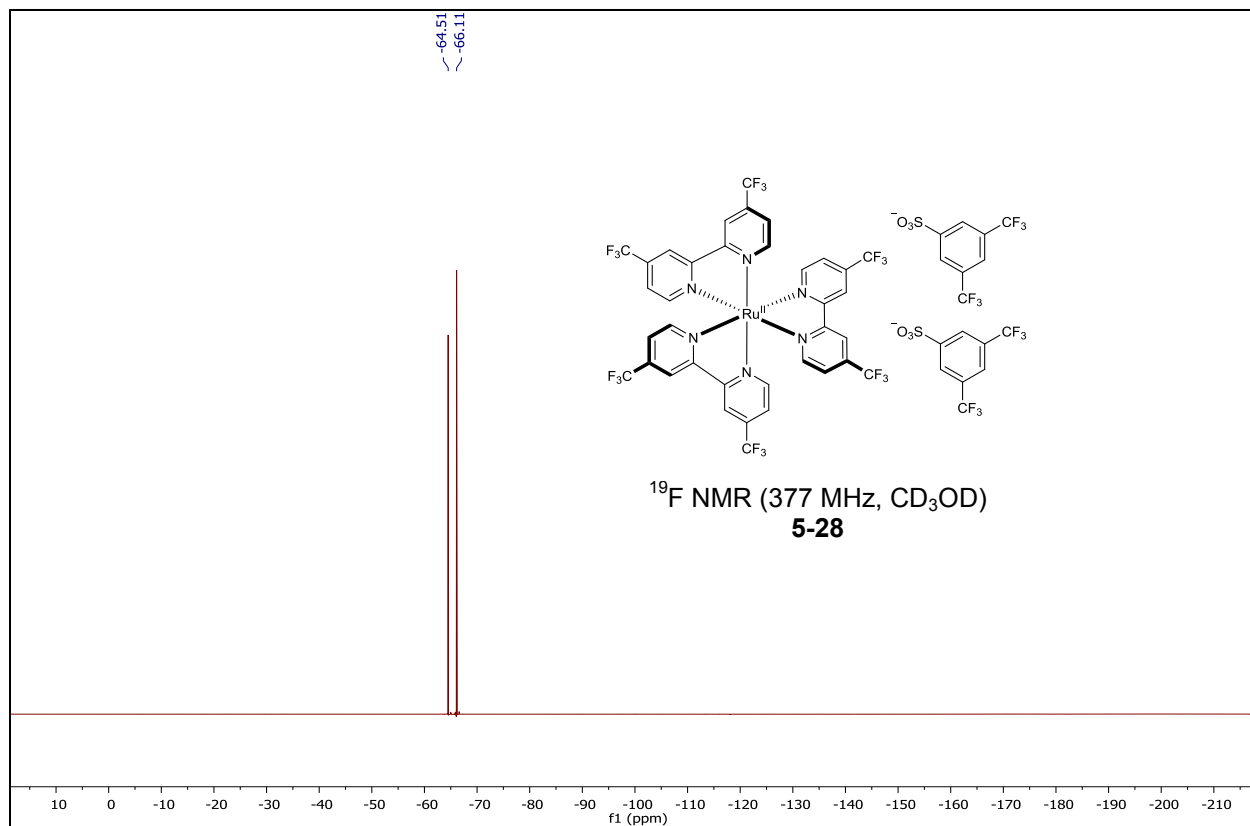


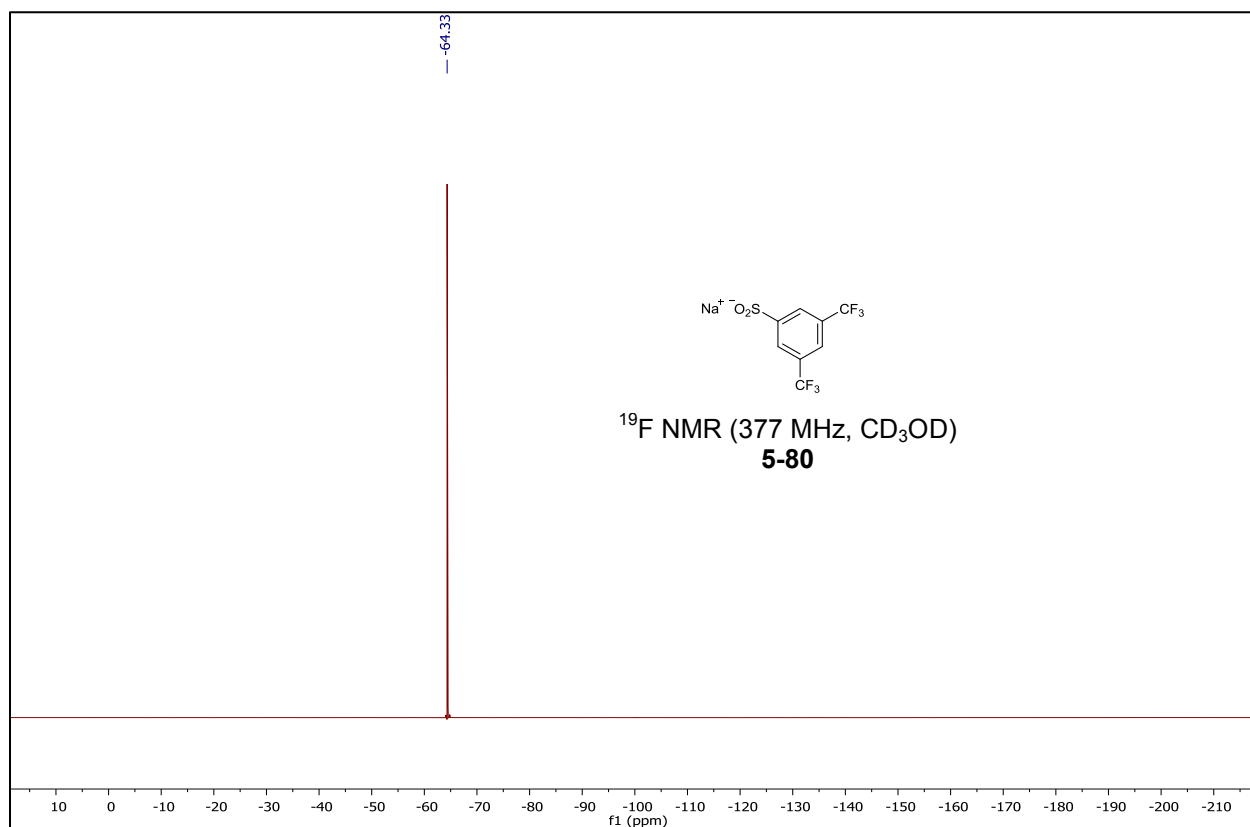
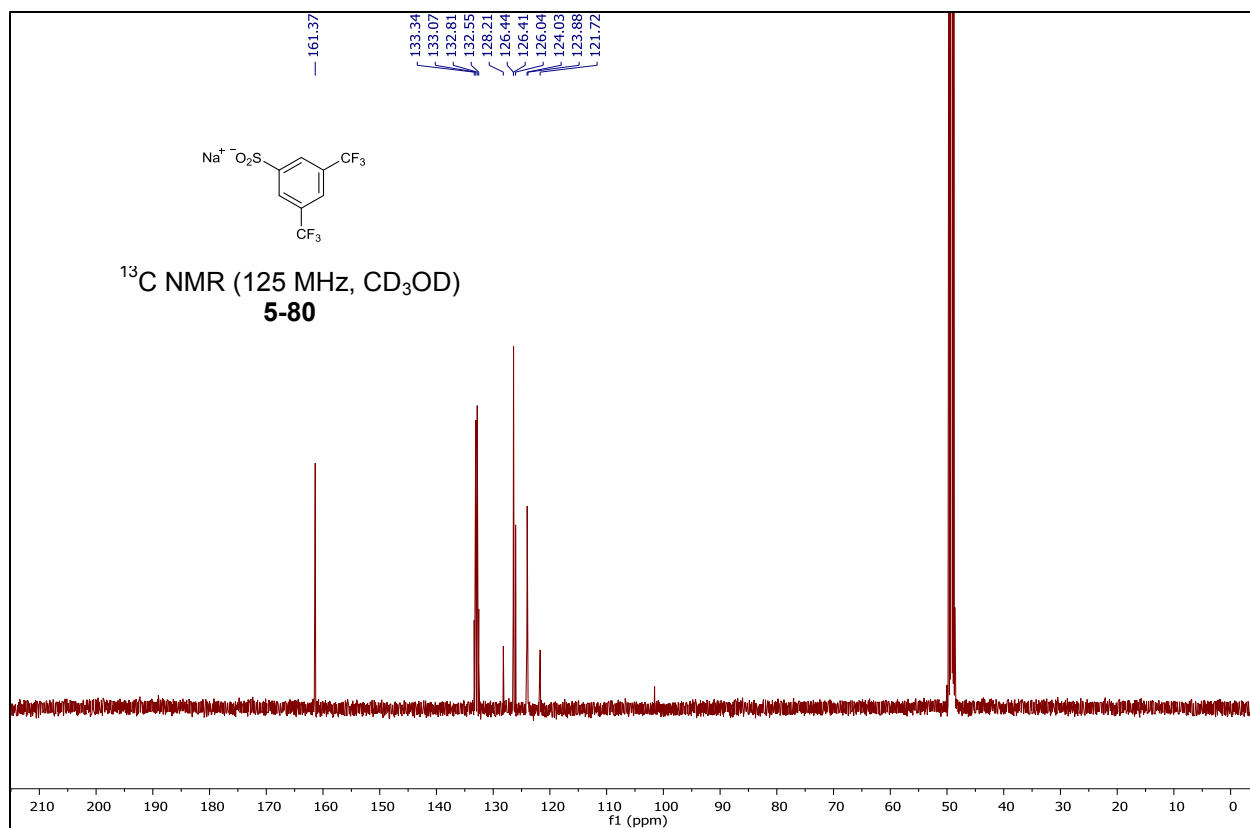


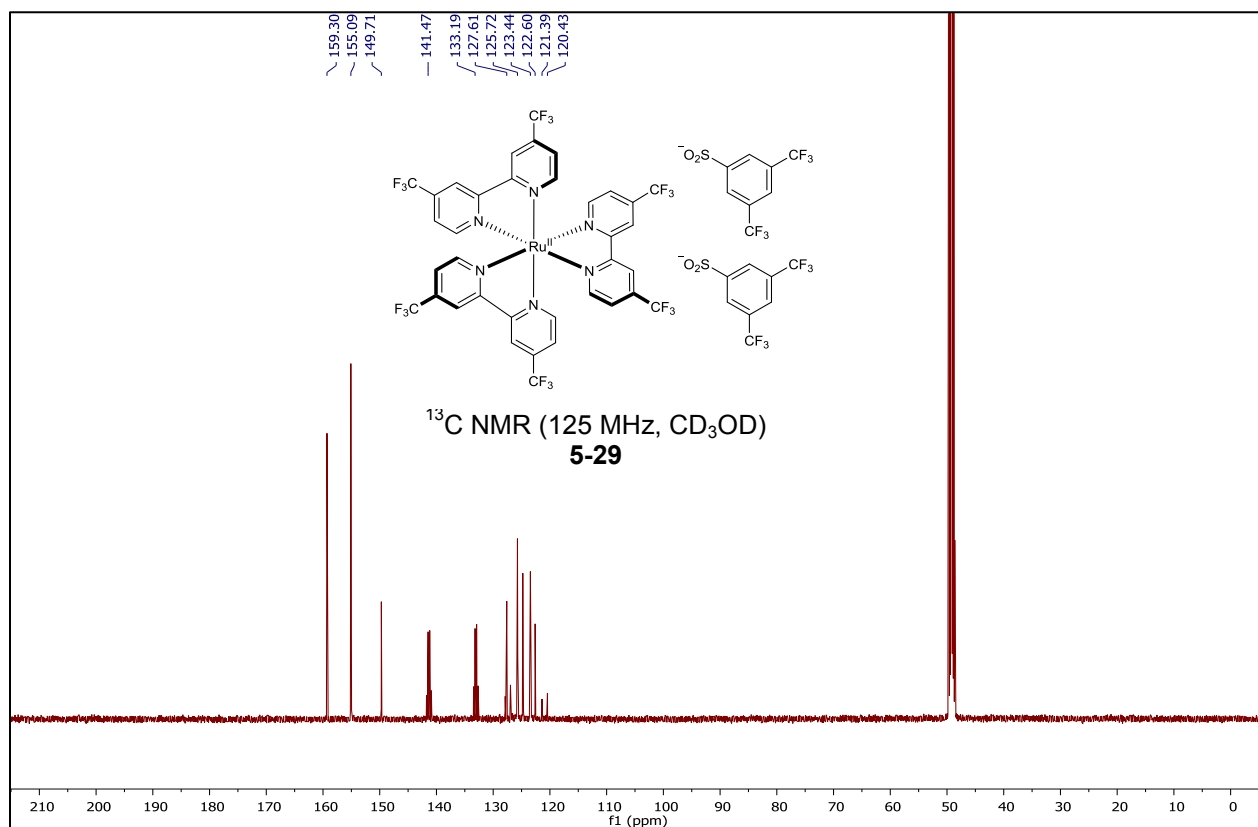
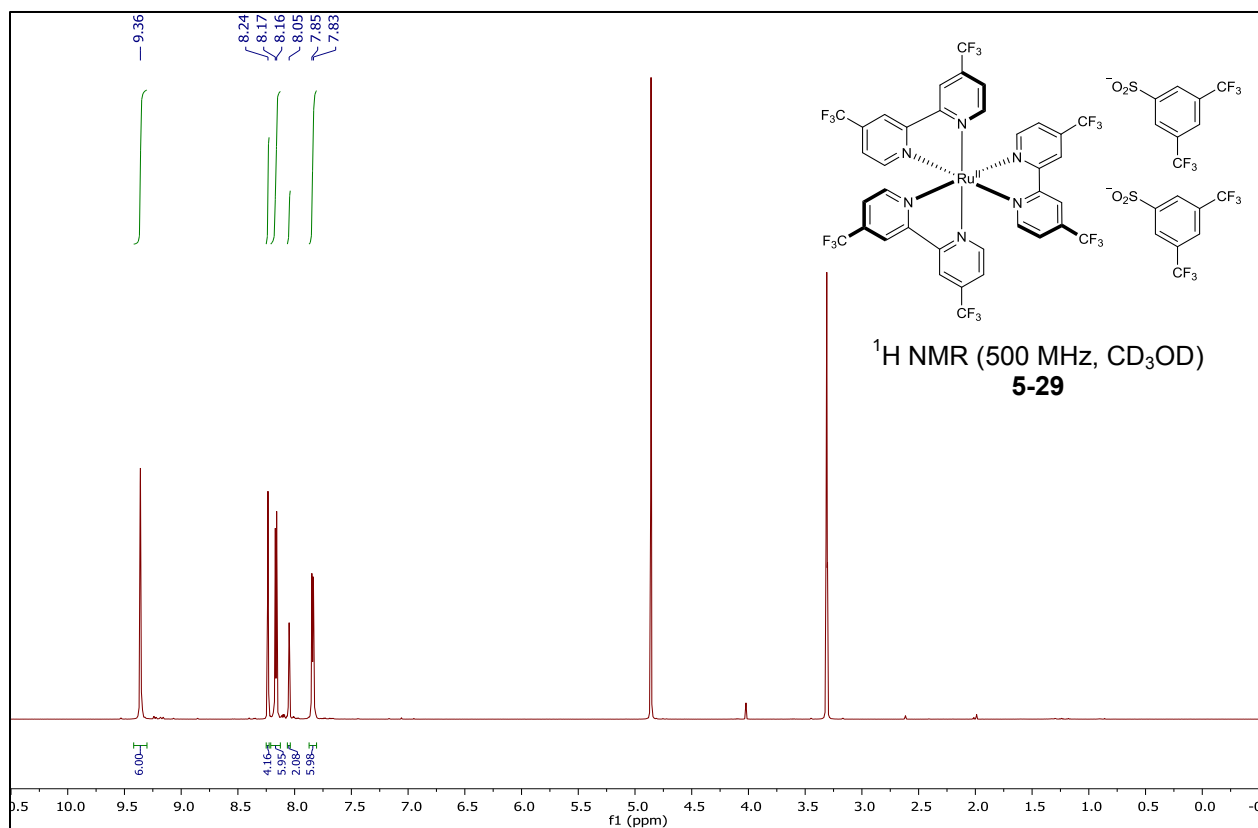


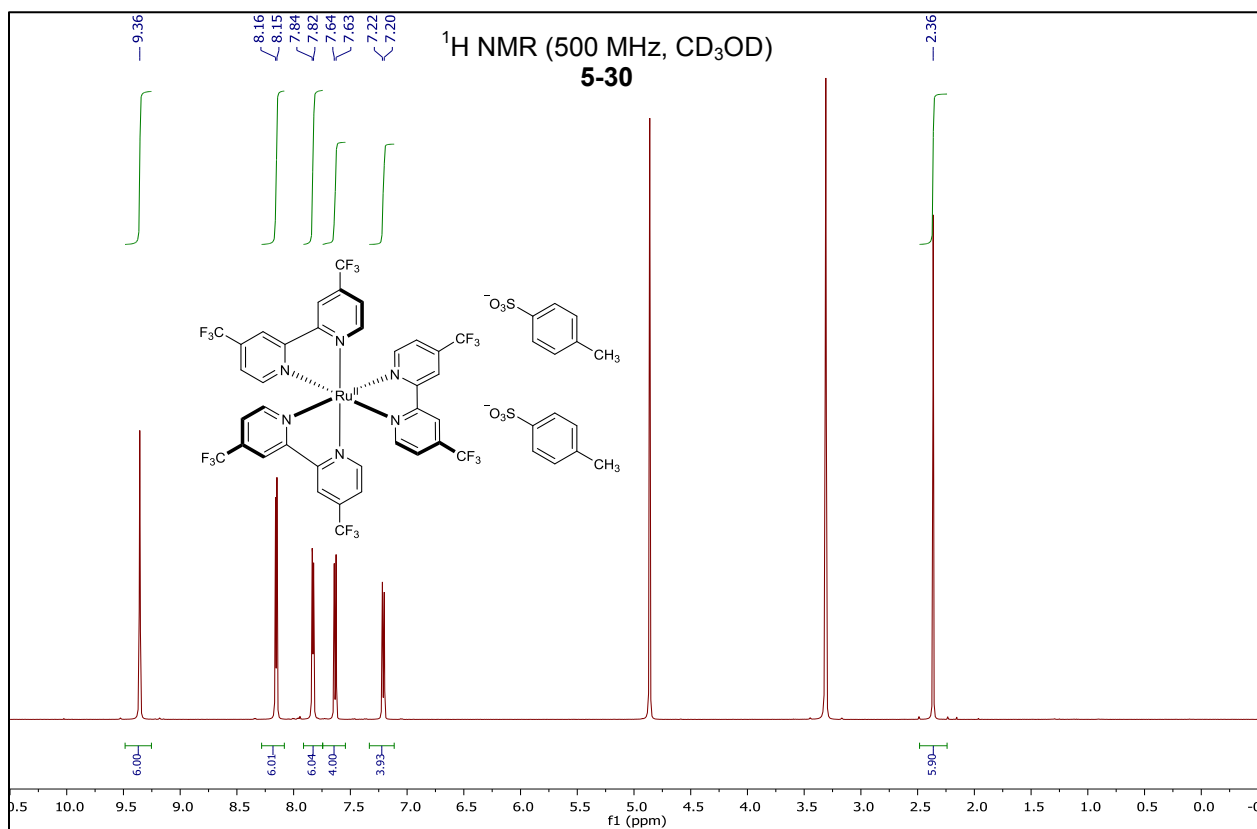
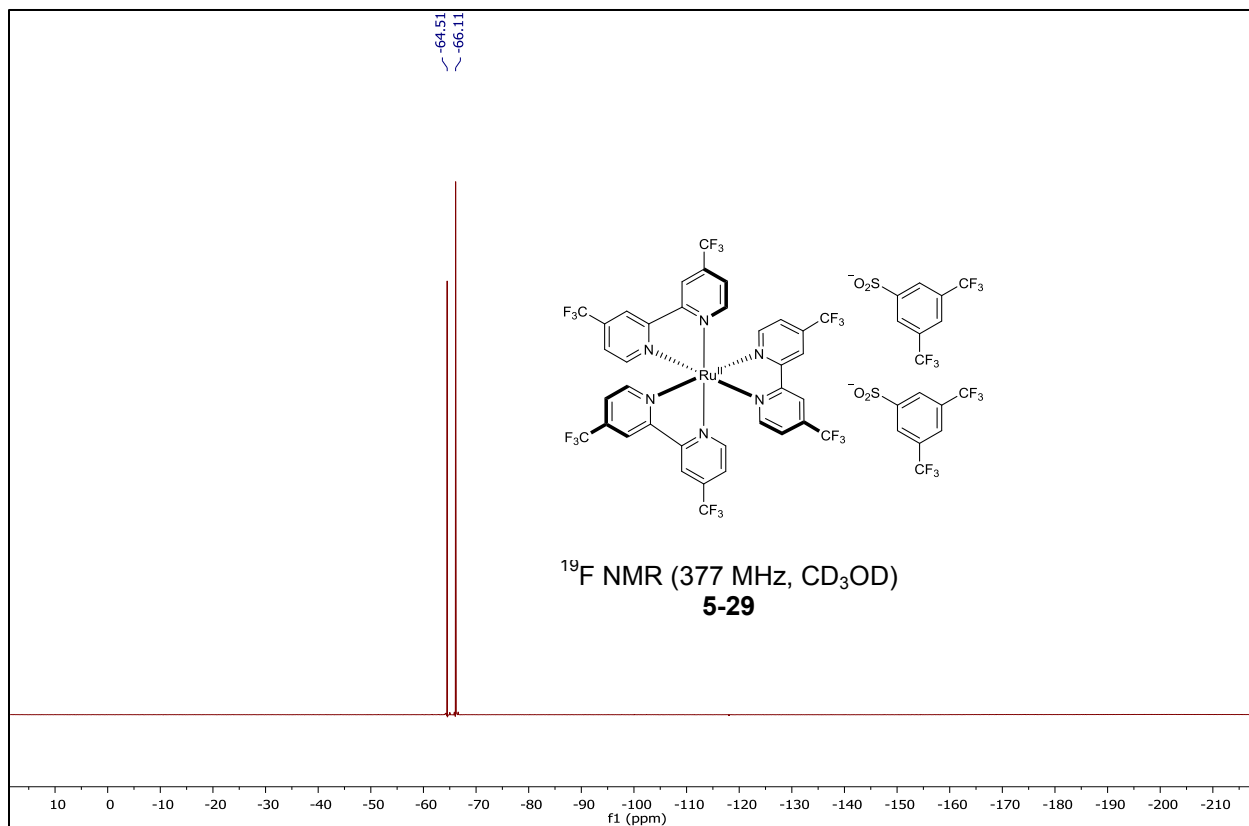


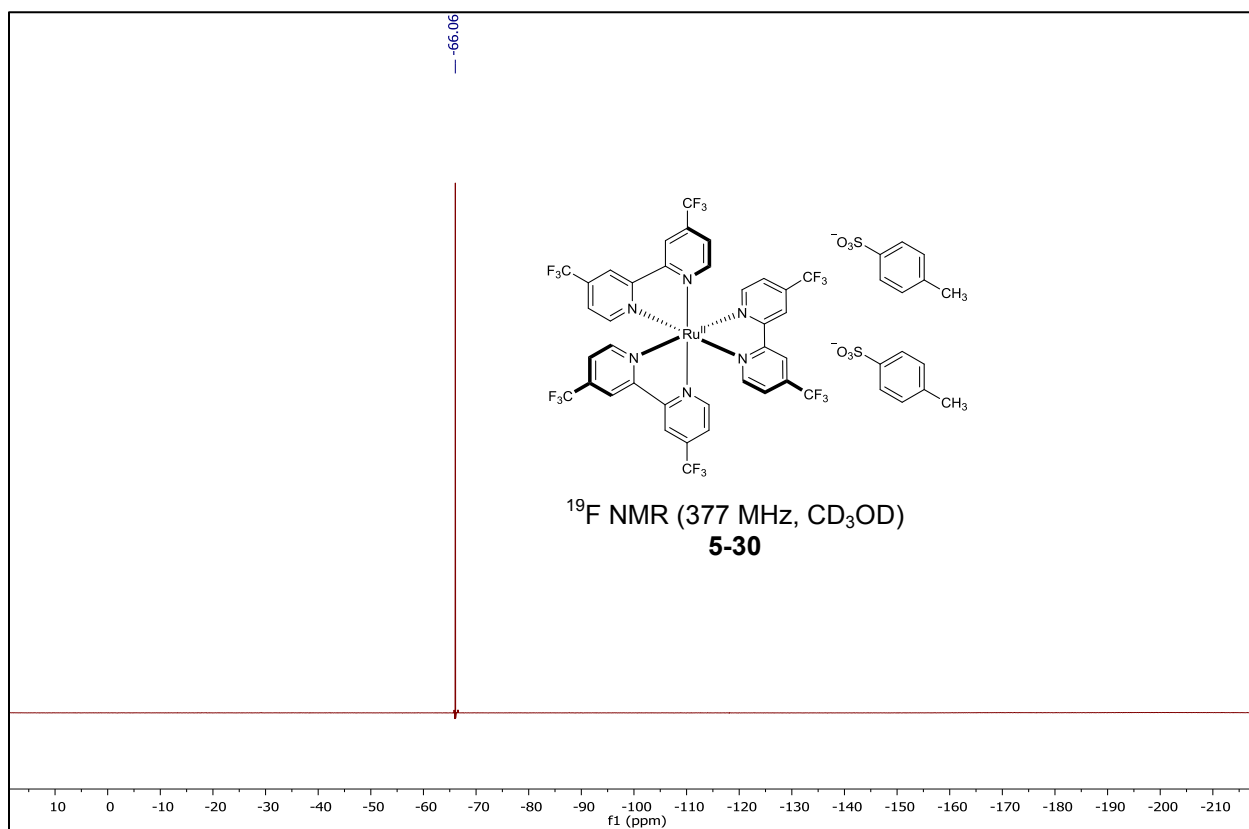
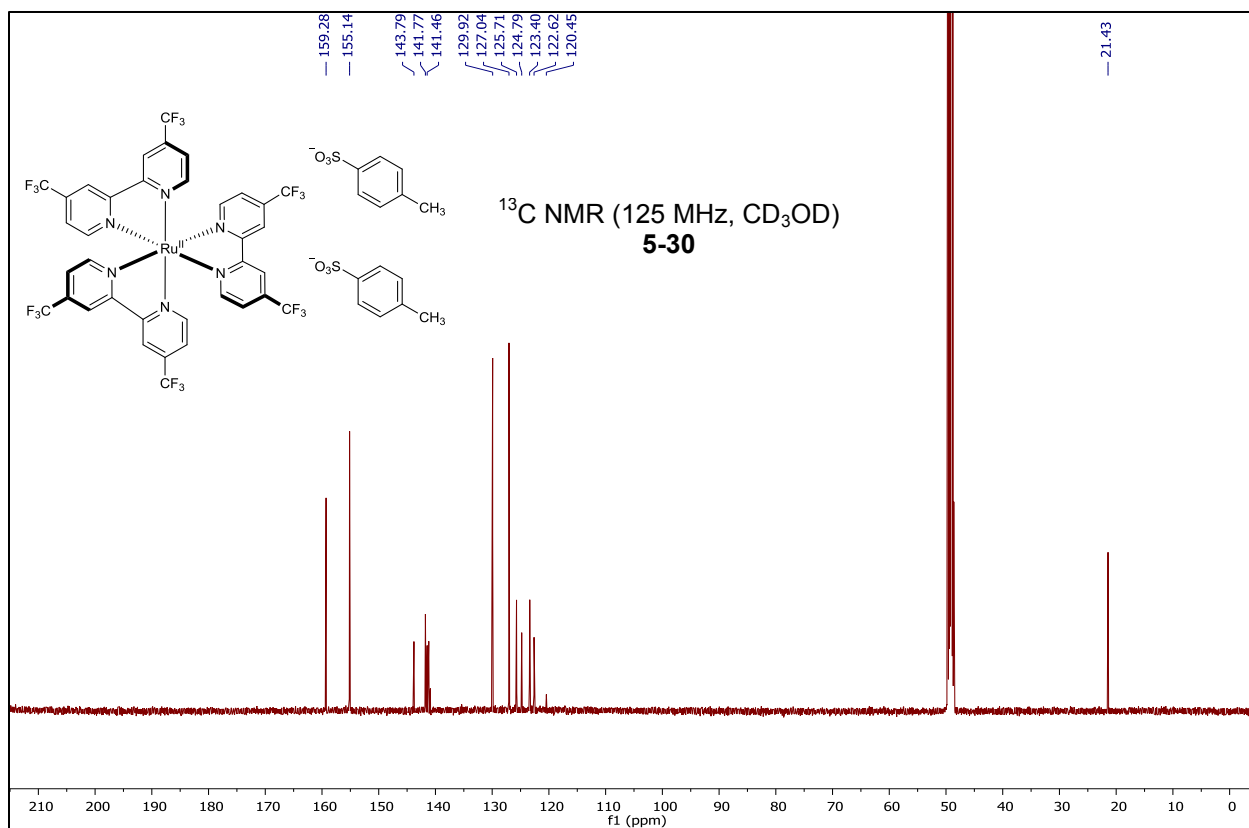


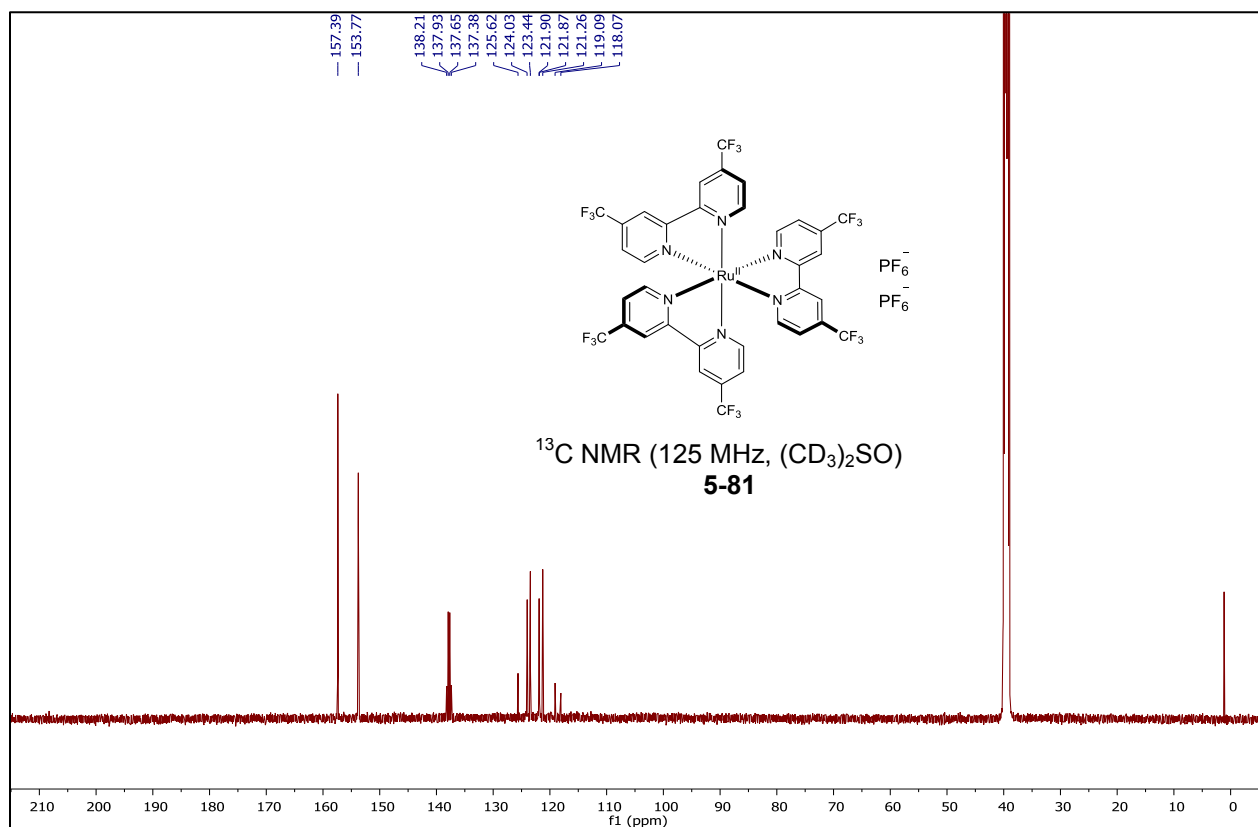
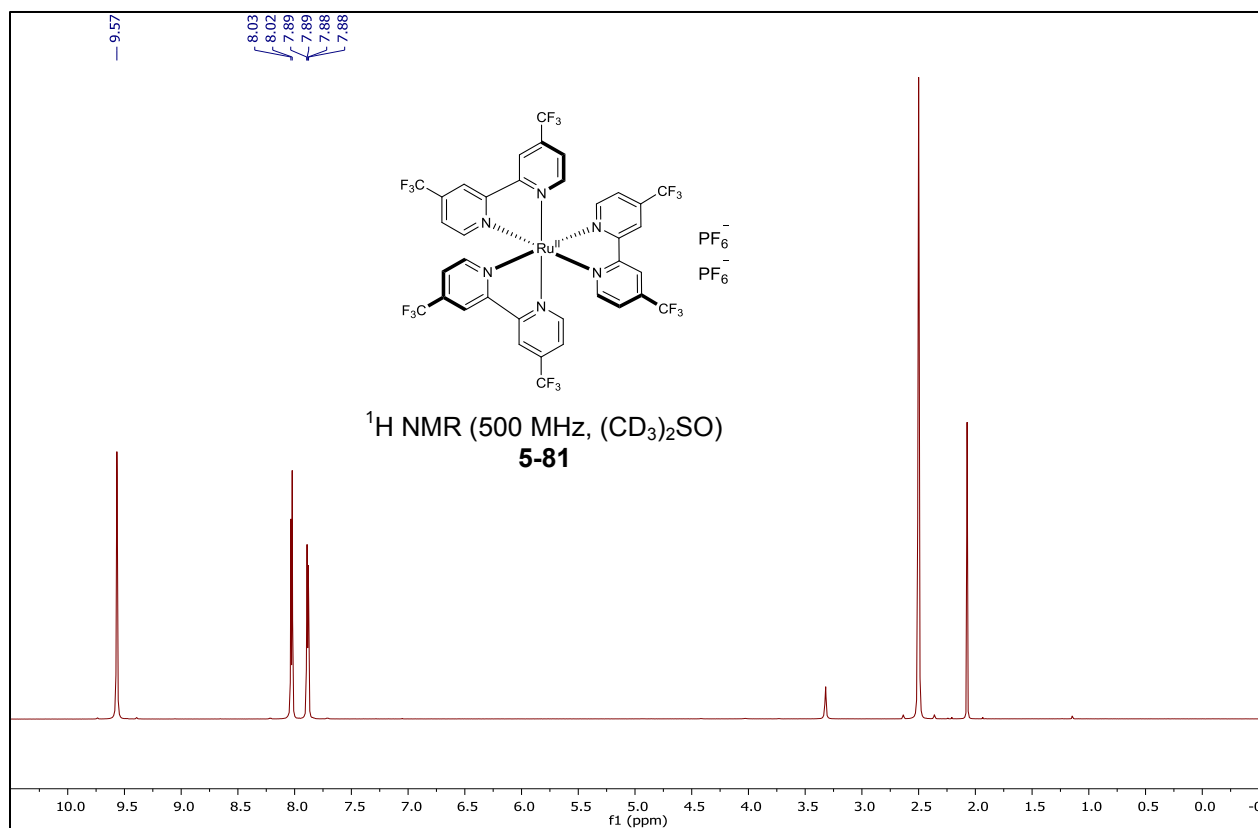


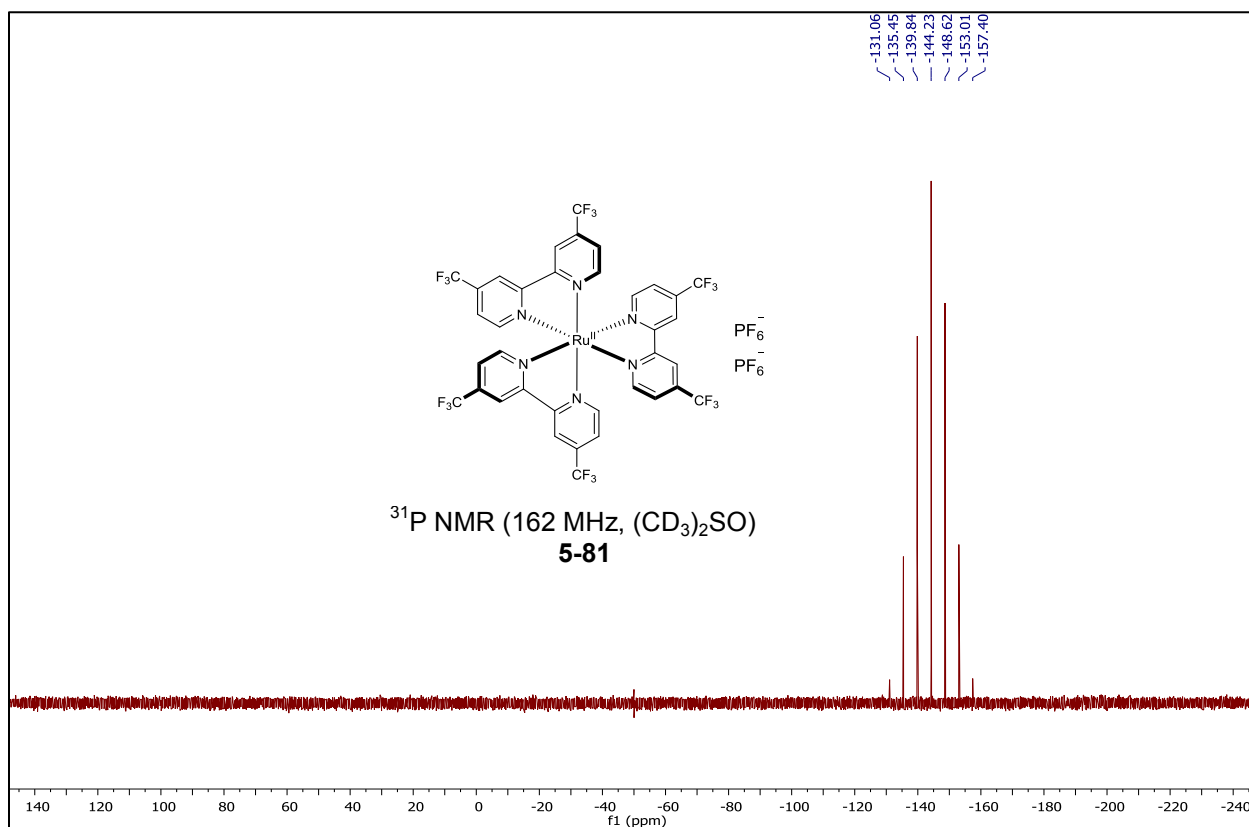
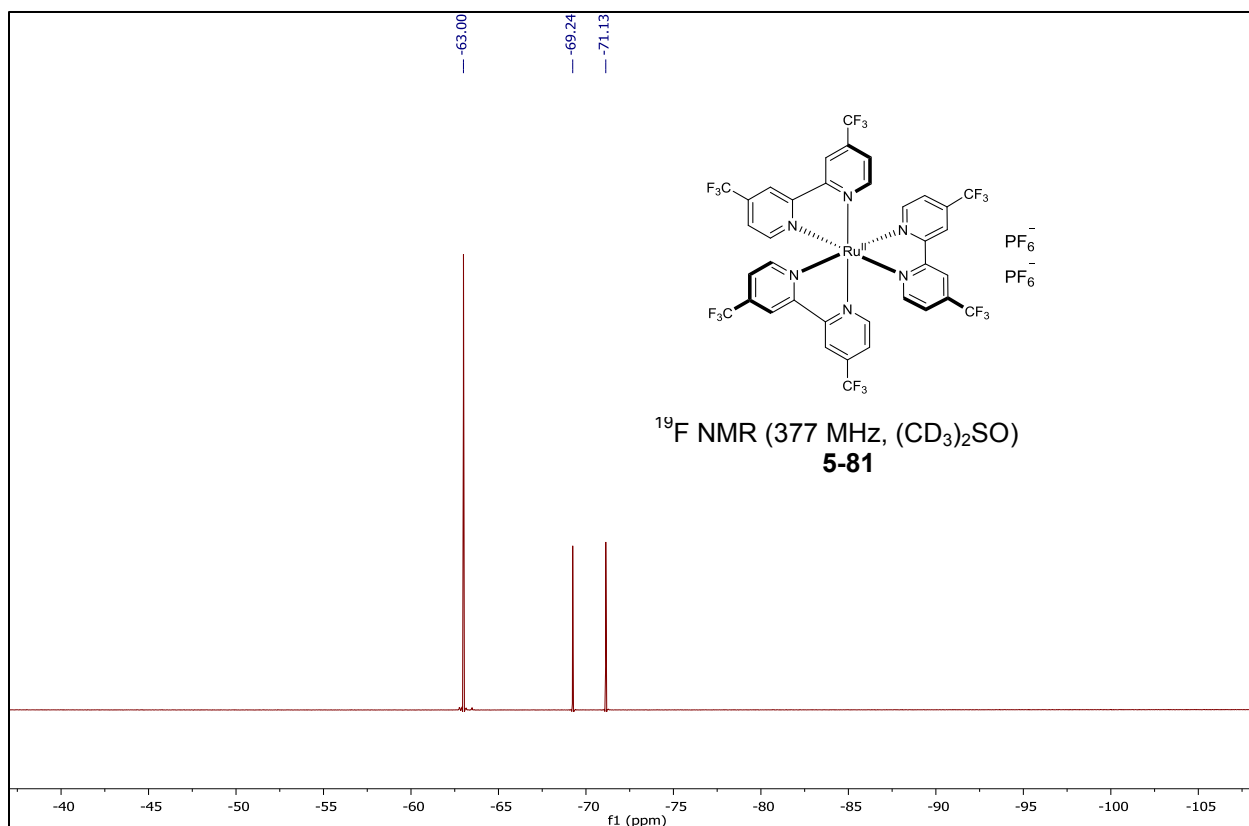












A.4 List of Compounds for Chapter 6